The Structure of the Eye

PROCEEDINGS OF THE SYMPOSIUM
HELD APRIL 11-13, 1960 DURING THE
SEVENTH INTERNATIONAL CONGRESS OF
ANATOMISTS, NEW YORK, NEW YORK

Edited by GEORGE K. SMELSER

College of Physicians and Surgeons
Columbia University

1961

ACADEMIC PRESS • New York and London

ACADEMIC PRESS INC.
111 FIFTH AVENUE
NEW YORK 3, N. Y.

United Kingdom Edition
Published by
ACADEMIC PRESS INC. (LONDON) LTD.
17 OLD QUEEN STREET, LONDON, S.W. 1

CONTRIBUTORS

T. Auerbach, *Department of Ophthalmology, College of Physicians and Surgeons, Columbia University, New York, New York*

Endre A. Balazs, *Retina Foundation, Department of Ophthalmology of the Massachusetts Eye and Ear Infirmary, and Harvard Medical School, Boston, Massachusetts*

Maurice H. Bernstein, *Department of Anatomy, Wayne State University College of Medicine, Detroit, Michigan*

A. I. Cohen, *Department of Anatomy, and the Beaumont-May Institute of Neurology, Washington University School of Medicine, St. Louis, Missouri*

Alfred J. Coulombre, *Department of Anatomy, Yale University School of Medicine, New Haven, Connecticut*

Jane L. Coulombre, *Department of Anatomy, Yale University School of Medicine, New Haven, Connecticut*

Eduardo de Robertis, *Instituto de Anatomía General y Embriología, Facultad de Ciencias Médicas, Buenos Aires, Argentina*

Anthony Donn, *Department of Ophthalmology, College of Physicians and Surgeons, Columbia University, New York, New York*

John E. Dowling, *Biological Laboratories, Harvard University, Cambridge, Massachusetts*

Olavi Eränko, *Department of Anatomy, University of Helsinki, Siltavuorenpenger, Helsinki, Finland*

M. Lynette Fleeney, *Francis I. Proctor Foundation for Research in Ophthalmology, University of California School of Medicine, San Francisco, California*

Carl Feldherr, *Department of Ophthalmology, College of Physicians and Surgeons, Columbia University, New York, New York*

H. Fernández-Morán, *Mixter Laboratories for Electron Microscopy, Neurosurgical Service, Massachusetts General Hospital, Boston, Massachusetts, and Department of Biology, Massachusetts Institute of Technology, Cambridge, Massachusetts*

Ben S. Fine, *Ophthalmic Pathology Branch, Armed Forces Institute of Pathology, Washington, D. C*

LEVON K. GARRON, *Francis I. Proctor Foundation for Research in Ophthalmology, University of California School of Medicine, San Francisco, California*

MARY ANN GAVIN, *Ophthalmology Branch, National Institute of Neurological Diseases and Blindness, National Institutes of Health, Public Health Service, U. S. Department of Health, Education and Welfare, Bethesda, Maryland*

I. R. GIBBONS, *Biological Laboratories, Harvard University, Cambridge, Massachusetts*

S. P. HAZLETT, *Department of Ophthalmology, College of Physicians and Surgeons, Columbia University, New York, New York*

CLIFFORD V. HARDING, *Departments of Ophthalmology and Physiology, College of Physicians and Surgeons, Columbia University, New York, New York*

HEINZ HERRMANN, *Department of Zoology, Institute of Cell Biology, University of Connecticut, Storrs, Connecticut*

MARIE A. JAKUS, *Retina Foundation, the Department of Ophthalmology, Massachusetts Eye and Ear Infirmary, and Harvard Medical School, Boston, Massachusetts*

JAN LANGMAN, *Department of Anatomy, McGill University, Montreal, Canada*

ARNALDO LASANSKY, *Instituto de Anatomía General y Embriología, Facultad de Ciencias Médicas, Buenos Aires, Argentina*

W. MANSKI, *Department of Ophthalmology, College of Physicians and Surgeons, Columbia University, New York, New York*

D. M. MAURICE, *Ophthalmological Research Unit, Medical Research Council, Institute of Ophthalmology, London, England*

L. MERCIER-PAROT, *Laboratoire d'Embryologie, Faculté de Médecine, Paris, France*

ESTERI MERENMIES, *Department of Anatomy, University of Helsinki, Siltavuorenpenger, Helsinki, Finland*

DAVID B. MEYER, *Department of Anatomy, Wayne State University College of Medicine, Detroit, Michigan*

NANCY L. MILES, *Department of Ophthalmology, College of Physicians and Surgeons, Columbia University, New York, New York*

FRANK MOYER, *Department of Biology, The Johns Hopkins University, Baltimore, Maryland*

MIKKO NIEMI, *Department of Anatomy, University of Helsinki, Siltavuorenpenger, Helsinki, Finland*

RONAN O'RAHILLY, *Department of Anatomy, Wayne State University College of Medicine, Detroit, Michigan*

GEORGE D. PAPPAS, *Departments of Anatomy and Ophthalmology, College of Physicians and Surgeons, Columbia University, New York, New York*

A. G. EVERSON PEARSE, *Department of Pathology, Postgraduate Medical School of London, London, England*

ANTOINETTE PIRIE, *Nuffield Laboratory of Ophthalmology, University of Oxford, Oxford, England*

JOHANNES ROHEN, *Anatomisches Institut der Universitat, Mainz, Germany*

W. SCHWARZ, *Forschungsabteilung fur Elektronenmikroskopie der Freien Universitat Berlin, Berlin, Germany*

RICHARD L. SIDMAN, *Laboratory of Cellular Neuropathology, Harvard Medical School, Boston, Massachusetts*

FRITIOF S SJOSTRAND, *Laboratory for Biological Ultrastructure Research, Karolinska Institutet, Stockholm, Sweden*[1]

GEORGE K. SMELSER, *Department of Ophthalmology, College of Physicians and Surgeons, Columbia University, New York, New York*

B. D SRINIVASAN, *Department of Ophthalmology, College of Physicians and Surgeons, Columbia University, New York, New York*

KATHARINE TANSLEY, *Institute of Ophthalmology, University of London, London, England*

A. J. TOUSIMIS, *Ophthalmic Pathology Branch, Armed Forces Institute of Pathology, Washington, D.C*

H. TUCHMANN-DUPLESSIS, *Laboratoire d'Embryologie, Faculté de Médecine, Paris, France*

FR VRABEC, *Eye Clinic of the Faculty of Hygiene, University of Prague, Prague, Czechoslovakia*

[1] *Present address* Department of Zoology, University of California, Los Angeles, California

George Wald, *Biological Laboratories of Harvard University, Cambridge, Massachusetts*

Fujiwara Wanko, *Ophthalmology Branch, National Institute of Neurological Diseases and Blindness, National Institutes of Health, Public Health Service, U. S. Department of Health, Education and Welfare, Bethesda, Maryland*

J. J. Wolken, *Biophysical Research Laboratory, Eye and Ear Hospital, University of Pittsburgh School of Medicine, Pittsburgh, Pennsylvania*

J. Reuben Wolter, *Department of Ophthalmic Surgery and Laboratory of Neuropathology, University of Michigan Medical Center, Ann Arbor, Michigan*

Eiichi Yamada, *Department of Anatomy, School of Medicine, Kurume University, Kurume, Japan*[a]

[a] *Present address:* Department of Anatomy, School of Medicine, Kyushu University, Fukuoka, Japan.

PREFACE

Investigations of fundamental problems in relation to the eye are in an astonishingly vigorous and expanding phase. This is due, in part, to a conviction of clinical ophthalmologists that advances in their specialty depend upon a more thorough understanding of ocular structure and function. However, vastly varied research efforts are also devoted to the eye in laboratories unrelated to ophthalmology—biochemistry, anatomy, physics, as well as in those of basic biology. Investigators in these diverse fields are discovering the opportunities for fundamental research presented by the eye. Within this organ, tissues are found which, because of simplicity of their organization, form almost perfect model systems, e.g., vitreous humor as a mucoid connective tissue, the cornea as the most regularly arranged fibrous tissue, and the near-crystalline organization of the rod outer segments. The eye also provides tissues (lens) so homogeneous and distinct from others, that basic problems in immunochemistry of tissue specificity can best be analyzed with its help. Because of the avascular character of the cornea, and the consequent simpler relationship of the epithelium to the underlying connective tissue, it is possible to investigate the metabolic interrelationships of these tissues more readily than elsewhere.

In addition to providing opportunities for investigating problems of wide application to other tissues, the eye also presents its own highly specialized problems. The transparency of various components—cornea, lens, and vitreous humor—challenges the physicist, while the biological problem of maintaining this condition puzzles the physiologist. One can hardly imagine a more fundamental problem than that presented by the reactivity of protoplasm to stimuli. The mechanism by means of which single quanta of light are detected and the effect produced converted to neural excitation, is certainly among the most challenging problems of modern biology.

These are but some factors contributing to the current spate of "eye research." Because of diversity of interests and techniques, little is known in one field, or laboratory, of the equally exciting studies in others. Anatomists, as well as ophthalmologists, may not treat the eye as isolated tissues, or reactions, but as a complete organ. Therefore, it seems proper that the older discipline should be the one to call home, at least occasionally, the various highly specialized investigators who are isolated by techniques as much as by geography. Segregation of their scientific efforts, caused by complications of problems and methodology, should not be allowed to progress without attempts to counteract it. This Symposium, held at Columbia University on the occasion of the Seventh International

Congress of Anatomists, is such an effort. The status of our concepts of eye structure, particularly with reference to those problems currently found to be the most challenging and amenable to study by modern methods, is reported here.

In this volume, the fine structure of ocular tissues is delineated by the leaders in electron microscopy from three continents. The most detailed description of the retina to date is made, which is, in part, based on refinements of this, the newest of the anatomical disciplines. Similarly, the techniques of histochemistry provide description of the distribution of enzyme systems in the various retinal elements, adding infinitely to our concept of their structure and purpose, which has heretofore depended upon the classic methods of Golgi and Cajal. The powerful tools of immunology allow the dissection of lens proteins into at least ten entities instead of the classic three, and these have been applied to the analysis of development and phylogenetic relationships. These problems, of prime importance in the eye, are no less so in the field of general biology. In addition, contributions to ocular anatomy are also presented, which are made possible by applications of radioautography to ocular problems. This technique permits following cells in their complicated migration from one region to another, identifying sites of cellular replacement—in short, adds "time" to the other parameters which can be studied.

Mid-twentieth-century anatomy will be found to have confirmed numerous findings, or suppositions, of the past; however, in many instances the newer methods have revealed undreamed-of structures and relationships. This Symposium, therefore, constitutes the "current events" of eye anatomy, supplementing "text-book" knowledge required by all biologists and clinicians alike, who wish a modern concept of eye structure. The invariable effort of symposium participants to relate the structure to its function answers their basic need.

The extreme diversity of tools used by modern anatomists in solving the problems of structure is impressive. Added to the older, classic techniques are those of the new anatomists. These diversified approaches used in solving problems of common interest, the enthusiasm of the participants tempered by their critical presentations, made this Symposium both significant and rewarding. It is, therefore, the participants who primarily deserve our thanks for demonstrating to us the effectiveness of the new tools of anatomy in revealing the structure of the eye. No less deserving are the five superb chairmen who kept us in order with the requisite firmness, and guided the discussions with skill—Bernard Becker, Russell Carpenter, Keith Porter, Ludwig von Sallmann, and Katharine Tansley.

GEORGE K. SMELSER

December, 1960

ACKNOWLEDGMENTS

The participants and the editor are deeply indebted to the following organizations which made the symposium and its publication possible:

National Science Foundation, Washington, D. C.

National Institute of Neurological Diseases and Blindness, National Institutes of Health, Bethesda, Maryland

National Council to Combat Blindness Inc., New York

National Society for the Prevention of Blindness, New York

and

The Institute of Ophthalmology, Columbia University, New York

CONTENTS

CONTRIBUTORS v

PREFACE ix

ACKNOWLEDGMENTS xi

Electron Microscopy of the Retina
FRITIOF S. SJOSTRAND 1

Ultrastructure and Chemical Organization of Photoreceptors
EDUARDO DE ROBERTIS AND ARNALDO LASANSKY 29

The Fine Structure of Vertebrate and Invertebrate Photoreceptors As Revealed by Low-Temperature Electron Microscopy
H FERNÁNDEZ-MORÁN 521
(Text starts on Page 521. The chapter is also listed here to indicate its original sequence in the structure of the volume.)

Localization of Oxidative Enzymes in Rat and Chick Retina in Various Physiological Conditions
A. G. EVERSON PEARSE 53

The Fine Structure of the Pigment Epithelium in the Turtle Eye
EICHI YAMADA 73

The Effect of Vitamin A Deficiency on the Fine Structure of the Retina
JOHN E DOWLING AND I. R GIBBONS 85

General Discussion of Retinal Structure in Relation to the Visual Process
GEORGE WALD 101

Silver Carbonate Techniques for the Demonstration of Ocular Histology
J REIMER WOLTER 117

Functional Architecture of the Retinal Epithelium
MAURICE H. BERNSTEIN 139

Some Preliminary Electron Microscopic Observations of the Outer Receptor Segments of the Retina of the *Macaca rhesus*
A I COHEN 151

Histochemical Observations on Esterases and Oxidative Enzymes of the Retina
OLAVI ERANKO, MIKKO NIEMI, AND ESTERI MERENMIES 159

A Structural Model for a Retinal Rod
J. J. Wolken 173

Comparative Anatomy of the Mammalian Retina with Respect to the Electroretinographic Response to Light
Katharine Tansley 193

The Development and Histochemistry of the Pecten Oculi
Regan O'Rahilly and David B. Meath 207

Cell Surfaces in the Crystalline Lens
Theodore Wanko and Mary Ann Gavin 221

The Appearance of Specific Antigens during Development of the Lens
Ivy Langman 235

Lens Antigens in Relation to Evolution
S. P. Hajdu, W. Manski, and T. Auerbach 249

Recovery from and Protection against Radiation Damage to the Lens
Antoinette Pirie 259

The Distribution of DNA-Synthesizing Cells in Lens Epithelium Following Injury
Clifford V. Harding, Carl Feldherr, and B. D. Srinivasan 273

Electron Microscopic Observations of the Human Vitreous Body
W. Schwarz 283

Molecular Morphology of the Vitreous Body
Endre A. Balazs 293

The Endothelium of the Anterior Chamber Angle of the Eye
Fr. Vrabec 311

The Topography of Encapsulated Terminal Sensory Corpuscles of the Anterior Chamber Angle of the Goose Eye
Fr. Vrabec 325

Morphology and Pathology of the Trabecular Meshwork
Johannes Rohen 335

The Fine Structure of the Human Cornea
Marie A. Jakus 343

Descemet's Membrane in the Human Peripheral Cornea: A Study by Light and Electron Microscopy
M. Lynette Feeney and Levon K. Garron 367

The Use of Permeability Studies in the Investigation of Submicroscopic Structure
D. M. Maurice 381

Electron Microscopical Studies of the Fibrillogenesis in the Human Cornea
W. Schwarz 393

The Development of the Structural and Optical Properties of the Cornea
Alfred J. Coulombre and Jane L. Coulombre 405

Tissue Interaction and Differentiation in the Corneal and Scleral Stroma
Heinz Herrmann 421

Incorporation of Tritium-Labeled Thymidine by Rabbit Corneal Endothelium
Nancy L. Mills and Anthony Donn 435

Electron Microscopy of the Pigment Epithelium of the Iris
A. J. Tousimis and Ben S. Fine 441

The Fine Structure of the Ciliary Epithelium in Relation to Aqueous Humor Secretion
George D. Pappas and George K. Smelser 453

Electron Microscope Observations on the Origin, Development, and Genetic Control of Melanin Granules in the Mouse Eye
Frank Moyer 469

Histogenesis of Mouse Retina Studied with Thymidine-H^3
Richard L. Sidman 487

Production of Congenital Eye Malformations, Particularly in Rat Fetuses
H. Tuchmann-Duplessis and L. Mercier-Parot 507

The Fine Structure of Vertebrate and Invertebrate Photoreceptors As Revealed by Low-Temperature Electron Microscopy
H. Fernández-Morán 521

Author Index 557

Subject Index 566

Electron Microscopy of the Retina

FRITIOF S. SJÖSTRAND[1]

Laboratory for Biological Ultrastructure Research, Karolinska Institutet, Stockholm, Sweden

THIS PAPER WILL SURVEY some of the work done on the ultrastructural organization of the retinal receptors in the eye.[2] Attempts will be made, based on morphological observations, to formulate hypotheses regarding certain fundamental biological problems which meet the investigator when analyzing the retinal components. Such problems deal with the molecular architecture of the various membranes and the development of membranous components, including the synthesis and the organization of the molecular constituents of the membranes. Furthermore, we find reason to discuss the functional significance of the principle of organization of the retina as well as the central nervous system with respect to neuronal and nonneuronal cellular elements, the latter being represented by the neuroglia, the Muller's cells in the retina, and the Schwann cells in the peripheral nerves

I shall allow myself to present certain hypotheses resulting from what might appear as rather wild speculations. Nonetheless, this seems appropriate at the present time when so many morphological observations have piled up that many conscientious researchers feel an intense pressure to test whether all these descriptive data can further our understanding of basic biological problems, or will merely remain examples of more or less artistic photography.

A Molecular Model for the Plasma Membrane[3]

One type of elementary structural component dominates the ultrastructural organization of the retinal receptors as well as many other types of cells There is a dominance of membranous components in the receptor cells, and we shall see that in the case of the receptor cells we are frequently dealing with the plasma membrane, or derivatives of the plasma membrane. It is therefore useful for our discussion of the prob-

---

[1] *Present address* Department of Zoology, University of California, Los Angeles, California.

[2] An earlier survey was published by the present author in *Ergeb. Biol.* 21, 128-160 (1959).

[3] Pictures illustrating this part of the paper have been published in "Modern Scientific Aspects of Neurology" (edited by J. M. Cumings; Arnold, London, 1960).

of the less opaque interspaces corresponds roughly to the thickness of one or two double layers of lipid molecules.

At the boundary between two closely packed cells the plasma membranes of the two cells appear as two osmiophilic layers about 60 Å thick separated by a light interspace about 100 Å wide. It was proposed that the regular and rather constant spacing of the two osmiophilic layers, one belonging to each of the two closely arranged plasma membranes, was due to some "cementing" material being interposed between the osmiophilic layers. It was proposed that this material consisted, at least partially, of two layers of lipids, one double layer belonging to each plasma membrane (Sjostrand and Rhodin, 1953).

With potassium permanganate fixation, Robertson (1957, 1959) observed that the plasma membrane which appears in osmium-fixed material as a single opaque layer about 60 Å thick showed a triple-layered structure with two opaque layers separated by a lighter interspace, each component measuring about 25 Å. Robertson assumed that this triple-layered component corresponded to the 60 Å thick osmiophilic layer described earlier by Sjostrand and Rhodin (1953). Robertson interpreted the light narrow interspace which separates the osmiophilic layers of the two plasma membranes when two cells are in close contact as representing an extracellular space, and he claimed (1957) to have disproven the interpretation proposed earlier for the layered membrane structures by Sjöstrand (1953c, e, f) and by Sjostrand and Rhodin (1953). However, a careful study of potassium permanganate-fixed myelinated and unmyelinated nerve fibers furnished evidence for the interpretation that the triple-layered component observed after potassium permanganate fixation corresponded only to a minor part of the osmiophilic layer of the plasma membrane (Sjostrand, 1960a, b).

First, it appeared on analyzing *the invaginations* of the plasma membrane of the Schwann cells through which the layered myelin sheath pattern is connected with the surface membrane of the Schwann cell, that most of the triple-layered component of the plasma membrane observed in potassium permanganate-fixed material is located in a position which corresponds to the light interspace which, in osmium-fixed material, separates the osmiophilic layers of the two adjacent plasma membranes. This conclusion is based on the fact that the invagination appears as a five-layered component in potassium permanganate-fixed material due to a close packing of the two triple-layered plasma membrane components.

Second, the triple-layered component of the plasma membrane in potassium permanganate-fixed material is continuous with the layered myelin sheath pattern as observed by Robertson (1957). The middle opaque layer, which is formed by a fusion of two permanganate-stained

lems mentioned above that we start with a presentation of a model for the molecular architecture of the plasma membrane (Sjöstrand, 1960a, b). Such a model can now be proposed since high resolution electron microscopy reveals structural components which are within the molecular range of dimension. The observed regular minute spacings are assumed to be due to ordered systems of molecules, and have been interpreted to a certain extent as representing layers of oriented molecules. The situation is similar to that of interpreting X-ray diffraction data which also give information of spacings existing in the object. The general principle for our interpretation of such ordered systems remains unchanged whether the structure, represented by dimensions and spacings, is deduced indirectly from X-ray diffraction patterns or can be observed directly by means of the electron microscope.

An electron microscopical analysis of the structure of the myelin sheath of peripheral nerve fibers has presented information of fundamental importance for the deduction of the model for the molecular architecture of the plasma membrane. This object is particularly suitable for such an analysis because it allows the pooling of data obtained with different methods of investigation; the electron microscope data are supplemented by X-ray as well as polarization optical data. The important observation by Ben Geren (1954) regarding the development of the myelin sheath from the Schwann cell plasma membrane shows the close relation between the layered structure of the myelin sheath and the plasma membrane. The direct continuity of the myelin sheath structure and the plasma membrane is retained in adult nerve fibers and, therefore, the layers which can be observed in the plasma membrane by means of electron microscopy can be related to the layered pattern of the myelin sheath.

The model for the molecular structure of the plasma membrane was derived from a comparative study of the structural patterns observed on material fixed with osmium tetroxide and with potassium permanganate.

Ever since the double character of most membrane components was observed in high resolution electron micrographs, which allowed measurements of spacings and thicknesses of the various layers, the present author has proposed that this monotonously repeated layered pattern corresponded to one basic principle of organization of these membrane components (Sjöstrand, 1953c, e, f). According to the proposed interpretation the opaque layers represent the location of the protein components, and the light interspaces between two pairs of opaque layers the location of layers of oriented lipid molecules. The myelin sheath pattern observed in the electron microscope would be easily understood by accepting these assumptions (Sjöstrand, 1953a). In most cases the width

of the less opaque interspaces corresponds roughly to the thickness of one or two double layers of lipid molecules.

At the boundary between two closely packed cells the plasma membranes of the two cells appear as two osmiophilic layers about 60 Å thick separated by a light interspace about 100 Å wide. It was proposed that the regular and rather constant spacing of the two osmiophilic layers, one belonging to each of the two closely arranged plasma membranes, was due to some "cementing" material being interposed between the osmiophilic layers. It was proposed that this material consisted, at least partially, of two layers of lipids, one double layer belonging to each plasma membrane (Sjostrand and Rhodin, 1953).

With potassium permanganate fixation, Robertson (1957, 1959) observed that the plasma membrane which appears in osmium-fixed material as a single opaque layer about 60 Å thick showed a triple-layered structure with two opaque layers separated by a lighter interspace, each component measuring about 25 Å. Robertson assumed that this triple-layered component corresponded to the 60 Å thick osmiophilic layer described earlier by Sjostrand and Rhodin (1953). Robertson interpreted the light narrow interspace which separates the osmiophilic layers of the two plasma membranes when two cells are in close contact as representing an extracellular space, and he claimed (1957) to have disproven the interpretation proposed earlier for the layered membrane structures by Sjostrand (1953c, e, f) and by Sjostrand and Rhodin (1953). However, a careful study of potassium permanganate-fixed myelinated and unmyelinated nerve fibers furnished evidence for the interpretation that the triple-layered component observed after potassium permanganate fixation corresponded only to a minor part of the osmiophilic layer of the plasma membrane (Sjostrand, 1960a, b).

First, it appeared on analyzing *the invaginations* of the plasma membrane of the Schwann cells through which the layered myelin sheath pattern is connected with the surface membrane of the Schwann cell, that most of the triple-layered component of the plasma membrane observed in potassium permanganate-fixed material is located in a position which corresponds to the light interspace which, in osmium-fixed material, separates the osmiophilic layers of the two adjacent plasma membranes. This conclusion is based on the fact that the invagination appears as a five-layered component in potassium permanganate-fixed material due to a close packing of the two triple-layered plasma membrane components.

Second, the triple-layered component of the plasma membrane in potassium permanganate-fixed material is continuous with the layered myelin sheath pattern as observed by Robertson (1957). The middle opaque layer, which is formed by a fusion of two permanganate-stained

layers when the plasma membrane surfaces reach in contact, is continuous with the intraperiod line of the myelin sheath pattern. If we now accept the interpretation of the myelin sheath pattern with regard to the relative location of the protein and lipid components which is generally agreed upon we find that the middle layer of the triple-layered plasma membrane component is continuous with the middle of the presumed lipid double layers in the myelin sheath. Therefore it seems proper to assume, as Robertson has done, that the triple-layered component contains a double layer of lipid molecules.

Third, in osmium-fixed material the light interspace separating the two osmiophilic layers, belonging one to each plasma membrane surface of the invagination, is continuous with the layer in the myelin sheath pattern in which the oriented lipid molecules have been proposed to be localized (Sjöstrand, 1953a, 1956c; Fernández-Morán and Finean, 1957). This interspace corresponds in width and relative position to two double layers in the myelin sheath.

As described above, the invagination of the Schwann cell plasma membrane appears as a five-layered component in potassium permanganate-fixed material and as a triple-layered component in osmium-fixed material. This striking difference could also be observed at regular cell boundaries between two Schwann cells of unmyelinated nerve fibers.

In analogy with the reasonable interpretation of the myelin sheath structure, it is assumed that the two layers of the plasma membrane, which appear stained after potassium permanganate fixation, correspond to the location of the polar end groups of the lipid molecules covered by a thin monomolecular layer of protein. This is in full agreement with the model for the structure of the plasma membrane proposed by Danielli and Davson (1934) and the interpretation proposed by Robertson (1957, 1959).

When superimposing the potassium permanganate picture onto the osmium picture, in the case of the myelin sheath as well as when dealing with boundaries between two closely packed cells, it is apparent that most of the triple-layered components of the plasma membranes in potassium permanganate-fixed material are located in what appears as light interspaces between osmiophilic layers in osmium-fixed material. Therefore, there is a clear possibility that the osmiophilic layer includes an additional membrane component which remains unstained in potassium permanganate fixation.

The model for the molecular architecture of the plasma membrane which I have proposed (Sjöstrand, 1960a, b) consists of a double layer of lipid molecules sandwiched between two very thin layers (monolayers) of protein molecules with extended peptide chains, and, in

addition to this complex, a layer of proteins of varying thickness in different types of membranes which would be located on the cytoplasmic side of the lipoprotein components (Fig. 1). In the plasma membrane the thickness of this protein layer would be of the order of 40 A. It might consist of globular protein molecules, and the enzyme molecules, which we assume are located in most membranes, might be located in this layer.

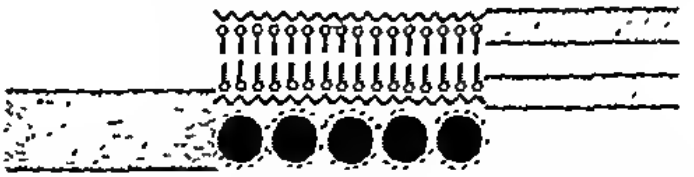

FIG. 1. Model proposed for describing the molecular architecture of the plasma membrane. (From Sjostrand, 1960a, b)

KEY: Small open circle attached to bar: Lipid molecule with the polar end indicated by the open circle. Wavy line: Protein molecules with peptide chain stretched. Filled circle: Globular protein molecules.

Robertson has proposed as an alternative that the double layer of lipid molecules is sandwiched between one protein layer (monolayer) and one polysaccharide layer. This assumption would allow a simple explanation for the fact that the peripheral permanganate-stained layer does not take any stain with osmium tetroxide fixation. The inner potassium permanganate-stained layer, as well as parts of adjacent lipid molecules, might well be included in the layer stained with osmium tetroxide and account for 10–20 A of the thickness of this layer.

The Molecular Architecture of the Outer Segments of Retinal Rods and Cones

After this discussion of a model for the molecular architecture of the plasma membrane we may turn to describing the structure of the outer segment of retinal rods and cones (Fig. 2). This jump will soon appear less abrupt than it might at first.

The shape and dimensions of the basic structural unit of the outer segment has been revealed by analyzing fragmented (Sjöstrand, 1949) as well as sectioned outer segments (Sjöstrand, 1953c) (Figs. 3 and 4). In the guinea pig retina each outer segment consists of a pile of 140 A thick disks, each disk consisting of two about 30 A thick layers separated by an interspace 70–80 A wide.

Since these dimensions are within the range of macromolecules it seemed reasonable to try to deduce a model illustrating an interpretation of the pattern in terms of the molecular architecture of these disks. The polarization optical analysis by W. J. Schmidt (1924, 1937, 1937)

furnished additional data on which to base this model. According to these latter data, the outer segment would contain lipid molecules oriented with their long axis parallel to the long axis of the outer segment. Protein components would be arranged in layers oriented perpendicularly to this direction.

The experiments of fragmentation of outer segments (Sjöstrand, 1949) had revealed that the height of a pile of a few disks corresponds to multiples of the thickness of an individual disk. It seemed unlikely, therefore, that the lipid molecules were located between the disks. Instead, the lipids were considered to be located within the disks in the interspace between the about 30 Å thick membranous layers. These membranous layers were proposed to represent the protein component of the outer segment. This interpretation seemed to fit in rather well with the dimensions of these various layers. The adjacent disks were assumed to be separated by an ionic aqueous medium.

The lipid concentration was estimated on very pure fractions of outer segments and was found to be about 40% of the dry weight of the segments (Sjöstrand and Cierer, 1959). The relative volumes of the light interspaces of the disks and of the osmiophilic layers are such that all the lipids could be located in the disks.

When analyzing thin sections it appeared that the width of the light interspace located within the disks was rather constant in contrast to the great variation in the width of the interspaces separating adjacent disks. This observation was considered to support the proposed model because the constant spacing between the osmiophilic layers was assumed to indicate the presence of some material which kept the osmiophilic layers glued together at a fixed distance.

The disk structure of the outer segments was described by other workers as "flattened sacs" (De Robertis, 1956). Furthermore, Robertson's interpretation that the lipids of the plasma membrane were located in its osmiophilic layer gave further impetus to investigate the appearance of the disk structure after fixation in potassium permanganate.

The disks of the outer segments show very different structural patterns in potassium permanganate-fixed and osmium-fixed material. After potassium permanganate fixation each disk appears to consist of five layers: three opaque layers separated by two less opaque interspaces (Fig. 5) (Sjöstrand, 1960b; Moody and Robertson, 1960). The middle

---

FIG. 2. Schematic drawing of retinal receptors (rods) in the guinea pig retina. One α-receptor in the middle flanked by two β-receptors. Interreceptor contacts as well as the synaptic connections between receptor cells and the neurons of the layer of the bipolars are presented schematically.

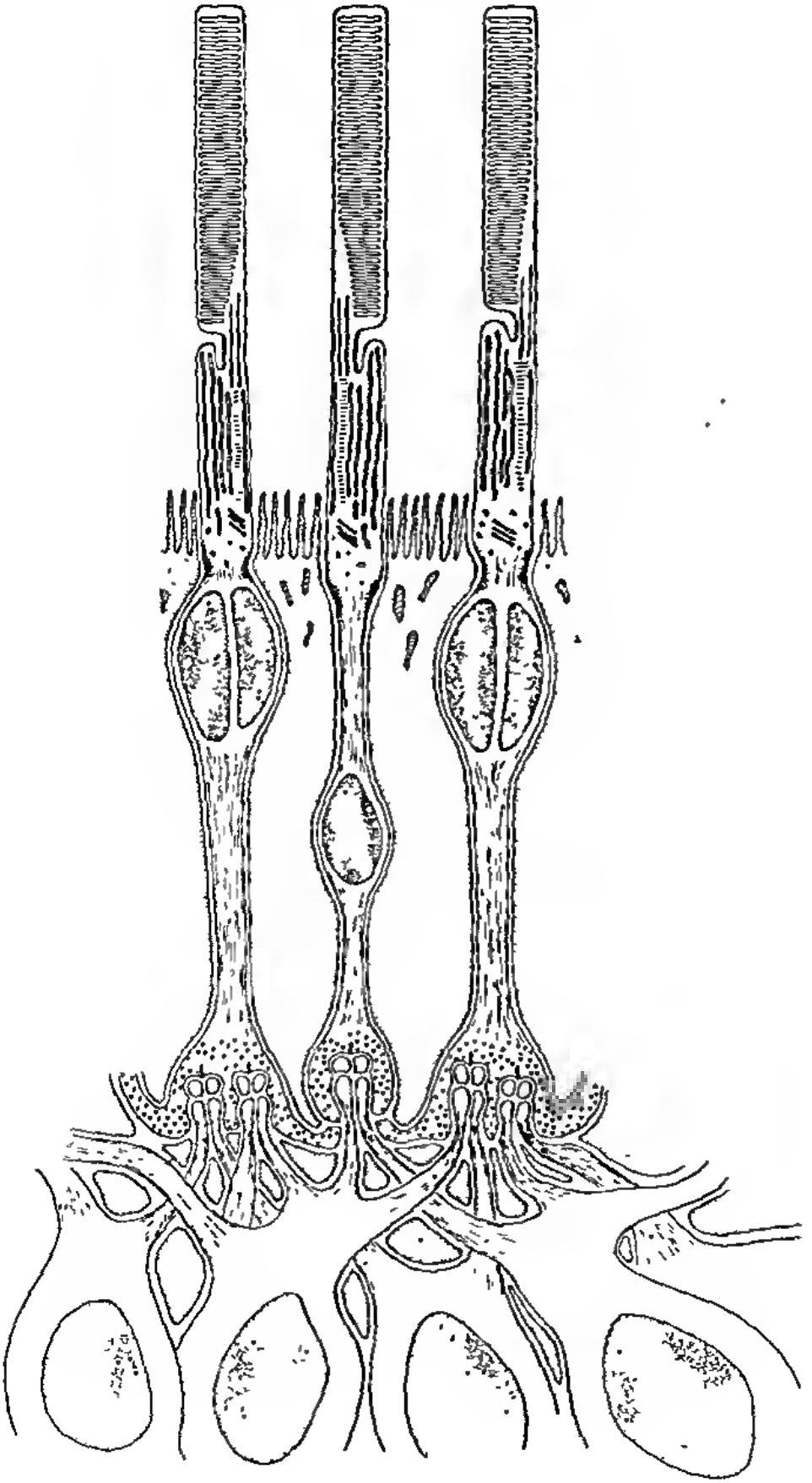

opaque layer is thicker than the other two opaque layers. Due to this multilayered appearance the disks give the impression of representing rather compact structures, and there is no indication that they represent flattened sacs. The total thickness of the disks as measured on potassium permanganate-fixed material is similar to that measured on osmium-fixed material. Therefore it seems likely that the about 30 Å thick osmiophilic layers of the disks correspond to the about 25 Å thick peripheral layers of the five-layered permanganate-stained disk, and that the osmium staining in this case does not reveal in any definite way the existence of a protein layer in addition to that which is assumed to be stained by potassium permanganate.

The following model for the molecular architecture of the unit disk will be tentatively proposed. Each disk consists of *two* double layers of lipid molecules sandwiched between two thin layers of protein molecules. The two double layers of lipid molecules are separated by a layer of protein or polysaccharides (Fig. 10). An alternative model with additional protein layers covering the free surfaces of the disk can, however, not be ruled out at present. These models will appear rather logical and plausible after the following discussion.

The Relation between the Outer Segment Disks and the Plasma Membrane

In the guinea pig retina the disks of the outer segments of the rods are interconnected through tubular connections (Sjöstrand, 1953c). These tubular connections are located at or close to the center of the disk at the inner end of a deep incision extending from the edge of the

---

FIG. 3. Low power picture of longitudinal section through parts of two outer segments of rod cells in the perch retina. Osmium tetroxide fixation. Magnification: × 8000.

FIG. 4. Longitudinal section through the two outer segments of a double cone in the perch retina. The triple-layered character of the individual disks is shown in this osmium-fixed specimen. Along the contour of the outer segment in the left side of the picture most of the light interspaces in the disks are closed by looplike connections between the two osmiophilic layers. For some adjacent disks, however, the osmiophilic layers are continuous leaving light space within the disks facing the extracellular space uncovered. At these places the osmiophilic layers of the disks are continuous with the plasma membrane. Along the contour of the outer segment in the right side of the picture all adjacent disks are mutually connected leaving uncovered the light interspaces in the disks facing the extracellular space. An examination of the contours on the opposite side of the two outer segments showed that all disks are closed along this edge. Osmium tetroxide fixation. Magnification: × 100,000. (From Sjöstrand, 1959b.)

disk to the center of the disk (Fig. 6). This structural continuity of the disks might be related to the mechanism through which the disks are formed.

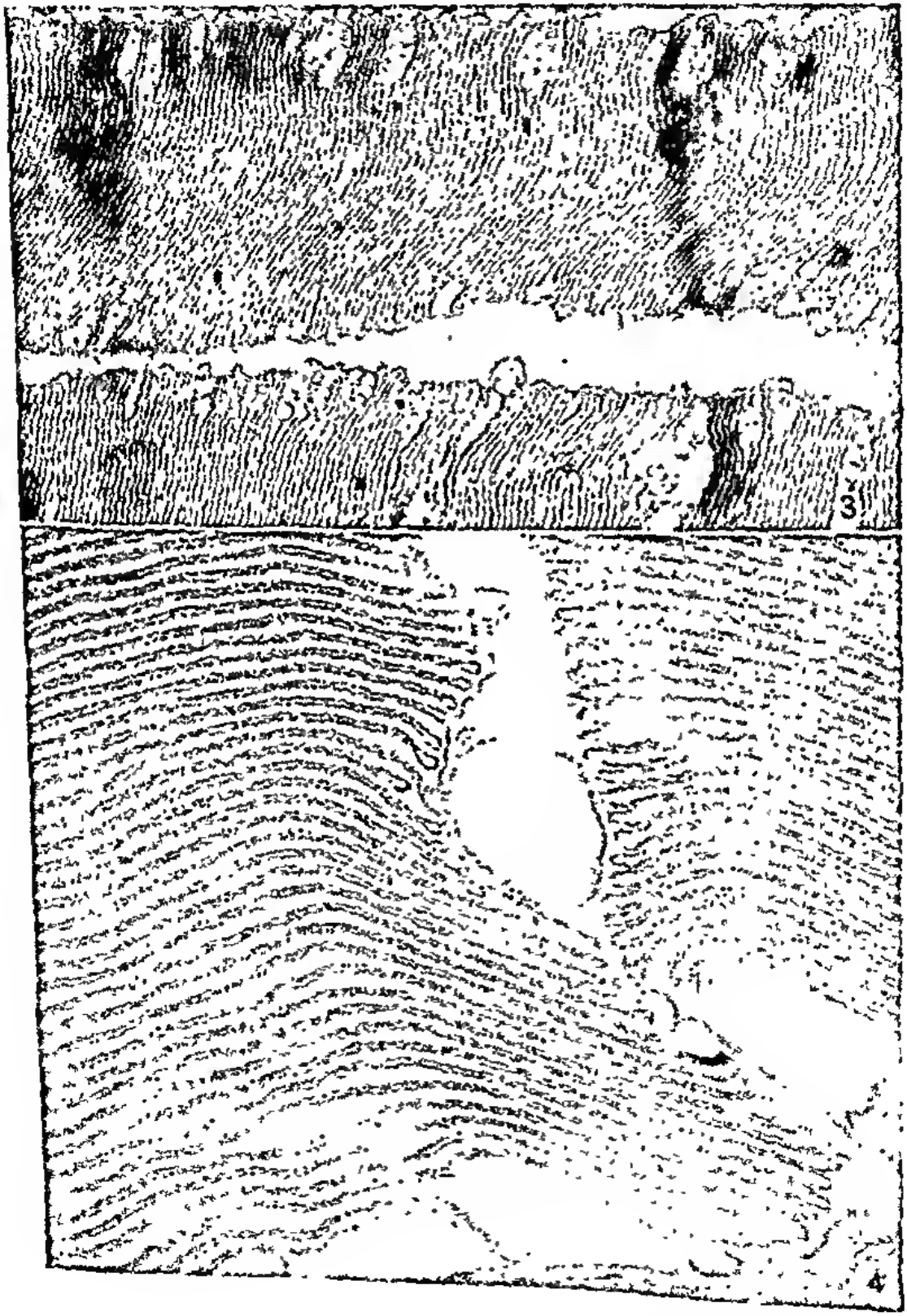

Some observations made on the structure of the outer segments of the cones in the perch retina and on developing rod outer segments in the cat retina are of interest in this connection. It was observed (Sjöstrand, 1959b) that the disk structure in the double cones of the perch retina represents infoldings of the plasma membrane of the outer segment. This becomes obvious when observing the disk edges in longitudinally sectioned outer segments fixed in osmium tetroxide when the plane of the section is properly oriented (Fig. 4). In such cases we find at one side of the outer segment that the edges of the two disk membranes are fused, frequently forming a small loop. On this side the outer segment is bounded by a plasma membrane. When looking at the edge on the opposite side of the outer segment, the pattern is different. The two opaque layers representing the two disk membranes are not fused, but diverge and are continuous with the nearest membranes of the adjacent disks above and below. This means that the interspaces separating adjacent disks appear closed at this edge, but the space bounded by the osmiophilic layers of the disk appears open. Along this side of the outer segment no plasma membrane covers the surface of the outer segment. Therefore it seems apparent that the disks represent folds of the surface membrane, and that in each fold the two membrane surfaces fuse to form the compact disk structure. That this is the case can easily be confirmed by direct observations of the relation between the plasma membrane and the disks. This type of outer segment lacks the tubular connections observed in the guinea pig rod outer segments. Furthermore, the disks are lacking any incisions. Due to this folded structure the pile of disks will form a continuous structure extending through the whole outer segment.

When studying the development of the outer segments the first days after the birth of kittens, preliminary observations (Sjöstrand, 1959b) indicated that the first unit disks were formed by a folding of the plasma membrane. The picture resembled that observed in adult perch cones. It therefore seems possible that the outer segments are formed through a repeated infolding of the plasma membrane (Figs. 7 and 8). In those outer segments where the connections between the disks are confined to tubelike structures, the base of the folds has been narrowed down and

---

FIG. 5. Longitudinal section through an outer segment of a retinal rod in the guinea pig eye fixed in potassium permanganate. Each disk appears as a five-layered structure with a thick middle opaque layer. Magnification: × 150,000. (From Sjöstrand, 1960b.)

FIG. 6. Cross section through outer segments of a cat retina showing the incisions at the edges of the disks and the tubular, stalklike connections between adjacent disks. Osmium tetroxide fixation. Magnification: × 35,000.

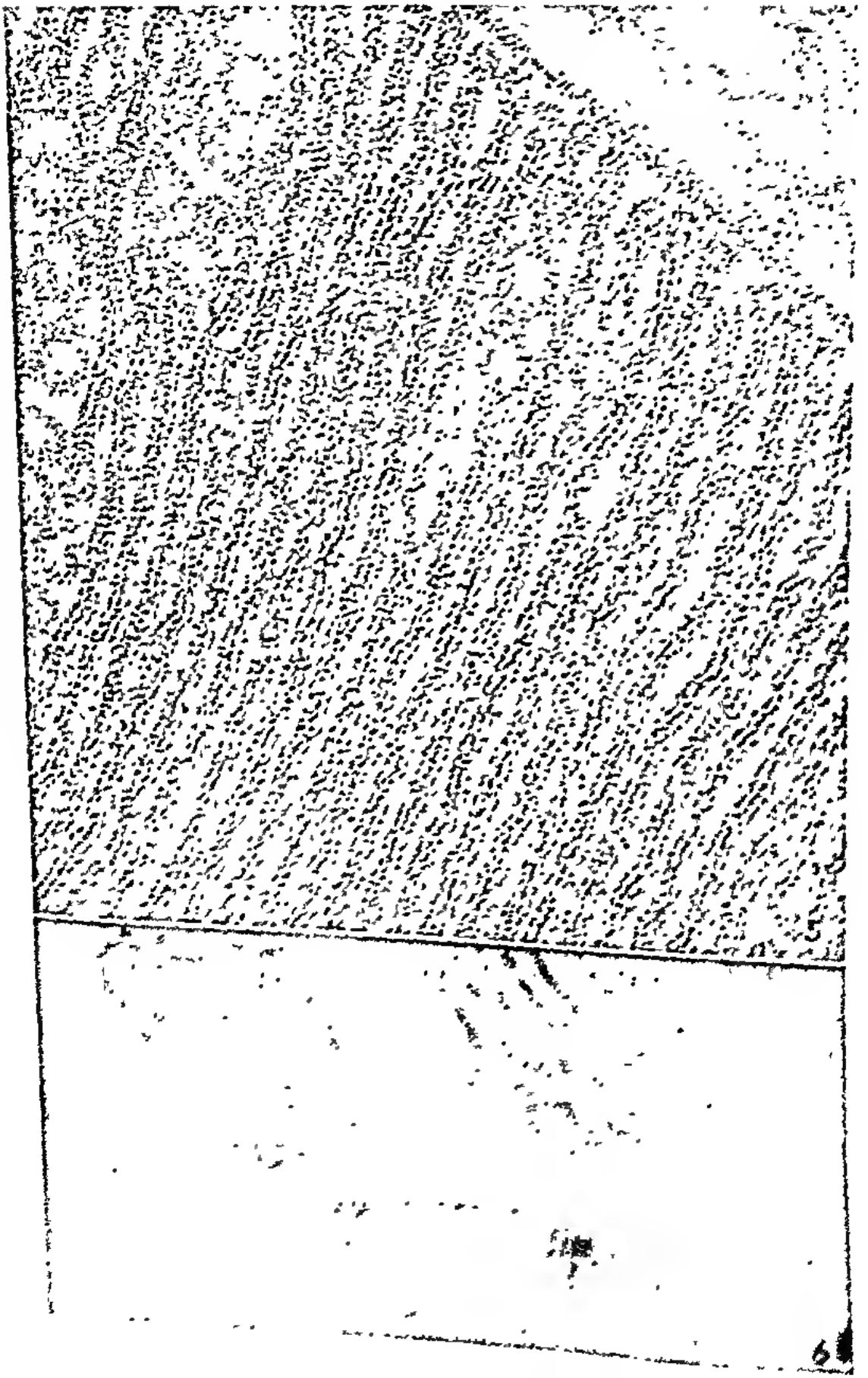
5
6

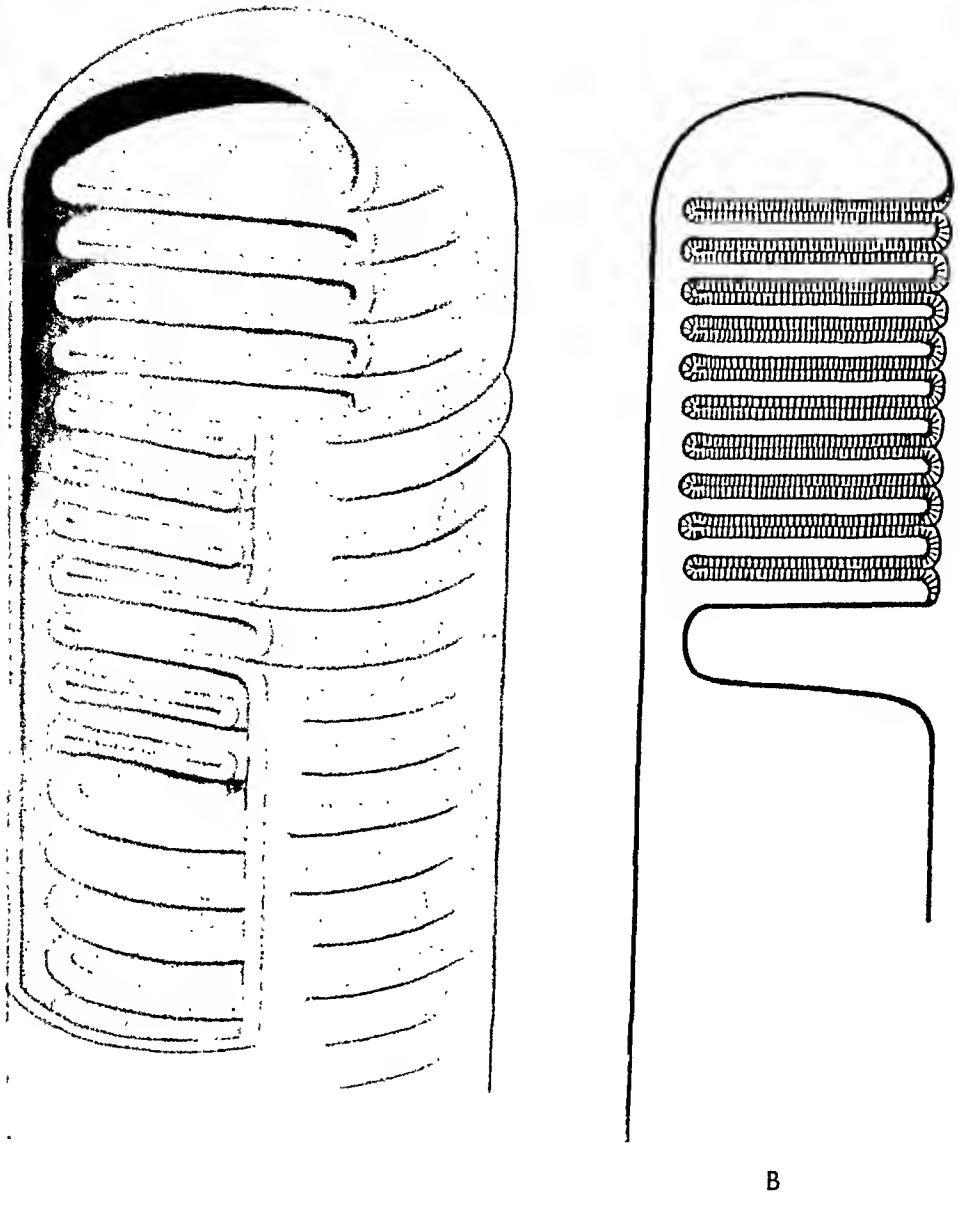

FIG. 7, A and B. Schematic drawings showing the arrangement of the outer segment disks in the perch cones. The disks extend as folds from the plasma membrane across the whole diameter of the outer segment. If a longitudinal section is oriented in such a way that it cuts through the centers of the area from which the folds extend (Fig. 7, B) one contour of the outer segment will appear like the contour of the outer segment on the right side of Fig. 4, this is represented in the upper area of Fig. 7, A. If the section was oriented in such a way that it cuts through the area of transition from folded to unfolded surface, one contour would appear like that of the outer segment on the left side of Fig. 4. This depends on the varying width of the folds. This case is represented in the middle portion of Fig. 7, A.

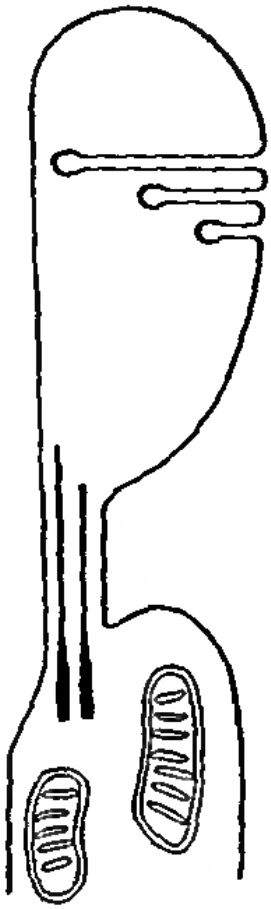

FIG. 8. Schematic drawing showing the formation of the outer segment disks as infoldings of the plasma membrane

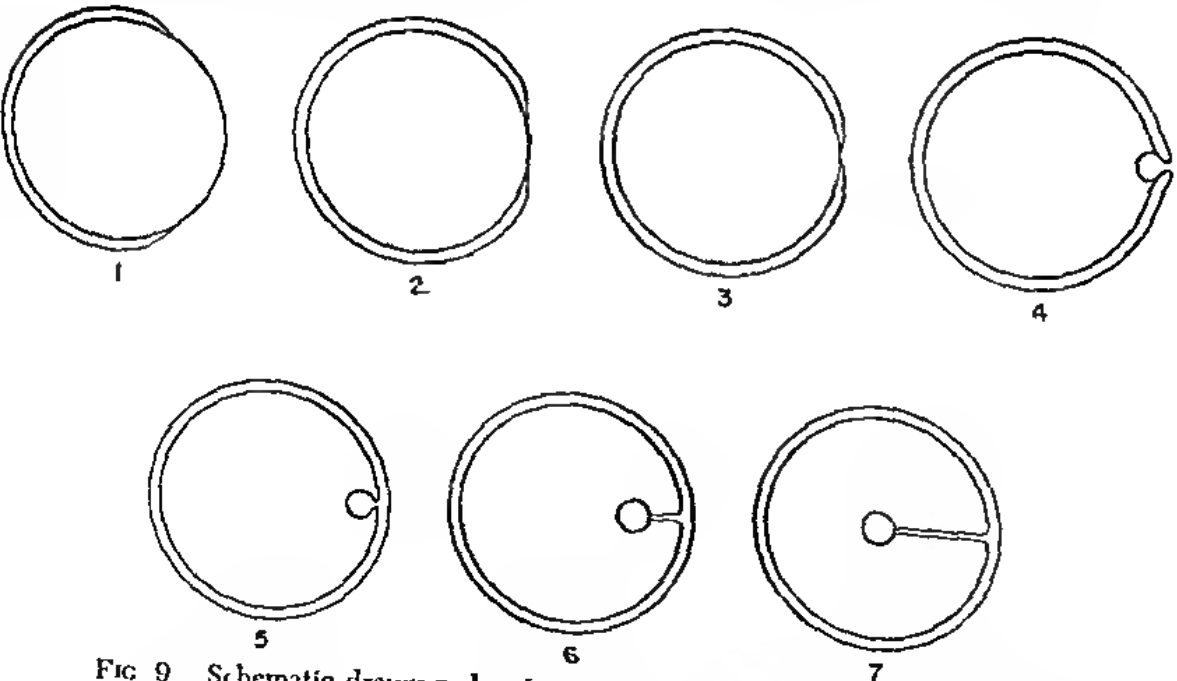

FIG 9 Schematic drawing showing a possible explanation for the formation of the stalklike connections between adjacent disks and the disk incision characteristic for mammalian rod cells.

displaced toward the center of the outer segment, leaving an open slit or incision extending from the edge to the center. This slit indicates the path along which the connection has moved (Fig. 9).

I would like to speculate a little about the mechanism of formation of these infoldings. There are some observations that seem to be of certain interest in this connection. The thickness of the osmiophilic layer of the plasma membrane of the outer segments is about 60 Å. The thickness of the osmiophilic layers of the disks is 30–40 Å. Therefore it seems reasonable to assume that the structural properties of the two membranes in the folds are not identical to the structural properties of the plasma membrane as is accounted for in the model discussed above. A great deal of the osmiophilic material in the plasma membrane seems to be lost in connection with the formation of the folds.

Let us imagine that it is the layer of protein in the plasma membrane, which was assumed to consist of globular protein molecules, that is missing in the folds, as proposed above. The edge region of the disks shows certain particular properties both in fragmented outer segments (Sjöstrand, 1949) and in sectioned retinas (Sjöstrand, 1953c). The fragmented disks are framed by an edge cord with a thickness of 140 Å. In the first electron microscopic study of thin sections through the outer segments of guinea pig rods the edge region was demonstrated to appear more intensely stained and more resistant to deformation than the rest of the disk membranes. In the perch cone outer segments, the edge region is characterized by a looplike appearance in cross section. Furthermore, the osmiophilic layer forming this loop is thicker than the osmiophilic layer extending along the flat surfaces of the disk. The thick-

---

FIG. 10. Schematic drawing illustrating the proposed model for the molecular architecture of the disks of the outer segments of rod and cone cells with the differentiation of these disks in an edge zone and a central zone. According to the proposed hypothesis, the edge zone would interfere with the formation of the rest of the disk and represent the region from which the disk grows. The edge zone appears as a part of the plasma membrane which has been dislocated through the growth of a fold which represents the first step in the development of the disk. The molecular architecture of the main part of the disk is proposed to be represented by four double layers of lipid molecules, each double layer being sandwiched between thin layers of protein. The edge zone is pictured to correspond to the complete membrane model proposed for the plasma membrane with a layer of globular proteins associated with a double layer of lipids sandwiched between two thin layers of proteins with extended peptide chains.

KEY: Small open circle attached to bar: Lipid molecule with the polar end indicated by the open circle. Jagged lines: Protein molecules with peptide chain stretched. Large open circles: Globular protein molecules.

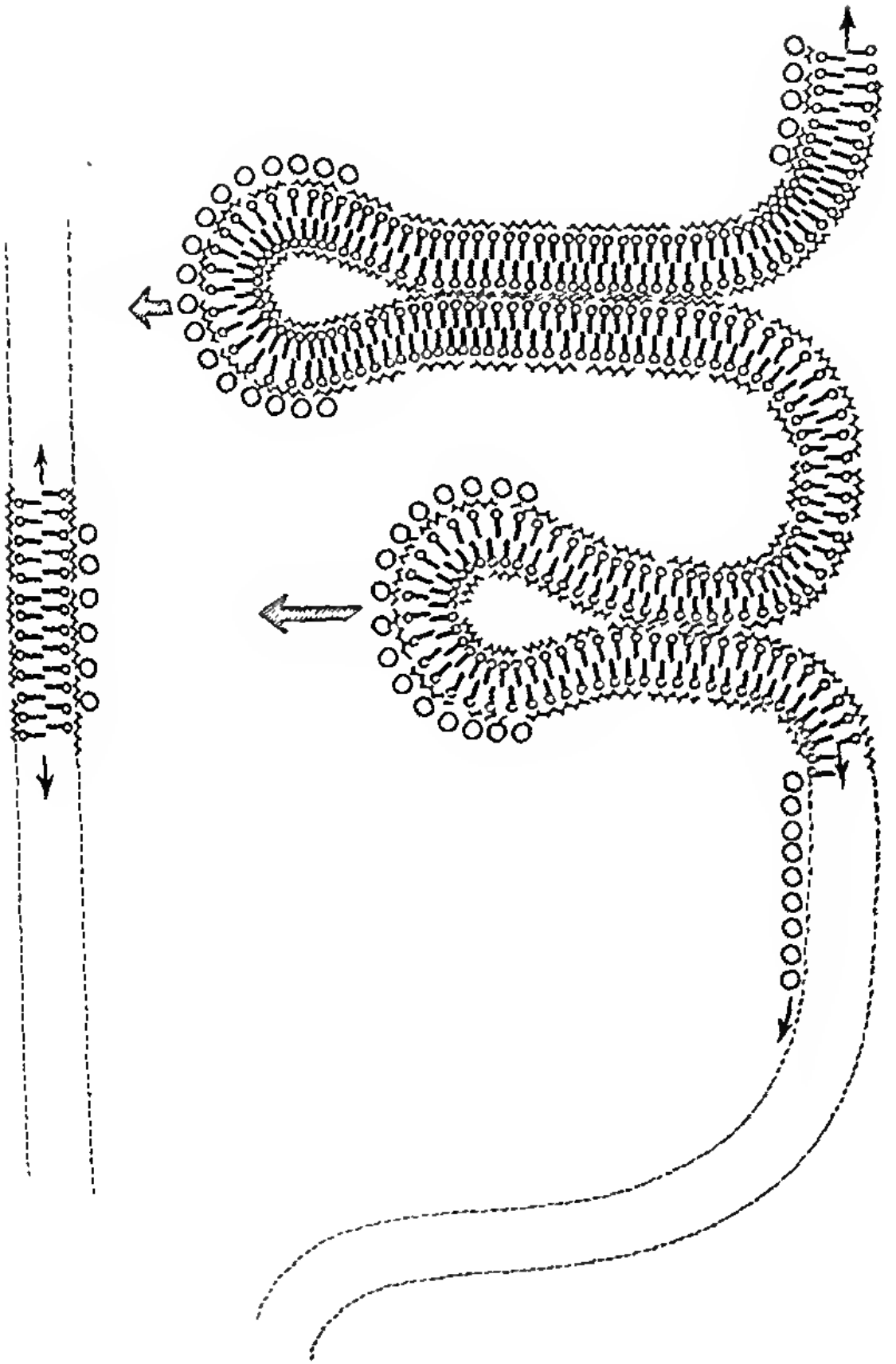

ness of the osmiophilic layer at the edge corresponds to that of the plasma membrane, that is, about 60 Å.

It was assumed that the protein layer, which was proposed to consist of globular protein molecules, contained enzyme molecules which were responsible for the enzymatic activity of the membranes. I would now like to propose the hypothesis that these enzymes contribute to the synthesis of certain key components in the lipoprotein membrane structure, and that the infoldings are formed by an intense synthetic activity of these enzyme systems. The synthetic activity, combined with transfer of substances from the cytoplasm, will, in this case, give rise to the formation of simplified membrane elements consisting of a double layer of lipid molecules sandwiched between very thin layers of proteins or proteins and carbohydrates (Fig. 10). With the growth of the membrane the region of the membrane which is responsible for the synthesis becomes dislocated, moving away from the surface of the outer segment. When reaching across the diameter of the outer segment and approaching the plasma membrane on the opposite side, this synthesis is brought to an end.

Regarding the localization of the rhodopsin in the rod outer segments, I have no direct observations to report. But I would not be surprised, particularly with this mechanism of formation of the outer segment disks in mind if the rhodopsin were located in the middle of the disks.

The "Extracellular Space" in the Retina

The outer segments of the receptor cells are connected with the inner segments through a thin stalklike connection (Sjöstrand, 1953d), which shows a certain similarity to the structure of a cilium. In the guinea pig retina this connecting structure consists of nine free filaments arranged in a ring, but without any central filaments. In addition to these filaments there are nine filaments which are fused with the plasma membrane. The nine free filaments pass for a certain distance through the apical part of the inner segment and form a structure which appears like a basal body. From this "basal body" a long, diffusely outlined filamentous structure extends through the inner segment. This structure is characterized by its cross-striated appearance.

The inner segment is characterized by the accumulation of mitochondria. Furthermore, in the vitreal part of the inner segment the Golgi apparatus can be observed. In most retinal receptor cells studied so far the mitochondria are confined to the inner segment.

The next segment of the receptor cells, the rod (or cone) fiber, is

surrounded by the glial element of the retina, the Müller's cells (Fig. 2). At the outer limiting membrane the peripheral region of the cytoplasm as well as the plasma membranes of both the receptor cells and the Müller's cells is specially differentiated. In osmium-fixed material the cytoplasm here appears very dense, and the plasma membrane is split up into several osmiophilic layers. The structure is similar to that of terminal bars as observed in different types of epithelial cells. From the free surface of the Müller's cells cylindrical processes extend between the inner segments of the receptor cells.

The close topographic relationship between the rod fibers and the Muller's cells is particularly striking when studying this part of the retina. Furthermore, the rod fibers show many morphologic features characteristic of nonmyelinated nerve fibers. The Müller's cells show a relationship to the rod fibers similar to that of the Schwann cells to the nonmyelinated nerve fibers. The boundary between rod fibers and Muller's cells consists of two osmiophilic layers about 60 Å thick, separated by a less osmiophilic interspace about 100 Å wide.

If we now apply the model we have deduced for the structure of the plasma membrane the light interspace separating the osmiophilic layers would correspond to the lipid layers of the two plasma membranes. This would mean that there would be no appreciable extracellular space separating the two cells. This is a relationship which is characteristic of all neurons in the retina as well as in the central nervous system. This is astonishing when considering that the extracellular space has been estimated to constitute about 30% of the volume of brain tissue. Even if we consider certain shrinkage during fixation and dehydration we can not account for any extracellular space of that order of magnitude in nervous tissue. Therefore the hypothesis has been proposed (Sjostrand, 1960a) that, in fact, the glial element in the retina, the Muller's cell, and the neuroglia in the central nervous system represent the extracellular space. The Muller's cells would then represent the outside of the excitable membrane. This idea is supported by the topographic relationships between the glia cells and the blood vessels in brain tissue as described by Maynard *et al* (1957) who, on morphologic grounds, proposed to locate the blood-brain barrier at the plasma membrane of the glia cells

The Synaptic Connections of the Receptor Cells

Let us now review some of the work done (Sjostrand, 1953b, 195[illegible], 1956a, b, 1958, 1959a, De Robertis and Franchi, 1956) on the synaptic connections between receptor cells and the neurons in the layer of the bi-

polar cells. The final step in the analysis was made possible by preparing three-dimensional reconstructions of the synaptic region from long series of serial sections. These three-dimensional reconstructions made it possible to reveal the complicated structure of the synaptic bodies of the receptors. The analysis was performed on guinea pig retinas.

When analyzing the synaptic bodies we can clearly distinguish between two types of receptor cells in the guinea pig retina. This retina is generally considered a pure rod retina, and this classification is justifiable if we define rods and cones with respect to the shape and structure of the outer segments of these receptors. However, when studying the synaptic bodies of the receptor cells we find one type of receptor cells, which I have proposed to call the α-cells, which show a shape and structure of the synaptic body characteristic of rod cells (Fig. 2) mixed with receptor cells characterized by synaptic bodies showing the conical shape and higher degree of complexity characteristic of cone cells. From electrophysiological studies of the guinea pig retina Granit (1947) has distinguished between the rodlike rods and conelike rods of the guinea pig retina. It seems likely that the two different types of receptors are the morphological counterparts to Granit's two types of retinal responses.

The study of the synaptic connections revealed rather extensive contact relations between the β-cells and the α-cells, contact relations identical from a morphologic point of view to those found in synapses. Therefore, it was proposed that these contacts represent interreceptor synapses. Not less than four β-cells seem to make contact with one α-cell (Figs. 11 and 12).

The synaptic relations between the α-cells and the nerve cells of the layer of the bipolars is structurally rather complicated. Each α-cell seems to be in synaptic contact with at least two nerve cells, one of which is

---

FIG. 11. Section through the outer plexiform layer showing several synaptic bodies (R1–R6) of receptor cells. R1 and R6 are of the α-type, R4 of the β-type. R4 sends a thin branchlet (arrow A) to contact the vitreal pole of R1. This section is one section in a series of 40 sections from which a three-dimensional reconstruction of the synaptic connections of receptor R1 was prepared (see Fig. 14). From this reconstruction it was revealed that R2 and R5 represent similar branchlets from other receptor cells making contact with R1. MC indicates Müller's cell cytoplasm characterized by randomly scattered opaque particles. V1 or V2 are synaptic vacuoles forming a pair. The osmiophilic synaptic ribbon, cross-sectioned, is located in the furrow between these vacuoles at left. Arrow B points to a receptor where a thin extension from one synaptic vacuole reaches the vitreal surface of receptor R4. Attention is called to the close relations between the plasma membranes of the receptor cells, the Müller's cells and the dendritic branchlet from the bipolars. These branchlets are located along the right edge of the picture. Osmium tetroxide fixation. Magnification: × 40,000. (From Sjöstrand, 1958.)


R6
MC
V2
R5
V1
R1
R4
MC
MC
R2
A
R4
B

definitely a bipolar cell. The second might be a horizontal cell or a bipolar cell.

The terminal branchlets of the dendrites of these nerve cells end in an invagination of the plasma membrane of the synaptic body of the α-cell which extends from the vitreal pole toward the center of the synaptic body. In the center of the synaptic body the dendritic branchlets make contact with two large vacuoles which also are located within the invagination of the receptor cell plasma membrane (Fig. 13). From one of these vacuoles a third large vacuole branches off, which extends in a scleral direction. A ribbon-shaped strongly osmiophilic component is located in the scleral furrough separating the two vacuoles of the first-mentioned pair (Figs. 11–15).

Small vesicles, the synaptic vesicles, are scattered all over the cytoplasm of the synaptic body (Sjöstrand, 1953b, 1954, 1955, 1956a) and are found to form a rather uniform layer along the surfaces of this ribbon-shaped component. Such vesicles are also observed in the synaptic vacuoles, but not in the rounded ends of the dendritic branchlets. Synaptic vesicles are, furthermore, found in those branches extending from the β-cells which make contact with the surface of the synaptic body of the α-cell. These branches also enter into contact with the dendritic branchlets of the nerve cells.

Synaptic vesicles were also found in the synaptic bodies of the inner plexiform layer on both sides of the presumed synaptic membrane. This fact was one reason why it seemed unlikely to me that the synaptic vesicles would contain transmitter substances, as proposed for the retinal receptors by De Robertis and Bennett (1955) and for the motor end plates in skeletal muscle fibers by Del Castillo and Katz (1956). Another observation that made this less likely at the time when the first observations regarding the structure of synaptic bodies were made, deals with the organ of Corti in the inner ear, where the synaptic vesicles were found only in the nerve endings making contact with the bases of the hair cells, that is on the postsynaptic side of the synaptic membrane (Sjöstrand *et al.*, 1955; Sjöstrand and Engström, 1954), but not on the presynaptic side in the hair cell cytoplasm.

The three-dimensional reconstruction of the synaptic bodies (Fig. 14) and of the outer plexiform layer made it possible to deduce a diagram illustrating the contact relations between receptor cells and be-

---

FIG. 12. Schematic drawing illustrating the interreceptor contacts in the guinea pig retina. Four receptors of the β-type enter into roving contact relation with one α-receptor. On the right side is a slightly simplified drawing of the synaptic body of an α-cell.

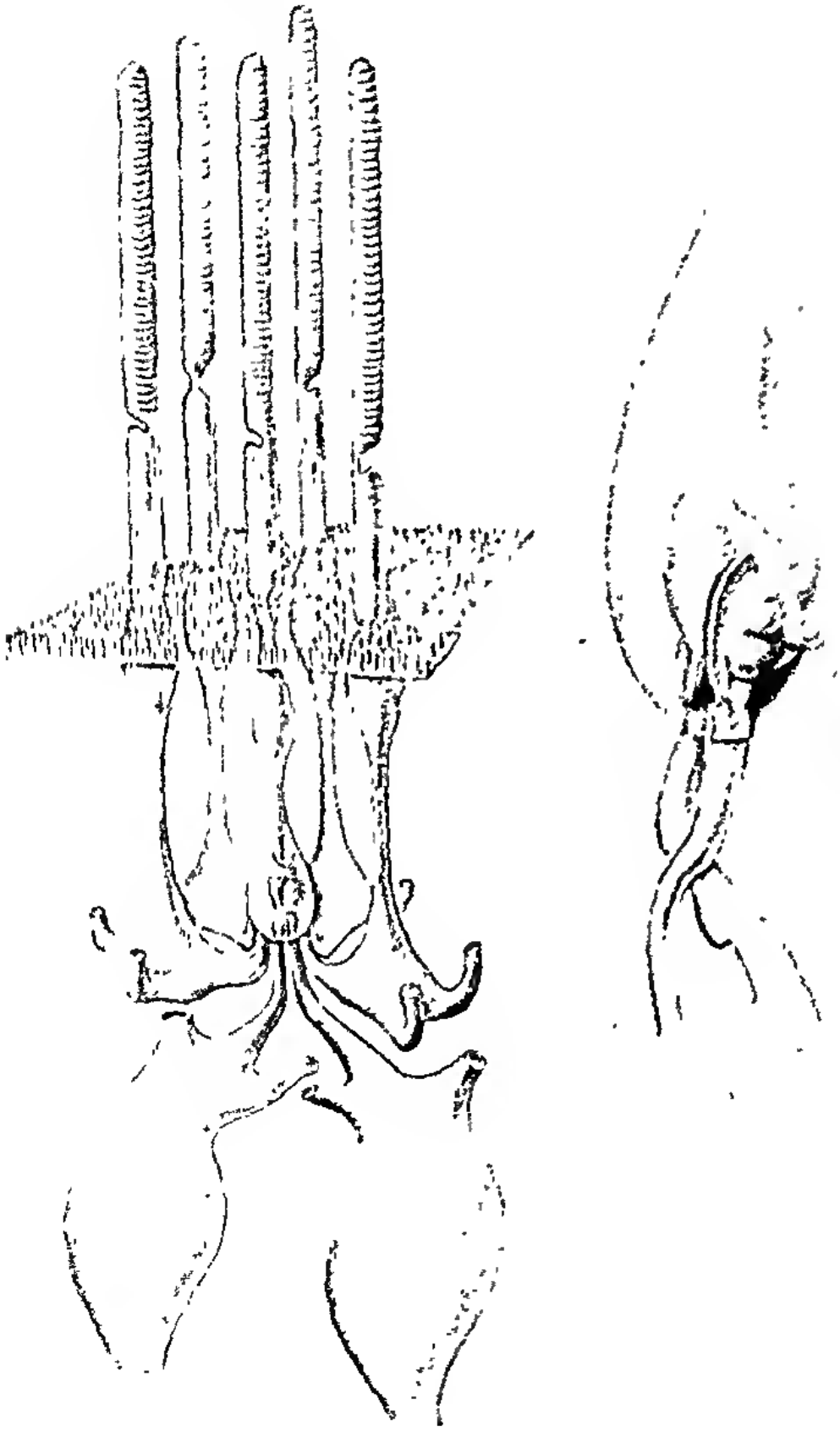

tween receptor cells and neurons in the layer of the bipolars. This diagram (Fig. 16) represents the first attempt to draw a circuit diagram for the first link in the chain of receptors and neurons connecting the retina with the visual centers in the brain.

The interreceptor synapses were interpreted to represent a mechanism by which inhibitory effects could be imposed on the α-cells (Sjöstrand, 1958). It was proposed that this inhibitor mechanism might explain some properties of the simultaneous brightness contrast because bright areas projected on the retina would activate β-cells, which would in their turn suppress transmission from the surrounding α-cells to the bipolars. This would effect an inhibition of adjacent α-cells located just outside the boundary of a brightly illuminated field in the retina, thereby increasing the contrast at that boundary. On the other hand, the α-cells located on the bright side close to that boundary would be less inhibited than those further inside the boundary, since some of the inhibitory connections would be represented by β-cells located outside the bright field. Therefore the bright field would appear brighter at the edge than at some distance from the boundary, and the less illuminated field darker at the boundary than in the rest of the less illuminated field. Such mutual inhibition has been recorded by Hartline *et al.* (1955/56; Hartline and Ratliffe, 1957) from the compound lateral eye of *Limulus*.

If we consider the synaptic vesicles as containing transmitter substances and note that synaptic vesicles can be observed on both sides of synaptic membranes or only on the presynaptic side or only on the postsynaptic side, as in the organ of Corti, we may assume that the synaptic vesicles located on the postsynaptic side are involved in antidromic inhibitory effects.

The Functional Significance of the Structural Organization in the Retinal Receptor Cells

When facing the problem of interpreting the functional significance of the various elaborate structural details which have been revealed thus far we find ourselves in a rather embarrassing position. The structural patterns do not unveil which mechanisms are involved in the fundamental processes of excitation. The language these patterns speak has

---

FIG. 13. Another section from the same series as that shown in Fig. 11. In this picture a dendritic branchlet (D) can be seen extending from a process of a nerve cell body (N) identified to belong to a bipolar, all the way to the synaptic body of receptor R_1 (α-type). The relations between the dendritic branchlet and the synaptic vacuoles (V) are shown. Osmium tetroxide. Magnification: × 40,000. (From Sjöstrand, 1958.)


V
V
R1
V
V
D
R4
N
13

not yet been deciphered. One way to reach toward an interpretation seems to be to try to guess what the functional significance is in order to find a starting point for designing experiments which might elucidate the correlation of structure and function. Such experiments certainly must involve other research methods than those applied in the analysis of the ultrastructural organization of the retina. We have already presented certain such guesses, some of which might well be tested by experiments involving principally chemical and biochemical methods of analysis. We have, however, not touched on the problem of the mechanism of excitation of the receptor cells.

In general terms it seems plausible to assume that excitation is initiated by the interaction between light and the outer segments of the receptor cells. The energy for the activity of the receptor cells might be delivered by the inner segments by the mitochondria located here. It has been proposed (Sjöstrand, 1953d) that the excited state develops in the inner segment, and that the events taking place in the outer segments act as a triggering mechanism on the inner segment. The function of the inner segment would then correspond to that of an amplifier.

The excitation is conducted down to the synaptic body through a process which might be similar to that of the conduction in a nonmyelinated nerve fiber, or there might be an electrotonic decremental conduction. This assumption is based on the structural similarity between the rod and cone fibers and nonmyelinated nerve fibers or dendrites. No electrophysiologist has yet been able to record any spike potential from retinal receptor cells.

We do not know anything about the mechanism of synaptic transmission at the vitreal end of the receptor cells. Nor does the morphology of this region furnish us with any clues regarding this mechanism.

The primary processes of excitation of the outer segments might be due entirely to the absorption of light quanta at discrete sites in the outer segment disks, resulting in the activation of a single or a number of disks (Sjöstrand, 1953d; Wald, 1954). It has, however, been proposed that the interaction between the regularly layered structure of the outer segments and the electromagnetic waves could be of a physical nature and be comparable to the mechanism involved in wave guides and wave receptor antennas (Ingelstam, 1956).

FIG. 14. Three-dimensional plastic reconstruction of the inner structure of a synaptic body of a rod cell of the α-type made from a series of 40 sections. The plasma membrane has been removed with the exception of that part which is bounding the vitreal pole of the synaptic body (indicated as the stippled component). (From Sjöstrand, 1958.)

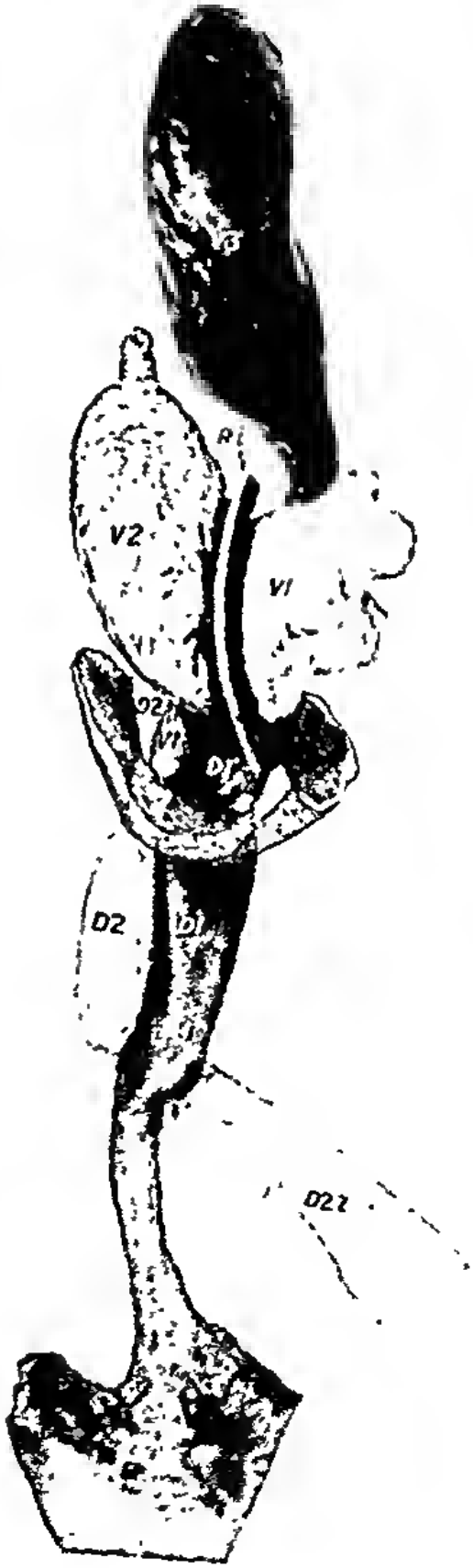
V2
VI
D2
D2
D22

The structural analysis of the retina represents a good example of the frustration of ambitious modern morphologists. At the same time it is a good example to show that when dealing with the very fundamental processes in living matter there is very little chance that any particular

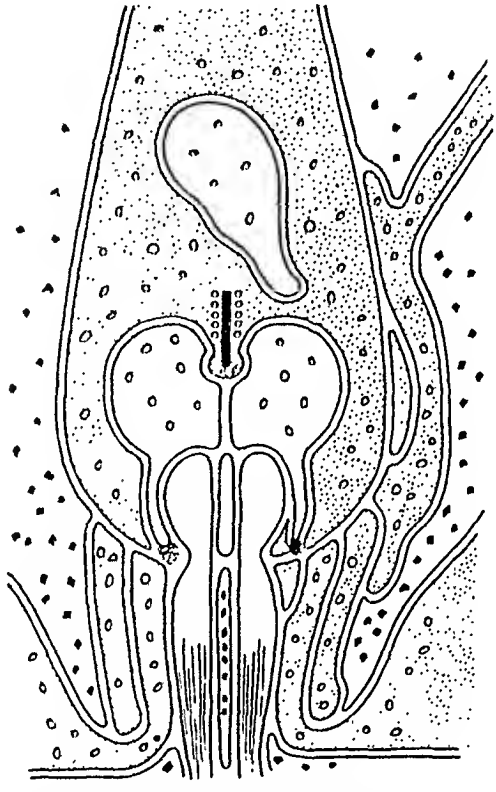

FIG. 15. Schematic drawing showing the structure of the synaptic body and interreceptor contents of a rod cell of the α-type in the guinea pig retina. (From Sjöstrand, 1958.)

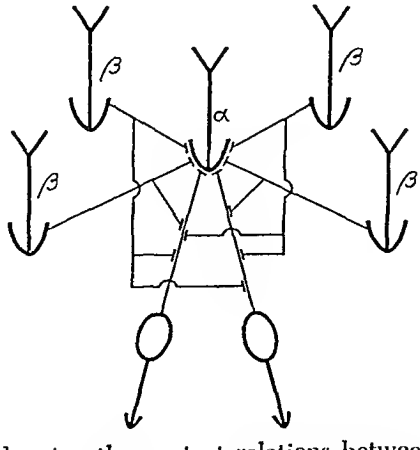

FIG. 16. Diagram showing the contact relations between receptors and neurons of one receptor of the α-type in the guinea pig retina. (From Sjöstrand, 1958.)

isolated method of investigation can furnish sufficient data for an understanding. The morphologist can only point to the type of structural components involved. We then find that membranous components are involved to a rather striking extent in connection with various functions of the cytoplasm. The morphologist contributes by directing attention to these membranous components and by stimulating further analysis from a chemical and physinlogical point of view. To reveal the functional significance of the organization of living matter in this particular type of supermolecular unit, the membrane, is a most basic biological problem.

References

Ben Geren, B. (1954). *Exptl Cell. Research* 7, 558-562

Danielli, J. F., and Davson, H. J. (1934) *J. Cellular Comp Physiol* 5, 495-508.

De Robertis, E. (1956). *J. Biophys Biochem Cytol* 2, 319-330

De Robertis, E., and Bennett, H. S. (1955). *J Biophys Biochem. Cytol* 1, 47-58.

De Robertis, E., and Franchi, C. M. (1956). *J. Biophys Biochem Cytol.* 2, 307-318

Del Castillo, J. and Katz, B. (1956). *Progr in Biophys. and Biophys. Chem.* 6, 121-170.

Fernández-Morán, H., and Finean, J. B. (1957). *J. Biophys. Biochem Cytol.* 3, 725-748

Granit, R. (1947) "Sensory Mechanism of the Retina," p. 252. Oxford Univ. Press, London and New York

Hartline, H. K., and Ratliff, F. (1957) *J Gen Physiol* 40, 357-376

Hartline, H. K., Wagner, H. C., and Ratliff, F. (1955/56). *J. Gen Physiol.* 39, 651-673

Ingelstam, E. (1956) *In* "Problems in Contemporary Optics, Proceedings of the Florence meeting, 10th-15th September, 1951" (Adriana Fiorentini, ed.), pp. 610-668 Istituto Nazionale di Ottica, Florence.

Maynard, E. A., Schultz, R. L., and Pease, D. C. (1957) *Am J Anat.* 100, 409-431

Moody, M. F., and Robertson, J. D. (1960) *J Biophys. Biochem. Cytol* 7, 87-92.

Robertson, J. D. (1957) *J Biophys. Biochem Cytol* 3, 1043-1048

Robertson, J. D. (1959) *Biochem. Soc Symposia (Cambridge, Engl.)* 16, 1-43.

Schmidt, W. J. (1928) *Arch exptl Zellforsch Gewebezucht.* 6, 350-366.

Schmidt, W. J. (1935) *Zool Anz* 109, 245

Schmidt, W. J. (1937) "Die Doppelbrechung von Karyoplasma, Zytoplasma und Metaplasma. Protoplasma-Monographien 11. Borntraeger, Berlin.

Sjostrand, F. S. (1949) *J Cellular Comp. Physiol* 33, 383-403

Sjostrand, F. S. (1953a) *Experientia* 9, 68-69

Sjostrand, F. S. (1953b) *J Appl Phys* 24, 1422

Sjostrand, F. S. (1953c). *J Cellular Comp. Physiol* 42, 15-44.

Sjostrand, F. S. (1953d) *J Cellular Comp. Physiol.* 42, 45-70

Sjostrand, F. S. (1953e). *Nature* 171, 30.

Sjostrand, F. S. (1953f). *Nature* 171, 31.

Sjostrand, F. S. (1954) *Z. wiss Mikroskop.* 62, 65-86.

Sjostrand, F. S. (1955). *In* "Symposium on the Fine Structure of Cells," 8th Congress of Cell Biology, Leiden, Holland, 1954, pp. 222-228. Noordhoff, Groningen.

Sjostrand, F. S. (1956a). *In* "Proceedings of the Third International Conference on Electron Microscopy, London 1954," pp. 428-431. Royal Microscopical Society, London.
Sjöstrand, F. S. (1956b). *Intern. Rev. Cytol.* **5**, 455-535.
Sjöstrand, F. S. (1956c). *Klin. Wochschr.* **35**, 237-250.
Sjöstrand, F. S. (1958). *J. Ultrastruct. Research* **2**, 122-170.
Sjöstrand, F. S. (1959a). *Ergeb. Biol.* **21**, 128-160.
Sjöstrand, F. S. (1959b). *Revs. Modern Phys.* **31**, 301-318.
Sjöstrand, F. S. (1960a). *In* "Modern Scientific Aspects of Neurology" (J. M. Cumings, ed.), pp. 188-231. Arnold, London.
Sjöstrand, F. S. (1960b). *In* "Symposium on Bioenergetics" Academic Press, New York. (In press.)
Sjöstrand, F. S., and Engström, H. (1954). *Acta Oto-Laryngol.* **44**, 490-501.
Sjöstrand, F. S., and Gierer, T. (1959). Unpublished report of F. S. Sjöstrand. *Ergeb. Biol.* **21**, 128-160.
Sjöstrand, F. S., and Rhodin, J. (1953). *Exptl. Cell Research* **4**, 426-456.
Sjöstrand, F. S., Engström, H., and Wersäll, J. (1953). *In* "Proceedings of the Fifth International Congress of Otorhinolaryngology, Amsterdam, 1953" (P. G. Gerlings and W. H. Straben, ed.), pp. 1-6. Van Gorcum, Assen.
Wald, G. (1954). *Science* **119**, 887-892.

Discussion

Dr. George Wald [Harvard University, Cambridge, Mass.]: Do you imply that the plasma membrane covers one side of the receptor outer segment and that the other side is naked? Does this mean, therefore, that the spaces between the disks are in direct continuity with the outer medium?

Dr. Sjöstrand [Stockholm, Sweden]: My data is based on study of developing perch cones and adult cat and adult guinea pig retina. In the perch cone outer segments, as well as in developing cat rod outer segments, part of the segments are "naked" due to the infolding of the plasma membrane. The plane at which the two membrane components of the disk are in contact and might have been glued together here can be projected out through the surrounding medium parallel to the plane without this projection cutting through the plasma membrane of the rod. According to my interpretation the disk is a compact structure and therefore there is no "space." In the guinea pig and adult cat the outer segment is covered by a complete plasma membrane. Adjacent disks are connected through tubular structures located at the end of a deep incision cutting through the disk from its edge to its center. This special structure can be imagined to develop according to the proposed scheme presented in Fig. 9 (see p. 13).

Ultrastructure and Chemical Organization of Photoreceptors[1]

EDUARDO DE ROBERTIS AND ARNALDO LASANSKY

Instituto de Anatomía General y Embriología, Facultad de Ciencias Médicas, Buenos Aires, Argentina

PHOTORECEPTORS of the vertebrate retina are highly differentiated cells in which the fundamental transformation of light energy to nerve activity takes place. Both rods and cones act as receptors of light quanta at the distal end and as transmitters of nerve impulses at the innermost extremity. These functions are carried out by two differentiated structures: a lipoprotein lamellar system involved in the photochemical mechanisms and a special synaptic junction.

Another interesting characteristic of photoreceptors is the compartmental arrangement of their structural and biochemical organization. Thus the visual pigments are exclusively located in the outer segments of both rods and cones while the enzymes for oxidative phosphorylation and the Krebs cycle are mainly distributed in the distal portion of the inner segments where mitochondria concentrate. Furthermore glycolytic enzymes are abundant in the most proximal portions of photoreceptors (Lowry *et al.*, 1956; Schimke, 1957).

Noell (1958a) has recently emphasized the importance of this enzymatic topography in relation to the action of certain poisons, such as iodoacetate, that specifically destroy photoreceptors. This type of study has also been carried out by us at the submicroscopic level demonstrating the susceptibility of all membranous components of the photoreceptor toward iodoacetate (Lasansky and De Robertis, 1959).

In a recent symposium on "Mechanisms of Vision" held in Caracas and now being published (De Robertis, 1960), we have summarized some of the latest results regarding the ultrastructure of rod and cone receptors of mammals in the adult and during differentiation.

In that report the submicroscopic organization of the rod and cone outer segments with their membranous flattened sacs, the connecting cilium with two basal centrioles, and the fine structure of the inner segments in the two types of visual cells were described (Fig 1).

The primary synapses between photoreceptors and bipolar cells will not be considered here. The submicroscopic characteristics of them

[1] Supported by Grant B-1549 from the US Public Health Service and Grant RF-59134 from the Rockefeller Foundation

and some changes in fine structure with darkness and intense illumination were previously described (De Robertis and Franchi, 1956; De Robertis, 1958).

In this presentation we shall discuss mainly recent unpublished work that refers (a) to the study of a genetic dystrophy of the visual cells in C3H mice in which there is an abnormal morphogenesis of photoreceptors. For this study DBA mice were used as controls. We shall also refer (b) to a study of the fine structure of the rod and cone outer segments of amphibia. This type of analysis will be discussed from the viewpoint of the chemical organization of the lipoprotein lamellar system present in those segments.

Morphogenesis of Visual Cells in DBA Control Mice

The process of morphogenesis observed in the DBA control animals confirmed the general description previously made in other strains (De Robertis, 1956b). The three main steps of morphogenesis corresponding to (a) the primitive cilium (Fig. 2), (b) the formation of the primitive sacs (Fig. 3), and (c) the remodeling and orientation of the sacs into the final disposition of the adult visual cells (Fig. 5) were also observed in DBA mice. However, it is now apparent that the surface membrane participates actively in the formation of the primitive rod sacs. In the membrane covering the end of the cilium there is a process of membrane synthesis and flow similar to that recently described by Tokuyasu and Yamada (1959). The primitive cilium with the "morphogenetic material" (De Robertis, 1956b) present in the apex probably exerts some kind of

---

KEY TO ABBREVIATIONS USED IN FIGS. 1-18

CC	connecting cilium	intra S	intrasaccular space
C_1	centriole 1	inter S	intersaccular space
C_2	centriole 2	m	membrane
cf	ciliary fibril	mi	mitochondria
es	cone sacs	OS	outer segment
dmi	degenerating mitochondria	PC	primitive cilium
dp	dense particles	ps	primitive sacs
IS	inner segment	rs	rod sac
is	intrasaccular space	vm	vesicular material

PLATE I

FIG. 1. Electron micrograph of a rod cell of the rabbit showing the connecting cilium with the two centrioles and the outer segment formed by a stack of bimembranous sacs. Magnification: × 65,000.

FIG. 2. Electron micrograph of the retina of a 10-day-old DBA control mouse. At the bottom the inner segment containing two centrioles. From C_1 emerges a primitive cilium. The ciliary fibrils end in a tubular and vesicular material in the apex (morphogenetic material). Magnification: × 46,000.

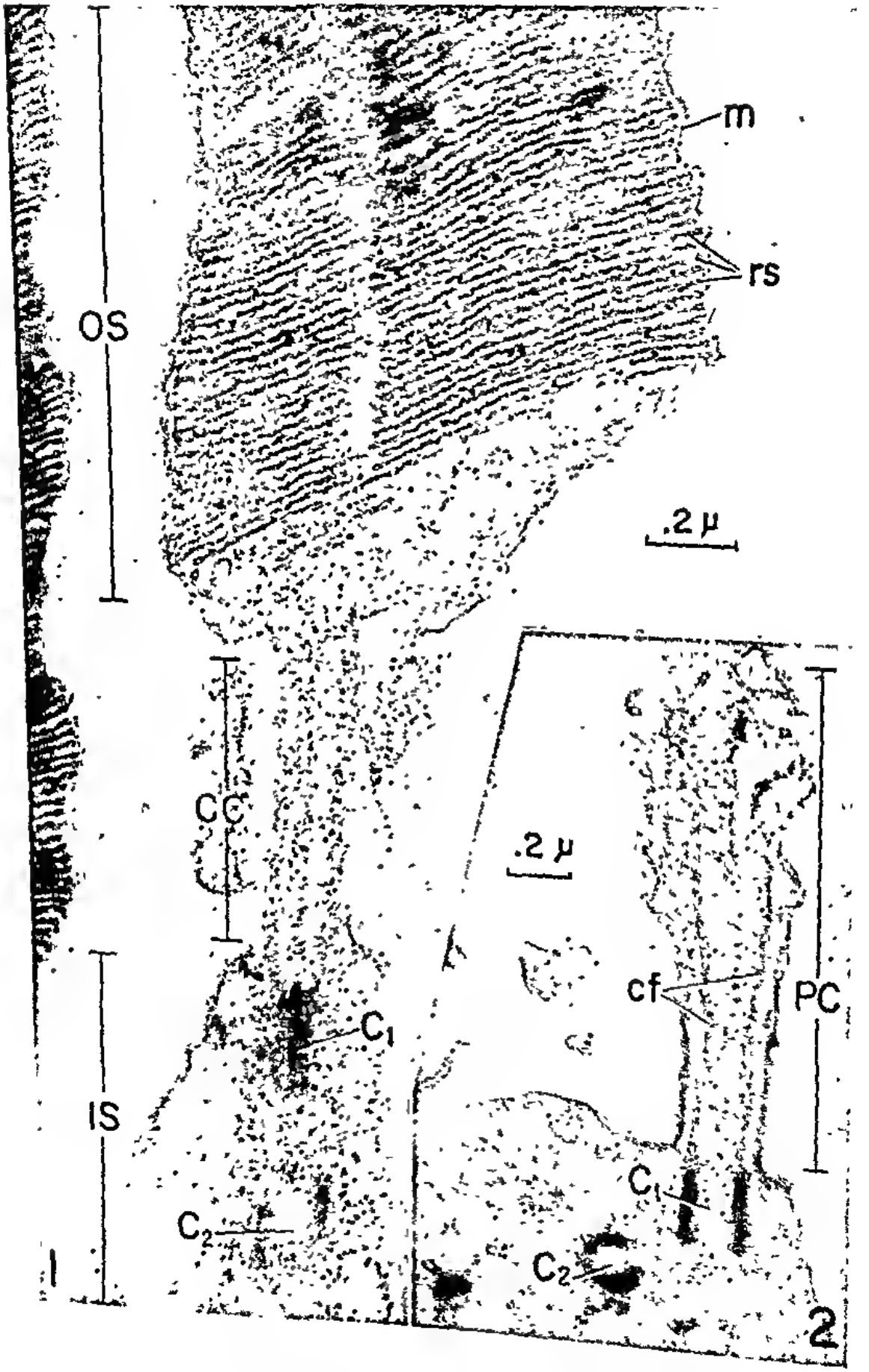
m
rs
OS
.2 μ
C
C
.2 μ
cf
PC
C1
IS
C2
C1
C2
1
2

"inductive" action on the membrane. It is interesting that this effect is from the very beginning asymmetrical, so that the primitive cilium remains unchanged on one side while on the other the sacs develop in great profusion (Fig. 3). While these morphogenetic changes take place in the outer segment, in the inner one there is a progressive axial lengthening with decrease in number of the RNA (ribonucleic acid) granules and appearance of neuroprotofibrils (De Robertis, 1956a,b). Simultaneously at the innermost end the primary synapse with the bipolar cell becomes differentiated (Lasansky and De Robertis, 1960).

Morphogenesis of Visual Cells in C3H Mice

The existence of an abnormal development of the retina leading to degeneration and disappearance of the photoreceptor cells has been known since the work of Keeler (1924), who interpreted the existence of "rodless" retina in mice as the result of an arrest in development. This visual abnormality was later observed by Karli (1952), Tansley (1954), and Sorsby *et al.* (1954) in albino mice, and recognized to be an inherited defect. The study of this degenerative process can be carried out better on pure strains of C3H mice (Noell, 1958a) in which it is inherited as a Mendelian recessive character.

Noell (1958a,b) recently described the histological and electrophysiological changes that take place. He has postulated that they occur in early stages of development of the visual cells and are closely related to metabolic changes associated with differentiation.

Histologically it has been observed that the postnatal development of the retina is apparently normal until the tenth day after birth. However, some differences with the controls are manifested by the deeper staining of the nuclei of the visual cells, a slight reduction in the width of this outer nuclear layer, and less definition of the photoreceptors. In later stages numerous visual cells die, and they almost disappear by the twentieth day. The electroretinogram, although showing some difference in the amplitude of the a-wave and a much higher threshold, develops

---

PLATE II

FIG. 3. The same as Fig. 2. Later stage of development showing the great enlargement of the apical portion of the cilium which is being filled with primitive sacs. Invaginations of the surface membrane that are forming sacs are indicated by arrows. See the scarcity of dense particles in the inner segment. Magnification: × 36,000.

FIG. 4. Developing visual cells of a C3H mouse at a stage similar to that of Fig. 3. The outer segment is being formed with some disorganization of the sacs. The most conspicuous changes observed in the inner segment are masses of vesicular material and a great increase in dense granules that are even found within the cilium. Magnification: × 32,000.


.5 μ
m
ps
cc
cf
C2
mi
dp
il
3
.5 μ
dp
mi
vm
cc
os
4

as in the normal animal until the fifteenth day, declining later when cell death becomes very marked in the total population.

These results are interpreted by Noell (1958a) as indicating that this genetic degeneration is not due to an arrest in differentiation of the visual cells but to a secondary alteration of elements which already have a certain degree of development.

Our electron microscope observations on developing visual cells in C3H mice show submicroscopic changes as early as in the eleventh day of postnatal life. The observations confirm and extend the concept that the hereditary visual alterations of the C3H mice are not the result of a primary arrested development, but of a secondary alteration of the differentiating photoreceptor. The early stages of morphogenesis of the visual cells start in the usual way. The outer segment originates from a primitive cilium as in the control DBA mice and then the formation of the membranous material starts and is very profuse (Fig. 4). However, it is soon apparent that the growth of the outer segment is disordered and does not reach the third stage of remodeling and reorientation of the sacs that finally builds up the definite regularly layered structure. On the contrary the exuberant and abnormal membranous growth "invades" the entire primitive cilium which may even disappear completely. The membranes are in this case in direct contact with the inner segment (Fig. 6). Furthermore, in more advanced stages stacks of parallel membranes, similar in aspect to the rod sacs, may be found in a completely abnormal location within the inner segment.

The earliest and most conspicuous changes occur in the inner segment where the main cytoplasmic components of the visual cells are located. The exuberant formation of vesicular material and the increase in dense particles that resemble the RNA granules of the normal are found from the very beginning of differentiation (Fig. 4). The ground cytoplasm becomes very dense and loaded with these dense granules. In later stages the mitochondrial alteration with vacuolization, disap-

---

PLATE III

FIG. 5. Later stage in differentiation of a rod cell of a DBA control mouse at the 13th day. See the connecting cilium and the rod sacs in their final orientation. Some formation of rod sacs still continues. The inner segment has mitochondria and a clear cytoplasm with only few particles. Magnification: × 41,000.

FIG. 6. Later stage in the degeneration of a developing visual cell observed at the 13th day. The outer segment shows a disorganized growth of rod sacs that invades the inner segment (arrows). The connecting cilium has probably disappeared because of this massive growth. The inner segment shows a great increase in dense particles which fill the entire hyaloplasm. Mitochondria are in stages of degeneration. Magnification: × 32,000.

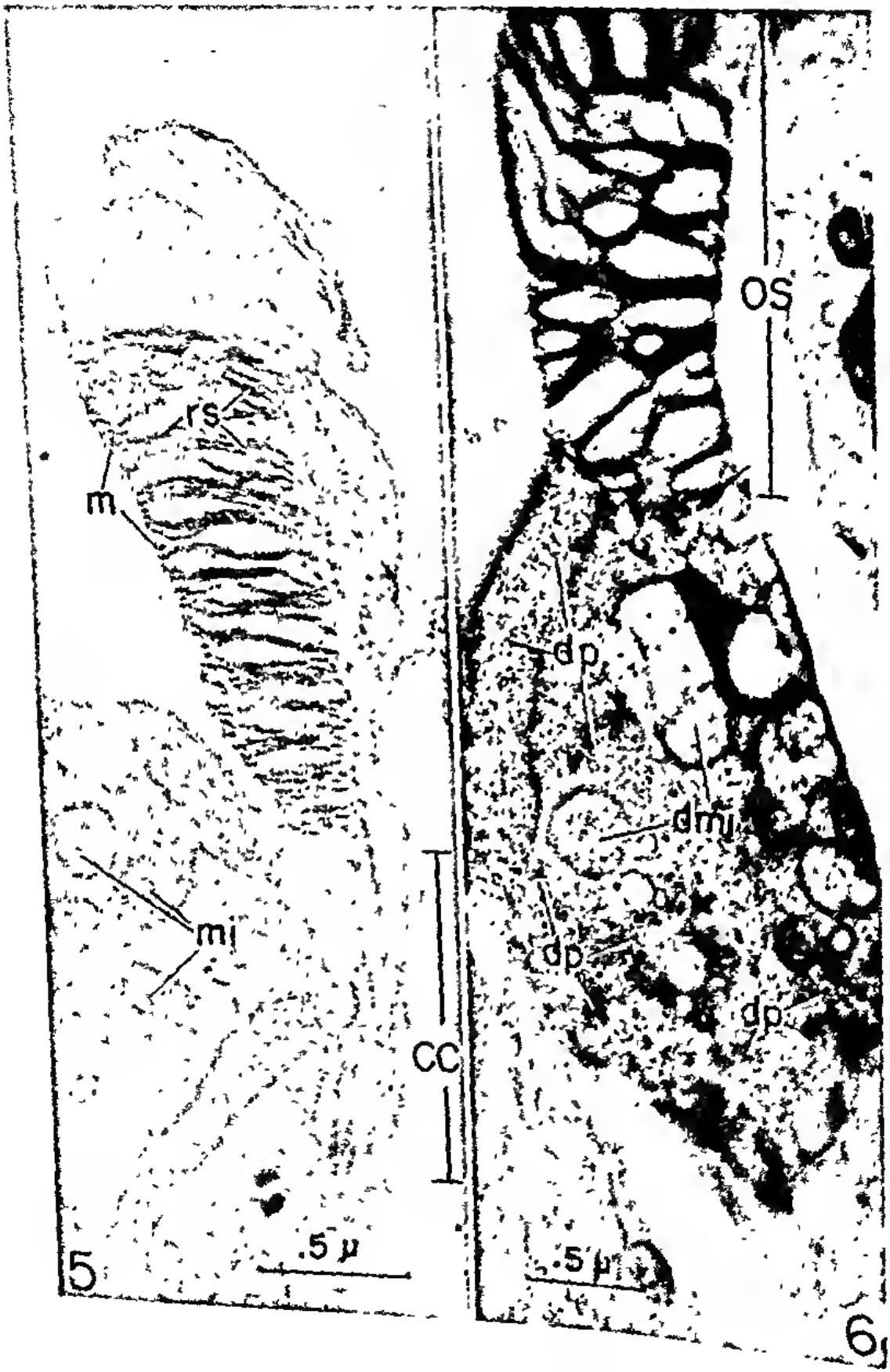
rs
m
mi
cc
.5 μ
5
os
dp
dmi
dp
dp
.5 μ
6

pearance of the crests, and final lysis becomes more and more apparent (Fig. 6). On the other end of the visual cell the development of the synaptic junction which starts normally, also undergoes profound alterations with lysis of the synaptic vesicles. For a more detailed description see Lasansky and De Robertis (1960).

The whole picture exhibited by a degenerating rod of the C3H mouse retina can be summarized by stating that the entire process of differentiation is exuberant and disordered and leads to final involution and cell death. These results should be correlated with the higher rate of oxygen uptake and glucose oxidation found in developing C3H retinas as compared with DBA control (Noell, personal communication, 1960). It can be hypothesized that because of the genetic alteration these abnormal visual cells are lacking some factor that controls the differentiation and growth of the subcellular components of the visual cell.

Because of the role that RNA particles play in differentiation and protein synthesis, the finding of a greatly increased number of them within the inner segment seems to be particularly important. However, it remains to be proven that these dense particles are exactly similar to the normal RNA ones.

Fine Structure and Chemical Organization of Lipoprotein Protein Lamellar Systems in Amphibian Photoreceptors

Since Schmidt (1935) studied the structure of retinal rods and cones by means of polarization microscopy, it has been known that the outer segment of both photoreceptors has a high degree of molecular orientation. The uniaxial positive birefringence, which changes to negative after lipid extraction, led to the interpretation of transversely oriented protein layers alternating with layers of lipid molecules longitudinally oriented along the axis of the photoreceptor. This type of layered organization with units smaller than the wavelength of light was confirmed by electron microscope studies of fragmented and sectioned rod outer segments (Sjöstrand, 1949, 1953). These observations indicated that the outer segment of the rod, in the guinea pig and other mammals (De Robertis, 1956a), is made of a stack of flattened "disks" or sacs having a double membrane structure (Fig. 1).

Sjöstrand (1953, 1959) postulated that the dense membranes observed in the outer segments are of protein nature and that the narrower spaces in between them are occupied by a bimolecular layer of lipid. Based on observations on cat and frog photoreceptors, Wolken (1956, 1957) reached the conclusion that the outer segments are made of double lipoprotein membranes and that the spaces in-between are occupied by soluble protein in an aqueous phase.

All these interpretations are handicapped by the fact that osmium fixation cannot be interpreted exactly in terms of the histochemical localization of protein and lipids. The reactivity of OsO_4 for sulfhydryl groups (Bahr, 1954), which are abundant in the outer segments of the visual cells (Bennett, 1951; Sidman and Wislocki, 1954, Wislocki and Sidman, 1954), is consistent with the concept of the protein nature of the membranes revealed by the osmium. However, recent work in pure lipid models has revealed a layered structure which was interpreted as a product of the reaction of OsO_4 with double bonds in the fatty acid chains (Stoeckenius, 1959). Therefore the role of lipids in the formation of the final image of the OsO_4-fixed material should not be disregarded.

In order to reinvestigate this problem on more precise histochemical grounds, a technique used for many years in light microscopy for the detection of phospholipids (Baker, 1958; Lison, 1953) was adapted in our laboratory for use with the electron microscope. This technique is based on a prolonged treatment of the tissue with dichromate. The staining of phospholipids is the result of the binding capacity for chromium which then acts as a mordant for hematoxylin (Baker, 1958, Lison, 1953). For the electron microscope, only a prolonged chromation with dichromate after fixation in formaldehyde is needed. With this technique we have demonstrated that at least 70 to 80% of the chromium is bound to the phospholipid fraction in peripheral and central nervous tissue (Lasansky *et al.*, 1960).

Furthermore, it is known that chromation stabilizes some lipid fractions by rendering them insoluble in organic solvents (Baker, 1958; Ciaccio, 1909). This last property was also judged advantageous for studying the lipoprotein systems of the visual cells with the electron microscope. Therefore, the fine structure of the cone and rod outer segments was reinvestigated and the results of OsO_4 fixation were compared with those obtained with prolonged chromation.

The lamellar structure revealed by these two techniques showed considerable differences in density distribution. The results which will be presented in more detail elsewhere (Lasansky and De Robertis, 1960), will be discussed here in terms of general molecular organization. A liquid crystalline structure as found in the myelin sheath will be proposed for retinal photoreceptors.

Fine Structure of the Rod and Cone Outer Segments

The observation of longitudinal sections of the rod and cone outer segment of the toad's retina, fixed in osmium tetroxide, reveals the fundamental similarities and differences that exist between both photoreceptors. The rod is formed by a stack of lobulated bimembranous

(Porter, 1957) flattened sacs that enclose a less dense space of 30 Å (Fig. 7). Apparently these sacs are osmotically very sensitive since in a hypotonic fixative the space in-between the sacs and especially the intrasaccular space increases considerably showing very neatly the continuity of the two membranes at the edges of the lobules (Fig. 8).

The cone outer segment is thinner and shows no lobulation. The pile of dense membrane is formed by the repeated folding of a continuous membrane as was found by Sjöstrand (1959) in the perch and Yamada (personal communication, 1960) in the turtle. In our description and for the purpose of homology the narrower space between the osmiophilic lines of the cone will be identified with the intrasaccular space of the rod and the wider space, with the intersaccular space of the rod (Fig. 9). The membrane thickness in both visual cells is 40 Å while the intersaccular space is 50 Å. The intrasaccular space is 20Å for the cone and 30 Å for the rod. Consequently the total repeating period is 150 and 160 Å, respectively.

In the chromated material the period is about 25% larger measuring 190 Å for the cone and 200 Å for the rod. The electron microscope image of the lamellar system in both photoreceptors is also very different when compared with that given by the osmium fixation. The layers appear to be more compact, lacking the clear spaces seen in the OsO_4 preparation (Figs. 10 and 11). Within this continuous background the repeating period contains two denser lines, l_1 and l_2, having differences in thickness and electron density. As can be observed in the cone shown in Figs. 11 and 12, l_1 *is thicker (approximately 70 Å), has a tendency to duplicate* and has less density than l_2, which is definitely single and approximately 30Å.

Interpretation of the OsO_4 and Chromium Patterns

The correlation of the patterns observed with both fixatives is made difficult by the repetitive character of the structure. There are several ways of matching the two patterns by a simple shifting of the bands.

PLATE IV

Fig. 7. Electron micrograph of a rod outer segment of the toad retina fixed in osmium tetroxide. The limits of two lobules are indicated with arrows. Within each lobule parallel stacks of rod sacs are observed. Each rod sac comprises two 40-Å thick membranes with a less dense inner space. The space between the sacs is larger than the sac inner space. Specks of osmium deposits are found on the rod sacs. Magnification: × 112,000.

Fig. 8. Electron micrograph of a rod outer segment of the toad retina fixed in osmium tetroxide. The rod sacs are greatly swollen showing a large clear cavity and the two membranes which are continuous at the edges (continuity indicated with small arrows). The lobules are more clearly visible. Magnification: × 65,000.

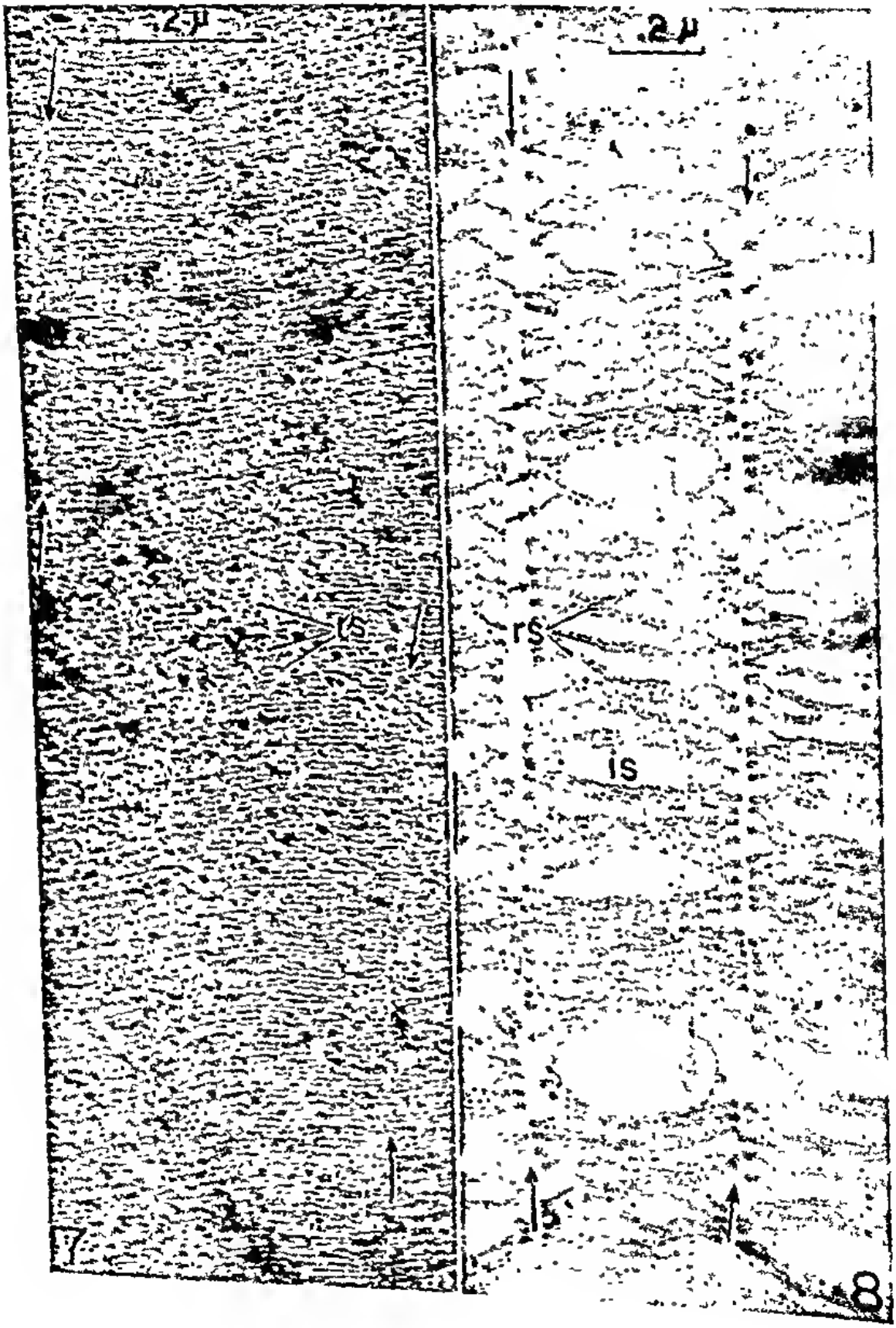
2μ
2μ
rS
rS
lS
lS
7
8

However, if one assumes that within this particular system lines of similar appearance and density correspond to layers of similar chemical nature there may be two ways, and probably only one, that is satisfactory.

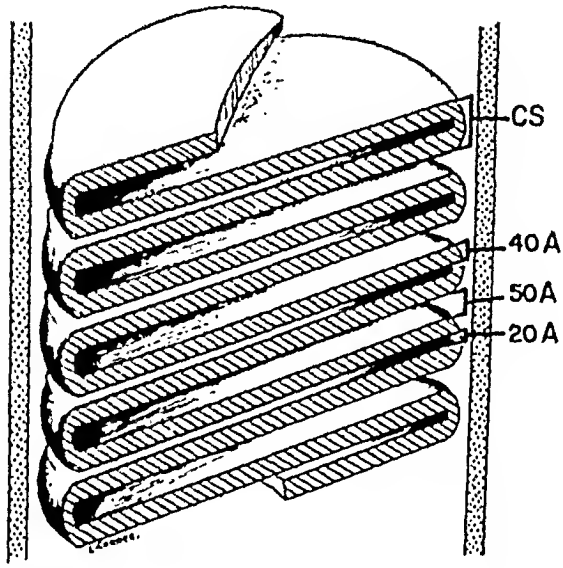

FIG. 9. Diagram showing the fine structure of the cone outer segment of the toad as revealed with osmium tetroxide. The zigzag continuity of the individual membranes with the adjacent ones is indicated. *CS* is interpreted as representing a single cone sac with an intrasaccular space of 20 Å and an intersaccular space of 50 Å.

In one interpretation, line l_2 would occupy the center of the intersaccular space of the OsO_4-fixed structure (Fig. 15, A). If this is the case l_1 would represent the two dense membranous constituents of a sac in the OsO_4-fixed structure. This interpretation, in order to be valid, has to explain a difference in thickness greater than 30 Å in-between l_1 and the sac plus the intrasaccular space.

The other interpretation involves the idea of the complementariness of both patterns. Taking into consideration a 25% shrinkage in the OsO_4, the 30-Å thick l_2 would occupy the intrasaccular space of 25 to 40 Å and l_1 of 70 Å would correspond to the intersaccular space also of about 70 Å (Fig. 15, B). In this second interpretation the matching is

---

PLATE V

FIG. 10. Electron micrograph of a cone outer segment fixed with formaldehyde and chromated. The dense l_1 and l_2 lines are visible on the less dense background. A split in l_1 is indicated by arrows. Magnification: × 315,000.

FIG. 11. Electron micrograph of a cone outer segment fixed in OsO_4 showing the stack of bimembranous cone sacs with the intrasaccular spaces (marked with arrows) and the larger intersaccular spaces. Magnification: × 315,000.

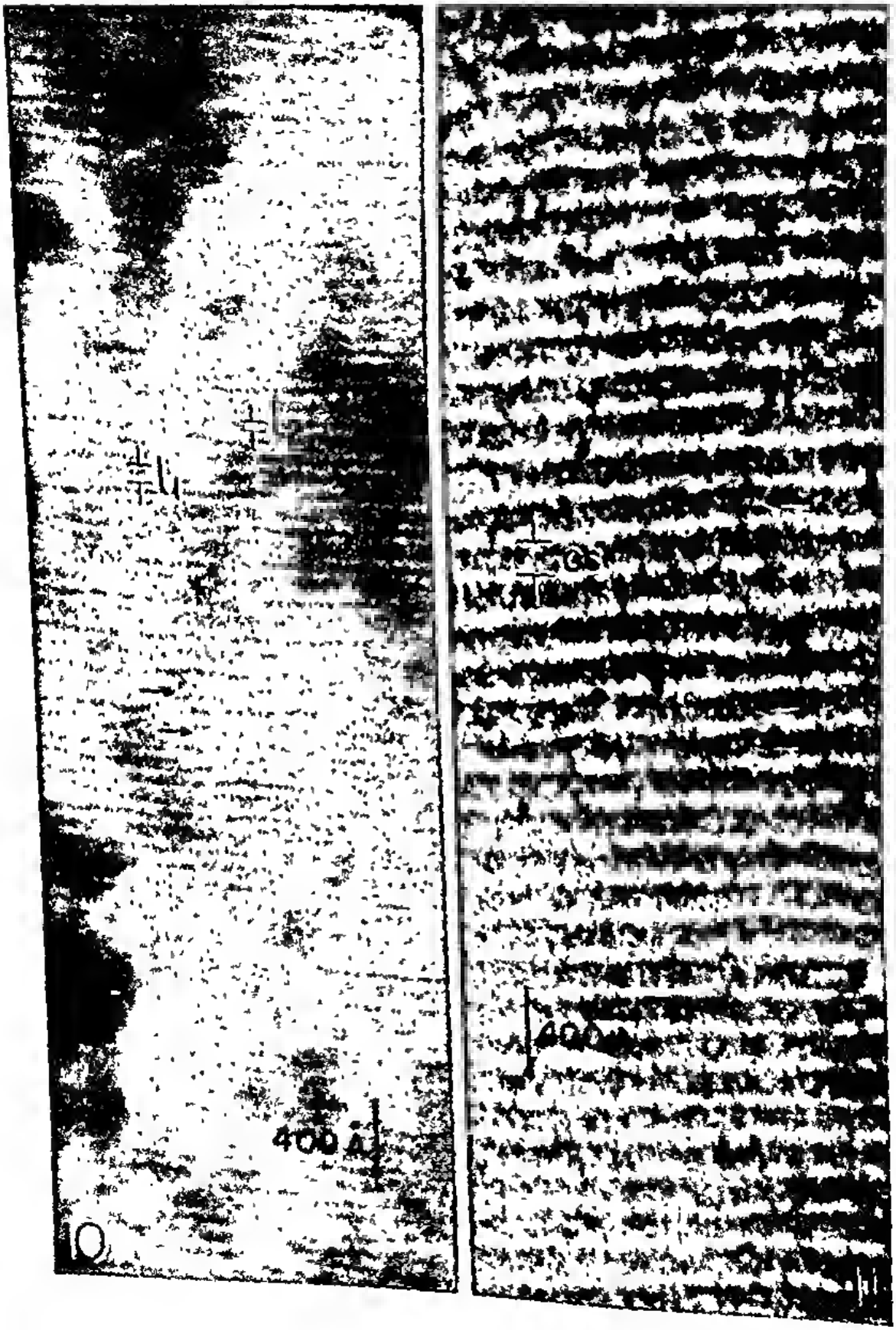
400 Å
400 Å

more exact. The lighter bands of the chromated tissue could be interpreted as a negative image of the membrane of the sac when osmium is not used. Similar findings have been described by Sjöstrand and Baker (1958) in frozen and dried tissues. In order to enhance the complementariness of the matching, in Figs. 16 and 17 the OsO_4 pattern is compared with the inverted image of the chromated specimen.

Chemical Nature of the Bands

The interpretation of the probable chemical nature of the bands is very difficult because of the complexity of the action of both osmium tetroxide and anionic chromium.

The reaction of OsO_4 with tissue components is still under discussion (Porter and Kallam, 1953; Bahr, 1954, 1955; Thornburg, 1958; Stoeckenius, 1959). While in light microscopy the blackening of unsaturated fatty acids dominates the picture, in electron microscopy the general background staining of the protein structure seems to be prevalent (Sjöstrand, 1956). Thornburg (1958) has stated that OsO_4 reacts with a variety of chemical radicals including unsaturated lipids, alcohols, and aldehydes and may form complexes with 1,2-diglycol sugars and nitrogen-ring compounds. Among the lipids there are some that only react weakly with OsO_4 (Bahr, 1954) and may be extracted by organic solvents.

In lipoprotein multilayered structures, i.e., rod and cone outer segments, myelin, chloroplasts, it is more frequently assumed that the electron-dense lines correspond to the deposit of OsO_4 in the protein layer or at the protein-lipid interface (Hodge *et al.*, 1955; Fernández-Morán and Finean, 1957; Sjöstrand, 1953).

The interpretation of the image obtained with anionic chromium is also difficult. Attempts made to establish the chemical significance of the dichromate reaction have shown that between 70 to 80% of the chromium binding is related to the lipid fraction. Within the lipids, cholesterol and tryglicerides are not reactive with dichromate while the relation to the phosphatides seems evident (Lasansky *et al.*, 1960). At the present time we do not know if the 20 to 30% of bound chromium,

---

PLATE VI

Fig. 12. Similar description as Fig. 10. Showing the edge of the cone. Magnification: × 260,000.

Fig. 13. Electron micrograph of rod cell of the toad fixed in formaldehyde, lipid-extracted with pyridine and chromated. The dense l_1 and l_2 lines are not present. Magnification: × 207,000.

Fig. 14. The same as Fig. 13 but treated with OsO_4 after lipid extraction. The bimembranous rod sacs are clearly visible as in Fig. 7. Magnification: × 153,000.

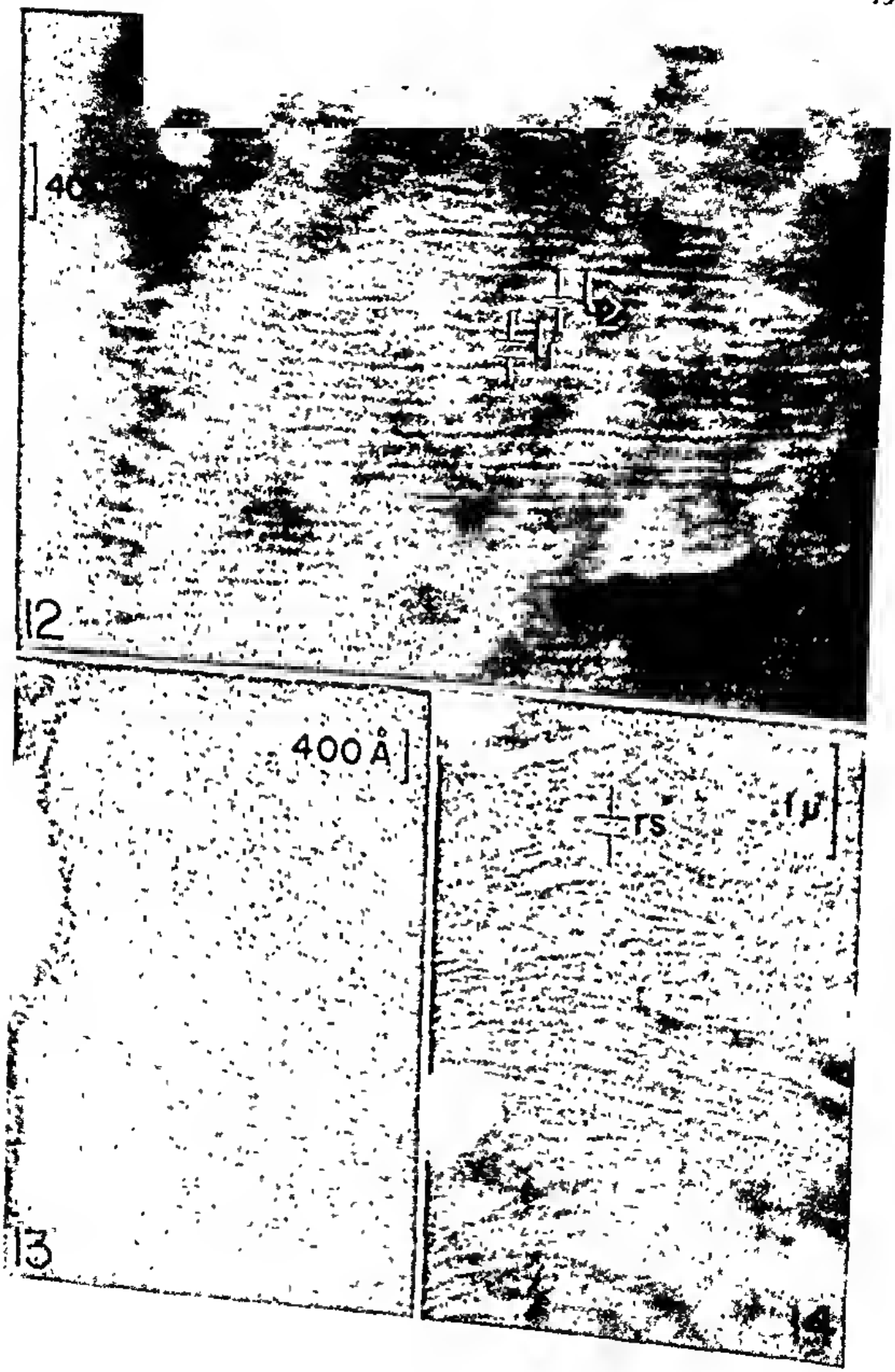
400 Å
rs
1μ
1
2
3
4

left after mild lipid extraction, is related to the proteins. This type of binding has not been clearly established with anionic chromium (dichromate) (Baker, 1958) while it is very evident with cationic chromium, frequently used as mordant of proteins.

The binding of chromium to the phosphatids may also stabilize the lipid structure preventing the extraction during dehydration and embedding. It seems possible to us that chromium may add to the final image of the electron microscope by the two mechanisms of binding to the phosphatids and by preventing lipid extraction. In favor of this is

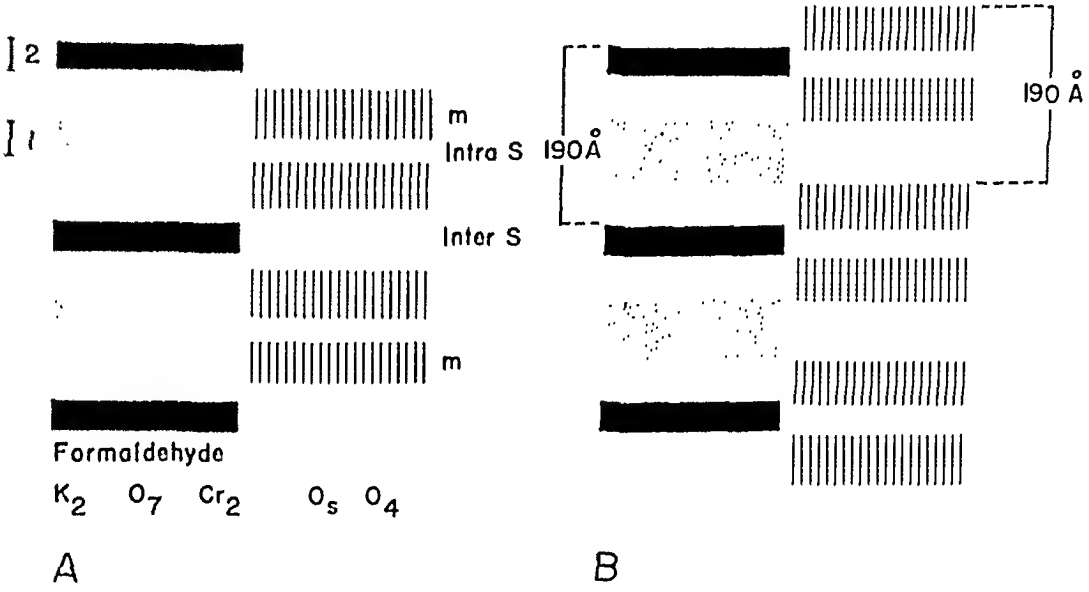

FIG. 15. Diagram showing the two settings A and B of the chromium and osmium patterns described in the text.

the fact that the period is 25% shorter in OsO_4 than in formaldehyde-dichromate indicating a certain collapse of the structure.

Furthermore, as is shown in Fig 13, if the tissue is treated with a lipid solvent, after formaldehyde fixation and then chromated, there is

PLATE VII

FIG. 16. Similar description as Fig. 10, but with inversion of the image. This photographic treatment permits a better comparison of the bands in the two materials and shows the correspondence of l_2 with the intrasaccular space and l_1 with the intersaccular space of the OsO_4 (see Fig. 17). Magnification: × 330,000.

FIG. 17. Similar description as Fig. 11. Magnification: × 315,000.

FIG. 18. Electron micrograph of the myelin sheath of the optic nerve of the toad fixed in formaldehyde-dichromate, showing the 50-Å period banding. Magnification: × 234,000.

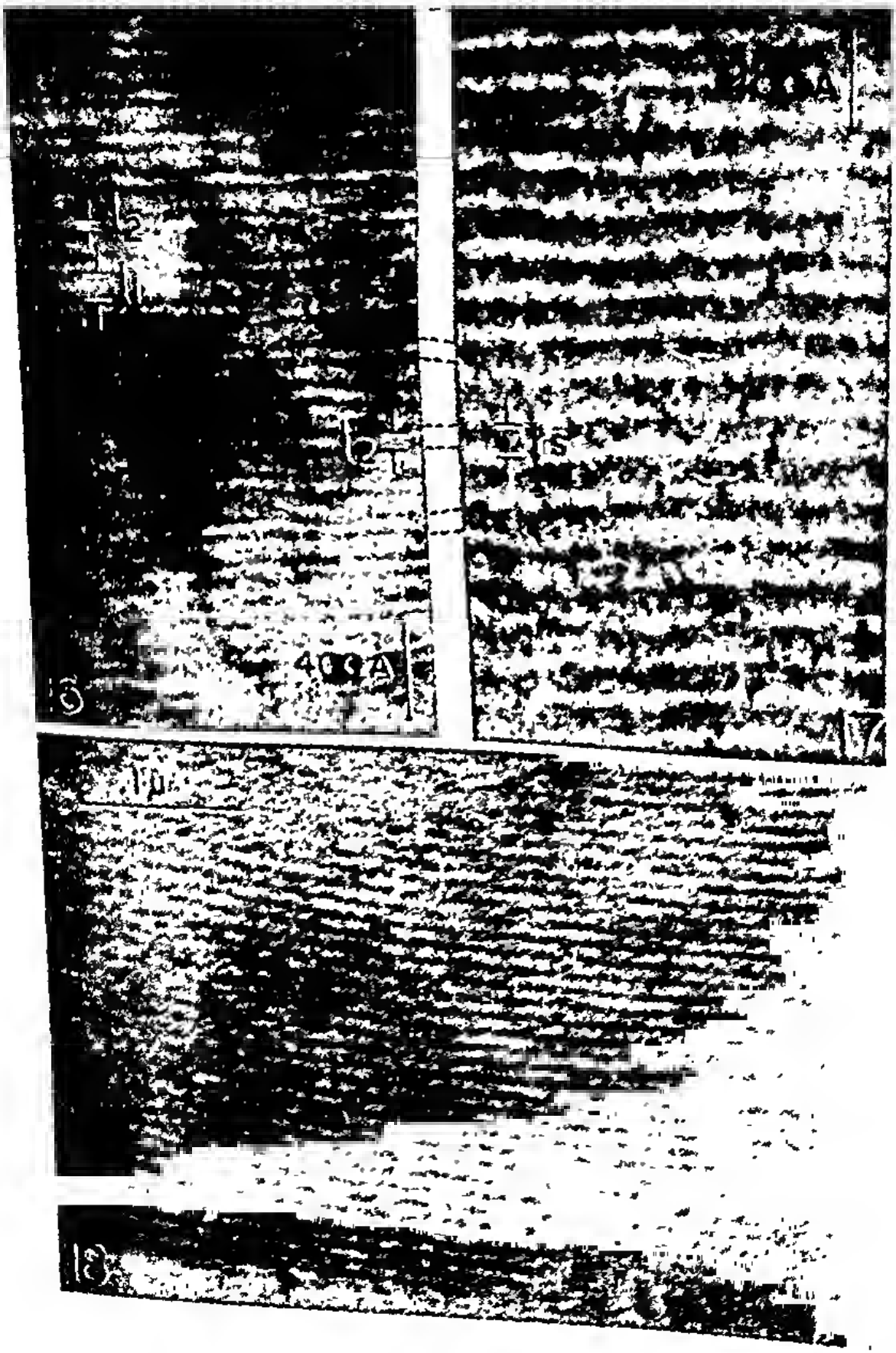
400 A
400 A
1 μ

practically no indication of dense lines. However, a similarly treated retina binds OsO_4 giving practically a normal membranous pattern (Fig. 11).

So far there is little information regarding the chemical nature of lipids in the rod and cone outer segments. Collins *et al.* (1953) calculated 30% of phospholipids by dry weight. More recently Krinsky (1958) has studied the effect of different solvents and enzymes on the lipoprotein structure of photoreceptors. Lillie (1952) has shown that in the rod outer segments of the guinea pig there are two lipid fractions. One is highly resistant to extraction with organic solvents and seems to be a galactolipid which is strongly bound to the protein. The other is a phospholipid which is rather easily extractable but is rendered insoluble after fixation in formaldehyde-dichromate.

The problem of the chemical nature of the bands, shown by the electron microscope in the lipoprotein systems of the visual cells, will be solved when more exact information becomes available about the mechanisms underlying chromation and osmium fixation. In the meantime we tentatively interpret both patterns to be complementary with l_1 and l_2 bands of lipid nature occupying, respectively, the intersaccular and the intrasaccular spaces in-between the osmiophilic membranes (Fig. 15B).

The Continuous Crystal-like Structure of the Rod and Cone Outer Segments

The molecular organization postulated above, with the dense lines l_1 and l_2 occupying the spaces in-between the membranes, suggests that the photoreceptor system may have a continuous crystal-like structure. As in the case of myelin (Fig. 18), a liquid crystal in a smectic state may be postulated for the rod and cone outer segments. If this is the case, extrapolating the data obtained in myelin by X-ray diffraction, there would be no "free fluid" space in the retinal photoreceptors and the water would be present mainly in an organized state.

Sidman (1957), who studied the concentration of solids in visual cell outer segments by refractometry, stated that "the values of 40 to 43 per cent obtained for concentrations of solids in rod outer segments are far higher than those found for ordinary cytoplasm and are among the highest measured for any biological material." The water content (1% of weight basis) of rod outer segments was calculated to be 64%; the value for cones was higher. On the other hand, Finean (1957) accepted a maximum of 50% water in myelin, but other authors have found a water content of 60 to 70% in the myelin sheath (Engström and Lüthy, 1950; Shanes and Berman, 1955). Thus, the data for photo-

receptors and myelin are reasonably close considering that several different techniques were used.

The hypothesis that the outer segments are organized as a continuous crystal-like structure requires studies by means of X-ray diffraction techniques in order to be confirmed. The existence of such a well-ordered organization would be of considerable interest in any possible explanation of the mechanism of origin and transmission of excitatory processes induced by light. Photochemical phenomena involving the transfer of energy throughout an orderly array of molecules have been considered in chloroplasts (Tollin *et al.*, 1958), and a similar mechanism might be involved in energy transfer in retinal photoreceptors.

Summary

New observations on morphogenesis of photoreceptors and macromolecular organization of lipoprotein systems in visual cells are described.

The differentiation of photoreceptors was studied in DBA normal mice and compared with that in C3H mice, in which there is a genetic dystrophy. The stages of development previously described by De Robertis (1956b) were confirmed, but an asymmetrical process of invagination of the surface membrane is recognized as the main source of the rod sacs in the rod outer segment.

Hereditary dystrophy in C3H mice is not the result of a primary arrest in development, but of a secondary degeneration of differentiating photoreceptors. The process of morphogenesis is exuberant and disordered, and leads to final involution and cell death. Because of an apparently uncontrolled growth, membranes may "invade" the connecting cilium and the inner segment of the rods. An increase in ribosome-like granules and mitochondrial alterations are also observed. These observations are correlated with recent biochemical findings and are discussed from the viewpoint of the genetic control of normal development.

A study of the fine structure of rod and cone outer segments of amphibian photoreceptors was carried out with fixation in OsO_4 and after formaldehyde followed by prolonged chromation in dichromate. With this technique certain lipid fractions are stabilized and chromium is preferentially bound to phospholipids.

The electron microscope image after chromation is very different than with OsO_4. The repeating period is 190 A for the cone and 200 A for the rod as compared with 150 and 160 A with osmium.

While in OsO_4 fixation there are clear (intra- and extrasaccular) spaces in-between the membranes, in chromium-fixed cells there is a more dense background with two denser lines. Of these l_1 is thicker

(70 Å), double, and less dense than l_2, which is definitely single and 30 Å thick.

The difficulties in correlating the two images were discussed. Of the several ways of matching, the interpretation of complementariness of both patterns is held as more probable. According to this I_1 and I_2 correspond, respectively, to the inter- and intrasaccular spaces and the bands of lower density in the chromated specimen to the membranes revealed by the OsO_4 (Fig. 15B).

The probable chemical nature of the bands is discussed and l_1 and l_2 are tentatively considered to be of lipid nature.

A continuous crystal-like organization of these retinal lipoprotein systems is suggested as a result of these observations and the similarity with the fine structure of myelin.

The possibility of energy transfer throughout an ordered and continuous array of molecules in photochemical systems is discussed.

References

Bahr, G. F. (1954). *Exptl. Cell Research* **7**, 457.
Bahr, G. F. (1955). *Exptl. Cell Research* **9**, 277.
Baker, J. R. (1958). "Principles of Biological Microtechnique." Wiley, New York.
Bennett, H. S. (1951). *Anat. Record* **110**, 231.
Ciaccio, C. (1909). *Anat. Anz.* **35**, 17.
Collins, F. D., Love, R. M., and Morton, R. A. (1953). *Biochem. J.* **53**, 632.
De Robertis, E. (1956a). *J. Biophys. Biochem. Cytol.* **2**, 319.
De Robertis, E. (1956b). *J. Biophys. Biochem. Cytol.* **2**, Suppl., 209.
De Robertis, E. (1958). *Exptl. Cell Research* **5**, Suppl., 347.
De Robertis, E. (1960). *J. Gen. Physiol.* (in press).
De Robertis, E., and Franchi, C. M. (1956). *J. Biophys. Biochem. Cytol.* **2**, 307.
Engström, A., and Lüthy, H. (1950). *Exptl. Cell Research* **1**, 81.
Fernández-Morán, H., and Finean, J. B. (1957). *J. Biophys. Biochem. Cytol.* **3**, 725.
Finean, J. B. (1957). *J. Biophys. Biochem. Cytol.* **3**, 95.
Hodge, A. J., McLean, J. D., and Mercer, F. V. (1955). *J. Biophys. Biochem. Cytol.* **1**, 606.
Karli, P. (1952). *Arch. Anat. Histol. Embryol.* **35**, 1.
Keeler, C. E. (1924). *Proc. Natl. Acad. Sci. U.S.* **10**, 329.
Krinsky, N. (1958). *A.M.A. Arch. Ophthalmol.* **60**, 694.
Lasansky, A., and De Robertis, E. (1959). *J. Biophys. Biochem. Cytol.* **5**, 245.
Lasansky, A., and De Robertis, E. (1960). *J. Biophys. Biochem. Cytol.* (in press).
Lasansky, A., De Robertis, E., Gomez, C. J., and Galfaso, C. (1960). Unpublished data.
Lillie, R. D. (1952). *Anat. Record* **112**, 477.
Lison, L. (1953). *In* "Histochimie et Cytochimie Animales." Gauthier-Villars, Paris.
Lowry, O. H., Roberts, N. R., and Lewis, C. (1956). *J. Biol. Chem.* **220**, 879.
Noell, W. (1958a). *Ann. N. Y. Acad. Sci.* **74**, 337.
Noell, W. (1958b). *A.M.A. Arch. Ophthalmol.* **60**, 702.
Porter, K. R. (1957). *Harvey Lectures, Ser.* **51**, 175.

Porter, K. R., and Kallam, F. (1953) *Exptl. Cell Research* **4**, 127.
Schmke, R. T. (1957). *Federation Proc.* **16**, 1468.
Schmidt, W. J. (1935). *Z. Zellforsch u. mikroskop. Anat.* **22**, 485.
Shanes, A. M., and Berman, M. D. (1955). *J. Cellular Comp. Physiol* **45**, 177.
Sidman, R. L. (1957). *J. Biophys. Biochem Cytol.* **3**, 15.
Sidman, R. L., and Wislocki, G. (1054). *J. Histochem. and Cytochem.* **2**, 413.
Sjostrand, F. S. (1949). *J. Cellular Comp. Physiol.* **33**, 383.
Sjostrand, F. S. (1953). *J. Cellular Comp Physiol.* **42**, 15.
Sjostrand, F. S. (1956). *Intern. Rev Cytol* **5**, 456
Sjostrand, F. S. (1959). *Rev Modern Phys.* **31**, 301.
Sjostrand, F. S., and Baker, R. F. (1958). *J. Ultrastructure Research* **1**, 239.
Sorsby, A., Koller, P. C., Attfield, M., Davey, J. B., and Lucas, D. R. (1954). *J. Exptl Zool* **125**, 171.
Stoeckenius, W. (1959). *J. Biophys Biochem Cytol* **6**, 225
Tansley, K. (1954). *J. Heredity* **45**, 123
Thornburg, W. (1958) *16th Ann. Meeting* E. M. Soc. of Am.
Tokuyasu, K., and Yamada, E. (1959). *J. Biophys Biochem. Cytol.* **6**, 225.
Tollin, G., Sogo, P. B., and Calvin, M. (1958). *Ann N.Y. Acad. Sci* **74**, 310.
Wislocki, G. B., and Sidman, R. L. (1954). *J. Comp. Neurol.* **101**, 53.
Wolken, J. (1956). *J. Cellular Comp Physiol* **48**, 349.
Wolken, J. (1957). *Trans N.Y. Acad Sci* **19**, 349.

Discussion

Dr. Hermann [Storrs, Conn.] May I ask whether the foregoing speakers considered the fact that energy production, which conventionally is attributed to activity in the mitochondria, is spatially separated from the synthesis of the membrane in the outer segment, and are we to assume that there may be energy transport from one segment of the rod to another?

Dr. De Robertis [Buenos Aires, Argentina] This is a difficult question because we know so little about energy transport. I wish to stress that the compartmental arrangement of rods and cones is very striking. All mitochondria are in a particular region of the cell that has a very slender connection with the outer segment. The injection of iodoacetate produces a specific degeneration of the outer segment without affecting the inner layers of the retina.

Dr. Sjostrand [Stockholm, Sweden]: Do you feel justified in assuming that everything which appears dark in your pictures represents lipids?

Dr. De Robertis: I don't believe I used that word but everything tends to show that this is so. It is very difficult to recognize lipids with the electron microscope, because many factors are involved in electron density. I think the main fact we have shown is that with pyridine treatment which extracts lipids these bands are no longer observed and the uptake of chromium has also almost disappeared.

The Fine Structure of Vertebrate and Invertebrate Photoreceptors As Revealed by Low-Temperature Electron Microscopy

H. FERNÁNDEZ-MORÁN

Mixter Laboratories for Electron Microscopy, Neurosurgical Service, Massachusetts General Hospital, Boston, Massachusetts, and Department of Biology, Massachusetts Institute of Technology, Cambridge, Massachusetts

See Page 521 for text of this chapter.

Localization of Oxidative Enzymes in Rat and Chick Retina in Various Physiological Conditions

A. G. EVERSON PEARSE

Department of Pathology, Postgraduate Medical School of London, London, England

Introduction

Until comparatively recently there were few recorded histochemical studies of the retinal dehydrogenases. These concerned mainly the succinate dehydrogenase system in a variety of animals (Francis, 1953; Wisłocki and Sidman, 1954, Tomita, 1958). The publication of two papers by Kuwabara and Cogan (1959) and Cogan and Kuwabara (1959) marked the first really comprehensive histochemical study of oxidative enzymes in the mammalian retina.

Earlier workers had used fresh frozen sections, with notably poor results Tomita (1958), for instance, recorded the presence of succinate dehydrogenase in chick retina but stated that accurate localization *was* impossible. Kuwabara and Cogan (1959) incubated full-thickness portions of human and rabbit retina in various media and subsequently, after fixing in formalin and embedding in gelatin, cut sections on a standard freezing microtome

Whatever other evidence may be adduced in favor of this method of preparatinn, it cannot be said to be easier or more convenient than the use of cold microtome (cryostat) sections. The latter have been employed for most of the work reported here.

While other workers studied only succinate dehydrogenase, Cogan and Kuwabara (1959) investigated also the localization of lactate dehydrogenase and diphosphopyridine nucleotide (DPN) diaphorase. In addition, they studied some activities which were manifestly unconnected with specific dehydrogenase activity.

Principles of Dehydrogenase Histochemistry

All modern histochemical methods for dehydrogenases and diaphorases are based on the reduction of colorless soluble tetrazolium salts to highly colored insoluble formazan pigments. This process is achieved by the transfer of hydrogen from the substrate (hydrogen donor) to the tetrazolium salt (hydrogen acceptor). When the substrate is succinate the final transfer is carried out by a flavoprotein attached to the dehydrogenase. This is not separately distinguished by name. If the substrate

is DPNH or TPNH (reduced diphospho- or triphosphopyridine nucleotide) the transfer of hydrogen goes through a separate flavoprotein, which is described as a diaphorase when the hydrogen acceptor is a dye, or as a cytochrome c reductase when cytochrome c is the acceptor. The latter is the normal state of affairs in the living cell.

When the substrate is any one of a number of compounds oxidized by specific dehydrogenases (e.g., malate, lactate, glutamate, etc.) the final pathway to the tetrazolium salt goes by way of DPN or TPN diaphorase. The specific dehydrogenases are thus either DPN-linked or TPN-linked or both.

We are now able to demonstrate in tissue sections at least eleven specific pyridine nucleotide-linked dehydrogenases, in addition to succinate dehydrogenase and the two diaphorases. From the results we can derive information about the predominant oxidative pathway employed by the cell under consideration, and we can estimate roughly the degree of activity exhibited. We can also obtain information about the distribution and number of mitochondria in the individual cells and about their physical state relative to other mitochondria. This process is known as "mitochondrial assay."

It is now considered that the final localization of formazan pigment in the tissues is to the sites of the diaphorase, except in the case of succinate dehydrogenase. When DPNH or TPNH are used as substrates all available sites of DPN or TPN diaphorase are revealed. With the specific dehydrogenase substrates the final pattern reflects the over-all localization of the dehydrogenase although the actual site, in the cell which contains the dehydrogenase, is that of the nearest diaphorase. Since the diaphorase is mainly intramitochondrial the localization of formazan should be (and is) intramitochondrial. If the dehydrogenase is extramitochondrial the histochemical localization is, in this instance, inaccurate.

Choice of Tetrazolium Salt

In the majority of studies in dehydrogenase histochemistry up to 1958 the most commonly used salt was blue tetrazolium (BT). In their studies on the retina Kuwabara and Cogan (1959) tested three other salts in addition to BT. These were neotetrazolium (NT), nitroneotetrazolium (NNT), and iodonitrotetrazolium (INT). They specifically stated that "the newer tetrazoliums (neotetrazolium, nitroneotetrazolium and iodonitrotetrazolium) were found to be too rapidly reactive." With BT they found, as other workers have done, that two formazans appeared as reaction products. One, a blue diformazan, was associated with cellular

structures and the other, a red monoformazan, with lipid and reticular structures.

Two different tetrazolium salts have been used in this investigation. They are 3-(4,5-dimethylthiazolyl-2)-2,5-diphenyltetrazolium bromide (MTT) and 2,2'-di-p-nitrophenyl-5,5'-diphenyl-3,3'-(3,3'-dimethoxy-4,4'-biphenylene) ditetrazolium chloride (nitro-BT). The former was synthesized by Beyer and Pyl (1954) and used in a cobalt chelation technique by Pearse (1957, 1960). The latter was produced by Tsou *et al.* (1956) and first used by Naehlas *et al* (1957).

There are strong objections to the use of BT or NT in dehydrogenase histochemistry, not only on account of their two reaction products (which lead to difficulties in interpretation) but also because they are inefficient hydrogen acceptors. The redox potential (half-wave reduction potential) of a tetrazolium salt is a measure of the ease with which it is reduced in biological systems. The tangent potential (the potential at which reduction first starts) is an even more accurate indicator. The redox potentials of BT and NT are —0.16 and —0.17 volts, respectively, while those of MTT and nitro-BT are —0 11 and —0 05 volts. The tangent potentials are in the neighborhood of —0.04 and 0.0 volts for these two salts Although the redox potential of INT is —0 09 volts the formazan derived from it is deposited as large crystals so that intracellular localization is impossible. Intracellular localization is possible with BT and NT but intramitochondrial localization is not. With nitro-BT and MTT intramitochondrial localization is regularly obtained.

Choice of Tissue Preparation

There are four alternative methods for producing thin, unfixed sections for histochemical studies If we exclude laborious cold knife procedures, which have been found wanting in the case of the retina, we are left with (1) cold microtome (cryostat) sections, (2) freeze-dried paraffin sections, and (3) freeze-substituted paraffin sections Of these, freeze drying yields excellent thin sections in which a number of intramitochondrial oxidative enzymes survive. After incubation, however, the final results are not very satisfactory. Freeze substitution also allows the production of thin sections, but activity of most of the dehydrogenases is destroyed by the processes of substitution With the cold microtome, thin (5μ) serial sections of retina are easily obtained and these are mounted directly on slides or cover slips. Preservation of structure, as far as the light microscope is concerned, is excellent. Preservation of oxidative enzymes is entirely satisfactory.

Material and Methods

Cryostat Sections (Rat Retina)

Whole eyes from young adult male rats (hooded and albino strains), and also from weanling rats of various ages, were removed as quickly as possible after killing the animals with coal gas. They were then quenched at —160°C in Freon 12 (Arcton 12) cooled by means of liquid air. The whole eye was then embedded in a block of rat liver, placed on a standard Cambridge rocking microtome chuck and, without allowing the eye to thaw, the block was frozen with dry ice. After rapid trimming with a sharp knife the block, and its chuck, were placed on the cold microtome.

Sections cut at 5 μ were mounted directly on cover slips inserted by means of a suction pickup through the operating port of the instrument.

Cryostat Sections (Chick Retina)

A similar method to that described above was used for the chick eye. In the case of the developing embryo (rat and chick), a block of tissue containing one or both eyes was embedded in rat liver and quenched with dry ice.

Freeze Substitution (Rat and Chick)

Small portions of retina were dissected out and quenched in Freon 12 cooled to —160°C with liquid air. Substitution was carried out in absolute acetone at —40°C for 5 to 7 days.

Media for Dehydrogenase and Diaphorase Studies

These were prepared according to the directions given by Pearse (1960) except that only in the case of alcohol and glutamate dehydrogenases was nitro-BT employed as hydrogen acceptor. The list of enzymes studied was as follows: DPN and TPN diaphorases, succinate, lactate, glutamate, β-hydroxybutyrate, α-glycerophosphate, glucose-6-phosphate, alcohol, isocitrate (TPN-linked), isocitrate (DPN-linked), and malate dehydrogenases. The incubation periods ranged from 15 min to 2½ hr, the average being 1 hr.

Stains Used for Comparative Preparations

Counterstains were infrequently used for the enzyme preparations. If necessary, brief staining in 1% aqueous methyl green (chloroform-washed) was used.

It was found more convenient to stain parallel or serial sections with hematoxylin and eosin or with Solochrome cyanine R (Pearse, 1960).

Results

With the exception of α-glycerophosphate dehydrogenase, which was practically absent in all cases, and β-hydroxybutyrate dehydrogenase, which was confined to a single region, oxidative enzyme activity in the retina of both chick and rat was found to be much more widespread than was anticipated. There were, in fact, few areas without activity. These findings are in conflict with those reported by other workers and can be attributed to the greater sensitivity of the methods employed in this study.

Adult Rat Retina

The localization in the retina of 9 specific dehydrogenases and 2 diaphorases is shown in Figs. 1 and 2. With the exception of Fig. 2e, which shows succinate dehydrogenase in the retina of a hooded rat, the illustrations in each case are from the pigment-free retina of the albino rat. It is thus possible to note the activity of the pigment epithelium in respect of the various enzyme systems. In Fig. 1a, for instance, the activity of alcohol dehydrogenase in the dark-adapted eye is shown. There is a strong reaction in the pigment epithelium (PE) and comparison with the control light-adapted eye (Fig. 1b) shows a considerable increase in activity. This finding suggests that the outer layer of the retina may play a part in the conversion of vitamin A to retinene by the mechanism suggested by Wald (1956).

In Fig. 1c the activity of glucose-6-phosphate dehydrogenase is shown. This enzyme, and 6-phosphogluconate dehydrogenase, which gives identical histochemical results, can be used as indicators of pentose cycle activity. It can be seen that in rat retina the latter is practically confined to the pigment epithelium and to the adjacent rod outer segments.

The activity of the DPN-linked isocitrate and malate dehydrogenases (Figs. 1d and 1e), on the contrary, is strong throughout the ganglion cell and inner plexiform layers, and moderately strong in the inner nuclear layer as well as in the outer layers of the retina. Glutamate dehydrogenase (Fig. 1f) is distinguished by very high activity in the outer plexiform layer (OP) where the rod-bipolar cell synapses are situated. As shown by Ladman (1958) each rod spherule in the albino rat possesses a single large oval or elongate mitochondrion measuring approximately 0.5 × 2.0 μ. This rod spherule region is characterized also by strong lactate dehydrogenase (Fig. 2f) and DPN diaphorase activities (Figs. 2d and 3C).

The remaining enzymes in Fig. 2 may need comment. The strongest TPN-linked isocitrate dehydrogenase activity (Fig. 2a) is in the rod and

cone inner segments and these show particularly strong DPN diaphorase (Figs. 2d and 5A) and lactate dehydrogenase (Figs. 2f and 5B) activity also. Succinate dehydrogenase (Fig. 2e) is generally much weaker than the other enzyme systems and almost totally lacking in the inner layers of the retina. It is present, however, in that portion of the rod and cone inner segments which lies immediately adjacent to the external limiting membrane. With the other systems (lactate, malate, DPN diaphorase) this area is weakly reacting.

It is worth noting that with several substrates, notably alcohol and glutamate (Figs. 1a and 1f), the external limiting membrane shows as a line of activity. TPN diaphorase (Fig. 2c) is much weaker than DPN diaphorase, particularly in the rod and cone inner segment (ellipsoid) region. The sole activity of β-hydroxybutyrate dehydrogenase, and hence presumably of fatty acid metabolism, is in the pigment epithelium and rod outer segment regions.

Since DPN diaphorase is preserved by freeze substitution it can be studied in freeze-substituted sections. Figures 3A and 3B show the result, in serial sections, of hematoxylin and eosin staining and of the diaphorase reaction. The structure of the rod and cone inner and outer segments is well shown and the diaphorase is seen to be restricted largely to the ellipsoid region. The gap between this and the border of the rod and cone nuclei (with the external limiting membrane seen in Fig. 3A) contains no diaphorase. The region of the rod-bipolar synapses, whose fine structure was studied by Ladman (1958) with the electron microscope,

---

FIG. 1. Albino rat, male, 200 gm. Fresh frozen (cryostat) 5-μ sections, incubated for oxidative enzyme systems as follows: (a) Alcohol dehydrogenase (dark-adapted eye); (b) Alcohol dehydrogenase (control eye); (c) Glucose-6-phosphate dehydrogenase; (d) Isocitrate dehydrogenase (DPN-linked); (e) Malate dehydrogenase; (f) Glutamate dehydrogenase. Magnification: × 250.

Key to abbreviations used in Figs. 1, 4, 5, and 7. G, Ganglion cell layer; IP, Inner plexiform layer; IN, Inner nuclear layer; OP, Outer plexiform layer; RCN, Rod and cone nuclei; RC, Rod and cone layer; PE, Pigment epithelium.

FIG. 2. As Fig. 1 except for Fig. 2c which is derived from a male 220-gm hooded rat. The enzyme systems shown are: (a) Isocitrate dehydrogenase (TPN-linked); (b) β-Hydroxybutyrate dehydrogenase; (c) TPN diaphorase; (d) DPN diaphorase; (e) Succinate dehydrogenase; (f) Lactate dehydrogenase. Magnification: × 250.

FIG. 3. Hooded rat, male, 180 gm. Freeze substitution in absolute acetone, —40°C, 5 days. Paraffin section, 5 μ. (A) Outer layers of retina with pigment epithelium below, and rod and cone nuclei above. Hematoxylin and eosin. (B) Serial section incubated for DPN diaphorase. (C) The same section as Fig. 3B showing rod spherules in the outer plexiform zone. (D) Outer plexiform zone. DPN diaphorase in fresh frozen section, purposely overincubated (1½ hr). Shows zone of swollen mitochondria. Magnification: × 2060.

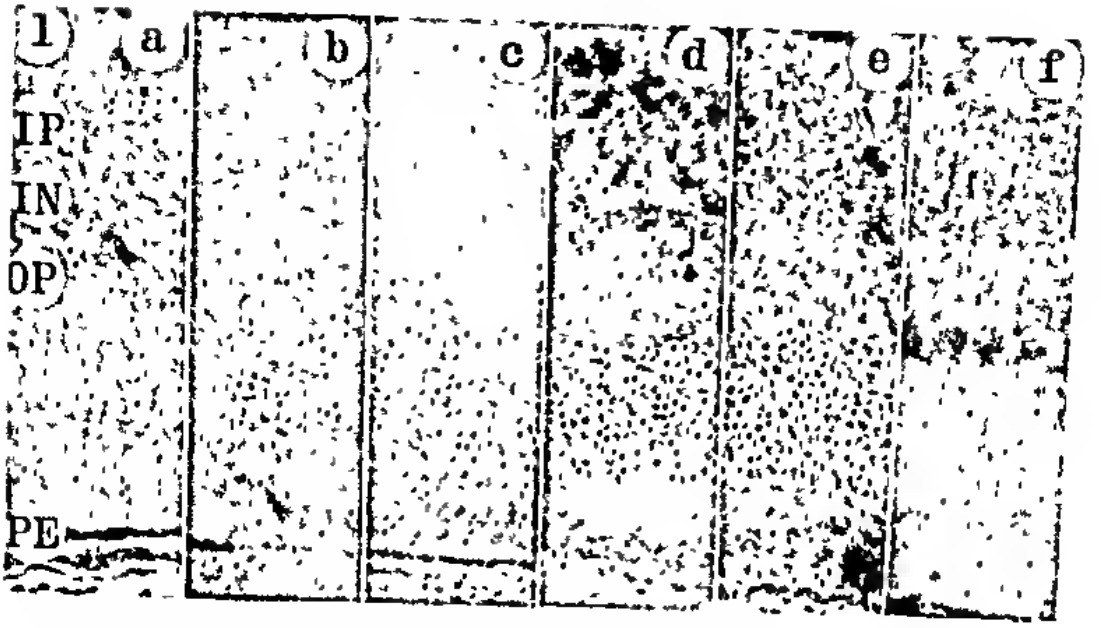
1
a
b
c
d
e
f
IP
IN
OP
PE

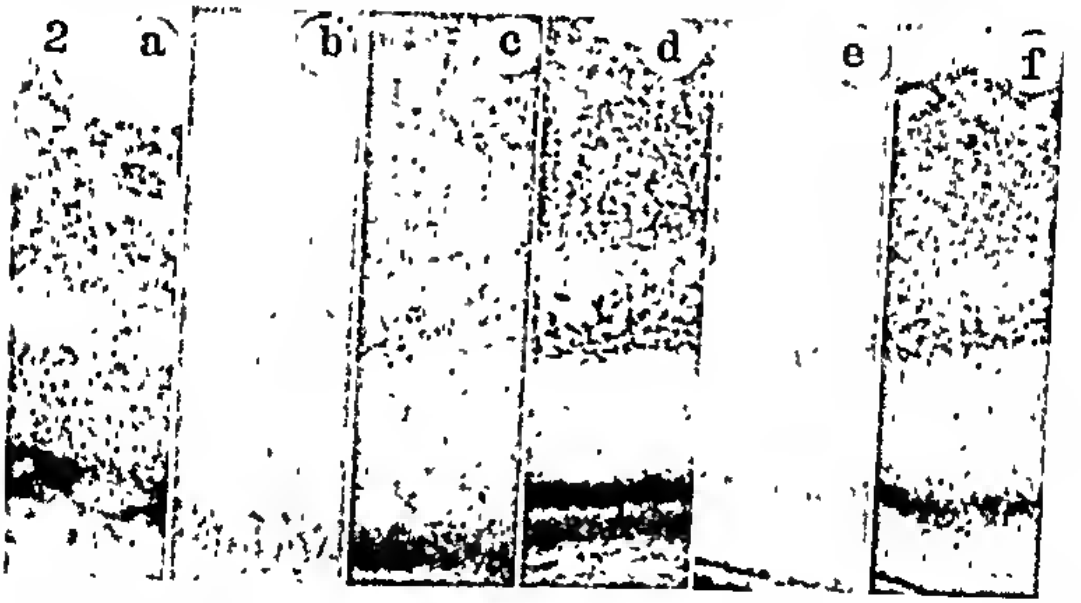
2
a
b
c
d
e
f


3
A
B
C
D

is shown in Fig. 3C. The bodies shown may represent the activity of the giant single mitochondria present in each synapse. Parallel studies of this region in fresh rat retina (Fig. 3D) show that the mitochondria of the rod synapses differ from those of the surrounding cells in that with slight overincubation (1½ hr) they react more intensely and begin to swell. This suggests that there are functional physical differences between their membranes and those of other retinal mitochondria.

The series of high-power photomicrographs (Figs. 4A,B,C, and 5A) represent the sites of DPN diaphorase activity in the fresh hooded rat retina. They should be compared with the same regions in the low-power photograph (Fig. 2d). In Fig. 5A between the ellipsoid zone, containing numerous formazan deposits, and the nuclei which appear as refractile spaces, weakly reacting mitochondria can be seen. It is these which are more easily seen in the succinate dehydrogenase reaction (Fig. 5C). The intervening illustration (Fig. 5B) shows lactate dehydrogenase activity in the ellipsoid zone with isolated foci of activity spreading into the outer segments.

Weanling Rat Retina

In the developing rat retina Graymore (1958), using biochemical methods, has described a sudden increase of glycolysis occurring at the time when the eyes are first opened. This is between the twelfth and fourteenth days of life. The only active glycolytic enzyme system demonstrable histochemically in rat retina is lactate dehydrogenase. As will be observed from Figs. 6A and 6B, there is a great increase of activity of this enzyme coincident with the opening of the eyes. The increase is a general one but the ganglion cells, the outer plexiform layer, and the ellipsoid zone of the rod and cone layer are particularly concerned. It appears to accompany a sudden increase in the rate of development of

---

Fig. 4. Hooded rat, male, 200 gm. 5 μ cryostat section. (A) Ganglion cell layer, labeled G, shows strong intramitochondrial activity; (B) Inner plexiform layer shows moderate activity throughout; (C) Junction of inner nuclear and outer plexiform layers with strong activity in the latter. DPN diaphorase. Magnification: × 2500. (For key to abbreviations, see legend to Fig. 1.)

Fig. 5. As Fig. 4. (A) Low activity in region of rod and cone nuclei with intense intramitochondrial activity in region of the ellipsoids of the rods and cones. DPN diaphorase. (B) Lactate dehydrogenase in the same region. (C) Succinate dehydrogenase in the same region. Magnification: × 2500. (For key to abbreviations, see legend to Fig. 1.)

Fig. 6. Fresh 5-μ cryostat sections. (A) Weanling hooded rat 10 days' old (eyes closed). (B) Weanling hooded rat 13 days' old (eyes open).

Incubated for the same time (1 hr) in the same medium. Lactate dehydrogenase. Magnification: × 170.

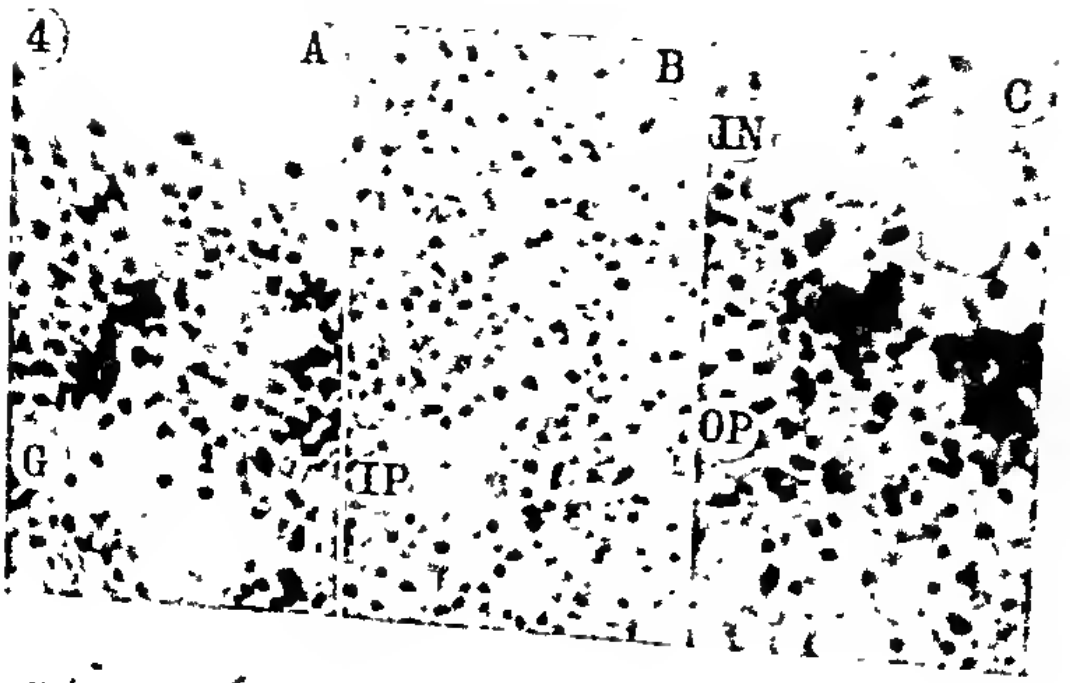
4
A
B
C
IN
G
IP
OP


5
A
B
C
RCN
RC
RC
RC


6
A
B

the ganglion cells, the rod synapses, and the ellipsoids (compare Figs. 6A and 6B).

Chick Retina (20-day)

The series of photomicrographs in Fig. 7 are of consecutive 5-μ fresh sections from the macular region of a 20-day-old chick. The nuclei are shown for convenience in Fig. 7a, and the other figures show, respectively, TPN diaphorase, and lactate and malate dehydrogenases.

Perhaps the most interesting feature of these enzyme reactions (as of others not illustrated) is the high over-all activity shown by every zone of the retina. Most of the zones can be subdivided, much as they are in the standard Golgi preparations. At least 3 "lines" of activity can be seen in the ganglion cell layer and in the inner plexiform region, 6 to 8 in the inner nuclear layer (in addition to the main division into 2 layers), 3 in the outer plexiform layer, and 2 in the rod and cone layer.

The external limiting membrane shows up clearly with DPN diaphorase (Fig. 8B), and to a lesser extent with the other systems shown. It seems probable that the strong lactate dehydrogenase activity in the inner region of the outer plexiform layer coincides with the situation of the cone synapses whose minute anatomy in rabbit retina was described by De Robertis and Franchi (1956). In this animal, however, no mitochondria were noted in the cone synapse.

Of the other enzyme systems studied (but not illustrated), the strongest were the DPN- and TPN-linked isocitrate dehydrogenases and glutamate dehydrogenase. There was a rise in alcohol dehydrogenase activity in the dark-adapted eye but the increase was mainly in the cone

---

Fig. 7. Chick retina (macular region), 20 days after hatching. 5-μ cryostat sections. (a) The three nuclear layers, stained with Solochrome cyanine R. (b) TPN diaphorase activity in a neighboring section. (c) Lactate dehydrogenase activity. (d) Malate dehydrogenase activity. Magnification: × 250. (For key to abbreviations, see legend to Fig. 1.)

Figs. 8A and 8B. As Fig. 7, but from whole retina treated by freeze substitution in absolute acetone at —40°C for 5 days. 5-μ paraffin sections. Note shrinkage by comparison with sections shown at identical magnification in Fig. 6. (A) Solochrome cyanine R. (B) DPN diaphorase reaction. Magnification: × 250.

Fig. 8C. High-power view of cone cell body region shown in Fig. 8B. Main activity appears in the ellipsoids but some activity is present in the myoids. Magnification: × 2500.

Fig. 8D. For comparison with Fig. 8C. Shows the DPN diaphorase reaction in a 5-μ cryostat section of a similar retina. A much smaller band of tissue is illustrated here (shrinkage being absent). Activity in lipid droplets (left, above ellipsoids) is absent from freeze-substituted retina (Fig. 8C) due to their solubility in acetone and chloroform. Magnification: × 2500.

ellipsoid region, not in the pigment epithelium as in the rat. There was only weak β-hydroxybutyrate dehydrogenase activity, and α-glycerophosphate dehydrogenase activity was not demonstrable.

Freeze substitution was shown by Feder and Sidman (1958) to be an excellent method for preserving retina. Figures 8A and 8B show the

macular region of chick retina prepared by this technique. Since the magnification (× 250) is the same as that of Fig. 7, it is evident that considerable shrinkage has occurred in the later stages.

High enzyme activity (Fig. 8B) is seen in the ganglion cell layer and in displaced cells in the inner nuclear layer. By far the highest activity, however, is in the so-called ellipsoid region of the cones which is shown at higher magnification in Fig. 8C. It is impossible to distinguish the activity of individual mitochondria in this region but there is a suggestion (Fig. 7c also) of small areas of lower activity at the junction of the ellipsoid with the outer segment.

A region of distinct intramitochondrial activity can be seen in the myoid region of the individual cone cells. In the fresh preparation (Fig. 8D) these features are less easily distinguished and an additional complication is provided by the presence of reacting lipid droplets (see also Fig. 7b).

Developing Chick Retina

Six-Day Incubation

At this stage of development (Fig. 9a) there is diffuse glycolytic activity, especially in the outer layers of the retina. It is possible already, however, to discern the position of the future inner nuclear and outer plexiform zones. At higher magnification the point at which the mass of developing nuclei (Fig. 9b) will divide to form the outer plexiform zone is visible in sections showing succinate dehydrogenase and DPN diaphorase activity (Figs. 9c and 9d). At still higher magnification (Fig.

Fig. 9a. Chick embryo retina, 6 days of development. 5-μ cryostat section. Shows diffuse activity throughout the retina with especially concentrated activity in the developing cones (below) and in the ganglion cell layer (above). Lactate dehydrogenase. Magnification: × 580.

Figs. 9b,c,d. As Fig. 9a. These figures show only the outer zones of the retina. (a) Solochrome cyanine R. (b) Succinate dehydrogenase. (c) DPN diaphorase. Magnification: × 820.

Fig. 9e. As Fig. 9a. Shows intramitochondrial DPN diaphorase activity, especially concentrated in developing cones. A tendency to parallel orientation of the formazan granules is observed. Other zones are evident also. Magnification: × 2560.

Figs. 10a,b. Chick embryo retina, 9 days of development. 5-μ cryostat section. (a) Solochrome cyanine R. (b) Malate dehydrogenase. The lowest layer is the pigment epithelium. In (a) separation of rod and cone nuclei is evident; (b) shows three layers of prominent activity. Magnification: × 820.

Figs. 10c,d,e. As Fig. 9, but after 13 days' development. (c) Solochrome cyanine R. (d) Malate dehydrogenase. (e) Lactate dehydrogenase. A broadening of the zones seen in Figs. 9a and b, has occurred. Both enzyme systems show similar localization of activity. Magnification: × 820.

9e), one can observe a tendency for the mitochondria in the future cone outer segments to line up in parallel rows.

Nine-Day Incubation

Observation of the retina after a further 3 days' development shows splitting of the mass of nuclei and a concentration of activity of a number

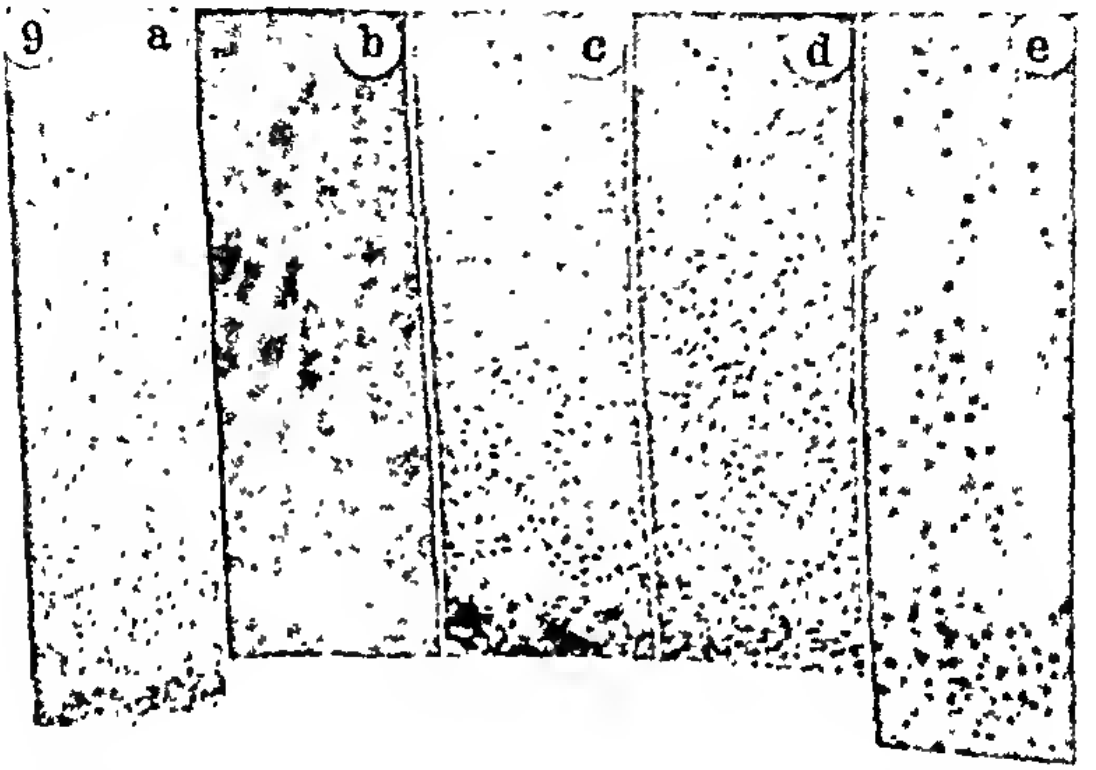

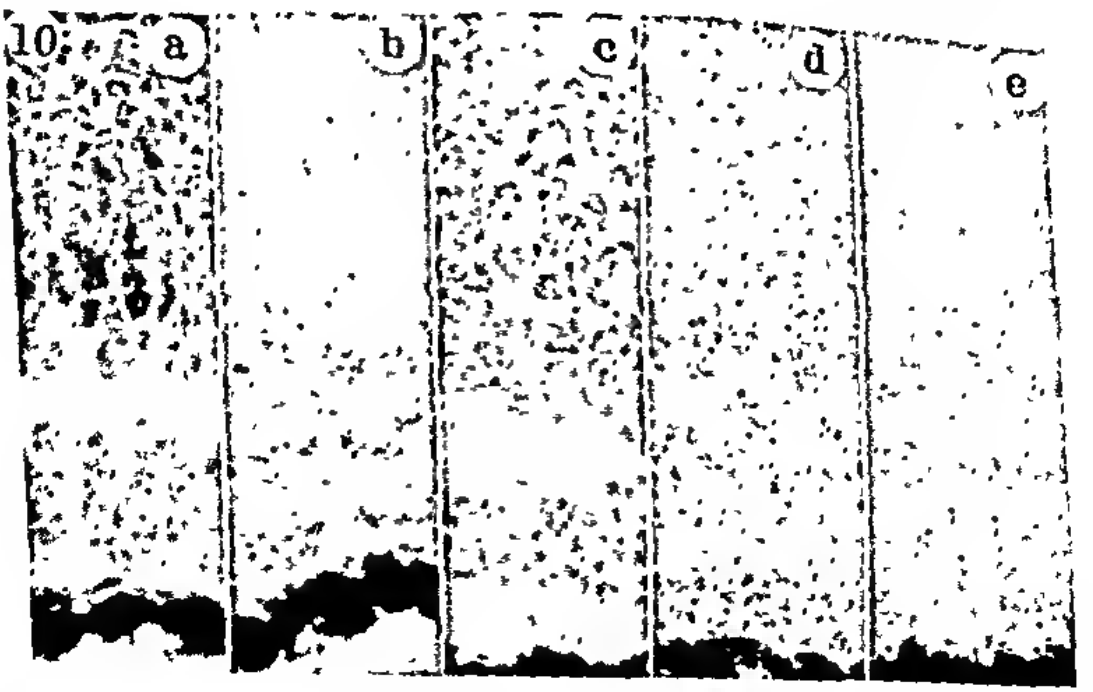

of oxidative enzyme systems in 3 particular regions (Fig. 10b). The outermost, in the future ellipsoids, is at this stage no stronger than the inner two which line the future outer plexiform zone.

Thirteen-Day Incubation

(Fig. 10c). Further development discloses no striking alteration in pattern or degree of oxidative enzyme activity. Figures 10d and 10e show the same 3 regions of high activity as the 9-day embryo retina.

Discussion

Little scope exists for comparison of the present results with those of other investigators because of the scarcity of reported work in this field. The elegant quantitative studies of Lowry and his co-workers (Lowry, Roberts, and Lewis, 1956) were made on rabbit and monkey retina. In the latter, lactate dehydrogenase was strongest in the outer plexiform zone and about half as strong in both the inner rod and cone segment and outer nuclear layers.

In the predominantly rod-containing retina of the rat and in the predominantly cone-containing chick retina (Figs. 2f and 7e), there is no doubt that the strongest lactate dehydrogenase is in the inner rod and cone segment. Activity in the outer nuclear layer is comparatively weak. Lowry's finding of equal activity in the ganglion cell and inner plexiform layers of the monkey retina is in keeping with the pattern (Fig. 2f) observed in the rat. In the chick, however (Fig. 7e), a manifest difference is present.

Malate dehydrogenase was found by Lowry to be strongest in the rod inner segments of both monkey and rabbit. In other zones of the rabbit retina this enzyme was weak but in the monkey a small peak was observed in the ganglion cell layer. Figure 7d shows that in the chick, malate dehydrogenase has two striking "peaks," one in the cone inner segments and the other in the ganglion cell layer. Activity in the rat (Fig. 1e) is somewhat similar. There is therefore, in view of the species differences, no great disagreement between the present findings and those of Lowry.

Comparing the present results with those of Cogan and Kuwabara, much greater differences are apparent though, once again, direct comparison is impossible due to the employment of different species. Kuwabara and Cogan (1959) found two basic types of formazan precipitation. One (lactate dehydrogenase) was said to be concentrated in Müller's fibers and other glial cells, and to a lesser extent in the ganglion cells. The other (succinate dehydrogenase) was characterized by a precip-

ZONES OF OXIDATIVE ENZYME ACTIVITY IN CHICK AND RAT RETINA

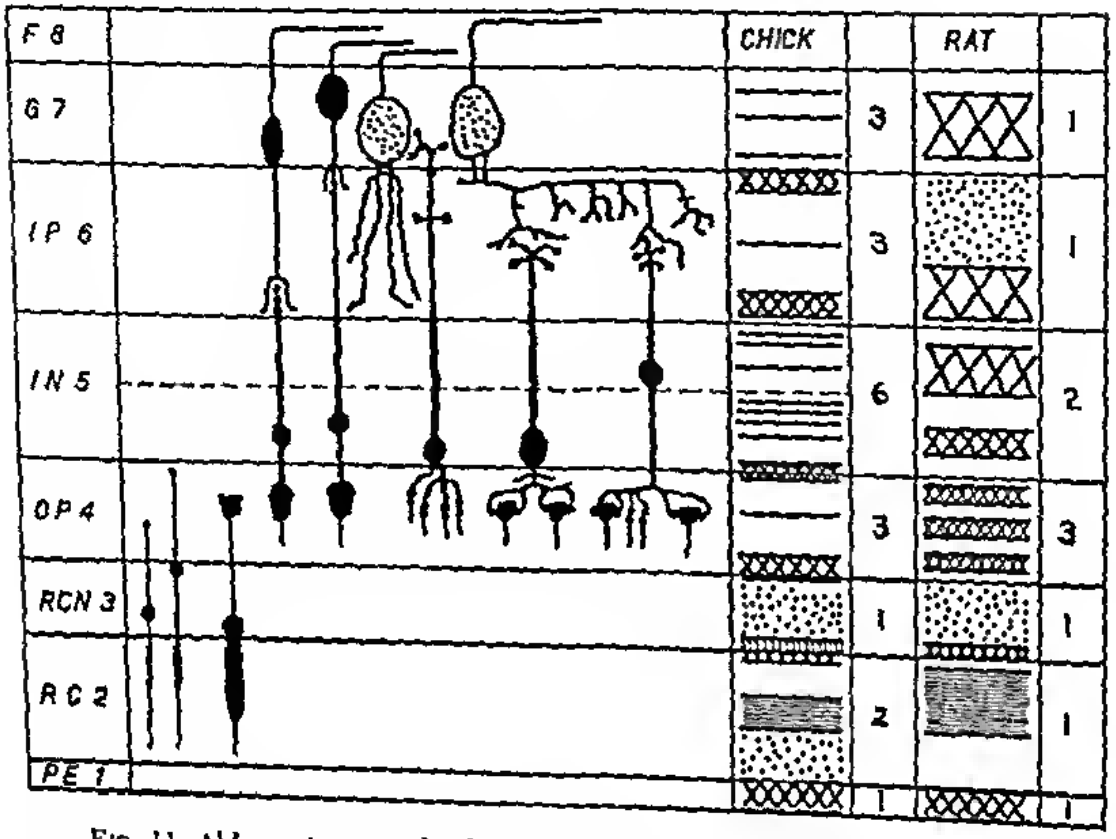

FIG. 11 Abbreviations in the first column: F = Fiber zone; G = Ganglion cell layer, IP = Inner plexiform layer, IN = Inner nuclear layer, OP = Outer plexiform layer, RCN = Rod and cone cell nuclei, RC = Rod and cone body layer, PE = Pigment epithelium

In the second column is a diagrammatic representation of cell bodies, axons, dendrites, and synapses in a composite retina, indicating their general arrangement within the numbered zones of "classical" histological practice.

Numbers in right-hand columns indicate the number of layers (of formazan pigment) visible with the light microscope or in photomicrographs taken with suitable filters. The other indications in the right-hand columns have the following significance: Single lines ——— = clearly separated, thin lines of activity, Two lines with crosses XXXX = much stronger activity in band form; Parallel lines ≡≡≡ = very strong activity. Diffuse dots . . . . . = background diffuse activity of greater than normal amount, Clear areas = low background activity or absence of activity.

Note that there is high oxidative enzyme activity of the *pigment epithelium*, in both chick and rat, which is second only to the very high activity of the *inner segments* of the photoreceptors. In each case a band of high activity marks the *external limiting membrane*. There is a suggestion that the synapses of the *outer plexiform layer* are grouped into three distinct bands. In the chick, but not in the rat, a similar grouping of synapses may occur in the *inner plexiform layer*. In the rat the inner nuclear layer is clearly divided into two zones while in the chick, where many lines of activity are visible, this division is only suggestive. The *ganglion cell layer*, in the rat, forms a single strong zone of activity but in the chick three distinct bands of activity are visible.

itate of formazan in the ellipsoids. No such localization is to be found in rat or chick retina. Although the location of the formazan product in the present study was in all cases intramitochondrial, and therefore intracellular, it was impossible to determine whether deposits arranged perpendicularly to the plane of the retinal surface were in Müller's fibers, or in the axons or dendrites of nerve cells.

Histochemical studies based on the incubation of whole retina fail to take into account the slow rate of penetration of tetrazolium salts into tissues. Cascarano and Zweifach (1959) showed that the only tetrazolium salt (in their series) which would penetrate 1-mm tissue slices in 1 hr was triphenyl tetrazolium chloride (TTC). This rate of penetration was achieved only with a concentration of 0.87% (average concentration in histochemical work is 0.02 to 0.05%). Patchy results were obtained by Kuwabara and Cogan, even after long (3 hr) incubation periods, and "ruptures of the inner layers of the retina increased the rate with which tetrazolium precipitation occurred in the vicinity of the rupture."

A so-called lactate dehydrogenase activity was observed by Cogan and Kuwabara at pH 8.8 to 9.5, in the absence of added DPN. This result cannot legitimately be ascribed to any specific enzyme activity. The use of high pH levels is not permissible in dehydrogenase histochemistry since it permits nonspecific reduction of tetrazolium salts, particularly by structures containing sulfhydryl groups. These may act directly, as in the alkaline tetrazolium reaction (Pearse, 1954), or indirectly through DPN or TPN in the "nothing dehydrogenase" effect described by Zimmermann and Pearse (1959). It is interesting to observe that Sidman and Wisloeki (1954) found a protein containing large amounts of SH groups in the rod outer segments of several species. For these and other reasons, the discrepancy between the present findings and those of Cogan and Kuwabara is considered to be largely due to very wide differences in the techniques employed.

The histochemical evidence of the present work suggests that the highest oxidative activity of retina is achieved by glycolytic pathways (lactate dehydrogenase) but that the activity of some other systems is of an almost equally high order. Malate, glutamate, and DPN- and TPN-linked isocitrate dehydrogenases are in this category. Succinate dehydrogenase activity is much lower. Linked activity of glutamate and isocitrate dehydrogenases (glutamate synthesis) and of malate and isocitrate dehydrogenases (conversion of isocitrate and pyruvate to α-ketoglutarate and malate) may thus be important pathways. Activity of the citric acid cycle seems to play a relatively subsidiary role in retinal metabolism; pentose cycle activity is minimal and fatty acid metabolism practically absent.

It is hardly surprising that actively respiring mitochondria are found to be distributed throughout the retina, although they are certainly concentrated into numerous bands or zones of higher than average activity. Some of these occur in the anatomical position of important structures such as the rod and cone synapses (3 bands in the chick), while others occur in the region of the bipolar-ganglion cell synapses (at least 3 bands in the chick). The sharp delineation of the external limiting membrane, by the majority of enzyme systems in both rat and chick, suggests a concentration of active mitochondria in this region of the rod and cone cells.

A diagrammatic representation of a composite retina from several species is shown in Fig. 11, in the left half of the illustration. In the right half are shown the lines or areas of higher than average oxidative enzyme activity in the retina of the chick and of the hooded or albino rat.

It is difficult, if not impossible, to consider these concentrations of activity as due to concentrations of activity in the supporting (glial) system of the retina, as presumed by Cogan and Kuwabara for lactate dehydrogenase. In the two plexiform zones the picture is probably produced by concentrations of specialized synapses while in the ganglion cell and inner nuclear zones it is manifestly due to segregation of the nuclei into layers so that the mitochondria of the perinuclear part of the cell body are similarly concentrated.

Correlation of oxidative enzyme histochemistry with conventionally stained preparations of the retina cannot afford much assistance. Correlation with silver techniques might be better but best of all would be accurate correlation with the results of electron microscopy. The results of such a study should provide a basis for further understanding of the mechanisms by which the first stages in the complex process of vision are carried out.

ACKNOWLEDGMENTS

I have to thank Mr. R. C. S. Hollands for a great deal of technical assistance in this study and Mr. V. [illegible] for taking the photomicrographs.

REFERENCES

[illegible], H., and Pyl, T. ([illegible]). *Chem. Ber.* 87, [illegible].
[illegible], J., and [illegible], B. W. ([illegible]). *J. Biophys. Biochem. Cytol.* [illegible], [illegible].
Cogan, D. G., and Kuwabara, T. ([illegible]). *J. Histochem. and Cytochem.* 7, [illegible].
De Robertis, E., and [illegible], C. M. ([illegible]). *J. Biophys. Biochem. Cytol.* 2, [illegible].
[illegible], C. M. ([illegible]). *J. Physiol. (London)* [illegible], [illegible].
[illegible], [illegible], and [illegible], [illegible]. ([illegible]). *J. Biophys. Biochem. Cytol.* 4, [illegible].
[illegible], C. N. ([illegible]). *Biochem. J.* 63, [illegible].
Kuwabara, T., and Cogan, D. G. ([illegible]). *J. Histochem. and Cytochem.* 7, [illegible].
[illegible], A. J. ([illegible]). *J. Biophys. Biochem. Cytol.* 4, [illegible].

Lowry, O. H., Roberts, N. R., and Lewis, C. (1956). *J. Biol. Chem.* **220**, 879.
Nachlas, M. M., Tsou, K.-C., de Souza, E., Cheng, C.-S., and Seligman, A. M. (1957). *J. Histochem. and Cytochem.* **5**, 420.
Pearse, A. G. E. (1954). *J. Pathol. Bacteriol.* **67**, 129.
Pearse, A. G. E. (1957). *J. Histochem. and Cytochem.* **5**, 515.
Pearse, A. G. E. (1960). "Histochemistry, Theoretical & Applied." Little Brown, *Boston, Massachusetts.*
Sidman, R. L., and Wislocki, G. B. (1954). *J. Histochem. and Cytochem.* **2**, 413.
Tomita, K. (1958). *Acta Soc. Ophthamol. Japan* **62**, 2547.
Tsou, K.-C., Cheng, C.-S., Nachlas, M. M., and Seligman, A. M. (1956). *J. Am. Chem. Soc.* **78**, 6139.
Wald, G. (1956). *In* "Enzymes: Units of Biological Structure and Function" O. H. Gaebler, ed., p. 355. Academic Press, New York.
Wislocki, G. B., and Sidman, R. L. (1954). *J. Comp. Neurol.* **101**, 53.
Zimmermann, H., and Pearse, A. G. E. (1959). *J. Histochem. and Cytochem.* **7**, 271.

Discussion

Dr. Cogan [Harvard University, Boston, Mass.]: Inasmuch as Dr. Pearse referred to our work, Dr. Kuwabara and I would like to show a few slides that may explain the differences between his results and ours.

We have found freezing and sectioning of the retina to be highly detrimental to subsequent dehydrogenase localization. Hence we have incubated the entire retina in a medium of tetrazolium and substrate prior to sectioning. Our preferred indicator is blue tetrazolium since this is not as sensitive as the other tetrazoliums and allows diffusion throughout the retina in the 2-hour incubation time. These are the main differences between our technique and that of Dr. Pearse.

Retinas incubated aerobically in this way with lactate DPN show abundant activity in Müller's fibers and only little activity in the photoreceptors (see A in Fig. 1 [Discussion]). There can be little doubt that it *is* Müller's fibers which are being outlined by the reduced tetrazolium. The pattern is the same as that obtained by Wolter with silver stains (*Am. J. Ophthalmol.* 40, 88, Part II, 1955) and by other conventional means of demonstrating Müller's fibers.

On the other hand, retinas incubated with succinate show activity predominantly in the ellipsoids of the rods and cones and in the reticular layers, but minimal or no activity in Müller's fibers (see B in Fig. 1).

Only minor variations are found in retinas from human, rabbit, cat, and beef sources. On the other hand, bird retinas, as exemplified by the turkey, are different (Fig. 1,C). Here almost all the activity is in the outermost layers, most especially in the photoreceptors, with a coarse or chunky type of tetrazolium precipitate in the myoids of the cones and a fine or granular type of precipitate in the ellipsoids.

Dr. Pearse [London, England]: I believe the differences reported are due to the techniques used. There is great danger in long incubation, in the presence of DPN.

Dr. Eränkö [Helsinki, Finland]: We have studied a number of species using Dr. Pearse's technique. We find that the differences described are to a great part species differences instead of due *only to the techniques* used.

Dr. Sjöstrand [Stockholm, Sweden]: It is possible to isolate outer segments and inner segments of the photoreceptors and work with them in rather pure prep-

Lowry, O. H., Roberts, N. R., and Lewis, C. (1956). *J. Biol. Chem.* **220**, 879.
Nachlas, M. M., Tsou, K.-C., de Souza, E., Cheng, C.-S., and Seligman, A. M. (1957). *J. Histochem. and Cytochem.* **5**, 420.
Pearse, A. G. E. (1954). *J. Pathol. Bacterial.* **67**, 129.
Pearse, A. G. E. (1957). *J. Histochem. and Cytochem.* **5**, 515.
Pearse, A. G. E. (1960). "Histochemistry, Theoretical & Applied." Little Brown, Boston, Massachusetts.
Sidman, R. L., and Wislocki, G. B. (1954). *J. Histochem. and Cytochem.* **2**, 413.
Tomita, K. (1958). *Acta Soc. Ophthamol. Japan* **62**, 2547.
Tsou, K.-C., Cheng, C.-S., Nachlas, M. M., and Seligman, A. M. (1956). *J. Am. Chem. Soc.* **78**, 6139.
Wald, G. (1950). *In* "Enzymes: Units of Biological Structure and Function" O. H. Gaehler, ed., p. 355. Academic Press, New York.
Wislocki, G. B., and Sidman, R. L. (1954). *J. Comp. Neurol.* **101**, 53.
Zimmermann, H., and Pearse, A. G. E. (1959). *J. Histochem. and Cytochem.* **7**, 271.

Discussion

Dr. Cogan [Harvard University, Boston, Mass.]: Inasmuch as Dr. Pearse referred to our work, Dr. Kuwahara and I would like to show a few slides that may explain the differences between his results and ours.

We have found freezing and sectioning of the retina to be highly detrimental to subsequent dehydrogenase localization. Hence we have incubated the entire retina in a medium of tetrazolium and substrate prior to sectioning. Our preferred indicator is blue tetrazolium since this is not as sensitive as the other tetrazoliums and allows diffusion throughout the retina in the 2-hour incubation time. These are the main differences between our technique and that of Dr. Pearse.

Retinas incubated aerobically in this way with lactate DPN show abundant activity in Müller's fibers and only little activity in the photoreceptors (see A in Fig. 1 [Discussion]). There can be little doubt that it is Müller's fibers which are being outlined by the reduced tetrazolium. The pattern is the same as that obtained by Wolter with silver stains (*Am. J. Ophthalmol.* **40**, 88, Part II, 1955) and by other conventional means of demonstrating Müller's fibers.

On the other hand, retinas incubated with succinate show activity predominantly in the ellipsoids of the rods and cones and in the reticular layers, but minimal or no activity in Müller's fibers (see B in Fig. 1).

Only minor variations are found in retinas from human, rabbit, cat, and beef sources. On the other hand, bird retinas, as exemplified by the turkey, are different (Fig. 1,C). Here almost all the activity is in the outermost layers, most especially in the photoreceptors, with a coarse or chunky type of tetrazolium precipitate in the myoids of the cones and a fine or granular type of precipitate in the ellipsoids.

Dr. Pearse [London, England]: I believe the differences reported are due to the techniques used. There is great danger in long incubation, in the presence of DPN.

Dr. Eränkö [Helsinki, Finland]: We have studied a number of species using Dr. Pearse's technique. We find that the differences described are to a great part species differences instead of due only to the techniques used.

Dr. Sjöstrand [Stockholm, Sweden]: It is possible to isolate outer segments and inner segments of the photoreceptors and work with them in rather pure prep-

aration. Some years ago we did such experiments and found that the more pure the outer segment fraction was the less enzyme activity we could find.

DR. PEARSE: There is no disagreement on this. Drs. Cogan, Kuwabara, Eränkö, and I find very little difference and very little activity in the outer segments. Occasionally there appears to be a mitochondrion much further out than normal. This is my explanation of the occasional focus of activity in the outer segment.

The Fine Structure of the Pigment Epithelium in the Turtle Eye[1]

EICHI YAMADA[2]

Department of Anatomy, School of Medicine, Kurume University, Kurume, Japan

THE PIGMENT EPITHELIUM is a simple cuboidal epithelium constituting the outermost layer of the neural part of the eye in vertebrates. During the development of the eye, the pigment epithelium and the retina are derived essentially from the same origin, namely the outer and inner layers of the optic cup. It has long been known that the cells of the epithelium play an important role in visual function and in the differentiation of the visual cells (Wald, 1958). Electron microscopy of these cells revealed that they had a characteristic feature in their fine structure, especially in the structure of the highly developed smooth-surfaced endoplasmic reticulum within the cytoplasm. In certain vertebrates (the bat, frog, and bird), the peculiarly lamellated myeloid bodies were also observed (Porter, 1957; Yamada *et al.*, 1958; Yamada, 1958, Porter and Yamada, 1960). In this paper, the pigment epithelium of the turtle eye is studied by means of the electron microscope, and the several morphological features in which it differs from other animals will be described.

Materials and Methods

Fresh-water turtles (*Chrysemys picta*) were used for this study. Methods of the tissue preparation and of the observation were essentially similar to those described in a previous paper (Porter and Yamada, 1960)

Observations

GENERAL APPEARANCE

The pigment epithelium of the turtle eye is a single layer of low cuboidal epithelial cells which rests on the rich capillary network of the choroid (lamina choriocapillaris) which is separated from the epithelium

---

[1] This report covers work done at the Rockefeller Institute, New York, and was supported in part by a grant from the National Science Foundation.

[2] *Present address*, Department of Anatomy, School of Medicine, Kyushu University, Fukuoka, Japan

by a thin layer of connective tissue, the so-called Bruch's membrane or lamina basalis. The cell is perfectly flat on its basal surface and is formed into numerous processes or pseudopodia on its apical surface: these processes are interdigitated with the outer and inner segments of the visual cells (mostly cones). A large ovoid nucleus, with a prominent nucleolus located usually at its center, can be observed about the middle of the cell. Figure 1 shows a photomicrograph of sectioned turtle pigment epithelium taken from a methacrylate-embedded block and stained with periodic acid-Schiff (PAS) and fast green. Figure 2 is an electron micrograph of the same epithelium taken from the same block. It is possible, in both figures, to divide the pigment epithelial cell along its plane into four zones or strata: basal zone, nuclear zone, apical zone, and cell processes. The basal zone presents a homogeneous appearance under both the light and the electron microscope and is about 1 μ thick. The nuclear zone contains diverse cell organelles such as nucleus, mitochondria, lipid granules, and myeloid bodies and occupies a large part of the cell.

The apical zone is a thin layer covering the nuclear zone and contains small myeloid bodies and pigment granules which are also found within the cell processes, or pseudopodia extending from the apical zone. The structure of each zone is described in detail below.

Capillaries of the Choriocapillary Layer; and the Bruch's Membrane (Figs. 1–4)

These two structures are essentially the same as those existing in frog's retina (Porter and Yamada, 1960). The capillary is rather large in diameter and is covered by a thin endothelial cell measuring about 50

FIG. 1. Photomicrograph of sectioned turtle pigment epithelium taken from a methacrylate-embedded block and stained with PAS and fast green. The picture represents a normal or slightly oblique section. The four zones, basal (bz), nuclear (nz), apical (az), and processary (ep) of the epithelial cell are recognizable. The round nucleus (N) with a nucleolus at its center and a lipid body (lb) are clearly seen. The myeloid bodies (mb) and mitochondria (m) in the nuclear zone are barely visible. Cell processes contain numerous fuscin granules (fg). Os: outer segment; is: inner segment; c: capillary of the choroid; and B: Bruch's membrane.

FIG. 2. Electron micrograph of turtle pigment epithelium taken from the same block as the photomicrograph in Fig 1. The four zones or strata of the cell are now clearly seen. Below on the left are seen the capillary lumen (c), a very thin endothelial cell (ed), and a piece of three-layered connective tissue with a prominent elastic lamina (el) in it. In the right upper corner is seen a part of the cone outer segment (os) surrounded by a number of cell processes (ep). Myeloid bodies (mb) and mitochondria (m) are the prominent structures within the cytoplasm. N: nucleus; Nl: nucleolus; fg: fuscin granule; bz: basal zone; nz: nuclear zone; and az: apical zone.


os
os
fg
az
nz
mb
N
m
lb
bz
B
B
C
C
1
5 μ
cp
fg
os
az
mb
cp
nz
N
bz
NL
mb
ed
el
m
2
μ
C

mμ thick in most parts. Fenestrations or interruptions are occasionally found (Fig. 4). The plasma membrane of the endothelial cell is relatively thick (about 10 mμ) and sometimes shows its three-layered nature (Fig. 4, insert). A feature is especially noticeable at its portion facing the pigment epithelium. The endothelial cell shows no distinct basement membrane along its basal surface. The connective tissue between the capillary and the epithelium is three-layered and the dense middle layer probably corresponds to the "elastic tissue." This intervening connective tissue, spread all over the retina, is about 0.7 μ thick.

Basal Zone (Figs. 1–4)

The basal cell surface appears perfectly flat (Figs. 1 and 2), but in high magnification, it has numerous minute tubular or vesicular invaginations on its surface, the basal plasma membrane presenting a finely irregular appearance (Figs. 3 and 4). The tubules or vesicles found in the basal zone are so densely packed together, in fact, that no other cell organelle can be observed here. This gives a homogeneous appearance to this zone in its light microscope image or in its low-power electron micrograph (Figs. 1 and 2). The tubules or vesicles range from 60 to 150 mμ in diameter, are gathered to make a layer about 1μ high from the basal surface of the cell, and then gradually decrease in number toward the nuclear zone. But some of them seem to be continuous with tubular elements of the endoplasmic reticulum found in the cytoplasm of the nuclear zone.

Nuclear Zone (Figs. 1–3, 5, and 6)

As described before, most of the cell organelles of the epithelial cell can be found in this area. The mitochondria of this cell are unique in some respects. They are extraordinarily long and slender (3 × 0.2 μ), and tend to arrange themselves vertically to the plane of the epithelium.

FIG. 3. Medium-power electron micrograph of sectioned turtle pigment epithelial cell showing the details of the four zones or strata. At the bottom of the figure is found a capillary lumen (c) with an endothelial cell (ed) forming its wall. The epithelial cell rests on a thin connective tissue layer with an elastic lamina (el) in the middle of it. The basal zone (bz) contains numerous tubules or vesicles, and many invaginations are found on its basal surface. The middle zone of this figure represents a nuclear zone containing long oriented mitochondria (m), myeloid bodies (mb), and a network of the tubular endoplasmic reticulum (sr). The prominent terminal bar (t) is also found in this zone. Note the presence of the rough-surfaced elements (er) of the endoplasmic reticulum. From the apical zone of the cell extend upwards cell processes which contain fusein granules (fg), tubular elements of the endoplasmic reticulum, and small myeloid bodies, os: outer segment (possibly rod); g: granules of unidentified character.

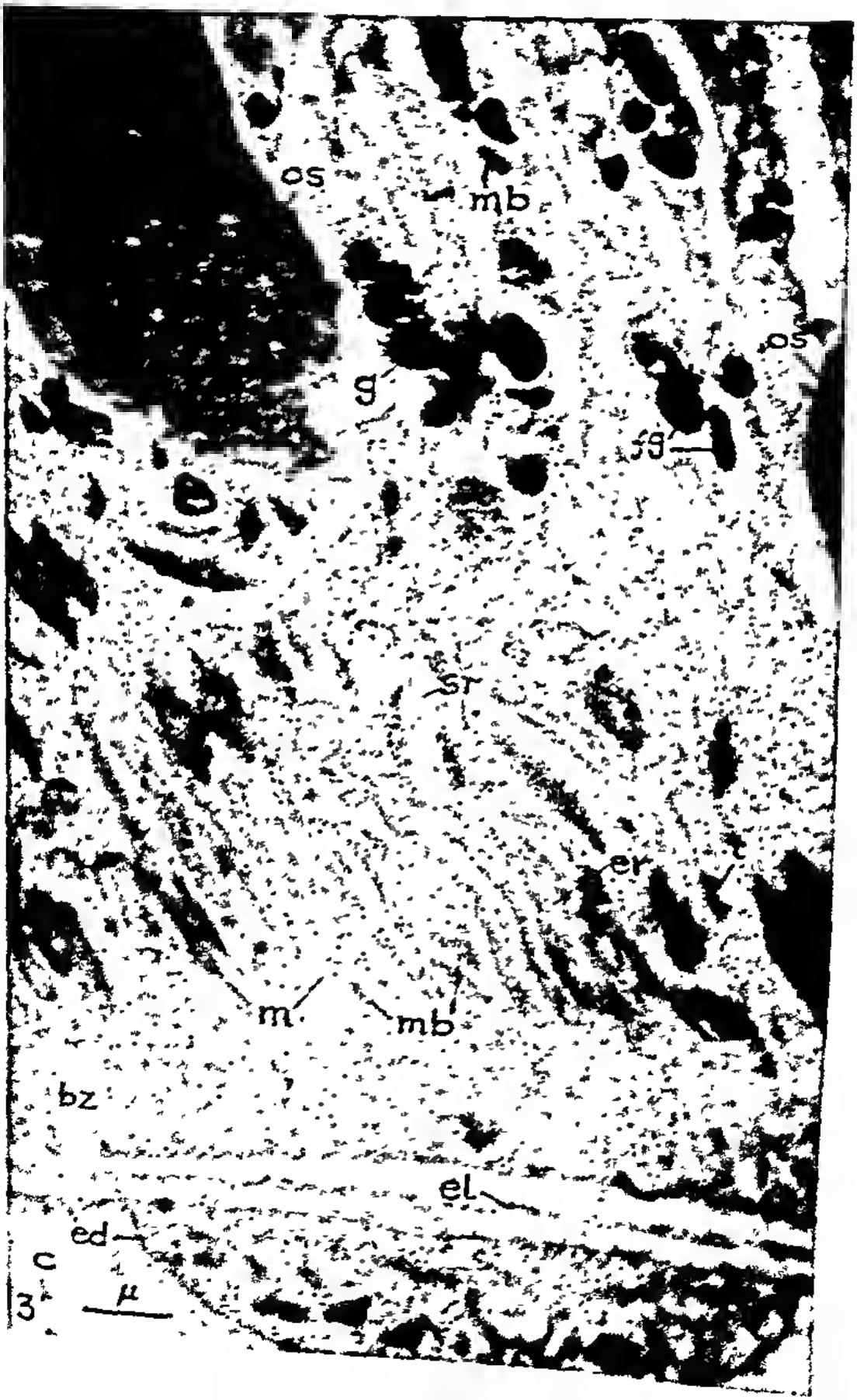
os
mb
os
g
sg
e
st
er
m
mb
bz
el
ed
c
3
μ

Their cristae mitochondriales are also found arranged parallel to the long axes of the mitochondria (Figs. 3 and 6). Another prominent structure in this zone is the myeloid body. These are present in large numbers. The myeloid bodies were the same in their fine structure in the frog's pigment epithelium (Porter and Yamada, 1960) and in the turtle's (Figs. 5 and 6). They are composed of a number of flattened sacs which, in turn, are continuous at their margin with the surrounding endoplasmic reticulum (Figs. 5 and 6). The long axes of the myeloid bodies are usually extended vertical to the plane of the epithelium, so that the mitochondria and myeloid bodies appear to be arranged parallel to each other. These two structures are often found quite close to each other as shown in Figs. 3 and 6, in which some of the myeloid bodies are surrounded very closely by large mitochondria. It is also common to find that myeloid bodies are aggregated and connected with one another on their convex faces (Figs. 2 and 5).

As mentioned earlier in this paper, the pigment epithelial cell is an extreme example of a cell with extensively developed smooth-surfaced endoplasmic reticulum in its cytoplasm. The cytoplasm of the entire cell body is filled with a network of membrane-limited tubules. As described before, the tubules are more densely distributed in the basal than in any other zone. Nevertheless, the reticulum in the nuclear zone occupies nearly half the volume of the cytoplasm. Most of the membranes limiting the tubules are devoid of ribonucleoprotein (RNP) particles and belong to the smooth-surfaced elements of the endoplasmic reticulum. The RNP particles, however, are found scattered in small clusters throughout the cytoplasm except the basal zone. Some of the particles are attached to the cytoplasmic surface of the tubular membrane and are of the rosette-like pattern in their arrangement (Fig. 3). The continuity between these tubular elements and the components of the myeloid bodies was already mentioned.

The terminal bar of this epithelium is always located about the

---

FIG. 4. Details of the basal zone and capillary endothelial cell. Tubules or vesicles in the basal zone and the invaginations of the basal cell surface are quite visible. The capillary endothelial cell (ed) has a relatively thick plasma membrane and is partially interrupted to form a pore (indicated by arrow). b: basement membrane of the epithelium; m: mitochondria; and mb: myeloid bodies.

Insert: Detail of the plasma membrane of the endothelial cell showing its three-layered nature.

FIG. 5. A part of the nuclear zone delineated in detail. Mitochondria (m), myeloid bodies (mb), and fusein granules (fg) are clearly shown. The continuity between the components of the myeloid bodies and the surrounding endoplasmic reticulum (sr) is clearly visible. Note a thin membrane around the pigment granules.

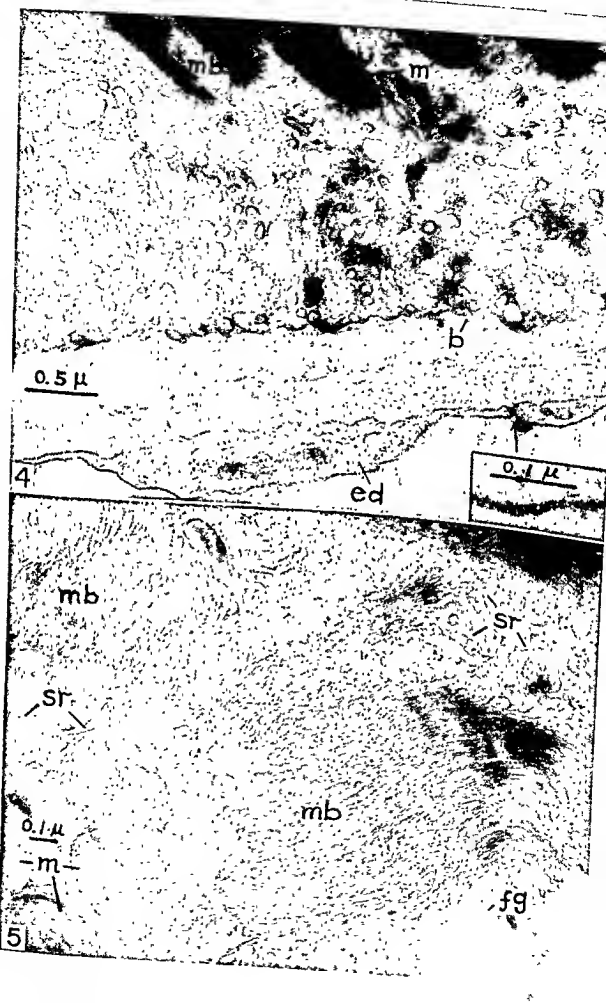
mb
m
b
0.5 μ
4
ed
0.1 μ
mb
sr
sr
0.1 μ
m
mb
fg
5

middle of the nuclear zone (Fig. 3) and represents one of the morphological features of this epithelium. The probable functional significance of the terminal bar being low in position relative to the cell surface was discussed previously (Porter and Yamada, 1960).

The Apical Zone (Figs. 3 and 7)

The network of the endoplasmic reticulum is somewhat less compact in the apical than in the nuclear zone of the cell and the pigment granules (fuscin granules) instead of the mitochondria are usually found as characteristic dense bodies in the apical zone. In addition, the small myeloid bodies and vesicular or vacuolar components about 0.1 μ in diameter, which are arranged in rows toward the free surface of the cell, are clearly seen in this area (Figs. 3 and 7). Occasionally, the outer segment of the visual cell is in direct contact at its tip with the free surface of the apical zone (Fig. 3).

Cell Processes (Figs. 2, 3, and 7)

In a single section, more than 20 cell processes extend from the free surface of one cell toward and between the outer segments of visual cells. Each process is about 0.7 μ in diameter, becoming smaller toward the tip, and ranging from 3 to 10 μ in length, reaches up to the level of the ellipsoid in the inner segment. The content of the process does not differ significantly from the cytoplasm of the apical zone. Each process contains dense pigment granules (0.2 × 1 μ) arranged, as a rule, parallel to its axis, and surrounded by a thin membrane (Fig. 7), as described for the frog's epithelium (Porter and Yamada, 1960). It contains, besides, tubular elements of the endoplasmic reticulum as well as small-sized myeloid bodies. There are some granules similar in size, different in internal structure, low in electron density, and finely granular in appearance (Fig. 3).

FIG. 6. Details of a part of the nuclear zone showing large slender mitochondria (m), myeloid bodies (mb), and smooth-surfaced endoplasmic reticulum (sr). The continuity of the membrane in the myeloid bodies to that of the endoplasmic reticulum is clearly shown by the arrow. Note the cristae mitochondriales and the intimate relationship between mitochondria and myeloid bodies.

FIG. 7. An oblique section through a part of the apical zone and the cell processes (cp). The latter contain tubular elements of the endoplasmic reticulum (sr) as well as fuscin granules (fg) encapsulated by a thin membrane. The vesicles (v) arranged in rows are recognized close to the free surface of the apical zone. The myeloid bodies (mb) are found within both the cell processes and the apical area of the cell.

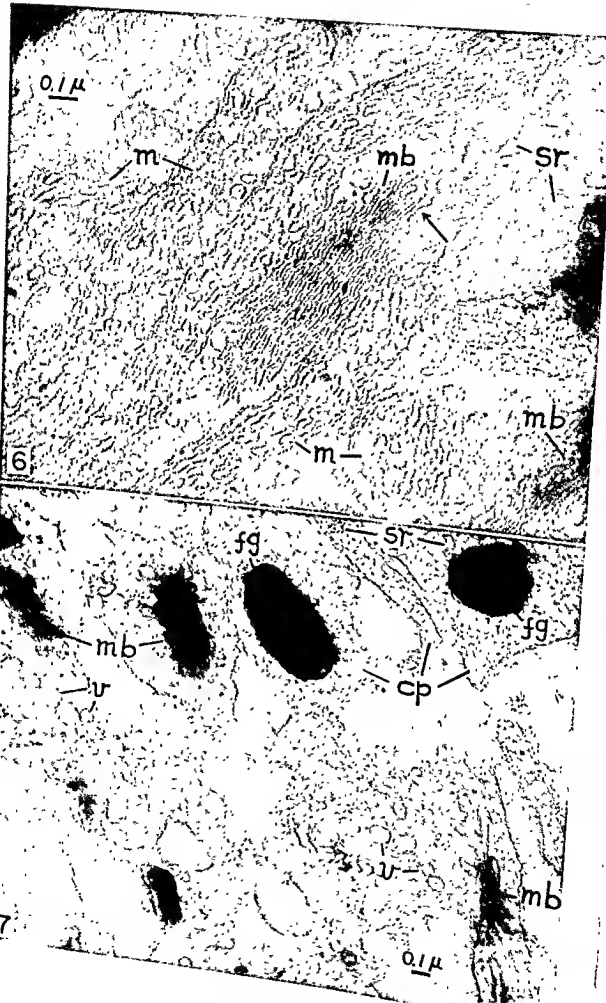
0.1 μ
m
mb
sr
mb
m
6
sr
fg
fg
mb
v
cp
v
mb
7
0.1 μ

Discussion

The retina of the turtle has been known as a retina which is composed mainly of cone visual cells. In this respect, it may be expected that there are some physiological and morphological features peculiar to the structure of the pigment epithelium. In addition, the retina of the chelonian eye is entirely avascular, lacking even a conus papillaris which is found in the ordinary reptiles (Duke-Elder, 1958). It is obvious, then, that all the metabolites required must be mediated by the vascular network of the choroid and through the pigment epithelial cells. For this reason, we could expect the pigment epithelium to be more specialized in structure in the turtle than in any other reptile.

The characteristic morphological features of the turtle pigment epithelium differ from those described in other animals and may be summarized as follows: (1) the existence of a distinct basal zone; (2) presence of myeloid bodies, even in the cell processes, and (3) that of large slender oriented mitochondria. First of all, the extremely numerous tubules and vesicles found in the basal zone are considered, at least some of them, to be derived from the basal cell membrane, possibly by the micropinocytic process, because there are a number of small or deep invaginations found along the basal surface. These findings suggest that a very active exchange of metabolites is taking place at this level of the pigment epithelial cell. It appears also that some of the tubules are continuous with the elements of the endoplasmic reticulum in the nuclear zone.

No specialized zone like this has been observed in the pigment epithelia of a mammal or a frog, but a similar area exists in birds (Yamada *et al.*, 1958). It is to be noted in this connection that the bird retina is also avascular although there is a specially vascularized pecten.

The characteristic development of the smooth-surfaced endoplasmic reticulum in the pigment epithelium in general, together with its probable significance in visual physiology, has been described and discussed in a previous paper (Porter and Yamada, 1960). It has been also mentioned that myeloid bodies, as a specialized part of the endoplasmic reticulum (Porter, 1957; Porter and Yamada, 1960), are to be regarded as some sort of membrane crystal and are assumed to be responsible for the sensitivity to light of these cells.[3] Therefore, it seems unnecessary to repeat

[3] Myeloid bodies are found in the pigment epithelial cells in the turtle, frog, and bird, but not in most mammals. Excepting in mammals migration of pigment granules has been observed. The fine structure of the myeloid body is quite similar to that of the outer segments of cones and rods. In preliminary electron microscope study on the dark-adapted frog retina, it seems clear that the pigment granules migrate toward the apical portion of the cells, but the cell processes or pseudo-podia containing the

those discussions here, but the presence of myeloid bodies in the cell body, even in its processes, is worth mentioning. It is probable that this might help the quick response of the epithelial cell to light stimulation, and possibly correlate with the abundance of cones in the turtle retina.

The intimacy in location of myeloid bodies and mitochondria suggests some functional relationship between these two structures. There might also be some functional significance in the fact that both structures are oriented in arrangement, namely, that these arrange themselves perpendicular to the plane of the epithelial sheet and Bruch's membrane. It is assumable that the functional organization of the epithelial cell is polarized in that direction.

Summary

The pigment epithelium of the turtle (*Chrysemys picta*) was studied with the electron microscope. The morphological features of the epithelium, different from those of other vertebrates, were (1) that the distinct basal zone contains numerous tubules and vesicles; (2) that the epithelial cell contains myeloid bodies, especially in its processes or pseudopodia, and (3) that it contains large oriented mitochondria. The smooth-surfaced endoplasmic reticulum was found characteristically developed in this epithelial cell. The probable functional significance of these findings was discussed.

References

Dake-Elder, W. S. (1938), "System of Ophthalmology," Vol. I, The Eye in Evolution, pp 333-395 Mosby, St Louis, Missouri.

Porter, K. R. (1957) *Harvey Lectures, Ser* **52**, 175-228

Porter, K. R., and Yamada, E. (1960) *J. Biophys. Biochem. Cytol.* **7** (in press).

Wald, G. (1958) *Exptl. Cell Research* **5**, Suppl., 369.

Yamada, E. (1958) *J. Biophys Biochem. Cytol* **4**, 329.

Yamada, E., Tokuyasu, K., and Iwaki, S. (1958). *J. Electron-microscopy (Tokyo)* **6** 42-46

Discussion

Dr. Carpenter (Tufts University, Medford, Mass.): Have you studied the distribution of pigment granules in light- and dark-adapted eyes? How do they move?

Dr. Yamada (Kurume, Japan): We were able to show the migration of pigment granules still remain at their position between the rods and cones. The tubular element of endoplasmic reticulum is still found within the processes. Possibly the changes in the retina (cones and rods) caused by light stimulation are of importance for the pigment epithelial cell. The reaction or function of these cells might depend on the retinal condition. However, the pigment granule migration could be only a manifestation of those reactions. The strongly developed smooth-surfaced endoplasmic reticulum might be correlated with the active lipid metabolism of these cells.

granules in the frog eye very clearly, but found no difference in the granule structure in light- and dark-adapted eyes. The mechanism of the movement, I can not tell yet.

CHAIRMAN PORTER [Rockefeller Institute, New York]: The epithelial cell processes (pseudopodia) do not move; only the pigment granules migrate.

DR. YAMADA: Pigment granule migration *seems* to be accompanied by a shift of the endoplasmic reticulum.

DR. FERNÁNDEZ-MORÁN [Cambridge, Mass.]: In our studies there was no indication that pigment granules accumulated around the tips of the external segments more markedly in the dark- than in the light-adapted frog eye. In thin sections the pigment granules are often found in close contact with the outer membranes and unit layers of the retinal rods.

DR. CARPENTER: Are you suggesting that the granules leave the pseudopodia?

DR. FERNÁNDEZ-MORÁN: That is difficult to answer. In some cases there seems to be no membrane around the granule, and then these "naked" pigment granules appear to make direct contact with the lamellar components of the external segments. These preliminary observations are now being followed up.

DR. ROBERTSON [London, England]: Mr. Moody and I have found that a unit membrane does cover the surface of pigment granules in octopus' retina.

DR. MCCONNELL [Ohio State University, Columbus, Ohio]: Our studies are not in agreement with the observations of Dr. Fernández-Morán, that the pigment accumulates around the external segments in the dark. Sometimes this is true and sometimes not, depending on the pH, blood, ammonium ions, etc. Pigment granules creep between the rod segments when the frog's eye is stimulated by light after several hours dark adaptation. This movement requires 10–30 seconds, at a minimum.

DR. FERNÁNDEZ-MORÁN: The dark-adapted frog's eyes, mostly of the bull frog, which I referred to, had been kept in the dark for 12 hours and were then frozen *in situ* while dark-adapted. Although the sudden freezing could introduce certain artifacts, we find that this fixation *in situ* yields excellent preservation of the pigment epithelium–retinal receptor relationships.

DR. WALD [Harvard University, Cambridge, Mass.]: Please, could we not confuse the audience any further? It is my conviction that the pigment granules move in between the outer segments of the visual receptors in light adaptation, and move away from them in dark adaptation. If my ears did not deceive me, that is the opposite of what Dr. Fernández-Morán told us, but I believe it to be true.

DR. FERNÁNDEZ-MORÁN: While there are certainly differences, depending on various factors as already pointed out by Dr. McConnell, we find that the pigment granules are associated mainly with the tips of the rod outer segments in dark-adapted frog retinas. This close structural relationship of the pigment granules with the adjoining rod tips does not necessarily conflict with the established data on pigment localization in dark- and light-adapted retinas. It would essentially imply that close contact is still preserved with the outer parts of the receptors when the pigment granules move away from the spaces in between the external segments of the visual receptors during dark adaptation. I trust, therefore, that the higher resolving power of the electron microscope when applied together with improved preparation techniques will contribute to clarify and elucidate rather than to confuse the basic issues in this important *functional relationship*.

CHAIRMAN PORTER: Of course other factors besides light can cause pigment granule migration.

MR. FRANK MOYER [Johns Hopkins University, Baltimore, Md.]: Did Dr. Yamada observe any difference in the myeloid bodies in light- and dark-adapted retinas?

DR. YAMADA: I have not found any difference.

The Effect of Vitamin A Deficiency on the Fine Structure of the Retina[1]

JOHN E. DOWLING[2] AND I. R. GIBBONS

Biological Laboratories, Harvard University, Cambridge, Massachusetts

Introduction

FOR MANY YEARS it has been known that severe vitamin A deficiency causes histological degeneration in the retina (Tansley, 1933; Johnson, 1939), and it has been suggested that this structural damage might be responsible for the long lasting or permanent effects of night blindness that persist after the deficiency has been relieved (Johnson, 1943; Wald, 1955). However, experiments to examine this point have been limited by the fact that vitamin A has a function in general body metabolism in addition to its specific function in the retina. When animals are maintained on a diet completely free of vitamin A, they lose weight and die soon after the onset of retinal degeneration (Johnson, 1943; Dowling and Wald, 1958).

Recently, we have found that vitamin A acid, when fed to rats on a vitamin A-free diet, keeps them healthy and growing normally, but does not support the visual cycle (Dowling and Wald, 1960). Thus, rats maintained on a vitamin A-free diet, supplemented with vitamin A acid grow normally, but gradually become extremely night-blind.

The result of one such experiment is shown in Fig. 1. After exhaustion of its stored vitamin A, the rat given no supplement lost weight rapidly and died. The rat receiving vitamin A acid grew normally and appeared healthy throughout the experiment. Electroretinograms of this animal after 5 months are shown at the right of the figure compared with those of a normal rat. The deficient rat is highly night-blind; his visual threshold is 3.25 log units (about 1600 times) above normal. Independent measurements have shown that this rise of threshold corresponds to the loss of 96 to 98% of the rhodopsin content of the eye.

In such animals, therefore, we can study the effects of a dietary night blindness uncomplicated by other somatic symptoms.

In this paper we shall describe the effects of this deficiency and its

[1] This investigation has been supported by grants from the National Science Foundation and United States Public Health Service.

[2] Part of this work was done while J. E. D. held a Post-Sophomore Fellowship of the Public Health Service, on leave from Harvard Medical School (1959-1960).

relief on the structure of the retina. Detailed correlation of these histological changes with the simultaneous changes in biochemical composition and physiological activity has been made elsewhere (Dowling and Wald, 1960), and will be mentioned only briefly here.

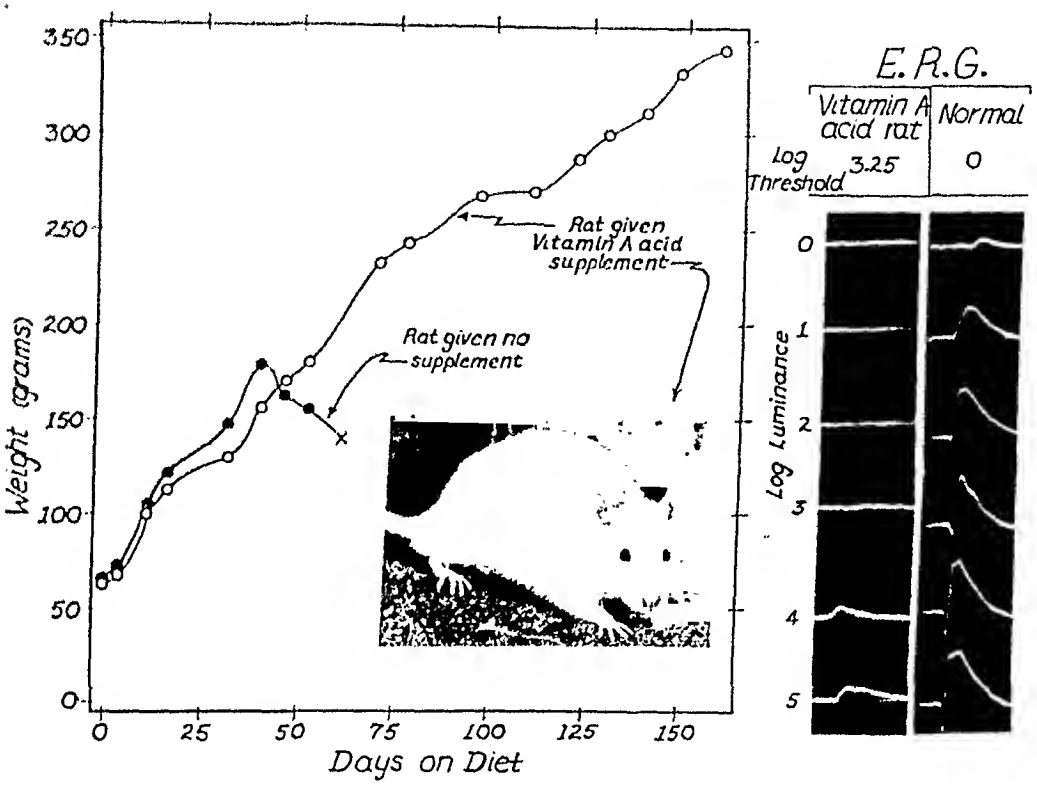

FIG. 1. Biological activity of vitamin A acid.

Litter mates were placed on vitamin A-deficient diet. The animal receiving no supplement grew until vitamin A stores were exhausted, then lost weight rapidly, and died on the 57th day of the experiment. The animal given vitamin A acid grew throughout the experiment (5 months) and remained in good condition. The picture of this animal was taken at the end of the experiment, as were the electroretinograms shown at the right, compared with those of a normal animal. They show that this rat is highly night-blind: it has a visual threshold 3.25 $\log_{10}$ units above normal, corresponding to loss of 96 to 98% of the rhodopsin from the eye (from Dowling and Wald, 1960).

Experimental

REARING OF THE RATS

Groups of albino, weanling rats were raised on Standard U.S.P. vitamin A-test diets supplemented orally with 50 μg/day of vitamin A acid, dissolved in vegetable oil. As controls, litter mates were raised

similarly on vitamin A-free diets, supplemented with vitamin A alcohol. The animals were sacrificed at times ranging from 2 to 10 months after having been placed on the diet.

In certain cases, deficient rats were fed large doses of vitamin A to permit us to examine the course of recovery from the deficiency.

Preparation for Light and Electron Microscopy

Without regard to conditions of light or dark adaptation, animals were anesthetized with Nembutal and the eyes enucleated. The cornea and the lens were removed and the whole back of the eye fixed for 1 hr in a 2% solution of osmium tetroxide, buffered to pH 7.8 with Veronal acetate, and containing 45 mg per milliliter sucrose and 0.002 *M* calcium chloride. The specimens were dehydrated in graded acetone-water mixture and embedded in Araldite epoxy resin (Glauert and Glauert, 1958). The whole back of the eye was embedded in an attempt to retain the normal relationship of the retina to the pigment epithelium. However, some separation usually did occur, and only in occasional areas was the normal approximation preserved.

Thin sections were cut with a Porter-Blum microtome and stained with saturated uranyl acetate in 50% ethanol. They were examined in an RCA EMU-3D electron microscope operated at 100 kv.

For light microscopy, thick (2–4 μ) sections were cut from the same specimens with the same microtome. The sections were mounted on slides with Mayer's albumen, and stained for 6 to 24 hr with 2% Giemsa blood stain. They were then washed briefly with ethanol, allowed to dry in the air and mounted in paraffin oil.

Observations

Retinal Degeneration

The changes observable with the light microscope during the course of degeneration are shown in *Fig. 2*. The retina of a control animal that had been kept 10 months on a vitamin A-free diet supplemented with vitamin A appears entirely normal (*Fig. 2a*).

In rats on the diet supplemented with vitamin A acid, the first signs of degeneration are noted after about 2 months, when the outer segments of the visual cells begin to stain less intensely than the normal and present a somewhat fragile and broken appearance (*Fig. 2b*). The inner segments and the nuclei appear normal, along with the other retinal tissues.

After 6 months on the diet (*Fig. 2c*), the visual cell layer has the

show no tendency to separate in the course of the preparation. (Unlike normal or slightly deficient eyes, in which some separation almost always occurs.)

Before considering the changes in fine structure that occur during degeneration, we must first mention certain features of the normal retina. Figure 3 shows a longitudinal section through part of a rod outer segment from the control retina shown in Fig. 2a. As in other animals (Sjöstrand, 1953), the outer segment consists of a stack of flattened transverse disks enclosed by the cell membrane. Each disk is itself composed of an outer membrane enveloping a less densely stained internal space.

Figure 4, a cross section cut near the proximal end of an outer segment, shows that the disks are approximately circular in face view, with a single incision. The incisions of adjacent disks are all stacked in line, so that together they form a small channel running up the interior of the outer segment. Rather numerous, short tubules extend from the body of the disks into this interior channel (Fig. 4). When these tubules are cut in cross section, as frequently occurs in longitudinal sections of the outer segment, they appear as small circles, of about the same diameter as the thickness of a disk (Fig. 3).

In the course of vitamin A deficiency, this highly ordered structure of the outer segment gradually breaks down. The degeneration begins with a marked swelling of the transverse disks, which pinch off to form large vesicles and tubules (Fig. 5). At this early stage, one frequently finds small stacks of apparently normal disks separated by others that are swollen and have broken into vesicles.

After a high proportion of the disks has degenerated in this way, the outer segment begins to lose its normal elongated, cylindrical shape, and may end by rounding up to become almost spherical. Figure 6 shows the fine structure of one such sphere. It cannot be confused with the cross section of a normal outer segment, since the latter is only about 1.5 μ in diameter, whereas such spherical remnants of rods are 3 to 5 μ across. Most of the interior is filled with distended vesicles and tubules, and only a very few intact disks remain. It is not clear to what extent

---

FIG. 6. A late stage in the degeneration of an outer segment. The structure is almost entirely filled with distended tubules and vesicles. With few intact disks remaining, the outer segment has assumed the characteristic spherical shape of a highly degenerate rod. Magnification: × 12,500.

FIG. 7. An apparently normal inner segment alongside a deteriorated, spherical outer segment, from an animal that had been on the diet for about 6 months. The mitochondria, cytoplasmic membranes, and cytoplasmic granules all look normal. Magnification: × 12,500.


1 μ
6
1 μ
7

such highly distorted outer segments retain contact with the inner segments. We have frequently observed them lying loose in the space between the retina and pigment epithelium, but this may have been an artifact of preparation.

The change in shape of the inner segments and their gradual reduction in number have already been mentioned. Their fine structure, however, appears to remain quite normal. The mitochondria, the cytoplasmic granules, and the cytoplasmic membranes seem unaffected by the drastic changes going on in the outer segments (Fig. 7). We have sometimes seen inner segments and degenerating outer segments in direct continuity with each other, without the ciliary constriction that normally intervenes. This would seem to imply the degeneration of the connecting cilium. However, in other cases, such as Fig. 7, the cilium is still present.

As the deficiency progresses, the terminal processes of Müller's fibers become highly conspicuous in the spaces left between the remaining inner segments (Fig. 9). In the normal retina these terminal processes are long cylindrical structures, about 0.1 μ in diameter, which envelop the proximal portion of the inner segment, forming what has been called the "fiber basket" (Polyak, 1941). In electron micrographs they are difficult to trace beyond the outer limiting membrane, but it is known from light microscopy that they are derived from glial cells deep in the retina (Polyak, 1941).

In the most highly deficient animals we have examined, after 10 months on the diet, almost all the visual cells have disappeared. Figure 8 shows a low magnification electron micrograph of part of the retina from such an animal. The visual cell nuclei are reduced to one irregular row. Those that remain, however, still appear normal. Only small fragments of inner and outer segments are visible, pressed against the processes of the pigment epithelium. On the right in the figure is a gap in

---

FIG. 8. A general view of the retina, pigment epithelium (PE), and choroid (Ch), of an animal maintained on deficient diet, supplemented with vitamin A acid for 10 months. Scattered fragments of inner and outer segments are tightly pressed against the processes of the pigment epithelium. Only one irregular row of visual cell nuclei (RCN) remains. At the right of the micrograph is a gap in this row of nuclei, where the rod-bipolar synapse layer (SYN) extends to the pigment epithelium. Even at this stage, the remaining synapses and visual cell nuclei appear as they usually do, although both are drastically reduced in number. At the lower left is part of a bipolar cell nucleus (BCN). Magnification: × 3000.

FIG. 9. An electron micrograph showing the base of the inner segments and a region of the external limiting membrane, in a 6-month deficient rat. Many of the visual cells have disappeared, leaving gaps between the remaining inner segments. The figure shows one such gap in which the terminal processes of Müller's fibers are highly conspicuous. Magnification: × 11,000.


Ch
PE
RCN
SYN
RCN
15μ
8
Ch
1μ
9

the row of rod nuclei. Here the rod-bipolar synapses (outer plexiform layer) are in direct contact with the pigment epithelium. This synaptic layer looks as it usually does but is much reduced in thickness—presumably through the loss of afferents from the visual cells.

Retinal Recovery

If the degeneration of the visual cells has not progressed too far, structural and physiological recovery can be induced by giving vitamin A to the deficient animals.

We have found that animals maintained on the deficient diet for about 6 months are the most suitable for observing regeneration. At this stage, there are very few intact outer segments left, and the number of visual cells has been reduced to about one-half.

In a typical experiment, three litter mates were raised on a vitamin A-free diet for 6½ months. The control animal was fed vitamin A throughout the experiment, while the other two animals were fed vitamin A acid. The recovery animal was fed a large dose of vitamin A (500 μg) and then periodically fed further vitamin A for 16 days.

Sections of the retinas from these animals are shown in Fig. 10. The control (Fig. 10a) has a normal retina. The deficient animal (Fig. 10b)

Fig. 10. Recovery from deficiency. Three litter mates were raised on vitamin A-free diets for 6½ months; one was supplemented with vitamin A, the other two with vitamin A acid. Sixteen days prior to the end of the experiment, the recovery animal was fed a large dose of vitamin A.

Fig. 10a. The retina from control animal maintained on vitamin A throughout the experiment.

Fig. 10b. The retina from the deficient animal. Almost all of the outer segments have disappeared along with about half of the visual cell nuclei and inner segments. The inner segments that remain are shorter and wider than normal.

Fig. 10c. The retina from the recovery animal. New outer segments, normal in length and width, have regenerated. There has been no increase in number of visual cell nuclei or inner segments, and the inner segments have remained squat. The number of regenerated outer segments, therefore, is only about half the normal number.

Fig. 11. An early stage in the regeneration of an outer segment. A cilium, extending from the inner segment at the bottom of the figure, has expanded at the distal end; a few vesicles are present in the structure; and the ciliary fibers extend much of its length. At the far distal end, are small membranous saccules, oriented longitudinally with respect to the rest of the cilium. Magnification: × 11,500.

Fig. 12. A later stage of outer segment regeneration. Many more membranous saccules are present. The saccules are mostly oriented longitudinally but, at the proximal end, appear to be assuming the normal transverse arrangement. Magnification: × 11,500.

shows typical changes as described previously. The animal fed vitamin A (Fig. 10c), however, has regenerated new outer segments that appear normal. There has been no increase in the number of visual cells, so that

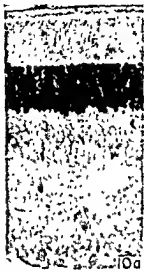

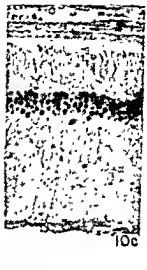

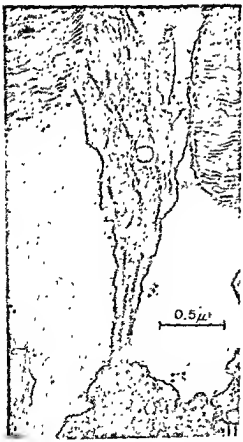

only about one-half the normal number of inner and outer segments are present. The inner segments have remained short.

In order to discover the detailed process by which the outer segments regenerate, we have examined the fine structure of retinas from recovering animals, 3 to 16 days after beginning to feed vitamin A.

After 3 days of recovery, one finds elongated cilia protruding from occasional inner segments. The ends of these cilia are enlarged, and contain many vesicles. At a later stage, the distal end of the cilium has broadened further, and contains a number of small membranous saccules at the distal end (Fig. 11). Later, the number of saccules has greatly increased, and they have begun to assume the form of transverse disks (Fig. 12). After 16 days of recovery, the outer segments appear essentially normal, and no further regeneration is apparent. The fully regenerated outer segments have the same dimensions as the normal (about 1.5 μ diameter and 15 μ long).

It is difficult to deduce the dynamic sequence of events from static micrographs, and our observations on regenerating visual cells are not sufficiently numerous for a detailed hypothesis concerning the mechanism of the process. We can, however, point out the resemblance between our micrographs of regenerating outer segments and the published micrographs of other workers who have studied the normal embryological development of the visual cells (De Robertis, 1956; Tokuyasu and Yamada, 1959). The process by which the outer segments regenerate after vitamin A deficiency is very similar to their normal morphogenesis.

Pigment Epithelium

It has been known for many years that a very close relationship exists between the outer segments of the visual cells and the pigment epithelium, and that the retina is incapable of functioning without this association. Wald (1958) has recently discussed this subject.

Many features of the fine structure of the pigment epithelium have been described by previous workers (Porter, 1957; Yamada *et al.*, 1958). We have extended these observations, and our detailed findings will be reported later. For the present we will mention only one feature that is directly related to our present subject. This concerns the disappearance of the myeloid bodies in vitamin A deficiency.

The myeloid bodies occur frequently in the pigment epithelium cells of normal rats. Their over-all shape varies, but they have a uniform fine structure consisting of a number of flattened, more or less parallel saccules, which resemble the disks of the rod outer segment. Each myeloid body is bounded by a single densely staining membrane. No instances of continuity have been observed between the internal saccules

and the general system of membranes in the cytoplasm, as described for the myeloid bodies of the frog pigment epithelium (Porter, 1957).

In the pigment epithelium of vitamin A-deficient rats, we have found no typical myeloid bodies. How they disappear is not yet known. When the deficiency is relieved, the myeloid bodies quickly reappear, becoming conspicuous within 3 days after beginning to feed vitamin A.

Discussion

Detailed measurements (Dowling and Wald, 1958, 1960) on the biochemical composition of the outer segments have shown that the level of rhodopsin (vitamin A aldehyde-opsin complex) begins to fall early in vitamin A deficiency, declining to 5 to 10% of normal after 2 months. The visual protein, opsin, declines more slowly, about 50% remaining after 2 months. No histological changes occur during the early phase of deficiency, when the level of rhodopsin is falling. This was to be expected, for the level of rhodopsin decreases also in normal light adaptation. The anatomical degeneration of the rod outer segments appears, rather, to parallel the loss of the visual protein, opsin, that occurs later in deficiency. Opsin is a major component of the outer segments [e.g., 14% of the dry weight in cattle, and 40% of the dry weight in frogs (Wald, 1955)], so that its loss may well be directly responsible for the breakdown of structure.

It is less clear why whole visual cells should die following the loss of their outer segments. The cells begin to disappear only late in the deficiency, when the outer segments have almost gone. It may be that the cells die as the result of lack of stimulation. However, the possibility that vitamin A may be necessary for a further specific role in the life of the visual cell must also be considered.

It has been suggested that certain types of primary retinal degeneration, as in *retinitis pigmentosa*, might be the result of a highly localized vitamin A deficiency (Cogan, 1950), caused perhaps by a metabolic defect involving one of the enzymes of the visual cycle. This hypothesis has been criticized on the grounds that the effects of vitamin A deficiency occur throughout the animal, and that no one has shown that deprivation of vitamin A can cause specific degeneration of visual cells (Noell, 1953). The present results show that lack of vitamin A alone does cause the death of visual cells, and that animals maintained on the vitamin A-deficient diet supplemented with vitamin A acid come to mimic closely the condition observed in *retinitis pigmentosa*.

Both the inner and outer segments characteristically change their shapes during the course of vitamin A deficiency and recovery. The inner

segments, normally forced to maintain an elongated, cylindrical form by the pressure of the surrounding inner segments, assume a more globular form, without any change in fine structure, when the number of surrounding inner segments decreases. Relief of the deficiency does not increase the number of the inner segments, and they remain squat and rounded. The outer segments, on the other hand, lose their normal shape during deficiency because of the breakdown of their internal structure. This internal structure is reformed after giving vitamin A, and the segment then regains its normal shape and size.

The disappearance of the myeloid bodies during vitamin A deficiency and their reappearance in recovery demonstrates that these structures, like the outer segments, are dependent on vitamin A for their maintenance and formation. This, and their morphological resemblance to part of a rod outer segment, suggests a functional activity in the life of the pigment epithelium cell.

Summary

Rats raised on a vitamin A-free diet and supplemented with vitamin A acid appear normal and grow well, but develop a high degree of night blindness. With time, the visual cells display anatomical changes and eventually disappear. The initial anatomical disturbance seems limited to the outer segments, and consists of a swelling and segmenting of the disks to form large vesicles and tubules. Eventually these remnants of outer segments disappear completely. At a late stage of deficiency, the inner segments and visual cell nuclei decrease in number; no obvious changes in fine structure have been observed prior to their loss.

Provided that deficiency has not been allowed to progress too far, outer segments of the visual cells can be regenerated by feeding vitamin A to the deficient animals. The development of the regenerating outer segments is very similar to their normal morphogenesis. However, once a visual cell has been completely lost, it is not replaced.

Acknowledgment

We should like to thank Professor George Wald for many helpful discussions concerning this study.

References

Cogan, D. G. (1950). *Trans. Am. Acad. Ophthalmol. and Otolaryngol.* July-August, p. 629.

De Robertis, E. (1956). *J. Biophys. Biochem. Cytol.* **2**, 319.

Dowling, J. E., and Wald, G. (1958). *Proc. Natl. Acad. Sci. U.S.* **44**, 648.

Dowling, J. E., and Wald, G. (1960). *Proc. Natl. Acad. Sci. U.S.* **46**, 587.

Glauert, A. M., and Glauert, R. H. (1958). *J. Biophys. Biochem. Cytol.* **4**, 191.

General Discussion of Retinal Structure in Relation to the Visual Process

GEORGE WALD

Biological Laboratories of Harvard University, Cambridge, Massachusetts

When Dr. Smelser asked me to discuss this afternoon's papers, I had only a vague idea of what was going to happen specifically, but a rather good idea of what might happen generally, and so got ready for it by bringing along a few figures. These are not an attempt to give another paper, but merely to remind me of the things I should like to discuss, that came up in the course of the afternoon.

This is the first time I have had the heady experience of taking part even to this extent in a meeting of anatomists. But this is the new anatomy, jumping off as always from gross and microanatomy, but then entering the world of dimensions opened by the electron microscope, dimensions shared with the larger organic molecules, and hence chemistry, and revealing at times changes in structure which themselves constitute physiological function. Furthermore, the lamellae that Sjöstrand first demonstrated to constitute the basic structure of the outer segments of the rods and cones are a manifestation of crystallinity, involving such a regular orientation of molecules as characterizes the solid state; so that the considerations that begin in anatomy now range through chemistry and physiology to the quantum mechanics of the solid state. I should like in these few minutes to remark upon some of these problems.

Let me begin at the level of simple microanatomy. In the course of his lecture, Dr. Pearse remarked that the pigment epithelium has been a neglected tissue in the eye. It has indeed been all too much neglected, and one of the things that I particularly enjoyed today is the amount of attention it has received from several of the speakers, and of course most notably from Dr. Yamada.

The pigment epithelium contains many of the secrets, I think, of visual organization and function. Listening today to Dr. Fernández-Morán, I was reminded that he was our host at an extraordinary meeting on nerve structure and function, held in March, 1957, at what was then his research institute on a mountain top overlooking Caracas. At that meeting I listened with great interest as a group of nerve physiologists and anatomists discussed another neglected tissue, the so-called sheath of Schwann or neurolemma. They seemed rather suddenly to have awakened to the realization that this neglected tissue, which plays a

central role in forming the myelin sheath and in nerve regeneration, may well have much to do also with generating the nerve impulse.

I realized then that much that was said reminded me of the pigment epithelium in the eye; and I should like to suggest here, as I did then, that the pigment epithelium may represent the sheath of Schwann of

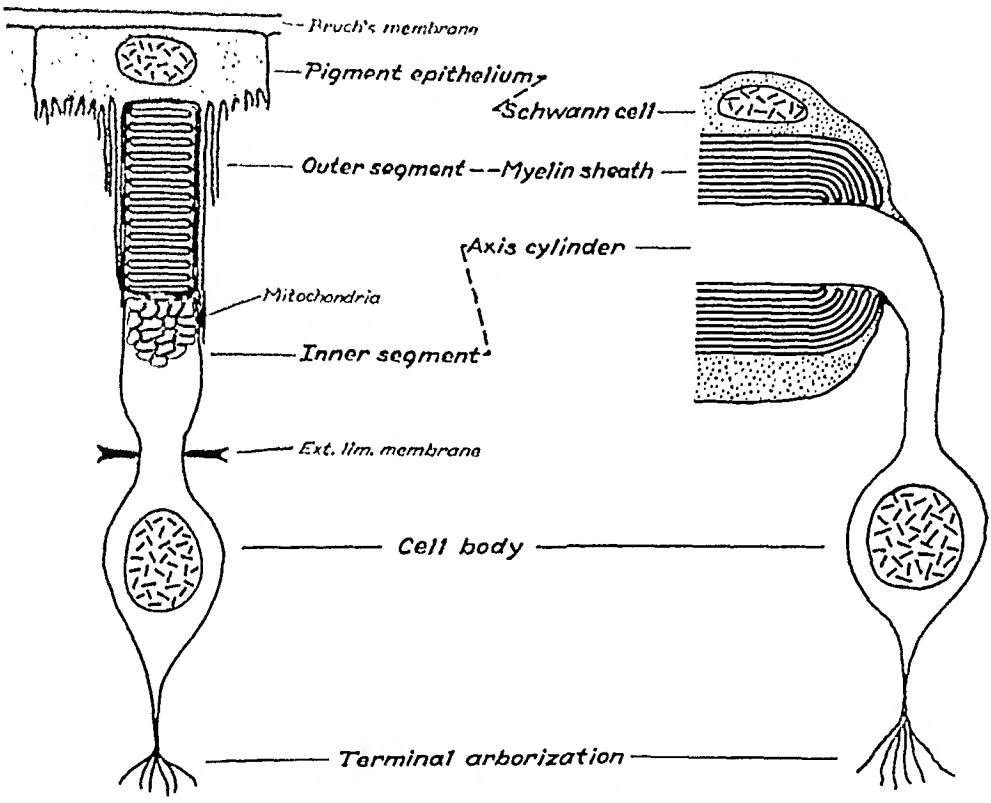

FIG. 1. Structural relations between a retinal rod and a peripheral nerve cell. The pigment epithelium of the retina, with its long protoplasmic processes in which the outer segments of the visual receptors are embedded, bears much the same intimate relation to the outer segment of a rod, as does the Schwann cell to a nerve axon. Both tissues are neuroglial. The outer segment is comparable in structure with the myelin sheath, both being composed of double layers. The inner segment of the rod is comparable with the axis cylinder of nerve. Both cells possess comparable cell bodies with nuclei; and both end in arborizations which make synaptic contact with other nerve cells. From Wald (1958).

the retina, and that its very intimate relationship with the outer segments of the visual cells may be somewhat comparable to the intimate relationship of the Schwann cells with nerve axons (Wald, 1958).

The diagram of Fig. 1 is intended to suggest this parallelism. It has already been remarked in this meeting that in the pigment epithelium we have what looks like a highly metabolic tissue. I like to think of it

I should like in this connection to add a word to John Dowling's paper. In rats on a vitamin A-deficient diet supplemented with vitamin A acid, though after several months the cells of the pigment epithelium look as good as ever, their myeloid bodies which Dr. Yamada described have vanished. If one feeds such an animal vitamin A, within a couple of weeks—the same length of time it takes to reconstruct the outer segments of the rods—the myeloid bodies also return. That is, in the first 4 to 6 months of such a vitamin A acid regime, only two structures disintegrate in what appears to be an otherwise intact animal: the outer segments of the visual cells, and the myeloid bodies of the pigment epithelium, and on readministration of vitamin A, both these structures repair together.

I should like to say another thing that impresses me, though I am not an anatomist, so please forgive it. The pigment epithelium and the layer of visual cells originated identically as adjoining areas of ependyma, lining the inner surface of the primary optic vesicle. In further development, the pigment epithelial cells remained relatively simple, while the layer of visual cells differentiated in the extraordinary way that we have been discussing all afternoon. Mr. Dowling showed us, however, that in animals kept for 10 months on a vitamin A-deficient diet supplemented with vitamin A acid, the entire layer of visual cells is finally reduced to a single row of nuclei, no longer surrounded with any special structures, so that it looks like a simple, cuboidal epithelium. At this point it faces another such simple epithelium, the pigment epithelium. These two tissues, which had the same embryonic origin, have come, as the result of this nutritional regime, to resemble each other again to a remarkable degree.

A retina in this state resembles closely the condition found in certain cases of primary optic degeneration associated with genetic mutations in rats and mice [e.g., the C3H mutant in mice (cf. Noell, 1958)] and

with the human disease *retinitis pigmentosa* (cf. Cogan, 1950). It might be thought that these latter conditions may for this reason also involve some localized disorder of vitamin A metabolism. It takes two components, however, to make a visual pigment: vitamin A, but also a specific type of retinal protein, an opsin. We think that the restricted type of retinal degeneration seen in animals on a vitamin A-deficient diet supplemented with vitamin A acid results secondarily from the instability and eventual disintegration of opsin in the absence of the vitamin A aldehyde with which it ordinarily combines (Dowling and Wald, 1960). The genetic mutants referred to, however, and perhaps also *retinitis pigmentosa*, may achieve the same effect directly through interference with the synthesis of opsin, without involving any disturbance in the metabolism of vitamin A. This seems the more reasonable view; for our present idea of gene action is that it is concerned directly with determining protein structure ("one gene, one protein"); and in the diseases mentioned, this protein is probably opsin.

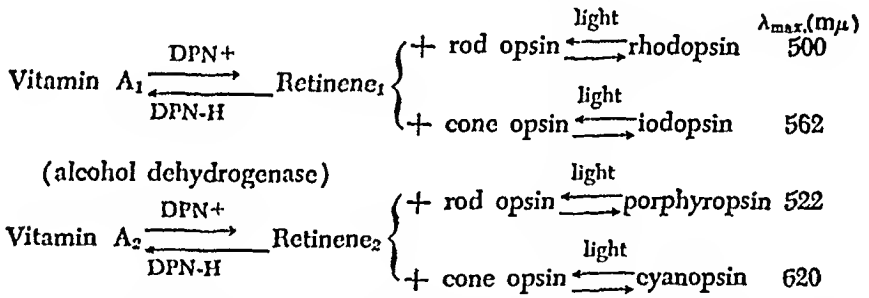

FIG. 2. Diagram of the over-all reactions in the four principal visual systems of vertebrates. At the right are given the most usual positions of the absorption maxima (λ_{max}) of the visual pigments. From Wald (1958).

As you see, the retinal anatomy has come to be closely bound up with its chemistry. Figure 2 is a diagram that shows the over-all chemical equations of the principal visual systems of the vertebrate eye. The visual pigments found in the outer segments of the rods and cones all are formed by the combination of vitamin A aldehyde, or retinene, with a specific type of protein called an opsin. We have two types of vitamin A—A_1 and A_2—and the corresponding aldehydes, the retinenes 1 and 2. We have also two great families of opsins, one found in rods, and the other in cones. The four combinations formed from these substances are the four principal pigments of vertebrate vision (Wald, 1956, 1958, 1960).

That is, vitamin A_1 is oxidized to retinene$_1$ by the enzyme alcohol dehydrogenase and DPN (diphosphopyridine nucleotide). Retinene$_1$ can combine with rod opsin to yield rhodopsin, or with cone opsin to yield

iodopsin. Similarly, vitamin A_2 is oxidized to retinene$_2$ by the same enzyme system; and this can combine with rod opsin to yield porphyropsin, or with cone opsin to yield cyanopsin.

Ruth Hubbard showed some years ago that the apparent molecular weight of cattle rhodopsin is about 40,000 (Hubbard, 1953–1954). A considerable fraction of this has since been shown to be lipid, and perhaps could be removed in large part without destroying the pigment (Krinsky, 1958); so that a number somewhere between 30,000 and 40,000 for the molecular weight seems at present to be about right. Several other rhodopsins that we have examined seem to have similar molecular weights.

If this molecule were spherical or roughly cuboidal, its diameter would be 30–40 A units. This is perhaps a significant number, because the membranes that form the lamellae of the outer segments of rods and cones are of that order of thickness (Sjöstrand, 1953, 1958). We think that the membranes are largely made of visual pigment; not entirely, for there does not seem to be enough pigment to make the membranes entirely. What we think is that the visual pigment is laid mosaically in the structure of the membranes, and constitutes a large portion of that structure (Wald, 1954).

Figure 3 introduces a special problem in anatomy, not indeed the relatively coarse anatomy revealed in the electron microscope, but the very much finer anatomy revealed by X-ray diffraction, the anatomy of vitamin A.

Vitamin A occurs in a variety of shapes, *cis-trans* or geometric isomers of one another. The most common and stable shape is the all-*trans* configuration shown at the top of Fig 3; but all the visual systems we know, whether rod or cone, made with vitamin A_1 or A_2, in vertebrate or invertebrate eyes, are made by joining the lowermost, hindered *cis* configuration of vitamin A or retinene—the 11-*cis* isomer called neo-b—to the opsins. When a visual pigment is bleached by light, however, the retinene that emerges is all-*trans*, and it has to be bent and twisted back into the 11-*cis* configuration before the visual pigment can be regenerated. That is, a cycle of *cis-trans* isomerization is an intrinsic part of every visual system we know.

This, I think, is still anatomy, though at its furthest reach. Why is the shape of vitamin A or retinene so important for forming a visual pigment? The recent work of Hubbard and Kropf (1958, 1959; Hubbard *et al.*, 1959) has shown that, quite the contrary of being merely an interesting complication in the operation of visual systems, this geometrical isomerization is in fact the heart of the process.

Let me state the situation as plainly as I can: *The only thing that*

light does in vision is to isomerize retinene. Figure 4 shows a simple diagram of what this means. The reason that the shape of retinene is so important in making a visual pigment is that the 11-*cis* isomer has the particular shape that *fits* a portion of the surface of opsin. It is only when this condition of close fit is achieved, that it is possible to form a stable visual pigment. The retinene is anchored to the protein through

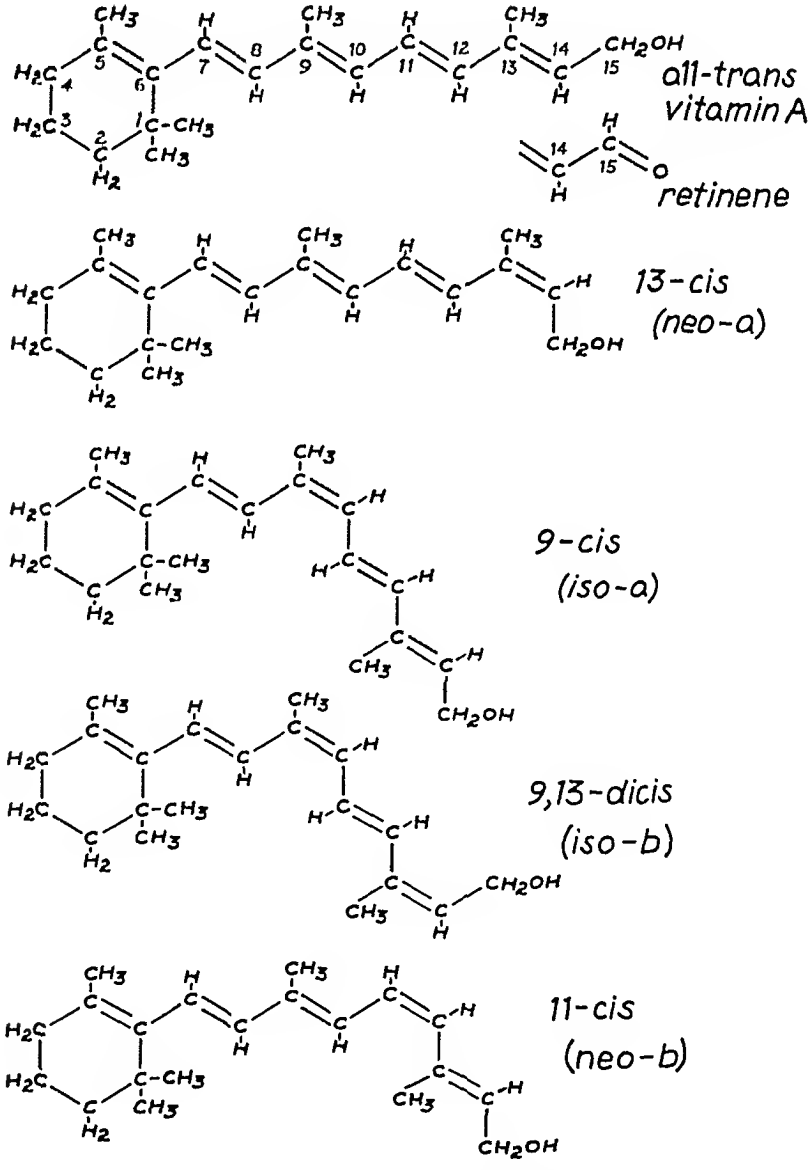

FIG. 3. Geometric isomers of vitamin A and retinene. The upper four structures represent the unhindered, and hence most probable configurations. The lowermost structure is the sterically hindered *cis* isomer from which all known visual pigments are formed.

a Schiff base linkage formed by condensing the aldehyde group of retinene with an amino group of opsin ($C_{19}H_{27}HC = O + H_2N\text{-}opsin \rightarrow C_{19}H_{27}HC = N\text{-}opsin$). Along with this, however, the hydrocarbon chain of retinene must achieve closeness of fit to form the pigment.

A quantum of light absorbed by such a visual pigment does nothing but isomerize the retinene to the *all-trans* configuration, i.e., it straightens out the side chain. All that follows represents ordinary thermal ("dark") reactions. Now the retinene no longer fits the protein, and under ordinary conditions hydrolyzes off. *This is the mechanism of bleaching.*

By going to low temperatures one can identify two intermediate stages in this process. The first effect of absorbing light, isomerizing the retinene to all-*trans*, yields a transitory *product called lumirhodopsin*, stable only below about —50°C. On warming this slightly, the configuration of the protein opsin opens up, exposing two new sulfhydryl (SH) groups not previously accessible to our reagents, and also one H^+-binding group with a pK of about 6.6. This product, which we call metarhodopsin, is stable only at temperatures below —20°C. *If this is* allowed to warm up, *in the presence of water*, the linkage that *binds* the retinene to the protein spontaneously hydrolyzes, liberating the retinene.

It is clear from the speed with which a visual excitation occurs that this must depend upon the conversion of the visual pigment to the lumi-pigment, or at most to the meta-pigment. It cannot wait upon the relatively slow hydrolysis of retinene from opsin.

I should like now to ask how this kind of process might lead *to a* nervous excitation? May I say at once that I cannot answer this question, I can at most talk about it. We do not yet know the mechanism of any biological excitation, and are in that regard as badly off in vision as elsewhere.

As it happens, in vision this problem involves a particularly rigorous condition, first made plain by my former teacher, Selig Hecht (Hecht *et al.*, 1941–1942). It lies in the fact that a dark-adapted rod—and *probably* also a dark-adapted cone—is stimulated by the absorption of a single quantum of light. A *single* quantum of light is absorbed by a single molecule of rhodopsin, and we must attempt to understand how so small an event *can have so large* an effect.

The fact itself can be demonstrated in a number of ways. In Table I it is demonstrated, so to speak, anatomically. Here I have computed from the known optics of the human eye the number of quanta per second that reach a retinal rod, and that are absorbed by rhodopsin in a dark-adapted rod, at various brightnesses of illumination.

It should be stated at once that the threshold of vision in the dark-adapted eye lies at about 10^{-6} millilamberts, some ten times below the

lowest brightness shown here. Even at 10^{-5} millilamberts, therefore, at about ten times the minimum visual threshold, a single rod absorbs a quantum of light on the average about once every 2 min. As the light grows brighter, rods receive quanta more often than this. By 10^{-2} millilamberts, however, cones have already begun to take over the principal function in vision; yet even at this brightness an individual rod absorbs on the average only about 7 quanta per second.

TABLE I

ABSORPTION OF LIGHT BY RHODOPSIN IN HUMAN RODS AT VARIOUS LUMINANCES

Field brightness (millilamberts)	Flux density at retina		Quanta/sec/rod	
	Lumens/sq mm	Quanta/sec sq mm	Incident	Absorbed
10^{-5}	7.0×10^{-12}	10^{4}	0.0254	0.0085
10^{-3}	6.4×10^{-10}	9.2×10^{5}	2.33	0.78
10^{-2}	5.8×10^{-9}	8.35×10^{6}	21.2	7.1
0.1	4.7×10^{-8}	6.8×10^{7}	173	58
1.0	3.3×10^{-7}	4.75×10^{8}	1210	403
10	1.9×10^{-6}	2.7×10^{9}	6860	2287
100	9.7×10^{-6}	1.4×10^{10}	35,500	11,833
1000	5.6×10^{-5}	8.1×10^{10}	206,000	68,667

NOTE: The first two columns show the flux density at the retina, corrected for the opening of the natural pupil, as computed by Blanchard (1918). Converted to quanta/sec on the basis that for scotopic vision at 507 mμ, 1 lumen = 5.72×10^{-4} watt = 1.37×10^{-4} cal/sec = 1.47×10^{15} quanta/sec. Cross-sectional area of human rod outer segment, 2.54×10^{-6} mm^2. The outer segment contains about 4×10^{7} molecules of rhodopsin, on the assumption that it absorbs about 30% of incident light of wave length 507 mμ (compare Rushton, 1956). The last column ("Absorbed") is computed as though there were no bleaching. To the extent that rhodopsin is bleached, the absorption is lowered.

I think one must conclude from such a computation that if the rods were not single quantum detectors, they would do little for us in vision. Throughout the entire range in which the rods mediate scotopic vision, they must respond to the absorption of single quanta of light, for within their reaction times this is all they are offered.

We have, therefore, in the outer segments of the rods and cones, structures so finely poised that a change in a single molecule of visual pigment can trigger them to respond. Only a finely contrived machine could behave in this way, and this is probably the significance of the elaborate ultrastructure that we have been discussing all afternoon. Certainly also this initial event must be greatly amplified, for without such amplification the transformation of a single molecule probably could do nothing.

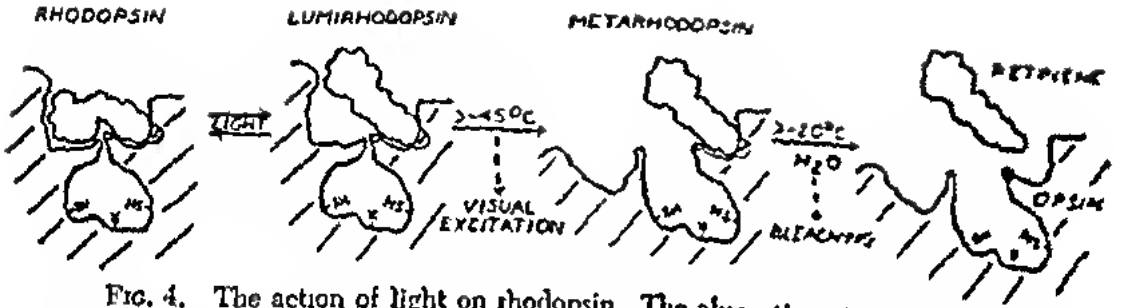

FIG. 4. The action of light on rhodopsin. The absorption of light by rhodopsin isomerizes its 11-*cis* chromophore to the all-*trans* configuration, yielding at first product the all-*trans* chromoprotein, lumirhodopsin. This labilizes the protein, opsin, which rearranges to a new configuration, yielding a second all-*trans* chromoprotein, metarhodopsin. This second process exposes reactive groups on opsin and may be responsible for triggering visual excitation. Vertebrate metarhodopsins are unstable and above —15° hydrolyze to opsin and all-*trans* retinene, the process that corresponds to bleaching. From Hubbard and Kropf (1959).

so far analyzed, in a zymogen the active catalytic center is covered over with an amino acid or a small peptide, so that it is unavailable for catalysis. In every case, activation involves the removal of the covering group by hydrolysis, so exposing the catalytic center.

We can toy with the idea that in such a visual pigment as rhodopsin, 11-*cis* retinene covers a potential catalytic center. The absorption of a quantum of light, by straightening out the retinene to the all-*trans* configuration, exposes this center, initiating the catalysis. If we only knew what reaction we should like to catalyze to produce a nervous excitation, we could proceed to test this suggestion. Unfortunately, we have no idea *what* we want such an enzyme to do, and hence no idea what to test.

This, however, is only one of several possibilities. A second possibility rests on the realization that the molecules of visual pigment form part of the lamellae of the rods and cones. The absorption of a quantum of light by *one such molecule* may produce a unimolecular hole in the lamellar membrane, permitting a leakage of ions that might result in a small change of potential across the outer segment, exciting the receptor.

The changes of visual threshold in light and darkness constitute the phenomena of light and dark adaptation. Dowling, whom you have heard from earlier this afternoon in other connections, has recently measured in groups of rats, by means of the electroretinogram, the depression of visual threshold that results from exposure to intense light, and the recovery of the visual threshold during a subsequent interval in the dark, i.e., dark adaptation. In the same and other groups of animals, he has extracted rhodopsin from the retinas at various intervals during dark adaptation, so that he can correlate the fall of visual threshold in dark adaptation with the rise in concentration of rhodopsin in the rods.

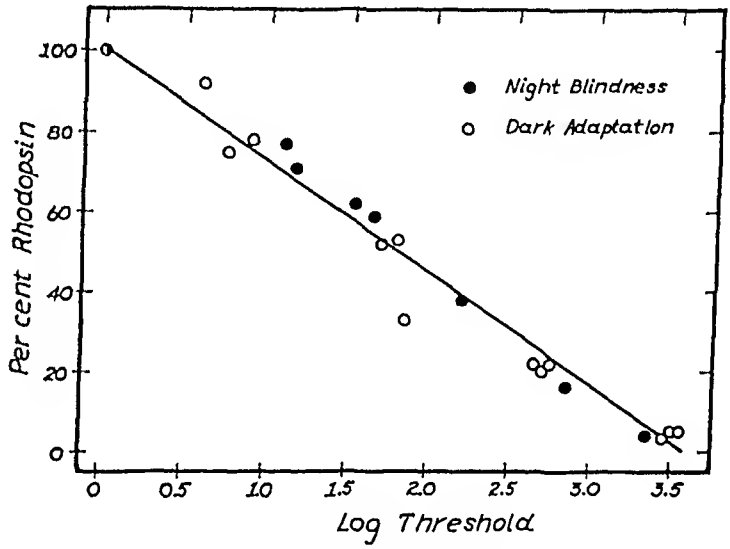

FIG. 5. The relation between the rhodopsin content of the rat retina and the logarithm of the visual (electroretinographic) threshold, in animals night-blind owing to vitamin A deficiency, and in normal animals during dark adaptation. The relationship is essentially identical in both cases, implying that the night blindness due to vitamin A deficiency in itself is accounted for completely by the loss of rhodopsin from the retina. From Dowling (1960a).

It has turned out that both these processes take 2 hr to complete in the rat, and that throughout the course of dark adaptation the logarithm of the visual threshold falls linearly as the rhodopsin concentration rises (Dowling, 1960a).

Figure 5 summarizes this relationship, and brings it together with another phenomenon, night blindness. One can make a rat night-blind in either of two ways: by exposure to bright light, which light-adapts it; and, as Dowling showed you earlier this afternoon, as the result of vitamin A deficiency. In both cases one can ask the question, what is the relationship between the concentration of rhodopsin in the retina

and the visual threshold? Figure 5 shows that in both cases one obtains the identical relationship, a linear rise in the logarithm of the threshold, with lowering of the rhodopsin concentration (or vice versa). The identity of this function in both cases is one evidence that the rise of visual threshold in night blindness owing to vitamin A deficiency, in itself is accounted for completely by the fall in rhodopsin concentration.

The processes of light and dark adaptation involve still another phenomenon, best demonstrated in another recent experiment by Dowling, and bringing us back directly to the anatomy of the retina (Dowling, 1960b). Figure 6 shows that the processes of light and dark

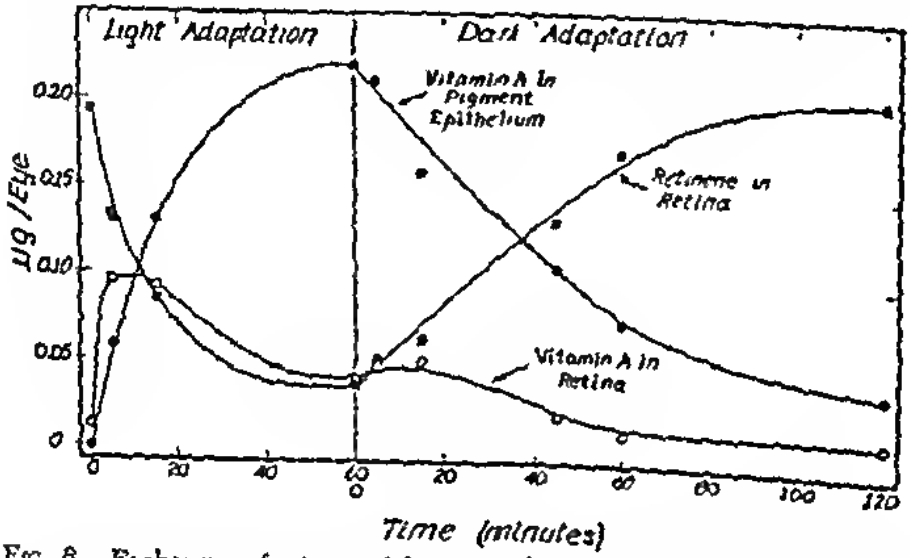

FIG. 6. Exchanges of vitamin A between the retina and the pigment epithelium during light and dark adaptation in the rat. The "retinene" in this figure represents retinene bound to opsin in the form of rhodopsin. At the beginning of light adaptation, as light bleaches rhodopsin, the retinene that is liberated is rapidly reduced to vitamin A. The concentration of vitamin A therefore rapidly rises, then falls again as the vitamin A leaves the retina to enter the pigment epithelium. During dark adaptation the retina recaptures vitamin A from the pigment epithelium by binding it in the form of rhodopsin. From Dowling (1960b).

adaptation involve exchanges of material between the outer segments of the rods and the pigment epithelium, though little if any vitamin A leaves the eye (cf also Hubbard and Colman, 1959). During light adaptation, as rhodopsin is bleached, the retinene which is liberated is rapidly reduced to vitamin A. As a result, the vitamin A concentration in the retina first rises rapidly, then falls again as most of this vitamin A migrates out of the outer segments of the rods, not into the inner segments, but into the pigment epithelium. Then during dark adaptation, the outer segments recapture vitamin A from the pigment epithelium by binding it again in the form of rhodopsin.

In the outer segment, as repeatedly emphasized today, we have a quasi-crystalline structure. Many of its molecules are highly oriented in what amounts to an approach to the solid state. No proteins can move in such a structure, and many other molecules that compose it are fixed in position. What this experiment shows, however, is that something does move in and out, and that is vitamin A. This constant interchange of vitamin A between the outer segments and the pigment epithelium constitutes part of their functional interrelationship.

Having wandered in this summary through various levels of anatomy, physiology, and chemistry, I should like to end with energetics, and the physics of the solid state as it applies to the outer segments.

During today's session we have seen again and again the lamellated ultrastructure of the outer segments of the rods. There is much in this structure that reminds one of the structure of another cellular organ, the chloroplast, which mediates the most important of all photobiological reactions, photosynthesis. Figure 7 shows one of Alan Hodge's electron micrographs showing a portion of a chloroplast in a mesophyll cell of corn, *Zea mays* (Hodge *et al.*, 1955). In this structure one sees certain dense, heavily pigmented regions, the so-called grana, which appear to contain the bulk of the chlorophyll, and are probably prineipally concerned with the light reaction in photosynthesis.

It is striking to see what a close relationship exists between the way the grana are spun out of the more widely spaced lamellae that form the stroma of the chloroplast, and Dr. Yamada's pictures of the way in which the myeloid bodies of the pigment epithelium condense out of the endoplasmic reticulum.

There is a widespread tendency to foist the properties of chloroplasts upon the outer segments of the rods and cones. We have, for example, already heard several thoughts expressed today about energy migration inside the rod. Let me just say a word about this problem. Every anat-

---

FIG. 7. Portion of a mesophyll chloroplast from a 3–4-week-old maize leaf, showing the lamellar structure of the grana (the denser regions, G_1–G_4) and of the stroma. The grana are derived from the fundamental lamellar structure of the stroma, involving among other things a doubling of the lamellation (see forking at 2). Where the plane of the section is accurately normal to the lamellar plane, the compound nature of the individual lamellae (1) is visible. The lamellar structure of the grana, however, can scarcely be distinguished when they are cut obliquely (G_3, G_4). A number of dense spherical bodies (*DSB*) are present in the stroma, and the limiting membrane of the chloroplast (*CM*) shows indistinctly at the lower left. cy, cytoplasm; st, starch grain. A striking similarity is evident between the grana and the stroma of the chloroplast and the relationship of the myeloid bodies with the endoplasmic reticulum of the pigment epithelium, as shown by Yamada elsewhere in this volume. From Hodge *et al.* (1955).

omist who shows a picture of a lamellated structure nowadays, provided there is a physicist in the room—and since we haven't heard, I guess that there is not one here—is promptly invited to begin to discuss phenomena of solid state physics, for lamellae of these dimensions are

themselves an expression of some degree of crystallinity. Such discussions tend to go at once to questions of semiconductivity, photoconductivity, and exciton transfer. Sometimes one is virtually told that though the anatomist may be the proper man to cut sections, it takes an expert in quantum mechanics to say what they mean.

It is probably true that a large amount of radiationless transfer of molecular excitation goes on in the grana of the chloroplasts. It may also be true that they exhibit photoconduction. There is a strong temptation to transfer either or both these phenomena into the outer segments of rods and cones.

What I should like to say is that there is no compelling reason to assume such a position. These are interesting phenomena to speculate about, but we have as yet no evidence that they occur in rods and cones, and there is, I believe, no necessity that such evidence will ever be provided.

The point is that vision and photosynthesis are intrinsically very different kinds of process. The job of photosynthesis is to convert the energy of light into chemical work; and the more efficiently it accomplishes that conversion, the more it does for plants, and eventually for animals.

There is no evidence whatever that light does work in vision. What we want of light in vision is a molecular excitation, the excitation of a visual pigment from its ground electronic state to its first electronically excited state. Even the isomerization of retinene that results from this excitation does not *use* the energy of the absorbed quantum. The isomerization from the 11-*cis* to the all-*trans* configuration is an energy-*yielding* process, the all-*trans* configuration representing the lower energy state. The subsequent transformation of lumi- to metarhodopsin, and the hydrolytic cleavage of retinene from opsin are all spontaneous—i.e., energy-yielding—processes. Also the combination of 11-*cis* retinene with opsin to make a visual pigment is a spontaneous reaction that goes to completion at room temperature, and hence also is energy yielding. Indeed, the only energy-demanding process we know in the whole cycle of visual reactions is the re-isomerization of all-*trans* to 11-*cis* retinene; and we now know that that has ways of proceeding in the dark.

It is wrong, therefore, to use uncritically such a phrase as "light does work in vision." So far as we know, it does not do work; it merely produces a molecular excitation. To put it colloquially, in vision light has only a triggering function. The work done is in *loading* the excitable structures, by ordinary thermal (i.e., "dark") reactions.

The only direct attempt I know of to find radiationless intermolecular energy transfer in the lamellar structure of the rod outer segments

is in the recent experiments of William Hagins, at the National Institutes of Health at Bethesda (Hagins and Jennings, 1960). He approached this problem in a number of ingenious ways, but concluded that he had not found the phenomenon.

I should like to say a final thing. We do not know the mechanism of nervous excitation in the rods and cones, any more than in other excitable structures. There is, however, the naive notion that if the molecular excitation produced by the absorption of light in the body of the outer segment could somehow be transmitted from molecule to molecule until it reached some molecule on the border of separation between the outer and inner segment, that would solve the problem of nervous excitation. Let me say for myself that I have no more idea what to do with an excited molecule at the boundary between the outer and inner segment than in the body of the outer segment. The concept of intermolecular energy migration can do very little for us at present. What we need to understand is how that energy is used; and its migration without a clear concept of what we need to do with it, leaves us in as great a quandary as ever.

References

Blanchard, J (1918) *Phys. Rev* [2] **11**, 81.

Cogan, D. G. (1950) *Trans Am. Acad. Ophthalmol Otolaryngol.*, July–Aug., 629.

Dowling, J E. (1960a) *Nature* In press.

Dowling, J. E. (1960b) *Nature* In press

Dowling, J. E., and Wald, G *(1960).* *Proc. Natl Acad Sci U. S.* **46**, 587.

Hagins, W. A., and Jennings, W. H. (1959). *Discussions Faraday Soc. No.* **27**, 180

Hecht, S, Shlaer, S, and Pirenne, M. H (1941-1942). *J. Gen. Physiol.* **25**, 819.

Hodge, A J, McLean, J D, and Mercer, F. V. (1955). *J. Biophys. Biochem. Cytol* **1**, 605.

Hubbard, R (1953-1954) *J. Gen Physiol* **37**, 381.

Hubbard, R., and Colman, A D. *(1959).* *Science* **130**, 977.

Hubbard, R, and Kropf, A (1958) *Proc. Natl Acad. Sci. U. S.* **44**, 130.

Hubbard, R, and Kropf, A (1959) *Ann. N. Y. Acad Sci.* **81**, 388.

Hubbard, R, Brown, P K., and Kropf, A. (1959). *Nature* **183**, 442

Krinsky, N I (1958) *A M A Arch Ophthalmol.* **60**, 688.

Noell, W K (1958). *Ann N. Y Acad. Sci* **74**, 337.

Rushton, W A. H (1956). *J. Physiol.* (London) **134**, 30.

Spostrand, F. S (1953) *J. Cellular Comp. Physiol.* **42**, 15

Spostrand, F S (1958). *Ergeb. Biol.* **21**, 128.

Wald, G (1954) *Science* **119**, 887.

Wald, G. *(1956).* *In* "*Enzymes· Units* of Biological Structure and Function" (O Caebler, ed.), p 355. Academic Press, New York.

Wald, G (1958). *Exptl. Cell Research, Suppl.* **5**, 389.

Wald, G. *(1960).* *In* "Handbook of Physiology, Neurophysiology," Vol. I, p. 671. American Physiological Society. Washington, D C.

Silver Carbonate Techniques for the Demonstration of Ocular Histology

J. REIMER WOLTER

Department of Ophthalmic Surgery and Laboratory of Neuropathology, University of Michigan Medical Center, Ann Arbor, Michigan

The Glia of the Human Retina and Optic Disk

THE RETINA, as a part of the central nervous system, has its neurons supported by an elaborate system of glia, as do neurons in general The neurons of the retina were much studied by early authors (Ramón y Cajal, 1893; Polyak, 1941), and details of their intricate structure and arrangement have been known for more than a hundred years. The supporting system of the brain contains three types of glia the astroglia, the oligodendroglia, and the microglia, all of which are well known. In the human retina, on the contrary, with the exception of the cells of Müller (radial fibers), not much is known of the glia

This gap in our knowledge is due to technical difficulties, since with conventional histologic procedures or the older metallic impregnation methods it is impossible to visualize the retinal glia. However, some of these difficulties were recently alleviated by Scharenberg and Zeman (1952) who perfected a silver carbonate technique of del Rio Hortega and developed a new astroglia method, both simple and reliable This method permits the impregnation and photomicrographic recording of the retinal glia under normal and pathological conditions

Three main types of neuroglia are found in the human retina the radial fibers of Müller, the astroglia, and the perivascular glia It must be emphasized that the neuroglia—in contrast to the fibrovascular structures of the retina—are *not* mesodermal in origin and have nothing in common with the mesodermal connective tissues. Neuroglia have been shown to develop from the primitive medullary epithelium of the optic vesicle, which in the early phases of embryonal development differentiates into neuroblasts and glioblasts. Glioblasts are precursors of the retinal neuroglia

It is somewhat confusing that another element of the human retina, very different from the neuroglia in its structure and functions, is also termed glia. These are the microglia which, it must be emphasized, undoubtedly are mesodermal in origin, and are found in all parts of the central nervous system. First described by del Rio Hortega (1932), they

Silver Carbonate Techniques for the Demonstration of Ocular Histology

J. REIMER WOLTER

Department of Ophthalmic Surgery and Laboratory of Neuropathology, University of Michigan Medical Center, Ann Arbor, Michigan

The Glia of the Human Retina and Optic Disk

THE RETINA, as a part of the central nervous system, has its neurons supported by an elaborate system of glia, as do neurons in general. The neurons of the retina were much studied by early authors (Ramón y Cajal, 1893; Polyak, 1941), and details of their intricate structure and arrangement have been known for more than a hundred years. The supporting system of the brain contains three types of glia: the astroglia, the oligodendroglia, and the microglia, all of which are well known. In the human retina, on the contrary, with the exception of the cells of Müller (radial fibers), not much is known of the glia.

This gap in our knowledge is due to technical difficulties, since with conventional histologic procedures or the older metallic impregnation methods it is impossible to visualize the retinal glia. However, some of these difficulties were recently alleviated by Scharenberg and Zeman (1952) who perfected a silver carbonate technique of del Rio Hortega and developed a new astroglia method, both simple and reliable. This method permits the impregnation and photomicrographic recording of the retinal glia under normal and pathological conditions.

Three main types of neuroglia are found in the human retina: the radial fibers of Muller, the astroglia, and the perivascular glia. It must be emphasized that the neuroglia—in contrast to the fibrovascular structures of the retina—are *not* mesodermal in origin and have nothing in common with the mesodermal connective tissues. Neuroglia have been shown to develop from the primitive medullary epithelium of the optic vesicle, which in the early phases of embryonal development differentiates into neuroblasts and glioblasts. Glioblasts are precursors of the retinal neuroglia.

It is somewhat confusing that another element of the human retina, very different from the neuroglia in its structure and functions, is also termed glia. These are the microglia which, it must be emphasized, undoubtedly are mesodermal in origin, and are found in all parts of the central nervous system. First described by del Rio Hortega (1932), they

are also called Hortega cells. These wandering phagocytes may be considered the histiocytes of the central nervous system.

A demonstration of the different types of glia found in the human retina follows. Sections used are frozen human retina stained with the silver carbonate methods (Scharenberg and Zeman, 1952), and all microphotographs are unretouched.

Radial Fibers of Muller

The radial fibers of Müller with their inner and outer limiting membranes form the coarse skeleton which supports the neurons, various other glial elements, and blood vessels of the retina. The inner portion of Müller's radial fibers forms brushlike ends firmly anchored in the inner limiting membrane which membrane is considered a product of Müller's fibers. It is composed of a hyalinelike homogeneous substance and the inner processes of Müller's fibers, which form a mosaiclike pattern within it (Figs. 1 and 2).

The inner surface of the inner limiting membrane is partly covered by a discontinuous sheet of flat cells with long interconnected processes (Wolter, 1956a). These cells are most obvious in an area around the optic disk, and are found to proliferate in eyes with pathological degeneration involving the retina, and normally in senescence. I believe that these cells are a special type of astroglia growing out of the optic disk onto the inner retinal surface (Wolter, 1959a).

The inner limiting membrane covers all of the central and intermediate retina with the exception of the inner surface of the optic disk.

Fig. 1. Flat section through inner brushlike processes of Müller's radial fibers close to inner limiting membrane of normal human retina. Frozen section, Hortega method, photomicrograph.

Fig. 2. Flat section through inner limiting membrane. Only the mosaiclike arranged inner endings of Müller's fibers in this membrane are stained. The connecting homogenous substance of the inner limiting membrane remained unstained. Frozen section, Hortega stain, photomicrograph.

Fig. 3. Extension of fibrillar structures of vitreous (upper half of picture) into structures of peripheral retina (lower half of picture). The fibrils form rootlike structures in the retina. No inner limiting membrane is visible. Eye of 70-year-old man. Frozen section, Hortega stain, photomicrograph.

Fig. 4. Neurites of the nerve fiber layer of a normal human retina. Parts of ganglion cells are seen among the fibers. Flat frozen section, Hortega stain, photomicrograph.

Fig. 5. Typical lemmocyte of nerve fiber layer in flat section of normal human retina. One process of the lemmocyte is attached to the wall of a blood vessel (arrow). Frozen section, Hortega stain, photomicrograph.

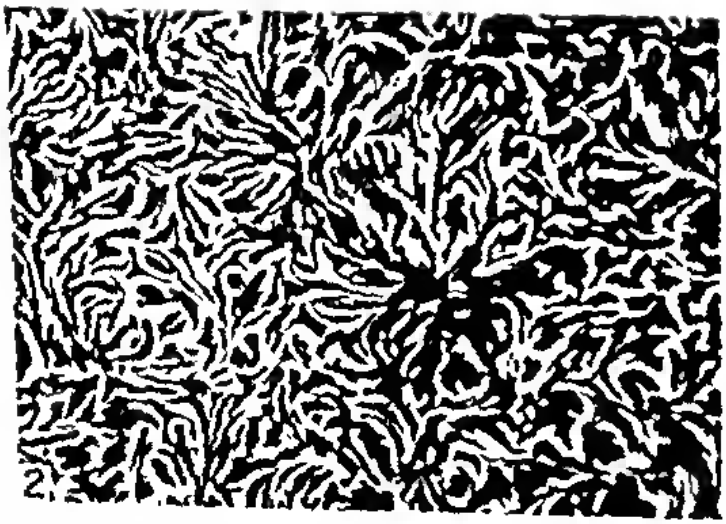

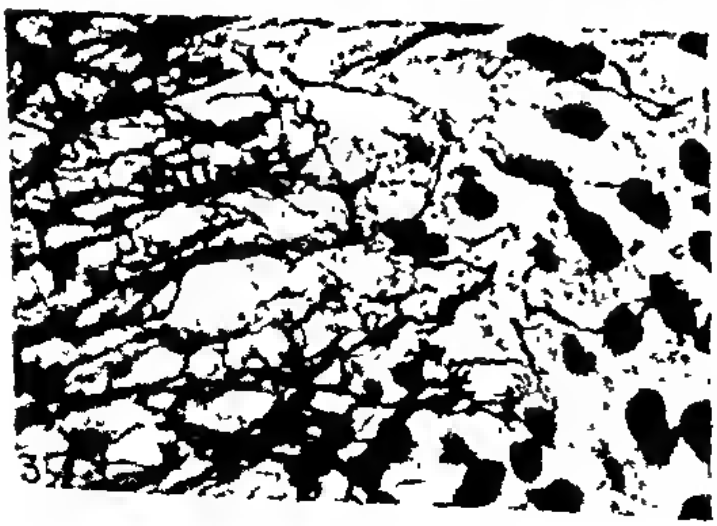

Absence of this membrane on the disk is explained by absence of Müller's radial fibers in the disk. It is very difficult to demonstrate a well-developed inner limiting membrane in the peripheral retina, especially in eyes of old people. In normal senescence this area shows layers of dense jellylike vitreous firmly attached to the inner retinal surface. It is usually not possible to remove this vitreous from the retina without damaging the latter. Silver stains show rather coarse fibrillar structures and cellular nuclei in this dense vitreous (Wolter and Wilson, 1959). Clearly visible rootlike processes of vitreous fibrils extend into the peripheral retina of these eyes (Fig. 3). There is no doubt that these "senile peripheral vitreoretinal adhesions" are most important in understanding the occurrence of retinal detachment in otherwise normal eyes.

The outer processes of Müller's radial fibers form a complicated system of glial fibers which surrounds and supports the neurons of the outer retina (Fig. 8) and forms the outer limiting membrane. Beautiful demonstrations of this portion of the framework of the radial fibers can be found in Polyak's book. It may be mentioned that the radial fibers of Müller are the only glia in the outer retina, since the astroglia and perivascular glia are limited to the inner retina where the retinal blood vessels are found.

Astroglia

It is important to emphasize that the retinal astroglia are not very different from those of other parts of the central nervous system. All astroglia are arranged as a dividing system between the neurons, (neuroectodermal) and the blood vessels and their connective tissues (mesodermal). Under normal conditions there is no direct contact between neurons and blood vessels. It seems to be the function of the astroglia not only to support the neurons and their processes, but also to select the nutritional fluids for the neurons from the blood vessels and to transport them within their protoplasm to the neurons. This must be valid for the retinal astroglia, since astroglia are only found in those retinal layers where there are blood vessels: the nerve fiber layer, the ganglion cell layer, and the inner plexiform layer. The inner nuclear layer has no astroglia of its own, although processes of the astrocytes of the inner plexiform layer always surround and accompany the capillaries as they enter it.

The astroglia of the nerve fiber layer differ distinctly from those of the other layers of the inner retina as well as from those of the brain. The nerve fiber layer contains the neurites of the neurons of the ganglion cell layer which run toward the optic disk and up to the brain. The astroglia of this layer are adjusted to support these neurites (Fig. 4). They are bipolar cells with elongated nuclei and two long straight proc-

esses which are attached to the nonmyelinated neurites (Fig. 5). One of the two processes may form a sucker footlike formation on the wall of a blood vessel (Fig. 5). These cells are identical with the so-called elements of Remak or lemmocytes (Wolter, 1955a). Not all lemmocytes of the nerve fiber layer are of the simple bipolar structure seen in Fig. 5. Some of them may show branching processes and there are transitional forms at the limit between nerve fiber layer and ganglion cell layer which look somewhat like typical astrocytes. When lemmocytes proliferate under pathological conditions, they take a star-shaped form and cannot be differentiated histologically from the astroglia of the deeper layers.

Typical star-shaped astrocytes are found in the ganglion cell and inner plexiform layers. They have a rather small nucleus and long cellular processes, commonly called glial fibers, and form a networklike fiber system in the inner layers of the retina, which is built into the coarser framework of the radial fibers of Müller. Some of the processes surround the ganglion cells, also having close contact with their neurites and dendrites. Other processes form sucker footlike formations on the wall of small blood vessels. Figure 6 shows typical astroglia in a flat section through the inner plexiform layer of a normal human retina. The star-shaped cell body and its long fiberlike processes are well stained. Normal astroglia of the white matter of the human brain also show the typical long processes (glial fibers) and sucker footlike endings at the wall of blood vessels. It is obvious that the astroglia of the retina are closely related to those of the brain. However, they are somewhat modified and adjusted to the special layerlike arrangement of the retina. Figure 7a represents a photomicrograph of another astrocyte of the inner plexiform layer of the normal human retina seen in a flat section. In this cell the rather delicate sucker footlike ending of one process on a capillary is easily visible. Figure 7b is a drawing of the same astrocyte to explain the photomicrograph.

In the normal adult the astroglia form a very regular honeycombed system of fibers all through the inner retinal layers. Their sucker feet have close relations to the retinal blood vessels. This network of glial fibers is somewhat denser and more cellular in babies. In senescence the astroglia show a decreased number of glial processes, and the remaining processes become coarser and more irregular. A multitude of pathological changes of the retinal astroglia can be observed under pathological conditions (Wolter, 1955b, 1957a, 1959a).

A dense interlacing network of glia fibers can be shown in the outer plexiform layer (Wolter, 1955a). These fibers could not be traced to cell bodies (Fig. 8), and I am now certain that they are part of the complicated fiber system of the outer parts of Müller's radial fibers.

Perivascular Glia

This peculiar type of glia is found only around the capillaries of the human retina. Because of staining characteristics, shape, and arrangement it would seem that the perivascular glia represent a special type of neuroglia (Wolter, 1957b), probably of neuroectodermal origin. Liss (1956, 1958) has found the same perivascular cells around the capillaries of the olfactory bulb and neurohypophysis.

Figure 9 shows a typical cell of the perivascular glia on a small blood vessel of the normal human retina. These cells have a star-shaped cell body and many long processes surrounding the blood vessel wall. Normally they do not extend into the retinal tissues. The cells have a rather small round or oval nucleus. Figure 10 shows our conception of the normal arrangement and relations of the astroglia and perivascular glia around the capillaries of the retina. It was pointed out above that nowhere in the normal retina is there direct contact of the neurons or their processes with the mesodermal tissues of the blood vessels. The limitation of these two tissues of different origin is achieved in part by the sucker footlike processes of the astroglia which cover most of the wall of the blood vessels. It appears that those areas of the capillary wall that are not covered in this way are surrounded by a network of processes of the perivascular glia. This conception would explain why the perivascular glia show such extensive proliferation and hypertrophy in many diseases accompanying degeneration of retinal astroglia. It seems that the perivascular glia try to cover more of the vascular surface to prevent direct contact of neurons with the blood vessel wall under these conditions.

Proliferation of the perivascular glia is very common in retinal degeneration in senescence and in chronic eye diseases. The processes of the perivascular glia then become hypertrophic, coil around the blood vessels and may extend into the retinal tissues. Finally these thick hypertrophic processes may become hyalinized and the cells degenerate. Hy-

---

Fig. 6. Typical astrocyte (arrow) in flat section through inner plexiform layer of normal human retina. Frozen section, Hortega stain, photomicrograph.

Fig. 7a. Normal astrocyte of inner plexiform layer of human retina with ending at capillary wall. Frozen flat section, Hortega stain, photomicrograph.

Fig. 7b. Drawing of the same astrocyte. a: cell body, b: process on blood vessel wall, c: capillary with erythrocytes.

Fig. 8. Network of glial fibers in outer plexiform layer of normal human retina. This probably represents processes of the outer parts of Müller's radial fibers. Frozen section, Hortega stain, photomicrograph.

Fig. 9. Perivascular glia cell of retinal blood vessel in normal human eye (arrow). Frozen section, Hortega stain, photomicrograph.

6

9

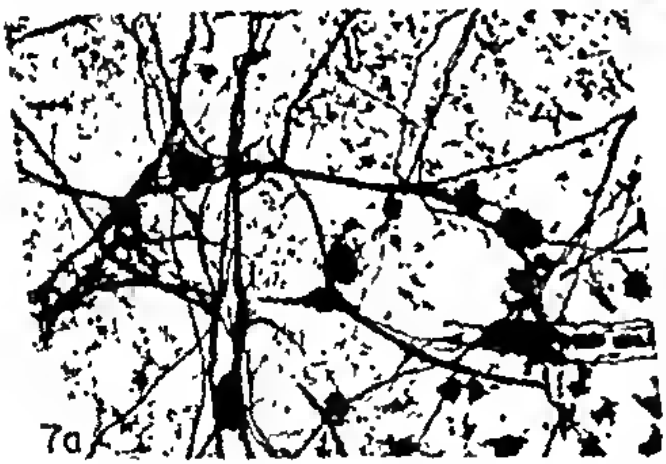

7a

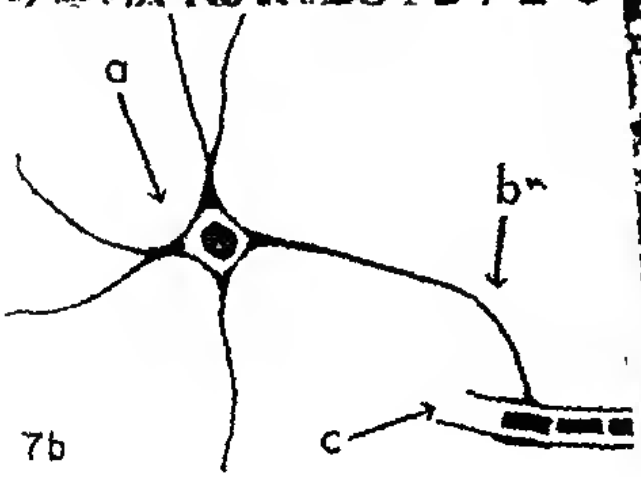

7b

8

alinized remnants of hypertrophic perivascular glia are common in the degenerated retinal periphery of normal eyes in senescenee (Wolter and Wilson, 1959).

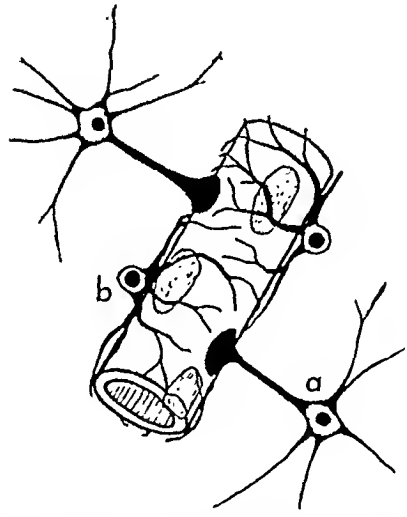

FIG. 10. Author's conception of the relations of astroglia (a), perivascular glia (b), and capillaries (center) in normal human retina. Drawing.

The presence of oligodendroglia in the human retina is not established definitely, but if they are there, they are more diffieult to stain than in the human brain.

MICROGLIA

It was emphasized above that mieroglia represent the only type of retinal glia not neuroeetodermal in origin, and are eonsidered mesodermal, whieh seems somewhat eonfusing. However, neuropathologists aceept the term *mieroglia* for these eells all through the central nervous system, and it would be even more confusing to use another term for these elements in the retina and optic nerve.

Microglia are the phagocytes (macrophages) of the central nervous system. It is easy to remember their functions when we recall that they really are the histioeytes of the nervous tissues. Mieroglia are normally small cells with a round nucleus and few short branching processes. They are wandering cells whose number increases tremendously when destruction of retinal neurons has occurred under pathological conditions. They not only funetion within the retina but also migrate into the pre- and retroretinal space for action (Wolter, 1960a). Their only known function is phagocytosis after which they appear as large round eells which still have the small nucleus and are filled with the phagocytized substances. In the retina these cells are easily detected by a fat stain, since the phagoeytized substances usually are lipids from destroyed retinal neurons. The fat-filled microglia are also known as gitter cells, ghost cells, or

granular compound corpuseles. Their accumulations in the retina explain the ophthalmoscopical findings of deep hard exudates and the *macular* star-figure in some pathologieal conditions (Wolter *et al.*, 1957).

The Glia of the Optic Disk

The optic disk (papilla) has a very complicated architecture (Wolter, 1956b, 1957c), composed of neurites, glia, connective tissue, blood vessels, and is a round sievelike structure at the posterior pole of the eye. This provides for a well-protected outlet for the bundles of neurites (Fig. 11) of the nerve fiber layer which form the adjacent optic nerve. The sclera has its direct continuation in the lamina cribrosa of the optie disk so there is as little weakening of the dense outer layer of the eye ball as possible.

The supporting structures of the optie disk consist of a posterior and an anterior portion. The posterior portion is formed by the sievelike intertwined connective tissue fibers of the lamina cribrosa. Astroglia are built into this coarse framework to surround and support the neurites on their way through it. This is again evidence for the principle that neurons and their processes have no direct contact with mesodermal tissues in the normal eye.

The anterior portion of the supporting structures of the optie disk resembles a shallow caplike wieker basket, composed of special retinal astroglia The function of this wicker basket is to protect and support the bundles of neurites (Fig. 11) at this vulnerable 90-degree flexion of the retinal fibers into the optic nerve. The glial basket is closely connected to the lamina cribrosa posteriorly, and is also firmly connected to Bruch's membrane of the choroid This latter membrane unites at the disk margin with a ring-shaped spur of the sclera. The anterior portion of the disk actually is a part of the retina. However, it contains no radial fibers of Muller. A special type of retinal astroglia is found in this area: the spider cells These were first described by Marchesani (1926), and are small star-shaped cells, with many long processes (glial fibers). Their bodies are arranged in columns along the blood capillaries of the disk. Their processes form an elastic meshwork which allows for mechanical changes of the eye movements, as well as for swelling of the disk in papilledema and neuritis.

The Glia of the Optic Nerve

The silver carbonate methods permit good demonstration of the astroglia in the normal human optic nerve The astrocytes are arranged in columns in both the center and periphery of the nerve bundles. They have star-shaped cell bodies and many processes, of which some form

sucker footlike endings on the blood vessels, and others surround the neurites (Fig. 12). The glial processes form a dense fiber network throughout the optic nerve, the main direction of which is across that of the neurites. Figure 16 is a drawing reconstruction of the arrangement of the astrocytes and of their relations to the neurites and the blood vessels. Several types of astroglia occur, differing in shape and arrangement of processes.

There are numerous oligodendroglia in the normal human optic nerve, although it is difficult to obtain a complete stain of these cells. They have close relations to the blood vessels, and beautiful stains of the more primitive ones may be easily obtained from cases of glioma of the optic nerve, most of which are oligodendrogliomas (Liss and Wolter, 1957).

There are always microglia in the normal optic nerve. Just as in the retina, they are normally small cells with a round nucleus and few branching processes. They have the same phagocytic functions as in the retina, or brain, and increase tremendously in destructive optic nerve pathology.

Further Evidence for the Existence of Centrifugal Nerve Fibers in Human Optic Nerve and Retina

There can be no doubt that most of the nerve fibers of the human optic nerve come from the cells of the ganglion cell layer in the retina and run through the optic nerve to the brain. However, the question of the existence of centrifugal nerve fibers in the human optic nerve has been repeatedly discussed in the literature. Some text books of ophthalmology and anatomy consider the existence of such fibers questionable (Lauber, 1936; Polyak, 1941; Friedenwald *et al.*, 1952; Kappers *et al.*, 1936). Other authors believe in the existence of such centrifugal (efferent, antidrome) nerve fibers (for example: Greff (1877); Cone and MacMillan, 1932; Duke-Elder, 1940). Recently Dodt (1956) revived the old discussion in finding electrophysiological evidence for centrifugal

---

FIG. 11. High-power view of nerve fiber bundles running through lamina cribrosa of normal human optic disk. Frozen section, Hortega stain, photomicrograph.

FIG. 12. Astrocyte of normal human optic nerve. Good stain of the numerous delicate glial processes. Frozen section, Hortega stain, photomicrograph.

FIGS. 13 and 14. Remaining nerve fibers (centrifugal) in optic nerve stump, 11 years after enucleation of the corresponding eye. Frozen section, Hortega stain, photomicrograph.

FIG. 15. Nerve ending on wall of retinal blood vessel. Frozen section, Hortega stain, photomicrograph.

13 14

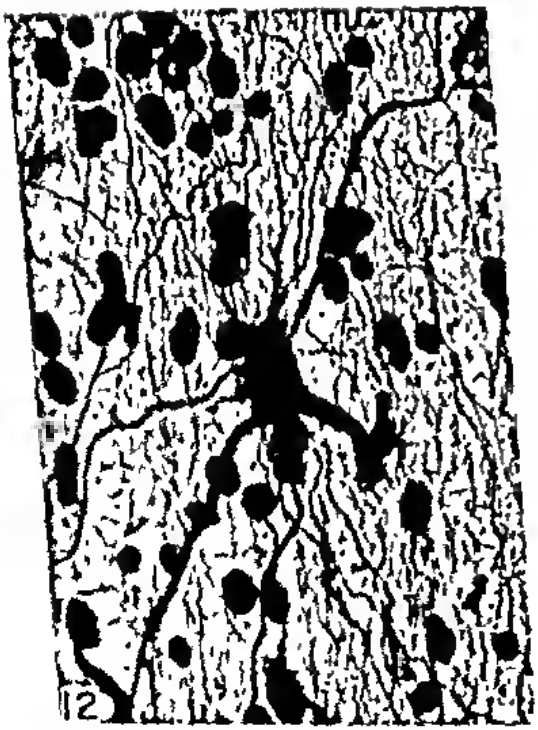

12

15

fibers in the optic nerve of the rabbit. Following is a short summary of our histological findings indicating that centrifugal nerve fibers exist in the optic nerve of man (Wolter and Liss, 1956; Wolter, 1956c, 1957d).

Centrifugal nerve fibers of the optic nerve are those fibers having their ganglion cell somewhere in the brain—and not in the retina, as centripetal fibers do. The basic fact that neurites (nerve fibers) soon degenerate after the ganglion cell to which they belong is destroyed, or after they become separated from this cell, is important for this discussion. This fact has been widely used in tracing the origin of nerve fibers by nerve cutting experiments. Our definite conclusion that centrifugal nerve fibers do exist in man comes from two cases.

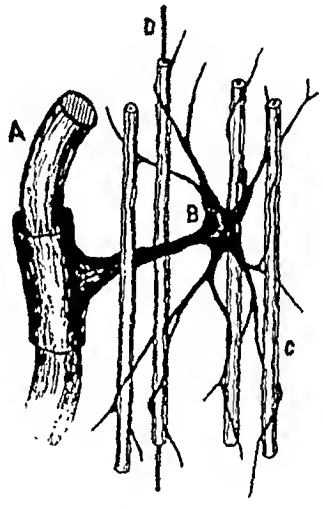

FIG. 16. Drawing reconstruction of the relations of the elements of the human optic nerve. A: blood vessel, B: astroglia, C: nerve fiber, and D: neurite in the myelin sheath.

The optic nerve stumps of two patients, the corresponding eyes of which had been enucleated 11 and 16 years before, were obtained for histological examination. Frozen sections of these were stained with the nerve fiber stain of del Rio Hortega (Scharenberg and Zeman, 1952). Surprisingly both nerve stumps still contained quite a number of nerve fibers (Figs. 13 and 14), which could only mean that these nerve fibers did *not* have their origin in the retina, which was removed years ago. These fibers must have come from the brain and be centrifugal in character.

Further studies show that the retina contains dichotomically branching nerve fibers which enter at the optic disk and form branching endings on the retinal blood vessels (Fig. 15). These fibers are probably vascular

The Pericytes of the Human Choroid and the Connection Between Choroid and Bruch's Membrane

Silver carbonate techniques are a valuable aid in anatomical examinations of the eye. This is not only true for the neurocetodermal tissues of the retina and optic nerve but fascinating things are also found with these techniques when the mesodermal tissues of the eye are stained.

Anatomists do not seem to be sure whether the cells known as pericytes really exist or, if so, what they are. They were discovered by Rouget (1873) and were later confirmed by Zimmermann (1923) and Schaly (1926) to occur in human tissues. Pericytes are hard to stain, but with silver impregnation they can be quite clearly stained in the human retina and choroid. Figure 20 shows a pericyte in the normal human choroid. It has a rather small nucleus and many branching processes of a very bizarre pattern which are closely attached to the wall of a precapillary blood vessel. Several types of pericytes are found in the human choroid which were discussed in detail in a recent paper (Wolter, 1956d).

Among other structures around the blood vessels of the normal human choroid, which can be beautifully stained with silver carbonate, are the extensive perivascular nerve plexus and—with the connective tissue method (Scharenberg and Zeman, 1952)—the perivascular connective tissues (Fig. 21). The perivascular nerves are branches of large choroidal nerve bundles mixed with originally perivascular nerve networks. In a good stain of these two structures it is impossible to doubt which are nerves and which connective tissue. Doubts can occur only after poor staining.

Silver carbonate methods also help explain the firm attachment of Bruch's membrane to the choroid. A network of coarse intertwined con-

---

FIG. 17. Terminal swellings of nerve fiber stumps in the nerve fiber layer of the retina in a case of recent venous occlusion. Frozen flat section, Hortega stain, photomicrograph.

FIG. 18. One of several terminal swellings of interrupted nerve fibers of human retina in retinal detachment shows an attempt at regeneration (arrow). Frozen section, Hortega stain, photomicrograph.

FIG. 19. Flat section of human retina through nerve fiber layer in a case of recent occlusion of central vein. Two small nerve fibers show interruption and formation of terminal swellings which point away from the disk (arrows). Frozen section, Hortega stain, photomicrograph.

FIG. 20. Pericyte around small blood vessel of normal human choroid. Modified Gross Schultze silver nitrate stain, frozen section, photomicrograph.

FIG. 21. Connective tissues fibers surrounding blood vessels of normal human choroid. The coarse supporting fibers of the choroid are unstained. Frozen section, Hortega stain, photomicrograph.


17
18
20


19
21

nective tissue fibers represents the skeleton of the choroid. This skeleton contains and supports all the other choroidal elements: vessels, nerves, and melanocytes. These fibers can be seen to extend into the outer layer of Bruch's membrane (Fig. 22), where they form regularly arranged root- or anchorlike structures (Fig. 23), resembling tree roots, and explaining the firm attachment of Bruch's membrane to the choroid. It is interesting that silver carbonate stain also shows a dense network of very delicate fibrils in the inner layer of Bruch's membrane, which is considered neuroectodermal in origin. These fibrils appear to be continuous with similar fibrils found in the outer layer of the membrane of Bruch (Wolter, 1955c).

The Cells and Nerves of the Cornea and the Corneoscleral Trabeculum

The so-called panoptic variants of the silver carbonate techniques of del Rio Hortega (Scharenberg and Zeman, 1952) permit demonstration of the corneal cells and their reactions in the stroma of man and animals (Wolter, 1958). Figure 24 shows stroma cells in a phase of traumatic irritation as seen in a flat section through rabbit cornea.

It is also possible with the same techniques to demonstrate nerve fibers and Schwann cells in the cornea. Three distinctly different nerve fiber types are demonstrable in the corneal stroma of rabbit and man (Wolter, 1956e). One is rather coarse and forms distinct endings in the stroma. Another is more delicate and ends with very fine networklike branches in the stroma. A third forms cobweblike strands which seem to be without endings and run through the stroma together with the other nerve fibers. All three types are well demonstrated in Fig. 25.

Studies of the corneal stroma in different phases of trauma provide new evidence for the old theory that there are preformed channels (Bow-

---

FIG. 22. Transitional section from choroid into Bruch's membrane (upper part of picture). The coarse supporting connective tissue fibers of the choroid are seen to extend into the membrane of Bruch and end there with rootlike formations. Frozen section, Hortega stain, photomicrograph.

FIG. 23. High power of the rootlike anchorage of the choroidal fibers in Bruch's membrane. Frozen section, Hortega stain, photomicrograph.

FIG. 24. Flat section of rabbit corneal stroma after experimental trauma. The stroma cells with their numerous processes are well shown. Hortega stain, frozen section, photomicrograph.

FIG. 25. Branching of nerves in normal rabbit corneal stroma. All three nerve types are seen. a: thick fibers, b: thinner dichotomically branching fibers, and c: cobweblike fibers. Frozen section, Hortega stain, photomicrograph.

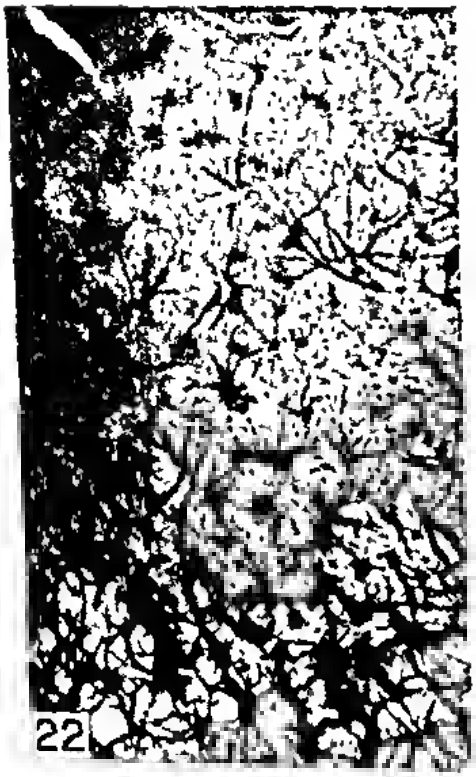

22

24

23

25

man's channels) present in the normal corneal stroma (Wolter, 1958, 1955d). The fact is that invading white blood cells are often found in long straight chains through the stroma and their direction often does not correspond with that of the surrounding corneal lamellae. These chains are approximately radially arranged. This observation has not been made in man, but often in the rabbit.

The corneal endothelium can also be stained with the panoptic silver carbonate techniques. Vacuolization is a typical finding in the corneal endothelium of human eyes, occurring only in the endothelium of the cornea itself. There is a sharp limit at Schwalbe's line; the endothelium of the corneoscleral trabeculum on the other side of this line shows no vacuolization (Fig. 26). It is quite possible that vacuolization of the human corneal endothelium represents an artifact, but it is at least a very interesting artifact, since it points out that the corneal and the trabecular endothelium are somewhat different (Wolter, 1959b).

Another interesting observation is that the endothelium of the rabbit cornea contains large branching nerve fibers which end within the protoplasm of endothelial cells (Wolter, 1957b). Small, but not as extensive, peripheral branches of nerve fibers can also be seen in the human corneal endothelium. However, I have been unable to find such extensive nerves in the human.

Silver carbonate techniques are also well suited to demonstrate the structures of the corneoscleral trabeculum (Wolter, 1957b, 1959e, 1960b). Figure 27 shows the uveal meshwork of the trabeculum of the normal eye of a child in which the architecture of the trabecular beams and endothelium can be seen. Figure 28 shows part of the scleral trabeculum of the same child in a tangential section. The branching nerves of the human trabeculum are demonstrated in Fig. 29. It is important to realize that the human trabeculum has an extremely rich nerve supply.

Limitations in time and space do not allow for demonstration of further histological details of the normal eye obtainable with the silver carbonate techniques of del Rio Hortega. However, it is hoped that this presentation may initiate new interest in old methods among anatomists.

FIG. 26. Left side of picture: corneal endothelium. Right side of picture: trabecular endothelium. The limit between cells with and without vacuoles is at the level of Schwalbe's line. Frozen section, Hortega stain, photomicrograph.

FIG. 27. Uveal meshwork of the trabeculum of a child. The endothelium is seen on the trabecular beams. Frozen section, Hortega stain, photomicrograph.

FIG. 28. Scleral meshwork of the same trabeculum as seen in Fig. 27.

FIG. 29. Branching nerve fibers in human trabeculum. Frozen section, Hortega stain, photomicrograph.

26

27

28

29

Every detail of ocular anatomy is of tremendous importance in understanding the functions and pathology of the eye, and every available method should be used to discover all these details.

References

Cone, W., and MacMillan. (1932). The optic nerve and papilla. *In* "Cytology and Cellular Pathology of the Nervous System" (W. Penfield, ed.), Vol. II, p. 890. Hoeber, New York.

del Rio Hortega, P. (1932). Microglia. *In* "Cytology and Cellular Pathology of the Nervous System" (W. Penfield, ed.), Vol. II. Hoeber, New York.

Dodt, E. (1956). Centrifugal impulses in rabbit's retinae. *J. Neurophysiol.* **19**, 301.

Duke-Elder, Sir St. (1940). "Text Book of Ophthalmology," Vol. I, p. 102. St. Louis, Mosby, Missouri.

Friedenwald, J. S. *et al.* (1952). "Ophthalmic Pathology: an Atlas and Textbook," p. 12. Saunders, Philadelphia, Pennsylvania.

Greff, R. (1877). Die mikroskopische Anatomie des Sehnerven und der Netzhaut. *In* "Handbuch der gesamten Augenheilkunde Graefe-Saemisch," Vol. I, Sect. 2. Engelmann, Leipzig.

Kappers, C. U., Huber, C. C., and Crosby, E. C. (1936). "The Comparative Anatomy of the Nervous System of Vertebrates Including Man," Vol. II, p. 60. Macmillan, New York.

Lauber, H. (1936). Der. Sehnerv. *In* Möllendorff's "Handbuch der mikroskopischen Anatomie des Menschen," p. 493. Springer, Berlin.

Liss, L. (1956). Astroglia and perivascular structures of the human olfactory bulb. *Ann. Otol. Rhinol. & Laryngol.* **65**, 937.

Liss, L. (1958). Die perivaskulären Strukturen der menschlichen Neurohypophyse. *Z. Zellforsch. u. mikroskop. Anat.* **48**, 283.

Liss, L., and Walter, J. R. (1957). The histology of the glioma of the optic nerve, *A.M.A. Arch. Ophthalmol.* **58**, 689.

Marchesani, O. (1926). Die Morphologie der Glia im Nervus opticus und in der Retina. *Arch. Ophthalmol. Graefe's* **117**, 575.

Polyak, S. L. (1941). "The Retina." University of Chicago Press, Chicago, Illinois.

Ramón y Cajal, S. R. (1893). "Histologique du système nerveux de l'homme et des vertébrés," p. 298. Norbert Maloine, Paris.

Rouget, C. (1873). Mémoire sur le développement, la structure et les propriétés physiologiques des capillaires sanguiniques et lymphatiques. *Arch. physiol. norm. & pathol.* **5**, 603.

Schaly, G. A. (1926). Over het Voorkomen van de Cellen van Rouget op den Wand van de Capillairen in het Oog van den Mensch, Proefschrift ter Verkrijking van den Graad van Doctor aan Rijks-Universiteit te Groningen, Groningen-Den Haag.

Scharenberg, K., and Zeman, W. (1952). Zur Leistungsfaehigkeit und zur Technik der Hortega'schen Silberkarbonatmethoden. *Arch. Psychiat. Nervenkrankh.* **188**, 430.

Wolter, J. R. (1955a). The cells of Remak and the Astroglia of the normal human retina, A.M.A. *Arch. Ophthalmol.* **53**, 832.

Wolter, J. R. (1955b). The astroglia of the human retina and other glial elements of the retina under normal and pathological conditions, *Am. J. Ophthalmol.* **40** (5) 88.

Wolter, J. R. (1955c). Histologic character of connection between Bruch's membrane and choriocapillaris of human eye, *A.M.A. Arch. Ophthalmol.* **53**, 285.
Wolter, J. R. (1955d). Ein Beitrag zur Frage der Existenz und Bedeutung der Bowmanschen Rohren der Hornhaut. *Klin. Monatsbl. Augenheilk.* **127**, 183.
Wolter, J. R. (1956a). Über besondere Astroglia an der Innenfläche der Retina. *Klin. Monatsbl. Augenheilk.* **129**, 224.
Wolter, J. R. (1956b). Die Struktur der Papille des menschlichen Auges. *Arch. Ophthalmol. Graefe's* **158**, 268.
Wolter, J. R. (1956c). Ein weiterer Beweis für die Existenz zentrifugaler Nervenfasern in der menschlichen Netzhaut. *Arch. Ophthalmol. Graefe's* **158**, 240.
Wolter, J. R. (1956d). The pericytes of the choroid of the human eye. *Am. J. Ophthalmol.* **41**, 990.
Wolter, J. R. (1956e). Über den Aufbau der Nervenbündel in der Hornhaut des Kaninchenauges. *Klin. Monatsbl. Augenheilk.* **129**, 20.
Wolter, J. R. (1957a). Das Verhalten der Astroglia bei fortgeschrittener Degeneration der Netzhaut. *Klin. Monatsbl. Augenheilk.* **130**, 498.
Wolter, J. R. (1957b). Perivascular glia of the blood vessels of the human retina. *Am. J. Ophthalmol.* **44**, 766.
Wolter, J. R. (1957c). The human optic papilla. *Am. J. Ophthalmol.* **42**, 45.
Wolter, J. R. (1957d). Über Endigungen zentrifugaler Nervenfasern an den Blutgefässen der menschlichen Netzhaut. *Arch. Ophthalmol. Graefe's* **158**, 524.
Wolter, J. R. (1957e). Innervation of the corneal endothelium of the eye of the rabbit. *A.M.A. Arch. Ophthalmol.* **58**, 246.
Wolter, J. R. (1958). Reactions of the cellular elements of the corneal stroma. *A.M.A. Arch. Ophthalmol.* **59**, 873.
Wolter, J. R. (1959a). Glia of the human retina. *Am. J. Ophthalmol.* **48** (5), 370.
Wolter, J. R. (1959b). The trabecular endothelium. *A.M.A. Arch. Ophthalmol.* **61**, 928.
Wolter, J. R. (1959c). Neuropathology of the trabeculum in open angle glaucoma. *A.M.A. Arch. Ophthalmol.* **62**, 99.
Wolter, J. R. (1960a). Macrophages of the human vitreous. *Am. J. Ophthalmol.* **49**, 99.
Wolter, J. R. (1960b). Pathology of the trabeculum in glaucoma. *Am. J. Ophthalmol.* **49**, 3.
Wolter, J. R., and Liss, L. (1956). Zentrifugale (antidrome) Nervenfasern im menschlichen Sehnerven. *Arch. Ophthalmol. Graefe's* **158**, 1.
Wolter, J. R., and Wilson, W. W. (1959). Degeneration of the peripheral retina. *Am. J. Ophthalmol.* **47**, 153.
Wolter, J. R., Goldsmith, R. L., and Phillips, R. I. (1957). Histopathology of the star figure of the macular area in diabetic and angiospastic retinopathy. *A.M.A. Arch. Ophthalmol.* **57**, 376.
Zimmermann, K. W. (1923). Der feinere Bau der Blutcapillaren. *Ztr. Anat. Entwicklungsgeschichte* **68**, 29.

Discussion

Dr. Cohen [Washington University, St. Louis, Missouri]: One of the interesting problems that has come up revolves about the mutually exclusive definitions of the term "internal limiting *membrane*" as either a cellular or noncellular structure. In the electron microscope all we see is a basement membrane, an acellular structure interposed between the glial cells of the retina and the vitreous body. This basement

membrane disappears at the optic papilla because it passes into the optic nerve. Anteriorly it just goes around the cup concavity onto the surface of the ciliary body and posterior iris, and its further continuation would be that of a basement membrane below the mesodermal component of the anterior iris. I think that ophthalmologists who use the term to refer to a sheet of contiguous cell processes on the vitreal surface of the retina might do well to reconsider the utility of this designation since the glial cell "feet" facing the vitreous humor are quite variable in thickness and appearance and do not constitute a uniform sheet. I am not sure that the concept of a membrane of cell "feet" is of value.

Dr. Wolter [University of Michigan, Ann Arbor, Michigan]: Dr. Verhoeff was asked the same question a few days ago at a meeting in Washington. His answer was: "If you cannot see the inner limiting membrane of the retina with the electron microscope this only shows that there is something wrong with the electron microscope." I agree with Dr. Verhoeff, since this membrane can be well stained with several methods including the silver carbonate method and is then well visible with the light microscope.

Dr. Cohen: I am not questioning the observation that there is a membrane on the retina, between it and the vitreous body. There is a controversy concerning what is meant by "internal limiting membrane." Apparently, what is meant by some (e.g., Polyak) is a sheet formed by closely approximated contiguous cell "feet" occupying the face of the retina. There is no continuous extra-retinal sheath of cells as the term sheath is usually employed in histology.

Chairman Carpenter [Tufts University, Medford, Mass.]: Do you mean that the internal limiting membrane is of cellular nature?

Dr. Cohen: No! There are retinal cells. Before them there is a basement membrane, an acellular membrane.

Functional Architecture of the Retinal Epithelium[1]

MAURICE H. BERNSTEIN

Department of Anatomy, Wayne State University College of Medicine, Detroit, Michigan

EXTENSIVE INVESTIGATIONS OF THE RETINA by means of electron microscopy (Sjöstrand, 1953; De Robertis, 1956) have largely focused on the photoreceptor elements. Porter (1957) and Yamada *et al.* (1958) have reported their observations on the pigmented epithelium of the retina. The critical importance of the retinal epithelium in visual function, as well as the variety of its spatial relations and contacts, has prompted a more extensive investigation of this portion of the retina.

Most of the observations to be reported here have been made on cats, utilizing the routine procedures of buffered osmium tetroxide fixation and methacrylate embedding.

The several functional aspects of the pigmented epithelium of the retina have been considered under three arbitrary headings; supportive, nutritional, and secretory. These subdivisions have no significance other than to facilitate this presentation. These functions are certainly interrelated and interdependent.

Supportive Functions of the Retinal Epithelium

The retinal epithelium follows the general planar organization of the retina and of a typical sheet of epithelial cells. In cross section in a low-power survey electron micrograph (Fig. 1), the rectangular cells rest on a basement membrane. They are 7 to 10 μ high and 20 to 25 μ across. The nuclei are roughly spherical, 3.5–4 μ in diameter, usually with a single nucleolus. The basal surface of these cells overlies either the vessels of the choriocapillaris or an extremely thin single cell layer which is interposed between the epithelium and the choroid. In tangential section (Fig. 2), the lateral faces of the epithelial cells are seen in close apposition, the cells forming a dense covering sheet, but with no indications of interdigitation. Polyak (1957) refers to an intercellular cement cap over the outer surface and reaching down between the cells

[1] The work reported here represents a continuation of work begun while the author was in the Department of Anatomy, University of California Medical Center, Los Angeles, California.

This work is currently supported by Grant No. B-2010 from the National Institute of Neurological Diseases and Blindness, United States Public Health Service.

of the retinal epithelium. This is probably an interpretation of the distribution of the basement membrane of the chorio-capillaries.

The inner aspect of the retinal epithelium presents a ragged fringe-like appearance. The terminal portions of the outer segments of the photoreceptors protrude into the epithelial cells which present two distinct surface modifications relating to the photoreceptors. The end of each outer segment is met by a short thick process of epithelial cytoplasm. From the sides of these short thick processes, long slender extensions envelop the terminal portion of each outer segment (Fig. 1). These extensions appear to be reflections of the epithelial cell surface. This particular facet of epithelial morphology is not as well developed in mammals as in some birds and amphibia. Nonetheless, it is important to note that the retinal epithelium serves to anchor the outer end of the extremely elongated photoreceptor structures. The photoreceptors are modified cilia (De Robertis, 1956), divided into inner and outer segments. The outer segments are composed of a stack of disklike elements, which may attain a height of 12 to 15 μ. The inner and outer segments are joined by a short bar with the structure of a typical cilium, but this bar apparently does not extend very far into either segment. The inner segment is a dense aggregation of mitochondria, comparable in length to the outer segment. Its inner (vitreal) end is held in place by the external limiting membrane. Thus four factors maintain the structural rigidity of the photoreceptor elements: the external limiting membrane, the short bar (cilium) joining the inner and outer segments, the finger-

---

PLATE I

FIG. 1. Low-power survey electron micrograph of a cross section through the outer rod segments (ors), the pigmented epithelium of the retina (per), tapetum (tap), and choroid (ch). The section is at the periphery of the tapetum, which is seen here diminishing from two layers to one. Two profiles of blood vessels of the choriocapillaris are seen outside the retinal epithelium. The even row of the rectangular epithelial cells forms the outer limit of the retina. The outer segments of the photoreceptors are inserted into the epithelium which sends out short thick processes to receive the photoreceptor elements and long slender processes to enclose them. The sharp oval lipofuscin pigment granules (fg) of the retinal epithelium are seen in the areas close to the outer rod segments.

FIG. 2. Tangential section through the pigmented epithelium of the retina. The polygonal cells are tightly packed but do not show any special adhesions or interdigitations. The ramifications of the choriocapillaris (cap) under the basal surface of the retinal epithelium (per) are apparent. The plications of the epithelium can be seen in the regions adjacent to the capillaries. A number of dense spherical granules (sg) are visible in the cytoplasm, as well as the large prominent nuclei (nuc). The section is too deep in the epithelial cells to show any of the characteristic lipofuscin granules.


top
per
fg
ch

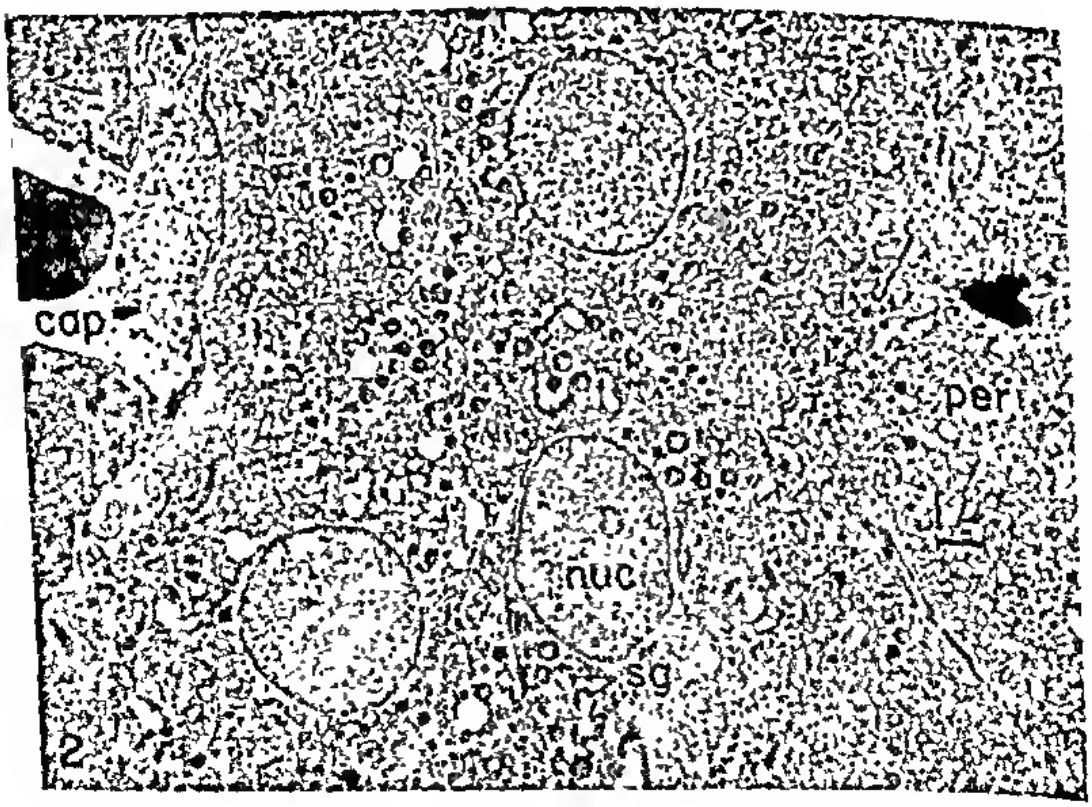
cap
per
nuc
sg
2

like extensions of the retinal epithelium, and the insertion of the outer segments into the surface of the epithelium.

The characteristic pigment of the retinal epithelium serves a protective rather than a strictly supporting function for the rods and cones. The pigment is considered to be a lipofuscin (Walls, 1942) in contrast to the melanin pigment of the choroid, and the granules are elongate ovals rather than the spheres seen in the choroidal cells. Migration of this pigment in light and dark adaptation is a notable feature of retinal function in many reptiles and amphibia, but is greatly reduced or absent in most mammals. As previously reported for the cat (Bernstein and Pease, 1959), the pigment granules are not conspicuous in that portion of the retinal epithelium overlying the tapetum.

Nutritional Functions of the Retinal Epithelium

The nutritional aspects to be considered here relate primarily to the question of fluid transport. In view of the high level of metabolic demand seen in the retina, its circulatory pattern is strangely constricted. The two main sources of blood supply are the central artery of the retina and the vessels of the choroid. According to Adler (1959), the central artery of the retina provides two capillary nets, a superficial (inner) one in the optic nerve fiber layer and a deep net between the inner nuclear layer and the outer plexiform layer. These are largely two-dimensional nets which follow the planes of the retina in their respective locations. The next vascular element found is the choriocapillaris on the external surface of the retinal epithelium. More than half of the total mass of the retina lies between these capillary networks and the choriocapillaris. Apparently the bulk of the blood supply comes from the choriocapillaris, which, according to Michaelson (1954), can supply nutrition to the retina for a distance of 130 μ. These capabilities find a morphological reflection in the appearance of the choriocapillaris vessels and the adjacent epithelium (Fig. 3), as compared to a vessel from the superficial network derived from the central artery of the retina (Fig. 4) and its surroundings. The choriocapillaris vessels form a dense anastomosing network with the endothelial cell nuclei most commonly seen oriented to the choroidal surface. This permits the plicated basal surface of the retinal cells to come into contact with the attenuated endothelial surface, which is characterized by extensive fenestrations. Figure 3 is typical in showing these fenestrations to be areas of membrane reduction rather than patent openings.

The importance of this interface in fluid transport is further indicated by the marked plications and folds seen in the basal surface of the retinal

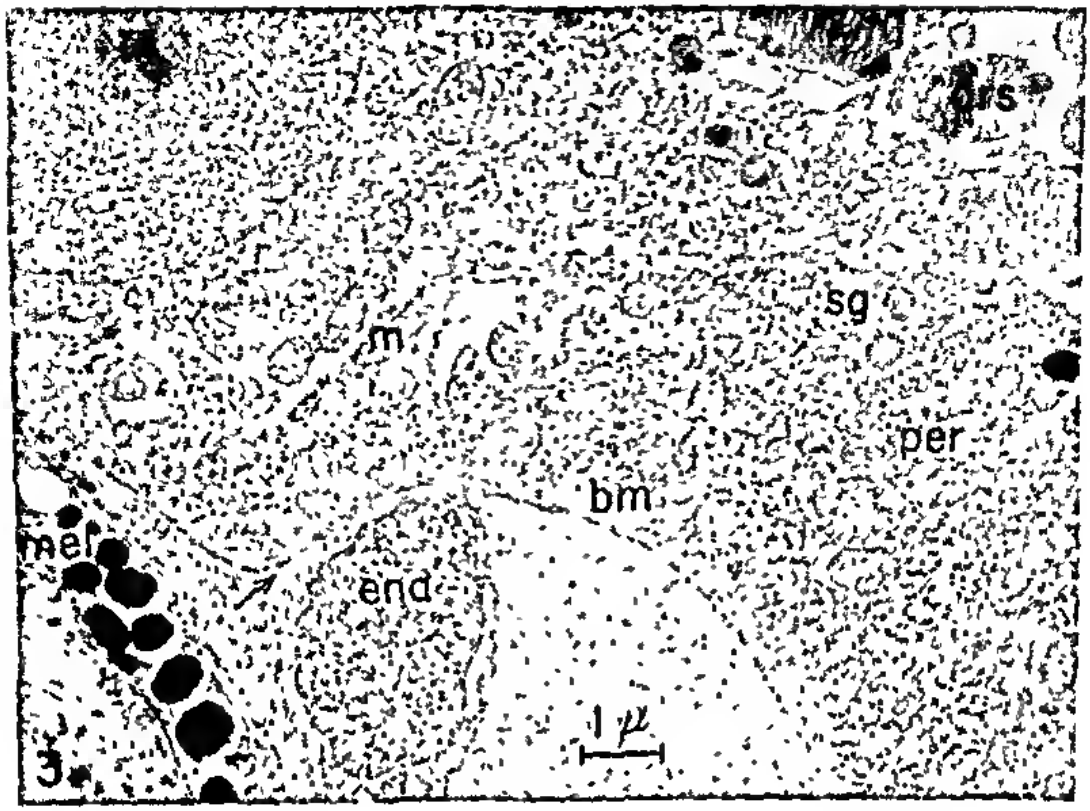
ors
sg
m
per
bm
mel
end
1 μ
3

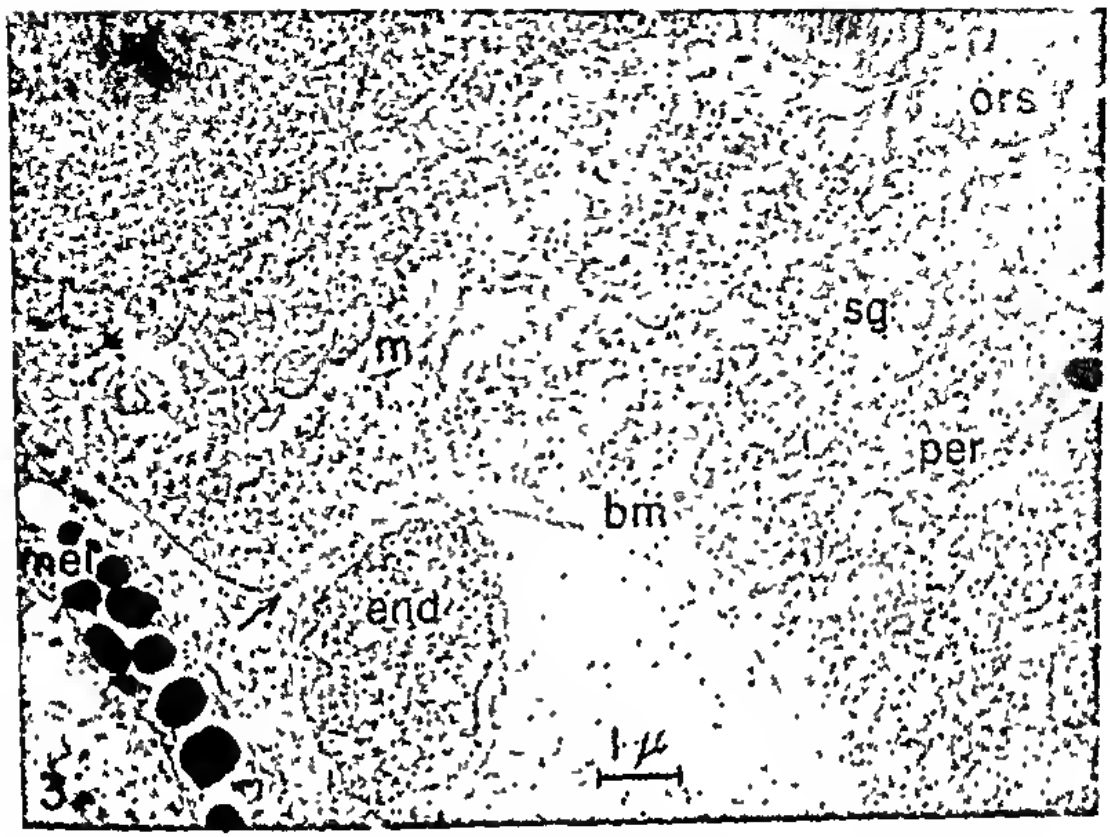
ors
sg
m
per
bm
mel
end
1 μ

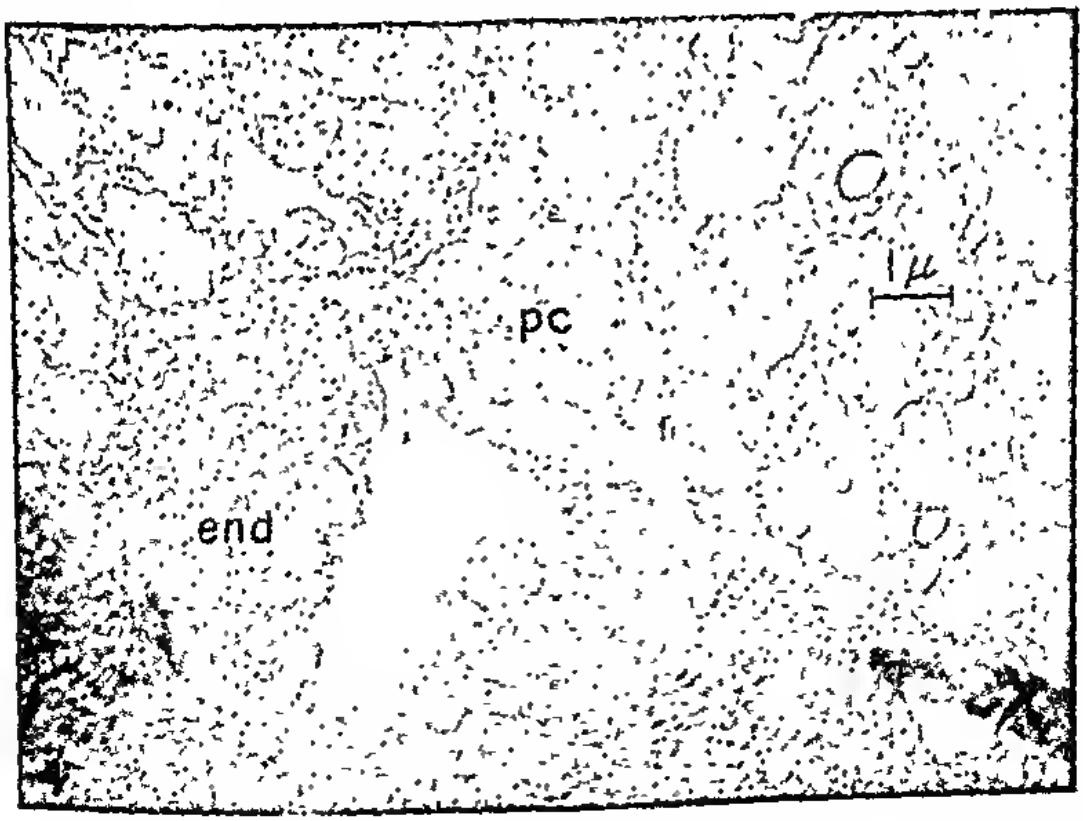
1 μ
pc
end

like extensions of the retinal epithelium, and the insertion of the outer segments into the surface of the epithelium.

The characteristic pigment of the retinal epithelium serves a protective rather than a strictly supporting function for the rods and cones. The pigment is considered to be a lipofuscin (Walls, 1942) in contrast to the melanin pigment of the choroid, and the granules are elongate ovals rather than the spheres seen in the choroidal cells. Migration of this pigment in light and dark adaptation is a notable feature of retinal function in many reptiles and amphibia, but is greatly reduced or absent in most mammals. As previously reported for the cat (Bernstein and Pease, 1959), the pigment granules are not conspicuous in that portion of the retinal epithelium overlying the tapetum.

Nutritional Functions of the Retinal Epithelium

The nutritional aspects to be considered here relate primarily to the question of fluid transport. In view of the high level of metabolic demand seen in the retina, its circulatory pattern is strangely constricted. The two main sources of blood supply are the central artery of the retina and the vessels of the choroid. According to Adler (1959), the central artery of the retina provides two capillary nets, a superficial (inner) one in the optic nerve fiber layer and a deep net between the inner nuclear layer and the outer plexiform layer. These are largely two-dimensional nets which follow the planes of the retina in their respective locations. The next vascular element found is the choriocapillaris on the external surface of the retinal epithelium. More than half of the total mass of the retina lies between these capillary networks and the choriocapillaris. Apparently the bulk of the blood supply comes from the choriocapillaris, which, according to Michaelson (1954), can supply nutrition to the retina for a distance of 130 μ. These capabilities find a morphological reflection in the appearance of the choriocapillaris vessels and the adjacent epithelium (Fig. 3), as compared to a vessel from the superficial network derived from the central artery of the retina (Fig. 4) and its surroundings. The choriocapillaris vessels form a dense anastomosing network with the endothelial cell nuclei most commonly seen oriented to the choroidal surface. This permits the plicated basal surface of the retinal cells to come into contact with the attenuated endothelial surface, which is characterized by extensive fenestrations. Figure 3 is typical in showing these fenestrations to be areas of membrane reduction rather than patent openings.

The importance of this interface in fluid transport is further indicated by the marked plications and folds seen in the basal surface of the retinal


tap
per
1 μ
m
sg
5

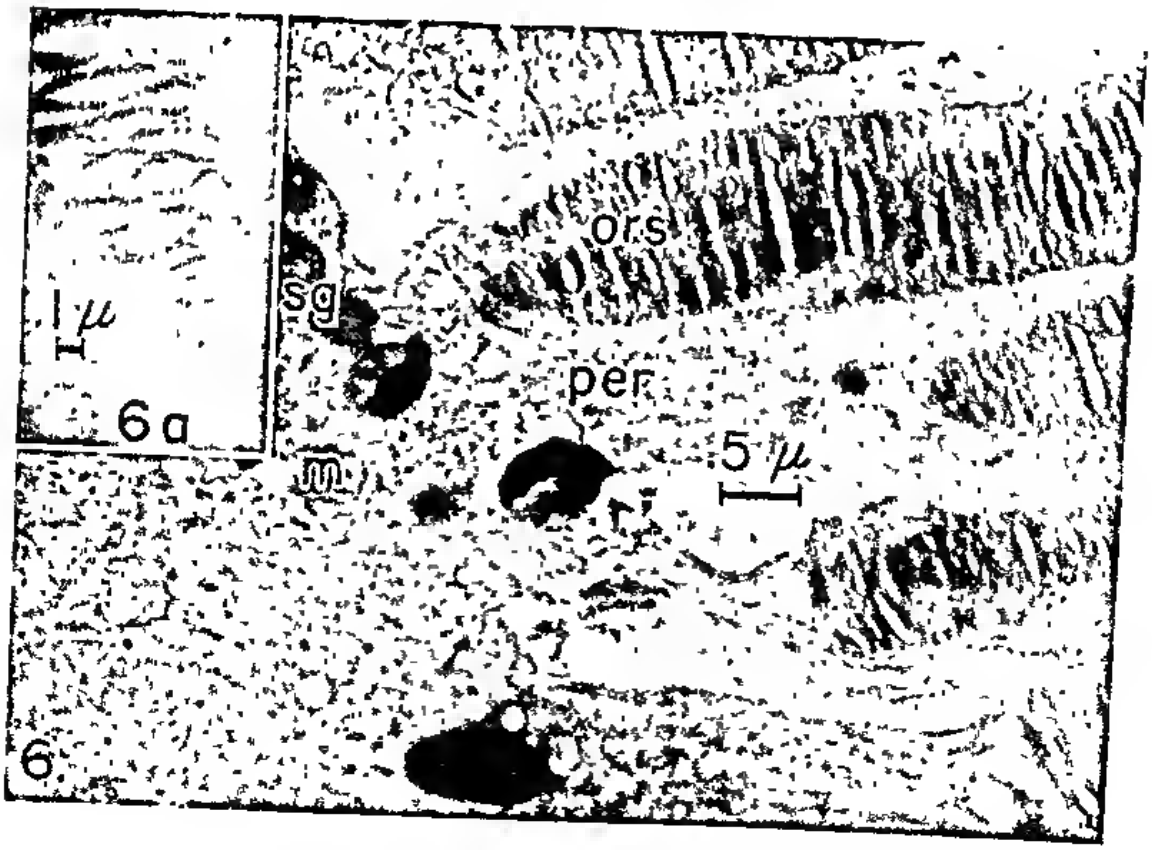
1 μ
6a
sg
ors
per
5 μ
m
6

The suggestive evidence for a synthetic (secretory) role of the pigmented epithelium of the retina is further supported by the histological interpretations of Mawas (1953), indicating this to be a secretory epithelium. That the particular fine structure of the epithelium is intimately involved in the visual process is further supported by the sharp contrast in the appearance of this same epithelium in its anterior extent, beyond the ora serrata, in the region identified as the non-neural retina. In Fig. 7 it can be seen that the choroid is covered here by a layer of epithelial cells quite different in their fine structure from the epithelial layer we have been considering. The marked interdigitations of the epithelial cells (Fig. 8) are a prominent feature. The dense ground substance packing the cytoplasm is no longer evident, nor do we see any indications of the characteristic organelles peculiar to the epithelium of the neural retina.

Discussion

Our consideration of the nature and structure of the pigmented epithelium of the retina leaves us with several unresolved anomalies. A remarkable degree of polarization indicates that the principal path of nutrient materials is from the vessels of the chorioeapillaris into the retina. This leaves the most striking concentration of metabolic machinery, the aggregation of mitochondria in the inner segments of the photoreceptor cells, in a state of spatial isolation from its main source of nutrient supply. The direct photoreceptor structures, the outer segments of the rods and cones, are apparently dependent on contact with the

---

PLATE III

FIG. 5. Cross section through the pigmented epithelium of the retina (per) in the region of the tapetum (tap). Mitochondria (m) and spherical granules (sg) are present in the epithelial cytoplasm. Note the absence of recognizable entities of the endoplasmic reticulum. The dense cytoplasm has the appearance of a featureless "ground substance."

FIG. 6. Electron micrograph of a thin section through the junctional region of the outer rod segments (ors) and the pigmented epithelium of the retina (per). Two types of epithelial processes are seen. Short thick protrusions meet the end of each outer segment. Their lateral margins continue as reflections of the epithelial cell surface to envelop the terminal portion of the outer rod segment. An intimate relationship of the outer segments and the retinal epithelium is thus established. The characteristic lipofuscin granules are present in close proximity to the outer segments. Mitochondria (m) and the dense spherical granules (sg) (see text) are seen in the cytoplasm.

FIG. 6a. At higher magnification, the reflection of the epithelial cell surface over the terminal portion of the outer rod segment is seen.


rap
1 μ
sg
5


1 μ
6a
sg
m
6

epithelium for the mechanics of regeneration of visual function. Yet the fine structure of this epithelium is unlike that of characteristically synthetic or secretory epithelial cells (Palade, 1955; Scott and Pease, 1959), which are packed with membranes of the granular reticulum.

The large spherical granules (Figs. 3 and 5) seen in the retinal epithelium are similar to the secretion granules (Scott and Pease, 1959) of glandular tissues. The work of Miyamoto and Fitzpatrick (1957) shows the pigment granules to be present and essentially complete in very early embryos, and tends to obviate any relation of these granules to pigment formation.

It is conceivable that the concentration of mitochondria seen in the inner segments of the rods and cones may relate more to the electrical transmission of the impulse initiated by light reception than to the direct metabolic maintenance and function of the photoreceptors. Furthermore, the biochemical data are indicative of a cyclic regenerative process, rather than a synthetic process involving the *de novo* production of materials destined for release or secretion. Such a regenerative process may require relatively little synthetic activity of the cells of the retinal epithelium.

PLATE IV

FIG. 7. Section through the epithelium of the non-neural retina. A portion of a choroidal melanocyte (mel) is also visible. The vacuolated cytoplasm (epi) contains an abundance of mitochondria, but none of the characteristic organelles of the epithelium of the neural retina. Recognizable elements of the endoplasmic reticulum and nuclei (nuc) are also visible.

FIG. 8. At higher magnification, the extensive interdigitation of the epithelial cells of the non-neural retina is shown. A substantial increase in the amount of intercellular substance is apparent. Conspicuous clear vacuoles indicate the site of materials lost in the normal preparation of materials for electron microscopy. Multitudinous cell membranes (cm) are present as folds, reflections, and insertions.


Cut
1 μ

References

Adler, F. H. (1959). "Physiology of the Eye." Mosby, St. Louis, Missouri.
Bernstein, M. H., and Pease, D. C. (1959). *J. Biophys. Biochem. Cytol.* **5**, 35-39.
De Robertis, E. (1956). *J. Biophys. Biochem. Cytol., Suppl.* **2**, 209-216.
Heydenreich, A. (1957). *Arch. Ophthalmol. Graefe's* **159**, 162-179.
Kühne, W. (1880). *Untersuch. physiol. Inst. Univ. Heidelberg* **3**, 221.
Mawas, J. (1953). *Ann. oculist. (Paris)* **186**, 488-506.
Maximow, A. A., and Bloom, W. (1957). "A Textbook of Histology." Saunders, Philadelphia, Pennsylvania.
Michaelson, I. C. (1954). "Retinal Circulation in Man and Animals." C. C Thomas, Springfield, Illinois.
Miyamoto, M., and Fitzpatrick, T. B. (1957). *Science* **126**, 449-450.
Palade, G. E. (1955). *J. Biophys. Biochem. Cytol.* **1**, 59-68.
Pease, D. C. (1956). *J. Biophys. Biochem. Cytol., Suppl.* **2**, 203-208.
Polyak, S. L. (1957). "The Vertebrate Visual System." University of Chicago Press, Chicago, Illinois.
Porter, K. R. (1957). *Harvey Lectures, Ser.* **51**, 175-228.
Scott, B. L., and Pease, D. C. (1959). *Am. J. Anat.* **104**, 115-161.
Sjöstrand, F. S. (1953). *J. Cellular Comp. Physiol.* **42**, 45.
Wald, G. (1958). *Exptl. Cell Research, Suppl.* **5**, 389-410.
Walls, G. L. (1942). "The Vertebrate Eye." Cranbrook Institute of Science, Bloomfield Hills, Michigan.
Yamada, E., Tokuyasu, K., and Iwaki, S. (1958). *J. Electronmicroscopy (Chiba)* **6**, 42-46.

Discussion

Dr. Dowling [Harvard University, Cambridge, Mass.]: Recently we have been studying the fine structure of the pigment epithelium in relation to our studies on vitamin A deficiency. Some of our findings may have some bearing here.

Dr. Bernstein noted difficulty in distinguishing the lateral boundaries of the pigment epithelial cells. In the rat, these boundaries are very clear and are emphasized by a characteristic alignment of mitochondria along them.

We also see several types of particles in the apical portion of the pigment epithelial cell cytoplasm. The myeloid bodies are the most conspicuous of these. In the rat, as in other animals, these are membranous structures, somewhat resembling the rod outer segments. These myeloid bodies are enclosed within a single membrane and show no continuity with the endoplasmic reticulum.

We also see smaller particles, enclosed by a membrane and granular in appearance. Often these smaller particles contain small areas of densely staining material and membranes like those in the myeloid bodies. Occasionally we see intermediate sized particles containing some granular material and many membranes. This sequence suggests that the myeloid bodies are formed from these smaller particles.

In vitamin A deficiency the myeloid bodies disappear but the smaller granular particles remain. When vitamin A is given the myeloid bodies reappear within a few days. Thus, the myeloid bodies, like the rod outer segments, seem dependent on vitamin A to maintain their structural integrity.

Some Preliminary Electron Microscopic Observations of the Outer Receptor Segments of the Retina of the Macaca rhesus[1]

A. I. COHEN

Department of Anatomy, and the Beaumont-May Institute of Neurology, Washington University School of Medicine, St. Louis, Missouri

Recent reports on the fine structure of retinal receptors have supplied comparative information for the mouse (Cohen, 1960), guinea pig (Sjöstrand, 1959), rabbit (De Robertis and Lasansky, 1958), perch (Sjostrand, 1960), frog (Moody and Robertson, 1960), and kitten (Tokuyasu and Yamada, 1959). These reports have emphasized that in both rods and cones the outer segments apparently contain a linear array of membranes which, on closer inspection, are revealed to occur in pairs, each member of which is the wall of a flattened sac. More recently, Moody and Robertson (1960) and Sjostrand (1960) have shown that in the cones of the frog and perch, the flattened sacs are in fact, infoldings of the cell membrane. While some studies on the developing outer segments have related the forming rod sacs to vesicles derived from the cell membrane (Tokuyasu and Yamada, 1959), the persistence of this physical relationship in the fully developed rod is less obvious.

In this preliminary note, we wish to confirm for the rhesus monkey, some general features described by Moody and Robertson for frog rods and cones, as well as to indicate some points of difference.

Rhesus retinas were fixed in Dalton's (1955) chrome osmic saline mixture, embedded in Araldite epoxy resin, and the sections stained with $KMnO_4$ by the method of Lawn (1960). The study has thus far been confined to the edge of the macular area. An RCA 2-E electron microscope was employed.

In the micrographs obtained herewith, the receptors were well separated by glial processes basally (Fig. 2) and by intimately associated pigmentosal filaments at their apical ends (Fig. 1). The inner segments differed principally in diameter, those of the cones being about three times the rod diameter. Both are rich in mitochondria, but a mitochondria-free zone was found at the apex of the inner segments. The

[1] This investigation has been aided in part by grant B-425 from the United States Public Health Service, National Institutes of Health.

FIG. 1. This micrograph shows an area of insertion of rod outer segments between pigment-bearing processes of pigmentosa (PIG) cells. A terminal bar (T) between two such cells and mitochondria (M) are shown. Magnification: × 16,000.

FIG. 2. This micrograph shows rod inner segment bases at the level of the external limiting membrane. At this terminal bar (T) line, evidences of intercalated glial cells (G) are seen. The penetration of rootlet fibrils (F) to this level is also evident. Magnification: × 30,000.

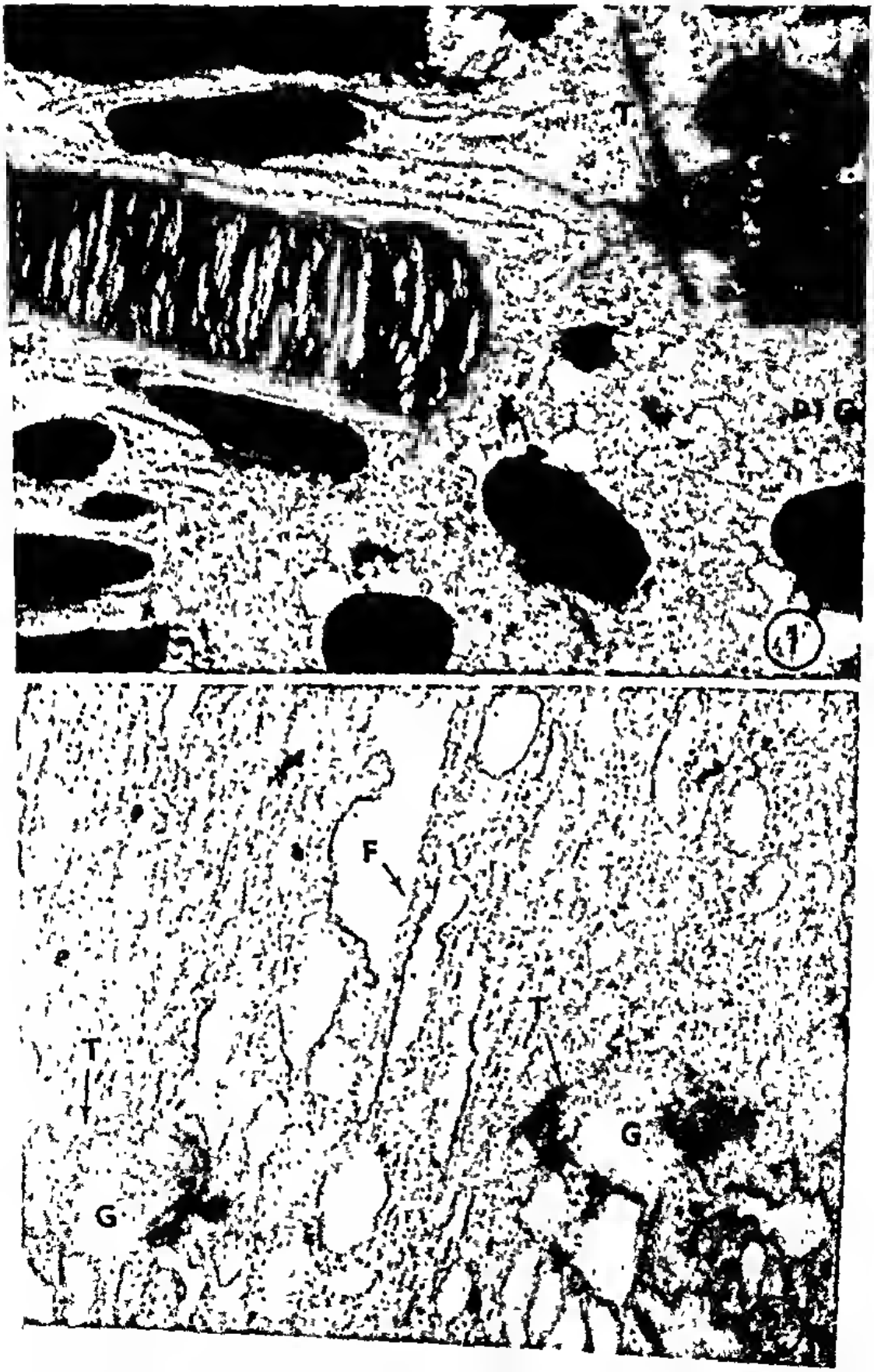
T
F
T
G
G

periphery of this apical zone enveloped the outer segment base as a calyx or cup (Figs. 3, 4, and 5).

The narrow segment between the outer and inner segment contained a flagellar stalk which ended in a basal body set in the inner segment and near a second basal body at right angles to the first. Bundles of filaments exhibiting striations were found in the inner rod segments in frequent association with vacuoles and extending in the vitreal direction at least to the level of the terminal bars constituting the external limiting membrane (Fig. 2).

In the rods, over the greater length of the outer segments, the flattened sacs did not appear to contact the cell membrane; however, evidences of infoldings of the cell membrane to form sacs were seen near the rod base (Fig. 3, arrow).

In the case of the cones, the saccular loops facing the flagellar "backbone" of the outer segment resembled the general situation in the rods, but at other points on the circumference of approximately the basal third of the outer segment of the cone, the sacs often but not always, were seen to be formed by cell membrane infoldings. The inconsistency in a particular section in the formation of sacs by membrane infolding may, in part, result from the infolding sites being confined to limited and staggered arcs of the circumference so that in any section some sacs would always be closed at both ends (Figs. 4 and 5) and, in part, to some basal sacs being discontinuous from the cell membrane. Proceeding sclerally along the distal portion of the outer segments of cones, the points of cell membrane infoldings became rarer and finally were not observed.

While some basal rod sacs were continuous with the cell membrane, others were not. It is possible that those which appeared discontinuous might fuse with the cell membrane in another plane than that of the section. It is also possible that the sacs might communicate with one another by villous processes of the kind seen in the incisures of the sacs of the rods of the mouse (Cohen, unpublished observations). Some cross-sectional views of rods have shown a scalloping of rod sac perimeters.

The continuity of cell membrane and saccule membrane may be of theoretical importance with reference to the path by which the information that a photochemical reaction has occurred reaches the receptor

---

FIG. 5. This micrograph shows membranal infoldings (INF) at a rod outer segment base but not in evidence either at the backbone (BB) or near the calyx (C). Magnification: × 55,000.

bipolar junction. This pertains even if outer segments have semiconductor properties. The information concerning the photochemical event must then traverse the narrow segment containing the flagellar stalk and then the inner segment if the transmission is intracellular.

References

Cohen, A. I. (1960). Some new observations with the electron microscope of the rods of mouse retina. *Anat. Record* **136**(2), 177 (Abstract).

Dalton, A. J. (1955). A chrome osmic fixative for electron microscopy. *Anat. Record* **121**, 281 (Abstract).

De Robertis, E., and Lasansky, A. (1958). Submicroscopic organization of retinal cones of the rabbit. *J. Biophys. Biochem. Cytol.* **4**, 743.

Lawn, A. M. (1960). The use of potassium permanganate as an electron-dense stain for sections of tissue embedded in epoxy resin. *J. Biophys. Biochem. Cytol.* **7**, 197.

Moody, M. F., and Robertson, J. D. (1960). The fine structure of some retinal receptors. *J. Biophys. Biochem. Cytol.* **7**, 87.

Sjöstrand, F. S. (1959). The ultrastructure of the retinal receptors of the vertebrate eye. *Ergeb. Biol.* **21**, 128.

Sjöstrand, F. S. (1960). Electron microscopy of the retina. *Anat. Record* **136** (2), 278 (Abstract).

Tokuyasu, K., and Yamada, E. (1959). The fine structure of the retina studied with the electron microscope. IV. Morphogenesis of outer segments of retinal rods. *J. Biophys. Biochem. Cytol.* **6**, 225.

Histochemical Observations on Esterases and Oxidative Enzymes of the Retina[1]

OLAVI ERÄNKÖ, MIKKO NIEMI, AND ESTERI MERENMIES

Department of Anatomy, University of Helsinki, Siltavuorenpenger, Helsinki, Finland

THE RETINA is known to be enzymatically very active (Pirie and Van Heyningen, 1956) and, as was pointed out by these authors, "it is more important to know the distribution of substances within the retina than to know the total in the tissue." Our work was designed to study the distribution of retinal enzymes interesting from the point of view of the impulse transmission, i.e., esterases, particularly cholinesterases, and amine oxidase, as well as enzymes involved in the oxidative metabolism of the retina, i.e., dehydrogenases, diaphorases, and cytochrome oxidase.

Material and Methods

Eyes of the following species were examined: the frog, the rat, the mouse, the guinea pig, and the rabbit. The animals were killed either by decapitation or by a blow on the head, and the eyes were either immersed as a whole in the fixative or frozen fresh. With a cryostat, sections were conveniently cut (Pearse, 1960) at 15 to 30 μ from the freshly frozen eyes, and the fresh sections mounted on cover slips. Sections from formalin-fixed eyes were cut at 20 to 30 μ with an ordinary freezing microtome, and then were rinsed in distilled water and mounted on slides. Fresh-frozen sections were used as such or after fixation in formalin and/or in ice-cold acetone. As fixatives, 3.5% formaldehyde with 1% of calcium chloride or with *M*/15 phosphate buffer, pH 7.4, were used.

For the demonstration of esterases, α-naphthyl acetate, 5-bromoindoxyl acetate, acetylthiocholine iodide, and butyrylthiocholine iodide were used. The esterase methods with the two first-mentioned substrates were essentially those given by Pearse (1953, 1960), while both Koelle's (1951) technique and Gomori's (1952) modification were used for the demonstration of cholinesterases. Eserine, 62C47 [1:5-bis-(4-trimethyl-ammonium-phenyl)-pentan-3-one di-iodide], iso-OMPA (tetraisopropyl-pyrophosphoramide), and E 600 (*p*-nitrophenol diethyl phosphate) served as selective inhibitors.

[1] This work was supported by a grant (A-1725) from the National Institute of Arthritis and Metabolic Diseases of the National Institutes of Health.

Monoamine oxidase was demonstrated both with the method of Koelle and Valk (1954) and with that of Glenner *et al.* (1957), using tryptamine hydrochloride as a substrate and iproniazide (isonicotinyl-2-isopropyl hydrazine phosphate), nialamide [1-(2-benzylcarbamyl-ethyl)-2-isonicotinyl hydrazine], and potassium cyanide as inhibitors.

Dehydrogenases and diaphorases were made visible with the methods of Hess *et al.* (1958), Scarpelli *et al.* (1958), and Novikoff and Masek (1958), using diphosphopyridine and triphosphopyridine nucleotides, sodium succinate, sodium lactate, glucose-6-phosphate, β-hydroxybutyrate, ethyl alcohol, and α-glycerophosphate as substrates. MTT [3-(4,5-dimethylthiazolyl-2-)2,5-diphenyltetrazolium bromide] and nitro-BT[2,2′-di-*p*-nitrophenyl-5,5′-diphenyl-3,3′-(3,3′-dimethoxy-4,4′-biphenylene)ditetrazolium chloride] served as color-forming electron acceptors.

Burstone's (1959) modification of the original "Nadi" reaction was used for the demonstration of cytochrome oxidase.

Results and Discussion

Esterases[2]

Nonspecific Esterases

The distribution of the reaction with α-naphthyl acetate, which is given by all esterases, was in all species strongly positive in the outer nuclear layer (Figs. 1 and 3). In the mammalian retina, intense reactions were also seen in the ganglion cell layer, in the inner plexiform layer, and the inner portion of the visual cell layer, which were less reactive in the frog retina. Species-dependent differences were further seen in the inner nuclear layer, which was moderately positive in the eyes of the mouse, the guinea pig, and the rat, but weakly stained or negative in the eyes of the frog and the rabbit.

The reaction with 5-bromoindoxyl acetate was studied only in the eyes of the mouse, the guinea pig, and the rat. It was strongly positive in all retinal layers except for the outer nuclear layer and the outer portion of the layer of rods (Fig. 5). The inner plexiform layer and the ganglion and amacrine cell layers around it exhibited the strongest reaction.

E.600 in a concentration of 10^{-4} *M* abolished altogether the reaction obtained with both acetates thus indicating that only esterases were involved. Eserine in a concentration of 10^{-4} *M* selectively inhibited the reaction in the inner plexiform layer (Figs. 2, 4, and 6), showing that it

[2] O. Eränkö and E. Merenmies are responsible for the work on esterases and amine oxidase and M. Niemi and E. Merenmies for that on dehydrogenases, diaphorases, and cytochrome oxidase.

was caused by cholinesterase activity, but did not much affect the other layers. In sections incubated in the presence of eserine, the ganglion cells and the amacrine cells stood out clearly on both sides of the almost negative inner plexiform layer.

Cholinesterases

As has been previously shown (Pepler and Pearse, 1957; Friedl, 1959) the combination of acetylthiocholine and 62C47 is particularly suitable for the histochemical demonstration of specific acetylcholinesterase, while butyrylthiocholine together with iso-OMPA selectively demonstrates nonspecific cholinesterase.

Acetylcholinesterase was positive in the inner plexiform layer in all the species examined (Figs. 7–9). Definite inner layering was often observed in it (Fig. 7), probably corresponding to the layering of the synapses. In some species, such as the guinea pig, a positive reaction was also seen in cells, presumably amacrine cells, immediately outside the inner plexiform layer. After a short incubation (1 hr with the Koelle technique, 3 hr with the Gomori technique), all other retinal layers were essentially unstained. With prolonged incubation, however, a positive reaction was seen also in the outer plexiform layer. In the frog retina, the acetylcholinesterase activity of the inner plexiform layer was much weaker than in the mammals. Prolonged incubation was therefore necessary, and it brought out a positive reaction also in the amacrine cells, the inner portion of the inner nuclear layer, and the outer plexiform layer (Fig. 9). Keeping the animals in the dark for 1 to 2 days did not affect the distribution or the activity of acetylcholinesterase.

The reaction for nonspecific cholinesterase was essentially negative after a short (see above) incubation time in all species. In some species, such as the frog, the guinea pig, and the rat, a weak reaction was seen after prolonged incubation in both plexiform layers. In the rabbit, a weak reaction became visible, in addition, in the region of the external limiting membrane and in fine fibers in the nuclear layers (Fig. 10).

Significance of Esterases

The results obtained with α-naphthyl acetate, 5-bromoindoxyl acetate, and the thiocholines as substrates clearly indicate that the inner plexiform layer is the main site of cholinesterase activity in the retina, and, furthermore, that specific acetylcholinesterase is the enzyme responsible for the reactions in this layer. This is in keeping with several earlier studies with different species (Anfinsen, 1944; Koelle and Friedenwald, 1950; De Roetth, 1950, Koelle *et al.*, 1952; Francis, 1953; Hebb *et al.*, 1953; Eichner, 1955, 1958; Leplat and Cerebtzoff, 1958; Shen *et al.*,

1956) and is strong evidence of a cholinergic transmission mechanism in this layer.

The presence of a less intense acetylcholinesterase activity in the outer plexiform layer has also been observed earlier (e.g., Koelle *et al.*, 1952; Francis, 1953), but in view of the low enzyme activity it appears questionable whether acetylcholine serves as a mediator in the synapses of this layer. For the same reason the significance of nonspecific cholinesterase in the retina seems to be rather small.

Reports on the presence of acetylcholinesterase outside the plexiform layers are in some cases explained by the use of early inadequate techniques (Koelle and Friedenwald, 1950; Hebb *et al.*, 1953) or by erroneous interpretation of the effect of inhibitors such as DFP (Eichner, 1958). However, our observations together with the studies by Koelle *et al.*

KEY TO ABBREVIATIONS ON FIGS. 1–24

gc:	ganglion cell layer	v:	visual cells
ip:	inner plexiform layer		i: inner segment
in:	inner nuclear layer		o: outer segment
on:	outer nuclear layer	p:	pigment epithelium
op:	outer plexiform layer	ch:	choroid

PLATE I

FIG. 1. Esterases in the retina of the rat. Formalin fixation, α-naphthyl acetate as a substrate. The retina (right) is detached from the choroid. The reaction is particularly strong in the inner and outer parts of the inner plexiform layer. Retinal blood vessels are also strongly stained. Magnification: × 130.

FIG. 2. Nonspecific esterases in the retina of the rat. Technique as in Fig. 1, but incubated with 10^{-4} *M* eserine, which inhibits the cholinesterases present in the inner plexiform layer. Magnification: × 130.

FIG. 3. Esterases in the retina of the mouse. Technique as in Fig. 1. Magnification: × 130.

FIG. 4. Nonspecific esterases in the retina of the mouse. Technique as in Fig. 2. Magnification: × 130.

FIG. 5. Esterases in the retina of the mouse. Formalin fixation, 5-bromoindoxyl acetate as a substrate. The distribution is otherwise almost the same as in Fig. 3, but the outer nuclear layer is essentially negative. Magnification: × 130.

FIG. 6. Nonspecific esterases in the retina of the mouse. Technique as in Fig. 5, but cholinesterases inhibited with 10^{-4} *M* eserine. Magnification: × 130.

FIG. 7. Acetylcholinesterase in the retina of the rat. Formalin fixation, acetylthiocholine and 10^{-6} iso-OMPA, the Koelle method. The reaction in the retina is limited to the inner plexiform layer, in which synaptic layering is clearly visible. Magnification: × 130.

FIG. 8. Acetylcholinesterase in the retina of the rat. Technique as in Fig. 7 but using Gomori's modification. A slight reaction is visible also in the outer plexiform layer. The strongly positive reaction on the left is in the choroid. Magnification: × 130.

(1952), Francis (1953), and Shen *et al.* (1956) show that this enzyme may also be present in the ganglion and amacrine cell layers.

The significance of nonspecific esterase activity, which was shown to be intense in several retinal layers, is as yet uncertain. Wislocki and Sid-

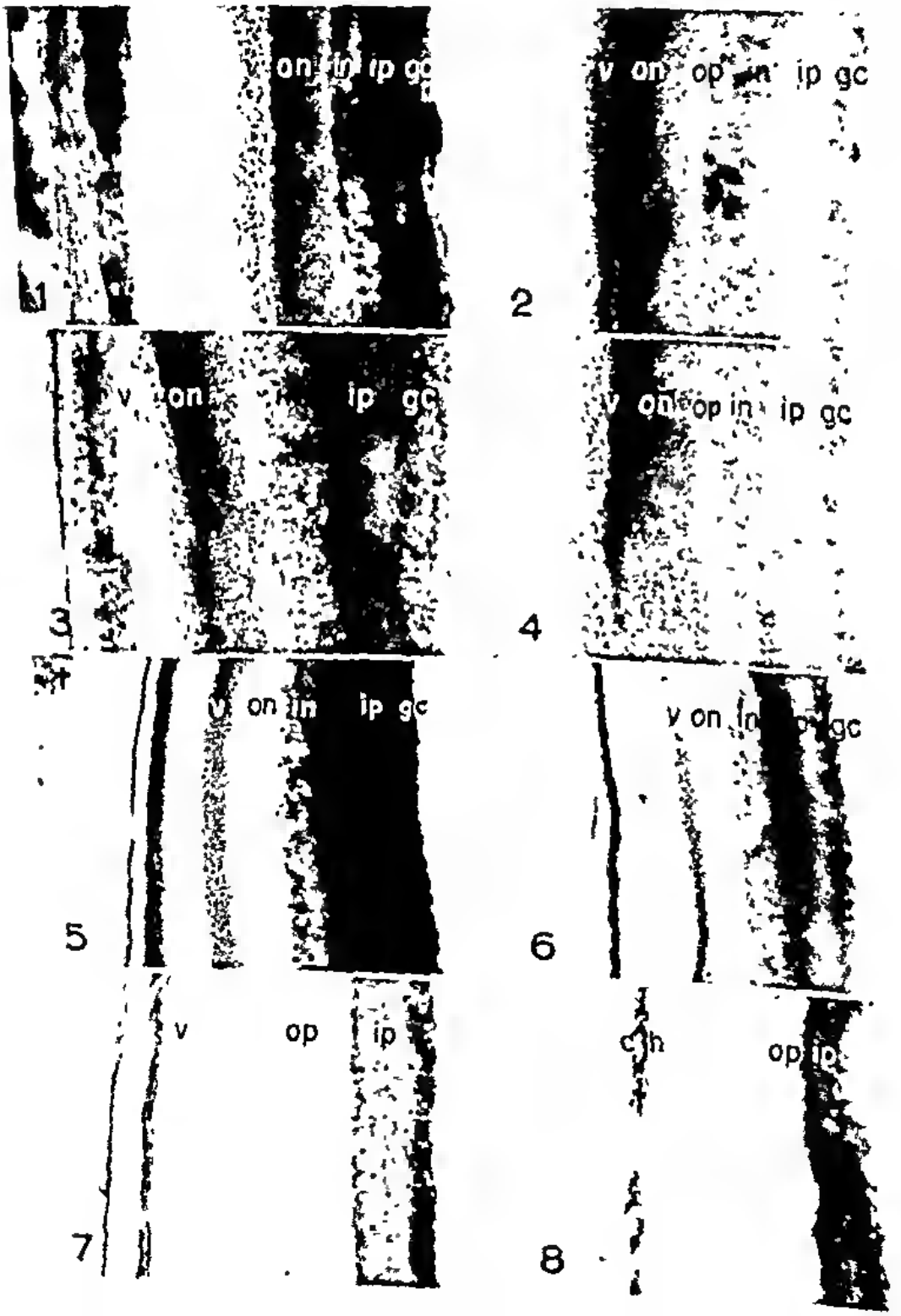

man (1954) also found a reaction which was most intense in the rods and cones and in the plexiform layers of the frog retina, but was also positive in the perinuclear cytoplasm of the nuclear layers. They did not offer any suggestions of the significance of this finding. Our observation that the enzyme is inhibited with E.600 shows that true esterases are involved. It is of interest to note that the distributions obtained with α-naphthyl acetate and 5-bromoindoxyl acetate were not identical, the former giving an intense reaction in the outer nuclear layer which was essentially negative with the latter substrate, which suggests that several types of aliesterases may be involved (cf. Pearson and Defendi, 1957).

Monoamine Oxidase

Essentially similar results were obtained with the method of Koelle and Valk (1954) and that of Glenner *et al.* (1957). A positive reaction was seen in all layers, particularly in the plexiform layers and in the inner part of the layer of rods (Figs. 11–13 and 15). In the frog retina (Fig. 11), the whole rod layer was strongly positive, while the outer

---

PLATE II

Fig. 9. Acetylcholinesterase in the dark-adapted retina of the frog. Fresh section, acetylthiocholine and 10^{-6} *M* iso-OMPA, Gomori's modification. Both plexiform layers, the amacrine cells, and a part of the inner nuclear layer exhibit enzyme activity. Magnification: × 130.

Fig. 10. Nonspecific cholinesterase in the retina of the rabbit. Fresh section, butyrylthiocholine and 10^{-5} *M* 62C47, Koelle's method. A weak reaction is visible in both plexiform layers, a part of the outer nuclear layer, and the outer limiting membrane. Magnification: × 130.

Fig. 11. Monoamine oxidase in the dark-adapted retina of the frog. Fresh section fixed in cold acetone, Glenner's method. All layers positive, the photoreceptor cells react very strongly. Magnification: × 130.

Fig. 12. Monoamine oxidase in the retina of the mouse. Fixation in formalin for 2 days, method of Koelle and Valk. Distribution as in Fig. 11, but only the inner part of the rod layer is strongly reactive. Blood vessels visible. Magnification: × 130.

Fig. 13. Monoamine oxidase in the retina of the mouse. Fixation in formalin for 2 hr, Glenner's method. Distribution as in Fig. 12, but a granular precipitate is seen in the outer limb of the rods. Magnification: × 130.

Fig. 14. Monoamine oxidase in the retina of the mouse. Technique as in Fig. 12, but incubated with 10^{-3} *M* nialamide. No essential change is apparent. Magnification: × 130.

Fig. 15. Monoamine oxidase in the retina of the rat. Technique as in Fig. 12. All layers variably positive. Magnification: × 130.

Fig. 16. Monoamine oxidase in the retina of the rat. As in Fig. 15, but incubated with 10^{-3} *M* nialamide, which did not cause any change. Magnification: × 130.

portion of the mammalian rod layer reacted but weakly (Figs. 13 and 15). Concentrations as high as 10^{-3} *M* of specific monoamine oxidase inhibitors iproniazide and nialamide had no significant effect on the intensity or the distribution of these reactions (Figs. 14 and 16). Potassium

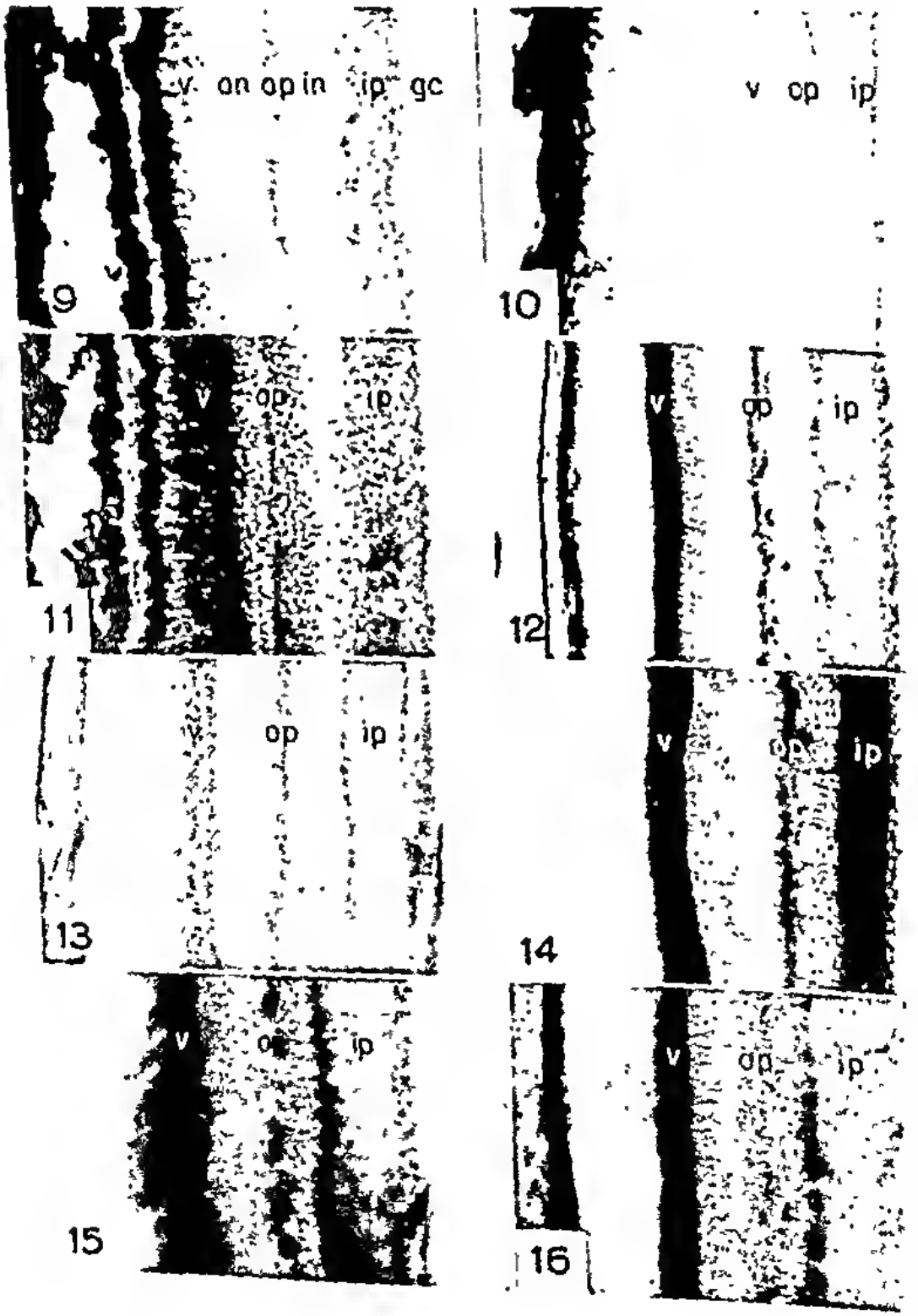

cyanide was also without effect in the same molar concentration. After incubation overnight without any substrate, a weak reaction was obtained with Glenner's method, the distribution being the same as that obtained with the substrate. However, a 3-hr incubation period with the substrate was sufficient to produce an intense reaction.

The failure of monoamine oxidase inhibitors to abolish or weaken the histochemical reactions renders it somewhat doubtful that monoamine oxidase is responsible for these reactions. However, the possibility cannot perhaps be altogether ruled out that the retinal enzyme, though a true amine oxidase, is resistant against these inhibitors. If this were so, the strong reactions in the synaptic layers of the retina might be taken to suggest that mediators other than acetylcholine, e.g., noradrenaline or hydroxytryptamine, are involved in the transmission of retinal nerve impulses. We are not aware of earlier studies on the amine oxidase activity of the retina, but it is of interest to note that Leplat and Gerebtzoff (1956) report that they have been able to demonstrate histochemically cyclic dihydroxy compounds in the layer of rods and the outer nuclear layer of the rabbit.

Dehydrogenases, Diaphorases, and Cytochrome Oxidase

Succinic Dehydrogenase

In all the species examined, a strong reaction of succinic dehydrogenase was observed in the inner segment of rods and cones (Fig. 17). The reaction was clearly localized in small, perhaps intramitochondrial granules. A moderate to strong reaction of the same granular type was observed in the outer plexiform layer of the frog, the mouse, and the rat, while this layer was colorless in the guinea pig and the rabbit. A weakly positive reaction was also seen in the inner plexiform layer of the first three mentioned species. Other regions, including the outer segment of rods and cones, were weakly reactive or negative.

DPN and TPN Diaphorases

A strong reaction was again encountered in the inner segments of rods (Figs. 18–21), with the exception of TPN diaphorase in the guinea pig. Both diaphorases exhibited a strong reaction also in the ganglion cell layer, with the exception of the frog retina, in which this layer was unstained. In other layers, marked species-dependent differences were noticed. Thus, the outer plexiform layer was strongly positive in the retina of the mouse (Fig. 19) but almost negative in the retina of the frog (Fig. 20) and the rabbit (Fig. 18). However, the distributions of DPN and TPN diaphorases resembled each other closely in each species, but may differ widely from that in other species (cf. Figs. 19 and 21).

DPN- and TPN-Linked Dehydrogenases

The nucleotide-linked dehydrogenases generally followed the localization of the corresponding diaphorases exhibiting two sites of intense activity in the inner segment of rods and in the ganglion cells (Fig. 22). In the ganglion cell layer of the frog retina, which was devoid of diaphorase activity, these dehydrogenases were naturally negative (Fig. 23); likewise, diaphorase-negative sites in any layer of any species were negative for these enzymes. In addition, negative reactions were obtained in some sites where the diaphorase reactions were positive. Thus, for example, the whole outer plexiform layer of the mouse retina showed a positive reaction for both DPN diaphorase (Fig. 19) and TPN diaphorase (Fig. 21), but lactic dehydrogenase was sharply localized only in the outer part of this layer (Fig. 22). Other notable exceptions of this type were the almost negative reactions for β-hydroxybutyrate and glucose-6-phosphate dehydrogenases in the layer of rods.

In some species, notably the guinea pig and the rabbit, thick fibers passing through the whole retina, presumably Müller's fibers, exhibited strong reactions for diaphorases and lactic, glucose-6-phosphate, and alcohol dehydrogenases. Such fibers were lacking, or were few, in the other species.

Cytochrome Oxidase

A strong reaction was observed in the outer part of the photoreceptor cells in all the species examined (Fig. 24). The inner segment of these cells was also regularly positive but usually the reaction was less intense. In the retina of the mouse and the rat, both plexiform layers and the ganglion cell layer were likewise positive, while in the frog, the guinea pig, and the rabbit these layers were weakly reactive or negative. Potassium cyanide inhibited the reaction completely in a concentration of 10^{-3} *M*. Acetone treatment before incubation did not affect the reaction.

Significance of Dehydrogenases, Diaphorases, and Cytochrome Oxidase

The inner segment of the photoreceptive cell layer was shown to contain, in all the species examined, a strong activity of succinic dehydrogenase, both diaphorases, many phosphopyridine-nucleotide-dependent dehydrogenases, including lactic dehydrogenase, and cytochrome oxidase. Strong succinic dehydrogenase activity has been observed earlier in this layer by several authors (Francis, 1952; Wislocki and Sidman, 1954; Kuwabara *et al.*, 1959; Kuwabara and Cogan, 1959; Cogan and Kuwabara, 1959). Kuwabara and his co-workers studied also lactic de-

hydrogenase and diaphorases but failed to observe them in this area, in contrast to our observation, which agrees well with the studies by Lowry *et al.* (1956), who detected biochemically lactic dehydrogenase in this region.

Obviously the inner photoreceptor cell segment is an exceedingly active area metabolically, and it is therefore not surprising that we found cytochrome oxidase there. High activity of oxidative enzymes and their apparent mitochondrial distribution fits in well with the electron microscopic observations demonstrating rich aggregations of mitochondria in this region (Sjöstrand, 1953, 1958; De Robertis, 1956; Ladman, 1958).

The strong cytochrome oxidase activity in the outer limb of the photoreceptive cells of our material confirms Akiya's (1952) observation made using the simpler type of "Nadi" reaction, and completes the observation made by Hubbard (1954) that isolated outer limbs of frog eye exhibit a high oxygen consumption. On the other hand, it is somewhat amazing that diaphorases and dehydrogenases, notably alcohol

---

PLATE III

FIG. 17. Succinic dehydrogenase in the retina of the mouse. Aggregations of formazan dots in the inner segments of the rods, the outer segments negative. Both plexiform layers reactive, the outer one strongly. Ganglion cells virtually inactive. Magnification: × 225.

FIG. 18. DPN diaphorase in the retina of the rabbit. MTT-cobalt method. Intense reactions are visible in the inner limbs of the photoreceptor cells and in the ganglion cells, whereas of the plexiform layers only the outer one shows some staining. Magnification: × 210.

FIG. 19. DPN diaphorase in the retina of the mouse. MTT-cobalt method. Both plexiform layers exhibit a definite activity, the outer one being more active. Magnification: × 200.

FIG. 20. DPN diaphorase in the retina of the frog. The intramitochondrial granules in the ellipsoids are clearly visible. The other layers are almost inactive. Magnification: × 450.

FIG. 21. TPN diaphorase activity in the retina of the mouse. The distribution is almost the same as that in Fig. 19. Magnification: × 200.

FIG. 22. Lactic dehydrogenase activity in the retina of the mouse. The eye was fixed overnight in cold formol-calcium before sectioning. The reaction is precisely localized in the ellipsoids and in the outer part of the outer plexiform layer. The latter site of reaction presumably represents the rod outer spherules. The ganglion cell layer is partly visible and exhibits activity also. Magnification: × 225.

FIG. 23. Alcohol dehydrogenase in the dark-adapted retina of a frog. The ellipsoids are most intensely stained. The outer segments of the photoreceptor cells are negative but both plexiform layers are positive. Magnification: × 130.

FIG. 24. Cytochrome oxidase in the retina of an albino guinea pig. The retina has become slightly detached from the underlying epithelium. The only active parts in the retina are the rods which are homogeneously stained. Magnification: × 225.

dehydrogenase, whose role in the rhodopsin synthesis is well known (Wald, 1956), could not be histochemically demonstrated in the outer limb.

The absence of succinic dehydrogenase from the ganglion cell layer,

which in the mammalian eye exhibited a strong activity of both diaphorases and several dehydrogenases, particularly those actively participating in glycolysis, suggests that metabolic pathways are different in the inner and outer parts of the retina. Lowry *et al.* (1956), who found little malic but much lactic dehydrogenase in the inner parts, and much malic but little lactic dehydrogenase in the outer parts of the retina, suggested that lack of oxygen in the inner layers was the reason for higher glycolytic activity in it. In this connection it must be remembered, however, that moderate activity of many diaphorases and dehydrogenases were in most species seen also in the intermediate layers. This suggests a more complicated pattern of oxidative metabolism than can be postulated on the basis of oxygen supply alone.

References

Akiya, H. (1952). *Acta Soc. Ophthalmol. Japon.* **56**, 764-779.

Anfinsen, C. B. (1944). *J. Biol. Chem.* **152**, 267-284.

Burstone, M. (1959). *J. Histochem. and Cytochem.* **7**, 112-122.

Cogan, D. G., and Kuwabara, T. J. (1959). *J. Histochem. and Cytochem.* **7**, 334-341.

De Robertis, E. (1956). *J. Biophys. Biochem. Cytol.* **2**, 319-330.

De Roetth, A., Jr. (1950). *A.M.A. Arch. Ophthalmol.* **43**, 1004-1025.

Eichner, D. (1955). *In* "Auge und Zwischenhirn," pp. 29-35. Ferdinand Enke, Stuttgart.

Eichner, D. (1958). *Z. Zellforsch. u. mikroscop. Anat.* **48**, 137-186.

Eränkö, O. (1959). *Histochemie* **1**, 257-267.

Francis, C. M. (1952). *J. Physiol. (London)* **119**, 38P.

Francis, C. M. (1953). *J. Physiol. (London)* **120**, 435-439.

Glenner, G. G., Burtner, H. J., and Brown, G. W., Jr. (1957). *J. Histochem. Cytochem.* **5**, 591-600.

Gomori, G. (1952). "Microscopic Histochemistry." University of Chicago Press. Chicago, Illinois.

Hebb, C. O., Silver, A., Swan, A. A. B., and Walsch, E. G. (1953). *Quart J. Exptl. Physiol.* **38**, 185-191.

Hess, R., Searpelli, D. G., and Pearse, A. G. E. (1958). *J. Biophys. Biochem. Cytol.* **4**, 753-760.

Hubbard, R. (1954). *J. Gen. Physiol.* **37**, 373-379.

Koelle, G. B. (1951). *J. Pharmacol. Exptl. Therap.* **103**, 153-171.

Koelle, G. B., and Friedenwald, J. S. (1950). *Am. J. Ophthalmol.* **33**, 253-256.

Koelle, G. B., and Valk, A. de T. (1954). *J. Physiol. (London)* **126**, 434-447.

Koelle, G. B., Wolfand, L., Friedenwald, J. S., and Allen, R. A. (1952). *Am. J. Ophthalmol.* **35**, 1580-1584.

Kuwabara, T., and Cogan, D. G. (1959). *J. Histochem. Cytochem.* **7**, 329-333.

Kuwabara, T., Cogan, D. G., Futterman, S., and Kinoshita, J. H. (1959). *J. Histochem. Cytochem.* **7**, 67-68.

Ladman, A. J. (1958). *J. Biophys. Biochem. Cytol.* **4**, 459-466.

Leplat, G., and Gerebtzoff, M. A. (1956). *Ann. oculist.* **189**, 121-128.

Lowry, O. H., Roberts, N. R., and Lewis, Ch. (1956). *J. Biol. Chem.* **220**, 879-892.

Novikoff, A. B., and Masek, B. (1958). *J. Histochem. Cytochem.* 6, 217.
Pearse, A. G. E. (1953). "Histochemistry, Theoretical and Applied." Churchill, London.
Pearse, A. G. E. (1960). "Histochemistry, Theoretical and Applied," 2nd ed. Churchill, London.
Pearson, B., and Defendi, V. (1957). *J. Histochem. Cytochem.* 5, 72-83.
Pepler, W. J., and Pearse, A. G. E. (1957). *J. Neurochem.* 1, 193-202.
Pirie, A., and Van Heyningen, R. (1956). "Biochemistry of the Eye." Blackwell, Oxford.
Scarpelli, D. G., Hess, R., and Pearse, A. G. E. (1958). *J. Biophys. Biochem. Cytol.* 4, 747-752.
Shen, S.-C., Greenfield, P., and Bovell, E. J. (1956). *J. Comp. Neurol.* 106, 433-462.
Sjostrand, F. S. (1953). *J. Cellular Comp. Physiol.* 42, 15-44.
Sjostrand, F. S. (1958). *J. Ultrastruct. Research* 2, 122-170.
Wald, G. (1956). *In* "Enzymes: Units of Biological Structure and Function (O. H. Gaebler, ed.), pp. 355-367. Academic Press, New York.
Wislocki, G. B., and Sidman, R. L. (1954). *J. Comp. Neurol.* 101, 53-99.

Discussion

Dr. McConnell [Ohio State University, Columbus, Ohio]: Have you observed any effect of dark or light adaptation in your studies?

Dr. Enäkö [Helsinki, Finland]: We have not found any great difference after 48 hours in the dark or light.

Dr. McConnell: We have investigated the effect of intensity and duration of exposure to light on retinal staining with methylene blue. There is a distinct difference between light- and dark-adapted retinas, particularly in the inner plexiform and outer nuclear layers. The differences are related systematically to the intensity and duration of light.

A Structural Model for a Retinal Rod[1]

J. J. WOLKEN

Biophysical Research Laboratory, Eye and Ear Hospital, University of Pittsburgh School of Medicine, Pittsburgh, Pennsylvania

IN SEARCH FOR A STRUCTURAL BASIS for photoreceptor function we are investigating the structure and the photosensitive pigment complex, in molecular dimensions.

The application of the electron microscope to the photoreceptor structure of a variety of invertebrate and vertebrate photoreceptors, has unveiled their *fine structure*. Some of these photoreceptors have already been described by Drs. Sjostrand (1959), E. De Robertis (1956), and H. Fernández-Morán (1959), as well as presented and discussed by them in this symposium. What has been revealed is that the photoreceptors, so far studied, are ordered structures of dense lamellae varying from 50 to 100 Å in thickness, the total thickness of these dense layers being of the order 200 Å, that are separated by less dense material. Professor Wald has also summarized the relation of the biochemistry of the visual complexes to the photoreceptor physiology (Wald, 1959).

Therefore it is intended to only review briefly our own electron microscopy studies of photoreceptor structures from a phylogenetic point of view; and from the experimental data, to indicate a structural model for a retinal rod. In considering the structure of the retinal rod, some experiments will be described that may have an analogy to the orientation of pigment molecules on surfaces in an ordered array similar to that found, by electron microscopy, for the photoreceptors.

In the vertebrate eye, the receptor cells of the retina are rods and cones, that lie side by side forming a mosaic of light-sensitive elements Each is composed of an inner segment and a rod- or cone-shaped outer segment These outer segments are packed plates or disks, of the order 200 Å in thickness, containing as their photosensitive pigments, either retinene$_1$ or retinene$_2$ (the aldehydes of vitamin A_1 or vitamin A_2) linked with a protein or lipoprotein opsin Such extracted pigment complexes are identified by their absorption spectra as rhodopsin (retinene$_1$ + rod opsin) or porphyropsin (retinene$_2$ + rod opsin) for the rods and iodop-

[1] Aided in part by the United States Public Health Service Institute of Neurological Diseases and Blindness (B-397-C6), the National Council to Combat Blindness (C-199-C8), and the McClintic Endowment Eye and Ear Hospital, Pittsburgh, Pennsylvania.

sin (retinene$_1$ + cone opsin) or cyanopsin (retinene$_2$ + cone opsin) for the cones (Wald, 1959).

Animals, in the course of evolution, have used various kinds of eyes for forming images. These photoreceptors are seen in the invertebrates, in which eyespots, sensory cells, ocelli, and compound eyes have arisen among annelids, mollusks, and arthropods, in each instance with differences in gross physical organization. A variety of such photoreceptors, that we have studied, are illustrated schematically in Fig. 1A-E.

In the protogoan flagellate *Euglena*, for example, the eyespot is a photoreceptor for light perception. The eyespot is an orange-red structure that is intimately linked to its flagellum. It is about 2 × 3 μ and consists of about 50 tightly packed grana of the order 0.1 μ in diameter forming a mosaic (Wolken, 1956a). The flagellum is a sensory structure into which sensitivity to physical or chemical stimuli has been incorporated. The flagellum is structurally similar to the fibril that penetrates from the outer through the inner segment of the vertebrate retinal rod (De Robertis, 1956). *Euglena* phototaxis and photokinesis (rate of swimming irrespective of direction) indicates that selective absorption by the eyespot is linked to its photomotion (Wolken and Shin, 1958). The eyespot + flagellum then acts as a receptor-effector system, directing the organism toward light, a "simple eye." The eyespot can then be considered structurally and functionally analogous to a retinal rod.

Let us next examine the *sensory cells* of the flatworm *Planaria*. Their two eyes consist of pigment granules that shade the sensory cells from light, in all directions but one, and so enable the animal to respond in a negative way to the direction of light. The sensory cells are about 5 μ in diameter, with a more variable length of approximately 35 μ, and each sensory element appears as packed tubules of the order 400 Å in diameter and each is surrounded by a wall structure of 100 Å in thickness. The appearance of tubes or lamellae depends on the angle at which the tissue is cut. These sensory cells are also structurally similar to the retinal rods (Wolken, 1958a).

The structure of the compound eye is of considerable interest in the organization of its visual cells. The compound eye consists of ommatidia; in the insect each ommatidium has a distal cone and lens, and a sheath of pigment cells which extend throughout its entire length. Each ommatidium consists of retinula cells, of which the differentiated structures are the rhabdomeres (Fig. 2). The rhabdomeres contain the photosensitive pigments and are the photoreceptors (retinal rods) in which the visual process is initiated. For example, the eye of *Drosophila* is composed of approximately 700 ommatidia; each ommatidium contains

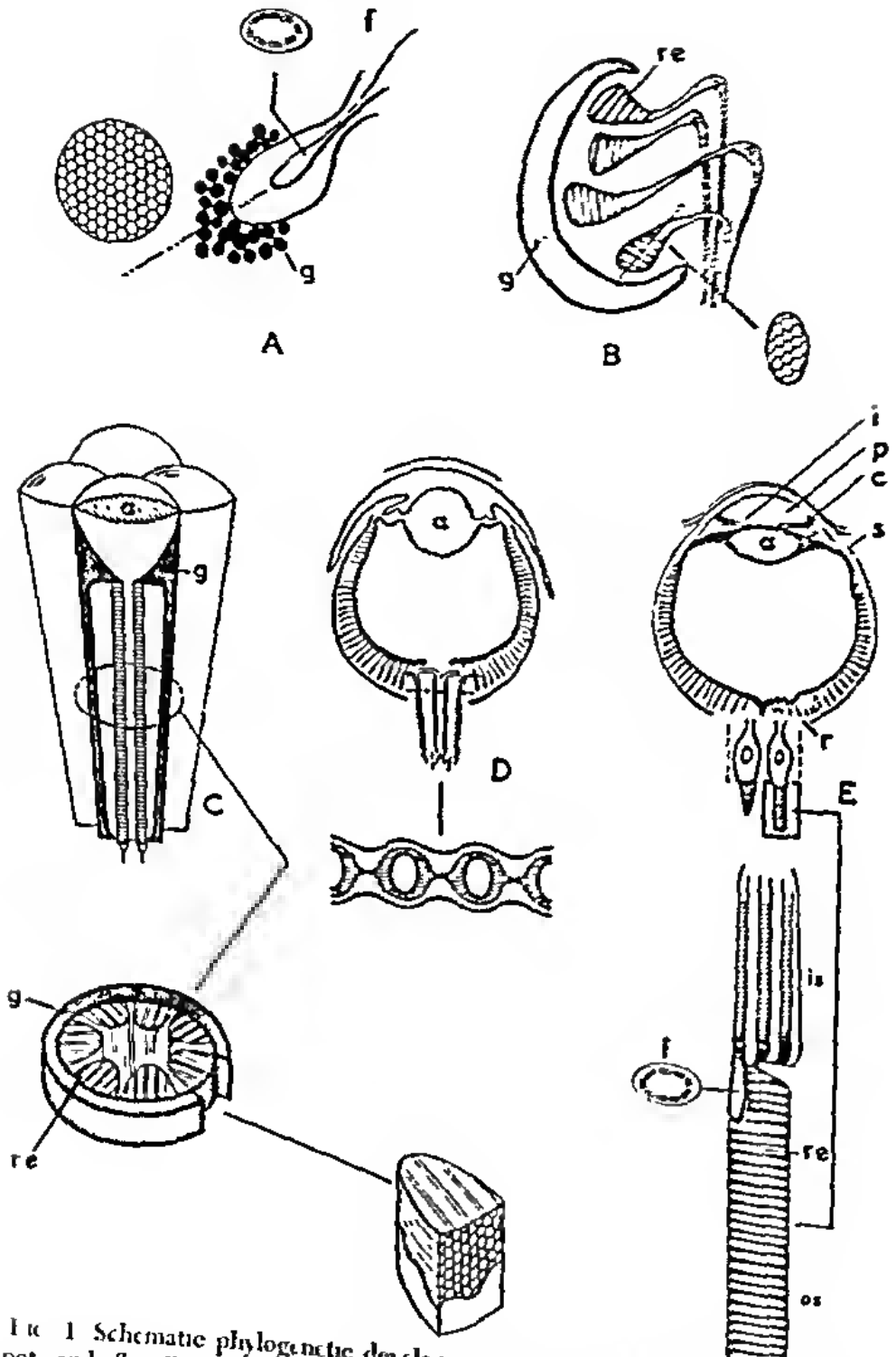

FIG. 1 Schematic phylogenetic development of the photoreceptor structures, A, eyespot and flagellum (f) (*euglena*), pigment granules (g), B, sensory cells (re) (*planaria*), surrounded by pigment granules (g); C, insect compound eye, lens (a), pigment granules (g); D, mollusk cephalopod eye showing compound retina, lens (a); E, vertebrate eye, iris (i), lens (a), pupil (p), ciliary muscle, sclera (s), and retina (r) showing an enlarged rod (re) outer segment (os) and inner segment (is). It is to be noted the structure connecting the inner with the outer segment (f) is similar to that of the eyespot with flagellum of Fig 1A.

seven retinula cells with seven rhabdomeres that are radially arranged to form a cylinder. The rhabdomeres are of the order 60 μ in length and 1 μ in diameter; they consist of tubules from 200 to 400 Å in diameter, whose walls are of the order 100 Å in thickness (Wolken *et al.*, 1957). A similar arrangement with similar dimensions is found for the housefly (Fernández-Morán, 1958; Khalaf, 1958). The visual pigment, retinene$_1$ has been isolated from the rhabdomeres of the housefly (Wolken *et al.*, 1960) and also from the honeybee (Goldsmith, 1958a, b). This would indicate that the insects too contain a rhodopsin. Many of the organisms that possess compound eyes exhibit orientation relative to the direction of vibration of polarized light, and such sensitivity to plane-polarized light, suggests the existence of a polarized light analyzer within the eye. A number of insects also show photosensitivity to the ultraviolet, and have been shown to have color discrimination. That they may possess other photosensitive pigments cannot be excluded since several photosensitive pigment complexes have been isolated (Bowness and Wolken, 1959).

We next examine the mollusks and find that their eyes resemble those of the vertebrates. However, the eye of the cephalopod *Sepia* and *Octopus* is a single lens eye, provided with a mechanism for accommodation. The lens is formed out of two halves joined together; the photoreceptors of the retina are not inverted as in the vertebrate eye, but are directly exposed to the incident light. The retina of the *Octopus* is made up of rhabdomes in which there are four rhabdomeres radially arranged forming a rhabdome (Wolken, 1958b). A central space separates the rhabdomes, that contains pigment-screening granules that migrate, depending on the light intensity (Fig. 3). Each retinal rhabdomere (rod) is of the order of 1 μ in diameter and 60 μ in length, and is made up of densely packed tubules, similar to those of the flatworm and the insects. Each tubule is of the order of 200 Å in diameter. The orientation of the rhabdomeres in the rhabdome and their internal structure are illustrated schematically in Fig. 1D. It will be noted in Fig. 1C how the retina resembles the insect compound eye.

Electron microscopic studies then distinguish an ordered structure

---

FIG. 2. The rhabdome of an ommatidia.

a. Electron micrograph showing the arrangement of the seven rhabdomeres. Magnification: × 21,500.

b. R_7 further enlarged to show the lamellae. Magnification: × 37,000.

c. A reconstructed section from electron micrograph through a rhabdomere to indicate a three-dimensional structure (as diagrammed in Fig. 1C and D). Magnification: × 46,000.


a
R1
R2
1 μ
R3
R7
R6
R4
R5
b
1 μ
0.5 μ
1
2
c

for all the photoreceptors investigated. However, they are *plates* or *disks* for the vertebrate retinal rods; *tubes* or *rods* for the invertebrate photoreceptors, all packed as a mosaic and having molecular dimensions of the order 50–200 Å (Table I and Figs. 1–4).

Geometry of the Retinal Rod

The principal components of the retinal rods are pigment, protein, and lipids. In terms of wet weight the pigment-protein rhodopsin accounts for 4 to 10%, the lipids for 20 to 40%, and the proteins for 40 to 50%. To be more specific, cattle rhodopsin constitutes 3.6% of its wet weight and 13% of its dry weight. However, frog rhodopsin constitutes 10% of its wet weight and more than 35% of its dry weight.

In order to reconstruct a structural model for the retinal rod it was necessary to visualize a geometric structure that would resemble the *in vivo* rod. One of the largest retinal rods is that of the frog which is about 6 × 55 μ and can be observed easily by light mieroscopy prior to fixation for electron microscopy. It was previously demonstrated, using polarized light, that the freshly isolated rods are ordered systems of lamellae (Schmidt, 1935). The retinal rods of the frog were isolated in dim red light and suspended in physiological saline. Upon examination in red light, they appear made-up of longitudinal fibers, 1 μ in diameter, that extend throughout the length of the entire outer segment. As soon as the white light is switched on, the outer segment swells and begins to break transversally, rather than longitudinally; when "bleached" the whole outer segment then appears as if these plates have fallen apart (Fig. 5).

The precise locations of the pigment, lipid, and protein within the outer segment of the rod can only be assumed from the chemical reactions of the tissue with the fixing agent and/or with various stains. Some experimental evidence indicates that the pigment molecules most probably reside in the (osmium-fixed) dense layers. For the geometry of the retinal rod we have taken the measurements from numerous electron micrographs of fixed (in 1% osmium tetroxide) retinal rod outer segments. The photoreceptor geometry (length, diameter, thickness, and

---

FIG. 3. *Sepia.*

a. An oblique section, electron micrograph to show the general pattern of the four rhabdomeres and their structure (refer to diagram Fig. 1C and D). Magnification: × 7000.

b. Higher magnification of rhabdomere area to show tubular packing. Magnification: × 33,000.

c. Higher magnification to show lamellar packing. Magnification: × 33,000.

number of dense layers) as determined from the electron micrographs (Table I) can be used together with the rhodopsin concentration to calculate the cross-sectional area of the rhodopsin molecule (Table II).

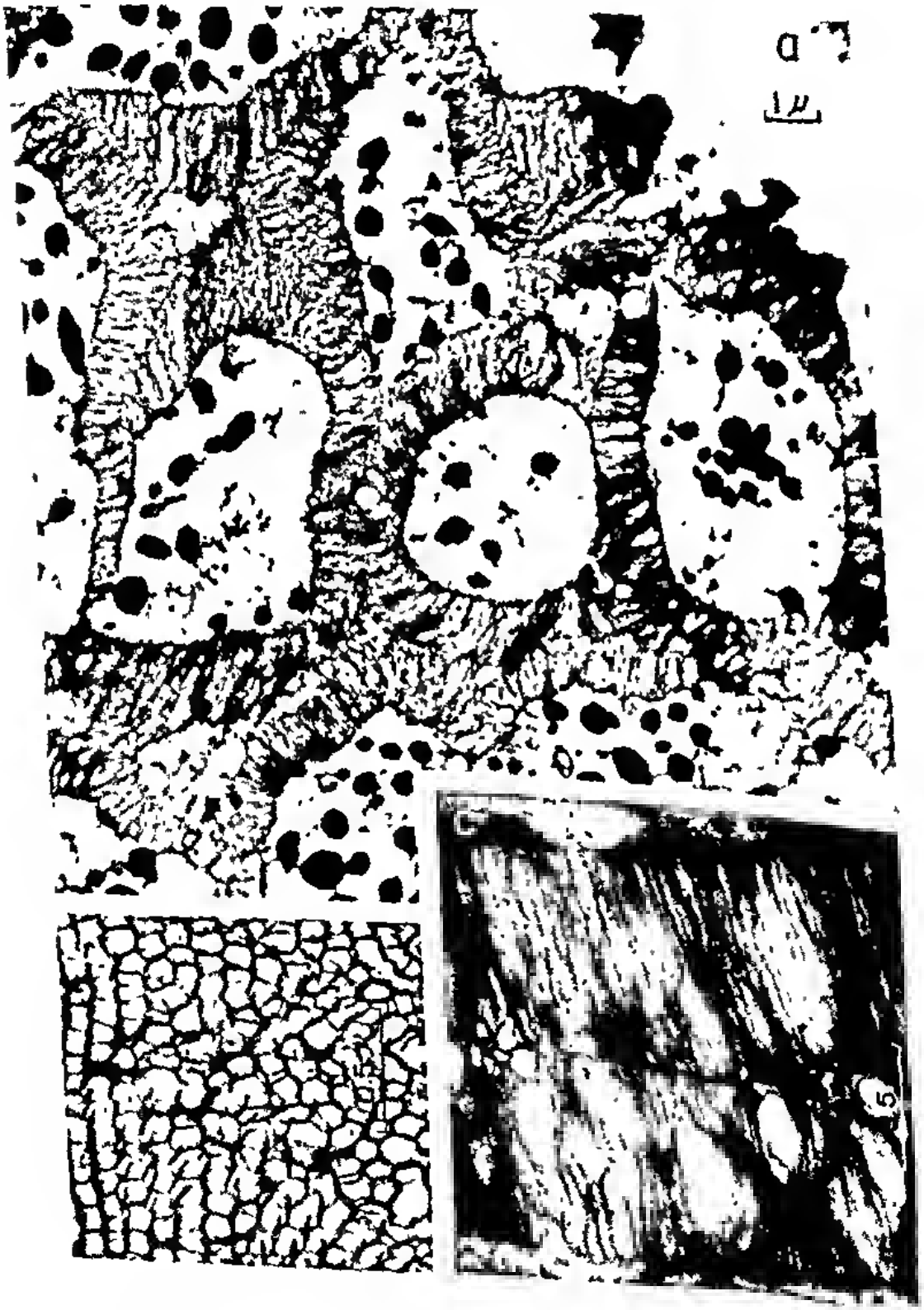

The dense layers consist of double layers of lipids and lipoproteins. A double layer is then structurally represented as lipoprotein macromolecules; the low-molecular weight lipids would then occupy the interstitial spaces. Monomolecular layers of pigment molecules occur at the interfaces between these layers. This is shown by the electron micrograph of the cattle rod (Fig. 4) and is illustrated schematically in Fig. 6. The cross-sectional area A (Table III), which would be associated with each macromolecule and therefore with each pigment molecule is

$$A = \frac{\pi D^2}{4P} \tag{1}$$

where D is the diameter of the photoreceptor and P is the number of pigment molecules in a single monolayer. The maximum cross-sectional area A with each rhodopsin molecule can be derived from the above equation, where P is replaced by $N/2n$, in which N is the pigment concentration in molecules per retinal rod and n is the number of dense layers per outer segment, then

$$A = \frac{\pi D^2 n}{2N} \tag{2}$$

The cross-sectional area calculated for cattle and frog rhodopsin was found to be 2500 Å^2 and 2620 Å^2, respectively. The diameter of the rhodopsin molecule would then be of the order 50 Å. This would be about the right order of magnitude since a rhodopsin molecule (cattle, frog) if symmetrical would have a diameter of the order 40 Å (Wald, 1954). A small area is greatly enlarged in Fig. 6, to show the molecular packing of retinene with opsin in the retinal rod-dense layers in which there would be one retinene molecule per opsin molecule. The area available therefore indicates that there would be sufficient space for all of the pigment molecules to cover all of the electron-dense surfaces. The orientation of retinene to the opsin follows from the kinetic studies of rhodopsin by Hubbard and Kropf (1959).

The rhodopsin molecular weight M can also be calculated from:

$$M = \frac{\pi D^2 TsLn}{4N} \tag{3}$$

FIG. 4. A cattle retinal rod outer segment electron micrograph.

a. Low magnification. Magnification: × 26,000.

b. An area further enlarged to show membrane and lamellae. Magnification: × 88,000.

c. A smaller area further enlarged to show the structure of the double lamellae. Magnification: × 160,000.

where D is the diameter of the photoreceptor; T is the thickness of the dense layers; s is 1.3 the density of the protein; L is Avogadro's number 6×10^{23}; n is the number of dense layers; and N is the number of pig-

TABLE I[a]

ANIMAL PHOTORECEPTORS: AVERAGE MEASUREMENTS FROM ELECTRON MICROGRAPHS

Animal	Photoreceptor	Diameter, μ	Length, μ	Volume, cm³	Total[b] thickness, Å	Kind of packing
Invertebrates						
Protozoa						
Euglena gracilis	Eyespot	2.0	3	9.4×10^{-12}	—	Rods
Platyhelminth						
Planaria	Sensory cell (retinal rod)	5.0	35	6.9×10^{-10}	140	Tubes
Arthropod						
Drosophila melanogaster	Rhabdomere	1.2	60	6.8×10^{-11}	120	Tubes
Housefly	Rhabdomere	1.2	60	6.8×10^{-11}	100	Tubes
Mollusk						
Octopus vulgaris	Rhabdomere	1.0	60	4.7×10^{-11}	200	Tubes
Sepia officinalis	Rhabdomere (retinal rod)	1.0	60	4.7×10^{-11}	200	Tubes
Vertebrates						
Frog	Retinal rod outer segment	6.0	55	1.5×10^{-9}	150	Plates
Perch	Retinal rod outer segment	1.5	40	6.2×10^{-11}	150	Plates
Chicken	Retinal rod outer segment	3.5	35	3.4×10^{-11}	250	Plates
Whale	Retinal rod outer segment	1.4	—	—	200	Plates
Cattle	Retinal rod outer segment	1.0	10	7.5×10^{-12}	220	Plates
Monkey	Retinal rod outer segment	1.3	22	2.3×10^{-11}	250	Plates
Man	Retinal rod outer segment	1.0	28	1.6×10^{-10}	250	Plates

[a] Modified from Wolken (1958a).

[b] Each lamella of the double membrane is from 50 to 100 Å in thickness. There is of the order of 1×10^6, as in the cattle rod, to 1×10^9, as in the frog rod for the number of rhodopsin molecules per retinal rod.

ment molecules per photoreceptor. The molecular weight calculated from this equation for frog and cattle rhodopsin is 60,000 and 40,000, respectively (Wolken, 1957, 1958a).

TABLE II
PHOTORECEPTORS[a]

Photoreceptor	D, photoreceptor, diameter, μ	T, thickness of dense layers, Å	n, number dense layers per photoreceptor	N, number pigment molecules per photoreceptor	M, calculated molecular weight pigment complex[b]
Frog retinal rod (*Rana pipiens*)	5.0	150	1000	3.8×10^9	60,000
Cattle retinal rod	1.0	200	180	4.2×10^8	40,000

[a] Structural data from electron microscopy.
[b] Calculated from equation (3).

TABLE III
RHODOPSIN MACROMOLECULE[a]

Retinal rods pigment macromolecule	A, cross sectional area of rhodopsin macromolecule Å^2	Diameter, d_m, Å	Length, macromolecule T/2, Å
Frog (*Rana pipiens*)	2620	51	100
Cattle	2500	50	100

[a] Calculated from the photoreceptor geometry

Calculation of the Size of Rhodopsin from Analytical Data

The visual complex rhodopsin, is prepared from the retinal rods by extraction with digitonin, a nonionic detergent ($C_{53}H_{90}O_{29}$). Rhodopsin possesses physiological activity in solution analogous to that of the intact retinal rod. It is difficult to measure the purity of these complexes, but rhodopsin can be estimated by the criteria of Wald and Brown (1953), using the ratio of its optical density, $m\mu$ $K \cdot \frac{400}{500}$, the minimum to that of the maximum. The purer the extract, the lower the ratio. Little is known chemically of the protein opsin and of how the pigment (retinene or other carotenoids) are linked with the protein. Retinene is yellow (λ max ~ 385) when it is complexed with a protein (opsin) as in rhodopsin, the shift in maximum absorption is toward the red to around 500 mμ. Retinene is attached to opsin probably through a Schiff-base linkage (Hubbard and Kropf, 1959).

The sedimentation of these complexes, rhodopsins, was studied in the analytical ultracentrifuge. From the sedimentation constant (S_{20}),

the molecular weight of rhodopsin was calculated from the Svedberg equation

$$M' = \frac{RTS_{20}}{D_{20}\ (1\text{-}p\bar{V}_{20})} \tag{4}$$

where R is the gas constant, T the absolute temperature, S_{20} the experimentally determined sedimentation, D_{20} the diffusion constant, p the density, and $\bar{V}_{20}$ the partial specific volume (Table IV). From analysis, the dry weight of frog rhodopsin averaged 20 mg/ml, of which 2.2×10^{-6} mole/liter was pigment and 0.026 mg/ml was nitrogen (Wolken, 1956b). With this information we can evaluate a molecular weight for frog rhodopsin, to be 67,000 (Table IV). The molecular weight calculated from the geometrical considerations is 60,000 (Table II). Using similar data a molecular weight of 40,000 was previously calculated by Hubbard (1954) for cattle rhodopsin. It is to be noted then the agreement between the molecular weight calculated from the geometry of the retinal rod (Table II) with that of the calculated molecular weight of rhodopsin (Table IV).

TABLE IV
RHODOPSIN[a]

Pigment complex in digitonin	Average sedimentation, S_{20}	Average complex micelle weight, M'	Average calculated molecular weight,[b] M
Cattle rhodopsin	9.77×10^{-13}	275,000	40,000
Frog rhodopsin	12.10×10^{-13}	295,000	67,000

[a] Analytical ultracentrifuge data.
[b] M is calculated from M' using the dry weights and per cent nitrogen.

Further, from the analytical data it is possible to show that one pigment molecule is most probably associated with each opsin macromolecule. This was done by demonstrating that the experimentally determined pigment concentration p is substantially the same as p' calculated from $p' = W/M'$, where W is the weight of the dried residue and M' is the pigment-complex micelle weight as determined with the ultracentrifuge (Wolken, 1956b). It cannot be excluded however that

FIG. 5. The frog retinal rod.

a, b, c, d. The "bleaching" of the frog retinal rod outer segment with light as observed with time through the light microscope. Magnifications: a, b, c, × 1800; d, × 1550.

e. A unit disk of the fixed thin-sectional retinal rod outer segment as seen with the electron microscope. Magnification: × 8000.

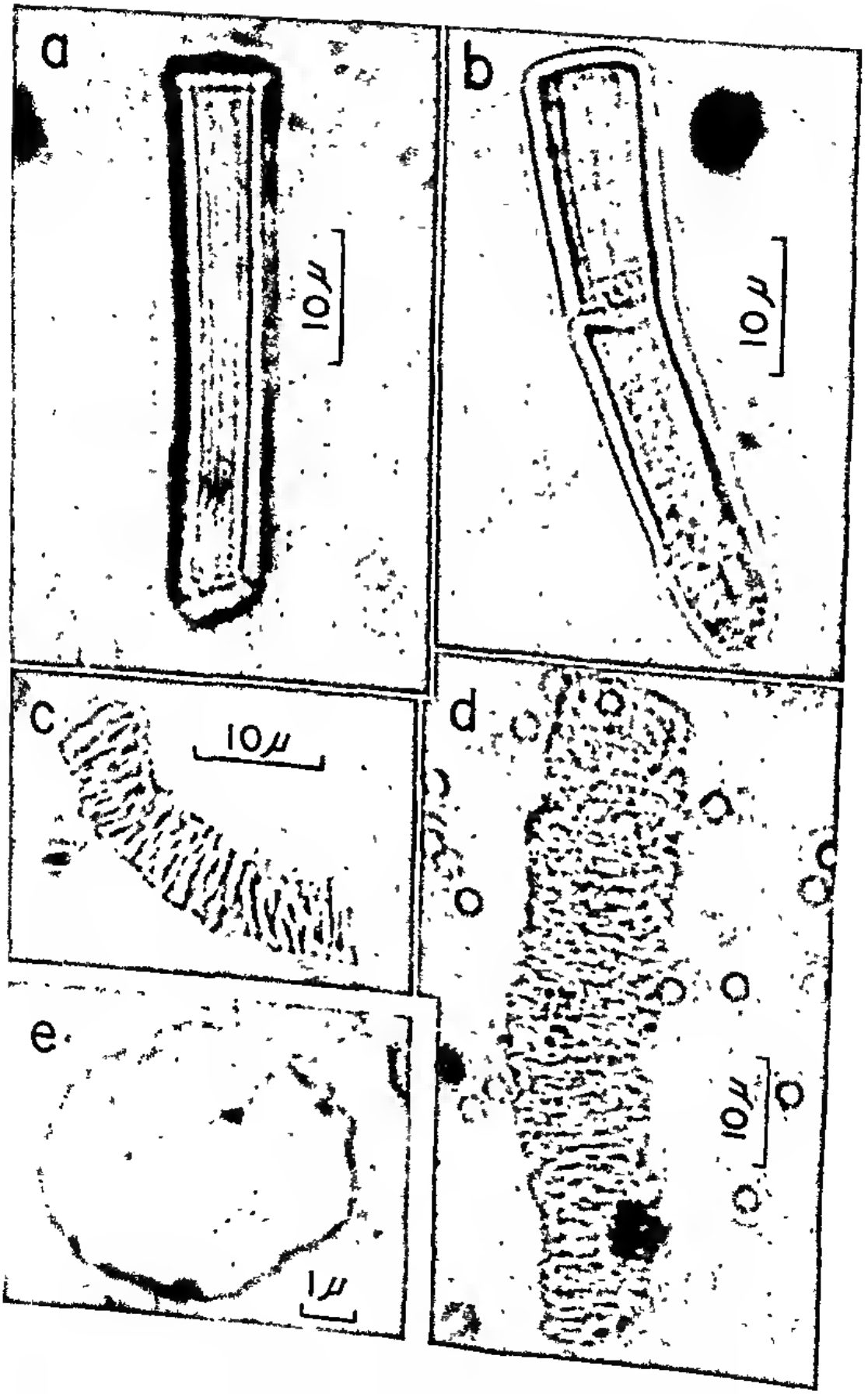
a
10μ
b
10μ
c
10μ
d
10μ
e
1μ

there may be more than one pigment molecule per macromolecule. All experimental evidence to date, though, indicates a 1:1 ratio. The maximum cross-sectional area was calculated to be of the order 50 Å for the rhodopsin molecule, indicating that retinene is loosely packed in the lamellae of the retinal rods (Fig. 6).

Periodicity

It will be remembered that in order to see the lamellae clearly the retinal rods are fixed for electron microscopy. The most widely used fixative is osmium tetroxide, although other metal-containing chemical compounds such as potassium dichromate, potassium permanganate, have been demonstrated to be effective fixatives for preserving their structure. What kind of systems then give rise to periodic structure as found for the photoreceptors? There are several such experiments on formation of periodic structures. Firstly there is the Liesegang ring phenomena; this was observed by Liesegang in the course of staining specimens for histological study by the Golgi technique (*i.e.*, the impregnation of potassium dichromate and silver nitrate into tissue). Liesegang's experiments and theories to explain the phenomena are given by Hedges (1932) and in a more recent review by Stern (1954). The formation of the ring structures can be observed if a drop of 15% silver nitrate is placed on a sheet of gelatin which has previously been impregnated with about 0.4% potassium dichromate. The silver slowly diffuses into the gelatin, there reacts with the potassium dichromate, and silver dichromate is precipitated in the gelatin. The precipitation is not continuous but forms a series of concentric rings separated by clear spaces in the gel (Fig. 7a). Another example of the same phenomena is that of gelatin saturated with ferric chloride and if a drop of potassium ferrocyanide solution should be placed in the center, blue rings of ferriferrocyanide would be formed. Light can modify these periodic precipitations if the precipitated molecules are light sensitive.

Another example of formation of periodic structures is salt crystallization in colloids or proteins. When molecules are in solution they take up configurations of lowest energy. This leads to crystallization when the number of molecules in the solution exceeds a certain minimum value characteristic of those particular molecules. An example of such a periodic crystallization is that of potassium dichromate in gelatin. The procedure is to place a drop of saturated potassium dichromate in gelatin solution on a microscope slide, warm gently, and quickly transfer the slide to the microscope. It will be observed that crystallization begins around the periphery of the drop and proceeds, by periods of rapid

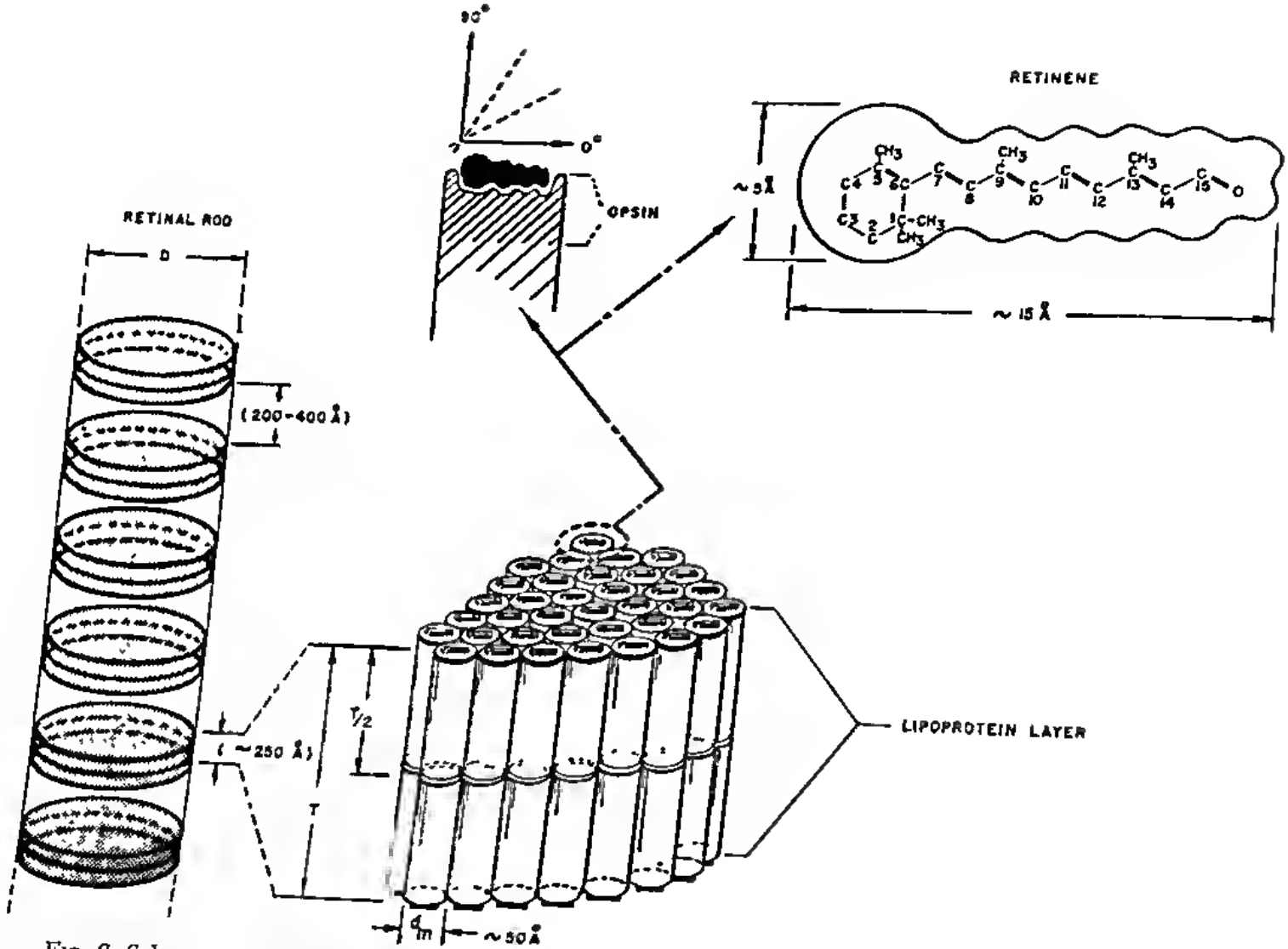

FIG. 6. Schematic model of retinal rod outer segments, indicating one retinene molecule per opsin molecule, their possible packing in the lamellae, and the attachment of retinene to opsin.

growth and slow growth, in a periodic manner. The distance between the rings decreases with the thickness of the film and with increasing rate of crystallization. The crystallization of sodium chloride is also affected by extremely small concentrations of most colloids (i.e., serum); as the ions are absorbed on the surface, the sodium chloride molecules are deposited in fine crystals on the glass surface, and at certain salt concentrations, periodic rings are formed (Lecomte du Noüy, 1926).

Now let us return to digitonin, used for extracting rhodopsin. Digitonin, a nonionic detergent, is a digitalis glycoside; its specific configuration permits combination with free cholesterol and with other natural sterols in the free state. Digitonin exhibits paracrystalline properties and when evaporated from a drop of solution on a surface, periodic rings will be formed (Fig. 7b). If a dye such as methylene blue, chlorophyll, or retinene is added to the digitonin solution and the same experiment is carried out, the dye will then be found concentrated within the rings (Fig. 7c and d). This was shown by scanning at the major absorption peak for the dye within the rings and interspaces with a microspectrophotometer (Wolken, 1960). Liquid crystals are generally divided into the smectic and nematic paracrystalline states. The more highly ordered of these is the smectic, where the molecules are arranged in equidistant parallel layers. Robinson and Ward (1957), have shown that when the synthetic polypeptide, polybenzoylglutamate L and D forms are mixed in dioxane, it then behaves as a liquid crystal. Although the solution was birefringent no regular orientation was observed with the polarization microscope, but after a short time orientation appeared on the walls of the capillary and spread toward the center with a regular orientation. If digitonin is caused to flow through a capillary, it becomes birefringent when observed through crossed polaroids; similarly when rhodopsin is caused to flow through the capillary, it too becomes birefringent.

Quantitative theories have tried to explain the formation of liquid crystals as resulting from the anisotropic interaction between long rod-like molecules. These theories indicate the essential feature that, if too many long rods are packed in a given space, they pack very poorly unless

---

FIG. 7. Periodic structures.

a. Liesegang rings formed by reaction of silver nitrate with a saturated potassium dichromate, gelatin. Magnification: × 73.

b. An aqueous 1.8% digitonin solution upon evaporation. Magnification: × 115.

c. A chloroplastin (chlorophyll-protein) in an aqueous 1.8% digitonin solution upon evaporation. Magnification: × 115.

d. Retinene in aqueous 1.8% digitonin solution upon evaporation. Magnification × 100.

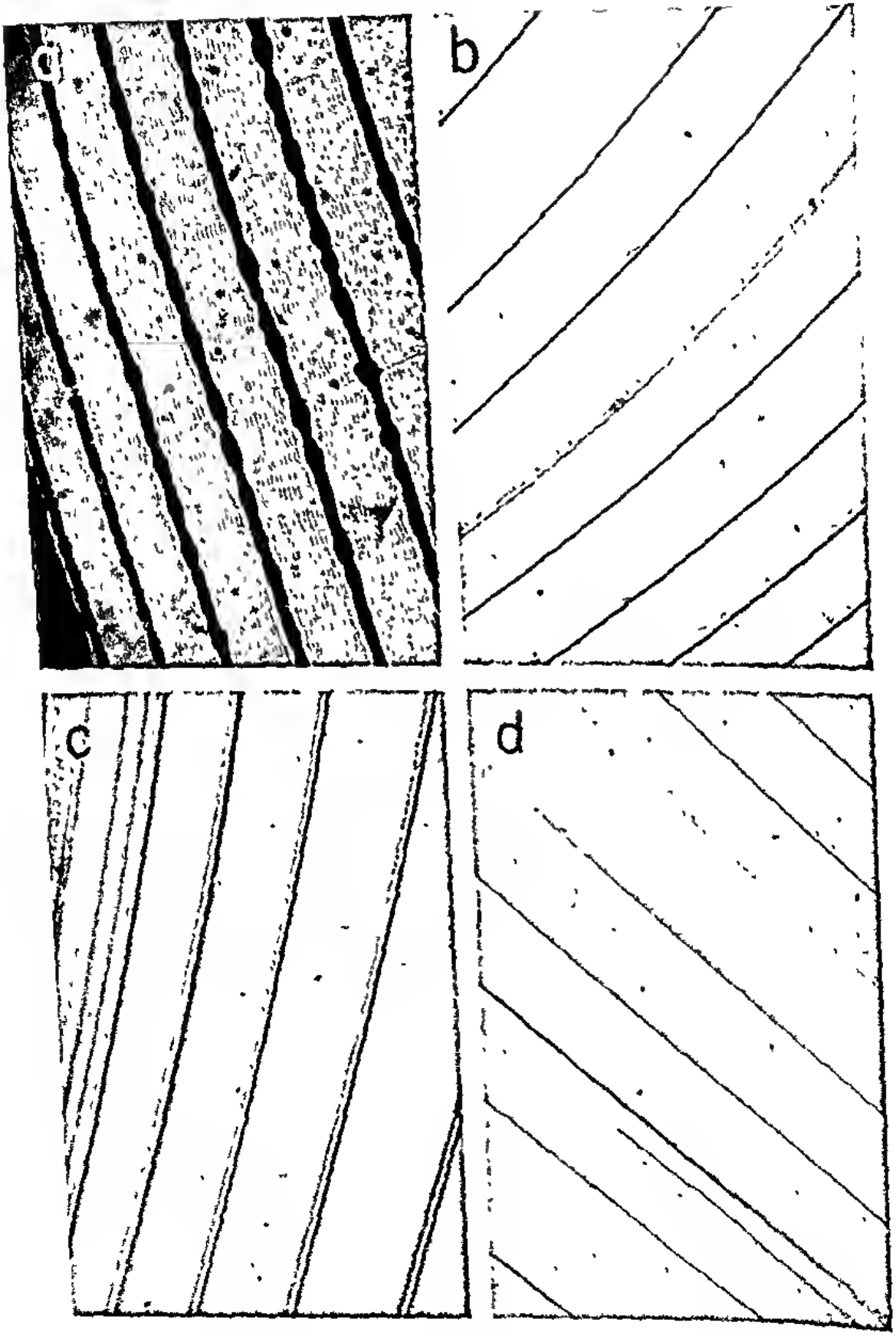
a
b
c
d

they are aligned; if aligned they can be packed more economically. Hence a concentrated solution of rod-like molecules tends to form liquid crystal structures, but if diluted, isotropic structures occur (Zimm, 1959). These experiments would indicate that the extracted rhodopsin molecules become aligned in solution with properties of a liquid crystal. Because of this behavior the structural integrity as well as the photochemistry of rhodopsin is possible.

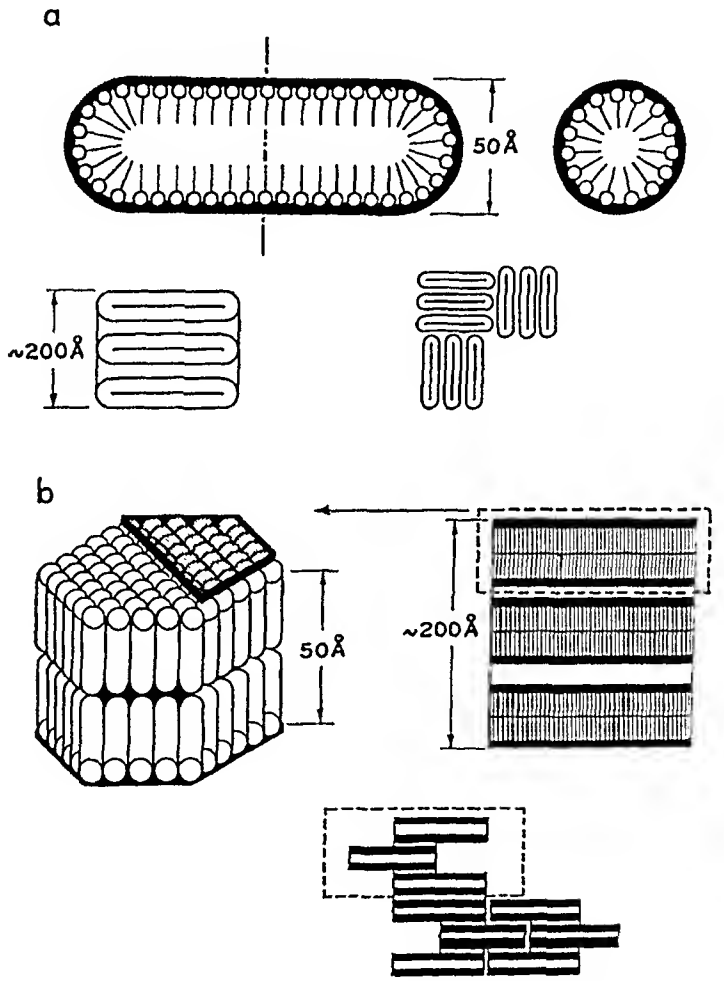

FIG. 8. Schematic model of rhodopsin digitonin micelle.

a, b. Depending on kind of packing of digitonin micelles. The rhodopsin would then be oriented on the surface of each micelle. Also showing how the micelles would pack if they formed larger units of three such micelles.

We visualize then that the orientation of rhodopsin in the digitonin micelles (Fig. 8) is similar to that of rhodopsin in the retinal rod (Fig. 6). The lamellar structure of the retinal rod may be an efficiency mechanism rather than a critical functioning device. However, this does not

exclude the probability that a liquid crystal type of matrix is necessary for orientation of the active photosensitive pigment complex.

References

Bowness, J. M., and Wolken, J. J. (1959). *J. Gen. Physiol* **42**, 779-792.
De Robertis, E. (1956). *J. Biophys. Biochem Cytol.* **2**, 319-329.
Fernández-Morán, H. (1958). "The Submicroscopic Organization and Function of Nerve Cells," pp. 566-643. Academic Press, New York.
Fernández-Morán, H. (1959). *Revs. Modern Phys.* **31**, No 2, 319-330.
Goldsmith, T. H. (1958a). *Ann N Y. Acad. Sci.* **74**, 223-229.
Goldsmith, T. H. (1958b). *Proc. Natl. Acad. Sci U. S.* **44**, 123-126.
Hedges, E (1932). "Liesegang Rings and Other Periodic Structures." Chapman and Hall, Ltd, London.
Hubbard, R. (1954). *J. Gen. Physiol.* **37**, 381-399.
Hubbard, R, and Kropf, A. (1959). *Ann. N. Y. Acad Sci.* **81**, 388-398
Khalaf, K. T. (1958). *Mikroskopie* **13**, 206-210.
Lecomte du Nouy, P. (1926). "Surface Equilibria of Biological and Organic Colloids" The Chemical Catalog Co, New York.
Robinson, C, and Ward, J. C. (1957). *Nature* **180**, 1183-1184.
Schmidt, W. J (1935). *Z. Zellforsch. u. mikroskop. Anat* **22**, 485-522.
Sjostrand, F. S. (1959). *Revs. Modern Phys.* **31**, No. 2, 301-318.
Stern, K H (1954). *Chem. Revs.* **54**, 79-99.
Wald, G. (1954) *Science* **119**, 887-892
Wald, G. (1959). "Handbook of Physiology" (Neurophysiology I), pp. 671-692. American Physiological Society, Washington, D C.
Wald, G, and Brown, P. K (1953). *J. Gen. Physiol.* **37**, 189-200.
Wolken, J J (1956a). *J. Protozool* **3**, 211-221.
Wolken, J J. (1956b) *J Cellular Comp Physiol.* **48**, 349-370.
Wolken, J J. (1957). *Trans. N Y Acad. Sci* [II], **19**, 315-327.
Wolken, J J. (1958a). *Ann. N. Y. Acad Sci.* **74**, 164-181.
Wolken, J J (1958b). *J Biophys. Biochem. Cytol.* **4**, 835-838.
Wolken, J J (1960) In "Origin and Role of Complex Macromolecular Aggregates in Development" (M V. Edds, Jr, ed.). Ronald Press, New York. In press
Wolken, J J, and Shin, E (1958) *J Protozool.* **5**, 39-46
Wolken, J J, Capenos, J., and Turano, A. M. (1957). *J. Biophys. Biochem. Cytol* **3**, 441-448.
Wolken, J J, Bowness, J M., and Scheer, I J (1960). *Biochim. et Biophys. Acta.* In press
Zimm, B M. (1959). *Revs. Modern Phys.* **31**, No. 1, 123-129.

Discussion

DU LIPETZ [Ohio State University, Columbus, Ohio]: I would like to add some evidence that the rhodopsin molecules are oriented in the rod outer segments. You will remember that Hagins attempted to test for orientation of the molecules and found that they showed no polarization of a test beam of light after an intense bleaching beam of plane polarized light had passed axially through the outer segments. This might mean that either the molecules were not oriented or that they were randomly distributed parallel to the disks in the outer segment.

Arden has found that the optical density of the rhodopsin, measured axially through the outer segments, is about twice that measure if you extract the rhodopsin or assume it is evenly distributed over the retina, or if you measure the outer segments randomly oriented in suspension. I have recently confirmed that the optical density of rhodopsin seen axially through the outer segments is about twice that seen, at an angle to the segment. This indicates that the rhodopsin molecules must be oriented within the outer segments.

Comparative Anatomy of the Mammalian Retina with Respect to the Electroretinographic Response to Light

KATHARINE TANSLEY

Institute of Ophthalmology, University of London, London, England[1]

MOST MAMMALIAN RETINAS, and all those belonging to the common laboratory mammals, have both rods and cones. Under most experimental conditions the responses of these retinas are dominated by their rod reactions There is, however, one mammalian family, the Sciuridae, the majority of whose members possess a pure-cone retina. This family embraces all the squirrel species, tree squirrels, ground squirrels, and flying squirrels as well as the chipmunks, marmots, and prairie dogs. Of all these only the flying squirrels are nocturnal in habit and are said to have a pure-rod retina. I have not examined them myself.

None of the seven squirrel and one chipmunk species so far examined from this point of view has been found to have a spectral sensitivity curve obviously associated with iodopsin (nor for that matter with rhodopsin), so that other criteria must be used in determining that these animals really do have pure-cone retinas. To begin with the general retinal structure and certain aspects of the visual cell structure are easily compatible with this view. I shall return to this point in more detail later. Their dark adaptation is rapid and not very great and their electroretinogram is of the classic cone type. Most important, none of them shows any evidence of a Purkinje shift on dark adaptation and so there is no evidence of a second scotopic mechanism, or at least not of one of any importance. All, with the possible exception of the American red squirrel *Tamiasciurus hudsonicus loquax*, are strongly diurnal in habit This is especially true of the ground squirrels and chipmunks.

In general, among vertebrates there are marked structural differences between primarily rod- and primarily cone-retinas. As an example of the rod-dominated retina we may take that of the rat or mouse (Fig. 1) Here we have many slender, tightly packed visual cells (rods), the large number of whose nuclei form a thick and prominent outer nuclear layer The inner nuclear layer is considerably thinner and the nuclei

[1] Some of the results incorporated here were obtained while the author was Visiting Scientist at the National Institute for Neurological Diseases and Blindness, National Institutes of Health, Bethesda, Maryland.

composing it are distinctly bigger than those of the rods. Thus there is a marked reduction of cells at this level, showing that there must be a convergence of many visual cells onto each bipolar cell of the inner nuclear layer. Besides bipolar cells this layer also contains the laterally orientated horizontal and amacrine cells as well as the nuclei of Müller's supporting fibers. There is a further reduction of cells when we come to the ganglion cell layer which is composed of a single row of cells not very closely packed. It is obvious that in a retina of this type there can be no question of a one-to-one relationship between visual cells and

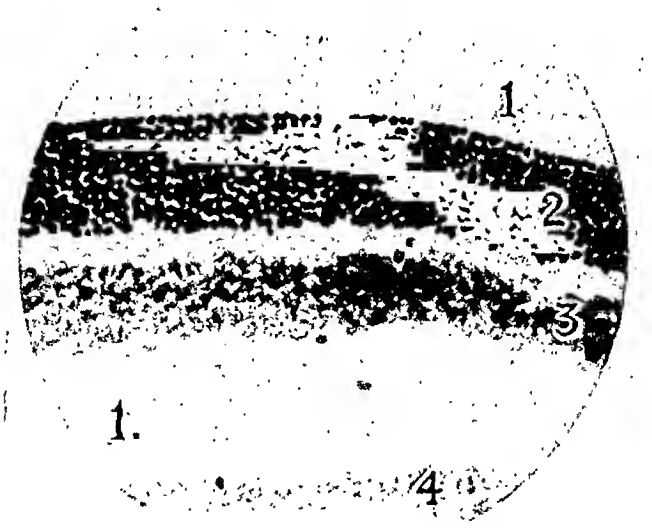

FIG. 1. Section through the nearly pure-rod retina of the rat. Bouin; hematoxylin and eosin. *Magnification:* × 325.

The following numbering applies to all retinal sections: 1, visual cells; 2, outer nuclear layer; 3, inner nuclear layer; 4, ganglion cell layer.

optic nerve fibers but that, on the contrary, a very large number of rods must finally be connected to each ganglion cell and so to each optic nerve fiber of which the ganglion cell is the nucleus. This arrangement provides for a high degree of summation of rod responses onto each optic nerve fiber, and this seems to be the basis of the high sensitivity of the rod retina.

In contrast let us look at a section of the pure-cone retina of a ground squirrel (Fig. 2). This section was taken from the central retina where the characteristic features of a cone retina are most marked. Here the visual cells per unit area are many fewer than in the rat. This fact is reflected in the comparative thinness of the outer nuclear layer, nowhere

more than about two cells thick and these cells are larger and perhaps less tightly packed than those of the rod retina. The inner nuclear layer, on the other hand, not only contains more cells than there are receptors but accommodates more than twice as many cells as there are in a comparable part of a rod retina. It is not known whether this increase is mainly due to an increased number of bipolar cells and, if so, of which type of bipolar cell. There is certainly some increase in the number of

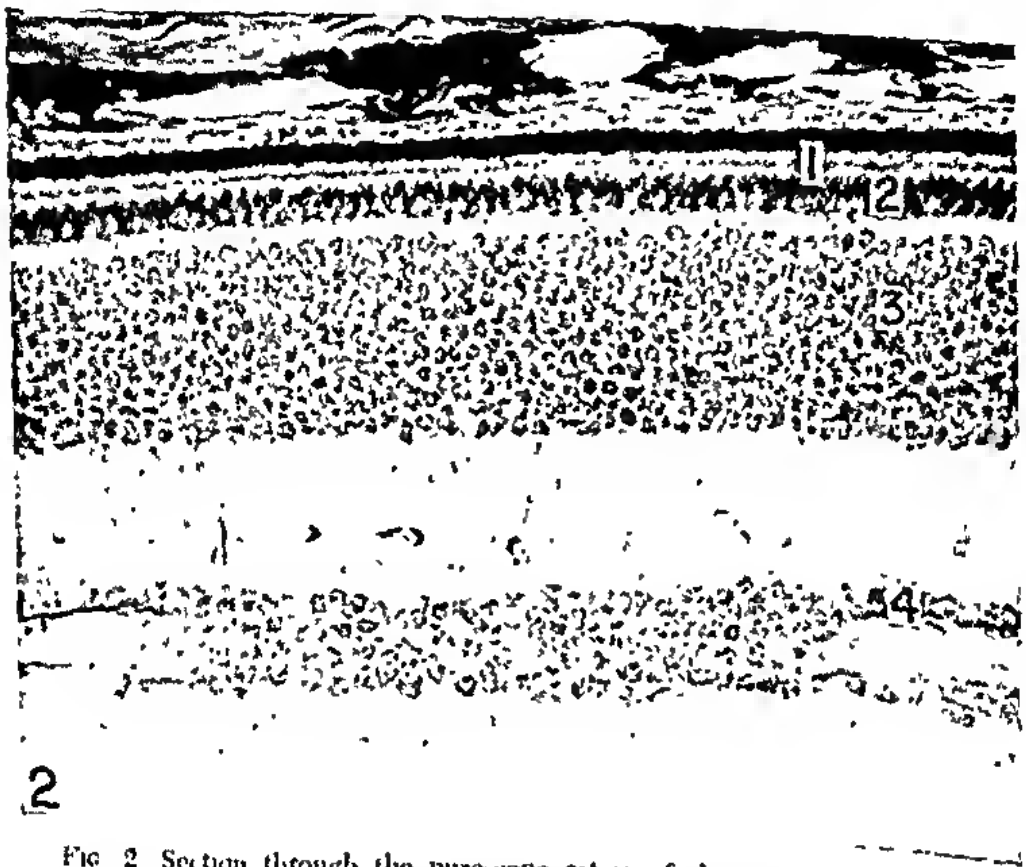

FIG. 2 Section through the pure-cone retina of the ground squirrel, *Citellus beecheyi* Boum. hematoxylin and eosin Magnification: × 285
For key to numbers, see legend to Fig. 1

horizontal cells and perhaps also of amacrine cells, but it seems probable that most of the extra cells are, in fact, bipolars of one type or another. Lastly, the ratio of ganglion cells to receptors is very much higher in a cone than in a rod retina. In the central area of the ground squirrel retina the ganglion cell layer is as much as five cells thick, giving a probable one-to-one relationship of cones to optic nerve fibers, and so the high visual acuity associated with a cone retina. This generous provision of bipolar and ganglion cells is not so marked in the peripheral retina, but the proportion of these nuclei to receptors is still high. The

additional cells which have to be accommodated in the central retina lead to a visible thickening of the retina in this area (Fig. 3).

Figure 2 was actually taken from a ground squirrel but the chipmunk retina is so similar that the figure could just as well be used to illustrate it. The tree squirrels, however, are rather different. Figure 4 shows a section through the central area of a tree squirrel retina. This section was most carefully chosen to be comparable to that from the ground squirrel shown in Fig. 2. In this retina the ganglion cell layer is never more than three cells thick and the inner nuclear layer, although

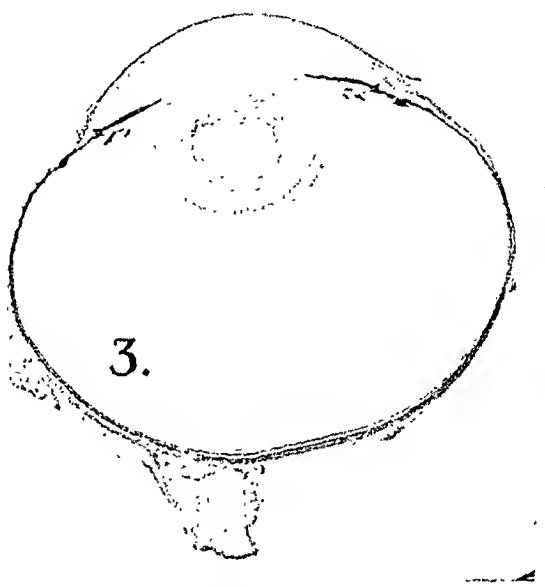

FIG. 3. Section through the whole eye of the ground squirrel, *Citellus variegatus buckleyi*. The section was cut at right angles to the linear-shaped optic papilla, typical of the diurnal squirrels. The increased thickness of the central retina can be seen to the left of the nerve head. This area is in the inferior (below) part of the fundus when the eye is *in situ*. Bouin; hematoxylin and eosin. Magnification: × 7.

always considerably thicker than the outer, is obviously smaller than that of the ground squirrel. Further, there is a most interesting modification of the visual cell layer. This is composed of a double row of cones not very obvious in Fig. 4 but well brought out with another stain and a higher power in Fig. 5. For comparison, a high power view of the ground squirrel visual cell layer is shown in Fig. 6. Thus, although the tree squirrel shows the characteristic features of a pure-cone retina, these features are not so extreme as they are in the ground squirrel and chipmunk. In this connection we have noticed that the two species of tree squirrel we have observed (the common gray squirrel, *Sciurus*

carolinensis leucotis and the American red squirrel, *Tamiosciurus hudsonicus loquax*) do not at all confine their activity to the hours between sunrise and sunset. This is particularly true of the red squirrel; three individuals kept in an outdoor cage regularly played on a revolving wheel in the evenings through the twilight until nightfall. Ground squirrels and chipmunks, on the other hand, are reported only to appear during the hours of full daylight. When we come to consider the dif-

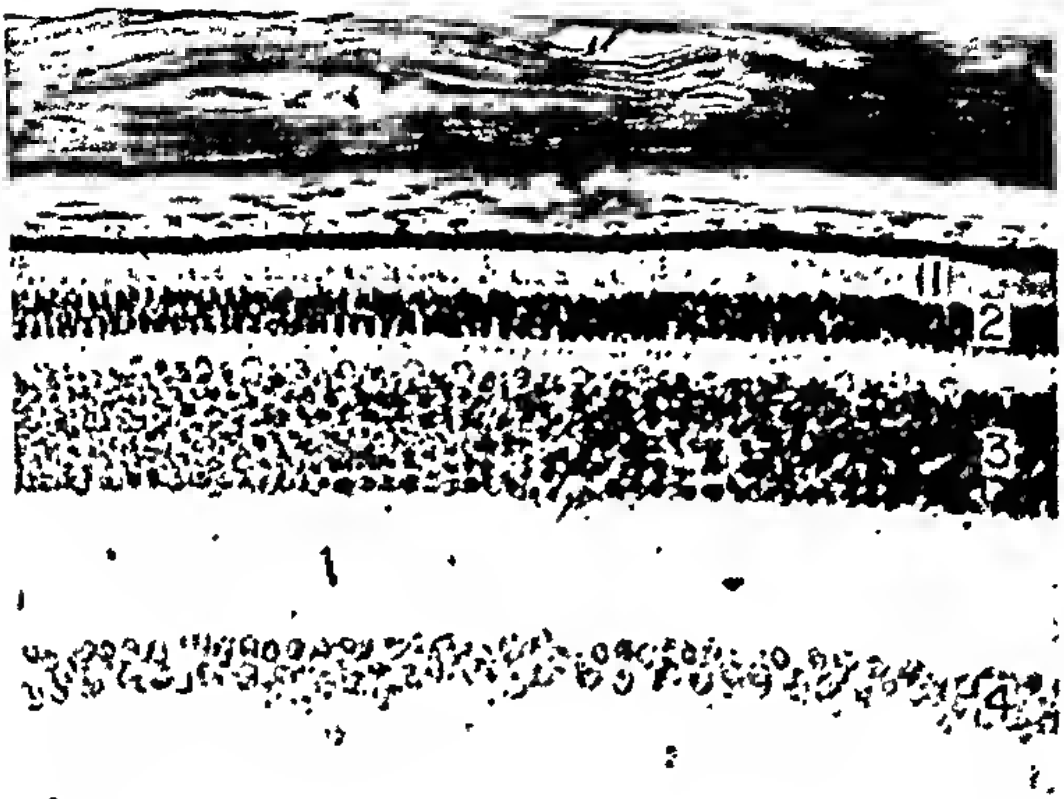

4

FIG. 4 Section through the retina of the American red squirrel, *Tamiosciurus hudsonicus loquax* Bonn, hematoxylin and eosin. Magnification: × 285.
For key to numbers, see legend to Fig. 1.

ferences between the rod and cone electroretinogram and how far the squirrel results in general, fit in with the usually accepted ideas on this subject we shall again find that, although most of its reactions are those of a cone animal, in some respects the red squirrel occupies an intermediate position between the two extremes. This does not appear to be because this animal does not have a truly pure-cone retina, for its spectral sensitivity curve is the same as that of the ground squirrels and, like them, it shows no Purkinje shift on dark adaptation. Personally I am inclined to think that the double row of visual cells in the tree squirrel

is a device for increasing the sensitivity of a pure-cone retina by increasing the number of visual cells converging onto each ganglion cell. Such a solution of the sensitivity problem would, of course, be expected to result in decreased visual acuity. We have no evidence one way or another on this point. The apparent complexity of the inner nuclear layer which is so striking in the ground squirrel retina is, in fact, a feature of other, nonmammalian, pure-cone retinas, and may be associated

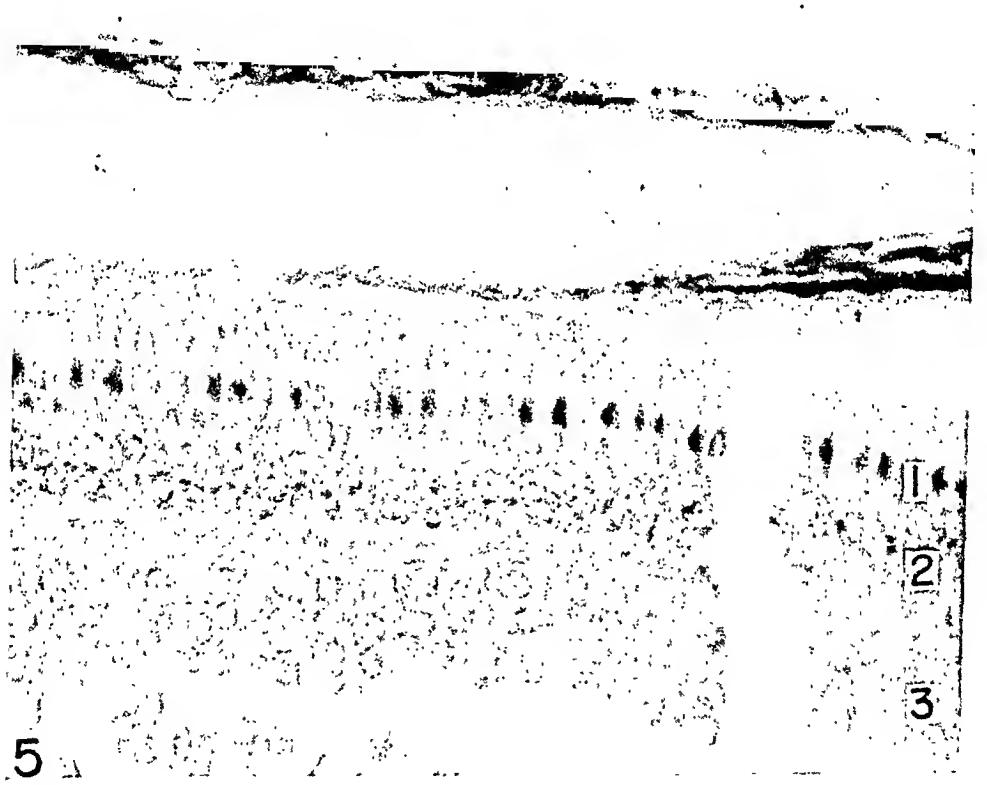

FIG. 5. Section through the visual cell layer of the gray squirrel, *Sciurus carolinensis leucotis*. Kolmer; Azan. Magnification: × 700.
For key to numbers, see legend to Fig. 1.

with some of the characteristics of the electroretinographic response to which we must now turn our attention.

Figure 7 shows electroretinograms from three animals with three different types of retina. A is from the highly rod-dominated eye of the rabbit, B shows dark- (left) and light-adapted (right) records from the mixed rod and cone eye of the frog, and C is from the gray squirrel. We have here a complete transition between an entirely rod response with *b*- and *c*-waves but no *a*-wave or off-effect and an entirely cone response with *a*-wave and off-effect, but no *c*-wave. With these stimulus intensities

the rabbit retina would give no response in light adaptation and, *except for the amplitude of the waves which would be increased*, dark adaptation does not change the characteristics of the squirrel *electroretinogram*. (We shall see shortly that dark adaptation associated with a much de-

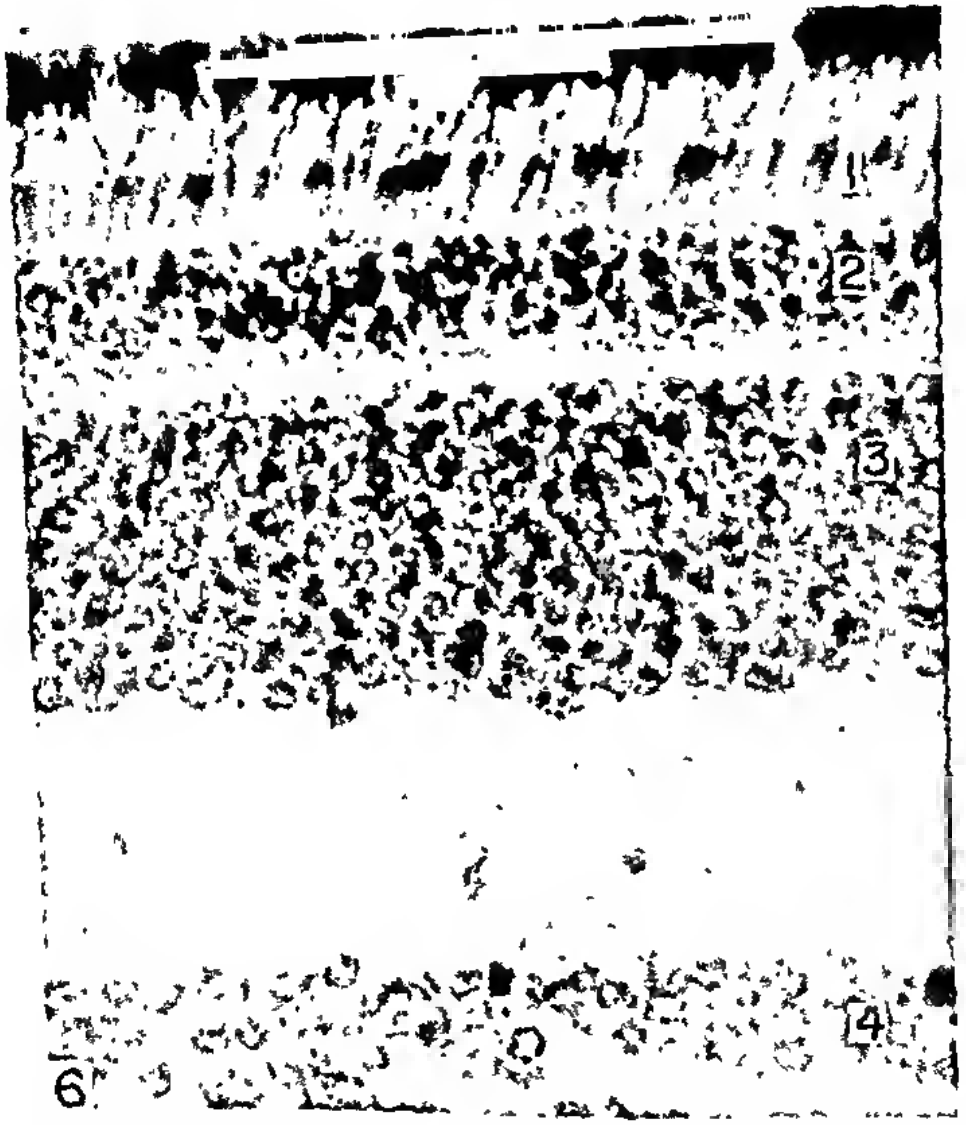

FIG. 6 Section through the visual cell layer of the ground squirrel, *Citellus lateralis* Zenker, Mallory's phosphotungstic acid hematoxylin Magnification: × 775. For key to numbers, see legend to Fig 1.

creased stimulus intensity *does* alter the squirrel response in rather a *surprising* way.) Intermediate between these two we have the mixed frog retina in which rod responses become more important in dark adaptation, and cone ones *in light* adaptation. In these two records we can see the shortening of the *b*-wave and the accentuation of the off-

effect with light adaptation, a change which, together with the large *a*-wave, is even more striking in the straight comparison between the pure-rod and the pure-cone response.

However, the differences between the rabbit and the squirrel eye do not seem to be due to a difference between rods and cones *per se*, but rather to differences in the neural organization of the two types of retina. Even the squirrel electroretinogram can be made to look like one from a rod eye by taking it in dark adaptation and with a low intensity

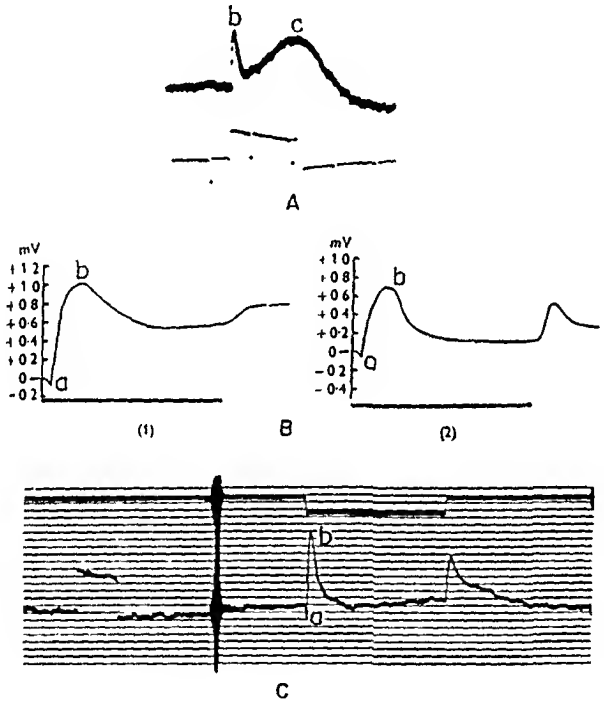

FIG. 7. Different types of electroretinogram. A, rod-dominated rabbit eye; dark adapted; one-second stimulus; B, mixed rod and cone frog eye; (1) dark adapted, (2) light adapted; two-second stimulus; C, pure-cone squirrel eye; light adapted; one-second stimulus; calibration, 100 μv.

stimulus. Figure 8 shows three gray squirrel responses to a decreasing light stimulus during dark adaptation. The disappearance of the *a*-wave and the progressive lengthening of the *b*-wave are very marked. In this experiment the stimulus was too short to give an off-effect, but even under conditions which do provide an off-effect this disappears very much sooner than the *b*-wave when the stimulus intensity is decreased.

FIG. 8. The squirrel electroretinogram. The effect of lowering the stimulus intensity on the *a*- and *b*-waves in dark adaptation. In this experiment the stimulus was too short to produce any off-effect. Time marking 50 cycles per second.

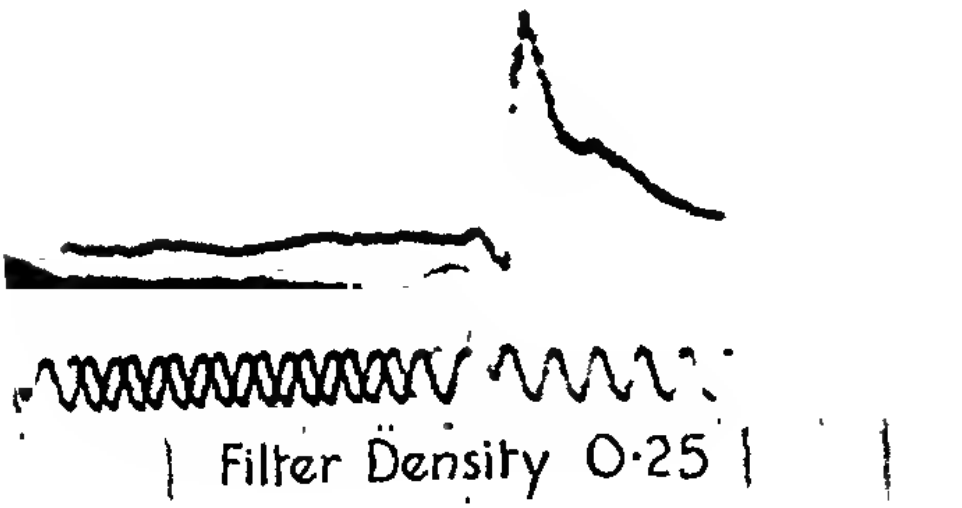
Filter Density 0·25

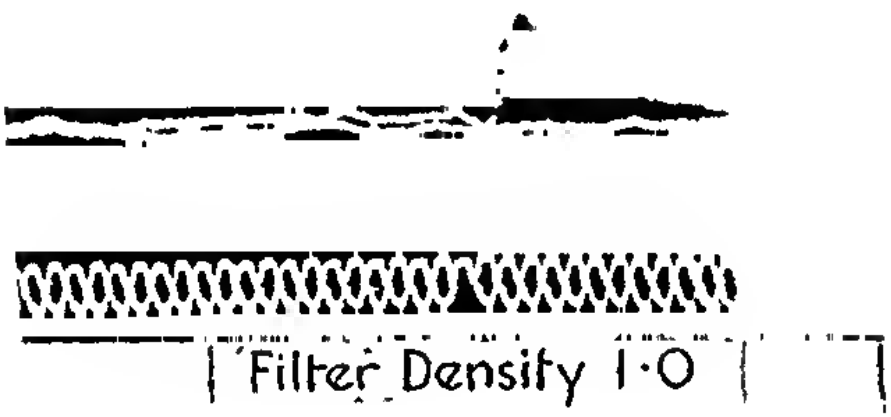
Filter Density 1·0

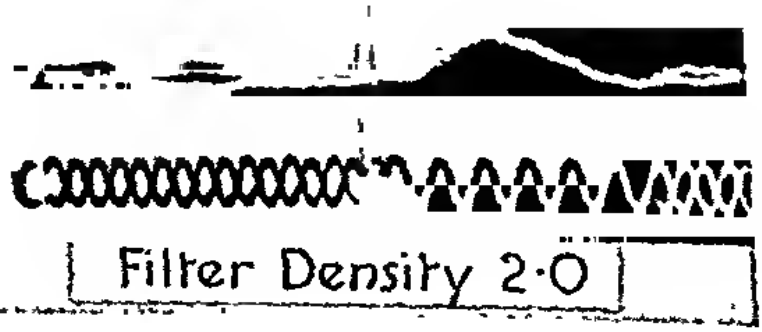
Filter Density 2·0

One finds a similar situation if one studies the flicker fusion frequency of different types of retina. Dodt (Dodt and Wirth, 1953) has shown that a pure- or nearly pure-rod retina like that of the guinea pig has a much lower fusion frequency as measured by the electroretinogram (in his experiments about 45 flashes per second) than that of the cone-dominated retina of the pigeon which can go up to about 140 flashes per second for the same stimulus intensity. In fact, Dodt uses the flicker fusion frequency as a means of differentiating between rod and cone responses. He believes (Dodt and Walther, 1958) that a fusion frequency above about 30 per second must be mediated by cones, and this may well be true, although there seems to be quite a lot of variation among cone retinas. This is not a very easy matter to work out from the literature. Dodt and Wirth found a fusion frequency of 140 per second for the pigeon using a one-to-one light-dark ratio at 8000 lux, while Bornschein and Szegvári's (1958) value for the European ground squirrel, *Citellus citellus* was around 100 per second. They used an electronic light flash of about 100 microseconds' duration and an intensity of about 300,000,000 lux. Our own values for a variety of ground squirrels and one chipmunk were also in the neighborhood of 100 per second. We used a one-to-one light-dark ratio and an intensity of about 7500 lux. Our experimental conditions were, therefore, comparable to Dodt and Wirth's, and our results to Bornschein and Szegvári's. For my present purpose it is of great interest that with exactly the same experimental conditions we were never able to record a fusion frequency of more than 65 per second for the red squirrel. So, although the value for this animal falls within Dodt's cone range, it is very markedly lower than that recorded for other cone-dominated retinas under comparable conditions. I am inclined to think that the reason may lie in the less well-differentiated neural structure of this retina with its greater convergence of visual cells onto ganglion cells, and also, perhaps to its less elaborate inner nuclear layer. The gray squirrel, however, also with a less elaborate retina but rather less at home in the dark than the red squirrel, shows a fusion frequency much nearer to that of the ground squirrels. Although superficially like that of the red squirrel, particularly in having the double row of cones, the gray squirrel retina does have more inner nuclear and ganglion cells per visual cell. Whether the increase is sufficient to account for the different flicker responses it is impossible to say. It is certainly true that the latency and the peak time of the *b*-wave of the electroretinogram of the gray squirrel falls between those of the red squirrel and the ground squirrel under comparable experimental conditions. The reactions of the red squirrel retina are a good deal slower than those of the ground squirrel and this, surely, is the reason for its lower flicker

does there seem to be much association between retinal structure and the size or speed of the off-effect, although over the whole range of vertebrate electroretinography there is an obvious link between the off-effect and cone responses. Unfortunately our recording techniques were not fast enough to provide data on the latency of the *a*-wave. So we come back to the *b*-wave, the latency and culmination time of which does, as we have just seen, seem to be associated with the retinal structure. We are now right back on the old question—where in the retina does the *b*-wave originate?

On the basis of his own and his collaborators' work Granit, as long ago as 1947, suggested that the *b*-wave arises in the bipolar layer, and later Noell (1953) obtained the only more or less direct evidence on this question in one experiment in which he cut off the central retinal artery in a monkey. Three weeks later the electroretinogram of the injured eye showed a much reduced *b*-wave but a more normal, though somewhat reduced, *a*-wave which was slower than in the control eye. Histological examination of the eye revealed that the ganglion cells had degenerated and that the inner nuclear layer was reduced to little more than one cell thick, while the visual cell layer was entirely normal. Dr. Richard Copenhaver and I have repeated this type of experiment on several ground squirrels with essentially the same result. We destroyed the retinal vessels as they left the nerve head by means of a photocoagulator. This is not a very easy operation in the squirrel for in these species the nerve head is not round but forms a long, thin, horizontal strip across the upper part of the retina with blood vessels emerging on both sides along its whole length. It is difficult to get the photocoagulator beam focused successfully onto the vessels at each end of the nerve head. However, in a few cases, the entire retinal circulation was satisfactorily destroyed. In these, much of the visual cell layer was histologically normal, although there was always considerable retinal detach-

One finds a similar situation if one studies the flicker fusion frequency of different types of retina. Dodt (Dodt and Wirth, 1953) has shown that a pure- or nearly pure-rod retina like that of the guinea pig has a much lower fusion frequency as measured by the electroretinogram (in his experiments about 45 flashes per second) than that of the cone-dominated retina of the pigeon which can go up to about 140 flashes per second for the same stimulus intensity. In fact, Dodt uses the flicker fusion frequency as a means of differentiating between rod and cone responses. He believes (Dodt and Walther, 1958) that a fusion frequency above about 30 per second must be mediated by cones, and this may well be true, although there seems to be quite a lot of variation among cone retinas. This is not a very easy matter to work out from the literature. Dodt and Wirth found a fusion frequency of 140 per second for the pigeon using a one-to-one light-dark ratio at 8000 lux, while Bornschein and Szegvári's (1958) value for the European ground squirrel, *Citellus citellus* was around 100 per second. They used an electronic light flash of about 100 microseconds' duration and an intensity of about 300,000,000 lux. Our own values for a variety of ground squirrels and one chipmunk were also in the neighborhood of 100 per second. We used a one-to-one light-dark ratio and an intensity of about 7500 lux. Our experimental conditions were, therefore, comparable to Dodt and Wirth's, and our results to Bornschein and Szegvári's. For my present purpose it is of great interest that with exactly the same experimental conditions we were never able to record a fusion frequency of more than 65 per second for the red squirrel. So, although the value for this animal falls within Dodt's cone range, it is very markedly lower than that recorded for other cone-dominated retinas under comparable conditions. I am inclined to think that the reason may lie in the less well-differentiated neural structure of this retina with its greater convergence of visual cells onto ganglion cells, and also, perhaps to its less elaborate inner nuclear layer. The gray squirrel, however, also with a less elaborate retina but rather less at home in the dark than the red squirrel, shows a fusion frequency much nearer to that of the ground squirrels. Although superficially like that of the red squirrel, particularly in having the double row of cones, the gray squirrel retina does have more inner nuclear and ganglion cells per visual cell. Whether the increase is sufficient to account for the different flicker responses it is impossible to say. It is certainly true that the latency and the peak time of the *b*-wave of the electroretinogram of the gray squirrel falls between those of the red squirrel and the ground squirrel under comparable experimental conditions. The reactions of the red squirrel retina are a good deal slower than those of the ground squirrel and this, surely, is the reason for its lower flicker

fusion frequency. All these findings suggest that when the ratio of visual cells to inner nuclear and ganglion cells increases in a retina its responses get slower. In other words, reactions which are the result of summation of stimuli take time to develop while those which are affected by the interplay of inhibitory influences are thereby speeded up. This, of course, is the old idea first put forward by Granit (1947). This speeding up of the retinal responses seems to be associated with a morphological elaboration of the inner nuclear layer.

Insofar as the electroretinographic technique is concerned, the responses that matter are apparently not at the ganglion cell level, since all the evidence suggests that this part of the retina is without effect on the electroretinogram (Granit, 1955). Nor, within our squirrel material, does there seem to be much association between retinal structure and the size or speed of the off-effect, although over the whole range of vertebrate electroretinography there is an obvious link between the off-effect and cone responses. Unfortunately our recording techniques were not fast enough to provide data on the latency of the *a*-wave. So we come back to the *b*-wave, the latency and culmination time of which does, as we have just seen, seem to be associated with the retinal structure. We are now right back on the old question—where in the retina does the *b*-wave originate?

On the basis of his own and his collaborators' work Granit, as long ago as 1947, suggested that the *b*-wave arises in the bipolar layer, and later Noell (1953) obtained the only more or less direct evidence on this question in one experiment in which he cut off the central retinal artery in a monkey. Three weeks later the electroretinogram of the injured eye showed a much reduced *b*-wave but a more normal, though somewhat reduced, *a*-wave which was slower than in the control eye. Histological examination of the eye revealed that the ganglion cells had degenerated and that the inner nuclear layer was reduced to little more than one cell thick, while the visual cell layer was entirely normal. Dr. Richard Copenhaver and I have repeated this type of experiment on several ground squirrels with essentially the same result. We destroyed the retinal vessels as they left the nerve head by means of a photocoagulator. This is not a very easy operation in the squirrel for in these species the nerve head is not round but forms a long, thin, horizontal strip across the upper part of the retina with blood vessels emerging on both sides along its whole length. It is difficult to get the photocoagulator beam focused successfully onto the vessels at each end of the nerve head. However, in a few cases, the entire retinal circulation was satisfactorily destroyed. In these, much of the visual cell layer was histologically normal, although there was always considerable retinal detach-

ment. The ganglion cells had disappeared but in no case did we succeed in destroying the whole of the inner nuclear layer. Figure 9 is a fairly representative example of what happened. The visual cell layer is apparently intact and healthy, but the inner nuclear layer has been reduced to less than half its original width and there are no ganglion cells left (compare Fig. 2 for a normal retina of the same species). So far as one can tell the lost cells are from the *inner* part of the inner nuclear

FIG. 9. Section through the retina of the ground squirrel, *Citellus beecheyi*, 2 weeks after destruction of the retinal circulation by photocoagulation. The ganglion cells have completely disappeared and the inner nuclear layer has been much reduced. Bouin; hematoxylin and eosin. Magnification: × 400.

For key to numbers, see legend to Fig. 1.

layer and would, therefore, be expected to be the amacrine and some of the bipolar cells. Figure 10 shows electroretinograms recorded from the same animal before and 2 weeks after photocoagulation. The fact that there was extensive retinal detachment and that some areas of this retina were completely degenerate, apparently as a consequence of the detachment, probably accounts for the general decrease of response. All the same it is clear that while the *b*-wave has been virtually destroyed, the *a*-wave has been less seriously affected and the off-effect,

although diminished is still well marked. This result suggests that, in any case in these squirrels, the off-effect must, to some extent at least, be independent of whatever mechanism is responsible for the *b*-wave.

The general result of these experiments was to confirm the old view that the *a*-wave arises in the outer part of the retina and the *b*-wave nearer to the inner surface. I think that problems arise with regard to the off-effect which we cannot consider in detail here. In these pure-cone retinas the off-effect not only shows considerable independence

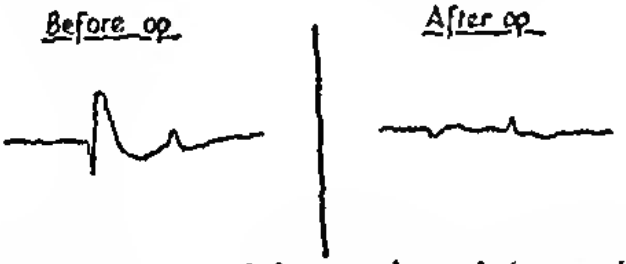

FIG. 10 Effect of destruction of the retinal circulation on the squirrel electroretinogram Records taken from the animal whose retina is shown in Fig. 9, left, before the operation, right, under the same experimental conditions 2 weeks later; 0.25 second stimulus

of the *b*-wave but also, under some conditions, of the *a*-wave as well. One interesting point is that even where the entire retinal circulation was destroyed we never managed to kill the outer part of the inner nuclear layer. It would seem that in the squirrels this part of the retina must derive its nourishment from the choroid rather than from the retinal circulation. This is not, perhaps, so very surprising when one considers how much less widely the inner nuclear layer is separated from the choroidal vessels than is the case in a retina containing many rods and, therefore, a really thick outer nuclear layer.

REFERENCES

Bornschein, H, and Szegvári, G (1958) Z Biol **110**, 285-290.
Dodt, E, and Walther, J B (1958) *Experientia* **14**, 142.
Dodt, E, and Wirth, A. (1953) *Acta Physiol Scand* **30**, 80-89.
Granit, R (1947) "Sensory Mechanisms of the Retina," Cumberlege and Oxford Univ Press, London and New York
Granit, R (1955) "Receptors and Sensory Perception" Yale Univ. Press, New Haven, Connecticut
Noell, W K (1953) USAF School of Aviation Med No. 21-1201-0004, Report No 1, 74-75

DISCUSSION

DR PRINCE [Ohio State University, Columbus, Ohio]: Would it not be helpful to investigate a squirrel with an all-rod retina? The African ground squirrel is possibly such an animal. It possesses a rectangular oblong pupil and is, I understand, completely nocturnal

CHAIRMAN CARPENTER [Tufts University, Medford, Mass.]: Do you suggest that the increase in the internal nuclear layer, with perhaps many more horizontal intraretinal neurons, may be a summation mechanism?

DR. TANSLEY [London, England]: No; summation, that is, a high ratio of receptors to optic nerve fibers, is a feature of the rod retina and the enormous amount that is possible in such a retina is one of the bases of its high sensitivity. In a cone retina, with its apparently complex inner nuclear layer, there appears to be a considerable amount of inhibition. It is an old idea of Granit's that inhibition cuts short a previous excitation and so clears the field for the next. In this way the retina can react faster, whereas it seems that summation takes time. The flicker results could be explained in these lines.

CHAIRMAN CARPENTER: Summation is usually at the expense of resolution, and a squirrel really needs good resolution.

DR. TANSLEY: It is probable that the red squirrel does not have as good resolution as the ground squirrels.

The Development and Histochemistry of the Pecten Oculi[1]

RONAN O'RAHILLY AND DAVID B. MEYER[2]

Department of Anatomy, Wayne State University College of Medicine, Detroit, Michigan

THE LATIN TERM PECTEN (*peigne* in French, *Fächer* in German) is used for a pigmented, intraocular projection which is peculiar to the avian eye.[3] It is believed that it was described originally in 1676 by C. Perrault (1613-1688). Further observations were made by Petit (1735).

In modern birds, the pecten is generally somewhat fan-shaped (for which reason it is termed *Fächer* in German) and the pleats, which are arranged as in corrugated iron, are commonly held in place by a crest or bridge of tissue (Fig. 1). The number of pleats,[4] which varies from about 3 to 30, is approximately 18 in *Gallus domesticus* (Mann, 1924a, b). The pecten projects from the optic disk into the vitreous body.[5] The base of the organ indicates the course of the embryonic retinal (or so-called "choroid") fissure, and the bridge is adherent to the vitreous body. The functional significance of the pecten, which is still in dispute, has been reviewed briefly by Mann (1924a, b), Baesich and Gellért (1935), Walls (1942), and Duke-Elder (1958). According to most writers, "the main function of the pecten is the nutrition of the retina . . ." (Mann, 1924b). Kauth and Sommer (1953) found, as a result of a biochemical investigation, that the pecten is extraordinarily rich in carbonic anhydrase and they refer to it as a respiratory organ for the interior of the eye. Baesich and Gellért, however, believe that the pecten acts as a heating element for the avian eye. A number of other functions have been proposed. Crozier and Wolf (1944a, b), for example, support the suggestion of

[1] This investigation was supported by research grant B-886 from the National Institute of Neurological Diseases and Blindness of the National Institutes of Health, U S Public Health Service

[2] U S Public Health Service Postdoctoral Research Fellow.

[3] A comparable vascular, pigmented projection (the *conus papillaris*) from the optic disk is found in lizards. The falciform process of teleostean fishes is a vascular, pigmented projection from the choroid through the retinal fissure.

[4] The number of pleats and the size of the pecten in various species of birds are given by Kajikawa (1923) and by Baesich and Gellért (1935).

[5] Lindahl and Jokl (1922), because of the close developmental relationship between the insertion of the optic nerve and the pecten, refer to the two structures as the "neuropecten."

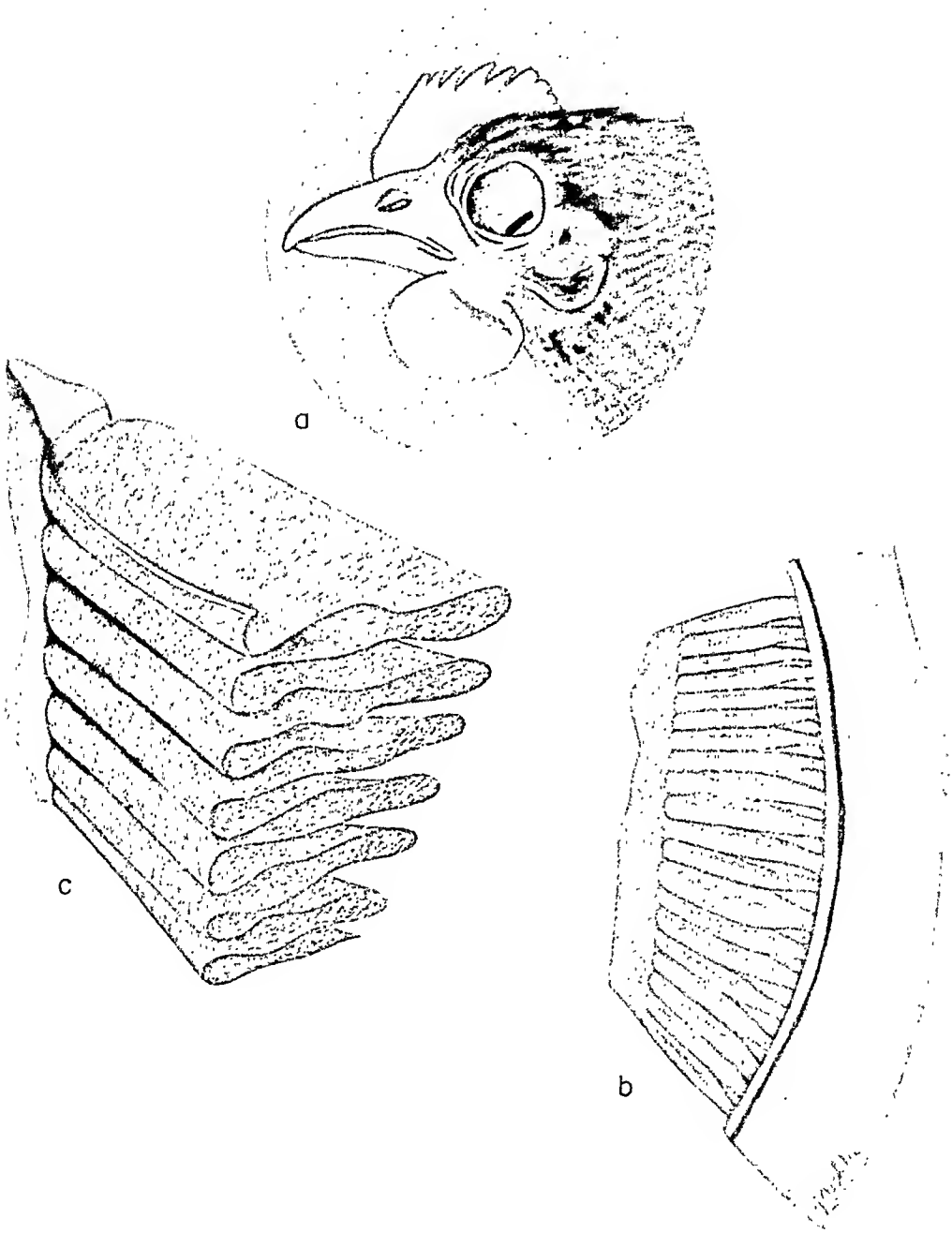

PLATE I

FIG. 1. General views of the pecten of *Gallus domesticus*. In (a), the pecten is shown in situ after removal of the lentieular half of the eye. In (b), the excised peeten is demonstrated on surfaee view. The line of attaehment to the optie disk is on the right, the bridge of the peeten is on the left side of the illustration. In (e), a small portion of the peeten, ineluding a part of the bridge, has been excised. The eharaeteristic arrangement of the pleats is evident.

Menner and believe that the pecten "increases the sensory action of small moving shadows."

Development

In 1901 Parreidt published a dissertation on the development of the pecten; he concluded, apparently without knowledge of the prior findings of Nussbaum, that the pecten is ectodermal in origin and arises from cells similar to those of the retina (Lindahl and Jokl, 1922). Slonaker (1921), however, adhered to the older view that the pecten is associated with the choroid and is mesodermal in origin. Important studies of the development of the pecten were undertaken by Bernd (1905), Lindahl and Jokl (1922), von Szily (1922), and Mann (1924a). The subject has been reviewed briefly by Romanoff (1960). Mann stresses that "the pecten is developed from ectoderm derived from the inner layer of the optic cup, secondarily vascularized by mesoderm."

The present authors have studied the development of the eye of the chick (*Gallus domesticus*) in serial sections at every stage (Hamburger and Hamilton, 1951) up to 43, and also in the newly hatched and the adult.

By stage 17 a relatively large vessel can be seen protruding through the retinal fissure into the vitreous cavity (O'Rahilly and Meyer, 1959). This is generally known as the "arteria cupulae opticae" and it is shown in Fig. 2 (stage 21). By stage 26 (4½–5 days of incubation) a clump of cells forms a low projection on the surface of the optic disk. This projection, known as Bergmeister's papilla (Mann, 1949), is the beginning of the pecten.[6] It is illustrated in Fig. 3 (stage 29), where a vessel can be seen at its base. The basal vessel appears to be derived from the extracupolar plexus and, at least in this specimen, does not seem to be connected within the wall of the optic cup with the arteria cupulae. The papilla soon becomes elongated (Fig. 4) and is termed the crista intraocularis (Mann, 1924a). In some specimens at stage 35 the pecten begins to fold slightly. Pigment granules are first seen at stage 36. The folds are well marked by stage 37 and the resemblance to the pecten of the adult is evident (Fig. 5). The pecten is still predominantly cellular rather than vascular, however, and pigment is scarce. In the newly hatched chick the degree of pigmentation is considerable and the vessels have the peculiar appearance noticeable in the adult.

[6] According to Slonaker (1921), the hyaloid membrane is invaginated by the developing pecten and "the hyaloid membrane completely envelops the whole structure in the adult." Both of these statements have been verified by the present authors on employing the PAS reaction.

It is of interest to record that Bergmeister's papilla can be detected in the human embryo at the end of the embryonic period proper. Thus one of the present authors (R. O'R.) has observed it in a human embryo of 30.7 mm crown-rump length (Streeter's stage 23). Its fate has been discussed by Mann (1949): "In man the size of this papilla is rather variable . . . . The cells forming the papilla are glial in nature and proliferate during the 5th month to form the glial sheath of the hyaloid artery . . . . This sheath and the papilla of Bergmeister atrophy with the hyaloid before birth. The exact amount of atrophy determines the depth of the 'physiological cup' in the centre of the disc, this being the depression left by the absorption of the cone of cells." Abnormally, excessive development of Bergmeister's papilla may "lead to the formation of strands of whitish, sometimes fluffy-looking tissue which veil the vessels on the disc" (see Fig. 76 in Mann, 1957).

Histology

The best accounts of the histological structure of the pecten are those of Mann (1924a, b) and Baesieh and Gellért (1935).

According to the former source, during development, "the blood capillaries rapidly increase in number, and finally come entirely to overshadow the original epithelial elements, which can, however, still be seen in the adult, though often widely separated by blood-vessels. Finally, pigment is developed in the remains of the neuro-epithelium."

PLATE II — Development of Pecten

These photomicrographs have been passed through a LogEtronics printer. The larger numerals in the upper right-hand corner of each photograph indicate the embryonic stage.

FIG. 2. The choroid fissure, stage 21. The cupolar vessel can be seen passing through the fissure and projecting into the vitreous cavity. Alum cochineal. Magnification: × 146.

FIG. 3. Bergmeister's papilla, stage 29. The converging nerve fibers of the retina have isolated a mound of cells that constitutes the beginning of the pecten. Note the basal vessel. Modified Papanicolaou's stain. Magnification: × 110.

FIG. 4. The developing pecten, stage 35. The pecten is now an elongated extension of Bergmeister's papilla. Basal vessels can be distinguished. Modified Mallory-Masson stain. Magnification: × 73.

FIG. 5. The developing pecten, stage 37. The characteristic pleats are now visible. The very slight degree of pigmentation present at this stage cannot be detected at this magnification. The partially detached internal limiting membrane of the retina can be seen at the right-hand side of the illustration. Modified Papanicolaou's stain. Magnification: × 73.

In summary, the pecten of the adult "consists of blood-vessels of a specialized type and pigment-containing cells representing the remains of the original ectoderm."

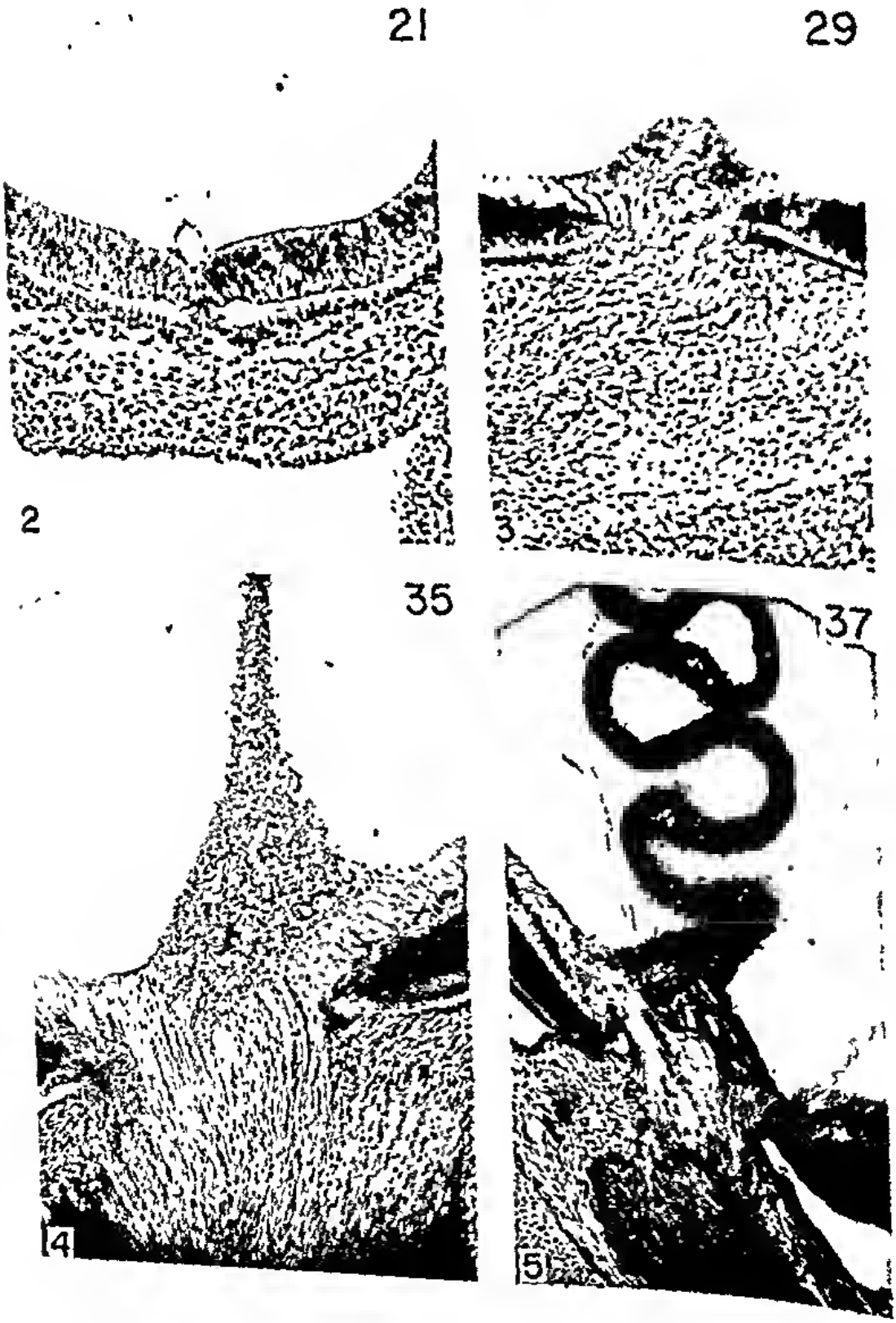

Thus the pecten comprises (1) a plexus of larger and smaller blood vessels (Figs. 6-9), and (2) pigmented intervascular tissue (Fig. 8).

The atypical structure of the vessels in the pecten has been emphasized by several workers, e.g., by Mann (1924a). The lining (presumably endothelial) cells possess nuclei that are "very large, oval, [and] do not stain darkly." Moreover, "the cytoplasm, instead of being thinned out almost into a film as generally in capillaries, appears swollen into a structureless, clear homogeneous mass in which the nuclei are embedded at intervals, no individual cell boundaries being seen." Externally, the cytoplasm is closely surrounded by "a perfectly clear hyaline and highly refractile limiting membrane, which completely invests every capillary." This membrane is apparently the same feature as the "homogeneous substance" or "hyaline substance" that Bacsich and Gellért describe around the endothelium of the "modified capillaries." According to the latter authors, the substance stains an intense blue color with Mallory's method and consists of "hyaline connective tissue" (*hyaline Bindegewebe*).

The cells of the intervascular tissue, believed by Mann to be neuroectodermal in origin, have been described as "glial" by most writers. Bacsich and Gellért, however, by the use of special silver methods, failed to demonstrate glia in the pecten. Moreover, these authors, again by the use of silver, found no nerve endings and no nerve fibers in the pecten. Elastic fibers and muscle fibers were also absent. They found (1) collagenous fibers, especially in the bridge, (2) reticular fibers, especially

---

PLATE III — Histology of Pecten

These photomicrographs have been passed through a LogEtronics printer.

FIG. 6. The region of attachment of a part of the pecten to the optic disk in an adult hen. Three of the pigmented pleats are visible. Note that optic nerve fibers reach, but do not penetrate, the base of the pecten. Modified Mallory-Masson stain. Magnification: × 38.

FIG. 7. The bridge of the pecten in an adult hen. The black pigment is evident. Most of the intervening tissue is stained (blue) with aniline blue. Modified Mallory-Masson stain. Magnification: × 64.

FIG. 8. A portion of an excised pecten, after the bridge has been removed and after the remainder has been extended on a slide, dehydrated, cleared, and mounted. The pattern of the larger and smaller vessels is outlined by the intervening pigment. Adult hen. Unstained preparation. Magnification: × 38.

FIG. 9. A portion of a pleat of the pecten of an adult hen. Note that the large vessel near the center of the illustration possesses a flattened endothelium, whereas the smaller vessels present bulky lining cells. The refractile (green) membrane surrounding each vessel is not easily distinguished in a black and white photomicrograph. The black areas are produced by the superimposition of small, spherical granules of pigment. Modified Papanicolaou's stain. Magnification: × 382.

around the blood vessels, and (3) pigment (melanin) granules, situated entirely within the cells of the intervascular tissue. According to Kajikawa (1923), some of the intervascular cells are free of pigment.

The present authors have studied the histological structure of the pecten of the adult by means of a modified Mallory-Masson technique and Papanicolaou's staining method. Some of the sections had been bleached by acidified permanganate according to the method of Chasterman and Leach (1958).

The smaller vessels, about 20–30 μ in diameter, are lined by cells that project into the lumen. The nuclei of these cells are round or oval

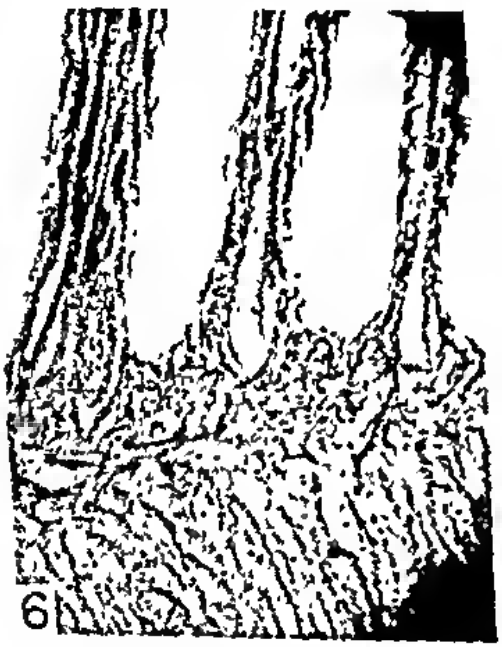

6

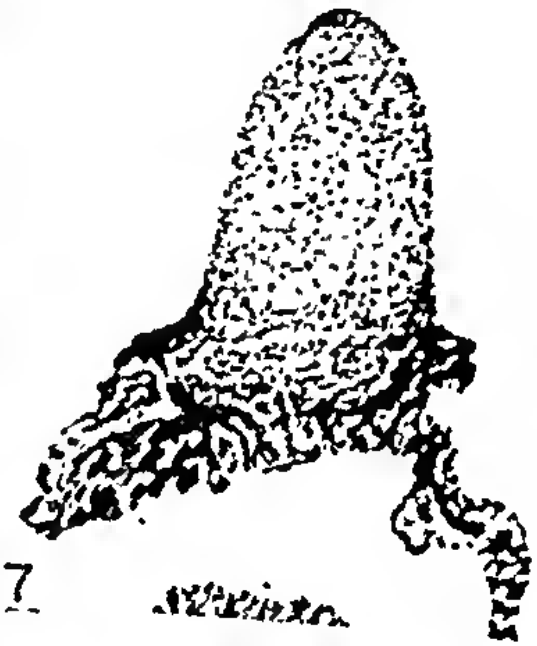

7

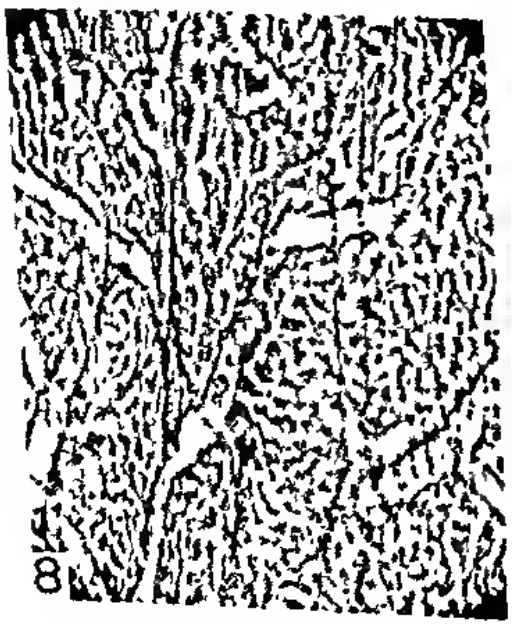

8

9

and they possess a distinct nucleolus. The cytoplasm appears pale and abundant, and cell boundaries are not evident. Externally, the lining cells are surrounded closely by a refractile, hyaline membrane which stains blue with aniline blue and green with fast green. The larger vessels, about 40–80 μ in diameter, frequently possess flattened lining cells. A hyaline membrane is present and is sometimes thicker, but, in the present preparations, is not as thick as that illustrated by Bacsich and Gellért (in their Fig. 1).

The intervascular tissue is most easily seen in the bridge of the pecten, where collagenous fibrils are found. The pigment granules are spherical in shape. They vary in size but are generally less than 2 μ in diameter. They are located mostly within the cells of the intervascular tissue (it is difficult to be certain that they are all intracellular; Mann points out that "the pigment granules very readily come out of the cells").

Histochemistry

The presence of 1,2-glycol groups, configurations that are most likely to be found in carbohydrate material, was demonstrated in the pecten by a positive periodic acid-Schiff (PAS) reaction which could be removed by prior acetylation and restored subsequently by saponification with KOH. In addition, no appreciable alteration in intensity of the PAS reaction was noted when either mild methylation (4 hr at 37°C) or diastase digestion was performed prior to oxidation. The localization and further identification of this material were studied also by the application of other polysaccharide techniques: alcian blue for acidic carbohydrates, metachromasia with azure A, colloidal iron (Mowry, 1958), mucihematein, aldehyde fuchsin, and methylene blue extinction.

Negative results were noted with mucihematein, and with methylene blue at pH values less than 5, and no metachromatic material was found when azure A was employed between pH levels 1.5 and 4.5 either alone or after sulfation (10 min at 25°C). Nuclei became orthochromatic at about pH 2.5 (calcium acetate formalin) or 3.5 (Bouin; Carnoy). Below these values the nuclei were unstained. The cytoplasm of the cells in the pecten is slightly orthochromatic at about pH 4.5 (calcium acetate formalin) and is unstained at lower pH values.

The cytoplasm of the lining cells of the small vessels was stained weakly with alcian blue, aldehyde fuchsin, and the PAS reaction. These cells were enveloped externally by a PAS-positive basement membrane (Fig. 11), which was surrounded by the highly refractile hyaline layer. The latter was relatively nonreactive to alcian blue, and the PAS reaction.

the vitreous body, which, in turn, was metachromatic (pH 4.5), PAS positive (diastase resistant), and distinctly stained by alcian blue and colloidal iron. In the combined AB-PAS reaction the bridge and the layer of the vitreous body adhering to it possessed a greater affinity for alcian blue. Prior mild methylation resulted in a decrease in the alcian blue staining, and a noticeable increase in the PAS reactivity of this tissue. Methylation supposedly hydrolyzes sulfate groups without esterifying hydroxyls. Thus, the increased PAS reactivity produced in the endothelial cytoplasm and in the bridge of the pecten by methylation prior to the AB-PAS procedure most likely indicates, according to Spicer (1960), the hydrolysis of sulfate groups attached to vicinal glycols of previously PAS-negative sites with the consequent accessibility of carboxyl groups.

Lipids were not demonstrated in the pecten, either by the use of oil-soluble dyes (oil red O, Sudan black B), or by the application of the performic acid-Schiff (unsaturated lipids) or Baker's acid hematein (phospholipids) reactions.

Developmental Histochemistry

The enormous task of applying histochemical procedures to embryos at each developmental stage has been initiated by employing the PAS reaction. Briefly, by stage 37, the pecten is covered by a strongly PAS-positive membrane, particularly prominent at the apical region of the organ. This membrane is continuous with that on the internal aspect of the retina, which is presumed to be the hyaloid membrane of the vitreous body, or perhaps a combination of internal limiting membrane and hyaloid membrane. The perivascular membranes of the pecten were scarcely visible at stages 37–41, at least in the pleats, but at stage 42, distinct membranes were observed around all the blood vessels. In the newly hatched chick the perivascular membranes are stained intensively; the cytoplasm of the cells of the pecten, as in the later embryonic stages, was very weakly, if at all, PAS positive.

PLATE IV — Histochemistry of Pecten

These photomicrographs have been passed through a LogEtronics printer.

FIG. 10. The bridge and several pleats of the pecten in an adult hen. Stained with alcian blue. The brightly stained alcian blue-positive material surrounding the bridge and the individual blood vessels appears here in light gray. Note the general distribution of the pigment granules. Magnification: × 140.

FIG. 11. A portion of a pleat of the pecten in an adult hen. The periodic acid-Schiff reaction after bleaching with acidified permanganate. PAS-positive, diastase-resistant membranes can be seen enveloping the pleat and surrounding each of the contained vessels. A weak reaction is also obtained in the endothelial cytoplasm. Magnification: × 140.

10

11

In the present study the precise localization of chemical substances or configurations in the various components of the pecten has yielded additional information on the structure of this organ. Moreover, the histochemical findings, when collated subsequently with enzyme and other protein distributions, may provide insight into the functional significance of this ocular enigma.

Acknowledgments

The writers are indebted to Mrs. Arlys Vettraino and Mrs. Rose Marie Caruso for the excellent preparation of the sections used in this study. Plate I is the work of Mrs. Geraldine Fockler. The photomicrographs were taken by Mr. Charles Pickard and were printed LogEtronically by Mr. Robert Wright.

References

Baesieh, P., and Gellért, A. (1935). *Arch. Ophthalmol. Graefe's* **133**, 448-460.
Bernd, A. H. (1905). Die Entwicklung des Peeten im Auge des Hühnehens aus den Blättern der Augenblase. Inaugural-Dissertation, Bonn.
Chesterman, W., and Leach, E. H. (1958). *Quart. J. Microscop. Sci.* **99**, 65-66.
Crozier, W. J., and Wolf, E. (1944a). *J. Gen. Physiol.* **27**, 287-313.
Crozier, W. J., and Wolf, E. (1944b). *J. Gen. Physiol.* **27**, 315-324.
Duke-Elder, W. S. (1958). "System of Ophthalmology," Vol. I, The Eye in Evolution. Kimpton, London.
Hamburger, V., and Hamilton, H. L. (1951). *J. Morphol.* **88**, 49-92.
Kajikawa, J. (1923). *Arch. Ophthalmol. Graefe's* **112**, 260-346.
Kauth, H., and Sommer, H. (1953). *Biol. Zentr.* **72**, 196-209.
Lindahl, C., and Jokl, A. (1922). *Z. ges. Anat., Abt. I* **63**, 227-342.
Lison, L. (1954). *Stain Technol.* **29**, 131-138.
Mann, I. C. (1924a). *Quart. J. Microsocp. Sci.* [N.S.] **68**, 413-442.
Mann, I. C. (1924b). *Brit. J. Ophthalmol.* **8**, 209-226.
Mann, I. (1949). "The Development of the Human Eye," 2nd ed. Brit. Med. Assoc., London.
Mann, I. (1957). "Developmental Abnormalities of the Eye," 2nd ed. Brit. Med. Assoe., London.
Mowry, R. W. (1958). *Lab. Invest.* **7**, 566-576.
Mowry, R., and Winkler, C. H. (1956). *Am. J. Pathol.* **32**, 628-629.
O'Rahilly, R., and Meyer, D. B. (1959). *Acta Anat.* **36**, 20-58.
Petit (1735). *Mem. acad. sci. Paris,* pp. 123-152.
Romanoff, A. L. (1960). "The Avian Embryo. Structural and Functional Development." Macmillan, New York.
Slonaker, J. R. (1921). *J. Morphol.* **35**, 263-357.
Spicer, S. S. (1960). *J. Histochem. Cytochem.* **8**, 18-35.
von Szily, A. (1922). *Arch. Ophthalmol. Graefe's* **107**, 317-431.
Walls, G. L. (1942). "The Vertebrate Eye and its Adaptive Radiation." Cranbrook Institute of Seienee, Bloomfield, Hills, Michigan.

Discussion

Chairman Carpenter [Tufts University, Medford, Mass.]: Have you a comment on the function of the peeten?

Dr. O'Rahilly [Wayne State University, Detroit, Michigan]: It is generally

suggested that it has something to do with the nutrition of the retina, which does not have its own vascular system in birds. We do not have any positive information about any other function. It has also been suggested that it may be a means of warming the eye. It contains a very marked concentration of carbonic anhydrase, which suggests that this is an intraocular respiratory organ.

DR. MCCONNELL [Ohio State University, Columbus, Ohio]: What do the PAS-reactive sites represent?

DR. O'RAHILLY: Actually pigment granules in the pigmented cells. I am not sure why they show. Possibly a histochemist would comment on this. The reaction is more marked as seen in the photographs than when observed with the microscope. The granules have a magenta color

Cell Surfaces in the Crystalline Lens

THEODOR WANKO AND MARY ANN GAVIN

Ophthalmology Branch, National Institute of Neurological Diseases and Blindness, National Institutes of Health, Public Health Service, U. S. Department of Health, Education and Welfare, Bethesda, Maryland

Introduction

Materials and Methods

Lenses from mature guinea pigs, monkeys, rabbits, and old rats were used. The animals were anesthetized with pentobarbital sodium (30 mg/kg) administered intravenously or intraperitoneally and with 0.2–1.0 cm³ of 2% lidocaine injected retrobulbarly. After removal of cornea and iris, the zonula fibers were carefully severed and the lenses were immediately immersed in the fixative. Fixation periods ranged from 1 to 3 hr in 1% OsO_4, buffered at pH 7.3 with Veronal acetate (Palade, 1952). The lenses were subsequently rinsed in buffer and rapidly dehydrated in a graded series of ethyl alcohols. Pieces from the regions of the lens cortex containing portions from the anterior and posterior lens sutures were dissected during dehydration in absolute alcohol. Selected specimens were embedded in a mixture of butyl- and methylmethacrylates in the ratio of 9:1 to which mixture 0.25% of the initiator, benzoyl peroxide, had been added before prepolymerization. They were incubated at 65°C for 24 hr. Alternately some tissue pieces were embedded in epoxy resin.[1] They were soaked in a mixture of equal parts of alcohol and plastic (casting resin, hardener, and plasticizer) at 65°C overnight. Further impregnation was carried out in a fresh plastic mixture without alcohol at 65°C for 24 hr. The tissue pieces were then infiltrated at room temperature for 24 hr with the epoxy mixture to which the accelerator had been added. They were embedded in a fresh change of the media

[1] As supplied by the New York Society of Electron Microscopy.

and polymerized at 65°C for 3 days. Sections were cut on a Sorvall-Porter-Blum microtome with a Vycor brand glass knife (Gavin and Lloyd, 1959), and were then transferred to grids filmed with collodion and carbon. Electron micrographs were recorded at magnifications ranging between 1200 and 15,000 × using an RCA electron microscope EMU 3C. The micrographs were photographically enlarged from 3.5 to 6 ×.

Observations

Three noticeably different patterns of intercellular relationship are observed in the lens cortex. Each variant is characteristically located in a particular area and will be described below.

The first example of these representative intercellular arrangements pertains to the cortical fibers in the periaxial and intermediate zones of the lens. Here, the lens fibers, hexagonal in cross section, are regularly arranged so that the over-all aspect resembles a honeycomb (Fig. 1). In both cross and longitudinal sections the closely opposed cell contours parallel one another and pursue a rectilinear course.

In contrast to the aforementioned region, a completely different form of cytoarchitecture distinguishes the monolayer of lens epithelium and the equatorial portions of the lens fibers. In the epithelium, the boundaries of the individual cells form a complicated system of interdigitations which become increasingly tortuous toward the equatorial zone (Fig. 3). The cell membranes enclosing the lens fibers in the same area are also characterized by a sinuous course which results from interdigitating cell processes (Figs. 4 and 5).

A third complex arrangement is observed at the lens sutures (Fig. 2). In their vicinity the regular array of the lens fiber membranes gradually changes to a system of many protruding cell portions of various sizes which are interposed between similar projections of the adjacent cells (Fig. 6). This occurrence of corrugated cell surfaces persists through varied orientations of the plane of sectioning. This indicates that the interdigitations occur anteriorly, posteriorly, and laterally be-

---

FIG. 1. Rat lens cortex. In cross section, cortical lens fibers (LF) are seen with hexagonal contours in a regular, honeycomb arrangement. This appearance is typical over the largest area of the fibers in the lens cortex. A nucleus (N) of the bow region is indicated. Methacrylate. Approximate magnification: × 12,000.

FIG. 2. Rat lens cortex. In the area of the lens sutures the cell contours (CM) are very irregular and exhibit many interlacing processes (arrows). Epoxy resin. Approximate magnification: × 6500.


LF
N
LF
5 μ
CM
M
5

tween lens fibers which belong to the same sector of the lens as well as between those lens fibers which meet at the suture and are located in opposite lens portions (Fig. 8).

In contrast to the pattern seen at the equatorial zone, the suture area also contains, besides the interdigitations, a few specialized contact areas of the cell boundary. In these instances, the opposing cell membranes which, in general, keep a distance of approximately 60 Å, separate to a distance of 200 or 250 Å over a length varying between 200 to 300 mμ. For this length, the membranes approximately double in thickness and display a high opacity (Fig. 9). In a slightly tangential section, it is observed that dark and light zones alternate for the length of the membrane thickening (Fig. 10). The space enclosed by the thickened membranes as well as the cytoplasm on either side of them is slightly more opaque than usual, but no further details are discernible with the methods employed.

The described pattern of interdigitations is maintained at the various depths of the lens cortex examined. The distribution of the cytoplasmic constituents varies, however. The more superficial fibers contain many small vesicular profiles; sometimes they are arranged in groups comparable to the components of the Golgi complex (Fig. 7). Occasionally, mitochondria are interspersed in the ground substance. The cytoplasmic inclusions gradually decrease in amount with the depth of the layers. The greater concentration of formed elements at the suture region (Fig. 7) is in contrast with the rest of the fiber where dense granules and low density elements predominate (Fig. 5).

Comments

From these data, together with previous observations on lens epithelium and lens fibers (Wanko and Gavin, 1958, 1959), it is apparent that in the lens cortex the intercellular relationship, characterized by numerous interdigitations, predominates in certain areas. These interdigitations occur throughout the epithelium and are maximally developed in its equatorial zone. A similar pattern prevails between the lens fibers in the same area and also at the sutures in the cortex of the mature lens.

In the center of the suture region exclusively, adjacent cell surfaces display over short distances a bipartite structure with two symmetrical

---

FIG. 3. Rabbit lens epithelium, intermediate zone. This micrograph depicts portions of epithelial cells which interdigitate (INT) extensively in the vicinity of the lens capsule (C). Cell membranes (CM) and part of a nucleus (N) are indicated. Methacrylate. Approximate magnification: × 93,000.

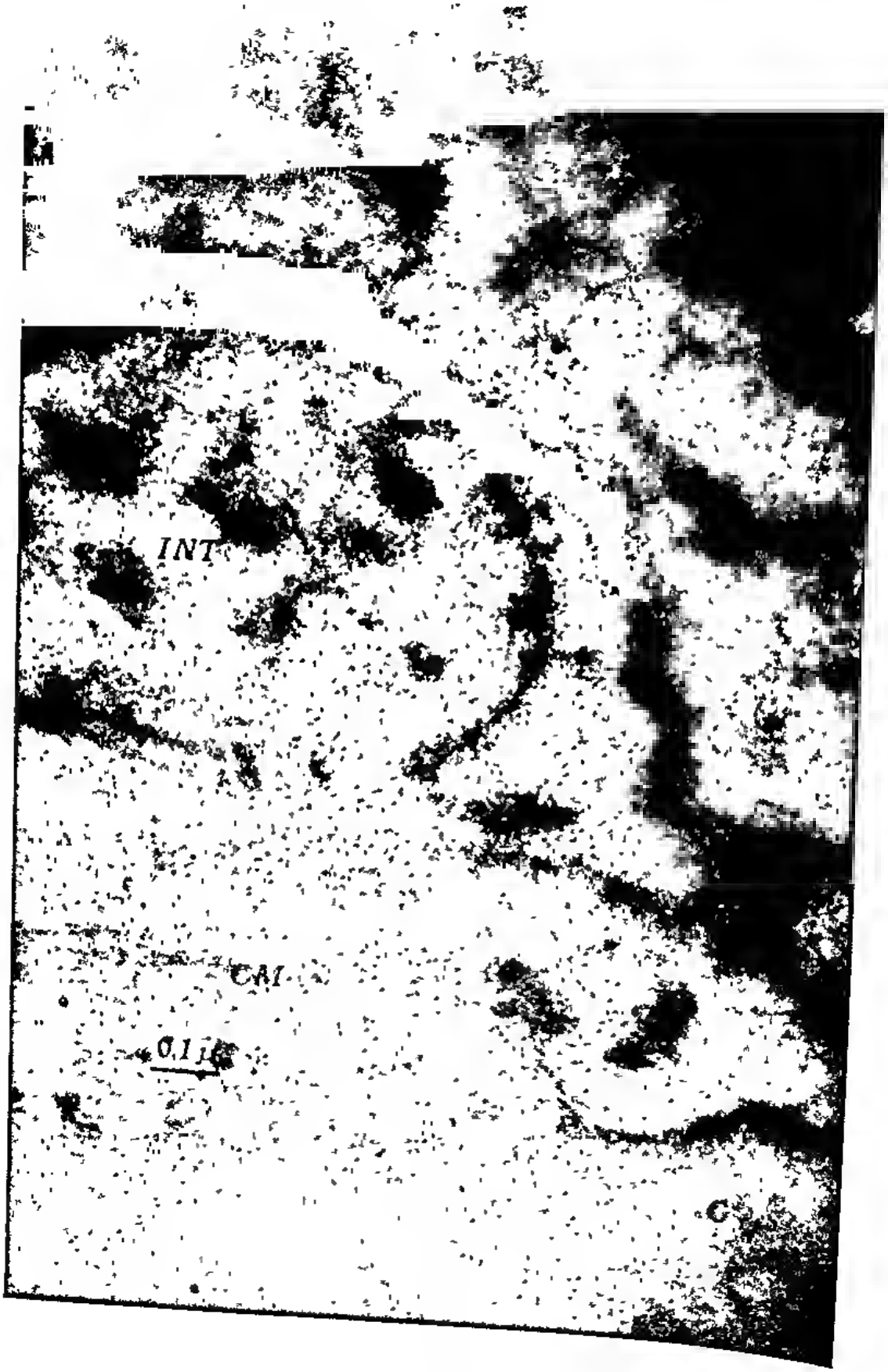
INT
CAI
0.1 μ
C

FIG. 4. Rabbit lens, young cortical fibers. Subcapsularly, at the equator, the cortical lens fibers (LF) exhibit tortuous interdigitating membranes (CM). A tangentially sectioned membrane (CM'), lens capusle (C), and a nucleus (N) are designated. Methacrylate. Approximate magnification: × 7500.

FIG. 5. Rabbit lens cortex. Corrugated cell surfaces (CM) with many longitudinal (INT) and cross-sectioned (INT') interdigitating cell processes outline the equatorial portions of the lens fibers. Clusters of dense granules (G) and small elements of low opacity (LD) are seen in the cytoplasm. Methacrylate. Approximate magnification: × 48,000.


C
LF
LF
5μ
LD
INT
INT
1

FIG. 6. Rat lens cortex. This micrograph illustrates the complicated pattern of numerous interdigitations (arrows) between two lens fibers (LF), in the suture region. Cell membranes are marked with CM. Epoxy resin. Approximate magnification: × 26,500.

FIG. 7. Rat lens cortex. In the superficial layers of the suture region the lens fibers (LF) contain a large number of vesicular profiles (V). Epoxy resin. Approximate magnification: × 48,000.


LF
LF
CM
1 μ
LF
V
V
LF
LF
1 μ
7

halves which enclose an enlarged interstice. These components of the cell surface correspond to similar entities described with slight variations in several tissues and can be classified as desmosomes (Fawcett, 1958; Karrer, 1959). Although there is little evidence, desmosomes are believed to function as accessories of intercellular cohesion.

Various physiological roles have been attributed to such highly corrugated cell surfaces in investigations of other tissues. The functional

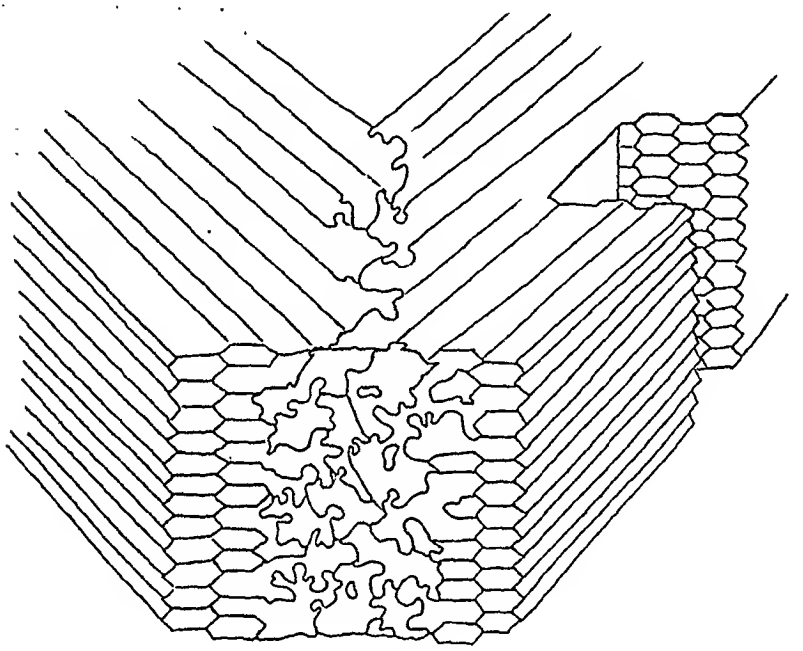

FIG. 8. Lens fibers in the suture area. This schematic diagram illustrates how the cortical fibers converge from opposite sectors at the lens suture, where they interlace and at the same time interdigitate with one another and also with the fibers located in the same lens sector.

interpretations range from one of stabilizing intercellular connections to that of ensuring continuous mobility of contours during metabolic activity. In the lens of mammals, birds, and reptiles other than snakes (Prince,

---

FIG. 9. Rat lens cortex. Occasionally in the suture area, two opposite cell membranes (CM) exhibit desmosomes in the form of circumscribed thickenings with high opacity and enlarged intercellular space (arrow). Epoxy resin. Approximate magnification: × 93,000.

FIG. 10. Rat lens cortex. In this instance a desmosome in the suture region is sectioned in a slightly tangential plane. Zones of high and low opacity alternate in the thickened portions of both cell membranes (arrow). Cell membranes (CM), a cross-sectioned mitochondrion (M), and vesicular profiles (V) are designated. Epoxy resin. Approximate magnification: × 93,000.

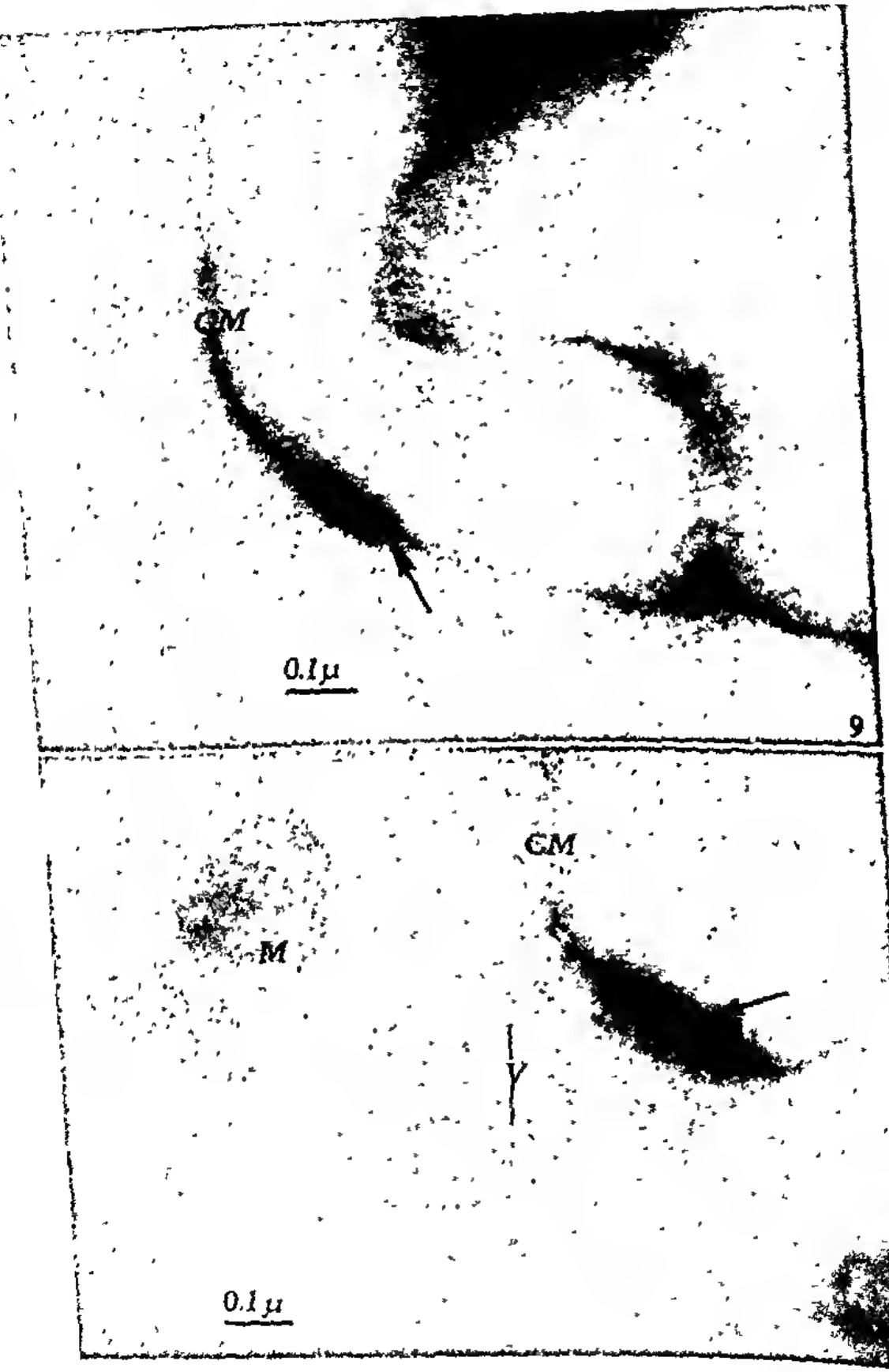
CM
0.1μ
9
CM
M
Y
0.1μ

1956), the change of shape is an essential function and the presence of such interdigitations might be associated with the mechanism of intracapsular accommodation. The lenses investigated in the present study are in complete accommodation due to the preparative proeedures. Therefore, different states of accommodation eannot be compared. It is probable, however, that during such an activity the shape of the individual cells is changed considerably. To aehieve this purpose, and at the same time preserve the morphological integrity of the cell, interdigitating cell processes might unfold in some plaees whereas new serpentine surfaces may be formed at other sites. This hypothesis is supported by the observations that the interdigitating cell proeesses oeeur mainly in those areas of the lens which undergo the greatest dimensional changes during accommodation, i.e., the anterior curvature, the periaxial zone, and the equator. If the desmosomes are a means of intereellular attachment they could, in this instance, effect a firm cohesion between the lens fibers subjected to transformation, and thus prevent their separation along the sutures.

Summary

Cell surfaees in the cortex of the crystalline lens are analyzed with special attention being given to the area of the sutures. They eonstitute a complicated system of interlacing lens fibers whieh, at the same time, interdigitate with one another on all sides and are in part eonneeted by desmosomes. A hypothesis coneerning the functional importance of cellular interdigitations in the lens is proposed.

Acknowledgment

We are indebted to Dr. Ludwig von Sallmann for constructive help with work and manuscript, and to Mr. H. Bartner, Medical Arts Section, Division of Research Services, who provided Fig. 8.

References

Fawcett, D. W. (1958). *In* "Frontiers in Cytology" (S. L. Palay, ed.), pp. 19-41. Yale University Press, New Haven, Connecticut.

Gavin, M. A., and Lloyd, B. J. (1959). *J. Biophys. Biochem. Cytol.* **5**, 507.

Karrer, H. E. (1960). *J. Biophys. Biochem. Cytol.* **7**, 181-184.

Palade, G. E. (1952). *J. Exptl. Med.* **95**, 285-298.

Prince, J. H. (1956). "Comparative Anatomy of the Eye," pp. 215-242. C. C Thomas, Springfield, Illinois.

Wanko, T., and Gavin, M. A. (1958). *A.M.A. Arch. Ophthalmol.* **58**, 868-879.

Wanko, T., and Gavin, M. A. (1959). *J. Biophys. Biochem. Cytol.* **6**, 97-102.

Discussion

Dr A. J. Coulombre [Yale University, New Haven, Conn.]: In your sections, gaps appear in the cell membranes separating adjacent lens fibers. Do they represent intercellular bridges?

Dr Wanko [National Institutes of Health, Bethesda, Md.]: We have also observed these but I am not sure that they are real

Dr. Pirie [Oxford, England]: What species were used in your study?

Dr. Wanko. We studied rabbit, monkey, guinea pig, and rat. No significant difference in the shape of fibers or other structures was seen. We are aware of the fact that some of these species can accommodate to a greater degree than others. The interdigitations are seen also in the newborn animal, at a time when there is no accommodation taking place.

Chairman Carpenter [Tufts University, Boston, Mass.]: You have described a most ingenious system of interdigitation which may provide strength during accommodation Would it not be interesting to study this in the fish eye, in which accommodation does not involve deformation of the lens.

Dr. Wanko I did not look at that

The Appearance of Specific Antigens during Development of the Lens[1]

JAN LANGMAN

Department of Anatomy, McGill University, Montreal, Canada

Introduction

Lens formation in the chick embryo is thought to be dependent upon "inductive" influences from the optic vesicle (Alexander, 1937; van Deth, 1940; Waddington and Cohen, 1936). This vesicle, an outpocketing from the rostral portion of the nervous system expands laterad in the direction of the surface ectoderm and establishes contact with this ectodermal layer at the 9-somite stage. During the subsequent period (9–20-somite stage), the two structures adhere tightly to each other.

At the beginning of this period (9–12-somites) the ectodermal cells —referred to hereafter as presumptive lens ectoderm—do not differ from those of the surrounding head ectoderm, that is they are cylindrical, have a vacuolated cytoplasm and a spherical or ovoid nucleus. During subsequent development (13–16-somite stage) the intracellular vacuoles disappear gradually and the nuclei become displaced toward the base of the cells, which is in contact with the optic vesicle. At the 18–19-somite stage, the cells become gradually more elongated (palisading phenomenon) and the nuclei directed perpendicularly to the basement membrane (nuclear orientation). These morphological changes, occurring only in those cells of the surface ectoderm which are in a direct contact with the optic vesicle (McKeehan, 1951, Langman, 1956), may suggest a rearrangement of the cellular components at a molecular level (Weiss, 1947)

To determine whether chemical substances characteristic of the lens arise in the presumptive lens cells during the induction period (9–20-somite stage), Langman *et al.* (1957) and Langman (1959a) explanted optic vesicles covered with presumptive lens ectoderm into a medium containing lens antiserum. It was hoped that in case lens antigens were present in the presumptive lens ectoderm cells a reaction between these antigens and lens antibodies present in the medium would cause a visible morphological reaction in the cells.

[1] This work was supported by grants from the National Research Council of Canada and the National Cancer Institute of Canada.

Experimental

Explants cultured in "normal" and "antimyosin" media (control media) gave rise to lens formation in 60 to 100% of cases, depending on the age of the embryo from which the tissue was obtained (Fig. 1). Failure of lens formation in some of the explants was attributed to factors such as mechanical and thermal damage during dissection, and to heterologous constituents in the media (Langman, 1953a, b). Explants cultured in "antilens" medium, however, showed 10 to 20 hr after the begin-

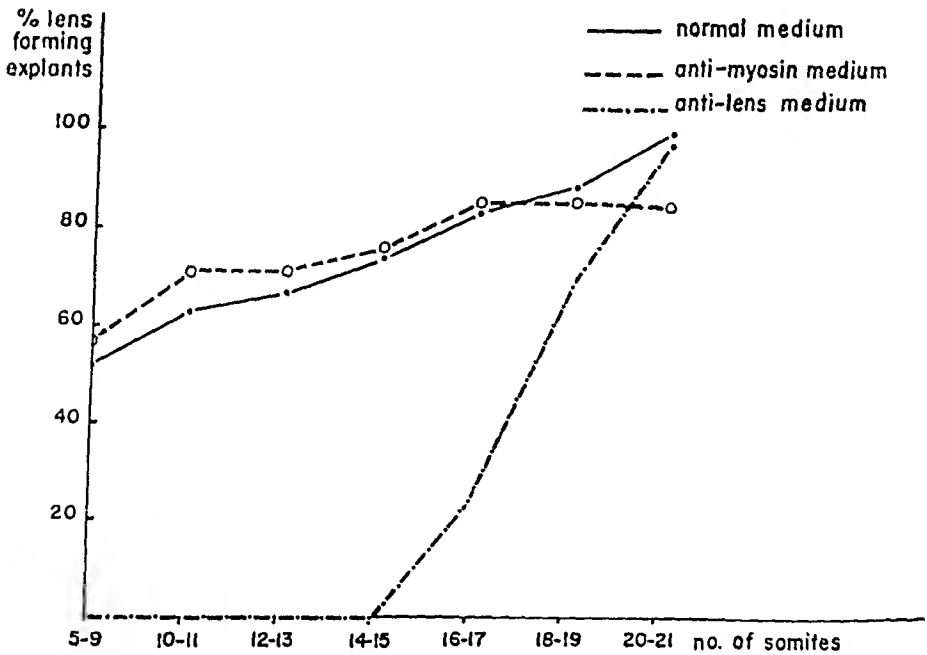

FIG. 1. Percentage of lenses developing in explants of optic vesicle and presumptive lens ectoderm in normal-, antimyosin-, and antilens media. At the horizontal axis is represented the age of the embryo in somites at the beginning of the explantation period.

ning of the tissue culture period a white, degenerating area in the presumptive lens ectoderm. This area grew larger during the next few hours and often broke off from the explant. The degeneration of the presumptive lens ectoderm in some of the cultures allowed the optic vesicle to protrude through a collar of nonpresumptive lens ectoderm, whereas necrotic fragments of the degenerated area were found at the bottom of the container (Fig. 2).

This pattern, however, was not followed by all explants. Whereas explants obtained from embryos with less than 17 somites were unable to form a lens in the "antilens" medium, those from embryos of 18 and more somites behaved like the controls and formed a normal lens (Fig.

1). The results of this experiment indicate that the control media do not interfere with lens formation *in vitro*; "antilens" medium, however, prevents lens development in explants obtained from embryos younger than 17 somites. It indicates that lens antibodies present in the medium react with constituents in the presumptive lens cells, which behave like lens antigens, in such a manner that the cells are unable to survive.

The above-mentioned experiment, however, does not decisively show whether lens antigen(s) are already present before induction starts or arise at some time during the induction period (9–20 somites). It could well be possible that lens antigens are not yet present in presumptive lens ectoderm cells of a 7-somite embryo, but arise under in-

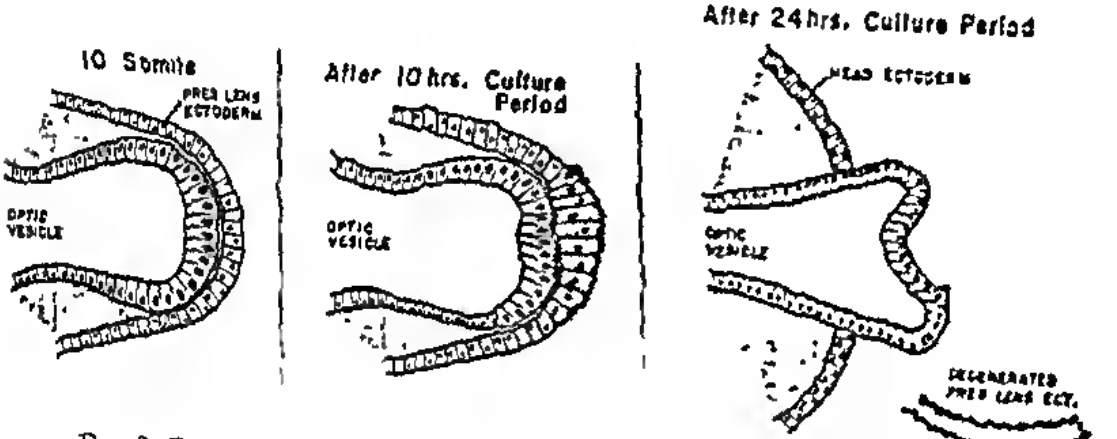

FIG. 2 Diagram showing the changes occurring in explants of optic vesicle and presumptive lens ectoderm, obtained from embryos with less than 16 somites and cultured in antilens medium On the left, at explantation Middle, degenerating presumptive lens area after 10 hr On the right, degenerate lens area lost, optic vesicle protruding through ectoderm

fluence of the optic vesicle at some time during the explantation period. As the total culture period is 72 hr the final result in both cases would be the same, namely, necrosis of the presumptive lens ectoderm. Therefore, to exclude the inductive influence of the optic vesicle during the tissue culture period, lens ectoderm from 7–20-somite embryos was dissected free from the optic vesicle (Langman, 1959a). The first attempts to do so were unsuccessful, since the ectoderm cells were so tightly adherent to the optic vesicle that separation led to damage of the presumptive lens cells. Success was achieved after dipping the heads of the embryos in trypsin solution (1.10,000) for 1 min and rinsing in Tyrode solution It was then possible to dissect the presumptive lens cells without damage, and subsequently to explant them on a clot, which was made up with the same constituents as in the previous experiment, but an equal amount of chicken plasma was added to obtain a coagulum.

Observing the explants under the dissecting microscope at regular intervals, it was noted that those cultured on a control medium showed migration and outgrowth in the form of an epithelial membrane in, or on, the medium 12 to 24 hr after the onset of the explantation period. Whatever the age of the donors, that is, regardless of whether or not the ectoderm had been exposed to the inductive influence of the optic vesicle prior to explantation, 80 to 100% of the explants showed outgrowth (Fig. 3). Explants grown on "antilens" medium behaved differently according to the age of the embryos from which the tissue was

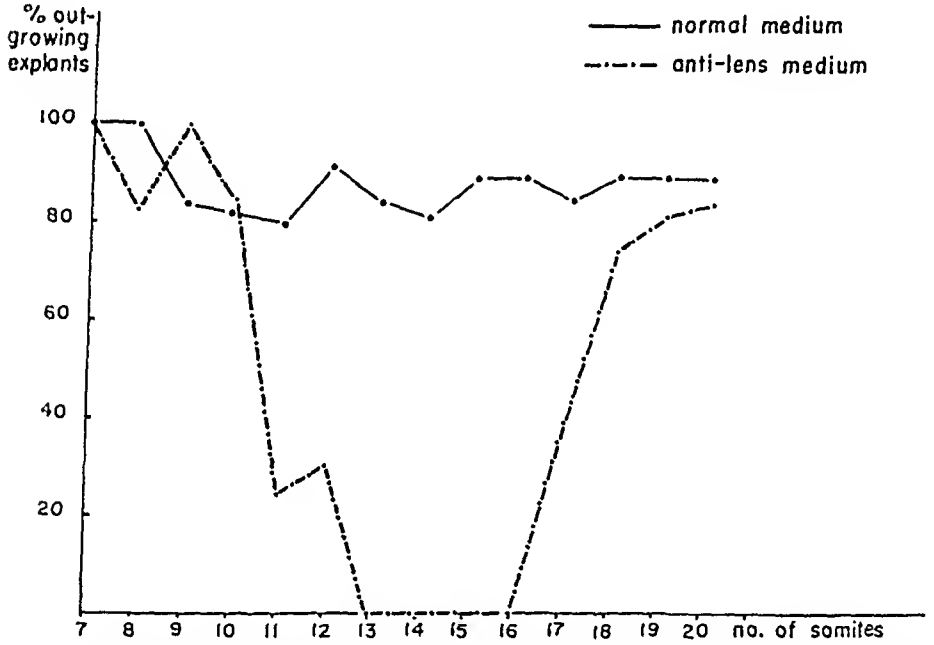

FIG. 3. Percentage of explants of presumptive lens ectoderm (optic vesicle removed) showing outgrowth after 72 hr in culture in normal or antilens medium. At the horizontal axis is represented the age of the embryo in somites at the beginning of the explantation period.

obtained. When the explants were obtained from 7–10-somite embryos, they showed outgrowth just as in normal medium. However, when they came from 11–12-somite embryos, they showed outgrowth in about 30% of the cases, while in those obtained from 13–16-somite embryos disintegration and death of the cells was observed in all cases. Explants obtained from embryos beyond the 17-somite stage again showed outgrowth and migration just as the control explants (Fig. 3). From this experiment, it can be concluded that a component behaving like a lens antigen is formed in the presumptive lens ectoderm cells at the 11-somite stage, that is, shortly after contact with the optic vesicle has started (9 somites) and shortly before the morphological changes characterized by loss of

vacuolization, nuclear orientation, and palisade phenomenon appear (13–19 somites). It is likely that, under the inductive influence of the optic vesicle, one or more components of the indifferent multipotent head ectoderm cells have acquired a new determining group specific for lens antigens.

Though lens antibodies administered in tissue culture indicated the presence of specific substances—lens antigens—in embryonic cells, this method does not give information about the number and nature of antigens arising in the lens in the course of its development. This problem was investigated by means of the double diffusion method of Ouchterlony (1949, 1953), applied in a slightly modified form (Langman, 1959b). This technique is based on the fact that various components of an antigen mixture migrate into an agar gel at different speeds, depending on their respective diffusion coefficient, which is determined by molecular weight, shape, and concentration of the molecules. When antigens (e.g., lens extracts) and corresponding antibodies (e.g., lens antiserum) are placed in two opposite wells in an agar plate, each substance will diffuse into the surrounding medium. When the diffusing antigen and corresponding antibody meet, a precipitin band becomes visible when a critical concentration is reached. Neither antigen nor antibody can diffuse beyond this precipitin zone, which acts as a virtual barrier to the particular antigen-antibody system. Antigens and antibodies unrelated to this system, however, will diffuse across this barrier and form their own precipitin lines (Ouchterlony, 1949, 1953; Wilson and Pringle, 1955; Korngold, 1956). When a mixture of several antigens and antibodies is used a series of bands is seen, each one of which corresponds to an antigen-antibody system.

To determine the number and properties of the antigens present in the adult chick lens, Maisel and Langman (1960) tested a 25% lens extract with lens antiserum at 4°C, according to Ouchterlony's technique, and recorded the appearance of precipitin lines during a 14-day period (Figs. 4–9, Plate I). It was noted that the first precipitin band became visible between the antigen well (top) and antibody well (bottom) 3 days after the start of the diffusion test (Fig. 4). The antigen corresponding to this band will be referred to as Fraction II. An additional, rather broad and vague precipitin band was apparent on the fourth day (referred to as Fraction III) (Fig. 5), while on day 5 of the test a third precipitin line became visible (Fig. 6) (Fraction I). During the following days, an additional number of precipitin lines appeared and on day 14 the total number of bands varied from 7 to 13, depending on the lens antiserum used. Thus, while at the end of the diffusion test Fractions I, II, and III could still be identified separately, it appeared

that each original fraction consisted of two or more closely related bands, which, it may be assumed, represent closely related antigens. It was concluded from this experiment that the adult chick lens contains three main fractions, which can be divided into a number of subfractions forming a total of 7 to 13 soluble lens antigens. Previous experiments, in which isoelectric, salt precipitation, and paper electrophoretic techniques were applied (Burky and Woods, 1928; Smelser and von Sallmann, 1949; Francois *et al.*, 1953, 1954), had shown the presence of only three distinct protein fractions in the lens of various animals. These protein fractions are known as "alpha" crystallin, characterized as a fast moving fraction in an electrical field; "beta" crystallin, a slower moving protein fraction; and finally "gamma" crystallin, a very slow moving fraction. In an attempt to correlate these three distinct lens proteins with the precipitin lines obtained with the agar diffusion method, Maisel and Langman isolated the alpha, beta, and gamma lens proteins by means of the Spinco continuous flow electrophoresis apparatus, using a 10% chick lens extract (unpublished). The fastest moving fraction isolated from the curtain, and known as alpha crystallin, was then tested in the agar plate and found to be identical with Fraction I (Figs. 10, 11, Plate II). Fraction II was similarly shown to be identical with beta crystallin (Fig. 12, Plate II) and Fraction III, with gamma crystallin (Fig. 13, Plate II).

The speed of diffusion of the various lens antigens and the localization of the precipitin lines in the agar plate led us to feel that the molecular weight of Fraction I (alpha crystallin) may be higher than that of Fraction II (beta crystallin), which in turn may be larger than that of Fraction III (gamma crystallin). When the sedimentation coefficient of the isolated protein fractions, giving an indication about their molecular weight, was determined by means of the ultra centrifuge, this value was found to be 17.7×10^{-13} for alpha crystallin, 9.5×10^{-13} for beta crystallin, and 4.2×10^{-13} for gamma crystallin. Comparing these values with the sedimentation coefficient of proteins of known molecular weight, it can be estimated that the molecular weights of alpha, beta,

PLATE I

FIG. 4. Precipitin band (Fraction II) found by testing 25% adult lens extract with lens antiserum, 3 days after the onset of the diffusion test. Distance between top well (antigens) and bottom well (antibodies) is 15 mm; temperature 4°C.

FIG. 5. The same plate at 4 days. Note the appearance of the second precipitin line (Fraction III).

FIG. 6. The same plate at 5 days. Note the appearance of a third precipitin line (Fraction I).

FIGS. 7, 8, 9. The same plate at 7, 10, and 14 days, respectively, after the onset of the diffusion test. Note the appearance of subfractions, especially in Fraction II.

and gamma crystallin are about 1,000,000, 300,000–200,000, and 60,000, respectively.

To determine whether all the soluble antigens demonstrated in the adult lens are already present at the earliest stage of lens development, or gradually arise in the course of lens formation, lens extracts of embryos of the following stages were tested with lens antiserum: (a) 50 hr

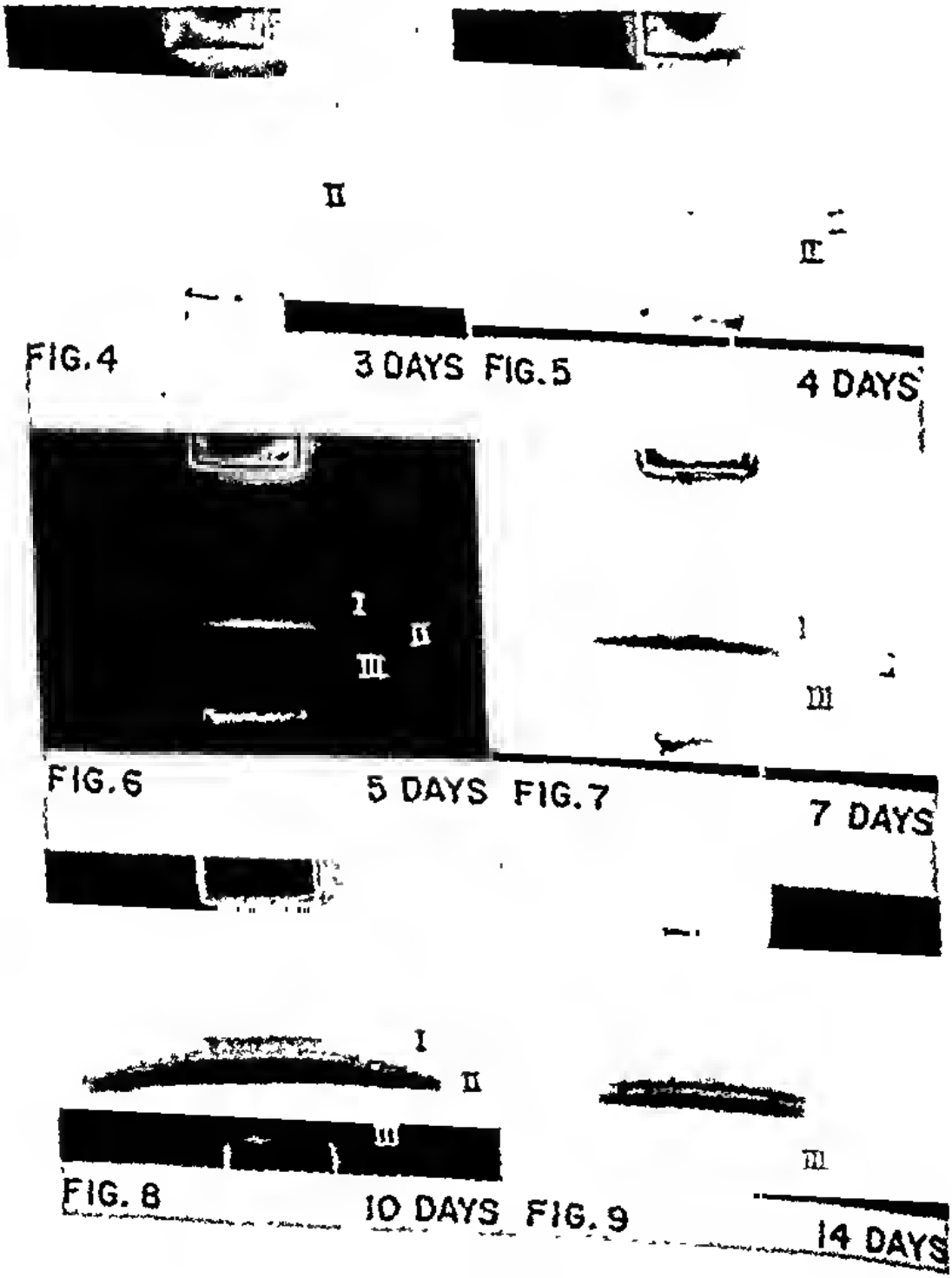

(19–24 somites); (b) 60 hr (28–32 somites); (c) 72 hr (35–37 somites); (d) 96 hr (43–44 somites) and 10 days (Langman, 1959b). A lens extract prepared from 50-hr embryos (19–24 somites) gave rise to one precipitin band when tested with lens antiserum, thus indicating the presence of a substantial amount of one lens antigen in the lens placode cells (Fig. 14, Plate II). During the 19–24-somite stage, the lens placode starts to invaginate (Fig. 15, Plate II), while at the cellular level small acidophilic fibers appear in the apical cytoplasm at the 23–24-somite stage (Fig. 16). In two experiments with 50-hr lens extract an additional faint band became visible closer to the antibody well in front of the first appearing band. It was noted that this band appeared only when the "mean somite age" of the embryos was closer to 24 than to 19 somites. Thus, while the first appearing lens antigen is located in the placode cells, the second lens antigen in all probability is formed at the 23–24-somite stage—that is at the time when the first acidophilic fibers appear in the cell. When lens extracts of 60-hr embryos (28–32 somites) and 72-hr embryos (35–37 somites) were tested with lens antiserum respectively, three and four precipitin bands (Figs. 17 of Plate II, 20 of Plate III) became visible, indicating the presence of substantial amounts of three and four lens antigens. The appearance of the additional antigens

---

PLATE II

FIG. 10. Precipitin bands found by testing 10% adult chick lens extract (Fractions I, II, and III) and isolated alpha crystallin (α) with lens antiserum. Note fusion between Fraction I and α, and crossing between Fraction II and α.

FIG. 11. Precipitin bands found by testing 10% adult chick lens extract (Fractions I, II, and III) and isolated alpha crystallin (α) with lens antiserum. Note the appearance of four subfractions in Fraction II and their crossing over with the α-crystallin band.

FIG. 12. Precipitin bands found by testing 10% adult chick lens extract (Fractions I, II, and III) and isolated beta crystallin (β) with lens antiserum. Note the fusion of Fraction II and the β-crystallin band.

FIG. 13. Precipitin bands formed by testing 10% adult lens extract (Fractions I, II, and III), isolated beta crystallin (β) and isolated gamma crystallin (γ) with lens antiserum. Note fusion between Fraction II and beta crystallin and between III and gamma crystallin.

FIG. 14. Precipitin band found by testing 50-hr lens extract with lens antiserum.

FIG. 15. Lens placode of 19-somite embryo.

FIG. 16. Invaginating lens placode from 24-somite embryo (50 hr); acidophilic fibers appear in cytoplasm of the cell (arrow).

FIG. 17. Precipitin bands found by testing 60-hr lens extract with lens antiserum.

FIG. 18. Invaginating lens placode from 28-somite embryo (60 hr); acidophilic fibers become longer.

FIG. 19. Lens vesicle from 32-somite embryo.

FIG. 10

FIG. 11

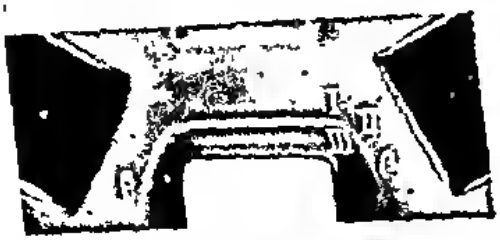

FIG. 12

FIG. 13

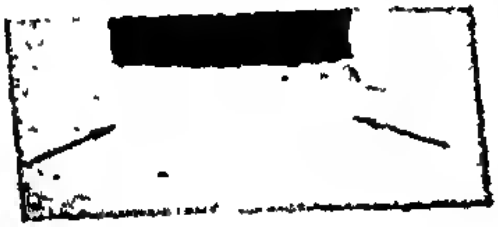

FIG. 14

FIG. 17

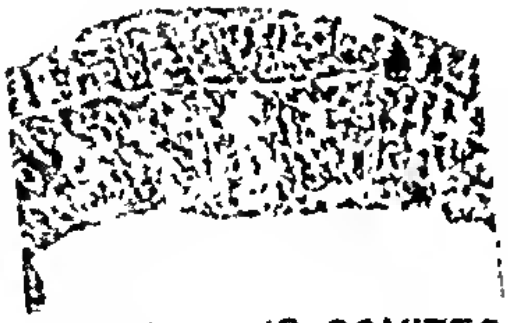

FIG. 15 19 SOMITES

FIG. 18 28 SOMITES

FIG. 16 24 SOMITES

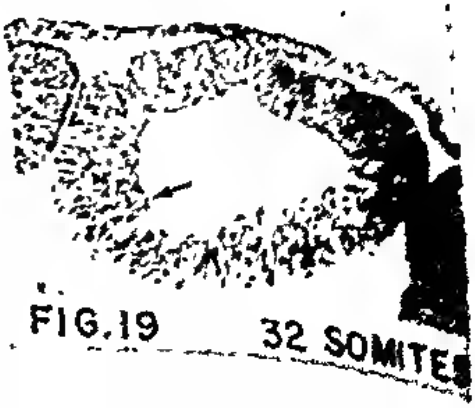

FIG. 19 32 SOMITES

coincides with the formation and growth of the acidophilic fibers in the cytoplasm, the appearance of basophilic granules at the base of the cells, and the formation of the first nuclear lens fibers (Figs. 18, 19, Plate II). By testing a lens extract from 80-hr embryos in which the lens fibers had reached their full length, the same number of precipitin bands was found as in 72-hr lens extract, indicating that the number of lens antigens did not increase during growth of the fibers. Hence, while the first appearing lens antigen is considered to be a lens placode antigen, the appearance of the following three antigens is presumed to be associated with the formation of nuclear lens fibers. At the 96-hr stage, elongation of the nuclei, mitotic activity, and the appearance of acidophilic fibers and basophilic granules in the cells of the marginal zone are the most characteristic morphological features (Fig. 23). Figure 22 shows that five precipitin bands were formed in the agar plate when a 96-hr lens extract was tested with lens antiserum. The new formed lens antigen is presumably located in the cells of the marginal zone and is considered to be one of the marginal lens fiber antigens. During the subsequent period of development, fiber formation in the marginal region of the lens is in full progress. When testing lens extracts of 10-day-old embryos (Fig. 24) and newly hatched chicks with lens antiserum, it appeared that some existing bands became dense and broad, while other new bands appeared, indicating increase in concentration of some of the existing antigens and formation of new antigens (Fig. 25). From this experiment, it can be concluded that in the course of lens development new antigens are formed one after another, preceding or coinciding with the formation of new morphological structures.

To determine whether the antigen found at the lens placode stage can still be demonstrated in lens extracts of 72- and 96-hr embryos and finally in the adult stage, lens extracts of these stages were tested side by side with lens antiserum. The results showed that the first formed lens antigen found at the lens placode stage is still present at the 72- and 96-hr stages and in the adult. It is represented in the agar plate by the precip-

---

PLATE III

FIG. 20. Precipitin bands found by testing 72-hr lens extract with lens antiserum.

FIG. 21. Lens vesicle 72-hr embryo (36-somites) shows beginning nuclear lens fiber formation.

FIG. 22. Precipitin bands found by testing 96-hr lens extract with lens antiserum.

FIG. 23. Lens from 96-hr embryo; nuclear lens fibers have filled the lumen of the lens vesicle and the cells in the marginal zone show beginning fiber formation.

FIG. 24. Lens from 10-day-old embryo.

FIG. 25. Precipitin bands found by testing 10-day lens extract with lens antiserum.

ıtin line closest to the antigen well, that is the line referred to above as Fraction I and found to be identical to alpha crystallin. Hence the first lens antigen to appear during lens formation is presumably alpha crystallin. Since beta crystallin is identical to Fraction II and this fraction arises during formation of the lens shortly after the appearance of Fraction I, it is presumed that beta crystallin is the second lens antigen to be formed.

FIG. 20 72 HOURS

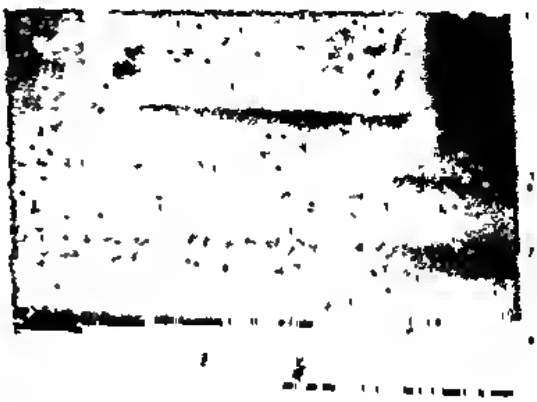

FIG. 22 96 HOURS

FIG. 21 36 SOMITES

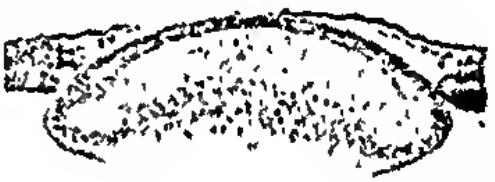

FIG. 23 44 SOMITES

FIG. 24 10 DAYS

FIG. 25 10 DAYS

Gamma crystallin was found to be the last fraction to arise during the development.

Summary

Summarizing the results of this experiment, it can be stated that the first lens antigen was found to arise in the presumptive lens ectoderm cells at the 11-somite stage, that is, shortly after the induction period has started (9 somites) and shortly before morphological changes in the cells, such as loss of vacuolization, palisade phenomenon, and nuclear orientation became visible (18 somites). This antigen, which could clearly be demonstrated in the lens placode cells (18–20 somites) by means of the agar-diffusion test, appears to be alpha crystallin and has an estimated molecular weight of about 1,000,000. The next antigens to be formed and identified as subfractions of beta crystallin (M.W. ± 200,000) arose at the 60–72-hr stage, when basophilic granules appeared at the base of the cells and the formation of the nuclear lens fibers became visible. When lens extracts of older embryos and newly hatched chickens were tested with lens antiserum, it appeared that some existing bands became dense and broad, while other new bands appeared, indicating increase in concentration of some of the existing antigens and formation of new antigens presumably located in the marginal lens fibers. Though it has not been possible to demonstrate the morphological substrate of gamma crystallin, it appears that this fraction (M.W. ± 50,000) arises as the last during development.[2]

References

Alexander H. E. (1937). *J. Exptl. Zool.* **75**, 41-73.

Burky, E. L., and Woods, A. C. (1928). *Arch. Ophthalmol.* **57**, 464-483.

Francois, J., Wieme, R. J., Rabaey, M., and Neetens, A. (1953). *Soc. Belge d'Ophthalmol.* **104**, 322-331.

Francois, J., Wieme, R. J., Rabaey, M., and Neetens, A. (1954). *Experientia* **10**, 79-83.

Korngold, L. (1956). *J. Immunol.* **77**, 119-122.

Langman, J. (1953a). *Proc. Koninkl. Ned. Akad. Wetenschap. Ser.* **56**, 17-28.

Langman, J. (1953b). *Proc. Koninkl. Ned. Akad. Wetenschap. Ser.* **56**, 214-218.

Langman, J. (1956). *Acta Morphol. Neerl.-Scand.* **1**, 1-12.

Langman, J. (1959a). *J. Embryol. Exptl. Morphol.* **7**, 193-202.

Langman, J. (1959b). *J. Embryol. Exptl. Morphol.* **7**, 264-274.

Langman, J., Schalekamp, M., Kuyken, M., and Veen, R. (1957). *Acta Morphol. Neerl.-Scand.* **1**, 142-154.

Maisel, H., and Langman, J. (1960). *J. Embryol. Exptl. Morphol.* Submitted for publication.

[2] The discussion for this article is combined with the discussion following the article by Drs. S. P. Halbert, W. Manski, and T. Auerbach.

McKeehan, M. S. (1951). *J Exptl. Zool.* **117**, 31-64.
Ouchterlony, O. (1949). Antigen-Antibody Reactions in Gels and the Practical Application of this phenomenon in the Laboratory Diagnosis of Diphtheria. Thesis. Karolinska Institute, Stockholm
Ouchterlony, O (1953). *Acta Pathol Microbiol Scand.* **32**, 231-240.
Smelser, G. K, and von Sallmann, L. (1949). *Am. J. Ophthalmol.* **32**, 1703.
van Deth, J. H. M. G. (1940). *Acta Neerl. Morph.* **3**, 151-155.
Waddington, C. H., and Cohen, A (1936) *J. Exptl. Biol.* **13**, 219-236.
Weiss, P. (1947). *Yale J Biol and Med* **19**, 235-278.
Wilson, M L, and Pringle, B. H (1955). *J Immunol.* **75**, 460-469.

See page 257 for Discussion

Lens Antigens in Relation to Evolution

S. P. HALBERT, W. MANSKI, AND T. AUERBACH

Department of Ophthalmology, College of Physicians and Surgeons, Columbia University, New York, New York

IT HAS BECOME QUITE CLEAR that during the many millions of years of evolutionary change, most proteins and other complex molecules of living organisms have progressively diverged in their composition and properties. The basic *function* of many of these proteins has been maintained intact throughout much of evolutionary history, as is evidenced, for example, by the remarkable similarity in enzymatically determined *metabolic steps* by which such diverse forms as bacteria, plants, and mammals derive energy. However, the progressive divergence of the detailed structure of particular proteins has readily been demonstrated by immunological techniques. For example, Nuttall (1904) has studied the cross relationships of serum proteins among various mammalian species. He found that antibodies against human serum proteins cross react strongly with serum proteins from apes (gorilla and orangutan), but cross-react less strongly with sera from monkeys, and progressively less with sera from species more widely removed in the phylogenetic scheme, until no reactions were seen with pig, rabbit, or kangaroo sera. Similarly, Heidelberger and Landsteiner (1923) showed that antibody against horse hemoglobin reacted with the immunizing antigen, but only cross-reacted weakly with hemoglobin of the closely related donkey. It failed to show any reaction with hemoglobins of ox, rabbit, rat, chicken, sheep, or pig. Similar data obtained by numerous investigators have demonstrated that tissues or fluids from one species of organism may contain numerous antigens whose immunological specificity is shared to varying degrees only by similar components from rather closely related species. This type of limitation of biochemical similarity has been termed *species specificity*.

In extreme contrast to this biochemical divergence is that observed with ocular lens, first noted by Uhlenhuth (1903). He showed that antiserum against vertebrate lens cross-reacted with many vertebrate lenses. This broad crossing of species lines with respect to the biochemical similarities of lens components has thus been appropriately called *organ specificity*. Hektoen and Schulhof (1924) and Woods and Burky (1927), among others, confirmed these observations and suggested on the basis of data then available that only one or two lens proteins were involved.

Unfortunately, the immunological techniques which had been developed at that period were quite uninformative with regard to the number of systems involved in the precipitin mixtures. The recent development of sensitive and potent methods for analysis of precipitin reactions in agar gels (e.g., Ouchterlony, 1949), with or without preliminary electrophoresis, has opened the way to a detailed study of this organ specificity, and of its significance.[1] In addition, the discovery by Freund and Bonanto (1944) of a valuable adjuvant vehicle for boosting antibody responses has greatly aided in these investigations.

The current status of our knowledge with regard to this subject may be conveniently divided into two aspects.

(1) The interrelationships of lens antigens among different vertebrates, and their meaning.

(2) The relationship of invertebrate and vertebrate lens antigens.

The Interrelationships of Vertebrate Lens Antigens

With the introduction of the newer methods of serological analysis, it soon became apparent that lens homogenates contained many more soluble antigens than had been heretofore suspected. Even using *homologous* lens antisera, by injecting adult rabbit lenses in Freunds adjuvants into adult rabbits, it was possible to show that at least 5 lens antigens could act as foreign substances in this species (Halbert *et al.*, 1957a, b) (See Fig. 1). With these homologous antisera, nonlens systems almost certainly were not complicating the picture.

With *heterologous* antilens sera (bovine lens injected into rabbits), Rao *et al.* (1955) found 6 bovine lens components, while François *et al.* (1956) using the immunoelectrophoretic method could detect 8 bovine lens antigens with such sera. Using the latter method, observations made in this laboratory have indicated that at least 10 bovine lens antigens can be detected in this way (Manski *et al.*, 1960). These are represented photographically and diagrammatically in Fig. 2.

With regard to organ-specific reactions, François *et al.* (1956) tested antibovine lens antisera against sheep, pig, horse, and human lenses.

---

[1] It may be recalled that these methods give clear and direct evidence of the number of immunologically distinct systems involved in a given reaction mixture, as revealed by the deposition of bands of precipitate. In the Ouchterlony technique, such bands will cross unrelated immunological precipitin systems ("nonidentity"), or merge with those which are related ("identity"). When complex mixtures are to be examined, preliminary electrophoresis of the antigens in the agar gel greatly facilitates the visualization of the minimum numbers of components. With this latter modification, the antisera is placed into a trench alongside the electrophoretically separated antigen.

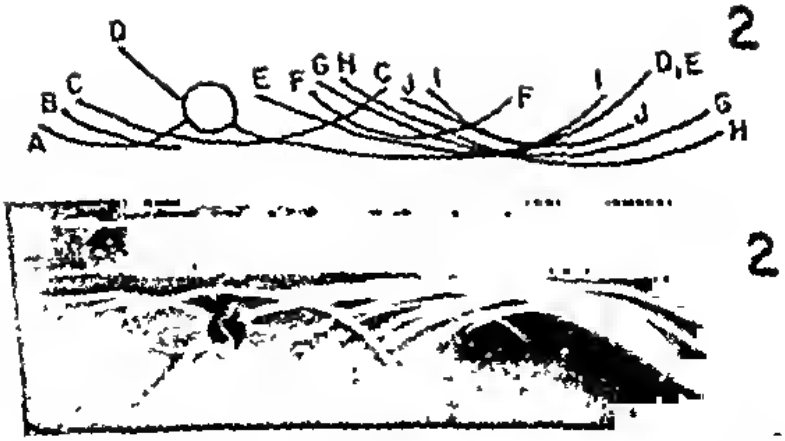

FIG. 2. Immunoelectrophoretic analysis of bovine lens homogenate and anti-bovine lens serum prepared in the rabbit.

experience of this laboratory, the organ-specific reactions are much more complex than this. Previously, antihuman lens antisera had revealed 6 cross-reactive fractions when tested with beef lens (Halbert and Fitzgerald, 1958). Using immunoelectrophoretic methods and taking care to use highly potent antilens sera, it has now been found that organ-specific

crossreactions among mammals may be due to similarity of 9 to 10 lens components (see Fig. 3). When antimammalian lens antiserum was tested against lenses from species lower in the evolutionary scale, the numbers of cross-reacting components were found to decrease, as exemplified in Fig. 4. In these tests, antihuman cataract lens sera were used,

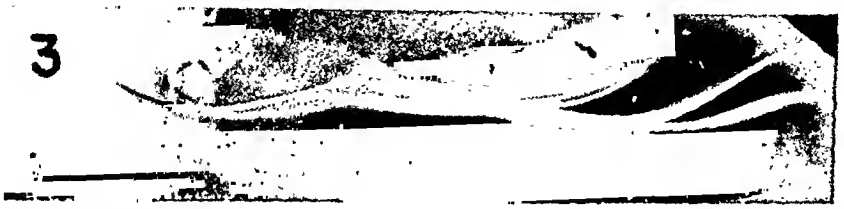

FIG. 3. Immunoelectrophoretic analysis of the cross reaction between antihuman cataract lens serum prepared in the rabbit, and Java monkey lens homogenate.

REACTION OF ANTIHUMAN (CATARACT) LENS SERUM WITH DIFFERENT VERTEBRATE LENSES

LENS	NO. of PRECIPITIN LINES IN DIFFERENT MOBILILITY GROUPS α	β	γ	TOTAL NO. OF PRECIPITIN LINES	IMMUNOELECTROPHORETIC PATTERNS
HUMAN	2	4	2	8	
RHESUS	2	5	3	10	
JAVA	2	5	3	10	
BOVINE	2	5	2	9	
RABBIT	2	4	3	9	
G.PIG	2	4	3	9	
RAT	2	4	3	9	
MOUSE	2	4	3	9	
WHALE	2	5	2	9	
CHICKEN	2	3	2	7	
FROG	2	3	1	6	
MENHADEN	1	3	1	5	
CARP	1	3	1	5	
SQUID	0	0	0	0	
LOBSTER	0	0	0	0	

FIG. 4. Diagrammatic summary of the cross reactions between antihuman cataract lens sera and lens from animals at different levels of the phylogenetic scheme.

but similar results have also been obtained with antibovine lens sera. In addition, homologous antirabbit lens sera, although much less potent, showed a similar pattern (Manski *et al.*, 1960). Interestingly, the cross reactions involved all three of the well-recognized electrophoretic *families* of lens proteins, the alpha, beta, and gamma crystallines. Such findings agree with those obtained by Witmer (1959).

At first glance it might be thought that the decreasing number of cross-reacting entities found in the above systems might be due to the simpler composition of lens substance as one goes down the phylogenetic scale. That such is not true is seen in tests between some of these other antisera and their immunizing lens antigens. A few of these results are shown in Fig. 5. Usually between 9 and 10 components were also found in these systems.

HOMOLOGOUS REACTION
OF SOME ANTIVERTEBRATE LENS SERA

LENS	Rabbit immune serum against lens of	IMMUNOELECTROPHORETIC PATTERNS
FISH	FISH	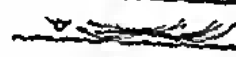
FROG	FROG	
CHICKEN	CHICKEN	
RABBIT	RABBIT	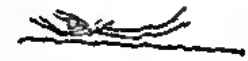
HUMAN	HUMAN	

Fig. 5. Immunoelectrophoretic analysis of some other lenses and the antisera prepared against them in the rabbit.

On the basis of the species thus far studied, the evolutionary pathways involved are indicated in the abbreviated diagram shown in Fig. 6. On the basis of this data, as examples, one should be able to predict that absorption of antimammalian lens antisera with bird lens should remove the amphibian lens and fish lens cross-reacting antibodies, while leaving some mammalian systems intact. Similarly, absorption of anti-mammalian lens with fish lens should remove fish cross reactivity and still leave cross reactions with amphibian lens as well as lenses of higher forms. That such appears to be the case is illustrated by a sample of such absorption tests shown in Fig. 7.

The data accumulated thus far, therefore, indicates that the origin of organ specificities would seem to lie in the retention by the lens of its evolutionary history. One may speculate that the relative stability of

these lens components may perhaps be due to the comparative isolation of the lens as a structure during development. It is also conceivable that the components involved are so well suited to their function that small

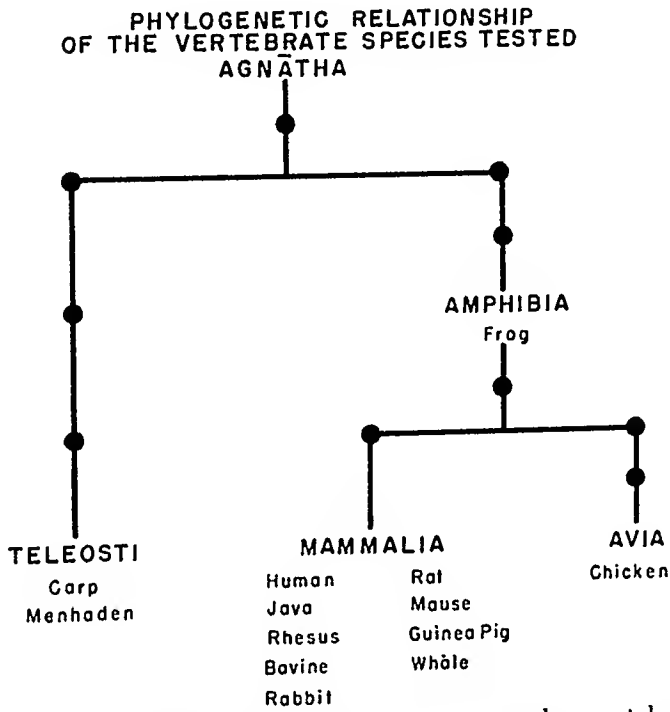

FIG. 6. Abbreviated diagram of the evolutionary pathways taken by some of the species included in these studies.

REACTION OF DIFFERENT VERTEBRATE LENSES
WITH ABSORBED ANTIHUMAN (CATARACT) LENS SERUM

LENS	ANTIHUMAN (CATARACT) LENS SERUM ABSORBED WITH LENS OF			
	WHALE	CHICKEN	FROG	FISH menhaden
HUMAN				
WHALE				
RABBIT				
CHICKEN				
FROG				
FISH				

FIG. 7. Results of absorption of antihuman cataract lens serum with lenses of several widely differing vertebrates.

chemical changes would have caused profound disturbances of use. At any rate, these observations are being extended to explore in great detail the possible evolutionary history of vertebrate lenses.

Vertebrate and Invertebrate Lenses

It is well known that the eyes of the cephalopod invertebrates bear a strong resemblance to vertebrate eyes in structure. Morphological and other evidence have indicated that the cephalopod eye has evolved along a distinct path from that of the vertebrates (Gregory, 1929). The similarity in structure has been considered an example of "convergent" evolution. Wollman *et al.* (1938) found that the octopus lens failed to cross-react with antisera against vertebrate lens, using simple tube precipitin methods. In this laboratory, it has been demonstrated that squid lens antisera prepared in the rabbit revealed 4 to 5 components when tested with squid lens in agar precipitin assays. One component formed a very dense band. No cross reactions whatsoever were noted with a number of vertebrate lenses. Similarly, several vertebrate lens antisera failed to show any cross reaction with the squid lens, while they cross-reacted freely among themselves as indicated above. Examples of these reactions are shown in Fig. 8. In addition, absorption tests carried out with the

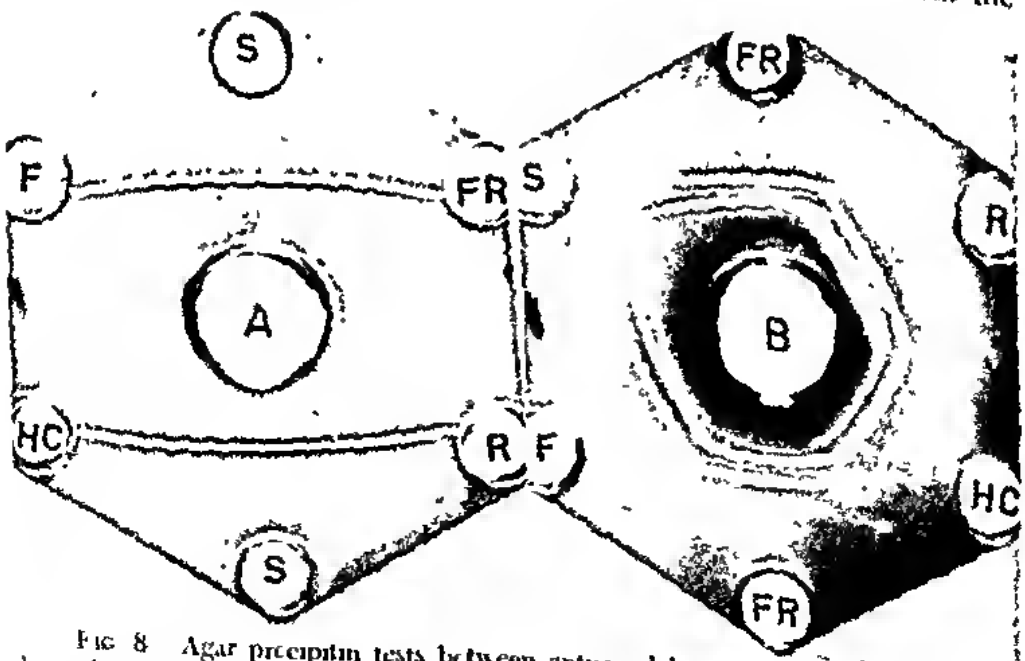

FIG. 8. Agar precipitin tests between antisquid lens serum, and several vertebrate lenses, and between antifrog lens serum and the same antigens. A = squid lens antiserum, center well (lens antigens in peripheral wells), B = frog lens antiserum, center well (lens antigens in peripheral wells); FR = frog (*Rana pipiens*) lens; F = marine fish (menhaden) lens, R = rabbit lens, HC = human cataract lens, S = squid lens.

squid lens antisera and vertebrate lenses, as well as the reverse, failed to demonstrate any similarities between the several invertebrate and numerous vertebrate lens components. It thus seems clear that the well-developed invertebrate lens does not share any chemical similarity in this respect with vertebrate lens. These observations support the view that the eye of the cephalopod did indeed evolve along a distinct path from that of the vertebrates. It is hoped that it may be possible to trace something of the evolutionary history of the invertebrate eye by using such antisera, and lenses or lens analogs from a wide variety of invertebrate species.

Summary

(1) It has been shown that the organ specificity of lens is quite complex and among mammalian lenses involves the biochemical similarity of at least 9 to 10 components.

(2) The number of components common between lenses of different vertebrates diminish according to the phylogenetic sequence of the vertebrate species tested using antimammalian lens sera.

(3) Absorption of antihuman lens serum with appropriate vertebrate lenses removed antibodies against all lens components of species which were lower in the evolutionary scale.

(4) The origin of organ specificity of the lens may lie in the retention by the lens of molecular structures acquired during successive stages of evolution.

References

François, J., Rabaey, M., Wieme, R. J., and Kaminski, M. (1956). *Am. J. Ophthalmol.* **42**, 577-584.

Freund, J., and Bonanto, M. V. (1944). *J. Immunol.* **48**, 325-334.

Gregory, W. K. (1929). "Our Face from Fish to Man." Putnam, New York and London.

Halbert, S. P., Locatcher-Khorazo, D., Swick, L., Witmer, R. H., Seegal, B., and Fitzgerald, P. (1957a). *J. Exptl. Med.* **105**, 439-452.

Halbert, S. P., Locatcher-Khorazo, D., Swick, L., Witmer, R., Seegal, B., and Fitzgerald, P. L. (1957b). *J. Exptl. Med.* **105**, 453-462.

Halbert, S. P., and Fitzgerald, P. L. (1958). *Am. J. Ophthalmol.* **46**, 187-195.

Heidelberger, M., and Landsteiner, K. (1923). *J. Exptl. Med.* **38**, 561-571.

Hektoen, L., and Schulhof, K. (1924). *J. Infectious Diseases* **34**, 433-439.

Manski, W., Auerbach, T., and Halbert, S. P. (1960). *Am. J. Ophthalmol.* (in press).

Nuttall, G. H. F. (1904). "Blood Immunity and Blood Relationship." Cambridge Univ. Press, London and New York.

Ouchterlony, O. (1949). *Acta Pathol. Microbiol. Scand.* **25**, 507-515.

Rao, S. S., Kulkarni, M. E., Cooper, S. N., and Radhakrishnan, M. R. (1955). *Brit. J. Ophthalmol.* **39**, 163-169.

Uhlenhuth, P. T. (1903). "Festchr. zum 60 Geburstag. Robert Koch," pp. 49-74. Fischer, Jena.
Witmer, R. H. (1959). *A.M.A. Arch. Ophthalmol.* **61**, 738-744.
Wollmann, E., Gonzalez, P., and Ducrest, P. (1938). *Compt. rend. soc. biol.* **127**, 668-670.
Woods, A. C., and Burky, E. L. (1927). *J. Am. Med. Assoc.* **89**, 102-110.

Discussion of Articles by Drs. Halbert, Manski, Auerbach, and by Dr. Langman

Dr Pirie [Oxford, England]: Did Dr. Halbert find any differences between the antigens in normal and cataractous human lenses with anticataract serum?

Dr. Halbert [Columbia University, New York]: We have carried out a few tests in which we placed the homogenate of normal human lens adjacent to that of cataractous lens, both being exposed to the anticataract lens antiserum. Very disappointingly, we found that all of the bands between the two merged. We had hoped that there might be some distinct immunological cataract components, so that one or more crossing bands would show up between the cataract lens and its antiserum. This did not occur.

Dr. Maisel [McGill University, Montreal, Canada]: We have used antisera prepared in rabbits against chicken lenses to study species specificity of the ocular lens. It was found that the alpha fraction is represented throughout the vertebrate series when this serum was tested against mammalian, turtle, frog, and fish lenses. In addition, in some cross reactions (e.g., with turtle lens) alpha, beta, and gamma fractions are all involved. This work, in conjunction with that of Dr. Langman's showing that the alpha crystallin is the first to develop embryologically, suggests that the alpha fraction is the basic protein in the evolution of the eye. Furthermore, the alpha fraction is always represented in all extra-lenticular tissue which can form a lens, although the beta and gamma material may be lacking. Also, we have found human fetal lens antigens which are not present in the adult mammalian lens.

How do you distinguish between the alpha, beta, and gamma crystallins in your study?

Dr Halbert: My feeling is that the time has come when we must very seriously consider abandoning the idea that there are distinct molecular entities of alpha, beta, and gamma crystallins. These are apparently families of different substances which tend to migrate together in an electric field. It is quite analogous to the situation with human serum which was previously divided into 5 components electrophoretically. We now know that human serum, by immunoelectrophoretic examination, is composed of many, many different and distinct entities. Why should we, therefore, continue to think of lens macromolecular components in these rather antiquated terms?

Dr Maisel: I cannot agree that we should abandon the terms alpha, beta, and gamma crystallin. Although there are many lens antigens, they seem to exist in three distinct groups. Each of these groups probably contains a series of closely related antigens.

Dr Halbert: In studying these systems, one must have potent antiserum. Even in the case of antiserum against human serum, if a potent antiserum isn't used, we might find only four or five components, instead of the 40 or more actually present. We must use extremely potent serum.

Also, one has to be very careful about band artifacts that apparently *can* develop when the gel precipitins are kept for prolonged periods. This has been demonstrated by many investigators, and caution must be observed in the interpretation of bands under certain conditions, especially when there are *relative* excesses of antigen or antibody for a given system. Some of the photographs shown by Dr. Langman suggested the possibility of this type of striation artifact.

In our experience, the separation of these lens antigens is not easy. With potent lens antiserum and immunoelectrophoretic analysis, the results are quite complex. We tested the alpha, beta, and gamma crystallins prepared by the most recent chemical fractionation procedures described by François, and the immunologic results reveal that all were complex mixtures. None is a "pure" moiety.

Dr. Herrmann [Storrs, Connecticut]: I am wondering whether the use of cellulose column chromatography, with or without pretreatment with hydrogen bond-disrupting compounds, may be recommended as an additional analytical tool in identifying antigenic proteins of the lens.

Dr. Halbert: We have done chromatographic separations of these electrophoretic fractions, and find that many of the peaks obtained are still mixtures of antigens. We get excellent protein elution peaks but similar antigens come off in many of the different peaks. We hope eventually to obtain some of these components as truly homogeneous moieties, using *all* currently available analytical techniques.

Recovery from and Protection against Radiation Damage to the Lens

ANTOINETTE PIRIE

Nuffield Laboratory of Ophthalmology, University of Oxford, Oxford, England

Introduction

Irradiation of the lens in mammals causes gradual development of cataract, the degree and type of opacity depending on the dose and type of radiation and the age and species of animal irradiated. Young animals are more susceptible than older ones. Poppe (1942), von Sallmann (1952a), and others have shown that irradiation of the lens damages the epithelial cells which lie in a single layer over the anterior surface. As in other tissues, radiation damage is histologically recognizable only in cells capable of division. In normal lens epithelium these cells lie in a ring at the periphery, about 1 mm in front of the lens equator and it is only if these cells are irradiated that cataract results.

The response of the epithelium of the lens to X-rays has been extensively studied histologically (Poppe, 1942; Cogan and Donaldson, 1951, von Sallmann, 1952a, von Sallmann *et al.*, 1955). Flat preparations of the whole epithelium and mitotic counts can be made (Howard, 1952) and cell distribution and nuclear damage can be examined. Von Sallmann (1952a) has shown that the characteristic response in a rabbit is an immediate fall in and then cessation of mitosis which may last up to a week depending on the dose of radiation given. This is followed for several weeks by an excess mitosis, together with the appearance of many fragmented nuclei. If the dose of X-rays has been insufficient to cause complete breakdown of the epithelium, this will still, many months later, show signs of damage, having fewer cells, whose arrangement and size are irregular (Poppe, 1942; von Sallmann 1952a).

The damaged epithelial cells form damaged lens fibers, misshapen and opaque to light. These get pushed, by subsequent cell divisions, round under the lens capsule to the posterior pole where they constitute the cataract. If the damage has been gross the epithelium degenerates completely and the whole lens may become opaque. Goldmann and Liechti (1938) found that X-rays damaged only the germinative epithelium of the lens. This has been confirmed by many later workers (Alter and Leinfelder, 1953, Puntenney and Shoch, 1954, von Sallmann *et al.*, 1955). Leinfelder and Riley (1956), Richards *et al.* (1956), and

Pirie and Howard-Flanders (1957) found that shielding a small part of the lens from the X-rays profoundly modified the development of opacity in the irradiated area. A dose of X-rays which, if given to the whole lens of a rabbit, would produce total opacity, produced only a partial opacity in the irradiated area when a quarter to a half of the lens was shielded.

Such a lessening of the injury might be due to one or more factors, such as, (1) replacement of damaged epithelium by migration of cells from the uninjured area, (2) protection of the epithelium during irradiation by factors from the shielded area, (3) recovery of damaged epithelium due to diffusion of substances from the uninjured area, as Devik (1955, 1957) considers may take place in the skin, (4) removal of toxic metabolites from the irradiated part by the cells of the shielded part, (5) maintenance of the lens fibers under the damaged epithelium in a healthy state by diffusion of metabolites from the uninjured area.

Modification of response to radiation is particularly interesting in the lens, as this is a mammalian tissue into which no outside cell penetrates and out of which no cell migrates owing to the impermeability of the lens capsule. Any modification of radiation damage must therefore be due to reaction of cells which are all present or have been derived from those present at the time of irradiation. There is no possibility of an influx of cells from elsewhere, of phagocytosis, or of cellular migration out of the tissue.

Effect of Part Shielding the Lens

To find out whether lessening of total damage by shielding a small part of the lens is due to cell migration from uninjured to irradiated area, to recovery of cells after irradiation, or their protection during irradiation by diffusible factors from neighboring healthy cells we have been studying the histology of lenses that have been only partly irradiated and by comparing histologically and clinically, the effect of partial shielding with that of a protective agent, cysteine.

In the experiments using part-shielded lenses one-half of the lens has been irradiated and the other half shielded with lead. Flat preparations of the epithelium of such half-irradiated lenses have then been examined at different times in an attempt to determine whether cell migration from healthy to irradiated area or recovery of cells in the irradiated area takes place. Mitotic counts have been made, the area in which damaged nuclei or abnormal cells are present has been measured, and the general distribution and density of cells has been assessed (Pirie and Drance, 1959).

A dose of 1400 to 1600 r, 200 kv X-rays, to the right eye of 6- to 12-week-old rabbits was used. To shield half the lens a contact lens with a

superstructure in which there was a semicircular lead shield was inserted into the right eye. The position of the shield was noted at start and end of irradiation. When the rabbit was ultimately killed a stitch was inserted at the limbus at the center of the shielded side before the eye was excised, and a tag of pigmented ciliary process was later left attached to the lens at this point. This tag remained on the epithelial preparation throughout.

Fixation and staining of nuclei with the Feulgen stain, followed by removal of the epithelium plus capsule to make a flat preparation, were carried out according to Howard (1952). The circular preparations were marked with India ink on the cover slip in either four sectors of 90° each or a larger number of smaller sectors. Mitotic counts were made in complete sectors and the total for the whole epithelium calculated. For assessment of cell density, photographs were taken of two comparable microscopic fields, one in the irradiated area and one in the shielded area, and the total number of cells in each were counted. The ink sectorial markings were invaluable in enabling two fields comparable in position to be found Comparisons were also made between the totally irradiated and the other nonirradiated eye of the rabbit, and, in litter mates, between the effect at any one time of half or total irradiation of their lenses. Lenses were examined at intervals between 1 day and 9 months after X-ray

The most interesting result is that there does not appear to be any cell migration from the unirradiated half of the epithelium into the irradiated area. This conclusion is based on the finding that the area of X-ray damage remained detectable for the whole period of observation and that it remained between 40 and 60% of the total. The area of damage can be mapped using different criteria at different times after irradiation at first, by determining the area in which mitosis is absent; later, the area containing fragmented nuclei; and many weeks after X-irradiation, the area of cell depletion. We have not found any progressive reduction in the size of the area which shows X-ray damage nor is there a change at any time in the number of mitoses in the nonirradiated half of the lens, compared with the number in the epithelium of the other nonirradiated lens, an increased cell division would have been expected had cell migration been taking place. We therefore conclude that the lessened severity of the X-ray damage in the half-irradiated lens cannot be due to cell replacement. It must then be due to diffusion of substances into or out of the irradiated area, with benefit to the epithelial cells or lens fibers or both. If replacement of damaged epithelium by migration of cells from the uninjured area were taking place, the area of damage should decrease with time. This does not occur.

As the *area* of epithelial damage did not decrease in the months following irradiation we next compared the *severity* of damage, using criteria laid down by von Sallmann (1952a). In the half-irradiated as in the wholly irradiated lens there is arrest of mitosis with complete disappearance of mitotic cells in the irradiated area for up to 5 days after X-ray. This is followed by overshoot of mitosis with many broken nuclei, micronuclei, and abnormal forms. This phase lasted 6 to 8 weeks being maximal at 3 to 4 weeks after irradiation. Both the half-irradiated and

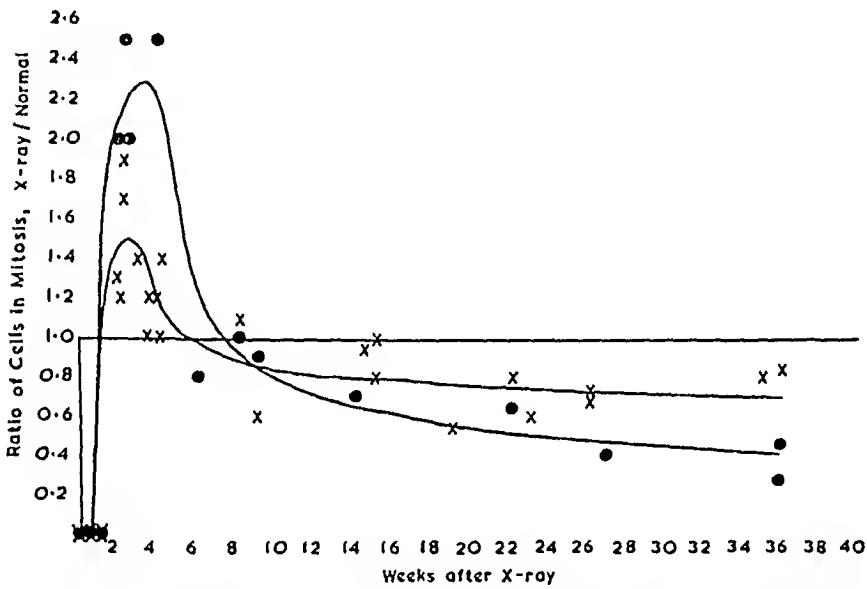

FIG. 1. Ratios of number of mitoses in the irradiated area of lens epithelium to the number in the nonirradiated area plotted against time after irradiation.

KEY: x———x Ratio of mitoses in irradiated half of lens to the mitoses in the shielded half of the same lens. ●———● Ratio of mitoses in the totally irradiated lens to the mitoses in the left lens of the same rabbit.

the wholly irradiated epithelia show these changes, but the overshoot of mitosis is greater in the wholly irradiated lens than in the irradiated half of the half-irradiated lens. From 8 to 30 weeks after X-ray the irradiated areas show fewer mitoses than the nonirradiated areas, but again the

---

FIGS. 2a and b. Cell depletion in the irradiated half of the lens 14 weeks after 1400 r. Magnification: × 250.

FIG. 2a. Shielded half, peripheral zone.

FIG. 2b. Irradiated half, peripheral zone.

FIGS. 3a and b. Cell depletion in the totally irradiated lens, 14 weeks after 1400 r.

FIG. 3a. Left, nonirradiated lens. Magnification: × 160.

FIG. 3b. Right, totally irradiated lens.

depression of mitosis appears to be greater in the wholly irradiated than in the half-irradiated lens. Figure 1, in which the ratios of the number of mitoses in the irradiated parts to the number in the respective control areas are plotted against time after X-ray, shows that after complete arrest of mitosis in both irradiated areas the totally irradiated lens shows

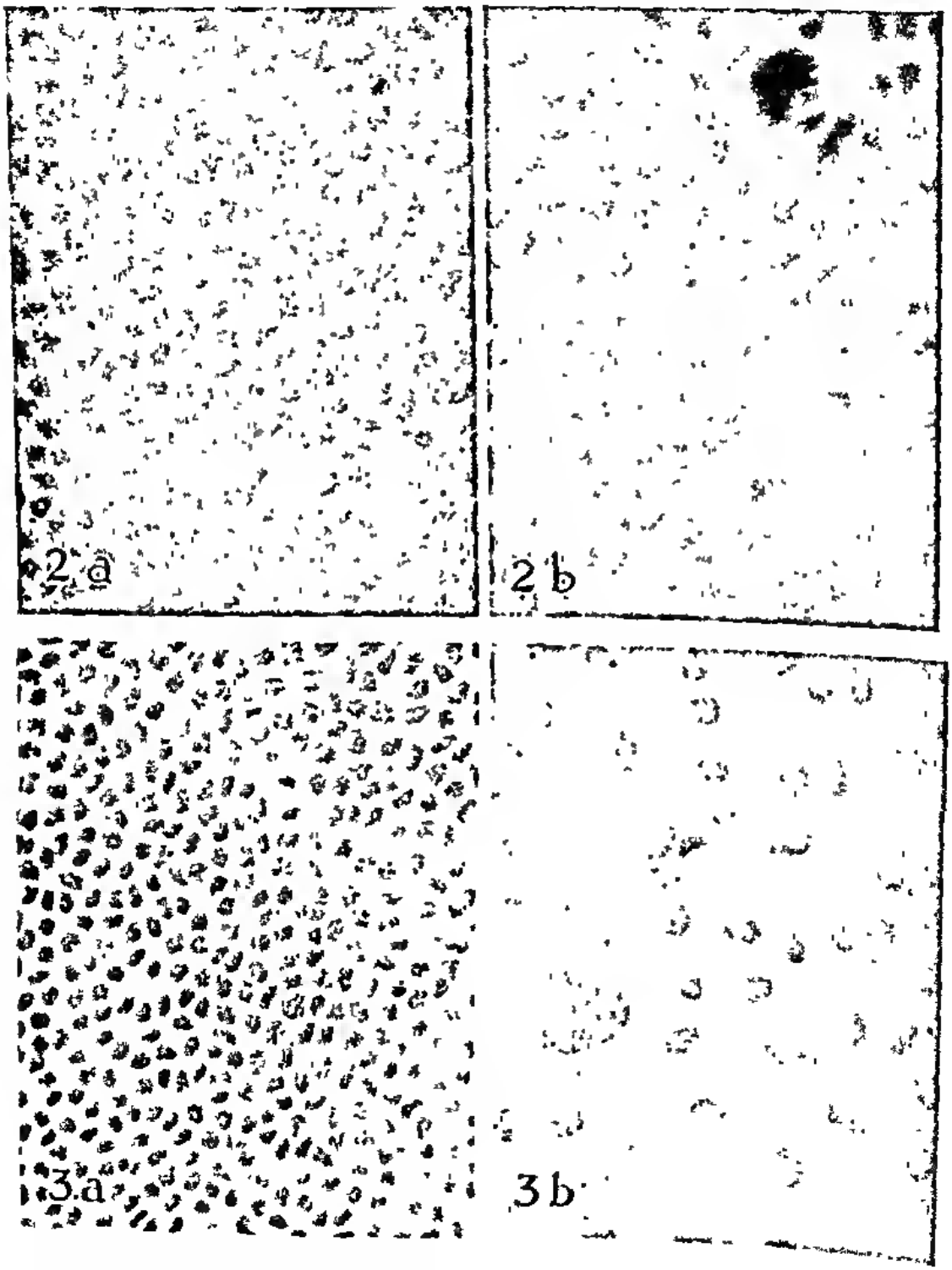

a greater overshoot of mitosis followed by a greater reduction in number of mitoses than the irradiated epithelium of the half-irradiated lens.

Poppe (1942) and von Sallmann (1952a) have noted cell depletion in lens epithelium after X-ray, persisting for as long as the period of observation. In the irradiated half of a half-irradiated lens, cell depletion was most obvious in the zone just central to the germinative zone. Figure 2 shows fields comparable in position from the two halves of a single epithelium, and shows that the cell nuclei in the irradiated area are sparser and more irregular in size and staining power than those in the nonirradiated area.

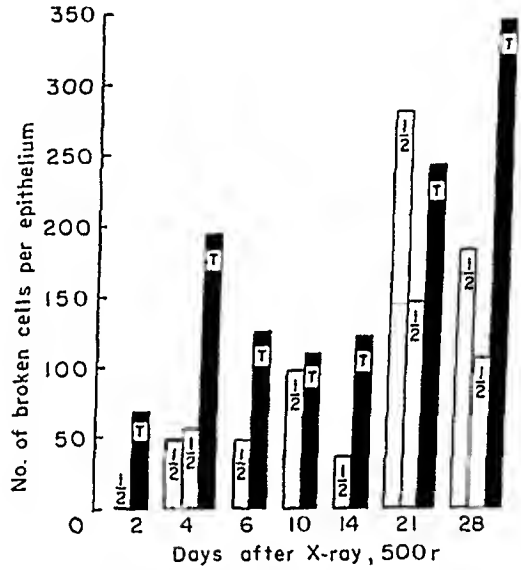

FIG. 4. Comparison of total number of fragmented nuclei in the half-irradiated and totally irradiated lens. Comparisons were made between litter mates after 500 r. The fragmented nuclei in the central 90° sector of the irradiated half of the half-irradiated lens and in one or more of such sectors of the totally irradiated lens were counted and the numbers multiplied to give the total in the full circle of 360° of the epithelium.

KEY: Solid bars "T" = totally irradiated. Empty bars "½" = half-irradiated.

But comparison showed that the epithelium of the irradiated area of the half-irradiated lens is much less abnormal than that of the wholly irradiated lens (Fig. 3). Few cells, and most of these abnormal, were left in the epithelium of the totally irradiated lens 16 weeks after irradiation, while although a loss of cells had certainly taken place in the irradiated half it was nowhere near so severe and the remaining cells looked fairly normal at this time.

Cell loss must be due to break up of the cell or its nucleus. Since fewer cells are lost from the irradiated area when half of the lens is shielded, one would expect to find fewer broken nuclei. We therefore

examined the number of fragmented nuclei in the totally and half-irradiated epithelia at different times after irradiation, using in this case a dose of 500 r. Figure 4 shows that in all cases but one, there were fewer broken nuclei (calculated for the whole epithelium) in the irradiated half of the half-irradiated lens than in the totally irradiated epithelium. The difference was manifest between 2 and 28 days after irradiation. This implies that the epithelium has either been "protected" or has "recovered," at least to some extent, in the first 2 days after irradiation.

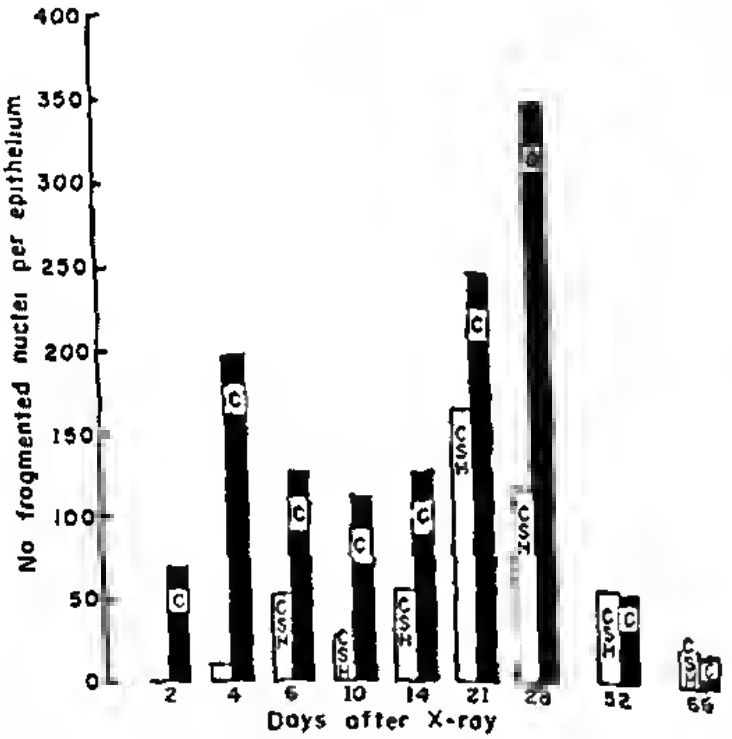

FIG 5 Comparison of fragmented nuclei in lens epithelium of rabbit given 500 r X-ray to eye with or without pretreatment with cysteine, 1.0 g/kg intravenous KEY Solid bars "C" = control Open bars "CSH" = cysteine treated.

Effect of Preirradiation Treatment with Cysteine

A histological comparison was therefore made between the effects of a protective agent, cysteine, with half-shielding of the lens. Von Sallmann (1952a, b) has shown that an injection of cysteine before irradiation will markedly reduce irradiation damage to the lens, and he found some evidence that the lens of the cysteine-treated rabbit showed fewer damaged nuclei than the one irradiated without prior cysteine. We have confirmed this observation When cysteine is injected about 5 min before irradiation with 500 r the number of broken nuclei that develop is considerably less than in the lenses of litter mates given 500 r without pretreatment with cysteine. Figure 5 shows the results up to 28 days after

irradiation. This is precisely the same picture that we obtained in our comparison of the half-irradiated and the totally irradiated lens (Fig. 4). Our experiments also seemed to show that injection of cysteine prior to irradiation with 500 r prolonged the mitotic arrest after irradiation, and lessened the excess mitosis that occurred at a later stage.

Effect of Cysteine Alone

This led us to examine the effect of cysteine alone without irradiation and we found that a single injection inhibits mitosis almost completely in the normal lens. This inhibition gradually develops during the 24 hr after cysteine injection and persists for up to 4 days (Fig. 6).

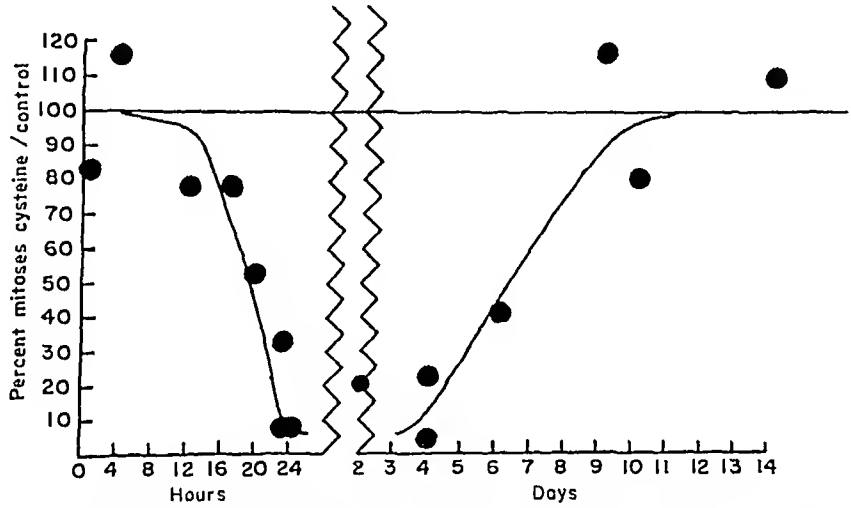

FIG. 6. Effect of a single cysteine injection on the numbers of mitoses in the lens epithelium of the rabbit.

Injections of saline or of glycine in comparable amounts have no effect (Pirie and Lajtha, 1959). Wachtl and Kinsey (1958) had found earlier that addition of cysteine to the medium in which they cultured rabbit lenses depressed mitosis.

It is generally agreed that cells are more sensitive to irradiation damage at some rather than other stages of the mitotic cycle. If cysteine arrests the cycle at a stage at which the cells are not sensitive or are less sensitive to radiation it would act as a radioprotector. This hypothesis gains support from Dr. Lajtha's observation that cysteine prevents deoxyribonucleic acid formation in bone marrow cells and from Dr. Stocken's observation that it prevents nuclear phosphorylation. If we assume that the two processes, arrest of mitosis and lessening of X-ray damage, are connected it seemed possible that a temporary arrest of mitosis by cysteine might benefit the cell even if it occurred after ir-

radiation rather than before it. Such a slowing down of the cell cycle might enable repair processes to get under way. The reasoning is not convincing but, since we know so little of either protectioo or repair in irradiated eells we considered it worth while to see whether prolonged cysteine treatment, begun *after* irradiation, affected the subsequent histological and clinical development of damage in the lens.

Effect of Postirrodiotion Treotment with Cysteine

The plan of the experiment has been to irradiate the right eyes of a litter of rabbits aged 8 to 12 weeks with 1400 r and half an hour *after* irradiation to inject cysteine intravenously into half the litter. A cysteine

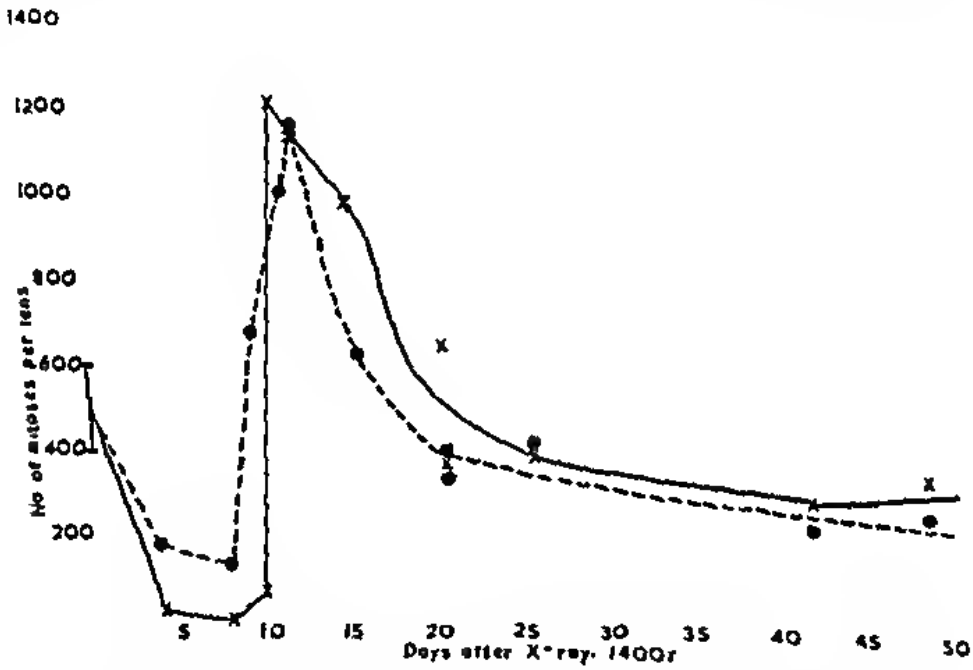

Fig 7 Total mitoses in lens epithelium of rabbit given 1400 r to right eye with or without treatment with cysteine for 28 days *after* irradiation.

Key ●——●——● Control, no cysteine, x——x——x Cysteine (CSH).

injection was then given to these same rabbits at 2-day intervals for the next month. Some litters were killed for histological examination of their lenses and some were preserved to follow the clinical development of cataract Litter mates were killed in pairs, one control and one cysteine injected rabbit at a time.

To state our results briefly, it seems that there is no clinical difference between the two groups, but the lenses of the cysteine-treated rabbits show less histological damage during the period of cysteine injections.

Figure 7 compares the total number of mitoses, whether normal or abnormal, in the epithelia at different times after irradiation with 1400 r.

For the first 10 days after X-ray there are very few dividing cells in the lens of the cysteine-treated rabbit. After that, even though treatment is continued, the mitoses start to rise, and reach, and may sometimes surpass, the numbers in the lens of the litter mate irradiated and given no cysteine. Although cysteine injections delay the start of mitosis they do not diminish the overshoot.

Postirradiation cysteine has a more marked effect on numbers of broken nuclei that develop in the lens than on mitoses. Figure 8 shows that there are fewer broken nuclei in those lenses that have been cysteine

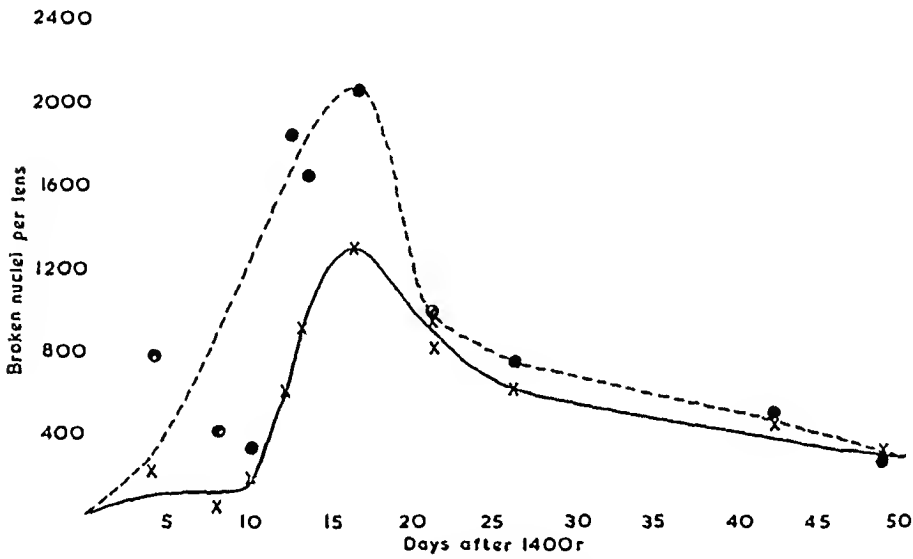

FIG. 8. Broken nuclei in lens epithelium of rabbit given 1400 r to right eye with or without treatment with cysteine for 28 days *after* irradiation.

KEY: ●— — —● Control, no cysteine; x———x Cysteine (CSH).

treated and that this difference is noticeable throughout the period of examination.

Owing to the technique used in this particular experiment the left lenses received approximately 600 r through the head when the right lenses were given a dose of 1400 r. The course of the beam could be tracked in the surviving animals by the development of gray fur, and the left eye was found always to have been within the beam. We have therefore compared the mitoses and the broken nuclei in the left eyes of rabbits with and without cysteine and again have found, first that cysteine completely blocks mitosis for 10 days but that thereafter there is a slight tendency for the lens of the cysteine-treated rabbit to show more mitoses than the control (Fig. 9), and second, from 2 to 49 days after irradiation

there are fewer damaged nuclei in the lens of the cysteine-treated rabbit (Fig. 10).

The fact that continuous cysteine treatment inhibited mitosis only for about 10 days after irradiation led us to investigate the effect of con-

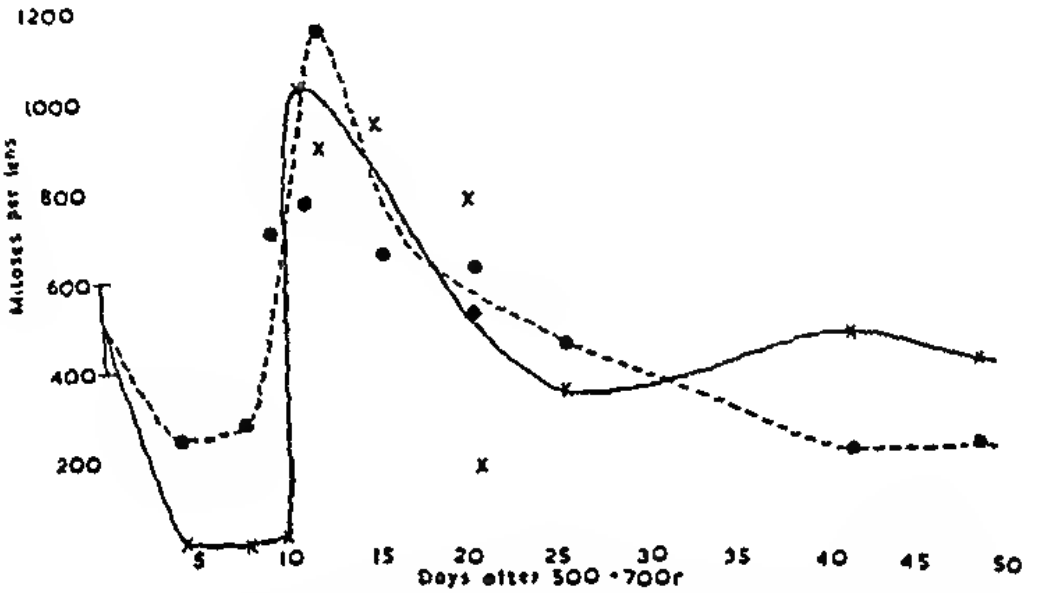

FIG 9 Total mitoses in lens epithelium of rabbit given approximately 600 r to left eye with or without treatment with cysteine for 28 days *after* irradiation.

KEY ●---● Control, no cysteine, x———x Cysteine (CSH).

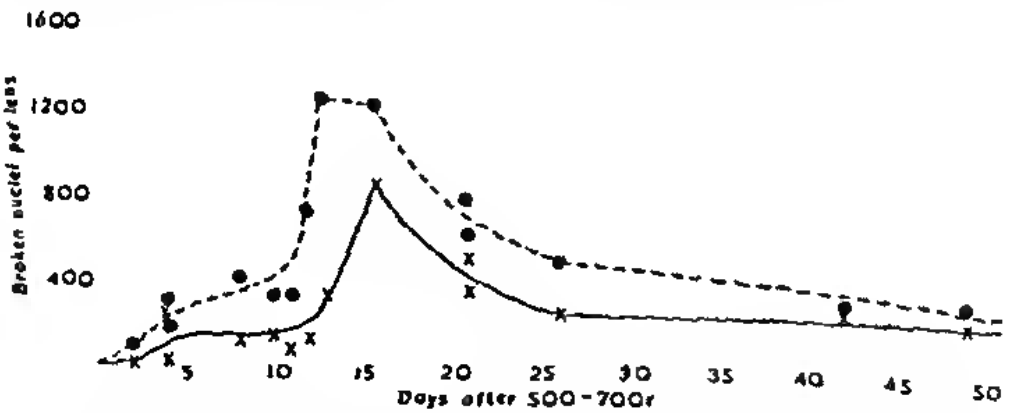

FIG 10 Broken nuclei of lens epithelium of rabbit given approximately 600 r to left eye with or without treatment with cysteine for 28 days *after* irradiation.

KEY ●---● Control, no cysteine, x———x Cysteine (CSH).

tinuous cysteine on mitosis in the normal rabbit. We found that inhibition only lasts for about 14 days; thereafter cell division occurs normally even though cysteine is still injected every second day.

Thus cysteine has the same inhibitory effect on mitosis in the already

irradiated cell as it has on the normal cell or on the cell which is subsequently irradiated. Cysteine also reduces the number of broken nuclei which develop in lens epithelium after irradiation and this reduction occurs whether the cysteine is given before or after irradiation. Yet the clinical result is entirely different. Given before irradiation, cysteine protects, given afterward it does not appear to do so.

Cataract Formation

A dose of 1400 r to the eye of an 8- to 12-week-old rabbit will cause severe if not complete opacity after several months. None of the 16 rabbits in our series has yet developed complete cataract but several have severe opacities and at present there is no difference between those that were given cysteine after irradiation and those that were not. Nor is there a clinical difference between the left eyes which received the lower dose of approximately 600 r through the head. In these lenses a posterior polar cataract is developing but no general opacity. It seems therefore that although giving cysteine has some effect in reducing the number of broken nuclei which develop after irradiation this does not alter the clinical course after these doses of X-rays.

These experiments with the protective agent cysteine have not therefore helped to explain why shielding a part of the lens so greatly diminishes the radiation damage in the irradiated area. Although both histologically and clinically the half-shielded lens reacts in the same way as the cysteine-protected lens, it is difficult to think that shielding is purely a protective measure rather than one that promotes recovery. This is particularly so when one considers Riley and co-workers' (1959) experiments in which they showed that if one half of the lens was irradiated with 6000 r, a subsequent irradiation of the second half would cause complete opacity of the whole lens if it was given within 4 months, but that if given more than 4 months after the irradiation of the first half of the lens, complete opacity did not develop. That is, recovery of the cells first irradiated had taken about 4 months to be established.

It is reasonable to consider that both protective and recovery factors are involved in the lessening of damage that is brought about by partial shielding. The lens epithelium affords a convenient tissue in which to study these processes.

Acknowledgments

I wish to acknowledge the collaboration of Dr. S. M. Drance, Dr. D. S. Thomson, and Mrs. M. Overall in part of the work. I also wish to acknowledge support from the National Council to Combat Blindness, New York and the Medical Research Council.

References

Alter, A. J., and Leinfelder, P. J. (1953). *A.M.A. Arch. Ophthalmol.* **49**, 257-260.

Cogan, D. G., and Donaldson, D. D. (1951). *A.M.A. Arch. Ophthalmol.* **45**, 508-522.

Devik, F. (1955). *Acta Radiol., Suppl.* **119**.

Devik, F. (1957). In "Advances in Radiobiology" (E. Forssberg and J. Abbott, eds.), pp. 226-229. Oliver and Boyd, Edinburgh.

Goldmann, H., and Luchti, A. (1938). *Arch. Ophthalmol. Graefe's* **138**, 722-736.

Howard, A. (1952). *Stain Technol.* **27**, 313-315.

Leinfelder, P. J., and Riley, E. F. (1956). *A.M.A. Arch. Ophthalmol.* **55**, 84-86.

Pirie, A., and Drance, S. M. (1959). *Intern. J. Rad. Biol.* **1**, 293-304.

Pirie, A., and Howard-Flanders, P. (1957). *A.M.A. Arch. Ophthalmol.* **57**, 849-854.

Pirie, A., and Lajtha, L. G. (1959). *Nature* **184**, 1125-1127.

Poppe, E. (1942). "Experimental Investigations of the Effects of Roentgen Rays on the Eye." Jacob Dybwad, Oslo.

Puntenney, I., and Shoch, D. (1954). *Am. J. Ophthalmol.* **38**, 673-682.

Richards, R. D., Riley, E. F., and Leinfelder, P. J. (1956). *Am. J. Ophthalmol.* **42**, No. 4, Part II, 44-50.

Riley, E. F., Richards, R. D., and Leinfelder, P. J. (1959). *Radiation Research* **11**, 79-89.

von Sallmann, L. (1952a). *A.M.A. Arch. Ophthalmol.* **47**, 305-320.

von Sallmann, L. (1952b). *A.M.A. Arch. Ophthalmol.* **48**, 276-291.

von Sallmann, L., Tobias, C. A., Anger, H. O., Welch, C., Kumura, S. F., Munoz, C. M., and Drungis, A. (1955). *A.M.A. Arch. Ophthalmol.* **54**, 489-514.

Wachtl, C., and Kinsey, V. E. (1958). *Am. J. Ophthalmol.* **46**, No. 5, Part II, 288-292.

Discussion

Dr. Kinsey (Kresge Eye Institute, Detroit, Michigan): Did the number of cells showing mitosis decrease and was there any increase in cells showing nuclear fragmentation in the protected area of the lens?

Dr. Pirie (Oxford, England). No.

Dr. Kinsey. Did you irradiate any eyes between the third and fifth day when mitosis had been reduced to zero?

Dr. Pirie. No. It takes 24 hours for it to be noticeable that the cysteine inhibition has started. If you give a dose of cysteine to a rabbit, the mitosis appears to be absolutely normal for 24 hours. It must be because it is a very long mitotic cycle, several days or weeks.

Dr. Cogan (Harvard University, Cambridge, Mass.). Dr. Pirie asked for alternative suggestions: Is it not possible that one might have back-scatter which would increase the exposure dosage to any one part when the whole lens is exposed as compared to exposure of only one-half the lens?

Dr. Pirie. You mean, going from one eye to the next?

Dr. Cogan. No, back-scatter from that half of the lens which would be presented when the shield was used. The effect would of course depend on the energy of the radiation.

Dr. Pirie. We used 250 kv X-rays. I don't know about back-scatter. We didn't find any sign of damage in the shielded area, that is, histological damage. We never found any damaged nuclei or micronuclei.

CHAIRMAN VON SALLMANN [National Institutes of Health, Bethesda, Md.]: During the past year, Dr. Curtis (Brookhaven National Laboratory) and I studied the recovery from lens injury produced by proton microbeams. The diameters of the beam were 25, 75, and 1000 microns. I have the impression that some regeneration of epithelium cells occurred. Obviously, the experimental conditions were different from yours, Dr. Pirie, but I think in small areas one may say recovery or regeneration from radiation injury did occur in the experimental animal (mice).

The Distribution of DNA-Synthesizing Cells in Lens Epithelium Following Injury[1]

CLIFFORD V. HARDING, CARL FELDHERR, AND B. D. SRINIVASAN

Departments of Ophthalmology and Physiology, College of Physicians and Surgeons, Columbia University, New York, New York

Introduction

It is possible, by means of autoradiography, to demonstrate the incorporation of tritiated thymidine in whole-mount preparations of lens epithelium. Thymidine incorporation is, in general, assumed to be an indication of DNA synthesis by a cell in preparation for division, and the number of cells in a given population which are undergoing incorporation has been used as an index of cellular proliferation (Hughes *et al.*, 1958). *In vitro* studies with rat, rabbit, and frog lenses have shown that thymidine incorporation is restricted, for the most part, to certain cells in the equatorial region (Harding *et al.*, 1960). Relatively few cells in the central region were found to incorporate thymidine. This distribution of DNA-synthesizing cells in the rabbit can be greatly altered by mechanical injury (Harding *et al.*, 1959). A puncture through the anterior capsule with adhering epithelium can result in eventual incorporation of thymidine and division in cells surrounding the wound, including areas of cells that under normal circumstances show very little DNA synthetic or mitotic activity.

In order to determine the nature of the stimulus which leads to DNA synthesis and mitosis, it was thought important first to get a clear picture of the distribution of DNA-synthesizing cells and the way in which this changes with time after injury.

In the present investigation the distribution of cells actively incorporating tritium-labeled thymidine was determined at different periods of time after mechanical injury to the lens epithelium. The specific results obtained are affected, to a certain extent, by the age and strain of rabbit used, as well as the characteristics of the injury. The results presented show the variety of effects on DNA synthesis and mitosis produced by injury. They emphasize the possible application of this monolayered, avascular, cellular system as a tool in studies on the mechanism by which injury leads to cell division.

[1] This work has been supported by Contract No. AT(30-1)2456 with the U. S. Atomic Energy Commission, and the Knapp Memorial Fund.

Methods and Materials

Preliminary experiments indicated the necessity of maintaining maximum constancy in experimental procedure. Variations in the age or strain of rabbit used, or changes in the method of injury appear to have definite effects on the results (which, in some cases, are quite marked). Two major difficulties were encountered, and had to be avoided: loss of cells during preparation of the whole mounts, and destruction of large irregular areas of cells following injury. In both cases, the pattern of DNA synthesis was obscured or unpredictably modified. Loss of epithelial cells during preparation of the whole mount seemed to depend to a certain extent on the strain of rabbit used, and in our hands, there was little loss of cells in the American Dutch rabbit. The unpredictable destruction of large areas of cells as a result of the injury was most obvious in the adult. Consequently, young (about 1½ lb) American Dutch rabbits were used in many of the experiments.

Attempts were made to reduce variations in experimental procedure to a minimum. Mechanical wounds were obtained by inserting a fine steel needle directly into the lens at right angles to the epithelial surface. In one set of experiments the needle was sharpened to a fine point, and the depth of penetration was kept at a minimum (depth of penetration from surface of cornea, approximately 3 mm; maximum diameter of portion of needle in lens approximately 0.1 mm). The loss of aqueous through the corneal wound was small. In another set of experiments a larger steel needle was used and the depth of penetration was greater (depth of penetration from surface of the cornea, approximately 8 mm; maximum diameter of needle in lens, approximately 0.3 mm). At various periods of time after injury the radioactive solution was injected into the anterior chamber.

This solution consisted of Eagle's basal medium [minus serum or glutamine (Eagle, 1955)] plus tritium-labeled thymidine at a concentration of 20 μC/ml. The specific activity of the thymidine was in the range of 1.9 to 3.0 C/mM. Since the total volume injected was about 0.10 to 0.15 ml, there was approximately 2–3 μC of tritium per eye. In all cases, the animals were killed 2 hr after the injection of tritium-labeled thymidine. The eyes were fixed immediately in Carnoy's fixative (3 parts absolute alcohol = 1 part glacial acetic acid) (Howard, 1952; von Sallmann, 1952), and prepared for autoradiography (Harding *et al.*, 1960).

Results

Whole mounts of lens epithelium prepared from eyes that were fixed 4, 8, and 12 hr after injury did not show detectable amounts of

thymidine incorporation in the vicinity of the wound. Incorporation did, however, appear in a small number of preparations from 14-hr injuries, and in the majority of preparations from 16-hr injuries. The cells which show incorporation at these times are relatively close to the wound (Fig. 1, for example, shows the distribution of radioactive nuclei around a 16-hr wound). Autoradiograms of older wounds (e.g., 18, 20, 22, 24, and 28 hr) show larger areas of cells undergoing incorporation. Preparations from wounds of 28 to 32 hr or more, typically show an arrangement of radioactive nuclei in the form of one or more well-defined bands which surround the injury site, and this is demonstrated in the autoradiogram shown in Fig. 3. It can be seen from a comparison of Fig. 1 (16-hr wound) or Fig. 2 (18-hr wound) with Fig. 3 (36-hr wound) where the radioactive bands are well defined, that the total area involved increases with increase in time after injury. This indicates the presence of a progressive mechanism which gradually affects cells at greater and greater distances from the wound.

The size of the wound appears to affect the course of events following injury. A fine sharp needle inserted only a short distance into the lens causes a very small and localized wound. Some of these wounds were so slight that only a small area of cells was affected. In these areas relatively small numbers of cells incorporated thymidine, and the time following injury during which DNA synthesis took place was apparently comparatively short. In those cases in which synthetic activity continued through the second day after a relatively small wound, a single band of radioactive nuclei was found. Preparations from the smallest wounds to show incorporation on the second day after injury had relatively distinct bands of radioactive nuclei. For example, Fig. 3 shows an autoradiogram of a 36-hr wound. The radioactive nuclei (C) form a very distinct band completely surrounding the wound (A). Also, the cells (B) between the injury site and radioactive nuclei appear to be more densely packed than those cells (D) outside the radioactive band. The cells in region D have the normal appearance of cells in this central region of epithelium from an uninjured lens. A higher magnification of the zone of radioactive nuclei is shown in Fig. 4. Here, the relationships pointed out above are more obvious, and also the relationship between cells with radioactive nuclei and cells in mitosis is evident. A zone of mitotic figures is found adjacent to the band of radioactive nuclei, on the side toward the wound. Such preparations from larger wounds tend to show a considerably greater scattering of the radioactive nuclei in the form of less well-defined bands.

Discussion

Thymidine incorporation is, in general, assumed to be an indication of DNA synthesis by a cell in preparation for division. This is based on the assumption that DNA undergoes little turnover (Hughes, 1959), and that thymidine incorporation reflects a true synthesis of DNA, asso-

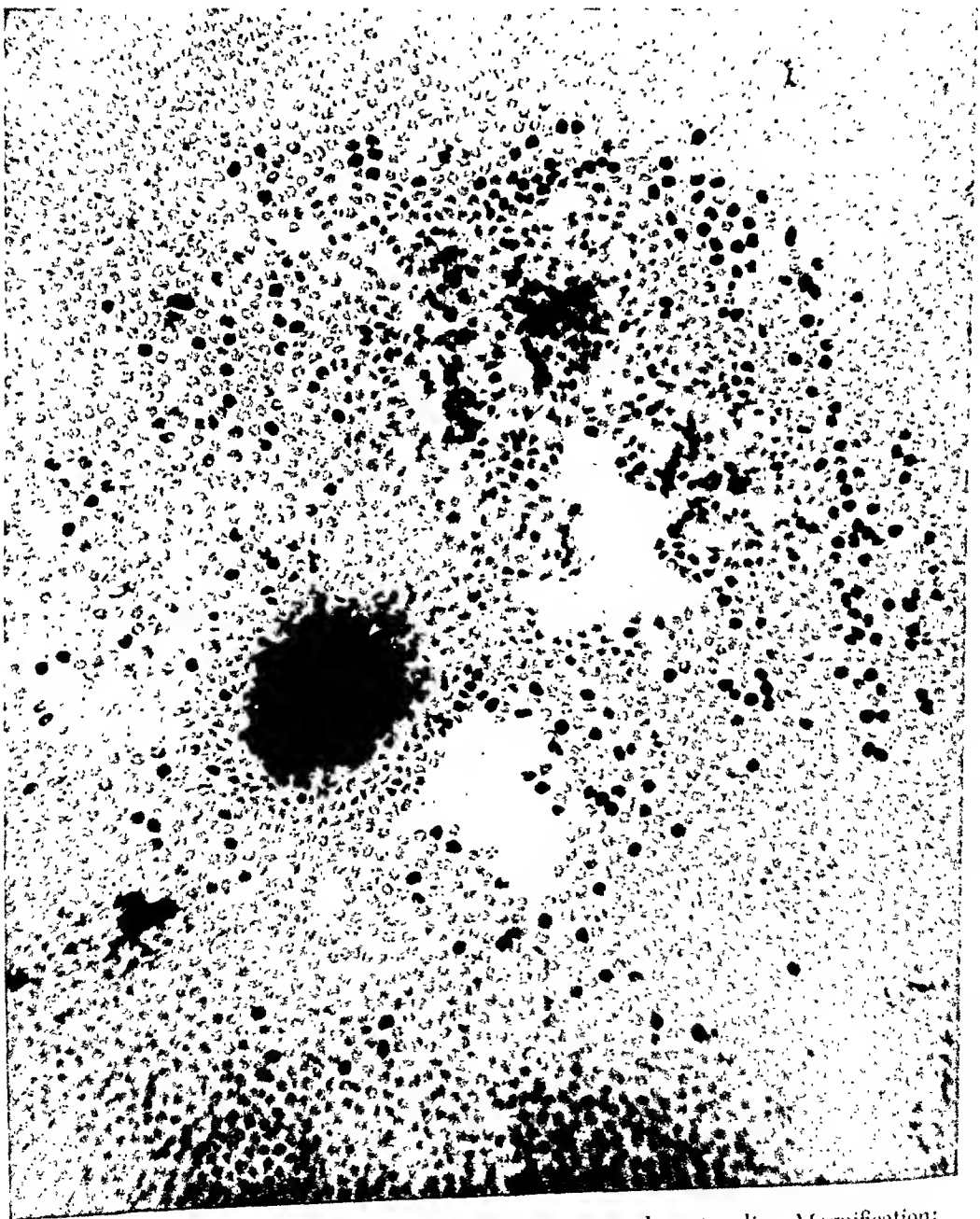

FIG. 1. Autoradiogram of 16-hr wound. Harris hematoxylin. Magnification: × 70. Note that the radioactive nuclei are restricted to the wound area.

ciated with chromosome replication. On this basis, thymidine incorporation has been used as an index of cellular proliferation (e.g., Hughes *et al.*, 1958; Leblond *et al.*, 1959, Quastler, 1959). The possibility that there is a metabolism of DNA, which takes place independently of cell division, has, however, been brought up (Pelc, 1959). It is not possible

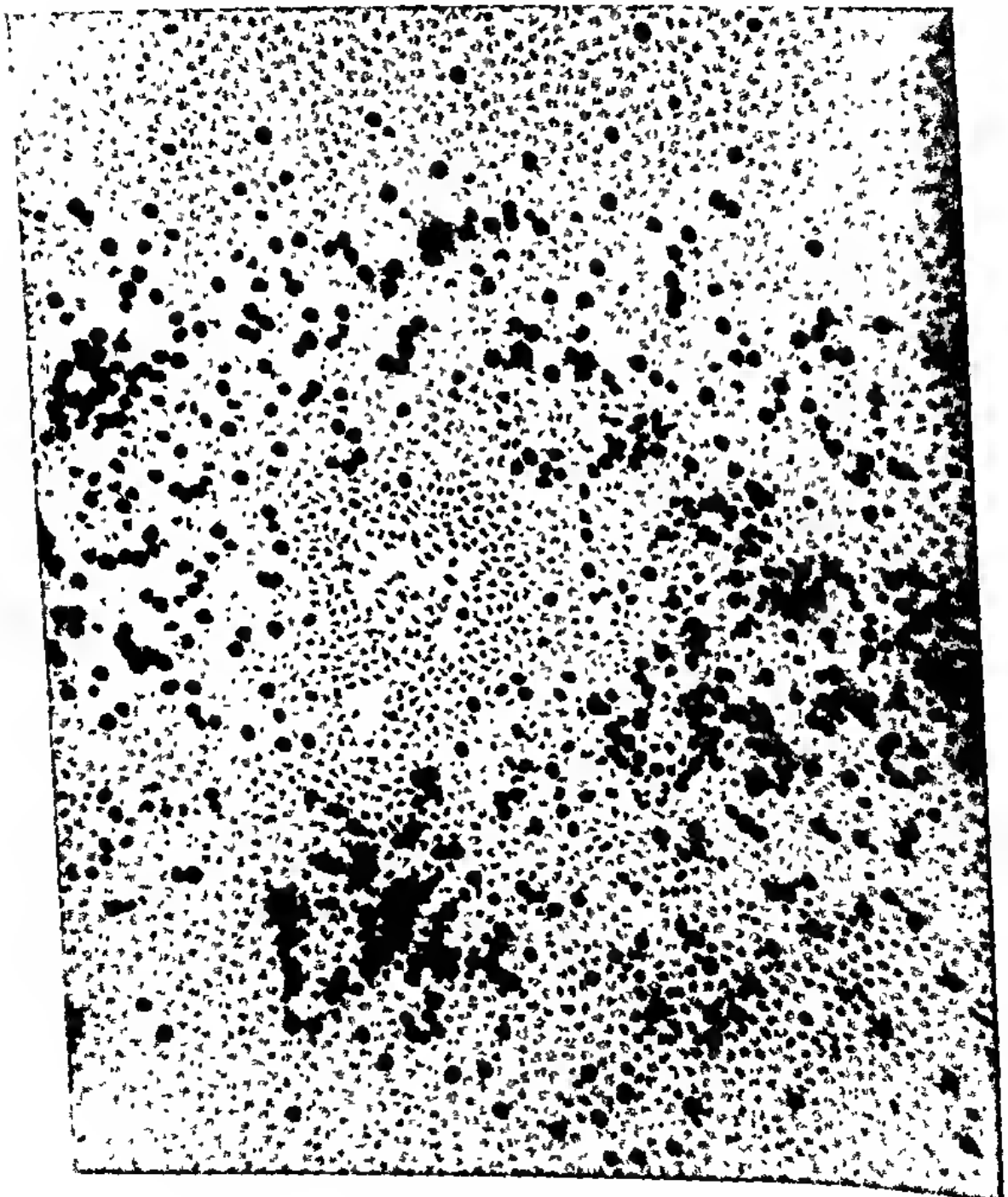

FIG. 2 Autoradiogram of 18-hr wound Harris hematoxylin. Magnification: × 70

as yet to say whether the thymidine incorporation, indicated in our autoradiograms of injured epithelium, indicates synthesis exclusively, or a combination of synthesis and turnover.

Evidence has been presented that in mammalian cells, DNA syn-

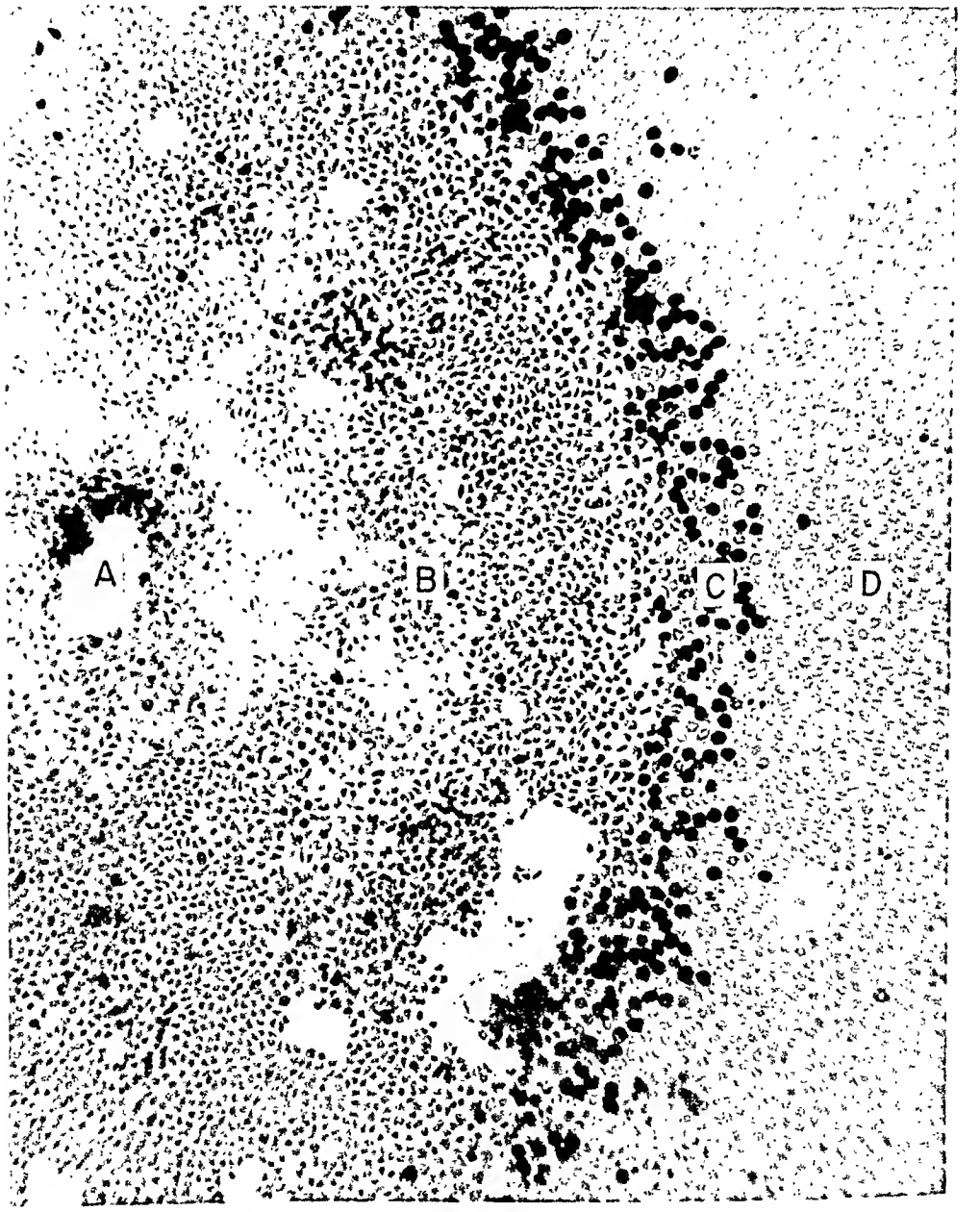

FIG. 3. Autoradiogram of 36-hr wound. Harris hematoxylin. Magnification: × 70. The wound (A) is surrounded by an area of densely packed cells (B). The band of radioactive nuclei (C) lies at the outer edge of this area. Cells (D) that lie further from the wound, have the appearance of normal cells from uninjured lenses.

thesis occurs only during a restricted portion of the cell cycle. Painter and Drew (1959) have presented evidence that this so-called synthetic phase in the HeLa cell lasts for approximately 8.5 hr, out of a total of 28 to 30 hr for the cell cycle. Mitosis occurs approximately 3 to 10 hr after the synthetic phase.

FIG. 1. Autoradiogram of 36-hr wound. Harris hematoxylin. Magnification: 175. Note that the mitotic figures lie adjacent to the radioactive band on the side toward the wound. The mitotic figures themselves are not radioactive.

On the assumption that thymidine incorporation represents DNA synthesis in preparation for cell division, it is appropriate to make certain comparisons between the distribution of cells undergoing incorporation and those undergoing mitosis.

With regard to the distribution of cells showing incorporation, it has been shown that the first cells to incorporate thymidine are restricted quite closely to the area near the wound. At later and later times, there is an increase in the area involved, and eventually the distribution of radioactive nuclei assumes the form of one or more bands encircling the wound. The mechanism by which this pattern arises is not understood. The tentative working hypothesis which we have adopted accounts for this pattern partly on the basis of synchronization of cell division. According to this concept, all cells at a given radius from the wound would have been stimulated simultaneously to undergo division, and would at any given time be synchronized at the same stage of the cell cycle. It is assumed that the greater the distance from the wound, the more recent the time of stimulation. All stages of the cell cycle could, therefore, be represented in one whole mount. Since DNA synthesis occurs in mammalian cells only at one restricted stage of the cell cycle (Painter and Drew, 1959), only the band of cells in that synthetic stage would show thymidine incorporation. Cells in the negative zone (the zone in which cells do not show radioactive nuclei, as seen in Fig. 3), therefore, are assumed to be in a nonsynthetic phase, and would be incapable of incorporating thymidine.

The next question is the pattern of distribution of mitotic figures. A prediction is possible on the basis of our hypothesis that various stages of the cell cycle are represented in one whole mount, and that the further the cell is from the injury, the more recent the stimulation. Since DNA synthesis precedes mitosis, it might be expected that the radioactive band would lie further from the wound than the mitotic figures. The tendency for the radioactive nuclei to lie further from the wound than the mitotic figures has been pointed out, and is indicated in Fig. 4.

A more complete picture of the relationship between thymidine incorporation and mitosis must await quantitative determination of the relationship of incorporating cells to dividing cells. The nature of the stimulus, which apparently progresses to greater and greater distances from the wound, is not understood. However, the above discussion of band formation is independent of the nature of the stimulus itself. The manner in which the stimulus progresses to greater distances from the wound may possibly be a reflection of the slow diffusion of an injury substance(s) from the site of injury (or possibly a reflection of the way in which a naturally occurring inhibitor to cell division is diluted or

inactivated). Although it seems less likely, this pattern may depend on an entirely different mechanism, such as a cell to cell interaction. Quantitative analyses of the injury reaction may be useful in distinguishing among these possible mechanisms.

Summary

Very few cells in the central region of normal rabbit lens epithelium are found to incorporate thymidine (a specific precursor to DNA synthesis). Mechanical injury to the epithelium results in the incorporation of thymidine by many of these cells. Incorporation is first detected at 14 to 16 hr after injury in cells immediately surrounding the wound. At later times, cells over larger areas of the epithelial layer become involved. Starting at approximately 28 to 32 hr, the cells showing thymidine incorporation are distributed in the form of one or more bands which encircle the wound. A zone of mitotic figures is associated with the band of incorporating cells, on the side toward the wound. The results suggest a mechanism for the stimulation of DNA synthesis which originates at the site of injury, and gradually moves outward.

References

Eagle, H. (1955) *Science* 122, 501-504

Harding, C. V., Dunn, A., and Srinivasan, B. D. (1959) *Expll. Cell. Research* 18, 582-585

Harding, C. V., Hughes, W. L., Bond, V. P., and Schork, P. (1960). *A.M.A. Arch. Ophthalmol.* 63, 58-65

Howard, A. (1952). *Stain Technol* 27, 313-315

Hughes, W. L. (1959) *In* "The Kinetics of Cellular Proliferation" (F. Stohlman, Jr., ed.), pp 83-94 Grune & Stratton, New York.

Hughes, W. L., Bond, V. P., Brecher, G., Cronkite, E. P., Painter, R. B., Quastler, H., and Sherman, F. C. (1958) *Proc. Natl. Acad. Sci. U. S.* 44, 476-483.

Lindsay, C. P., Messner, B., and Kopriwa, B. (1959). *Lab. Invest* 8, 296-308.

Painter, R. B., and Drew, R. M. (1959). *Lab. Invest.* 8, 278-285.

Polk, S. R. (1958) *Lab. Invest.* 8, 225-236.

Quastler, H. (1959) *In* "The Kinetics of Cellular Proliferation" (F. Stohlman, Jr., ed.), pp 218-222. Grune & Stratton, New York.

von Sallmann, L. (1952). *A.M.A. Arch. Ophthalmol* 47, 303-320

Discussion

Dr. Carpenter (Tufts University, Medford, Mass.): Did you find when longer time after injury was allowed before injection of the thymidine that the area of isotopically labeled nuclei increased, as one would expect?

Dr. Harding (Columbia University, New York): Yes, at different times after the injury the total area involved increased. From 14 to 16 hours after injury no cells incorporate thymidine. After that, incorporation begins and is fairly well restricted to the site of injury. Later, the area of incorporating cells becomes grea

On the assumption that thymidine incorporation represents DNA synthesis in preparation for cell division, it is appropriate to make certain comparisons between the distribution of cells undergoing incorporation and those undergoing mitosis.

With regard to the distribution of cells showing incorporation, it has been shown that the first cells to incorporate thymidine are restricted quite closely to the area near the wound. At later and later times, there is an increase in the area involved, and eventually the distribution of radioactive nuclei assumes the form of one or more bands encircling the wound. The mechanism by which this pattern arises is not understood. The tentative working hypothesis which we have adopted accounts for this pattern partly on the basis of synchronization of cell division. According to this concept, all cells at a given radius from the wound would have been stimulated simultaneously to undergo division, and would at any given time be synchronized at the same stage of the cell cycle. It is assumed that the greater the distance from the wound, the more recent the time of stimulation. All stages of the cell cycle could, therefore, be represented in one whole mount. Since DNA synthesis occurs in mammalian cells only at one restricted stage of the cell cycle (Painter and Drew, 1959), only the band of cells in that synthetic stage would show thymidine incorporation. Cells in the negative zone (the zone in which cells do not show radioactive nuclei, as seen in Fig. 3), therefore, are assumed to be in a nonsynthetic phase, and would be incapable of incorporating thymidine.

The next question is the pattern of distribution of mitotic figures. A prediction is possible on the basis of our hypothesis that various stages of the cell cycle are represented in one whole mount, and that the further the cell is from the injury, the more recent the stimulation. Since DNA synthesis precedes mitosis, it might be expected that the radioactive band would lie further from the wound than the mitotic figures. The tendency for the radioactive nuclei to lie further from the wound than the mitotic figures has been pointed out, and is indicated in Fig. 4.

A more complete picture of the relationship between thymidine incorporation and mitosis must await quantitative determination of the relationship of incorporating cells to dividing cells. The nature of the stimulus, which apparently progresses to greater and greater distances from the wound, is not understood. However, the above discussion of band formation is independent of the nature of the stimulus itself. The manner in which the stimulus progresses to greater distances from the wound may possibly be a reflection of the slow diffusion of an injury substance(s) from the site of injury (or possibly a reflection of the way in which a naturally occurring inhibitor to cell division is diluted or

inactivated). Although it seems less likely, this pattern *may* depend on an *entirely* different mechanism, such as a cell to cell interaction. Quantitative analyses of the injury reaction may be useful in distinguishing among these possible mechanisms.

Summary

Very few cells in the central region of normal rabbit lens epithelium are found to incorporate thymidine (a specific precursor to DNA synthesis). Mechanical injury to the epithelium results in the incorporation of thymidine by many of these cells. Incorporation is first detected at 14 to 16 hr after injury in cells immediately surrounding the wound. At later times, cells over larger areas of the epithelial layer become involved. Starting at approximately 28 to 32 hr, the cells showing thymidine incorporation are distributed in the form of one or more bands which encircle the wound. A zone of mitotic figures is associated with the band of incorporating cells, on the side toward the wound. The results suggest a mechanism for the stimulation of DNA synthesis which originates at the site of injury, and gradually moves outward.

References

Eagle, H (1955). *Science* **122**, 501-504.

Harding, C V, Donn, A, and Srinivasan, B. D. (1959). *Expll. Cell. Research* **18**, 582-585

Harding, C. V, Hughes, W. L., Bond, V. P, and Schork, P. (1960). *A.M.A. Arch. Ophthalmol* **63**, 58-65.

Howard, A (1952). *Stain Technol.* **27**, 313-315.

Hughes, W L. (1959) *In* "The Kinetics of Cellular Proliferation" (F. Stohlman, Jr, ed), pp. 83-94 Grune & Stratton, New York.

Hughes, W. L., Bond, V P, Brecher, G, Cronkite, E. P., Painter, R. B, Quastler, H, and Sherman, F C (1958) *Proc. Natl. Acad. Sci. U. S.* **44**, 476-483

Leblond, C P., Messier, B., and Kopriwa, B (1959). *Lab. Invest.* **8**, 296-308.

Painter, R B, and Drew, R. M. (1959). *Lab. Invest.* **8**, 278-285.

Pele, S R (1959) *Lab Invest* **8**, 225-230.

Quastler, H. (1959). *In* "The Kinetics of Cellular Proliferation" (F. Stohlman, Jr, ed), pp 218-222. Grune & Stratton, New York.

von Sallmann, L (1952). *A.M.A. Arch. Ophthalmol* **47**, 305-320.

Discussion

Dr. Carpenter (Tufts University, Medford, Mass.): Did you find when a longer time after injury was allowed before injection of the thymidine that the area of isotopically labeled nuclei increased, as one would expect?

Dr. Harding (Columbia University, New York): Yes, at different times after the injury the total area involved increased. From 14 to 16 hours after injury, no cells incorporate thymidine. After that, incorporation begins and is fairly well restricted to the site of injury. Later, the area of incorporating cells becomes greater

and greater, and after 32 hours the incorporating cells begin to form a well-defined band which completely encircles the wound itself. We have direct evidence, therefore, that the stimulus to cells causing them to incorporate thymidine is progressing outward from the wound.

Dr. Carpenter: Could you distinguish the effect of epithelial injury from that of perforation of the lens capsule?

Dr. Harding: In order to do this we would have to injure the epithelium without perforating the capsule. We have tried very hard to get a localized injury without perforating the capsule, but have not succeeded. It would be interesting to do this type of experiment in which the lens epithelium was injured locally but the capsule was not perforated.

Dr. Maurice (London, England): What is the nature of the repair of the injury?

Dr. Harding: At approximately 14 hours after injury, which is before the incorporation starts, the wound is evident as a localized perforation. Two or three days later the injury is completely healed over. In all cases the actual size of the injury is relatively small compared to the total area of the cells involved in thymidine incorporation.

Chairman Von Sallmann [National Institutes of Health, Bethesda, Md.]: Are these phenomena of waves of mitotic activity you have described similar to those observed in other cell populations, for instance by E. Jusélius (*Graefès Arch. Ophthalmol.* **76**, 350-400, 1910) in the corneal epithelium. The assumption has been made that there are stimulating substances produced by the injury.

Dr. Harding: This may be true. I believe that the lens has certain unique features for studies on the relationship between injury and cell division. We are dealing with a relatively isolated system, which is avascular and without a nerve supply and completely enclosed by a membrane. It is conceivable, therefore, that a stimulating substance produced by the injury might remain within the lens for a relatively long period of time and its effect, therefore, be exaggerated. In the similar experiments of Mills and Donn (reported in this volume) on corneal endothelium, injury causes an incorporation of thymidine by cells adjacent to the wound but not at greater distances from the wound as we found in the lens. In this tissue a stimulating substance might be diluted and carried away in the aqueous humor. However, it has certainly not been *proven* that the effects of injury on cell division in the lens are due to the production of stimulating substances. Other mechanisms could explain the results.

Electron Microscopic Observations of the Human Vitreous Body

W. SCHWARZ

Forschungsabteilung für Elektronenmikroskopie der Freien Universität Berlin, Berlin, Germany

THE NORMAL VITREOUS BODY possesses two physical qualities, a perfect transparency to light and a gelatinous consistency. The transparency to light facilitates the free passage of light between the lens and the retina, and is, therefore, a prerequisite for the visual capacity. The gelatinous consistency varies among the vertebrates. However, it is the same in each species The plasticity of the gelatinous vitreous body is necessary for the changes in shape of the lens and the ciliary body as well as for the position of the retina. The significance of the gelatinous consistency with respect to the intraocular pressure is not clear as yet.

The composition of the vitreous body has been a much debated issue The vitreous body in a fresh state appears structureless and entirely homogeneous under the light microscope. However, with the phase microscope there are several noticeable structures which differ from each other in different regions (Grignolo, 1953, 1954; Schwarz and Schuchardt, 1950, Bembridge *et al.*, 1952). With the ultra immersion microscope, thin threads have been visualized which crisscross each other and have no anastomoses (Lauber, 1936; Grignolo, 1954). Their width is too small to be determined with the ultra immersion microscope. However, their length is of light microscopical magnitude, and various lengths of the fibrils have been found by several investigators: Baurmann and Thiessen (1922), 3.8 μ; Duke-Elder (1930), 30 μ; Stromberg (1932), 50 μ. The average distance between these threads amounts to 2.1 μ (Baurmann, 1923) or 9.8 μ (Baurmann, 1929). In several regions of the vitreous body these values deviate from the mean su that the arrangement in the peripheral parts, in particular near the ora serrata, is more dense than in the central parts. The vitreous body in vivo viewed with the slit lamp microscope shows an entirely different appearance. Layers consisting of ramifying bands become visible. These bands are considered to form the anterior optical limiting membrane of the vitreous body. This membrane is folded, reflects the light well and has, therefore, been designated membrana hyaloidea plicata by Vogt (1942).

Whereas the vitreous body in the fresh state shows no structures under the light microscope, there are visible in the fixed state structures

of light microscopical magnitude. At present they are considered to be artificial products or agglutinations of the ultramicroscopically visible components of the fresh vitreous body (Lauber, 1936). The ultramicroscopically visualized threads have been mostly considered to be micellar colloid structures of a gel.

The development of electron microscopy has permitted the definition of these threadlike components as fine fibrils. The electron microscopic studies have been carried out mostly in the bovine vitreous body. Some specimens were prepared for electron microscopy by placing small fragments on the Formvar supporting film of the specimen grid, sometimes using a platinum loop, others after fragmentation in a Waring blendor or by sonic treatment. All investigators have found thin fibrils (Appelmans and Blockeel, 1952; Matoltsy *et al.*, 1951; Schuchardt and Knoch, 1950; Schwarz, 1951a). The width of these fibrils ranged from 150 to 200 Å according to Schwarz (1951a). Besides these fibrils other types, 250 Å and 500–800 Å in width, have been observed by Matoltsy *et al.* (1951). The human vitreous body has been investigated very rarely. Strampelli and Posarelli (1944, 1945) have taken specimens from several parts of the vitreous body with a platinum loop, which were dried on the specimen grid. Only a few fibrils have been found, but their width was not measured. However, many salt crystals were seen which were precipitated by the drying process. Schwarz (1951b, c) has demonstrated the fibrils of the human vitreous body using the technique of sectioning and sonic treatment described by Wolpers (1943). The fibrils were uniform, ranging in width from 270 to 320 Å. The nature of the fibrils is still a matter of controversy. Matoltsy *et al.* (1951) consider the fibrils of the vitreous body to belong to the collagen class. By defining them as vitrosin fibrils they wish to emphasize that they are different from the collagenous fibrils of the connective tissue. They have observed a cross-striation with a period of 610 Å in the fibrils which are 150 to 300 Å in width. However, there was no cross-striation visible in other fibrils 250 Å in width. The fibrils measuring 500 to 800 Å in width show a cross-striation of 640 Å, as has been found in fibrils of connective tissue. However, Schwarz (1951a, b, c) has not been able to confirm these periods of cross-striation in the fibrils of the vitreous body in the human and bovine eye. Between the fibrils there is an interfibrillar substance which contains besides other material hyaluronic acid. From these studies no conclusions can be drawn as to the distribution and arrangement of the fibrils in the vitreous body. Serial sections would be necessary. All fixatives except formalin cause considerable changes in consistency and transparency of the vitreous body accompanied by a distortion of its structures. In addition, removal of water which amounts to 99% in the

vitreous body causes shrinkage and precipitation. Therefore, the arrangement and the distribution of the fibrils in the vitreous body can be distinguished only in frozen sections from which the ice is removed by lyophilization. Those sections have been made from the bovine vitreous body (Schwarz, 1955, 1956; Fernández-Morán and Sylvén, 1956). The human vitreous body has not been investigated using this method.

Material and Methods

Left human eyes of various ages were fragmented in a Waring blendor. A drop of the suspension was placed on the specimen grid and treated with heavy metal salts as osmium tetroxide, phosphotungstic acid, and uranylacetate. Some specimens were shadowed. The corresponding vitreous bodies of the right eyes were cut with the Linde-Kryostat System Dittes-Duspiva. The sections ranged from 2 to 5 μ in thickness. They were lyophilized. Some sections were treated with hyaluronidase and subsequently with heavy metal salts. In order to enhance the contrast several sections were shadowed with palladium.

Results

The human vitreous body is composed of two electron microscopically visible structures, fibrils, and an interfibrillar substance. The fibrils are thin As the distribution curve shows, the width of the fibrils of a formalin-fixed vitreous body of a 50-year-old man ranges from 40 to 100 Å (Fig. 1), the maximum being 66 Å. The width measured in 200 fibrils averages 67 Å. In other specimens the distribution is similar, only minor shifts in the curves are noted. If the vitreous body is not fixed with formalin in time or the body is prepared in a fresh condition, thicker fibrils are obtained Probably they swell when being prepared in water by sonic treatment. The average of 200 unfixed fibrils from a 60-year-old man amounted to 103 Å and to 101 Å from a 70-year-old man. The shape of the distribution curve was the same. The fibrils stain with osmium tetroxide, phosphotungstic acid, and uranyl Some parts of the fibrils take up heavy metal salts more strongly. These parts alternate with the unstained parts of the fibrils. From this an impression of cross-striation is given which turns out to be most distinct when uranylacetate is used. One period consists of a light and dark area and is 120 Å in width (Fig. 2) A larger unit of several periods does not exist. The interfibrillar substance masks the fibrils and part of it is found between the fibrils. After treatment with hyaluronidase the fibrils become more distinct and the spaces between the fibrils contain less material. This substance is apparently identical with hyaluronic acid which is present to some extent

of light microscopical magnitude. At present they are considered to be artificial products or agglutinations of the ultramicroscopically visible components of the fresh vitreous body (Lauber, 1936). The ultramicroscopically visualized threads have been mostly considered to be micellar colloid structures of a gel.

The development of electron microscopy has permitted the definition of these threadlike components as fine fibrils. The electron microscopic studies have been carried out mostly in the bovine vitreous body. Some specimens were prepared for electron microscopy by placing small fragments on the Formvar supporting film of the specimen grid, sometimes using a platinum loop, others after fragmentation in a Waring blendor or by sonic treatment. All investigators have found thin fibrils (Appelmans and Blockeel, 1952; Matoltsy *et al.*, 1951; Schuehardt and Knoch, 1950; Schwarz, 1951a). The width of these fibrils ranged from 150 to 200 Å according to Schwarz (1951a). Besides these fibrils other types, 250 Å and 500–800 Å in width, have been observed by Matoltsy *et al.* (1951). The human vitreous body has been investigated very rarely. Strampelli and Posarelli (1944, 1945) have taken specimens from several parts of the vitreous body with a platinum loop, which were dried on the specimen grid. Only a few fibrils have been found, but their width was not measured. However, many salt crystals were seen which were precipitated by the drying process. Schwarz (1951b, e) has demonstrated the fibrils of the human vitreous body using the technique of sectioning and sonic treatment described by Wolpers (1943). The fibrils were uniform, ranging in width from 270 to 320 Å. The nature of the fibrils is still a matter of controversy. Matoltsy *et al.* (1951) consider the fibrils of the vitreous body to belong to the collagen class. By defining them as vitrosin fibrils they wish to emphasize that they are different from the collagenous fibrils of the connective tissue. They have observed a cross-striation with a period of 610 Å in the fibrils which are 150 to 300 Å in width. However, there was no cross-striation visible in other fibrils 250 Å in width. The fibrils measuring 500 to 800 Å in width show a cross-striation of 640 Å, as has been found in fibrils of connective tissue. However, Schwarz (1951a, b, c) has not been able to confirm these periods of cross-striation in the fibrils of the vitreous body in the human and bovine eye. Between the fibrils there is an interfibrillar substance which contains besides other material hyaluronic acid. From these studies no conclusions can be drawn as to the distribution and arrangement of the fibrils in the vitreous body. Serial sections would be necessary. All fixatives except formalin cause considerable changes in consistency and transparency of the vitreous body accompanied by a distortion of its structures. In addition, removal of water which amounts to 99% in the

vitreous body causes shrinkage and precipitation. Therefore, the arrangement and the distribution of the fibrils in the vitreous body can be distinguished only in frozen sections from which the ice is removed by lyophilization. Those sections have been made from the bovine vitreous body (Schwarz, 1955, 1956; Fernández-Morán and Sylvén, 1956). The human vitreous body has not been investigated using this method.

Material and Methods

Left human eyes of various ages were fragmented in a Waring blendor. A drop of the suspension was placed on the specimen grid and treated with heavy metal salts as osmium tetroxide, phosphotungstic acid, and uranylacetate. Some specimens were shadowed. The corresponding vitreous bodies of the right eyes were cut with the Linde-Kryostat System Dittes-Duspiva. The sections ranged from 2 to 5 μ in thickness. They were lyophilized. Some sections were treated with hyaluronidase and subsequently with heavy metal salts. In order to enhance the contrast several sections were shadowed with palladium.

Results

The human vitreous body is composed of two electron microscopically visible structures, fibrils, and an interfibrillar substance. The fibrils are thin. As the distribution curve shows, the width of the fibrils of a formalin-fixed vitreous body of a 50-year-old man ranges from 40 to 160 Å (Fig 1), the maximum being 66 Å. The width measured in 200 fibrils averages 67 Å In other specimens the distribution is similar, only minor shifts in the curves are noted. If the vitreous body is not fixed with formalin in time or the body is prepared in a fresh condition, thicker fibrils are obtained. Probably they swell when being prepared in water by sonic treatment. The average of 200 unfixed fibrils from a 60-year-old man amounted to 103 Å and to 101 Å from a 70-year-old man. The shape of the distribution curve was the same. The fibrils stain with osmium tetroxide, phosphotungstic acid, and uranyl. Some parts of the fibrils take up heavy metal salts more strongly. These parts alternate with the unstained parts of the fibrils. From this an impression of cross-striation is given which turns out to be most distinct when uranylacetate is used. One period consists of a light and dark area and is 120 Å in width (Fig. 2). A larger unit of several periods does not exist. The interfibrillar substance masks the fibrils and part of it is found between the fibrils. After treatment with hyaluronidase the fibrils become more distinct and the spaces between the fibrils contain less material. This substance is apparently identical with hyaluronic acid which is present to some extent

in the vitreous body. The heavy metal salts stain besides the fibrils some other particles which occur between the fibrils and are recognized even after treatment with hyaluronidase. These small spherical granules are 100 Å in width.

The sections through the anterior part of the vitreous body were made in a horizontal plane after the eye had been frozen in toto. Behind the lens the vitreous body contains only a few fibrils which are widely separated (Fig. 3). A layer of closely packed and intermingling fibrils follows. This layer is about 8000 Å in width. The fibrils run mainly

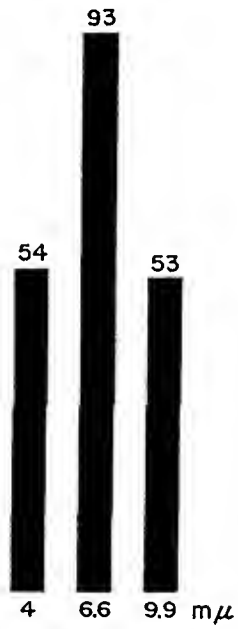

FIG. 1. Distribution curve of the width of fibrils of a formalin-fixed vitreous body of a 50-year-old man. Figures above bars indicate number of fibrils.

parallel to the surface of the vitreous body. The anterior surface of this layer shows fibrils arranged in bundles which take a winding course within this layer. Frequently an archlike bulging out of these fibrils at the anterior surface of this layer is observed. The interfibrillar substance of this layer is so great in amount that a portion of the fibrils is masked. From the back surface of this layer to the central part of the vitreous body, there are strands of fibrils which run across each other. The width of these bundles ranges from 1500 to 3000 Å. Between these bundles numerous single fibrils are noted which run irregularly in all directions (Fig. 3). Between the fibrils of the anterior limiting membrane, but also anterior and posterior to this layer, small spherical bodies stain with uranylacetate and are 100 Å in width (Fig. 4). Posterior to these densely packed fibrils, at small intervals, are other fibrillar layers running parallel

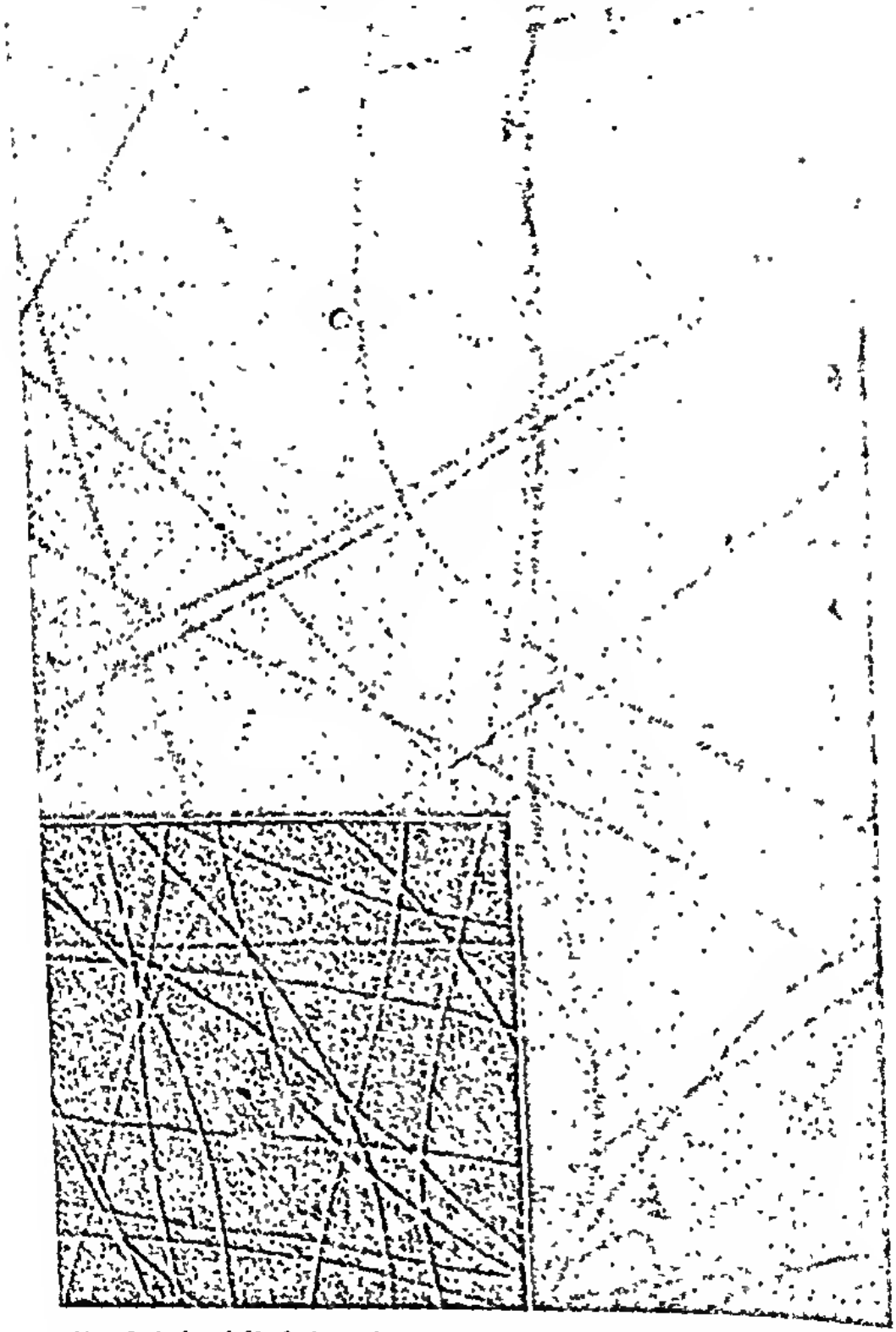

FIG. 2. Isolated fibrils from the vitreous body of a 57-year-old man, stained with uranylacetate. Periods 120 Å. Inset: isolated fibrils shadowed with palladium. Magnification: × 30,000

to the surface of the vitreous body. No difference in structure between the two fibrillar layers can be recognized.

FIG. 3. Frozen-dried preparation through the anterior region of the vitreous body of a 57-year-old man. Shadowed with palladium.

At the top a few fibrils in the postlenticular space. In the center a zone densely packed with fibrils (membrana hyaloidea plicata). Magnification: × 30,000.

Discussion

The pattern of cross-striation of the fibrils of the vitreous body is considerably different from the one of the collagenous fibrils. The periods of fibrils of the vitreous body described by others are in part identical with the periods of collagenous fibrils and are very likely due to an admixture of collagenous fibrils. Probably they enter the vitreous body

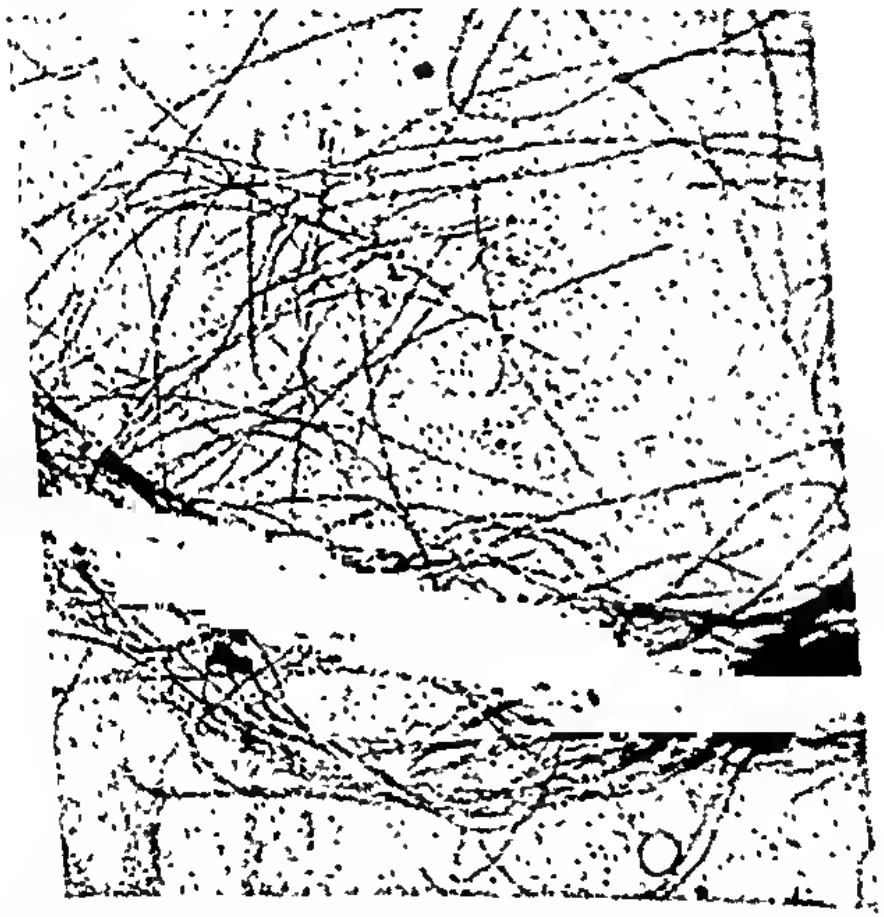

FIG. 4 Frozen section through the anterior region of a frozen-dried preparation of the vitreous body of a 57-year-old man. At the top is the postlenticular space, in the center the zone densely packed with fibrils (membrana hyaloidea plicata). Protein particles 100 Å in width. Magnification: × 30,000.

very easily at the time of its removal, because very frequently a whitish annulus of connective tissue remains attached to the base of it. If any admixture from the ciliary body and the retina is avoided, fibrils are obtained the width of which shows only small deviations from the mean. After staining with uranyl their period amounts to 120 Å. The treatment with hyaluronidase causes the fibrils to stand out more distinctly due to the removal of hyaluronic acid. As a result, small spherical particles become visible, which belong very likely to the soluble protein fraction of

the vitreous body (Balazs, 1953). The zone densely packed with fibrils within the region of the hyaloid fossa of the anterior part corresponds to the membrana plicata which can be seen with the slit lamp microscope. The postlenticular space anterior to it is mostly optically empty when observed with the slit lamp microscope. At times, a fine fibrillar structure can be recognized which corresponds to the horizontal section of the hyaloid fossa observed electron microscopically. Posterior to the zone, which is densely packed with fibrils, there are, at some distance, still other zones which are abundant in fibrils. Also this corresponds to the view obtained with the slit lamp microscope where several layers glint one after another.

Summary

The vitreous body of human eyes of various ages were examined by electron microscopy. Fibrils and the interfibrillar substance can be distinguished. The fibrils are very thin. Only small deviations from the mean width of 67 Å have been observed. Parts of the fibrils stain with heavy metal salts so that a kind of cross-striation is seen. After staining with uranyl the period is 120 Å, and differs from the collagenous period. The interfibrillar substance contains hyaluronic acid which can be removed easily with hyaluronidase. In addition, there are spherical particles 100 Å in width, which stain with heavy metal salts and belong to proteins. Frozen sections of the anterior part of the vitreous body have been lyophilized. Immediately posterior to the lens there is a zone which contains a few fibrils and corresponds to the postlental optically empty zone of the vitreous body which can be seen with the slit lamp microscope *in vivo*. Following this is a zone, 8000 Å in width, where the fibrils are packed densely. This zone corresponds to the membrana hyaloidea plicata. The number of zones where the fibrils are packed densely varies.

These electron microscopic results of sections of the anterior part of the human vitreous body correspond with the findings found by the slit lamp *in vivo*.

Acknowledgment

The work was supported by grants from the Deutsche Forschungsgemeinschaft.

References

Appelmans, M., and Blockeel, J. (1952). *Ophthalmologia* **124**, 297-302.
Balazs, E. A. (1953). *Am. J. Ophthalmol.* **38**, 21-28.
Baurmann, M. (1923). *Arch. Ophthalmol. Graefe's* **111**, 352.
Baurmann, M. (1929). *Arch. Ophthalmol. Graefe's* **122**, 415.
Baurmann, M., and Thiessen, R. (1922). *Nachr. Ges. Wiss. Göttingen. Math.-physik. Kl.* **1922**, 125.

Bembridge, B. A., Crawford, G. N. C., and Pirie, A. (1952). *Brit. J. Ophthalmol.* 36, 131.
Duke-Elder, S. (1930). *Brit. J. Ophthalmol. Suppl.* 4.
Fernández-Morán, H., and Sylvén, B. (1956). *In* "The Biochemistry and Physiology of Bone" (G. H. Bourne, ed.), pp. 53-80. Academic Press, New York.
Grignolo, A. (1953). *Progr. Ophthal.* 2, 1-35.
Grignolo, A. (1954). *Boll. oculist* 33 (ix).
Lauber, H. (1936). *In* "Mollendorffs Handbuch der mikroskopischen Anatomie des Menschen," Vol. III/2. Springer, Berlin.
Matoltsy, A. G., Gross, J., and Grignolo, A. (1951). *Proc. Soc. Exptl. Biol. Med.* 76, 857-860.
Schuchardt, E., and Knoch, M. (1950). *Naturwissenschaften* 37, 428.
Schwarz, W. (1951a). *Z. Zellforsch.* 36, 45-61.
Schwarz, W. (1951b). *Z. Zellforsch.* 36, 248-292.
Schwarz, W. (1951c). *Verh. Anat. Ges., Heidelberg*, p. 187.
Schwarz, W. (1955). *Congr. fédérative. intern. Anat., Paris* 1955.
Schwarz, W. (1956). *Anat. Anz.* 102, 434-442.
Schwarz, W., and Ruska, H. (1950). *Optik* 7, 318.
Schwarz, W., and Schuchardt, E. (1950). *Z. Zellforsch.* 35, 293-310.
Strampelli, B., and Posarelli, A. (1944/45). *Boll. accad. med. Roma* 70, 177.
Stromberg, R. (1932). *Zentr. ges. Ophthalmol.* 27, 44.
Vogt, A. (1942). "Atlas der Spaltlampenmikroskopie." Springer, Berlin.
Wolpers, C. (1943). *Klin. Wochschr.* 22, 624-625.

Molecular Morphology of the Vitreous Body[1]

ENDRE A. BALAZS

Retina Foundation, Department of Ophthalmology of the Massachusetts Eye and Ear Infirmary, and Harvard Medical School, Boston, Massachusetts

Our present concept of connective tissue is based on the simplified picture of a three-compartment system, viz., the fluid within the blood and lymph vessels, the matter within the cell membranes, and the substance filling the space between the cells.

The first compartment is in liquid state and is, structurally speaking, a fluid in which molecules and larger particles are dissolved or randomly dispersed. Dynamically, this compartment may be described by hydrodynamic events, the driving forces of which originate from the activity of the cells outside this compartment.

The second compartment, the intracellular matter, is in solid state and represents, structurally, a complex system of subcompartments with both a liquid and a solid state character. The extreme complexity of this system is further complicated by the dynamic processes dominated by energy-producing chemical events and resulting in self-duplicating synthetic processes as well as mechanical movements.

The third compartment, the space between the cells, is also in solid state and may be structurally described as a continuous framework of macromolecules organized in filaments, fibers, or lamellae. The free space in this fixed lattice is filled with a solution of other macromolecules and crystalloids. Dynamically, this system is characterized by the stored elastic energy in the lattice originating from active movements in neighboring compartments and by the translational diffusion of the molecules not fixed to the lattice.

The intercellular space as a tissue compartment is, first of all, a morphological concept, and its functional meaning needs amplification. In this paper an attempt will be made to describe the intercellular space of one of the simplest connective tissues, the vitreous body, in terms of molecular morphology and to explain some functional aspects by the interaction of the structural elements.

---

[1] This investigation was supported in part by a PHS research grant (B-1146) from the National Institute of Neurological Diseases and Blindness, Public Health Service, and by Fight-for-Sight Grant-in-Aid (3-180(C8) of the National Council to Combat Blindness, Inc., New York, New York. Paper 90, Retina Foundation.

The Gel State

The vitreous body is in solid state in most animals and in humans. It is properly called a gel because it fulfills all of the requirements for a gel structure as set forth by rheology and colloid chemistry, viz., (1) the solid phase is present in a finely dispersed "colloidal" state, and (2) the separated solid particles are not deposited by gravity nor are they present in a colloidal suspension as freely moving kinetic units, but interact to form a continuous coherent framework throughout the solution (Hermans, 1949).

The vitreous body also fulfills the conditions for a "biological gel," whereby a gel is a solid system in which a small volume of solid is dispersed in a relatively large volume of liquid by the property of mechanical rigidity and by its ability to support shearing stress at rest. Such a system has no finite viscosity and is not soluble in excess volumes of the solvent which forms its liquid phase without destroying the coherent framework of the gel-forming solid (Ferry, 1948).

In the vitreous body the liquid or the solvent is water and the solids dispersed in "colloidal" state are the macromolecules. It is practically cell-free, only approximately 1/1000th of its volume being occupied by approximately one million cells (in steers) (Szirmai and Balazs, 1958a). These cells are all located just beneath the surface of the vitreous body, next to the retina. Therefore, one should probably distinguish the gel proper from this cortical layer which, in addition to macromolecules, contains these cells. This part of the gel, consequently, should properly be called the cortical tissue layer of the vitreous body.

An important question in connection with a gel structure is as follows: Of the many macromolecules present in the gel, which ones are responsible for the continuous framework and, therefore, for the solid state? It has been known for some time that, after the removal of a fibrous component, the gel state of the vitreous disappears (Duke-Elder, 1933). This fibrous element of the gel has been identified by chemical (Pirie *et al.*, 1948; Matoltsy, 1952), electron optical (Schwarz, 1951a, b, 1956), and X-ray diffraction (Gross *et al.*, 1955b) methods as a collagen type of protein. It is consistent with these findings that proteolytic enzymes such as collagenase and pepsin, which hydrolyze collagen, liquefy the gel, while other proteolytic enzymes, such as trypsin and chymotrypsin, known to be less effective in hydrolyzing collagen, do not liquefy the gel (Pirie *et al.*, 1948).

The heat shrinkage of the vitreous body presents further evidence that a collagen-type protein is responsible for the gel structure. An example of this heat shrinkage is given in Fig. 1, which shows the volume

decrease of the gel when incubated at temperatures of 50°–65°C. In the course of the thermal denaturation of the collagen a shortening of the fibers occurs (Gustavson, 1956) which, in the case of the vitreous body, results in a volume decrease of the network of collagen-type filaments. In the course of the heat shrinkage all of the hydroxyproline-containing filaments remain within the contracting gel.

In increasing fields of gravity the network settles and a sediment is formed as the gel volume gradually decreases, leaving an increasing volume of liquid supernatant. This process is demonstrated in Fig. 2 in centrifuging steer vitreous bodies for various periods of time with increasing centrifugal force. Both the thermal shrinkage and the volume

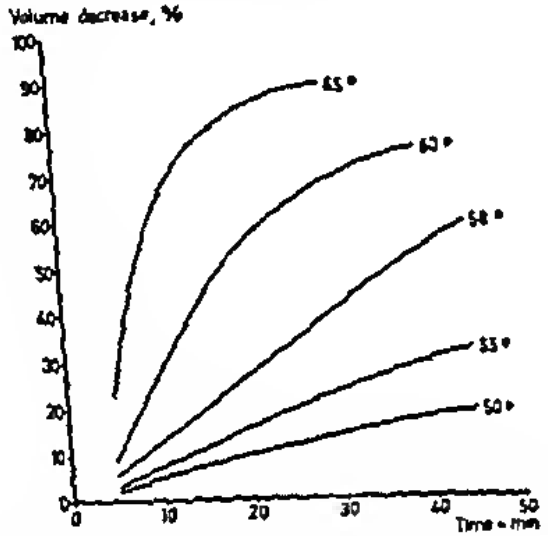

FIG 1. Thermal shrinkage of tuna vitreous body. Volume decrease, in per cent of original volume, is plotted against time of heating. Figures next to curves indicate temperatures used in °C

decrease on centrifugation indicate that the packing of the gel-forming network can be tightened either by shortening the length of the network filaments by heat or by compressing them to a denser structure by centrifugal force.

Shrinkage of the gel can also be achieved by increasing its hydrogen ion concentration. Between pH 2 and 3 an irreversible shrinkage and clouding of the gel can be observed which can be prevented by a simultaneous increase of the ionic strength (Baurmann, 1924; Goedbloed, 1935a). According to Goedbloed (1935a) the "complex aggregation of the mucoproteins" at low pH's squeezes the network, which results in a volume decrease of the gel. Pirie *et al.* (1948) found that the volume decrease in acid also occurs in the vitreous body of cattle after the hyaluronic acid is washed out. Therefore, they suggested that the shrinkage is due to the swelling and shortening of the collagenlike fibers.

A volume decrease of the vitreous gel also occurs when it is thoroughly washed with water or with dilute salt solution ($\Gamma/2 < 0.2$, pH 6–7) (Goedbloed, 1935b; von Sallmann, 1941). In the washing process most of the proteins and hyaluronic acid are removed from the gel (Pirie *et al.*, 1948). Repeating this experiment, we found, for example, that 43% of the hyaluronic acid was removed from the gel when approximately 10-ml pieces of steer vitreous gels were washed with 10 times their own volume of buffer (1/15 *M* phosphate buffer with 0.1 *M* NaCl, pH 6–8) for 24 hr under continuous shaking at 37°C. However, when 2000 U.S.P. units of testicular hyaluronidase[2] was added to the buffer

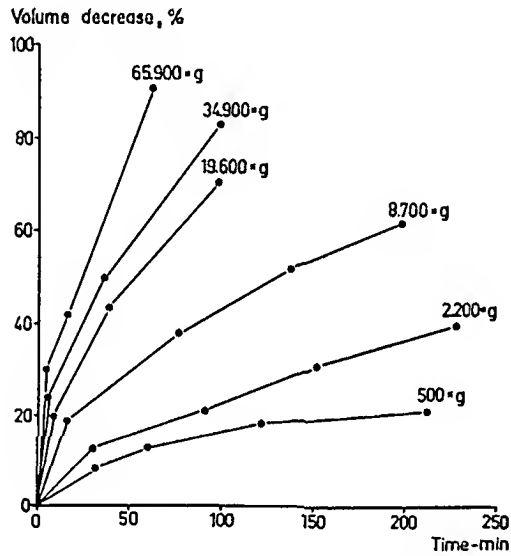

FIG. 2. Shrinkage of steer vitreous body in various centrifugal fields. Volume decrease, in per cent of original volume, is plotted against time of centrifugation. Figures next to curves indicate centrifugal force used.

and extraction was carried out under the same conditions and for the same length of time, 73% of the hyaluronic acid was removed. In both cases thymol was added as a bacteriostatic agent. In this process of extraction a volume decrease took place which was 12% in the case of the buffer and 26% in the case of the hyaluronidase treatment. A similar experiment using 2 to 3-ml pieces of cow vitreous gels is shown in Table I, where the volume decrease was measured after 24 hr and after 120 hr of continuous shaking at 37°C. In this case, too, a considerably greater decrease of the gel volume occurred with hyaluronidase than with the control buffer. Our interpretation of these experiments is that the volume decrease of the gel is a direct result of the removal or degradation of

[2] Wydase, Wyeth Laboratories, Inc., Philadelphia, Pennsylvania.

the hyaluronic acid molecules. With hyaluronidase treatment, the extraction is more effective and therefore the shrinkage is more evident. It should be pointed out that the hyaluronic acid in the gel will be slowly degraded even in buffer solution, which is probably another cause of volume decrease.

TABLE I

EFFECT OF HYALURONIDASE ON THE VOLUME DECREASE OF THE BOVINE VITREOUS BODY

Incubation medium	% Volume decrease	
	After 24 hr	After 120 hr
Buffer	11 ± 3	17 ± 5
Buffer + hyaluronidase	29 ± 5	48 ± 9

NOTE: 2–3 ml pieces of gel were incubated in 50 ml McIlvain's buffer (pH 7.0). The figures give the mean and the standard error of the mean of five samples in each group. 1000 U.S.P. units of testicular hyaluronidase (Wydase, Wyeth Laboratories, Inc., Philadelphia, Pennsylvania) was used in each sample.

A shrinkage of the vitreous gel can also be observed when it is placed in water solutions containing cationic molecules, such as cationic dyes, cetylpyridinium chloride, protamine sulfate, or colloidal iron.[3] This volume decrease is accompanied by precipitate formation on the surface of and within the gel. Under the light microscope this precipitate is identifiable as small globules or fibers containing the cationic dye or the other cationic molecules added to the solution (Balazs, 1958). When the hyaluronic acid had been previously removed from the gel by hyaluronidase treatment, no precipitate formation could be observed. The formation of this precipitate, the water-insoluble complex between the hyaluronic acid and the cationic molecules, depends on the hydrogen ion and salt concentration and on the relative amount of hyaluronic acid and cationic molecules in the solution. The appearance of this precipitate and the factors that influence its formation are very similar to those observed on mixing hyaluronic acid or other acidic polysaccharides with any of the above-mentioned cationic molecules (Balazs and Szirmai, 1958a, b; Szirmai and Balazs, 1958b). A similar precipitate can be seen when frozen sections of such tissues as cornea, umbilical cord, or rooster comb are placed in, or synovial fluid is dropped into, a water solution of the above-mentioned cationic molecules.

The volume decrease occurring simultaneously with the precipitate formation, using steer and calf vitreous bodies, is illustrated in Table II. A similar volume decrease can be demonstrated with any other cationic molecules that, under similar conditions, form a water-insoluble complex

[3] Saccharated iron oxide, Proferrin, Sharp & Dohme, Philadelphia, Pennsylvania.

TABLE II

EFFECT OF AZURE A ON THE VOLUME DECREASE OF THE BOVINE VITREOUS BODY

Washing medium	% Volume decrease	
	Steer	Calf
Water	16 ± 3	15 ± 2
4×10^{-4} *M* Azure A	67 ± 6	59 ± 5

NOTE: 5–10 ml pieces of vitreous gel were washed for 24 hr in 100 × their volume of water or dye solution at 4°C. under continuous shaking. The figures give the mean and the standard error of the mean of 5–10 samples in each group. Azure A, certification No:Naz.17, National Aniline Division, Allied Chemical Corp., New York, New York.

with hyaluronic acid. Cetylpyridinium chloride, in addition to precipitating hyaluronic acid, interacts with proteins. Therefore, cetylpyridinium chloride treatment of the vitreous gel causes a much more drastic volume decrease than a cationic dye like azure A does. When most of the hyaluronic acid is removed by washing or by hyaluronidase digestion, the volume decrease following cetylpyridinium chloride treatment is considerably less (Table III).

The mechanism of the volume decrease caused by treatment with cationic molecules can be explained by the interaction between the cationic molecules and the hyaluronic acid. As the polyacid-cation complex precipitates in the interfibrillar space, due to entanglement of the

TABLE III

EFFECT OF CETYLPYRIDINIUM CHLORIDE ON THE VOLUME DECREASE OF THE BOVINE VITREOUS BODY

Pretreatment	% Volume decrease in cetylpyridinium chloride after pretreatment		
	Calf	Steer	Cow
None	97 ± 1	96 ± 2	84 ± 1
Water extraction	68 ± 4	63 ± 2	64 ± 5
Hyaluronidase digestion	22 ± 4	23 ± 13	29 ± 2

NOTE: The volume of the gel pieces used was 2–6 ml.

Pretreatment under continuous shaking: In water, 10 × the gel volume, for 18 hr at 4°C. In Ringer's balanced salt solution, with 100 U.S.P. units testicular hyaluronidase (Wydase, Wyeth Laboratories, Inc., Philadelphia, Pennsylvania) per 1 ml gel, incubated at 37°C. for 18 hr. Merthiolate (1:10,000) used as bacteriostatic agent.

Washing in cetylpyridinium chloride: In 2.5×10^{-3} *M* cetylpyridinium chloride, 10 × the gel volume, under continuous shaking for 24 hr at 20°C.

The figures give the mean and the standard error of the mean of 5–8 samples in each group.

collagen filaments with the hyaluronic acid molecules, the network collapses, resulting in a volume decrease of the gel.

In summary, the shrinkage of the vitreous gel, occurring under the above-described conditions, can be the result of one of the following three mechanisms: (1) Changes in the network-forming collagenlike filaments either by shortening their length or by tighter packing of the network. (2) Removal of the hyaluronic acid from the network by washing with water or salt solution or by enzymatic hydrolysis or any other means of degradation. (3) Precipitation of hyaluronic acid with cationic molecules.

The Model Gel

It is obvious from the above section that, in addition to the collagenlike fibrous network, a soluble macromolecule, i.e., hyaluronic acid, must also play an important role in the volume changes of the vitreous gel. To gather more information on this point, studies were made on model gels prepared by heating collagen solutions as described by Gross *et al.* (1955a) and Jackson and Fessler (1955). The effect of various factors on the formation of these collagen gels was studied recently by Bensusan and Hoyt (1958) and by Gross (1959). The latter found that various mucopolysaccharides, including hyaluronic acid, do not affect the gel formation as judged from turbidity measurements. We were able to confirm this result, but noticed that the collagen gel formed in the presence of high-molecular weight hyaluronic acid has certain properties which are different from those of the controls.

Depending on the concentration of collagen, the newly formed gel, on standing at 20°–37°C., undergoes syneresis in the course of a few hours. The syneresis of collagen gels containing 0.1–2.0 mg/ml hyaluronic acid is considerably reduced (Table IV).

TABLE IV

EFFECT OF HYALURONIC ACID ON THE SYNERESIS OF COLLAGEN GELS

Collagen, mg/ml	Hyaluronic acid, mg/ml	Volume decrease, %
1.36	—	61
1.36	0.4	30
0.68	—	58
0.68	0.4	35

NOTE: Phosphate buffer, pH 7.0, I/2 0.14. Na-hyaluronate from human umbilical cord, $[\eta] = 4200$ cc/gm, in 0.2 *N* NaCl. Collagen prepared from calf tendon.

Another way to study the effect of large molecular polysaccharides on collagen gels is to subject gels containing various concentrations of

an acidic polysaccharide[4] to centrifugal force. As shown in Fig. 3, increasing concentrations of the mucopolysaccharide reduce the volume change produced by the centrifugal field.

This model, consisting of collagen fibers with hyaluronic acid filling the interfibrillar space, in view of the similarity in structure, can be considered an artificial vitreous body. This model gel will also shrink on heating, and its volume will decrease when washed in large volumes of water containing various cationic molecules.

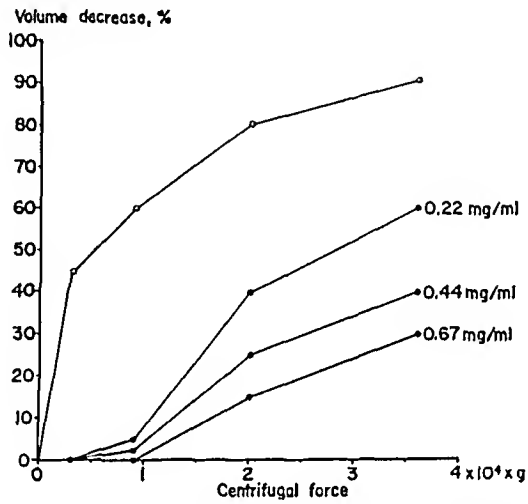

FIG. 3. Shrinkage of collagen gels containing polysaccharide of tuna vitreous body. Volume decrease, in per cent of original volume, is plotted against centrifugal force. O — Collagen gel without polysaccharide. ● — Collagen gels containing various concentrations of polysaccharide, indicated in figures next to curves.

The effect of hyaluronic acid or hyaluronic acidlike polysaccharides may be interpreted in terms of stabilization by these large polyacids of the collagen network. Hyaluronic acid, owing to its large molecular volume, fills the space between the filaments and braces the network elements.

Cortical Tissue Layer

This layer, which includes, but is not limited to, the hyaloid membrane, is approximately 100 μ thick and covers the whole vitreous body from the zonular region posteriorly. It contains three structural elements which are not common to other parts of the vitreous, viz., (1) sheets or

[4] A hexuronic acid-, glucosamine- and galactosamine-containing polysaccharide, or a mixture of polysaccharides, without ester sulfate groups, was found to be present in the aqueous humor and in the vitreous body of the tuna (E. A. Balazs, unpublished data).

membranes made of collagen-type fibers, (2) cells, and (3) an accumulation of proteins and mucopolysaccharides in the interfibrillar space.

In contrast, in the cortical layer of the retrolental area there are few or no cells in adult animals and the concentration of proteins and hyaluronic acid is lowest (Balazs, 1960). Schwarz (1960) was able to show in the electron microscope on frozen sections made from this area that the randomly distributed fibers of the gel are oriented in a membrane-like structure parallel to the surface.

The orientation and condensation of fibers on the surface of the vitreous body were suggested by several authors after studying the hyaloid membrane area in the light microscope (see review by Grignolo, 1953). Tousimis and Fine (1960) recently studied this area in the electron microscope on fixed and embedded samples. Their findings indicate that the fibers are packed in several layers of sheets or bundles running more or less parallel to the surface. Whether this packing of the fibers is a result of the fixation and embedding or whether it represents a situation existing *in vivo* is an open question.

The cells in this layer were recently studied in detail by Szirmai and Balazs (1958a) and by Hamburg (1959). The number of these cells per square millimeter of surface area varies considerably from species to species, with age, and topographically. In adult cattle there are 50–80 cells per square millimeter in the posterior part and 300–400 cells per square millimeter in the pars plana area.[5]

The high concentration of hyaluronic acid and proteins in the interfibrillar space of this area (Balazs, 1960) indicates that the cells are embedded in a more dense and probably a more rigid structure than the rest of the vitreous gel. Figure 4 gives a schematic picture of this cortical tissue layer. It considers two possibilities, viz., that the cells are embedded in a continuous random network which is denser on the very surface of the gel, or that several sheets of fibrous layers separate interlamellar spaces containing the cells. These spaces run parallel to the surface and contain hyaluronic acid in high concentration. The fibrous membrane on the surface of the gel above the cells is the so-called hyaloid membrane.

If the vitreous body is washed thoroughly with water, the surface layer can be separated with relative ease. In the electron microscope this surface layer gives the picture shown in Fig. 5a and b.[6] When the gels are washed in a dialysis membrane, in addition to the fibers, globular particles of various size are clearly visible between the fibers. Most likely macromolecules which could not diffuse through the dialysis mem-

[5] E. A. Balazs, L. Z. J. Toth, and E. A. Eckl, unpublished data.
[6] E. A. Balazs, and G. Bloom, unpublished data.

brane are retained in the gel (Fig. 5a). When the macromolecules diffuse freely out of the gel, no granular material appears on the electron micrographs (Fig. 5b). In both cases, however, the fibers seem to be embedded in a homogeneous matrix in which an occasional hole is visible. While these holes are probably artifacts caused by stress developed during drying, they also indicate the presence of this homogeneous matrix in which the fibers seem to be embedded. Such holes were not observed in gel samples taken from any other part of the vitreous and treated similarly. The morphological appearance of this

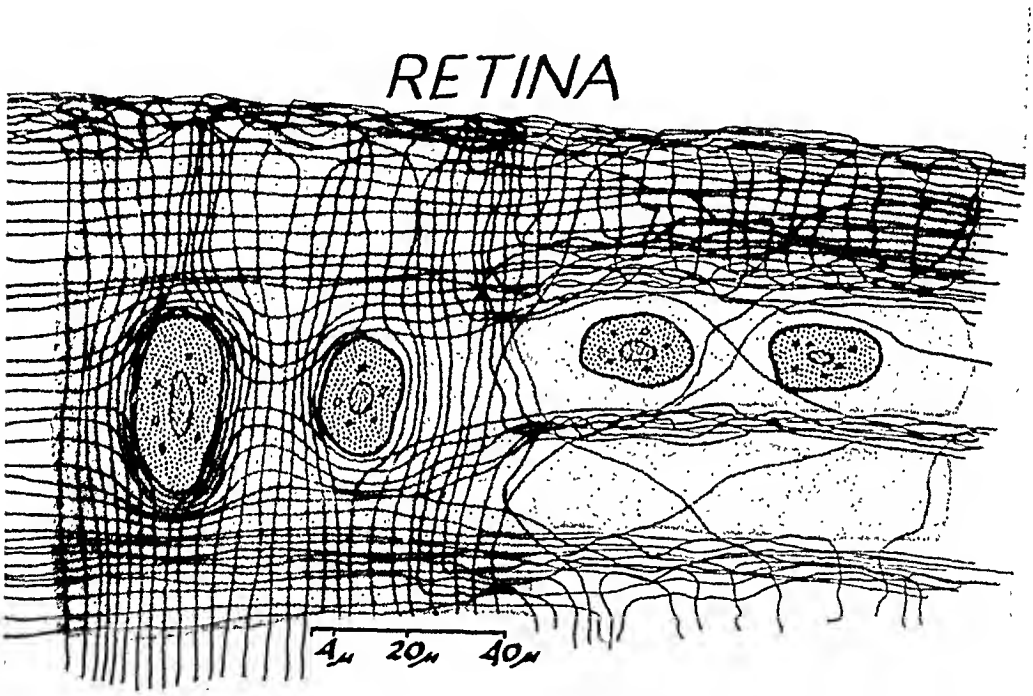

FIG. 4. Schematic picture of the cortical tissue layer of the vitreous body presenting two possible structural arrangements of the fibers and the cells as described in text. Dotted areas denote continuous hyaluronic acid meshwork.

unfixed, washed, and dried-in cortical layer is very similar to that obtained on fasciae (Day and Eaves, 1953). The structural complexity and the functional particularity of the cortical layer of the vitreous body clearly separate this area from the rest of the gel and justify the term cortical tissue layer.

The Biological Role of Hyaluronic Acid

Since hyaluronic acid or hyaluronic acidlike polysaccharides have been found in the vitreous bodies of all animal species studied, one can assume that this polyacid is consistently present in the interfibrillar space

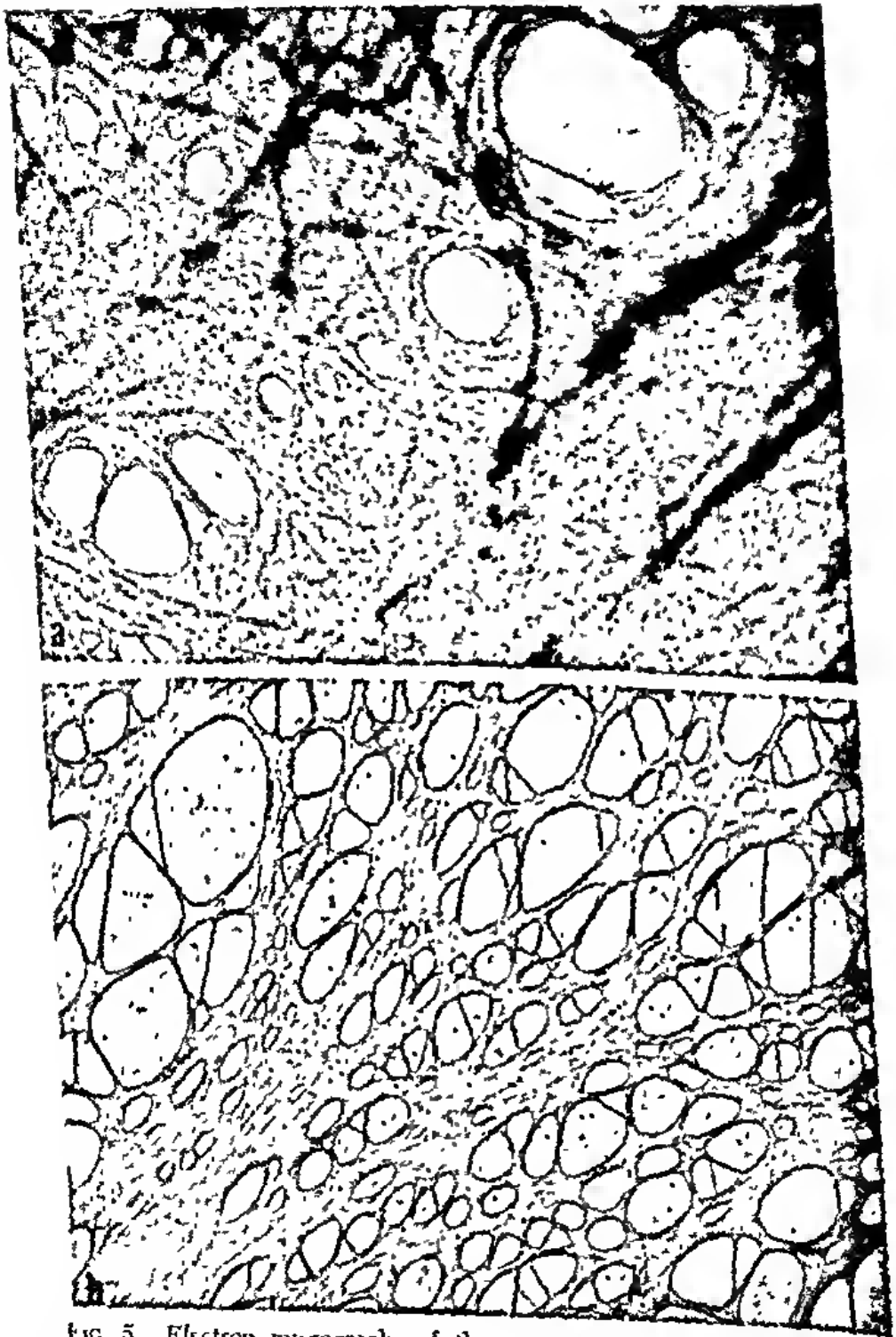

FIG 5. Electron micrographs of the posterior cortical layer of the vitreous body (cow). Unfixed, unstained preparations from water-washed gels. Surface of vitreous body is parallel to picture surface. Magnification: × 10,700 (E. A. Balazs and G. Bloom, unpublished data.)

(a) Fresh gel placed in dialysis bag and washed with large volumes of water at 4°C for 16 hr. 0.2–0.5 mm thick gel samples were taken from the surface layer, stretched on the grid, and dried. (b) *Same as (a)*, but gel placed directly in water.

of the vitreous body. There are considerable species differences and variations with age in both the qualitative and the quantitative aspects of this macromolecular component of the gel (Balazs *et al.*, 1959a, b). The complexity of the topographic distribution of the hyaluronic acid in the vitreous body further complicates this picture (Balazs, 1955). In comparing the intrinsic viscosity of the hyaluronic acid in the vitreous bodies of various animal species, Balazs and Sundblad[7] found that in all other animals studied and in humans the intrinsic viscosity of hyaluronic acid is much higher than in cattle. Laurent and co-workers (1960) fractionated the hyaluronic acid of the cattle vitreous body and found an extreme polydispersity with molecular weights ranging from 2×10^6 to 7×10^4. Also in cattle, Balazs and Sundblad[7] found that the intrinsic viscosity of hyaluronic acid varies, depending on the part of the gel from which it is prepared. The concentration of hyaluronic acid varies in different animal species between such extreme values as 10 μg/ml in the rooster and 556 μg/ml in the owl monkey. The intrinsic viscosity varies between 1040 cc/gm in the steer and 7250 cc/gm in the rooster.

The high intrinsic viscosity values indicate either a rigid rodlike molecule with a large dissymmetry or a random coil-type of molecule of large hydrodynamic volume. Experiments made on protein-containing hyaluronic acid prepared from synovial fluid (Ogston, 1953) and on protein-free hyaluronic acids prepared from various tissues (Laurent, 1957a; Balazs, 1958) indicate that this polysaccharide can be best described in terms of a spheroidal model of very large hydrodynamic volume. Thus, this polyacid, probably because of the highly charged polysaccharide chain, occupies in water a large, nearly spherical domain, which is up to 1000 times greater than that the polysaccharide chain would occupy in close packing. The internal structure of the molecule is not fully understood, but it is probably best described as a random coil with some degree of stiffness (Laurent, 1957b) and we must assume, therefore, that the average distance between the polysaccharide chains within the molecular domain is of the order of several hundred Å (in water, $\Gamma/2$ 0.1–0.2). The exact volume of the molecular domain will depend on such factors as the length of the polysaccharide chain, the ionization of the acidic group, the counterion, and the other ions and their concentration in the solvent. Interactions directly between the chain elements, or through other molecules present in the molecular array, will also greatly influence the volume and the internal configuration of the molecule.

The large domain of solution occupied by the spheroidal molecule should be regarded as a physical entrainment of the solvent by the ran-

[7] Unpublished data.

domly kinked coil of the long polysaccharide chain. The hydrodynamic specific volume of sodium hyaluronate (MW $2\text{–}3 \times 10^6$) in 0.2 *M* NaCl solution (pH 6–7) is at least 500–1000 ml/gm of dry material (Balazs *et al.*, 1957). A large hydrated volume (200–500 ml/gm) was also reported by Ogston (1953) on Na-hyaluronate preparations containing approximately 20% protein. This high hydrodynamic specific volume means that at concentrations greater than 0.2 mg/ml the domains occupied by the individual molecules overlap and the chains may become entangled. Solutions at this concentration are more properly described as a continuous network of polysaccharide chains than as freely moving individual molecules (Ogston and Woods, 1954).

The close packing of the molecules can be achieved experimentally by placing a dilute solution of hyaluronic acid on a filter membrane which permits the passage of the water and the small ions but not the macromolecules. The limiting concentration at the closest packing of the molecules is 2–5 mg/ml in 0.2 *M* NaCl solution, and it decreases in solutions of lower ionic strength. Similar limiting concentrations were found in electrodeposition experiments[8] where the hyaluronic acid accumulates as a paste on the dialysis membrane next to the anode in the course of a modified electrophoresis (Roseman and Watson, 1957).

It is of extreme biological importance that the concentration of hyaluronic acid in several connective tissues (comb, umbilical cord) and in certain parts of the vitreous body was found to be of the same order of magnitude as the concentration of solutions which have been described as a continuous molecular meshwork.

The biological role of hyaluronic acid in the intercellular space stems from the following two characteristics of the macromolecule: (1) As a polyacid, it carries a high net electric charge, resulting in considerable repulsion between the individual chain elements and also presenting a large surface for electrostatic interaction. (2) As a random coil, it has a large hydrodynamic volume, and therefore, at relatively low concentration, forms a continuous molecular meshwork with definite interchain spacing. The recognition of these two fundamental molecular characteristics and the various experimental findings give us a basis for further speculation about the biological role of this polyacid in the intercellular space of connective tissue in general and in the vitreous body in particular.

Structural and Form Resistance

In a random network of collagen fibers the size of the interfibrillar space can be estimated if the diameter of the fibers and the concentration

[8] E. A. Balazs, unpublished data.

of the fiber-forming macromolecule are known. Assuming a diameter of 100 Å for the fibers in the central part of the bovine vitreous body, and assuming that the concentration of the water-insoluble collagen in the gel is a close enough measure for the fiber-forming protein, the estimated distance between the network elements is 1–1.5 μ (Fig. 6). In most of the other animal species and in humans this distance is considerably less

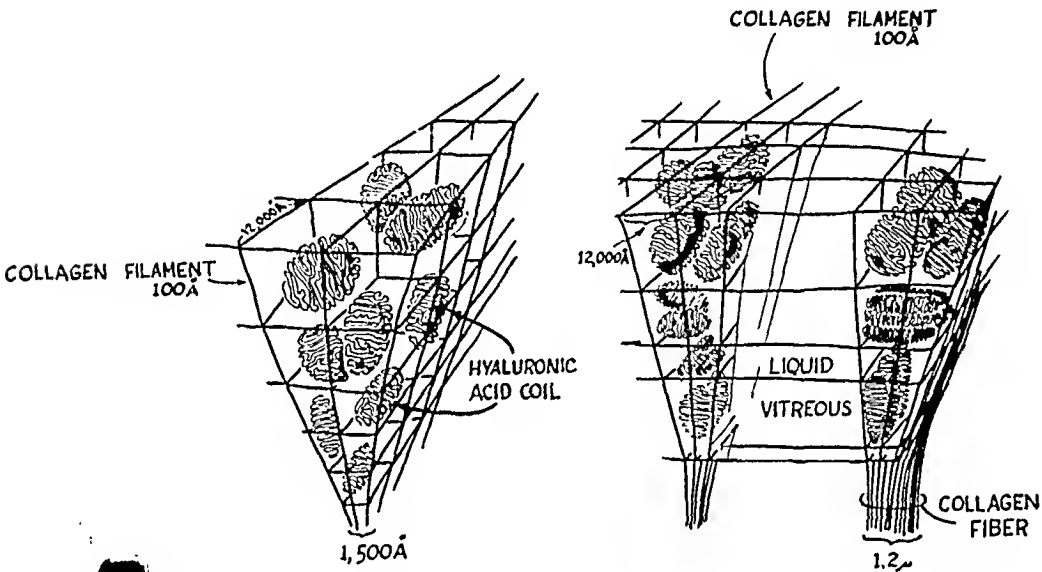

Schematic picture of the fine structure of the vitreous gel showing fib ork reinforced with hyaluronic acid molecules. *Left*—Random distribution of the structural elements. *Right*—Formation of liquid pool and partial collapse of the network.

because the collagen concentration of the vitreous body is higher. This interfibrillar space is filled with spheroidal hyaluronic acid molecules 0.2–0.5 μ in diameter (Balazs *et al.*, 1957; Laurent, 1957b). The space-filling contribution of the other macromolecules present in the interfibrillar space in about the same concentration as hyaluronic acid is negligible because of their low hydrodynamic specific volume.

It is evident that the stabilizing effect of the hyaluronic acid molecules will be considerable by virtue of the fact that their molecular volume and the size of the "holes" of the network are of the same order of magnitude. When the concentration of hyaluronic acid in a fibrous network gel is above the point where the space occupied by the individual molecules overlaps, the system is best described in terms of two interweaving continuous molecular networks, one represented by the network of collagen filaments and the other by the continuous molecular meshwork of hyaluronic acid. Such a two-component structure will have

greater mechanical stability than the collagen network alone, as manifested by the tendency to maintain its volume and to resist deformation under tensile and compressive forces. When one of the components, the hyaluronic acid, is removed from the gel, the stabilizing effect disappears and the collagen filaments under tensile and compressive forces may aggregate to large fibers, resulting in partial constriction of the network and simultaneous formations of liquid pools within the gel (Fig. 6). This mechanism may be the basis of pathological changes in the vitreous body described as formations of fibrous bands and liquid vitreous.

Our somewhat speculative interpretation of the experimental findings on the vitreous body and on the model gel is, in essence, not far removed from the explanation of the mechanical stability of connective tissue given by Fessler (1957). According to him, partial immobilization of water, occurring through a postulated chain of frictional interactions of structures ranging from molecular to cellular dimensions, is responsible for the elastic resistance to deformation and for the mechanical integrity of connective tissue.

Molecular Sieve

The flow of water and the passage of macromolecules through concentrated hyaluronic acid solutions is hindered. The translational diffusion of macromolecules through the continuous meshwork of molecular domains of hyaluronic acid coils is slowed down or completely [illegible], depending on geometric factors and charge effects.

The cortical layer of the vitreous body may well represent a molecular sieve and can be responsible for the low protein content of the gel. In this respect, it is interesting that the fine structure of this layer, as revealed by electron micrographs, is rather similar to that of fasciae. Moreover, Day (1950) has shown that the flow of salt solutions through sheets of fasciae is increased after hyaluronidase treatment, suggesting further similarities between fasciae and the cortical layer of the vitreous body.

Cell Barrier

The space-filling and stabilizing effect of hyaluronic acid in collagen gels such as the vitreous body has another important aspect: Cells in this network can move only if they dissolve the network elements or if they push their way through the network. There is no evidence that the invading cells in the vitreous body can dissolve the collagen filaments, and since strong junction points in the collagen network have not been demonstrated, the possibility of the cells displacing the filaments exists. The continuous meshwork of hyaluronic acid filling the space between the network elements is the main resisting structure remaining in the

path of the migrating cells. To break down this barrier the cells must degrade the hyaluronic acid, which can be accomplished either enzymatically or by oxidation-reduction systems. Thus, hyaluronic acid, as it fills the space between the collagen filaments, can be considered an important factor in the maintenance of the cell-free character of the vitreous body.

In conclusion, it should be emphasized that the intricate molecular morphology of the vitreous body has a functional meaning that not only determines the nature of the intercellular space but influences the function of the cells embedded in or adjacent to it. The vitreous is not like a cellular tissue, nor is it a gel structure with a continuous matrix of randomly distributed macromolecules, but rather a combination of the two, reflecting the complex functional interplay of neighboring tissues as well as a morphogenetic growth pattern.

References

Balazs, E. A. (1955). *Acta 17th Concilium Ophthalmol., 1954* II, 1019.

Balazs, E. A. (1958). *Federation Proc.* **17**, 1086.

Balazs, E. A. (1960). *In* "Importanee of the Vitreous Body in Retina Surgery with Special Emphasis on Reoperations," Proceedings of the Second Conference of the Retina Foundation (C. L. Schepens, ed.). Mosby, St. Louis, Missouri (in press).

Balazs, E. A., and Szirmai, J. A. (1958a). *J. Histochem. and Cytochem.* **6**, 278.

Balazs, E. A., and Szirmai, J. A. (1958b). *J. Histochem. and Cytochem.* **6**, 416.

Balazs, E. A., Varga, L., and Gergely, J. (1957). *Abstr. 9th Intern. Congr. Rheumatic Diseases, Toronto*, p. 30.

Balazs, E. A., Laurent, T. C., and Laurent, U. B. G. (1959a). *J. Biol. Chem.* **234**, 422.

Balazs, E. A., Laurent, T. C., Laurent, U. B. G., DeRoehe, M. H., and Bunney, D. M. (1959b). *Arch. Biochem. Biophys.* **81**, 464.

Baurmann, M. (1924). *Arch. Ophthalmol. Graefe's* **114**, 276.

Bensusan, H. B., and Hoyt, B. L. (1958). *J. Am. Chem. Soc.* **80**, 719.

Day, T. D. (1950). *Nature* **166**, 785.

Day, T. D., and Eaves, G. (1953). *Biochim. et Biophys. Acta* **10**, 203.

Duke-Elder, W. S. (1933). *Brit. J. Ophthalmol., Monograph Suppl. No.* 4.

Ferry, J. D. (1948). *Advances in Protein Chem.* **4**, 1.

Fessler, J. H. (1957). *Nature* **179**, 426.

Goedbloed, J. (1935a). *Arch. Ophthalmol. Graefe's* **133**, 1.

Goedbloed, J. (1935b). *Arch. Ophthalmol. Graefe's* **134**, 146.

Grignolo, A. (1953). *In* "Progrés d'Ophtalmologie" (E. B. Streiff, ed.), Vol. II. Karger, Basle.

Gross, J. (1959). *In* "Connective Tissue, Thrombosis and Arteriosclerosis" (I. H. Page, ed.), p. 77. Academic Press, New York.

Gross, J., Highberger, J. H., and Sehmitt, F. O. (1955a). *Proc. Natl. Acad. Sci. U. S.* **41**, 1.

Gross, J., Matoltsy, A. G., and Cohen, C. (1955b). *J. Biophys. Biochem. Cytol.* **1**, 215.

Gustavson, K. H. (1956). "The Chemistry and Reactivity of Collagen" Academic Press, New York.
Hamburg, A. (1959). *Ophthalmologica* **138**, 81.
Hermans, P. H. (1949). *In* "Colloid Science" (H. R. Kruyt, ed.), Vol. II, p. 451. Elsevier, Amsterdam.
Jackson, D. S., and Fessler, J. H. (1955). *Nature* **176**, 161.
Laurent, T. C. (1957a). *Arkiv Kemi* **11**, 457.
Laurent, T. C. (1957b). "Physico-chemical Studies on Hyaluronic Acid." Almqvist & Wiksells, Uppsala.
Laurent, T. C., Ryan, M., and Pietruszkiewicz, A. (1960). *Biochim. et Biophys. Acta* **42**, 476.
Matoltsy, A. G. (1952). *J. Cell. Physiol.* **38**, 29.
Ogston, A. G. (1953). *Trans Faraday Soc.* **49**, 1481.
Ogston, A. G., and Woods, E. F. (1954). *Trans Faraday Soc.* **50**, 635.
Pirie, A., Schmidt, G., and Waters, J. W. (1948). *Brit. J. Ophthalmol.* **32**, 321.
Roseman, S., and Watson, D. (1957). *Abstr. 5th Intern. Congr. Rheumatic Diseases, Toronto*, p. 29.
Schwarz, W. (1951a). *Z. Zellforsch u. mikroskop. Anat.* **36**, 15.
Schwarz, W. (1951b). *Z. Zellforsch u. mikroskop. Anat.* **36**, 284.
Schwarz, W. (1956). *Anat. Anz.* **102**, 434.
Schwarz, W. (1960). In this volume, p. 283.
Szirmai, J. A., and Balazs, E. A. (1958a). *A.M.A. Arch. Ophthalmol.* **59**, 34.
Szirmai, J. A., and Balazs, E. A. (1958b). *Acta Histochem. Suppl.* I, 50.
Tousimis, A. J., and Fine, B. S. (1960). Personal communication.
von Sallmann, L. (1941). *Arch. Ophthalmol.* **26**, 770.

Discussion

Dr. Wolter [University of Michigan, Ann Arbor, Michigan]: How do you identify the fibers you describe as collagen?

Dr. Balazs [Retina Foundation, Boston, Mass.]: They are called collagen-type fibers because of the existing evidence of their collagen nature obtained from chemical and X-ray diffraction studies. Since both studies were carried out only on the adult bovine vitreous body, we really don't have enough information to say that these fibers are of the collagen type in every part of the vitreous body, in animals of all ages, or in all animal species.

Dr. Pirie [Oxford, England]: I would like to ask Dr. Balazs how long he left his vitreous body in distilled water when he got shrinkage. I think I would rather emphasize the effect of the swelling and shrinking of fibers on the total volume of the vitreous, as having a greater effect than the removal or otherwise of hyaluronic acid. For example, if you leave vitreous body of cattle, which has normally a volume of about 18 cm^3 in distilled water for several days, its volume will rise to about 60 cm^3. It is terrifically swollen, a very solid gel, with all the hyaluronic acid gone. That, it seems to me, is simply because you have charged collagen fibers, which repel each other.

Similarly, when you add acetic acid, you get your precipitate of mucin, and you also shrink up the network of collagen fibers. I think either dispersion of the collagen fibers in the case of distilled water or their swelling and shortening in the case of acid has a greater effect on the vitreous gel volume than removal of hyaluronic acid or precipitation of hyaluronic acid. That is more of an opinion than a question.

DR. BALAZS: Our investigations on the shrinkage of the vitreous body were usually carried out in water, buffer, or hyaluronidase over a period of 1 or 2 days at 4° or 37°C. using bacteriostatic agents. I agree with your point, that swelling of the vitreous body may also occur under certain conditions. Factors which influence this swelling are the relative volume of the gel and the liquid used for washing, the hydrogen ion concentration, and the ionic strength of the solution. I must, however, disagree with your statement that in our experiments the collagen, rather than the hyaluronic acid, is responsible for the shrinkage. The collagen, which is a polyampholyte with an isoelectric point close to neutrality, will be less affected by the factors mentioned than a polyacid such as hyaluronic acid. As far as I know, there is no experimental evidence showing that at neutral pH in distilled water the volume of these collagen fibers will change significantly. The acid shrinkage of the vitreous body occurs at a pH at which one can expect a swelling, rather than a volume decrease, of the collagen fibers. The precipitation of hyaluronic acid with the proteins at this pH can actually be demonstrated, but the contribution of this precipitation and the shortening of the fibers to the shrinkage of the gel is a matter of degree. Both factors may participate in this process, but the main point that I should like to bring out is that hyaluronic acid, with its molecular characteristics, is more liable to volume changes at the ionic strengths and at the pH's I mentioned than the collagen fibers.

The Endothelium of the Anterior Chamber Angle of the Eye

FR. VRABEC

Eye Clinic of the Faculty of Hygiene, University of Prague, Prague, Czechoslovakia

Introduction

MANY PAPERS CONCERNING the anterior chamber angle of the eye have been published in the course of the last 100 years; however, at the present time many important questions remain unanswered. Due to the wide use of clinical gonioscopy, and to the discovery of the aqueous and laminated veins, interest in the problems of the filtration angle is still growing. It has been clearly shown that the canal of Schlemm is, in all normal circumstances, filled with aqueous humor, and the outflow of a large part of the aqueous takes place through this system to the episcleral circulation. Some possibility of an enzymatic control of this outflow was established by the perfusion experiments of Bárány (1955). These results have caused an increase in anatomical work endeavoring to clear up unknown factors of the functioning of the filtration angle. Electron microscopy has already contributed to this research (Garron *et al.*, 1958).

For a long time the author has been interested in the endothelial lining of the anterior chamber of the eye [see paper on the endothelium of the anterior surface of the iris (Vrabec, 1952) and other papers dealing with the problems of the corneal and trabecular endothelium (Vrabec, 1957, 1958a, b)]. Other authors have studied the endothelium of the trabecular meshwork in the course of research on the filtration angle (Ashton *et al*, 1956, Rohen, 1957; Speakman, 1959). As the endothelium of the trabecular meshwork represents, in my opinion, the most important tissue component of this intricate eye region, an outline of some of the results of studies of the comparative anatomy, evolution, and definite pattern of this interesting part of the eye seems important.

Material and Methods

The anterior chamber angle has been studied in 51 species of vertebrates using the usual histological methods. The eyes were fixed usually in formol or Susa solution, embedded in paraffin or celloidin-paraffin. Some sections were stained by routine methods, others were impreg-

nated by Gomori's method for reticular fibers; and still others were stained by PAS method, PAS-Hale method, etc.

For the purposes of the pseudoreplica[1] study, whole sectors of the cornea and trabecular meshwork of *Macaca mulatta, Ovis aries, Capra hircus,* and *Homo sapiens* were stained by the PAS method, with Harris' hematoxylin or by toluidine blue. Several layers of the trabecular meshwork were then removed by the pseudoreplica technique and mounted in cedar oil. Frozen sections of the trabecular meshwork, flat as well as sagittal, of *Capreolus capreolus, Pan troglodytes,* and *Homo sapiens* were impregnated by the Schultze method. India ink and colloidal silver were used for the study of phagocytosis in the rabbit's trabecular meshwork, with somewhat better results with the latter. Other material was embedded in Celodal to avoid changes caused by the paraffin embedding (*Delphinus delphis, Homo sapiens, Macaca mulatta, Capra hircus, Ovis aries, Phoxinus phoxinus, Perca fluviatilis,* two human fetuses, one of 22 mm and one of 310 mm). The corneal and trabecular endothelium has been investigated by the impregnation method of McGovern[2] in the following species: *Cyprinus carpio, Esox lucius, Trutta gairdneri iridexus, Rana esculenta, Lepus cuniculus, Felis domestica,* and *Homo sapiens.*

Results

Cyclostomata

Here, the first stage of the evolution of the well-known annular ligament of teleosts develops as a peculiar transformation of the inner layers of the corneoscleral junction. In lampreys this formation consists of epithelial-like elements with large, ovoid, and rather pale-staining nuclei. Here and there small vacuoles in the cytoplasm of some elements are seen. Fine threads of a reticular tissue crossing the anterior chamber angle are detected only with minute search.

---

[1] In the pseudoreplica method the tissue, after a suitable fixation, is washed and stained in block; then its surface is blotted dry with a smooth filter paper and covered with a 2% solution of celloidin in amylacetate, then dried in a current of air for the shortest time sufficient to make the surface dry. The celloidin film is removed with some superficial layers of the stained tissue by a tape and mounted on a slide, with the layer of the tissue below the tape and in a very small drop of the immersion cedar oil or other medium.

[2] The whole anterior segment of the eye without the lens is immersed in a 0.75% solution of $AgNO_3$, for 40 sec, then, without washing, in a mixture of 3% cobalt bromide solution with a 1% ammonium bromide solution ca. for 3–5 min. It is then briefly washed with distilled water and fixed in a dilute solution of formalin to harden the tissue for the freezing microtome. Frozen flat sections are mounted usualy in fructose syrup, but other mediums such as polystyrene are also suitable.

Teleosts

In this group increasing complexity and variation of the anterior chamber angle structures are found. One finds a reticular tissue filling the angle between the iris and the cornea (*Lota* or *Anguilla*), a compact enlargement of the corneal periphery, together with some connective and reticular tissue, in the chamber angle (*Esox lucius*, *Mollienisia*), or the typical well-known annular ligament (*Cyprinus carpio*, *Tinca tinca*, *Abramis brama*). This ligament occupies the whole anterior chamber angle sending processes of variable lengths along the anterior surface of the iris, as well as of the posterior surface of the cornea; moreover, it reaches behind to the ora *retinae*. Nevertheless, I was able to detect here a large gulf in the anterior chamber angle, penetrating, in the form of a flattened conical channel, through the solid mass of the annular ligament to the choroidal serious cavities (Fig. 1). This channel is situated in the lowest part of the anterior chamber, quite in front of the campanula (Figs. 2 and 3). The channel has solid endothelial walls separating it from the annular ligament, as well as from the iris. The channel entrance is slightly narrowed by an enlargement of the annular ligament. More equatorially the wall of this channel is surrounded by a reticular tissue which also forms its bottom. There Gomori's method has demonstrated very fine reticular fibers among the cells of the channel wall. In the black variety of *Mollienisia*, sections show a conspicuous reticular layer separating the iris from the enlarged corneal periphery. The framework of this tissue shows an unusual development (Fig. 4).

In a number of species, large amounts of glycogen fill the cytoplasm of vesicular elements of the annular ligament. In sections of tissue fixed with alcoholic solutions, the glycogen had a granular appearance; after fixation with ice-cold formalin, the vesicular elements were entirely filled quite uniformly by an amorphous mass of glycogen.

Amphibians

Caudata

Here the trabecular meshwork consists of two parts, a dense lamellar portion close to the inner surface of the corneoscleral boundary and a loose reticular tissue filling the bottom of the angle. Some capillaries and many melanophores are seen in the reticular tissue. The dense portion differs from the corneal and scleral tissue by numerous nuclei; its connective tissue fibers run mostly in a circular direction.

Ecaudata

In *Rana esculenta* I have seen, at least in the vertical meridian, a condition resembling that of the anterior chamber angle of sauropsids,

with its homolog of the canal of Schlemm lying close to the inner surface of the corneoscleral junction. A dense lamellar portion of the trabecular meshwork surrounds the inner wall of the venous channel; the uveal portion of the trabecular meshwork is composed of a beautifully developed loose reticular tissue. The anterior root of the dense lamellar portion reaches as far as the anterior surface of Descemet's membrane, similar to that of the anterior attachment of the scleral meshwork in higher vertebrates. A short smooth muscle runs from the choroid to the external wall of the posterior part of the channel (Fig. 5). Even this feature is reminiscent of the sauropsidian type. Gomori's method shows numerous reticular fibers in the dense lamellar portion, as well as in the loose reticular meshwork. In *Hyla arborea* the whole trabecular tissue is poorly developed.

The annular ligamentlike tissue filling the anterior chamber angle in *Xenopus* is well known; large amounts of glycogen are present in its vesicular elements (Fig. 6).

Reptiles

In serpents, a channel homologous to Schlemm's canal is deeply sunken in the scleral tissue; yet in serial sections many places are found where it approaches the reticular tissue of the anterior chamber angle

---

PLATE 1

Fig. 1. Anterior chamber angle in *Gobio gobio*. (a) Enlargement of the annular ligament above the entrance to the channel. (b) Gulf of the anterior chamber. Hematoxylin-eosin-orange G. Magnification: × 80.

Fig. 2. Frontal section of the lowest portion of the anterior chamber angle in *Cyprinus carpio*. (a) Sclera. (b) Channel between the ligamentum annulare and the iris. (c) Campanula. Hematoxylin-eosin-orange G. Magnification: × 8.

Fig. 3. A section of the same series, closer to the posterior end of the channel. (a) Sclera. (b) Channel, surrounded by a reticular tissue. (c) Campanula. Trichrome stain. Magnification: × 8.

Fig. 4. Reticular tissue between the iris and the enlarged periphery of the cornea in *Mollienisia sphenops*. (a) Cornea. (b) Reticular layer. Hematoxylin-eosin-orange G. Magnification: × 130.

Fig. 5. Anterior chamber angle in *Rana esculenta*. (a) Homolog of the canal of Schlemm with inner wall lined by a lamellar tissue. (b) Short smooth muscle running to the posterior portion of the external wall of the channel. Hematoxylin of Heidenhain. Magnification: × 130.

Fig. 6. Anterior chamber angle in *Xenopus* sp. The angle is filled by a large mass of vesicular elements similar to the annular ligament in teleosts. Hematoxylin-eosin-orange G. Magnification: × 80.

Fig. 7. Anterior chamber angle in *Vipera ammodytes*. (a) Intrascleral channels communicating with the choroidal circulation. Hematoxylin-eosin-orange G. Magnification: × 130.

and, simultaneously, sends large venous connections to the choroidal circulation (Figs. 7 and 8). In front of these venous channels a variable amount of reticular tissue is found. In *Python regius*, connections with the superficial episcleral circulation were found, as mentioned by Walls (1942).

In saurians a venous channel lying close to the inner wall of the

sclera reminds one again of the similar feature of the birds' anterior chamber angle. In *Lacerta agilis* this circular channel—which does not necessarily form a complete ring—fills up the whole bottom of the anterior chamber angle. Close to its posterior wall is found a large nerve trunk similar to nerve trunks in chelonians and birds (Fig. 9). A still greater likeness to the anterior chamber angle of birds is found in the anterior chamber angle in *Varanus;* here the ciliary body is divided deeply by the lateral development of loose reticular tissue (Fig. 10). The external wall of a large, flat canal of Schlemm touches the inner surface of the corneoscleral boundary. The inner wall of this channel is lined with denser, but not compact, reticular tissue. Between this denser tissue and the iris root, as well as in the anterior portion of the pars iridica of the ciliary body, a large mass of loose reticular tissue extends far behind to the ora retinae. In *Lacerta,* as well as in *Varanus,* the anterior attachment of the ciliary muscle reaches the posterior part of the external wall of Schlemm's canal. This feature corresponds to the relationship of the anterior end of Crampton's muscle in birds.

Birds

Here one should stress that the outflow of the aqueous evidently goes into the episcleral system. Also interesting is the invasion of the deep layers of the corneoscleral junction by numerous endothelial elements. These reach far from the anterior chamber along the conspicuous

---

PLATE II

Fig. 8. Anterior chamber angle in a fetus of *Coronella austriaca.* Two intrascleral channels approaching the reticular tissue filling the angle (a). Trichrome stain. Magnification: × 130.

Fig. 9. Anterior chamber angle in *Lacerta agilis.* (a) Scleral ossicle. (b) Canal of Schlemm. (c) Anterior chamber angle with the reticular tissue. Van Gieson stain. Magnification: × 80.

Fig. 10. Anterior chamber angle in *Varanus exanthematicus.* (a) Anterior chamber. (b) Canal of Schlemm. (c) Ciliary body. (d) Iris. A rich reticular tissue reaches far behind through the ciliary body. Heidenhain's hematoxylin. Magnification: × 80.

Fig. 11. Anterior chamber angle in *Turdus merula.* (a) Anterior chamber with some threads of the uveal meshwork. (b) Canal of Schlemm, with the well-known circular artery. (c) Large connective tissue channels penetrating through the sclera (d) to the episcleral circulation. Close to the external wall of Schlemm's canal, the anterior attachment of the striated Crampton's mucle (c) is to be seen. Azan stain. Magnification: × 130.

Fig. 12. Uveal meshwork of a sixth month human fetus. A very conspicuous reticulation of the tissue is seen. Held's hematoxylin. Magnification: × 330.

channels connecting the canal of Schlemm with the episcleral and conjunctival vessels (Fig. 11).

Mammals

The presence of a direct continuation of corneal endothelium with that of the anterior surface of the iris in *Cricetus* corroborates Rohen's

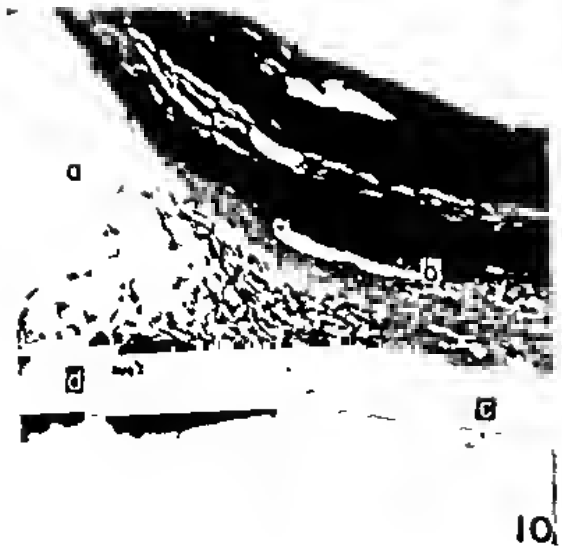

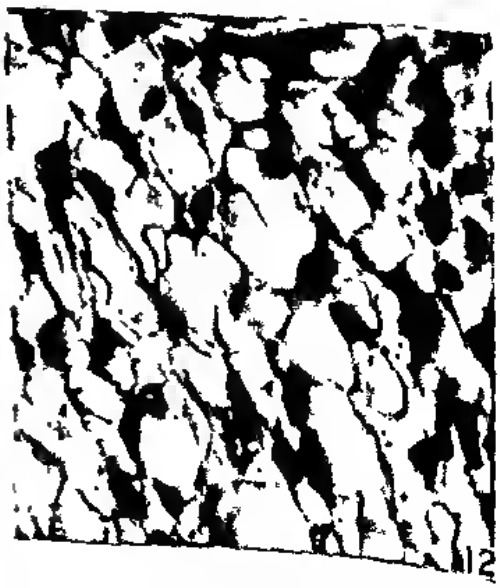

findings in other rodents. In *Foetorius furo* I was quite surprised to find a large intrascleral canal very similar to that in serpents, which seems quite unusual in carnivores.

The reticular and lamellar portions of the trabecular meshwork are found in varying degrees of development, and are most minutely described in the work of many authors.

The Development of the Structures of the Anterior Chamber Angle in Man

Some 40 fetuses ranging from a 5-mm embryo to one of 360 mm were studied. Moreover, the head of a human embryo of 22 mm and the anterior segment of the eye of another embryo of 310 mm were embedded in Celodal, in order to avoid gross deformations which necessarily accompany paraffin embedding. A fibrillar substance fills the whole anterior chamber in the first stages of development. However, with the Celodal embedding it can be demonstrated that at the 22-mm stage, the anterior chamber—so obvious in paraffin sections of this stage—is barely perceptible. The epithelium of the lens closely adheres to the corneal endothelium with only an insignificant layer of a slightly metachromatic substance between them. This metachromasia was seen in sections stained with cresyl violet. The endothelial elements not only migrate to the anterior chamber from the mesodermal tissue surrounding the anterior border of the optic cup, but are formed by local mitotic divisions of the endothelial elements themselves. In 26-mm stages and older, a striking difference appears between the compact mesoderm, close to the anterior border of the optic cup, and the loose fibrillar stroma of the cornea. Mesodermal condensation near the border of the cup is highly cellular, the nuclei are tightly packed together and fibrillogenesis is very poor. Even at the 60-mm stage fibrils are quite rare in the scleral meshwork in comparison to the rich collagen bundles of the deep scleral and corneal layers. Fibrils of the uveal, as well as the scleral, meshwork are mostly impregnated in black by Gomori's method, while in the corneal and scleral tissue collagen bundles are prevalent (Fig. 13). The reticulation[3] of the uveal meshwork, and somewhat later, of the scleral meshwork, is evident in paraffin sections from the middle of the fourth month (Fig. 12). In the Celodal sections of a 310-mm

[3] By "reticulation" I mean not only the formation of reticular fibers, but also the transformation of the compact endothelial tissue into an open spongy tissue of the trabecular meshwork and also of the anterior surface of the iris. This transformation is described as a characteristic property of the endothelial tissue by many authors (Bolck, F., "Die Endotheliome," Thieme, Leipzig, 1952).

fetus, however, this reticulation seems to be much less conspicuous (Fig. 15). It seems, therefore, that dehydration during the paraffin-embedding causes considerable shrinkage of the cellular content. Another striking difference appears between the deeper scleral and corneal layers and the trabecular meshwork in the series stained by the PAS method and with Best's carmine. A large amount of glycogen is found in the sclera and only a minimal amount in the trabecular meshwork, as well as in the choroid (Fig. 14). In later stages, when the fibers of the ciliary muscle are differentiating, glycogen appears to increase in the region of the ciliary muscle. This difference in the glycogen content strongly supports the concept of a fundamental difference in the nature of the trabecular meshwork and the scleral and corneal tissue, excepting, of course, the endothelium of the cornea and the trabeculae. The opinion of Redslob[4] (1935) about the common nature of the trabecular endothelium and the uveal tissue, particularly of the ciliary muscle, is supported by these observations. This view is also supported by Berggren's studies on the enzymatic activity of this region of the eye (Berggren, 1957).

Trabecular Meshwork of the Adult Human Eye

I wish to emphasize here the abrupt transition of the epitheliumlike corneal endothelium into the flat endothelial pattern and the increase there of the cement substance. This zone of transition is quite narrow. (See Chapter by Wolter, this volume, p. 117). The regular outlines of the flat elements are disturbed and they become irregularly shaped (Fig. 16). Nevertheless, the cell boundaries are to be seen even in the trabecular meshwork, in contradistinction to the view adopted by most previous authors. At the equatorial border of the transitional zone the large, flat endothelial cells diminish again, their outlines become irregular and in the cement substance of the outlines droplets of an argyrophil substance become visible. A minute pore appears in the center of many droplets, growing with enlargement of the droplets (Fig. 18). Three different methods are suitable for the study of these pores: firstly, flat, frozen sections impregnated by the Gros-Schultze method, where in some regions the endothelial membrane stretching across the large meshes of the inner layers of the scleral trabeculum happens to become visible and shows pores (Fig 19), secondly, similarly oriented sections impregnated

[4] Certains auteurs se sont interessés a l'origine exacte des cellules endotheliales [this means the corneal endothelium]. On les fait deriver de cellules de la membrane pupillaire ou celles qui entourent le cristallin. Nos recherches nous ont permis de constater, d'une façon absolue, que le groupe de cellules qui donne naissance aux elements endotheliaux sont celles qui representent l'ebauche du muscle de Brucke."

by the McGovern method; and thirdly, as an important supplementary control, pseudoreplica preparations of the meshwork stained by Harris's hematoxylin or toluidine blue. Comparison of preparations made by these techniques gives a far more complete picture of the pores than any single method. Such pictures have been published (Vrabec, 1957; Ashton *et al.*, 1956; Rohen, 1957; Speakman, 1959). Only with the pseudoreplica technique can we fully appreciate the surprisingly high number of cellular elements in the meshwork. This technique is decidedly better than the usual method of teased preparations in which the mechanical traction at the obliquely crossing trabeculae obviously changes their course, involving inevitable distortion of the delicate endothelial covering. By the pseudoreplica technique several layers of the meshwork are removed at one time without disturbing the relationship of their elements, except perhaps those of the bottom layer. The appearance of these preparations strongly confirms that given by McGovern's method (Figs. 18 and 21). In such specimens pores are clearly seen growing from the small circular openings between two adjacent elements (Fig. 22) to larger openings, the margins of which are crowded with numerous endothelial cells (Fig. 20). The pores of the most external layers of the meshwork are smaller and stretched more equatorially. The shape and outlines of the endothelial elements on the trabecular meshwork are irregular; which is only in accordance with the form of the connective tissue framework, forming the base of the endothelium. On the flat and almost solid plates of the

---

PLATE III

FIG. 13. Loose reticular tissue in the uveal portion of the meshwork in a human fetus at the beginning of the fifth month. Reticulin impregnation method of Gomori. Magnification: × 485.

FIG. 14. The same stage as Fig. 13, stained with the PAS-Hale combination for glycoproteins and acid mucopolysaccharides. (a) Sclera with a large amount of glycogen droplets. (b) Trabecular meshwork practically without glycogen. (c) Anterior chamber. Magnification: × 80.

FIG. 15. Human fetus of the 310-mm stage. Celodal embedding. The picture shows the compact trabecular meshwork with intact endothelial covering reaching the anterior surface of the iris in this late stage. Hematoxylin of Harris. Magnification: × 80.

FIG. 16. Human endothelium in the zone of transition. (a) Zone of transition with the increasing cement substance. (b) Irregular outlines of the trabecular meshwork zone. McGovern's method. Magnification: × 80.

FIG. 17. Phagocytosis of melanin granules in the endothelial elements of the trabecular meshwork of a 65-year-old woman. Masson's impregnation method. Magnification: × 130.

FIG. 18. Droplets of the cement substance in the outlines of the cells of a human trabecular meshwork. McGovern's method. Magnification: × 485.

anterior root of the scleral meshwork in front of the anterior surface of the periphery of Descemet's membrane, the endothelial elements are still regularly distributed; their outlines preserve a regular endothelial pattern, as shown in a previous paper (Vrabec, 1958b). They are large, flat elements with conspicuous oval nuclei and a large Golgi's net in the

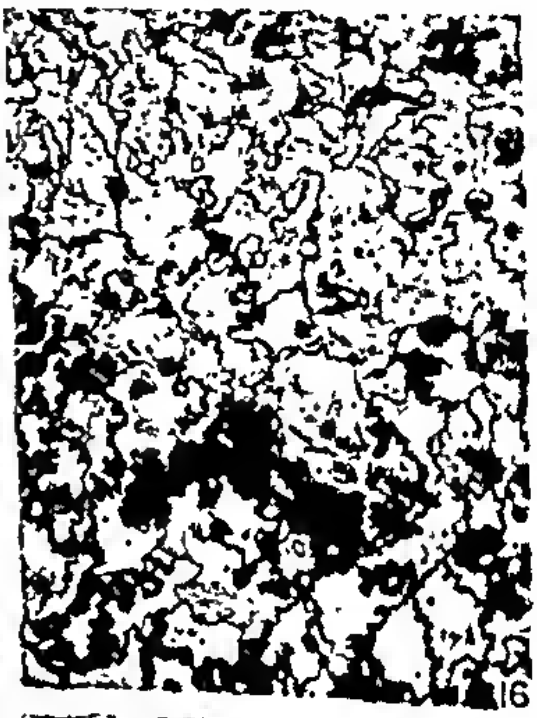

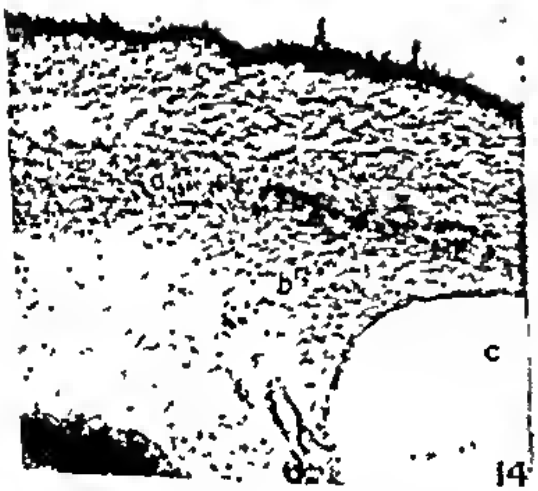

vicinity of the nucleus. Under normal conditions they multiply by amitotic divisions; in pathological conditions I have seen elements containing 2 to 3 and even more nuclei (Fig. 23). It seems possible, according to the work of Rohen and Unger (1958), that during a more active pathological process even a mitotic division can appear. The phagocytic activity of the elements of the trabecular meshwork has been long known; they can absorb large quantities of melanin in aged people, in glaucoma, or during inflammation (Fig. 17). It is not easy to study this storage experimentally, though I was able to follow the phagocytosis of colloidal silver or India ink particles. Their phagocytic power seems to be correlated with their ability to produce fresh quantities of cement substance, similar to that of the endothelial elements of blood vessels and peritoneum, as demonstrated by McGovern (1956), and also in reticulum cells in the beautiful storage experiments of Jancsó (1955). This fact clearly points to the pronounced metabolic activity and to the prime importance of the endothelial elements for the functioning of the whole trabecular meshwork.

Summary

The evolution of the structures of the angle was studied in 51 species of vertebrates by the use of usual as well as special, histological procedures. Moreover the ontogeny of this part of the eye was followed in

---

PLATE IV

Fig. 19. Human trabecular meshwork (scleral portion) showing the endothelial pores in the membrane stretching across the large meshes. (a) Trabeculum. (b) Endothelial membrane with pores. Silver impregnation by the Gros-Schultze method. Magnification: × 800.

Fig. 20. Trabecular meshwork in *Macaca mulatta* for comparison with the previous picture. (a) Trabeculum. (b) Numerous endothelial elements of a membrane stretching across the trabecular fibers. Giemsa azure-eosin stain, pseudoreplica method. A pore is seen in the endothelial membrane. Magnification: × 800.

Fig. 21. Human trabecular meshwork with several pores. (a) Surrounded by cement substance. McGovern's method. Magnification: × 485.

Fig. 22. Similar pores of the zone of transition and of the trabecular meshwork in *Macaca mulatta* in pseudoreplica stained by toluidine blue. (a) Pore between two adjacent endothelial elements; some other pores are to be seen in the neighborhood. In the top of the picture, the zone of transition to the corneal endothelium. Magnification: × 800.

Fig. 23. Flat section of the human trabecular meshwork in a case of uveitis. The anterior root of the trabecular meshwork (scleral portion). A large endothelial element with an oval nucleus and another nucleus (a) in the last stage of amitotic division is seen. Close to both nuclei two large Golgi's nets are situated. McGovern's method. Phase contrast. Magnification: × 540.

some 40 fetuses ranging from a 5-mm embryo to one of 360 mm. This study has revealed some new features of the organization of the anterior chamber angle. In the last portion of the paper dealing with the normal adult human trabecular meshwork special attention has been paid to the minute morphology and arrangement of the endothelial tissue component in the zone of transition and the trabecular meshwork.

References

Ashton, N., Brini, A., and Smith, R. (1956). *Brit. J. Ophthalmol.* **40**, 257-282.
Bárány, E. H. (1955). *In* "Glaucoma. A Symposium," pp. 91-104. Blackwell, Oxford.
Berggren, L. (1957). *Acta Soc. Med. Upsaliensis* **62**, 157-175.
Carron, L. K., Feeney, M. L., Hogan, M. J., and McEwen, W. K. (1958). *Am. J. Ophthalmol.* **46**, 27-35.
Janesó, N. (1955). "Speicherung" Akadémiai Kiado, Budapest.
McGovern, V. J. (1956). *J. Pathol. Bacteriol.* **71**, 1-6.
Redslob, E. (1935). *Arch. anat. hist. embryol.* **19**, 135-230.
Rohen, J. (1957). *Arch. Ophthalmol. Graefe's* **158**, 310-325.
Rohen, J., and Unger, H. H. (1958). *Am. J. Ophthalmol.* **46**, 802-813.
Speakman, J. S. (1959). *Brit. J. Ophthalmol.* **43**, 139.
Vrabec, F. (1952). *Ophthalmologica* **123**, 20-30.
Vrabec, F. (1957). *Am. J. Ophthalmol.* **44**, 7-12.
Vrabec, F. (1958a). *Brit. J. Ophthalmol.* **42**, 529-534.
Vrabec, F. (1958b). *Brit. J. Ophthalmol.* **42**, 667-673.
Walls, G. L. (1942). *Cranbrook Inst. Sci. Bull.* **19**.

The Topography of Encapsulated Terminal Sensory Corpuscles of the Anterior Chamber Angle of the Goose Eye

FR. VRABEC

Eye Clinic of the Faculty of Hygiene, University of Prague, Prague, Czechoslovakia

In a paper on the innervation of the trabecular system of the eye (Vrabec, 1954), the existence of terminal nervous corpuscles of Herbst found in the tissues of the anterior chamber angle of the goose eye was briefly mentioned. Up to that time no similar findings had been reported in the vertebrate eye apart from those described by Rochon-Duvigneaud (1943) in the ciliary body of the whale *Megaptera boops*. Some similar terminal corpuscles had been said to exist beneath the limbal conjunctiva in birds but since, in the same region in man and mammals, many special terminal corpuscles of the Krause type occur, this finding had been accepted without more detailed study.

However, since the function of these sensory endings in the chamber angle was not clear, a closer study of their topography has been made.

Material and Methods

The trabecular system, as well as all formations around the anterior chamber angle of the goose eye, has been studied very minutely. Some 20 eyes of adult birds and 4 of very young ones were used with different methods of impregnation. De Castro's method (Romeis, 1943), a variation of Cajal's method, indicated for the impregnation of bony tissues, has been principally used for sagittal sections of the anterior eye segment. This mixture both fixes and decalcifies. Other sagittal sections of material fixed in Boum and embedded in paraffin were impregnated by Palmgren's (1948) method, using colloidal silver. Both methods gave satisfactory results, but de Castro's was found more selective. In some sagittal frozen sections, and most of all with thick, flat frozen sections of this region, best results were obtained with the Gros-Schultze silver method. Gold toning was used following Palmgren's method and on only the best sections prepared by other methods. Ten to fifteen micron sections were prepared for de Castro's and Palmgren's methods, the flat and sagittal sections were impregnated by Gros-Schultze's method which were 40–60 μ thick and proved of great value in demonstrating the corpuscles. They showed the corpuscles in large areas, with many details

of their surroundings, and thus were most valuable for the topographical study.

Results

The sensory corpuscles of Herbst were numerous in all eyes examined, but their number seemed to vary from one bird to another and in various meridians of the same eye. This variability is best seen in flat sections involving the whole anterior segment of the eye. Possible causes of these local differences are discussed below.

Though the present paper deals especially with the question of terminal corpuscles, it is important to review the anatomy of the efferent venous system of the bird's eye before discussing more specifically localization of the terminal corpuscles. The anterior chamber of the bird's eye reaches further equatorially than that of mammals. Its lateral angle extends as an open slit equatorially between the pars scleralis and iridica of the ciliary body to the pars plana. Only some thin trabeculae covered by endothelial elements run from the pars scleralis to the pars iridica across the slitlike extension of the anterior chamber. The anterior part of the ciliary muscle runs to the external wall of Schlemm's canal. This venous canal consists of two larger venous channels almost entirely encircling the periphery of the sclerocorneal boundary. Between the venous channels runs a comparatively large artery, which seems to be present even in those meridians where the venous channels are far less conspicuous. This picture of the venous system of Schlemm's canal varies according to the meridian in which the sections of the examined eye are cut. The surrounding tissues (dense trabecular system, anterior end of Crampton's muscle, sclera and episclera) contain numerous vessels which comprise a simple endothelial tube. Some of them may represent, as many authors including Lauber believe, the afferent system of Schlemm's canal, the others are without doubt the efferent system connecting the canal of Schlemm with the episcleral venous system. The efferent vessels run in front of the anterior end of Crampton's muscle or through it, many of them forming a system of vessels parallel to the equator and then, in a rather steep course, penetrating the scleral wall of the eye in front of the ring of the scleral ossicles to the episcleral venous system (Figs. 1 and 2).

With the above anatomy in mind, the distribution of the terminal nervous corpuscles of Herbst may be described as they are found in very many localities. They were first seen between the scleral wall proper and the dense trabecular tissue in front of the anterior end of the ciliary muscle (Fig. 3), in a sagittal section impregnated by Gros-Schultze's

method, which therefore appeared entirely reliable. In the second specimen two associated corpuscles were found lying close to the large nerve bundles immediately behind Schlemm's canal (Fig. 4), and still other corpuscles were seen between Schlemm's canal and the sclera. A sagittal section impregnated by de Castro's method showed this localization very reliably, but in thin paraffin sections it is far more difficult to

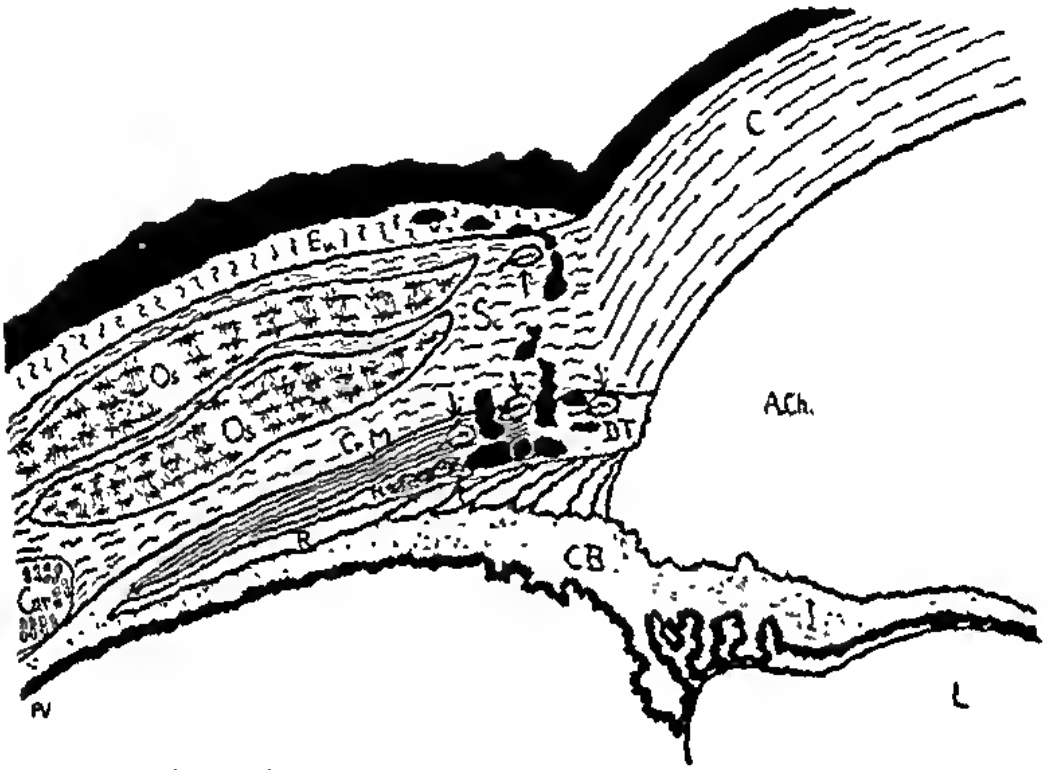

FIG 1 Sketch of the topography of the terminal corpuscles.

KEY. C, cornea, Sc, sclera, Os, scleral bone, Ep, episclera, Cr.M, Crampton's muscle, D.T, dense portion of the trabecular system; N, large nerve bundles behind the canal of Schlemm, R, lateral recess of the anterior chamber, C B., pars iridica of the ciliary body, I, iris, A Ch., anterior chamber, Car, scleral cartilage; L, lens.

Superficial conjunctival and corneal epithelium as well as the efferent venous system of the canal of Schlemm in black. The arrows indicate the terminal nervous corpuscles in the positions found on different sections

identify the corpuscles, as there they are much less conspicuous. Nevertheless even in such sections one can find some nerve bundles and simple endothelial channels accompanying them. Some corpuscles of peculiarly giant form were found immediately before the anterior end of Crampton's muscle (Fig 5), and still others even in the midst of its striated muscle fibers (Fig 6). A sagittal section impregnated by Palmgren's method showed a terminal corpuscle of Herbst's type in the external layers of the sclera close to a small empty endothelial channel. Both

structures were enclosed in loose connective tissue filling a channel in the strongly impregnated sclera.

Comment

At first sight these multiple localizations seem somewhat confusing. The corpuscles are most numerous in the dense tissue of the trabecular system and around the canal of Schlemm and its tributaries. The best way to study the relations and surroundings of the corpuscles is with thick sections impregnated by the Gros-Schultze method, where the efferent nervous fibers as well as the central glial mantle of the central nervous fiber are shown most prominently. In such sections it is possible to perceive simple, empty endothelial tubes of variable sizes in the immediate vicinity of such corpuscles (Figs. 8 and 9). In all layers through which the efferent venous vessels penetrate to the episcleral venous system, it seems possible to conclude that the corpuscles generally accompany the efferent vessels of Schlemm's canal. They are more numerous in some meridians than in others, very probably varying with the irregular distribution of the efferent channels of Schlemm's canal. This is another feature which emphasizes the relationship of the corpuscles to the efferent channels of the goose eye. Should these corpuscles register the action of the accommodation muscles, they would most probably show a more regular pattern of distribution in all meridians of the eye. Moreover, the existence of some of them in the outer layers of the scleral (Fig. 7), as well as in the deeper layers of the episcleral, tissues practically excludes the possibility of any relation to accommodation. The immediate contact of a corpuscle with the wall of a vessel makes it possible to register variations in the filling of the vessel. One must consider furthermore the possibility of registering also the pulse waves in the vessels. I had occasion to follow the pulsation of the aqueous content of the venulae aquasae of the human eye in two cases, as did Goldmann. The pulse wave most probably changes its amplitude with changes in intraocular tension.

FIG. 2. Sagittal section of the region of the corneoscleral boundary of the goose eye. The respective positions of the canal of Schlemm with its two venous channels (V) and central artery (A), of the anterior end of Crampton's muscle (Cr) and efferent venous channels (Ef) are to be seen. Gros-Schultze's methods. Magnification: × 150.

FIG. 3. Sagittal section of the anterior segment of the goose eye. Canal of Schlemm (Schl). The arrow indicates the terminal nervous corpuscle of Herbst between the sclera (Sc) and the dense portion of the trabecular system (T). Gros-Schultze's method. Magnification: × 150.

It is interesting to recall the work of some earlier authors who studied the disposition of Vater-Pacini's corpuscles and innervation of the lymphatics of the mesenterium of the cat (Dowgjallo, 1925/26 and Lawrentjew, 1925/26). These authors found great variability in the localization and number of such corpuscles in mesenteries, and their further

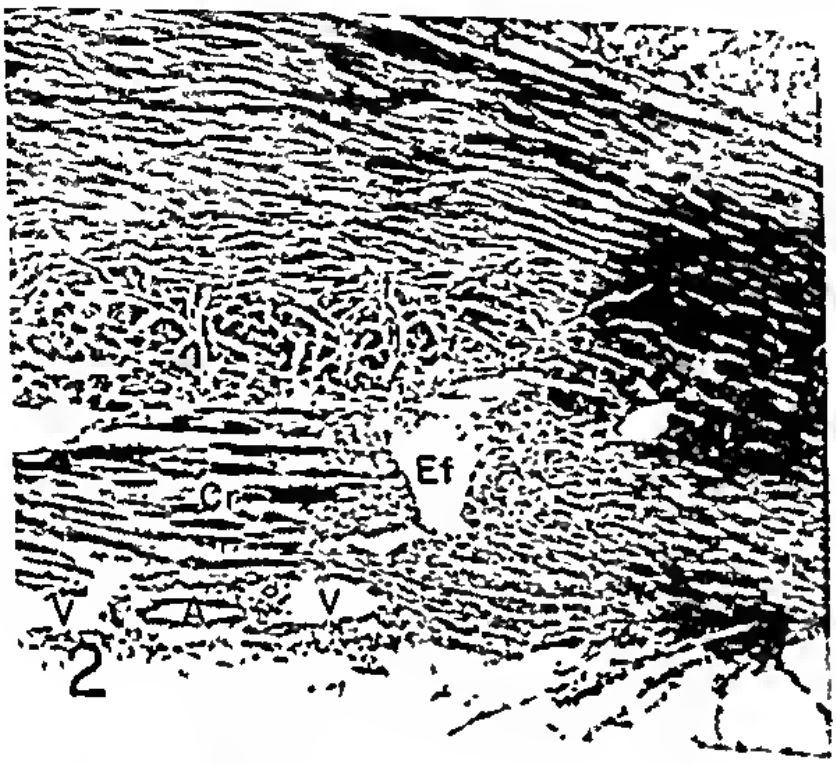

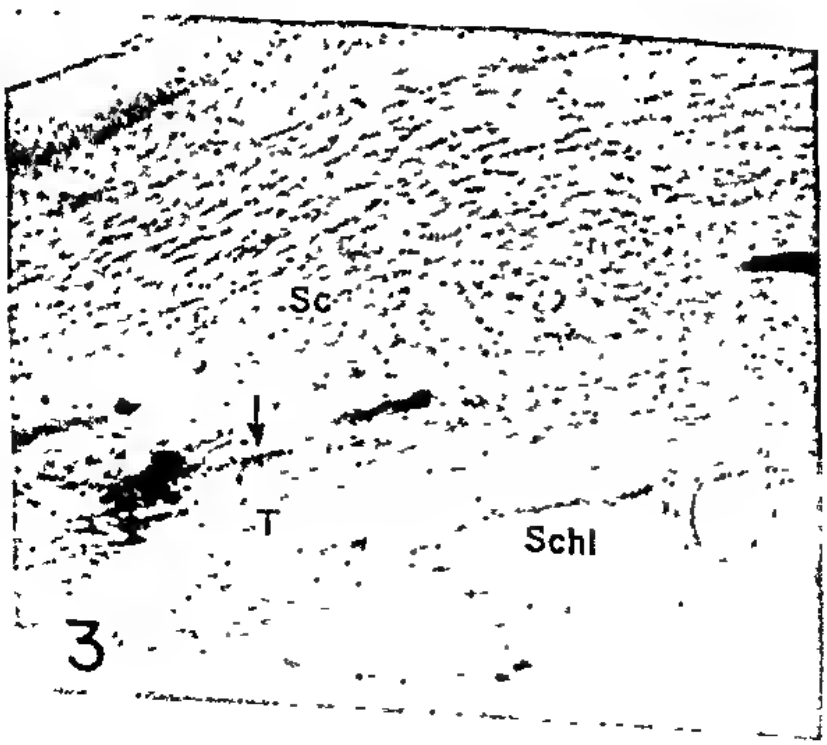

FIG. 4. Two associated nervous corpuscles immediately before the large nervous bundles encircling the anterior chamber behind the canal of Schlemm. Nerve bundles in black on the top of the figure. The arrow points in the direction of the cornea. Flat section impregnated by the method of Gros-Schultze. Magnification: × 150.

FIG. 5. A giant terminal corpuscle found immediately in front of the anterior end of Crampton's muscle. Flat section impregnated as above. Magnification: × 360.

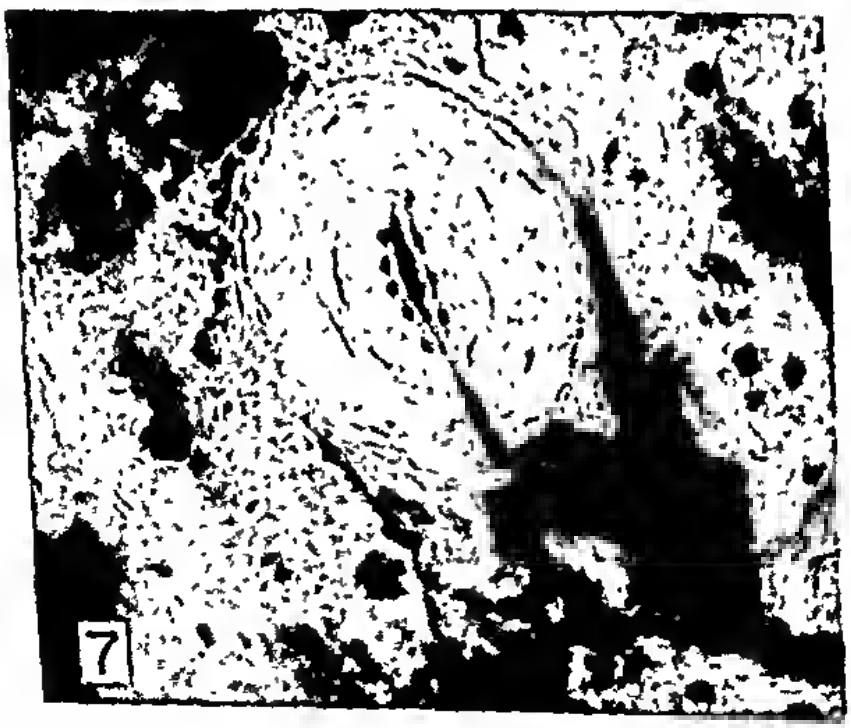

FIG. 6 A terminal corpuscle of Herbst enclosed in the midst of the striated muscle fibers of Crampton's muscle Flat section as in Fig. 4. Magnification: × 360.

FIG. 7 Terminal Herbst's corpuscle found in the superficial layers of the sclera. Flat section impregnated by Gros-Schultze's method. Magnification: × 360.

FIG. 8. Flat section of the tissue between the canal of Schlemm and the sclera. Efferent venous channels (V) with empty lumen. Thick nerve bundles in the neighborhood of the channel with associated nervous corpuscles. Gros-Schultze's method. Magnification: × 150.

FIG. 9. Another corpuscle in immediate contact with an empty endothelial tube. Gros-Schultze's method. Magnification: × 360.

work demonstrated the close relationship of those corpuscles to variations in the lymphatic system of the mesenterium. Kubik and Szabó (1955) observed that the corpuscles were situated in closest contact with the lymphatic vessels. We can consider this relation of terminal encapsulated nervous corpuscles in both systems, ocular as well as mesenterial, to be analogous.

Summary

Detailed study of the localization and relations of the encapsulated terminal sensory corpuscles of Herbst in the region of the anterior chamber angle of the goose eye showed their close relationship to the efferent venous system. Thus these corpuscles were found accompanying venous channels from the canal of Schlemm to the episcleral venous plexus. Their most probable function is to register pressure differences within those vessels.

References

Dowgjallo, N. D. (1925/26). Zur Frage uber die Vater-Pacinische Korperchen im Mesorectom der Katze. *Anat Anz.* **60**, 279.

Kubik, I, and Szabó, J. (1955) Die Innervation der Lymphgefasse im Mesenterium *Acta Morphol Med Sci. Hung T.VI*, 25

Lawrentjew, A P. (1925/26) Zur Topographie der Vater-Pacinischen Korperchen im Mesenterium des Dunn- und Dickdarms bei der Katze. *Anat. Anz.* **60**, 81.

Palmgren, A (1948) *Acta Zool.* **29**, 377-392.

Rochon-Duvigneaud, A (1943). "Les yeux et la vision des Vertébrés," p. 623. Masson, Paris.

Romeis, B. (1943) "Taschenbuch der mikroskopische Technik." Oldenbourg, Munich

Vrabec, Fr. (1954) L'innervation du système trabéculaire de l'angle iren. *Ophthalmologica* **128**, 359

Morphology and Pathology of the Trabecular Meshwork[1]

JOHANNES ROHEN

Anatomisches Institut der Universität, Mainz, Germany

Introduction

In the trabecular meshwork of primates, three different zones can be distinguished (Ashton *et al.*, 1956; Flocks, 1956, Rohen, 1957; Unger, 1957) (Fig. 1). The first zone contains a wide network of collagenous

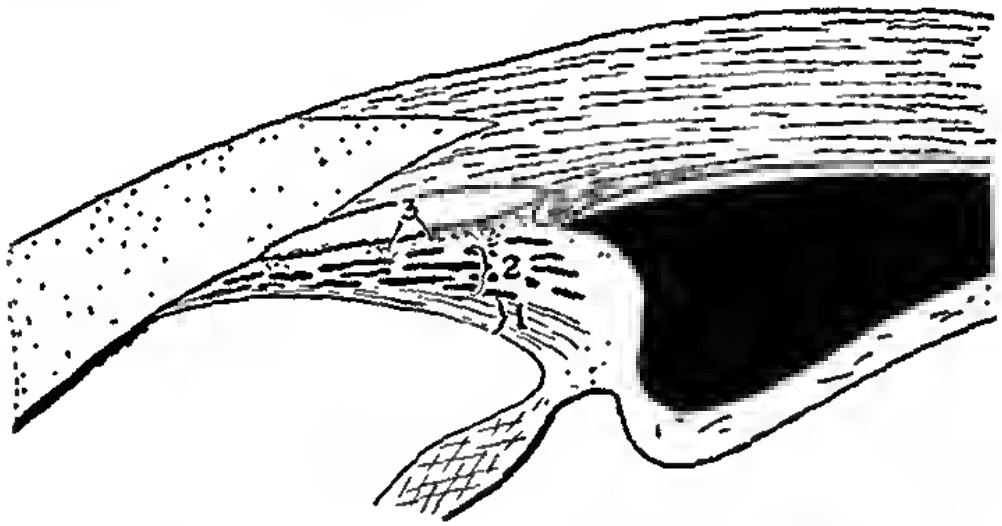

Fig 1. Schematic drawing of the chamber angle in primates, showing the three distinct parts in the trabecular meshwork Area 1 (uveal meshwork); area 2 (trabeculum corneosclerale), area 3 (inner wall or pore area).

strands connected with the tissue in front of the ciliary muscle and the iris root. The fibers are surrounded with concentric layers of homogeneous substances and endothelial cells. The second zone is the so-called trabeculum corneosclerale, itself consisting of lamellae with a central core of ground substance and a system of fibers, completely covered by "glass membranes" and cells. The most interesting area is zone three, the inner wall of Schlemm's canal. This area contains an argyrophilic fiber system which is embedded in a homogeneous inter-

[1] This report is based on research supported in part by Grant No. 137, Fight for Sight Fellowship, of the National Council to Combat Blindness, New York, and was done at the Oscar Johnson Institute, Department of Ophthalmology, Washington University, St Louis, Missouri.

fibrillar ground substance, rich in mucopolysaccharides (Zimmermann, 1957, 1958).

Experimental

By using enzymes *in vitro*, attempts have been made to determine the different natures of the fibers in the described areas. In addition, autolysis experiments were done. Human eyes were cut into several sectors and fixed at different intervals after storage at room temperature. After 2 or 3 days of autolysis, most parts of the glass membranes and collagenous structures in the meshwork had disappeared completely. The fiber system, however, remained intact and could be stained as in the control specimens which were fixed immediately. The reversed experiment was done with acetic acid. Several sectors of the same eye were put either in the fixative or in solutions of 0.5 and 1.0% acetic acid. After acetic acid treatment a marked thickening and swelling of the glass membranes was observed while the fibers of the trabeculae remained unchanged (Fig. 2). We, therefore, must assume the existence of fiber systems, different in structure and quality, within the three mentioned zones on the trabecular meshwork. The uveal meshwork (area 1) contains more collagen, the corneoscleral part (area 2) a specific fiber system, and the so-called pore tissue (area 3) mostly argyrophil or reticulin fibers.

We have studied the changes that occur with age in the inner wall of Schlemm's canal. Autopsy eyes were used as well as specimens of different species of monkeys. Localized proliferations of endothelial cells could be found on the inner wall, especially in specimens of younger age groups. Occasionally, such cell condensations were seen as tissue strands which divided Schlemm's canal into several parts. The illustrations selected, however, were from specimens which demonstrated no strands even in serial sections. It was apparent that in eyes, especially during the first decade of life, the endothelium of the inner wall of

---

Fig. 2. Effect of acetic acid on the trabeculae in a human eye. Two sectors of the same eye: (a) after immediate fixation; (b) after immersion in acetic acid (1%). Note the marked swelling of the trabeculae, specially the glass membranes. Goldner staining. Magnification: × 680.

Fig. 3. Cell proliferations on inner wall of Schlemm's canal in normal eyes: (a) human eye, 6 years old; (b) human eye, 4 weeks old; (c) monkey eye (Aotes triv.).

Fig. 4. Perfusion effect on the inner wall of Schlemm's canal in a human eye: (a) swelling and enlargement of the "pore area," marked by arrows; (b) vacuolization of the endothelial cells of Schlemm's canal. Note that no changes are observed on the other cell groups.

2a.

2b.

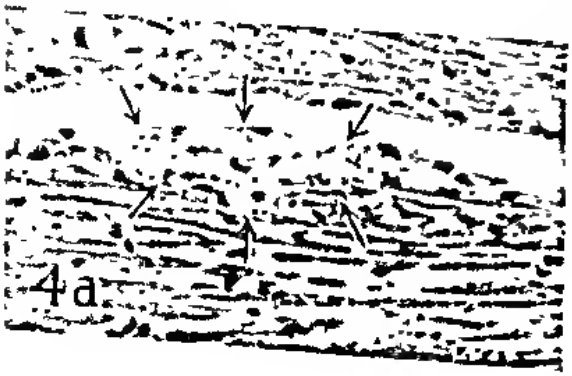

4a.

3a.

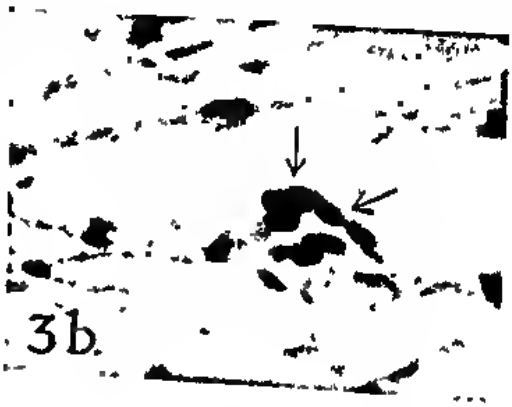

3b.

3c.

4b.

Schlemm's canal reveals localized areas of proliferated cells, sometimes piled up in several layers (Fig. 3b, c), and sometimes spread out in groups over the whole canal (Fig. 3a).

In order to explore the functional importance of the different zones in the trabecular meshwork, we compared the resistance to outflow, estimated by perfusion, with histological structure. After perfusion with Tyrode's solution [method used was the same as described by Bárány (1953)], one could observe frequently a marked swelling of area 3, i.e., the inner wall of Schlemm's canal (Fig. 3a). This area contained a homogeneous material which stained for mucopolysaccharides and was hyaluronidase-sensitive. After perfusion, this interfibrillar material was washed out, the resistance decreased, and the whole area developed a foamy appearance (Fig. 4a). On the other hand, the trabecular meshwork that was perfused often revealed vacuolated cells in the inner wall to a much higher degree than usually found in nonperfused material (Fig. 4b). Sometimes, the whole cell layer showed big vacuolated cells. This was, of course, an artifact. However, because of the fact that only these and not the other cells of the trabecular meshwork and Schlemm's canal appeared in this form it might be related to their specific function.

In order to further investigate the outflow mechanism, perfusions were carried out with different solutions (dextran of various molecular weights, hyper- and hypotonic solutions, cellulose, and pigment preparations from pigmented animals). In these experiments the perfused substances were found to be dammed up on the inner wall of Schlemm's canal or included within the vacuoles of the endothelium (Fig. 5). In addition, the shape of the cells was sometimes deformed. Artificial elongations or swelling were observed. The deformed cells frequently contained granules of the perfused material (Fig. 5). The resistance to outflow in these experiments increased markedly after 10 or 20 min. This effect occurred even when the perfused particles were much smaller than the probable pore size. Therefore, cellular changes may have occurred in the enucleated eyes during the experiment.

FIG. 5. Effect of perfusion with dextran or pigment solution on the inner endothelium of Schlemm's canal in human and monkey eyes. a,e,h—monkey; b,c,d,f,g—human eyes.

a,d—Pigment perfusion. *Note the condensation of pigment beneath* the endothelial layer or *within the cells* (d). b,f,g—Club-shaped cell deformations after perfusion of *dextran or protein*. The substances can be seen within the cells. f—Dextran (PAS-staining, see arrow). e,h—Cells with empty vacuoles lie beside cells which are filled with the perfused material (see arrows). c—Isolated endothelial cell of Schlemm's canal in which a large vacuole is filled with dextran (PAS-staining, see arrows).

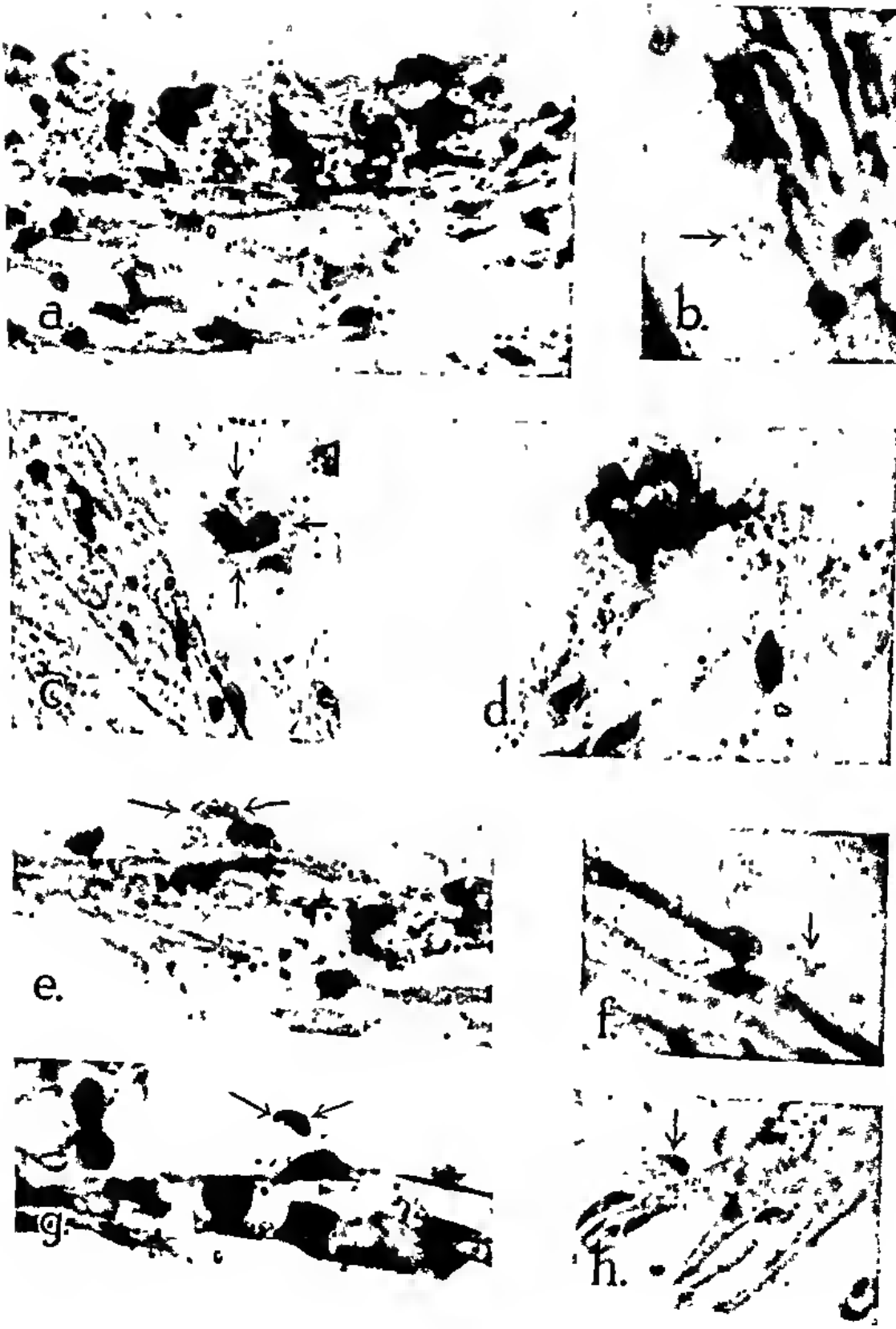
a.
b.
c.
d.
e.
f.
g.
h.

In addition we wish to report the findings on biopsy material from eyes with glaucoma obtained from trephine operations (Rohen and Unger, 1958). Histological sections of trephine buttons showed a high percentage of pathological changes in the inner wall of Schlemm's canal and the adjoining cell layer. A detailed description will be published elsewhere. It is conceivable that changes in form and function of the endothelial cells on the inner wall could lead to an obstruction of the pores. That may be the first step in the pathological destruction of the trabecular meshwork. The thickening of the glass membranes, loss or proliferation of cells, and narrowing of the intertrabecular spaces, as described previously (Rohen and Unger, 1958, 1959), may take place later and lead to a complete hyalinization of the entire tissue.

Summary

We believe that the outflow of aqueous humor really passes through the pores and holes in the endothelial cells lining Schlemm's canal (Holmberg, 1959) and that the main resistance is located in the inner wall itself.

References

Ashton, N., Brini, A., and Smith, R. (1956). *Brit. J. Ophthalmol.* **40**, 257-282.
Bárány, E. H. (1953). *Acta Soc. Med. Upsaliensis* **59**, 260-276.
Flocks, M. (1956). *A.M.A. Arch. Ophthalmol.* **56**, 708-718.
Holmberg, A. S. (1959). *A.M.A. Arch. Ophthalmol.* **62**, 956-976.
Rohen, J. (1957). *Arch. Ophthalmol. Graefe's* **158**, 310-325.
Rohen, J., and Unger, H. H. (1958). *Am. J. Ophthalmol.* **46**, 802-813.
Rohen, J., and Unger, H. H. (1959). "Zur Morphologie und Pathologie der Kammerbucht." Steiner-Verlag, Wiesbaden.
Unger, H. H. (1957). *Arch. Ophthalmol. Graefe's* **158**, 509-523.
Zimmermann, L. E. (1957). *Am. J. Ophthalmol.* **44**, 1-4.
Zimmermann, L. E. (1958). *Am. J. Ophthalmol.* **45**, 299-300.

Discussion

Dr. Teng [Manhattan Eye, Ear & Throat Hospital, New York]: I agree with the endothelial site. Recently we got some pictures which I think definitely show that the endothelial changes come first when the degeneration starts. The degeneration of collagen is probably due to the effect of aqueous humor. The relationship of endothelium protecting the collagen from the degenerative effect of aqueous humor, we have shown by animal experimentation and reported (*Am. J. Ophthalmol.* **46**, 534, 1958).

We have also seen cases where a defect in the endothelium of the trabecula may be covered by endothelial cells from the corneal side. Then you have obstruction of the trabecula or chamber angle by corneal endothelium and Descemet's membrane. Sometimes when there is an endothelial defect of the trabecula, the endothelial cells may proliferate from the trabecula, Schlemm's canal, or the

collector channels as a part of the healing process, as we reported years ago. Any of these can be a cause for obstruction of the outflow of the aqueous.

DR. ROHEN [Mainz, Germany]: I cannot comment on the sort of degeneration which occurs in glaucoma but can only describe the structures as seen without implication concerning the process of degeneration.

DR. LANGHAM [Wilmer Institute, Baltimore, Md.]: Do the endothelial changes observed correlate with age? This is important because of the controversy concerning the change in outflow resistance with age.

DR. ROHEN: I have the impression that the endothelial proliferation, demonstrated in normal eyes, can be correlated with age but this is not certain. We have perfused the eyes in which we found endothelial proliferation and found no relationship to the outflow. More data must be collected in order to answer this question.

DR. GARRON [University of California, Berkeley, California]. I am very pleased *that Dr. Rohen was able to demonstrate the vacuoles in the inner wall of Schlemm's* canal. Do you think they are truly present or are artifacts?

DR. ROHEN: The vacuoles are real, although they were demonstrated by perfusion which seemed to increase their number.

DR. WOLTER [University of Michigan, Ann Arbor, Michigan]: *Did you make* special nerve fiber preparations of the trabeculae in glaucoma and did you find evidence of nerve fiber pathology in the trabeculae of these cases?

DR. ROHEN. No.

CHAIRMAN BECKER [St. Louis, Missouri]: Is there any contradiction in the two pieces of information that Dr. Rohen has presented? Sections of trephine buttons from glaucomatous eyes showed characteristic cellular proliferations, whereas in two of the very young normal human eyes (1- and 6-month-old infants), as well as in the normal monkey eye even greater endothelial cell proliferations were found. Would you comment on the possible contradictions of these findings?

DR. ROHEN. I have only the impression that the cellular proliferation which occurs with age is different in histological appearance from that which we see in glaucoma.

The Fine Structure of the Human Cornea[1]

MARIE A. JAKUS

Retina Foundation, the Department of Ophthalmology, Massachusetts Eye and Ear Infirmary, and Harvard Medical School, Boston, Massachusetts

A BRIEF REVIEW of earlier literature dealing with corneal structure was given in a paper on the fine structure of the rat cornea (Jakus, 1954a). Other publications based on electron microscope examination of thin sections of corneal tissue include a preliminary report on human cornea (Jakus, 1954b), a study of the fine structure of Descemet's membrane (Jakus, 1956), and one of the Kayser-Fleischer ring in Descemet's membrane (Uzman and Jakus, 1957). Ishida (1958a) has written about spaces he observed between the epithelial cells and the connections between them; he has also described the basement membrane of the epithelium and Bowman's layer of the stroma (Ishida, 1958b), and has drawn essentially the same conclusions about their structure in the central cornea as did Jakus. Histochemical studies of the epithelial basement membrane include those of Teng and Katzin (1953) and of Offret and Haye (1959). Garron and Feeney have studied the trabecular meshwork and described long-spacing fibers in this region; their most recent paper (1959) summarizes their findings

This report will present some recent observations on the human cornea, both central and peripheral.

Experimental[2]

Corneas were fixed for 3 to 5 hr in cold 2% OsO_4 in Veronal acetate buffer, with 1% glycerine added, at pH's around 7.5. They were dehydrated in a graded series of methanol and cut into small pieces during dehydration To increase contrast, 0.5% phosphotungstic acid was added to the absolute alcohol. The tissue was then soaked in resin mixture,

[1] This investigation was supported by a research grant (B-454) from the National Institute of Neurological Diseases and Blindness, United States Public Health Service Equipment is on loan from the American Optical Company.

This is paper No 91 of the Retina Foundation

[2] The author wishes to acknowledge the kind co-operation of Dr. C. D. J Regan for making available human eye tissue; of Ciba Company, Inc., Shell Chemical Corporation, National Aniline Division of Allied Chemical and Dye Corporation, and Rohm and Haas Company, and of their chemists, for samples and information about their products, and for their interest in the problems involved in using epoxy resins as embedding media.

without accelerator, for about 3 days at 47°C., and embedded in gelatin capsules in the complete resin mixture. Polymerization was allowed to proceed at 47°C. for about 3 days, or until the blocks were considered to be adequately hardened. Sections were cut with a Porter-Blum, thermal-advance microtome, using glass knives, and examined with an RCA EMU-2D electron microscope equipped with an objective aperture.

Most of the tissue described here was embedded in Epon 815, although Araldites 6005, 502, and M have been used with equally satisfactory results. The formulation for the embedding mixture was based upon that published by Glauert *et al.* (1956), with modifications made as needed in the proportions of the plasticizer (dibutyl phthalate) and accelerator (tridimethylaminomethylphenol).

Observations

Central Cornea

Epithelium

The epithelium of human cornea resembles the corneal epithelia of other vertebrate species. The basal cells are columnar in shape and have roughly spherical nuclei (Fig. 1). Above them are several layers of flattened cells, which decrease progressively in thickness and have nuclei elongated in the plane of the cornea (Fig. 2). The outermost layer of squamous cells forms the smooth outer surface of the cornea. Mitochondria can be found in the epithelial cells but in the normal adult cornea they are small in size and few in number. The cytoplasm appears to consist chiefly of fine filaments (Fig. 3), less than 100 Å in width, the majority of which are perpendicular to the plane of the cornea in the basal cells and parallel to it in the squamous cells. As might be expected, the cells show birefringence positive with respect to these axes.

The surfaces of the epithelial cells form processes which fit snugly into corresponding indentations of adjacent cells. Along the membranes are attachment areas, or desmosomes, which look like black sutures holding together pieces of a jigsaw puzzle. In transverse section, each desmosome consists of a pair of dense plaques on opposing cell membranes, separated by a distance of about 125 Å (Fig. 4). Each plaque

---

Fig. 1. Basal cells of central corneal epithelium, showing nuclei (n), cell membranes with interdigitating processes (ip), and desmosomes (d). Magnification: × 6460.

Fig. 2. Superficial cells of corneal epithelium, showing a nucleus (n), cell membranes (cm), and desmosomes (d). The filamentous cytoplasm is more apparent here than it is in the denser basal cells. Magnification: × 6850.

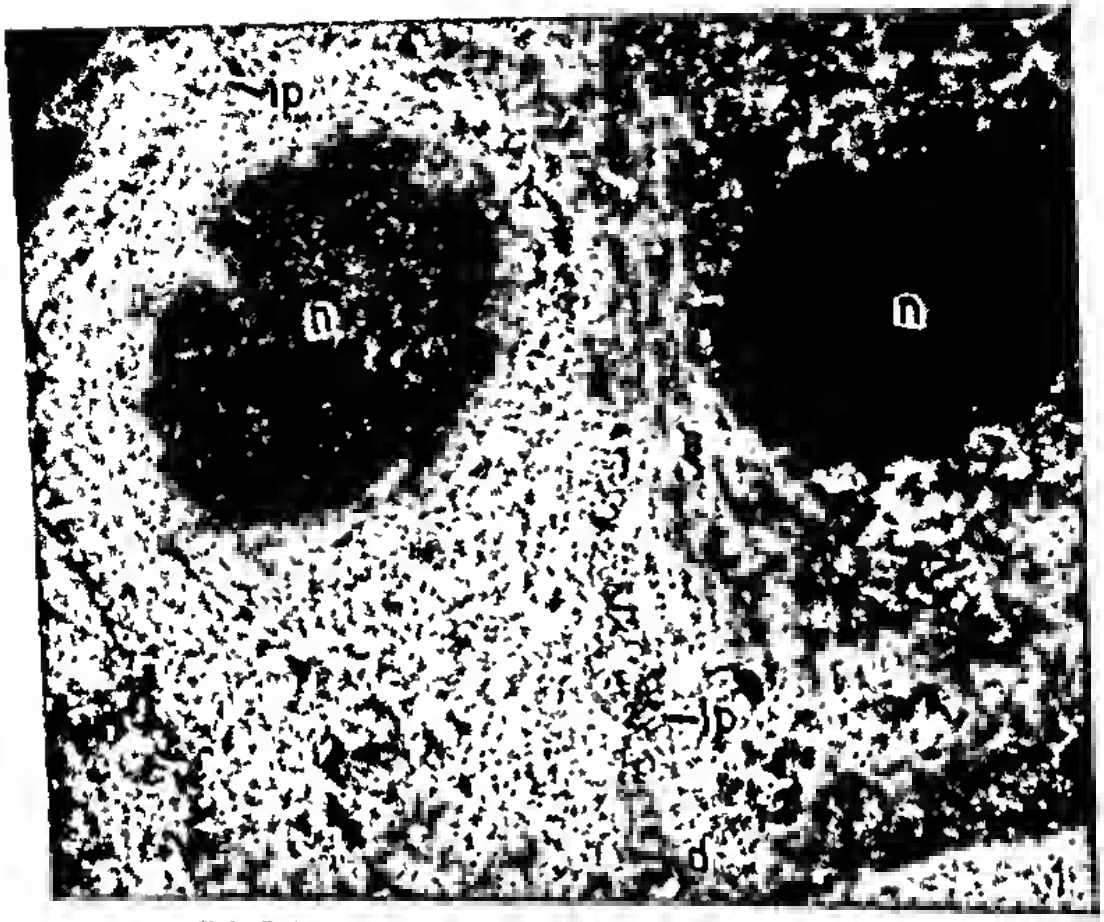
p
n
n
p
d


d
cm
n
2

appears to be the terminus of bundles of eytoplasmie filaments. The region between the plaques is somewhat darker than is the intereellular space between the desmosomes and ean sometimes be resolved into what look like fine connecting filaments. Within this region, midway between the plaques, there is often a line whieh appears to be a row of small granules. Sectioned tangentially, the desmosomal plaques appear as dark circular or oval struetures (Fig. 5). Widths of the plaques are generally between 500 and 1500 Å; some even larger ones may be eomposites of two or more smaller desmosomes.

The desmosomes faeing the stroma are asymmetrieal, with the basement membrane of the epithelium forming half of the strueture (Fig. 6). The dense plaque of the eell membrane is double, eonsisting of an outer thin layer and an inner thick layer, which probably represent the two halves of a double eell membrane (elsewhere this usually appears as a single line). The measured distanee between the two parts of this eomposite desmosome varies, depending in part upon the angle of sectioning, but the smallest values found, about 125 Å, were similar to those observed in the intercellular desmosomes. In this region, also, there is a moderately dense substanee which can oecasionally be resolved into filaments. Within the cytoplasm, adjaeent to the plaque, there is generally an aceumulation of dense material disposed in bands or clumps.

The basement membrane of the epithelium is 100 to 300 Å thiek in transverse sections and appears to eonsist of very fine, tightly paeked filaments. It is thicker and more dense at the desmosomes than between them. On the inner surfaee of the membrane thin filaments ean sometimes be seen, apparently leaving the membrane and wandering off into the stroma. Similar filaments have been found in larger numbers in the rabbit eornea.

Stroma

The stroma directly beneath the basement membrane of the epithelium eonsists of collagen fibrils elosely but randomly paeked into a feltlike layer whieh is not sharply demarcated from the remainder of

---

FIG. 3. Oblique section through superficial epithelial cells, showing cytoplasmic filaments (f), cell membranes with interdigitating processes (ip), and desmosomes (d). Magnification: × 9880.

FIG. 4. Intercellular desmosomes at higher magnification. Arrows point to row of granules in moderately dense region midway between desmosomal plaques. Magnification: × 33,850.

FIG. 5. Two clusters of intercellular desmosomes sectioned tangentially (arrows). Magnification: × 20,010.

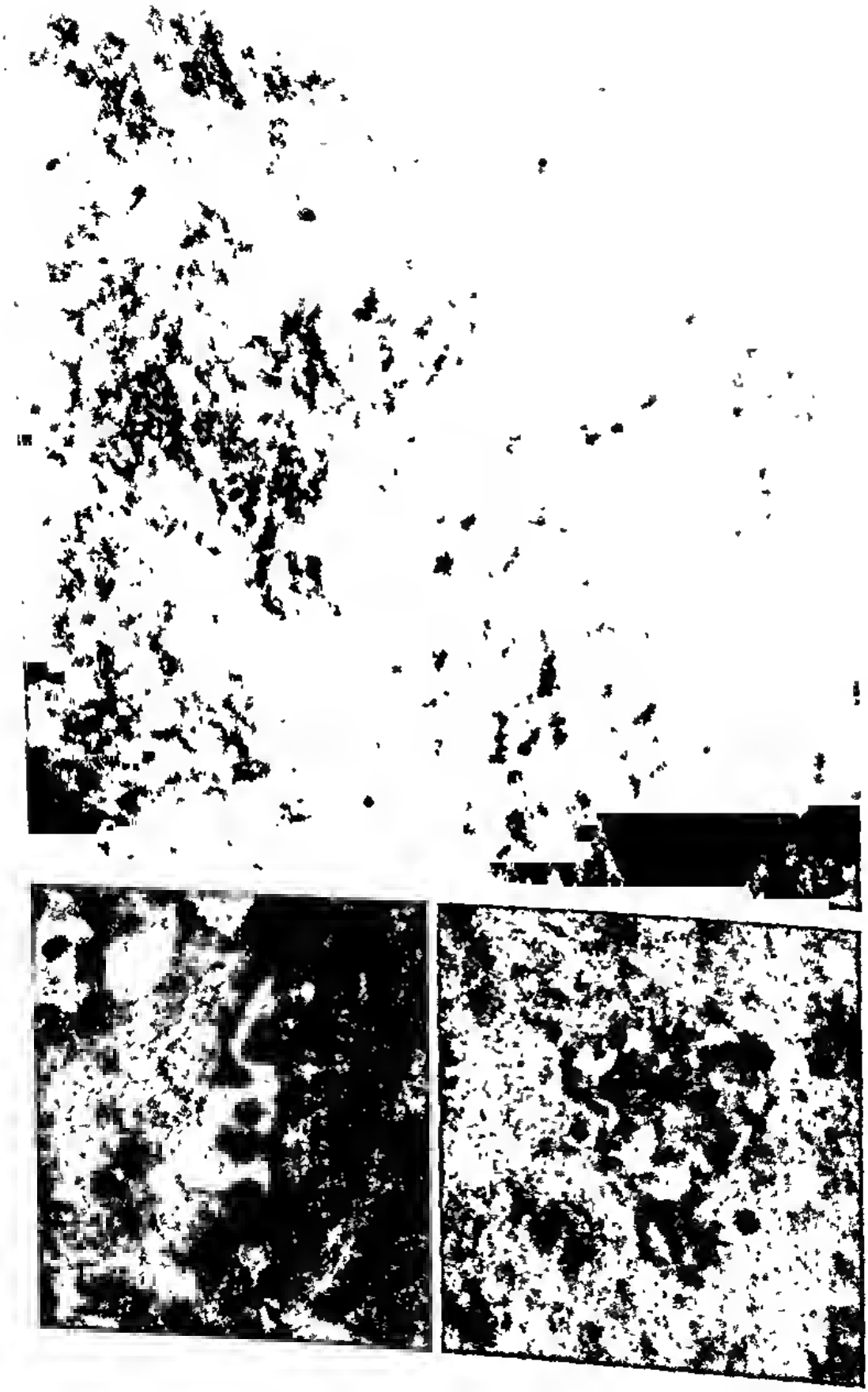

the stroma beneath it (Fig. 7). The characteristic collagen period is infrequently seen in these fibrils but, when observed, it is of the usual magnitude. Between the fibrils, here as elsewhere in the stroma, are fine filaments and what appears to be an amorphous matrix.

In the remainder of the stroma the collagen occurs in layers within each of which the fibrils run parallel to each other. In any field of a section cut from a suitably oriented block, the fibrils in one lamella form essentially right angles with those in adjacent layers (Fig. 8). In some regions the layers are straight and of nearly equal width, while in others they may vary from a single row of fibrils to layers several microns in thickness and may branch and anastomose with other lamellae running in the same direction (Fig. 9).

The fibril diameters of human stroma collagen fall within the range observed in the corneas of numerous other vertebrate species. There is some evidence, however, that a gradient exists, with the most frequent diameters gradually increasing in magnitude from the epithelium to Descemet's membrane. In Bowman's layer of the stroma most of the fibril diameters measured were between 160 and 240 Å, with a peak around 190 Å. Deeper in the stroma, the range was between about 240 and 280 Å, and near Descemet's membrane this increased to about 275 and 400 Å, with a peak around 340 Å. The repeating period along the fibril length was found to be between 550 and 600 Å, showing the usual shrinkage observed in embedded and sectioned collagen.

The stroma corpuscles are flattened cells which, in the human, appear to lie within rather than between the collagen lamellae (Fig. 9). There is little cytoplasm around the nuclei, and cytoplasmic inclusions are sparse but the cells have long, thin processes which make contact with those of adjacent cells in the same plane.

Descemet's Membrane

Descemet's membrane in the human does not show a high degree of organization. In transverse sections, only the portion of the membrane nearest the stroma resembles beef Descemet's membrane and even here the orientation is not very precise (Fig. 10). The average repeating

---

FIG. 6. Unusually long row of basal desmosomes in peripheral cornea, showing the basement membrane (bm), two-layered dense plaques (p), the moderately dense intradesmosomal material, and the dense cytoplasmic component adjacent to the plaques. *Magnification:* × 44,230.

FIG. 7. Bowman's layer (Bl) of the stroma, directly beneath the basement membrane (bm), merges smoothly with the remainder of the stroma (str). Magnification: × 14,000.

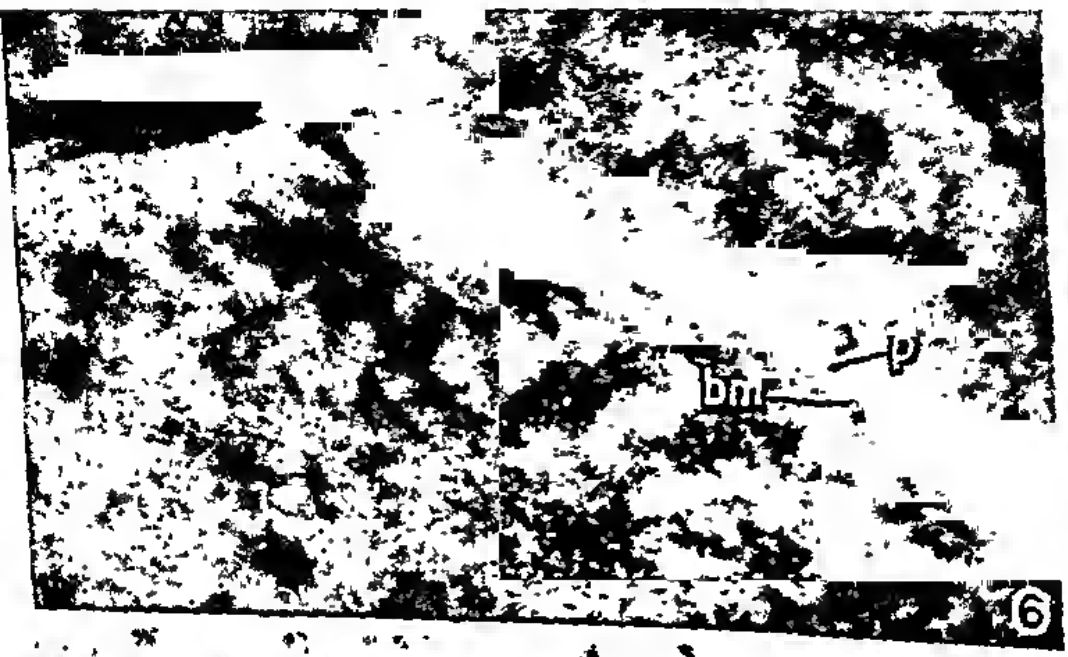
bm
6

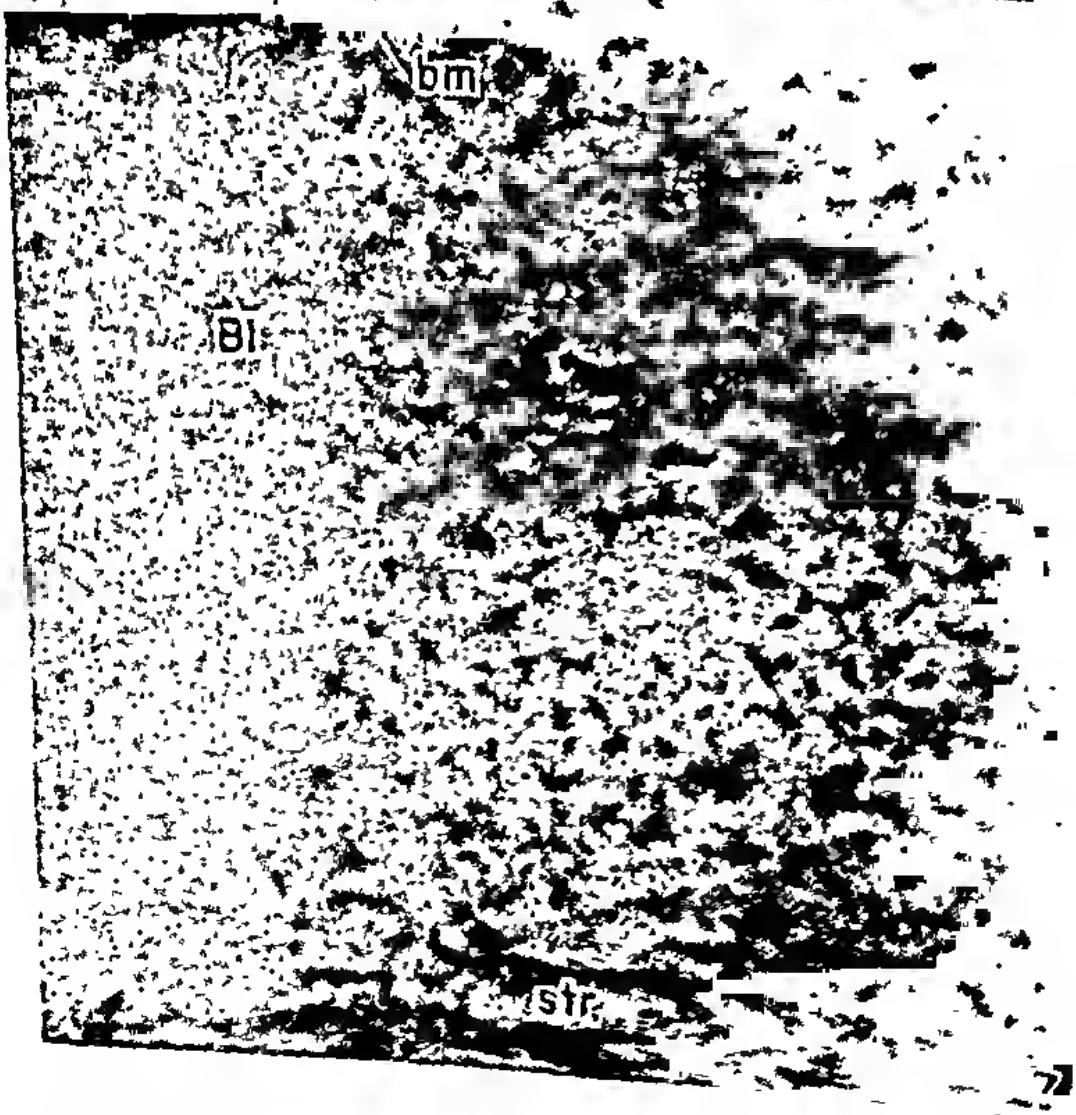
bm
Bl
str.
7

period of 1170 Å, however, is twice the average period of the collagen fibrils in the same corneas, thus exhibiting the same relationship to the stroma collagen as that found in other species.

Endothelium

The corneal endothelium consists of a flat layer of cells with fairly regularly spaced nuclei but with highly convoluted lateral surfaces (Figs. 10 and 11). Where the nucleus is thickest the depth of the cell increases correspondingly, and the resulting bulge is usually directed into Descemet's membrane rather than into the anterior chamber. This maintains the smooth, flat inner surface of the cornea. The endothelial cells contain vesicles and granules, and relatively larger numbers of mitochondria than do the epithelial cells, but they do not possess the abundant filamentous component of the epithelial cytoplasm. Desmosomes have not been observed between these cells.

Peripheral Cornea

In transverse sections of the central cornea, the innermost surface of the basal cells of the epithelium appears as a smooth line parallel with the plane of the cornea. Toward the limbus, however, this surface becomes increasingly irregular. Sections of this region are difficult to interpret because they cut through cytoplasm, cell membranes, desmosomes, basement membrane, and Bowman's layer collagen at all conceivable angles (Fig. 12). Bowman's layer itself changes markedly as it approaches the limbus. It gradually becomes thinner and more loosely packed (Fig. 13). Between the collagen fibrils can be seen many fine filaments and clumps of amorphous material or even finer filaments which have not been resolved. Cells which in the normal central cornea apparently could not penetrate Bowman's layer now invade this region (Fig. 14), and even capillaries approach within a few microns of the epithelium. At the same time the collagen fibrils exhibit an increased variability in diameter and a pronounced irregularity in cross-section contour (Fig. 15). The larger fibrils, 600 to 700 Å in diameter, have more sharply defined cross striations than do the narrower ones.

Fig. 8. Transverse section through the stroma, showing several lamellae (the fibers in stained sections), in each of which the collagen fibrils are oriented parallel with each other and perpendicular to those in adjacent layers. Magnification: × 10,230.

Fig. 9. Another section of the stroma, in which the layers of collagen fibrils vary widely in width and give off branches which join other layers of fibrils oriented in the same direction. Portions of three stroma cells (sc) are seen, each in its own lamellar lane. One was sectioned through its nucleus (n). Magnification: × 10,300.

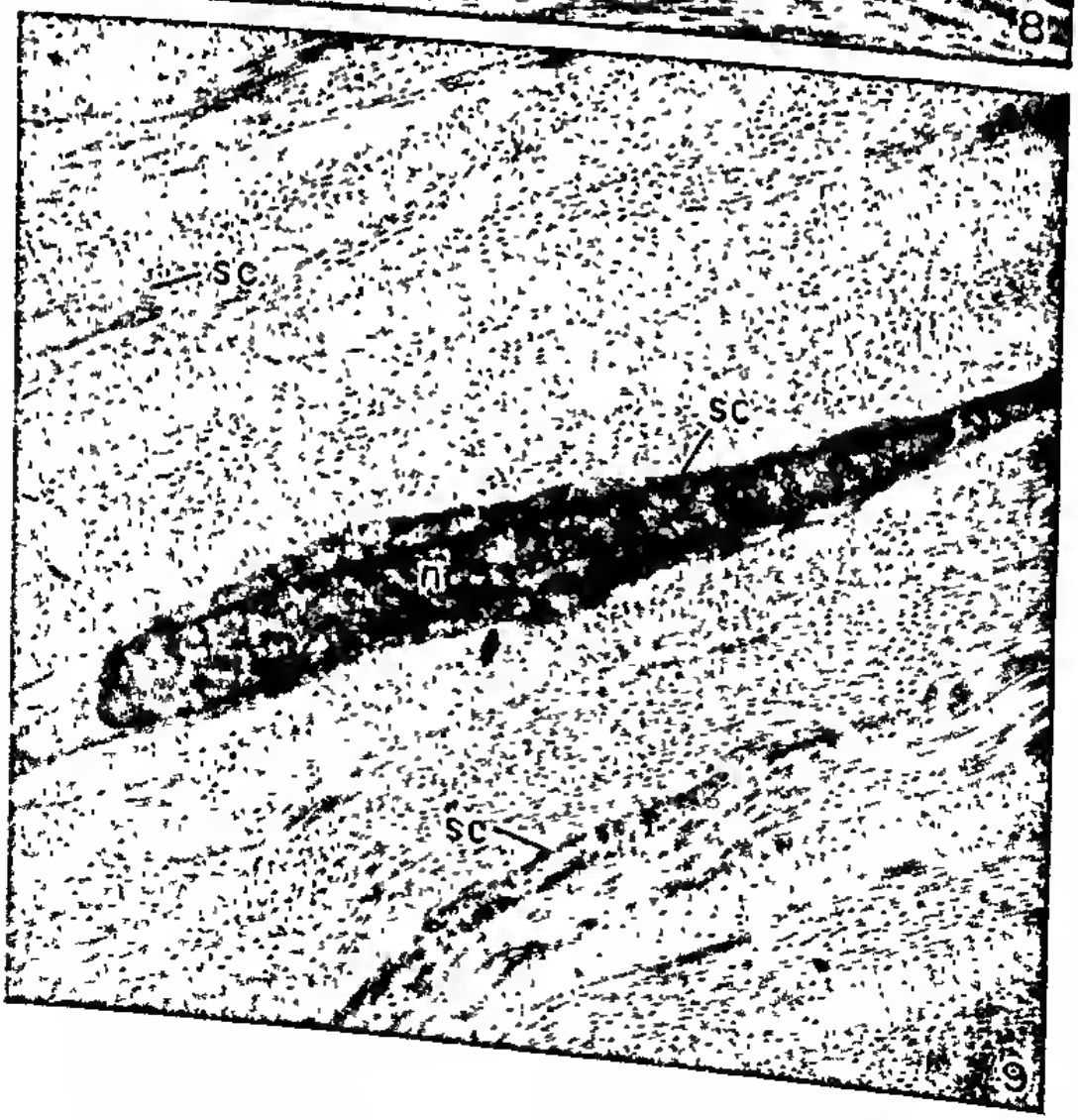
SC
SC
SC

The cells in this region fall into several categories. The most numerous type resembles the stroma cells in the central cornea (Fig. 14). There is, in addition, a cell which has a polymorphous nucleus and inclusions similar to those of cells which are seen also within the capillaries. The inclusions consist of vacuoles and solid, smooth-edged particles which are round, oval, or elongated in shape and which have diameters up to 1000 Å or more and lengths up to 4000 Å. A third type of cell has composite inclusions so numerous that they almost fill the cell, and pseudopodia-like processes around 500 Å in diameter. Some of the inclusions contain, or consist of, amorphous masses, but most of them are clusters of multiple membranes which assume the shapes of arcs, incomplete circles, complete circles or ovals, or short cylinders (these forms could all be interpreted as sections of randomly oriented cylinders with laminated walls and diameters around 900 Å) (Fig. 16). The identification of these two types of cells as, respectively, polymorphonuclear leucocytes and mast cells is in agreement with studies by Fawcett (1960).

Descemet's membrane also undergoes marked alterations in the peripheral cornea. Here are seen the Hassal-Henle bodies or "warts," posterior protrusions of the membrane which push into the endothelium until only a thin cytoplasmic layer remains to cover them (Fig. 17). Each body contains a complex network of branching and anastomosing tunnels which open on the endothelial surface of the membrane. Thin processes of the endothelial cells extend into the outermost portions of the tunnels while in the deeper regions are seen granules and fibers. The most prominent fiber type is a fusiform, long-spacing fiber which consists of regularly spaced dense bands connected by fibrils and resembles the oriented regions of mouse Descemet's membrane, although the connecting fibrils have diameters up to 150 Å. The average distance between the dense bands of this fiber is about 1050 Å, which is slightly (about 50 Å) and perhaps insignificantly less than the average value of the Descemet's membrane repeating period in this region. A series of nodes can often be seen on the connecting fibrils, midway between the dense bands.

Another type of fiber found in the tunnels resembles the connecting fibrils of the long-spacing type in width but is smooth and of uniform

---

FIG. 10. Inner edge of the central cornea, showing stroma (str), Descemet's membrane (Dm), and endothelium. In the endothelium are seen a nucleus (n), mitochondria (m) and cell membranes (cm). Magnification: × 10,240.

FIG. 11. Internuclear region of endothelium, showing tortuosity of lateral membranes seen in profiles of these cells. Magnification: × 24,800.

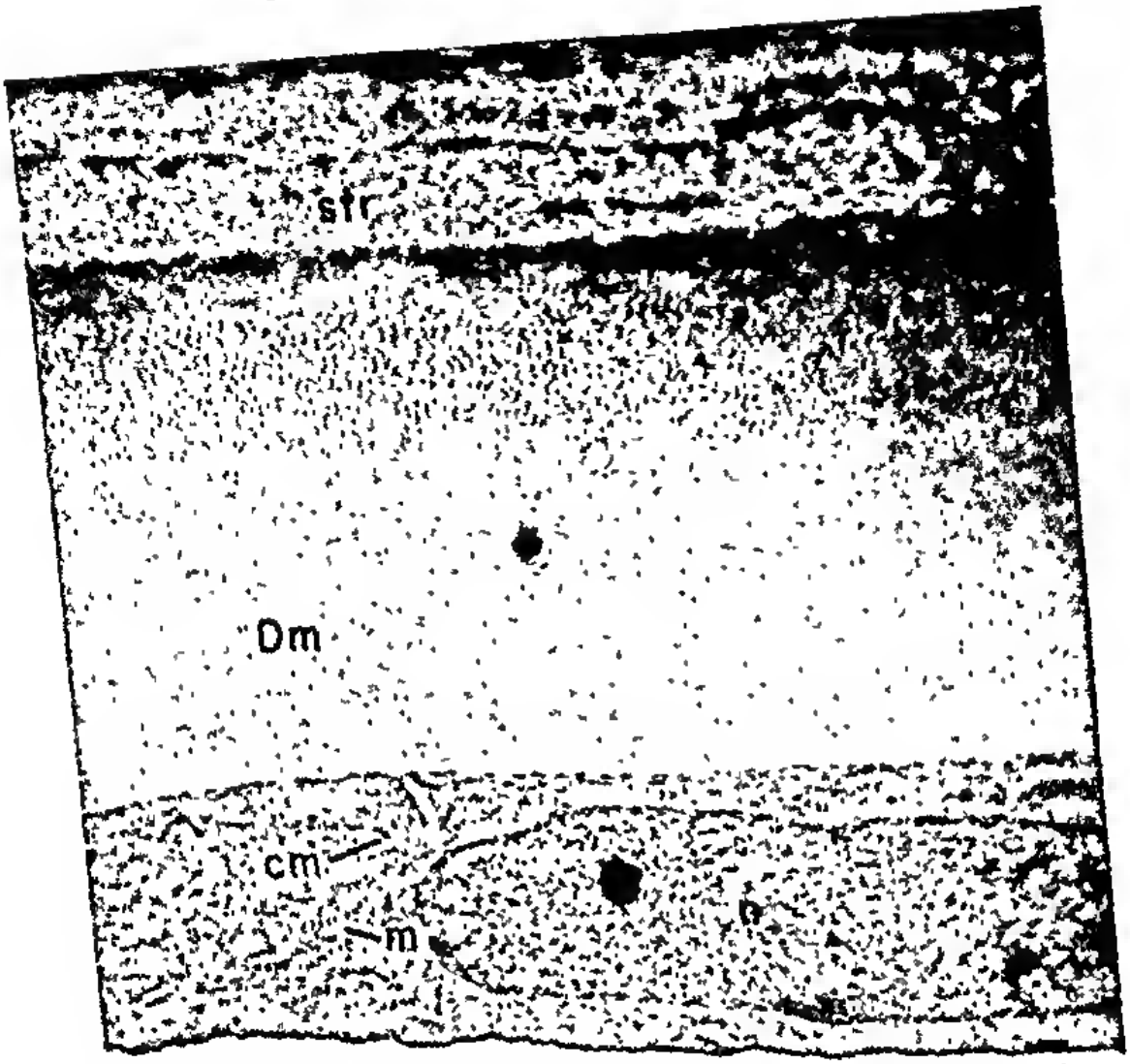

10

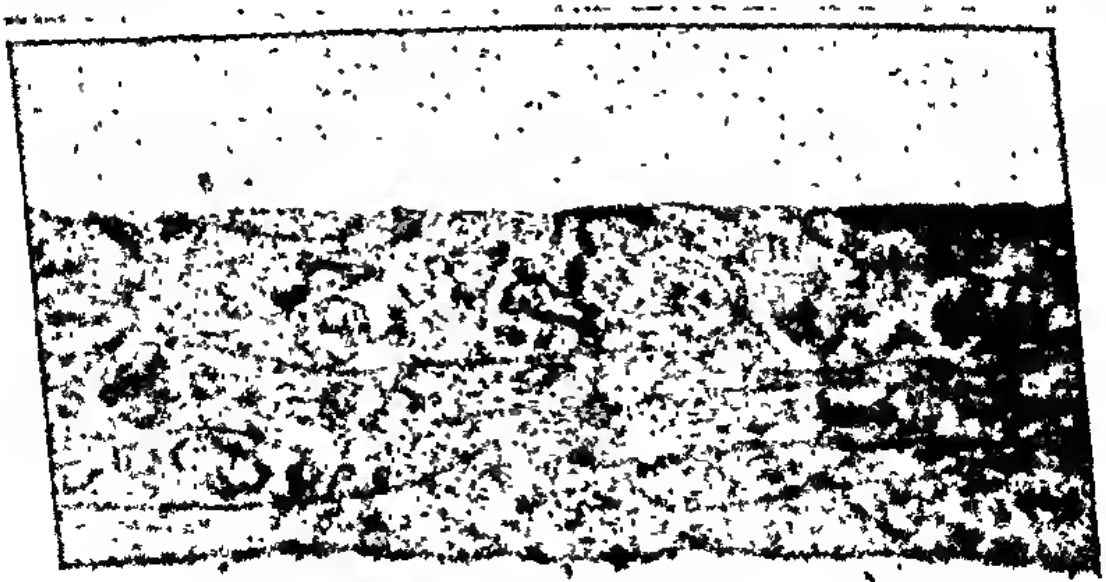

11

density. These fibrils frequently lie close to the long-spacing fibers and often appear to be continuations of the connecting fibrils of the latter.

Nearer the trabecular meshwork these two types of fibers are seen in larger numbers outside the channels as well as within them (Fig. 18). The long-spacing fibers within the substance of Descemet's membrane tend to form layers, one about midway between endothelium and stroma and another about 2 μ from the inner endothelial surface. In this same region Descemet's membrane begins to subdivide into layers. This appears to be accomplished by an intrusion of collagen into the membrane, separating it first into thin inner and thick outer portions. The division then continues, until a multiple-layered system is formed, with each layer usually identified by oriented regions and long-spacing fibers.

Meanwhile, still another type of fibril has made its appearance (Fig. 19). In bundles it is cross-striated, with a period like that of collagen, but its diameter is only about 75 Å. It can be seen first within Descemet's membrane and later it occurs along with the collagen bundles which are interposed between the thin layers of the membrane.

Finally, additional layers of cells appear, spaces form, and the organization of the tissue into the trabecular meshwork is well under way. A trabecular fiber cut in cross section looks like a roll of fibrous components surrounded by a layer of Descemet's membrane and a thin cellular sheath (Fig. 20). Within it can be found stroma-type collagen, limbal Bowman's layer-type collagen of variable diameter, the small-diameter fibrils, and long-spacing fibers. In longitudinal section, these fibrous components are seen in parallel bundles sandwiched between layers of Descemet's membrane and cells (Fig. 21).

Around the Hassal-Henle bodies, some regions of the endothelial cell membranes are thicker than usual and appear to show all stages of vesicle formation. Vacuoles surrounded by membranes of similar density are seen within the endothelial cytoplasm.

Discussion

One notable characteristic of the central, transparent cornea is that of regularity. The four chief layers (epithelium, stroma, Descemet's membrane, and endothelium) have smooth, parallel surfaces; the stroma

---

FIG. 12. Epithelium and Bowman's layer region of peripheral cornea, showing irregular inner surface of basal cells and basement membrane (bm). Magnification: × 14,400.

FIG. 13. Same region as that in Fig. 12, but slightly further out, showing variability in diameter and greater separation of collagen fibrils, and filamentous and other interfibrillar elements. Magnification: × 19,720.

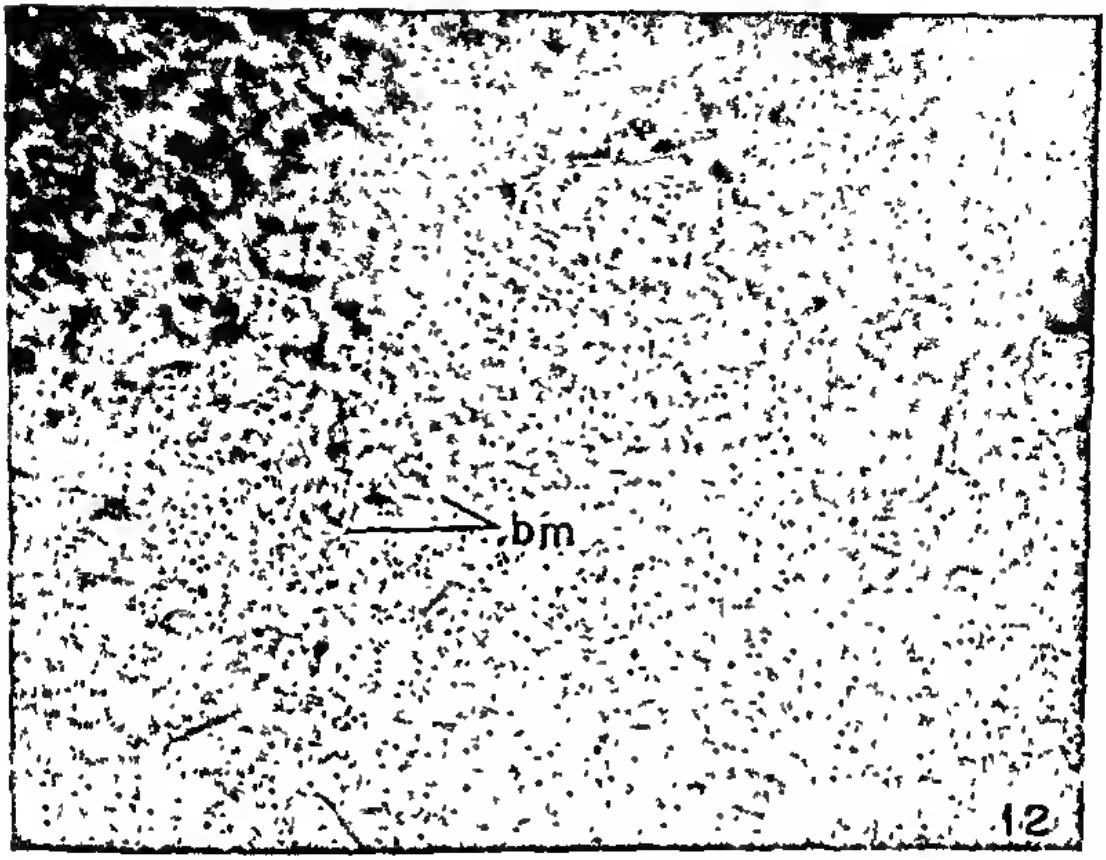
bm
12


bm
13

density. These fibrils frequently lie close to the long-spacing fibers and often appear to be continuations of the connecting fibrils of the latter.

Nearer the trabecular meshwork these two types of fibers are seen in larger numbers outside the channels as well as within them (Fig. 18). The long-spacing fibers within the substance of Descemet's membrane tend to form layers, one about midway between endothelium and stroma and another about 2 μ from the inner endothelial surface. In this same region Descemet's membrane begins to subdivide into layers. This appears to be accomplished by an intrusion of collagen into the membrane, separating it first into thin inner and thick outer portions. The division then continues, until a multiple-layered system is formed, with each layer usually identified by oriented regions and long-spacing fibers.

Meanwhile, still another type of fibril has made its appearance (Fig. 19). In bundles it is cross-striated, with a period like that of collagen, but its diameter is only about 75 Å. It can be seen first within Descemet's membrane and later it occurs along with the collagen bundles which are interposed between the thin layers of the membrane.

Finally, additional layers of cells appear, spaces form, and the organization of the tissue into the trabecular meshwork is well under way. A trabecular fiber cut in cross section looks like a roll of fibrous components surrounded by a layer of Descemet's membrane and a thin cellular sheath (Fig. 20). Within it can be found stroma-type collagen, limbal Bowman's layer-type collagen of variable diameter, the small-diameter fibrils, and long-spacing fibers. In longitudinal section, these fibrous components are seen in parallel bundles sandwiched between layers of Descemet's membrane and cells (Fig. 21).

Around the Hassal-Henle bodies, some regions of the endothelial cell membranes are thicker than usual and appear to show all stages of vesicle formation. Vacuoles surrounded by membranes of similar density are seen within the endothelial cytoplasm.

Discussion

One notable characteristic of the central, transparent cornea is that of regularity. The four chief layers (epithelium, stroma, Descemet's membrane, and endothelium) have smooth, parallel surfaces; the stroma

---

FIG. 12. Epithelium and Bowman's layer region of peripheral cornea, showing irregular inner surface of basal cells and basement membrane (bm). Magnification: × 14,400.

FIG. 13. Same region as that in Fig. 12, but slightly further out, showing variability in diameter and greater separation of collagen fibrils, and filamentous and other interfibrillar elements. Magnification: × 19,720.

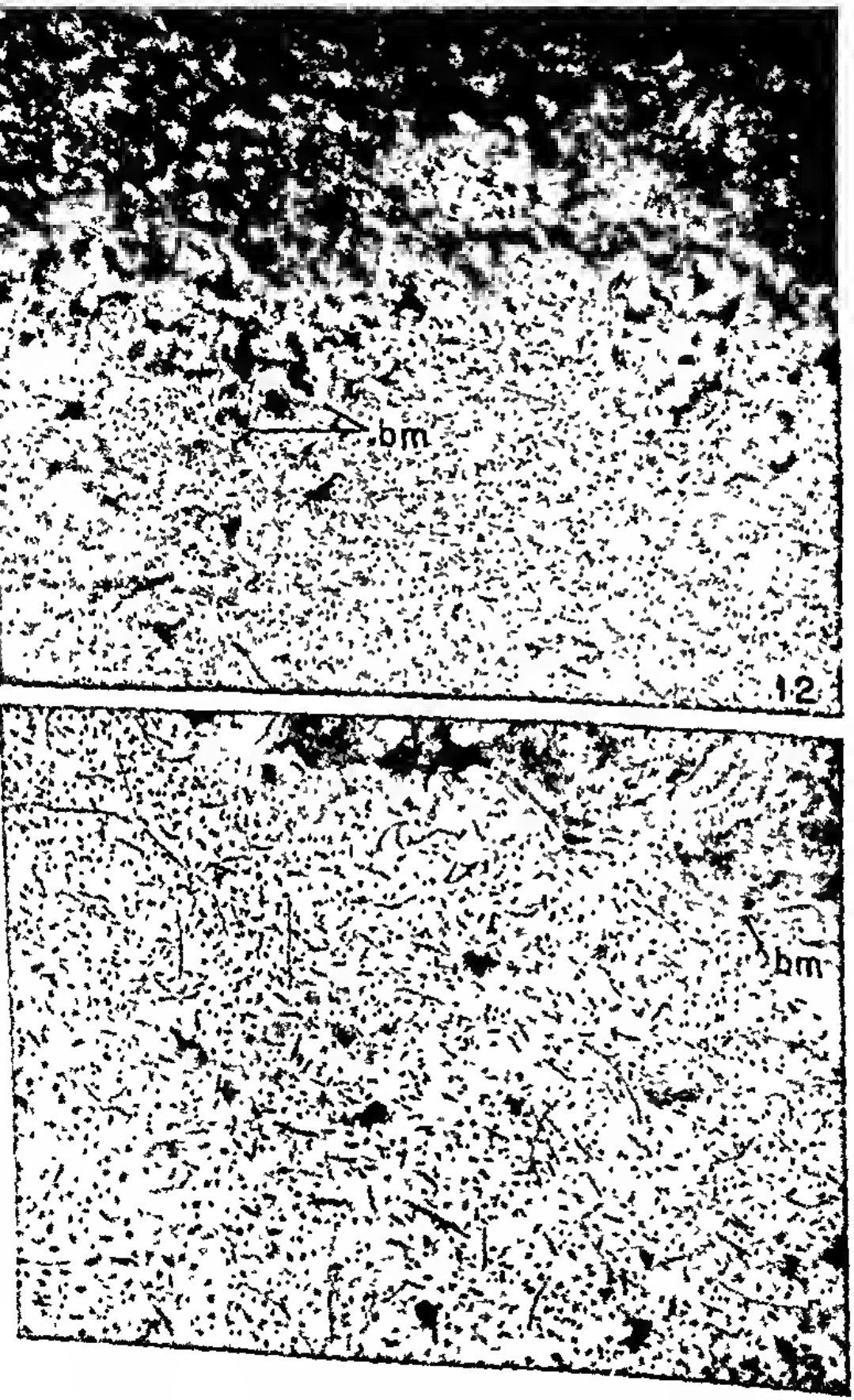
bm
12
bm

FIG. 14. Here a stroma-type cell is found about 2 μ from the epithelium (ep). Around it are collagen fibrils of different widths. Magnification: × 10,090.

FIG. 15. Many collagen fibrils in the peripheral cornea are stellate in cross section. When cut tangentially, they often appear to be twisted bundles of finer fibrils (arrows). Magnification: × 23,900.

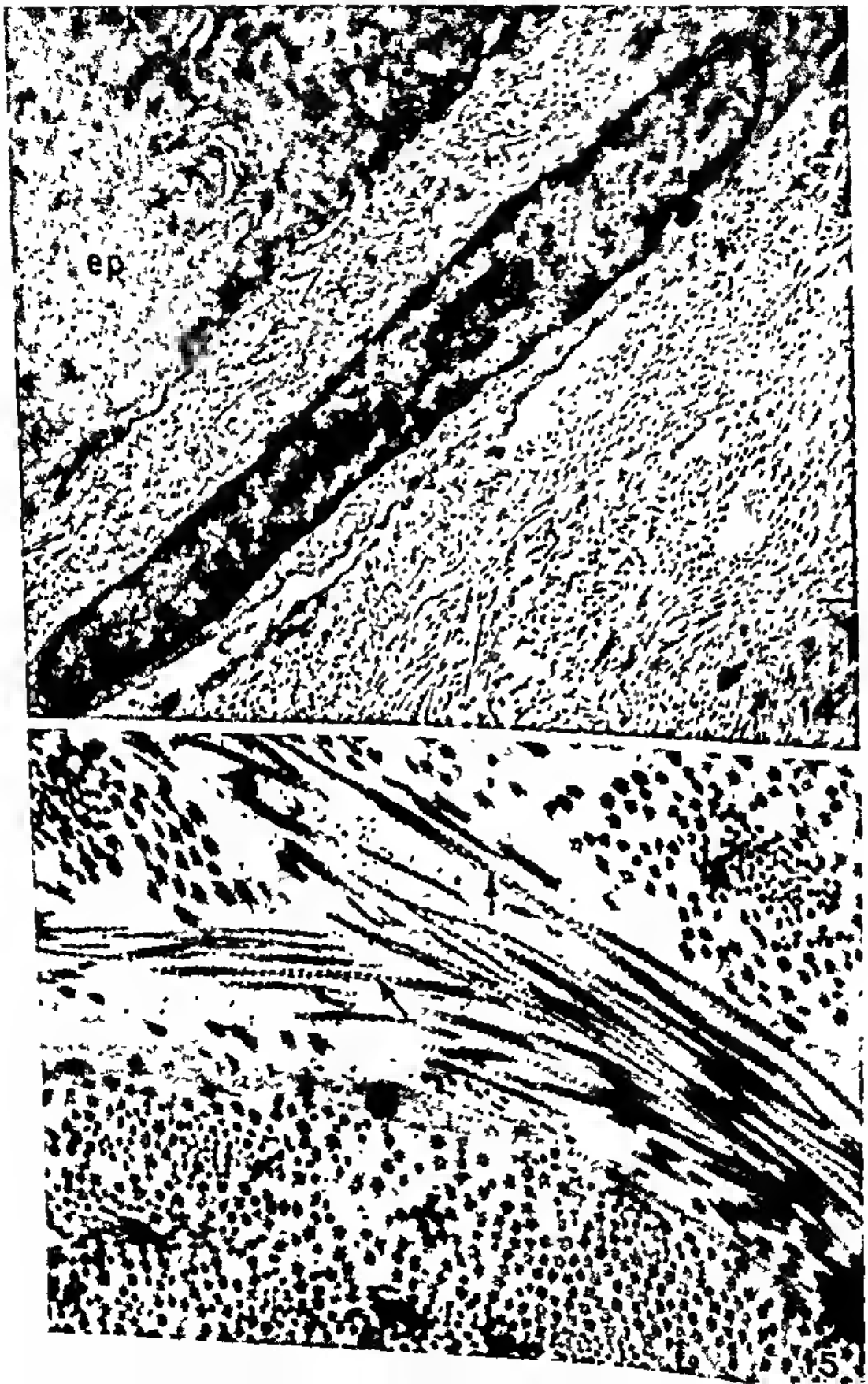
ep
14
15

FIG. 16. Peripheral stroma, showing a mast cell with composite inclusions and thin processes (p). Magnification: × 15,260.

FIG. 17. Peripheral Descemet's membrane, showing a Hassal-Henle body, or wart, with its network of tunnels (t), in which can be seen processes (p) of the endothelial cells, granules (g), long-spacing fibers (ls), and smooth fibrils (sf). Magnification: × 6610.


p
p
16
sf
ls
g
f
p

FIG. 18. Descemet's membrane showing its first split, with collagen fibrils between the two layers (Dm). Long-spacing fibers appear to be outside the tunnels as well as in them. Magnification: × 6650.

FIG. 19. Region above Descemet's membrane, showing typical stroma collagen fibrils (c) and the small-diameter fibrils (sdf) with a period like that of collagen. When sectioned obliquely or transversely, bundles of these fibrils may appear amorphous, particularly when viewed at low magnification. Magnification: × 20,850.

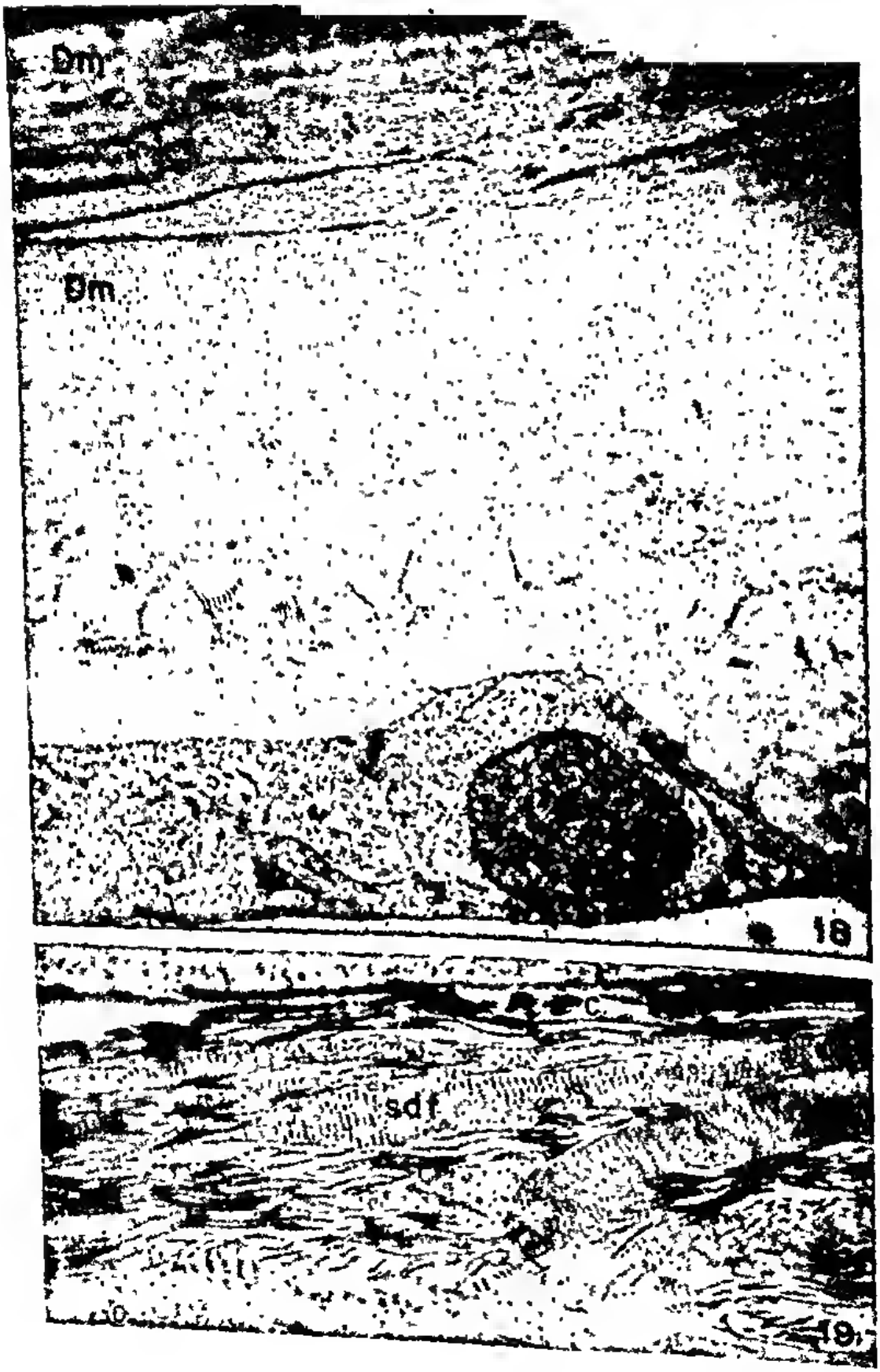
Dm
Dm
18
sdf
19

FIG. 20. Trabecular fiber in cross section, showing peripheral endothelial layer (en), Descemet's membrane layer (Dm), collagen fibrils of large diameter (c_1), stroma-type collagen fibrils of smaller and uniform diameters (c_2), small-diameter fibrils (sdf), and long-spacing fibrils (ls). Magnification: × 6790.

FIG. 21. Trabecular sheet, showing endothelial cells (en), layers of Descemet's membrane (Dm), collagen fibrils (c), and small-diameter fibrils (sdf), nucleus (n). Magnification: × 11,240.

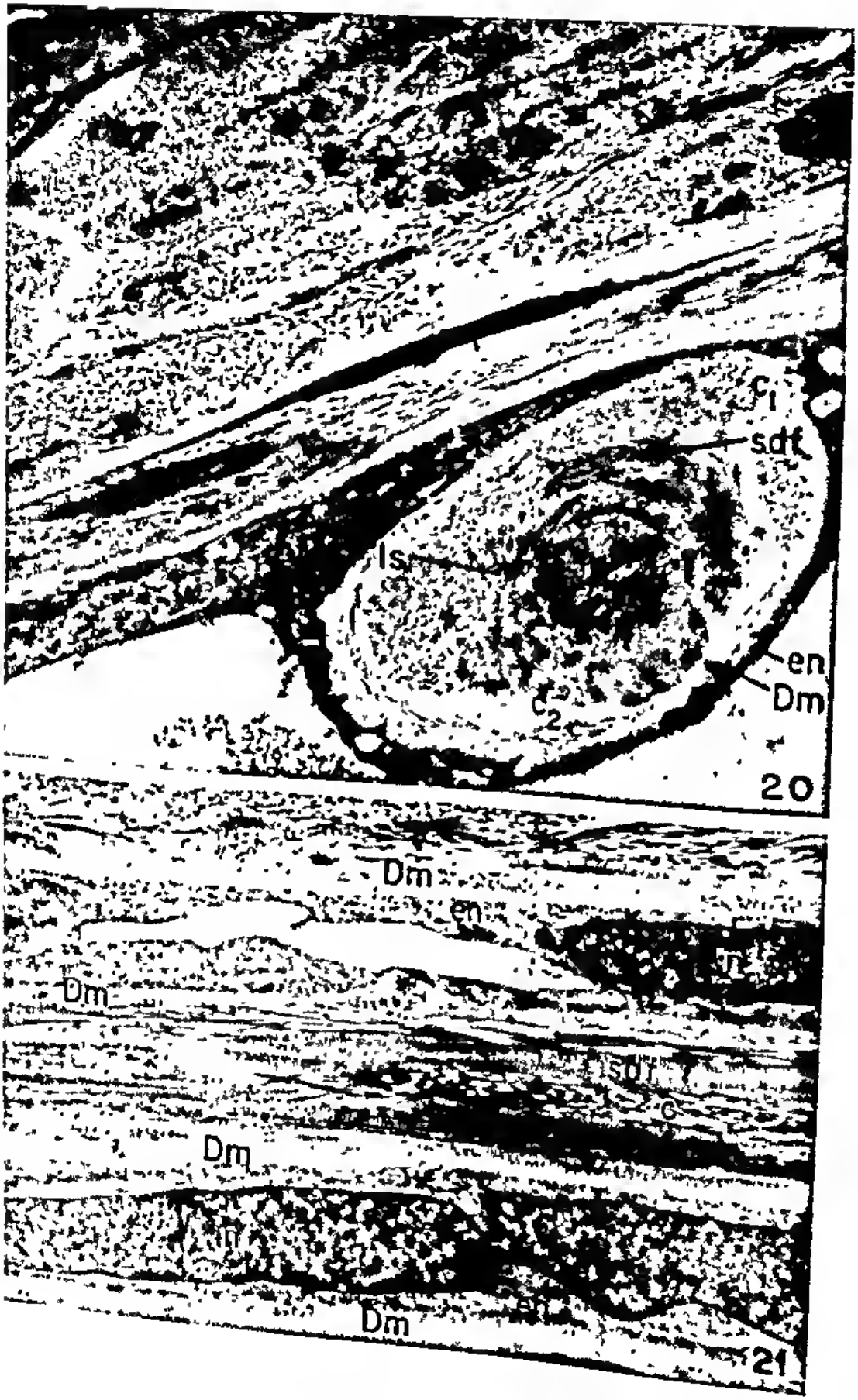
C_1
sdf
ls
en
Dm
C_2
20
Dm
en
Dm
sdf
C
Dm
Dm
21

collagen is oriented in layers which follow, for the most part, the plane of the cornea; and even the stroma cells are flat and scarcely disturb the contours of the lamellae within which they lie. The collagen fibrils of the stroma appear to be uniform in diameter and to be regularly spaced; the actual variations in both fibril diameter and distance between fibrils appear small when the entire structure is viewed. It should be remembered, too, that both sizes of structures and their spatial relationships were probably altered to some extent by the preparative procedures employed, and the living cornea may be an even more highly ordered tissue than it appears to be in these sections. Whether the other known protein and mucopolysaccharide components of the cornea are represented by the fine filaments or amorphous material seen between the collagen fibrils or whether they were completely extracted must be determined by further studies.

The fine structure of the central cornea gives the impression of stability, of activity just sufficient to maintain a state of equilibrium. Both the epithelial cells and the stroma cells are poor in endoplasmic reticulum and mitochondria, two cytoplasmic constituents associated with metabolic activity. Only the endothelium, which appears to be the main water pump of the cornea, has a high enough concentration of mitochondria to suggest that these cells are doing much more than just maintaining themselves.

In the limbus, by contrast, the picture is one of apparent flux. New surfaces have been created by the irregularity of the inner surface of the epithelium and its basement membrane, by the tunnels within the Hassal-Henle bodies, by the processes of the endothelial cells, and by the separation of Descemet's membrane into layers. The collagen fibrils in the outer portion of the stroma look very different, with their greater spread of widths, looser packing, and irregularity of shape. Capillaries penetrate this region and wandering leucocytes and mast cells appear in the stroma. Here the nutrients needed by the cornea are delivered and passed on to the cells or diffused into the stroma. Although the changes described occur near the two surfaces of the limbus, and much of the deeper stroma appears indistinguishable from the stroma in the central cornea, they are nevertheless sufficient to destroy transparency in this region.

The invaginations of the endothelial cell membranes and the vesicles in the cytoplasm, around the Hassal-Henle bodies, suggest that pinocytosis may be one of the mechanisms used by these cells to regulate the hydration of the cornea. This function of the endothelium is attested by the fact that injury to this layer results in edema and clouding of the cornea. But if the endothelial cells appear to be draining the cornea by

pinocytosis, they also appear to be adding something to Descemet's membrane by way of the processes they extend into the Hassal-Henle bodies. In support of this hypothesis, it can be recalled that the copper-*complex* granules comprising the Kayser-Fleischer ring of Wilson's disease are deposited in this region of Descemet's membrane. The membrane could act as a barrier by forming *complexes with and thus* precipitating certain *substances* released within it.

The variety of fiber types found in the peripheral cornea, and in particular within Descemet's membrane, is of interest. While no direct evidence exists that any of them, other than the stroma fibrils and Descemet's membrane, are species of collagen, *it is possible* that they all are, and that this region provides an environment in which collagen can assume a number of different forms. Several long-spacing varieties of collagen have been prepared *in vitro* but, so far as is known, *only* the eye has been shown to contain *similar structures in vivo*. The limbus can be thought of as a *transitional* zone between cornea, trabecular region, and sclera. The sclera and cornea are known to differ both *quantitatively* and qualitatively with respect to their mucopolysaccharide content and to have collagen fibrils which look *distinctly* different. On the other hand, the collagens *precipitated* from extracts of cornea and sclera appear to be identical, implying that the collagen components of these two tissues are not basically different and suggesting that *the* mucopolysaccharides are involved in producing the differences observed. If this conjecture is valid, and mucopolysaccharides are instrumental in determining the configurations which collagen assumes, then a mixture of them could account for the *diversity* of fiber types observed in the limbus.

A further complication is introduced by the fact that a wound in the adult *central* cornea stimulates the deposition *of collagen* fibrils resembling those found in the limbus or in other adult tissues, i.e., of dissimilar diameters, suggesting that *both the scar* and the limbus are more mature than the central cornea *and that* conditions in the adult central cornea are different from those which existed there during histogenesis of the stroma. In other words, adult corneal stroma *collagen can be* considered to be embryonic only in a limited sense; *or*, perhaps, the formed *collagen fibrils* are still morphologically embryonic but the stroma cells have meanwhile matured until they are able to produce only an adult type of collagen when called upon to repair an injury.

The fragmentation of Descemet's membrane into thin layers which become incorporated *into the* trabecular meshwork recalls the assumption that Descemet's *membrane is the* basement membrane of the endothelium and suggests that the thin layers also act as basement membranes for

the increased numbers of cells needed to cover the new surfaces formed in the trabecular region. It suggests also that these cells are endothelial in origin.[3]

References

Fawcett, D. W. (1960). Personal communication.
Garron, L. K., and Feeney, M. L. (1959). *A.M.A. Arch. Ophthalmol.* **62**, 966-973.
Glauert, A. M., Rogers, G. E., and Glauert, R. H. (1956). *Nature* **178**, 803.
Ishida, T. (1958a). *Acta Soc. Ophthalmol. Japon.* **62**, 1324-1331.
Ishida, T. (1958b). *Acta Soc. Ophthalmol. Japon.* **62**, 2220-2227.
Jakus, M. A. (1954a). *Am. J. Ophthalmol.* **38**(1), Part II, 40-52.
Jakus, M. A. (1954b). *Acta XVII Concilium Ophthalmol.* pp. 461-464.
Jakus, M. A. (1956). *J. Biophys. Biochem. Cytol.* **2**(4), Suppl., 243-255.
Offret, G., and Haye, C. (1959). *Arch. ophthalmol. (Paris)* **19**, 126-159.
Teng, C. C., and Katzin, H. M. (1953). *Am. J. Ophthalmol.* **36**, 895-900.
Uzman, L. L., and Jakus, M. A. (1957). *Neurology* **7**, 341-355.

[3] The discussion for this article is combined with the discussion following the article by Drs. M. L. Feeney and L. K. Garron (page 378).

Descemet's Membrane in the Human Peripheral Cornea[1]

A Study by Light and Electron Microscopy

M. LYNETTE FEENEY AND LEVON K. GARRON

Francis I. Proctor Foundation for Research in Ophthalmology, University of California School of Medicine, San Francisco, California

Introduction

THE AREA AROUND the termination of Descemet's membrane is of considerable interest to histologists because it is a transitional zone marking the juncture of corneal with scleral stroma and Descemet's membrane with trabecular meshwork. This area also contains the anterior border ring (*Schwalbe's line*) which is an important landmark in clinical ophthalmology. Our interest in Descemet's membrane grew out of studies of the adjacent trabecular tissue.

Salzmann's (1912) description of the histochemical and morphologic qualities of Descemet's membrane is still accepted from the standpoint of light microscopy His descriptions of various structural details in this area seem surprisingly accurate in the light of present-day knowledge obtained through the help of the electron microscope. Jakus (1951, 1956) has made the most comprehensive study of Descemet's membrane in recent years, utilizing the electron microscope with thin sections of the membrane Her findings in a variety of species, including the human, suggest Descemet's membrane to be a highly organized and ordered structure composed essentially of collagen in a dense ground substance. Our examination of the peripheral portion of Descemet's membrane by electron microscopy showed some interesting morphologic variations from the classic findings reported by Jakus. The purpose of this paper is to report these findings

Methods and Materials

Two embedding and sectioning techniques were employed for the light microscopic studies: (1) portions of normal tissue containing peripheral Descemet's membrane were fixed in formalin, embedded in paraffin, and 4 to 5-μ sections were cut in each of three planes, meridional, tangential, and frontal, (2) blocks of peripheral cornea were excised from celloidin-embedded eyes, reblocked in paraffin, and 1-μ

[1] This investigation was supported by Public Health Service research grants numbers B-1229 and B-1782 from the National Institute of Neurological Diseases and Blindness, Public Health Service

sections were cut in the same planes on the Porter-Blum microtome. Special stains were applied to all sections, including periodic acid-Schiff, Weigert's elastic stain, aldehyde fuchsin, Mallory's trichrome stain, and a Gomori-Van Gieson stain.

For the electron microscope studies, seventeen human eyes were utilized. Fifteen of these eyes were enucleated for malignant melanomas of the choroid, and two were obtained from the eye bank 20 min after death. The enucleated eyes were fixed immediately in 1% osmic acid prepared according to the method of Caulfield (1957). The anterior chamber of most eyes was perfused with the fixative for 10 min prior to dissection; the remaining eyes were opened immediately and immersed in fixative. Thin strips of tissue were cut and placed in fresh cold fixative for from 2 to 4 hr. Rapid dehydration was accomplished by standard methods in ethyl alcohol. The tissues were embedded in a mixture of *n*-butylmethacrylate and methylmethacrylate in proportions 8:2 or 9:1 and polymerized with ultraviolet light. Sections were cut on the Porter-Blum microtome at 1-μ thickness and stained for examination by bright field and phase microscopy; also at 0.05 to 0.025 μ thickness for electron microscopy. Some thin sections were floated on a drop of a saturated solution of uranyl acetate to enhance the contrast in the electron beam (Watson, 1958). Thin sections were placed on Formvar-coated copper grids and examined with the RCA EMU 3E electron microscope.

Results

In the meridional plane, Descemet's membrane becomes slightly thicker approximately one-half millimeter from its termination, following

---

FIG. 1. Electron micrograph near the termination of Descemet's membrane of human peripheral cornea. Two Hassal-Henle warts (HH) protrude into the anterior chamber (AC) and are covered by endothelium (EN). Branching fissures (F) are seen in the innermost portion of the warts. A wedge of light density material containing collagen fibers (W) separates the warts. Scattered islands of 1000-Å banded material (CC) are seen throughout these warts. Magnification: × 2800.

FIG. 2. Electron micrograph of the termination of Descemet's membrane (DM). The membrane is composed of a homogeneous ground substance in which islands of 1000-Å banded material (CC) are randomly dispersed. The homogeneous component continues over into the first trabecular sheet as a thin layer comparable to the basement membrane (BM) seen in the mid-trabecular sheets. In this specimen the endothelium was lost in preparation. The banded component appears to "separate" from the homogeneous ground substance (CC′) of Descemet's and is found embedded in a light density matrix. The collagen bundle (C) may be part of Schwalbe's line or the core of a trabecular sheet. Magnification: × 6500.

FIG. 2A. An island of 1000-Å banded material embedded in the dense homogeneous ground substance of Descemet's membrane. Magnification: × 28,000.

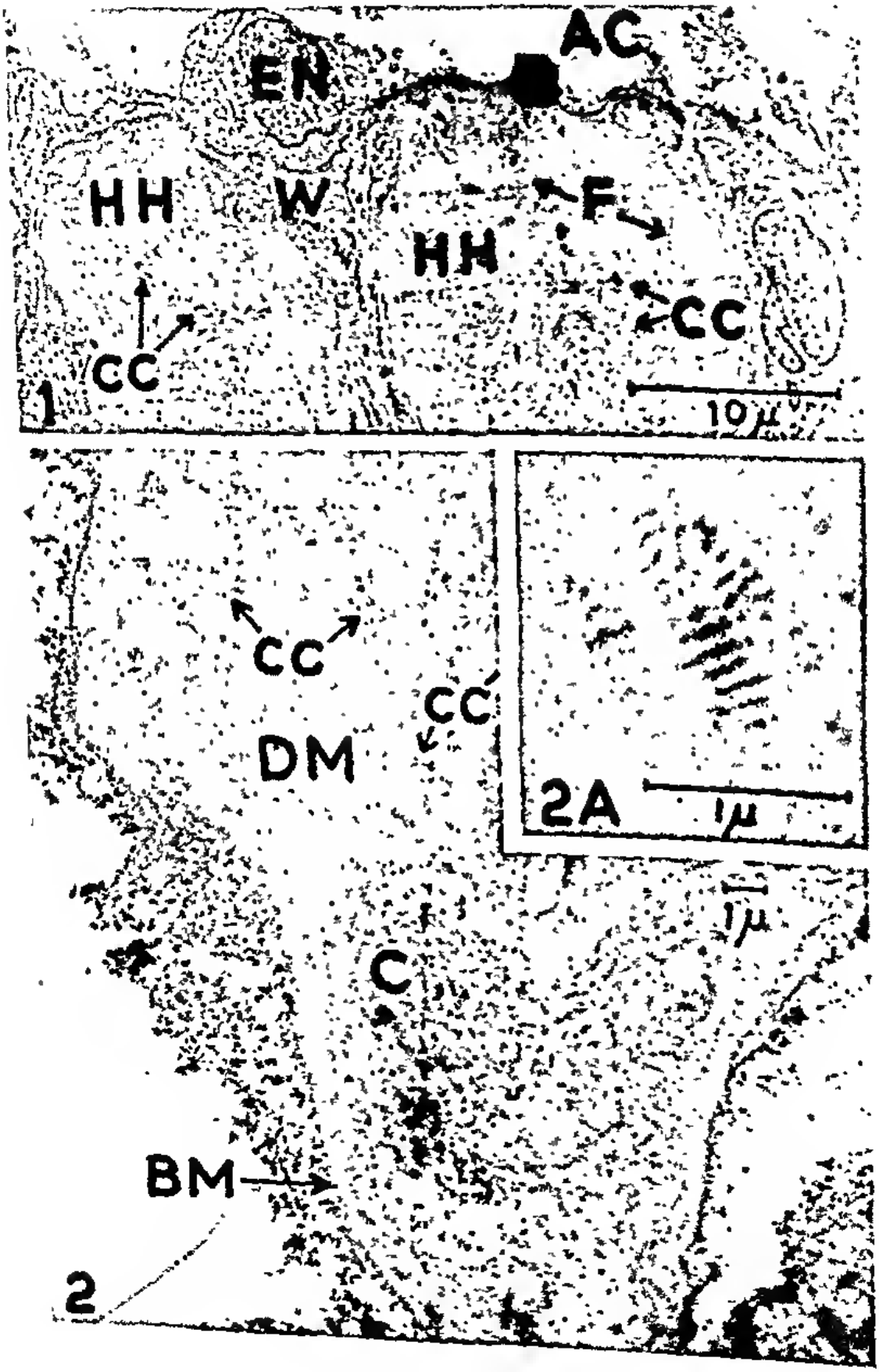
AC
EN
HH
W
F
HH
CC
CC
1
10 μ
CC
CC
DM
2A
1 μ
1 μ
C
BM
2

which it tapers, sometimes rather abruptly, and ends. The inner surface of the membrane is covered by corneal endothelium which is continuous with that of the trabeculae. The typical appearance of hexagonal shape and uniform size of the central endothelial cells, when viewed on the flat, is changed in the periphery. Here, the cells are irregular in size, shape, and arrangement, and they are interspersed by a varying number of nodular thickenings of the membrane which appear darker than neighboring cellular elements.

Electron micrographs of peripheral Descemet's membrane show it to have most of the characteristics of the membrane in the more central zone (Jakus, 1956). The ground substance, however, does show more variation in electron density (Fig. 1) and this is generally more intense in the inner half of the membrane. In addition, numerous small islands of banded material are seen in the ground substance of the membrane (Fig. 1, CC), increasing in number from the mid-periphery to the periphery. The two-dimensional profile of these islands is generally ellipsoidal or lenticular (Fig. 2A), and there is no special orientation of these structures within the membrane. The banded structures show a periodicity of approximately 1000 Å and resemble the material previously reported in the trabecular sheets (Garron *et al.*, 1958; Garron and Feeney, 1959). There is considerable variation in the amount of this banded material found in different eyes. In one eye, the periphery of Descemet's membrane showed large spiral formations (Fig. 3) composed of alternating layers of finely granular ground substance disposed between sheets of banded material and appearing somewhat like a coiled watchspring. In other eyes, only a scattering of these banded structures may be seen. As yet, we have not been able to relate their number or prominence to the age of the patient or any other factor.

As Descemet's membrane tapers down and apparently ends, electron micrographs show the continuation of a thin basement membrane beneath the endothelium toward the trabecular sheets (Fig. 2, BM). This basement membrane shows the same electron density as the ground substance of Descemet's membrane and apparently is a true continuation

---

FIG. 3. Electron micrograph of a spiral formation in peripheral Descemet's membrane. Layers of 1000-Å banded material are separated by a granular ground substance. Magnification: × 11,000.

FIG. 4. Electron micrograph of a meridional section near the termination of Descemet's membrane. Schwalbe's line (SL) is seen as a flattened bundle of collagen fibers cut on cross section. Numerous islands of 1000-Å banded material (CC) are scattered in the light density matrix between Descemet's membrane and Schwalbe's line. Endothelium (EN). Magnification: × 3000.


3
1μ

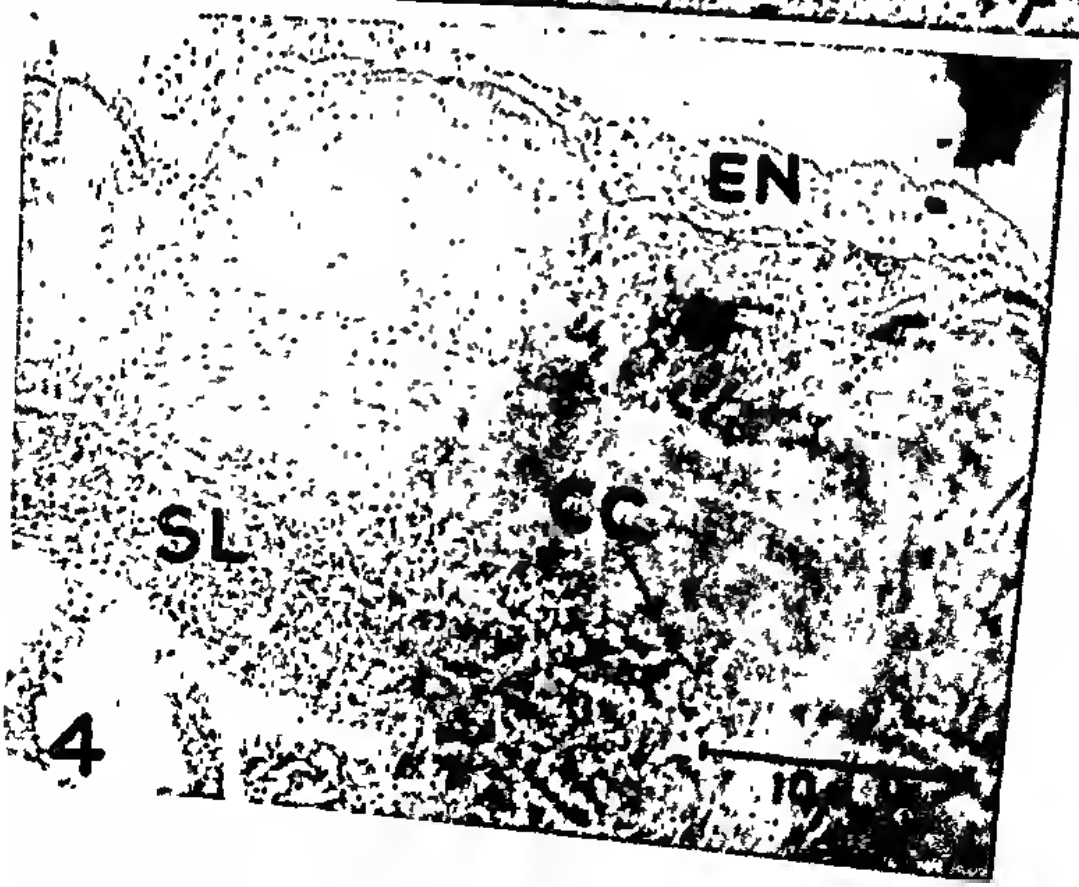
EN
SL
C
4
1μ

of it. It is also at this point that the 1000-Å banded material in Descemet's membrane appears in a light density matrix to participate in the formation of the trabecular sheets (Fig. 2, CC'). In a few eyes, wedges of collagen are seen in a light density matrix extending beneath the endothelium and between terminal outcroppings of Descemet's membrane (Fig. 1, Fig. 4, W). This collagen manifests similarities to that seen in the corneal stroma but may, however, originate from the nearby fibers of Schwalbe's line. The corneoscleral trabecular meshwork is thus formed out of the structures in this region, as noted above. In addition, a concentration of cells is noted in corneal stroma immediately external to the termination of Descemet's membrane. These cell appear to mark the "anterior root" of the trabeculae, and fibers extending back toward the trabecular meshwork assume all of the characteristics of the trabecular sheets.

The anterior border ring or Schwalbe's line is formed at the junction of the corneal stroma and the termination of Descemet's membrane (Fig. 4). In histologic sections it seldom is prominent in the normal eye and often cannot be distinguished from other fiber bundles of the corneal stroma. In meridional sections it appears as a bundle of fibers cut on cross section which indicates its course is circumferential about the eye. Schwalbe's line may be represented by a distinct rounded bundle of fibers or may be made up of small flat collagenous bundles disposed circularly around the termination of the membrane. In some eyes, Descemet's membrane appears to split to surround or embed these fibers. It is often difficult to identify Schwalbe's fibers in electron micrographs since they vary so little in appearance from the neighboring corneal stromal fibers. One can only presume their identification on the basis of location, orientation, and by the recognition of adjacent structures.

Hassal-Henle Warts

The most fascinating structures in this area are a number of dome-shaped protrusions from the periphery of Descemet's membrane into the

---

FIG. 5. Electron micrograph of portions of two Hassal-Henle warts showing the corneal endothelial cells filling the depression between warts. Numerous branching fissures (F) are seen in both warts. There are islands of 1000-Å banded material (CC) in the warts. Endothelium (EN). Magnification: × 7000.

FIG. 6. Photomicrograph of Descemet's membrane (DM) showing numerous fissures (F) into Deseemet's membrane and Hassal-Henle warts. S, stroma; EN, endothelium. Magnification: × 1400.

FIG. 6A. Photomicrograph of a flat section through the wart region of Descemet's membrane. Many branched fissures are seen ramifying across the Hassal-Henle warts. Magnification: × 500.

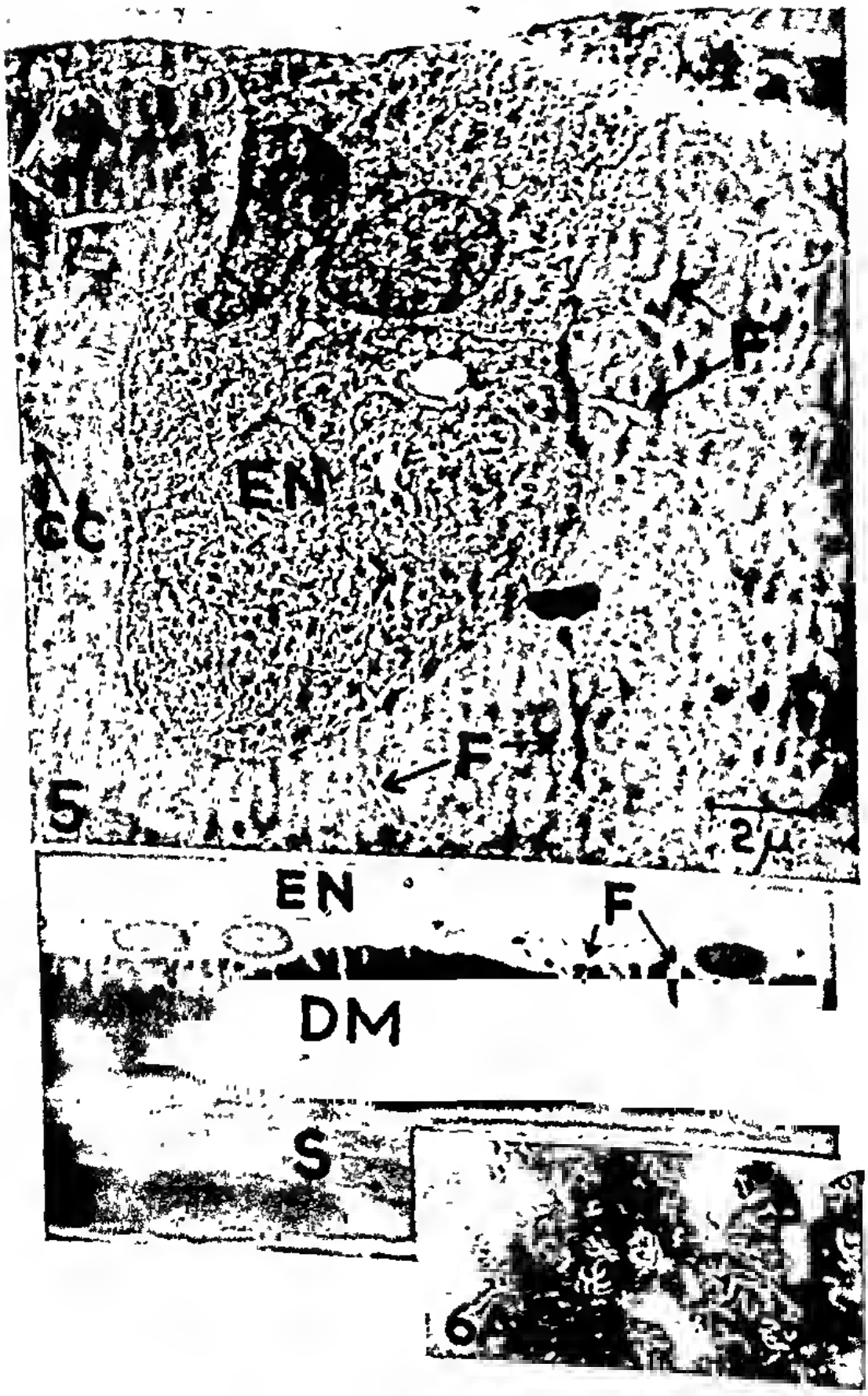
EN
C
F
F
5
2μ
EN
F
DM
S
6

anterior chamber, the Hassal-Henle warts. These warts have been known to histologists for over one hundred years. Originally, they were described by Hassal (1851) and Henle (1866). They rarely are found in the eyes of infants and children, but are seen with increasing frequency after age twenty. The breadth of this peripheral wart zone increases with age as does the thickness of the whole membrane.

These warts stain like Descemet's membrane and appear to be thickenings of the membrane. Endothelial cells fill the depressions between the warts and cover their surface, but the cytoplasm is thin over their crests (Fig. 5). Light microscopic studies of the Hassal-Henle warts failed to reveal details of their structure until improved techniques permitted sectioning this tissue at 1 μ. These sections through the wart region of Descemet's membrane show numerous fissures and channels across the crests and into the substance of the warts (Fig. 6). Tangential sections show numerous irregularly branched figures in this area (Fig. 6A), which represent the appearance of the fissures when viewed in this plane.

Electron micrographs show the mouths of the fissures to lie beneath the endothelial cell. In "normal" cornea adjacent to the wart-zone, it is possible to demonstrate simple clefts and indentations in the membrane, probably representing an early phase of wart formation. In most eyes the more peripheral the section the more elaborate the fissures become. Occasional eyes have peripheral warts without visible fissures. The fissures of some warts may penetrate the entire thickness of the membrane to the corneal stroma. The endothelial cell membrane is intact across the mouth of some fissures and in others it appears to be discontinuous. The fissures contain round or oval bodies approximately 0.1 μ

FIG. 7. Electron micrograph of a flat section across the head of a Hassal-Henle wart. Cytoplasm of the corneal endothelial cells (EN) surrounds the head of the wart. The fissures (F) in the wart contain dense staining granules and fibers. The cell membrane (CM) stretches across orifice of the fissure. The homogeneous substance of Descemet's membrane (DM) comprises the wart structure. Magnification: × 10,000.

FIG. 8. Electron micrograph of a wart from a case of cornea guttata. Absence of endothelium may be real or artifactual. Linear zone of dense particles (P) are seen in mid-Descemet's membrane. Magnification: × 4800.

FIG. 8A. Shows dense particles in higher power. Magnification: × 17,000.

FIG. 8B. Photomicrograph of transverse section of central cornea guttata. Magnification: × 400.

FIG. 8C. Photomicrograph of tangential section through warts of cornea guttata. Magnification: × 400.

Compare Figs. 8B and C with Figs. 6 and 6A.


F
DM
7
8C
2μ
P
8A
8B
8

in diameter in which no characteristic structural features have so far been resolved, and irregular strands of amorphous and fibrous material are also seen (Fig. 7).

Cornea Guttata

Cornea guttata is a bilateral corneal disease involving the central corneal endothelium and Descemet's membrane. The lesions of this disease have in the past been considered to be similar to Hassal-Henle warts since wartlike excrescences are found on Descemet's membrane. The disease is progressive with a spread of these lesions toward the periphery of the cornea.

We have studied tissue from one case of cornea guttata and have found the typical morphology of the lesion to differ considerably from that of Hassal-Henle warts. The warts of this guttata case are mushroomlike projections having flat tops (Fig. 8). They contain no fissures and apparently are not covered by endothelium. Between the warts, Descemet's membrane is covered by endothelium which appears to be poorly preserved in spite of rapid and careful fixation. A thin layer of dispersed, dense, fine particles is seen in the mid-zone of Descemet's membrane (Fig. 8, P). The layer is about 0.5 μ wide and the individual particles vary from 50 to 400 Å in diameter. Additional particles are scattered randomly on the stromal half of the membrane. The identity and nature of these particles are unknown.

Comments

From a morphologic study it appears that Descemet's membrane is composed of at least two substances: a homogeneous component or ground substance, and a component with 1000-Å periodicity. In the peripheral zone the banded component is present in higher concentration than in the central cornea, or at least its separation from the homogeneous component is more pronounced. The 1000-Å banded material continues over into the sheets of the trabecular meshwork, but the dense homogeneous component does not stay in close association with it. The islands of banded material in the trabeculae are found to be embedded in a homogeneous matrix whose density is much less than that seen in Descemet's membrane. It appears that the homogeneous component of Descemet's membrane continues over into the trabecular meshwork as a mere basement membrane to the endothelial cells. This confirms the observation of Salzmann (1912), that the trabecular sheets are "entirely covered over by a continuation of Descemet's membrane." This con-

tinuation, however, proceeds as two separate layers rather than an attenuation of the total membrane.

The transitional zone between Descemet's membrane and trabecular meshwork is the junction between a moving and a nonmoving part of the eye. It has been shown that contraction of the ciliary muscles exerts a pull on the scleral spur and the trabecular sheets resulting in a change in shape of the trabecular openings (Flocks and Zweng, 1957; Fortin, 1931; Heine, 1899). Because of the structural continuity between Descemet's membrane and the meshwork, it is possible that the peripheral region of Descemet's membrane receives some of the stresses of this motion. It is also possible that this stress stimulates the endothelial cells to produce the warts of Hassal-Henle. Whether the fissures in the warts result from a degenerative change or are the result of mechanical traction via the trabecular sheets are subjects for further study. Since the warts occur only in the extreme periphery of the membrane and the wart-bearing zone broadens with age, their occurrence suggests both a mechanical and degenerative pathogenesis.

References

Caulfield, J. B. (1957). Effects of varying the vehicle for OsO_4 in tissue fixation. *J. Biophys. Biochem. Cytol.* **3**, 827-829.

Flocks, M., and Zweng, H. C. (1957). Studies on the mode of action of pilocarpine on aqueous flow. *Am. J. Ophthalmol.* **44**, II, 360.

Fortin, E. P. (1931). Contributions to solutions of problems of glaucoma. *Arch. oftalmol., Buenos Aires* **6**, 219.

Garron, L. K., and Feeney, M. L. (1959). Electron microscopic studies of the human eye. II. Study of the trabeculae by light and electron microscopy. *A.M.A. Arch. Ophthalmol.* **62**, 966-973.

Garron, L. K., Feeney, M. L., Hogan, M. J., and McEwen, W. K. (1958). Electron microscopic studies of the human eye. I. Preliminary investigations of the trabeculae. *Am. J. Ophthalmol.* **46**, II, 27-35.

Hassal, A. H. (1851). "Microscopic Anatomy of the Human Body in Health and Disease," p. 513. Pratt, Woodford and Co., New York.

Heine, L. (1899). The anatomy of the accommodation of the eye. *Arch. Ophthalmol. Graefe's* **49**, 1.

Henle, J. (1886). "Handbuch der systematischen Anatomie des Menschen," Vol. II. Braunschweig, F. Viewig und Sohn.

Jakus, M. A. (1954). Studies on the cornea: I. The fine structure of the rat cornea. *Am. J. Ophthalmol.* **38**(II), 40-52.

Jakus, M. A. (1956). Studies on the cornea. II. The fine structure of Descemet's membrane. *J. Biophys. Biochem. Cytol.* **2**, Suppl., 243-252.

Salzmann, M. (1912). "The Anatomy and Histology of the Human Eyeball" (Translation by E. V. L. Brown). University of Chicago Press, Chicago, Illinois.

Watson, M. L. (1958). Staining of tissue sections for electron microscopy with heavy metals. *J. Biophys. Biochem. Cytol.* **4**, 475-478.

Discussion of Articles by Dr. Jakus and by Drs. Feeney and Garron

Dr. Tousimis [Armed Forces Institute of Pathology, Washington, D. C.]: Are the granules or inclusions you showed in the mast cells similar to any other pigment granules in the eye?

Dr. Jakus [Retina Foundation, Boston, Mass.]: They seem to be different. Each of these large inclusions is an aggregate of smaller, multilayered structures which vary from round to cylindrical in shape. Sections of randomly oriented, laminated cylinders would show such an apparent diversity in form.

Dr. Cogan [Harvard University, Boston, Mass.]: Did Dr. Jakus see a resemblance between that which she found in the Kayser-Fleischer ring and that which Miss Feeney has just reported?

Dr. Jakus: Yes, I see a great resemblance between the two, although the types of inclusions appear to be different. The ones in the Kayser-Fleischer ring are clusters of smaller particles, whereas the ones Miss Feeney showed look more like globules.

Miss Feeney [University of California, San Francisco, California]: They were between 50 and 400 Å in size, whereas those of Dr. Jakus were about 50 to 100 Å, I believe.

Dr. Jakus: The unit particles observed were about 50 Å in diameter but they aggregated to form clusters up to a third of a micron in diameter.

Dr. Cogan: Were they not in rows?

Dr. Jakus: Yes, there were two layers, the first about 0.6 micron and the second about 2 microns from the endothelial surface.

Dr. Carpenter [Tufts University, Boston, Mass.]: I understand from these two papers that the classical concept described by Salzmann is confirmed, that is, that Descemet's membrane extends out into the trabeculae, forming the basement membrane underlying the endothelium there. In addition, the so-called elastic component of the trabeculae is also derived from Descemet's membrane and that it is this portion which contains the fibers with 1000-Å periodicity. Is this correct?

Dr. Garron [University of California, San Francisco, California]: Yes, from our observations I would say that you have interpreted our findings correctly. Recently, we had the opportunity to perfuse the anterior chambers of two eyes with saccharated iron for 15 minutes prior to enucleation. In the trabecular tissue we were impressed by the finding that the fibers of the central collagen core and the fibers with 1000-Å periodicity were obscured by an overabundance of "ground substance."

Dr. Carpenter: Do you think the ground substance was increased by swelling?

Dr. Garron: No, it was our impression that the saccharated iron "fixed" the ground substance normally present in this location and prevented it from being washed away. Dr. Becker suggested that we try this some time ago. Holmberg has reported his findings with this technique using the eyes of monkeys.

Dr. Carpenter: Do you mean that after washing out the eye with the saccharated iron solution the extension of Descemet's membrane was more apparent?

Dr. Garron: Descemet's membrane seems to be continuous with the basement membrane of the endothelial cells covering the trabecular meshwork, whereas the 1000-Å banded material, which was also in Descemet's membrane, seems to be separate and continuous with the homogeneous matrix of the trabeculae. Each trabecular sheet, of course, has a collagen core which in turn seems to be continuous with the collagen of the substantia propria of the cornea.

Dr. Carpenter: Do the protoplasmic extensions of the endothelial cells enter

possibility that the type of mucopolysaccharides present in the cornea might be responsible for the diameter of the fibrils, or perhaps for their type of periodic spacing. Is it possible that the distance between adjacent fibrils, which is important in Dr. Maurice's hypothesis of transparency, might also be a function of the type of mucoid present? Is there a change in the regularity of fibril arrangement as you move peripherally to the edge of the cornea?

Dr. Jakus: The peripheral corneal fibrils do appear to be less regularly spaced than do the central ones, and mucopolysaccharides could very well be involved in the determination of interfibrillar distance as well as fibrillar diameter.

Chairman Becker: Dr. Jakus, have you examined the owl cornea? The owl has, according to Dr. Balazs, a high concentration of mucoid in the anterior chamber.

Dr. Jakus: The endothelial cells of the owl cornea contain large numbers of mitochondria and they have very irregular lateral surfaces which form complicated interdigitating processes.

The Use of Permeability Studies in the Investigation of Submicroscopic Structure

D. M. MAURICE

Ophthalmological Research Unit, Medical Research Council, Institute of Ophthalmology, London, England

Introduction

THE ELECTRON MICROSCOPE has enabled us to obtain a detailed view of submicroscopic morphology that was inconceivable with classic techniques However, since this method necessarily requires the use of dried sections, supplementary means must be used to relate the structures that can be seen to their condition in the living tissue. The study of diffusion and permeability is, in a sense, complementary to electron microscopy. The latter gives us the outlines of the denser structural elements in the dry tissue, the former provides us with information about the size of the spaces between these structures and the nature of the material filling them in the fresh tissue, but tells little about their shape.

The use of diffusional studies will be described in two situations in the cornea—the stroma and the endothelium. This tissue is particularly suitable because of its accessibility, regularity of structure, and freedom from blood vessels. These studies are not complete but are intended to illustrate the possibilities of the method.

Stroma

The stroma is made up of about 20% by weight of collagen and a further 5% of other organic material, principally mucopolysaccharide. The collagen is shown by the electron microscope to be divided into long uniform fibrils of about 250 Å diameter, which lie parallel to one another in bundles (Jakus, 1954, Schwarz, 1953). Calculation on this basis shows that the axes of the fibrils will be 600 Å apart on the average (Maurice, 1957). If the fibrils in their natural state were so swollen that their refractive index was equal to that of the ground substance surrounding them, the transparency of the tissue would be explained. If this explanation were correct, calculation shows that the fibrils would almost touch one another Whether this occurs, or whether spaces remain between the hydrated fibrils of the fresh stroma, cannot be decided on the basis of electron micrographs, it should be resolvable on the basis of its diffusional properties.

Methods

The technique employed for estimating the rate of diffusion was to introduce a very small depot of the concentrated test substance into the stroma and to allow it to spread along the tissue, that is, in the plane of the cornea. After a determined interval the distribution of the substance was measured and its diffusion constant calculated. Rabbits were used as the experimental animal throughout.

The experiment may be carried out *in vivo* or *in vitro*. The former method is convenient for slowly diffusing substances such as proteins and fluorescein, for the difficulty of maintaining the cornea in its normal state of hydration for protracted periods is automatically solved. This technique and its results will be described elsewhere (Maurice, 1960a, b).

For small ions, which rapidly leave the cornea across the endothelium in the living eye, the *in vitro* method is more applicable. The epithelium is scraped off and a strip of cornea of uniform width, 2–3 mm, is cut from limbus to limbus. The strip is quickly blotted, weighed, and covered with oil. The solution of the test substance is then applied with a thin glass rod to the center of the strip so that it forms a narrow band less than 1 mm wide across it. The strip is maintained at a constant temperature for a suitable period and then freed from oil, reweighed, and quickly dried.

The distribution of the test substance along the strip should have the form

$$C_a e^{-x^2/4Dt}$$

where t is the time of diffusion, D its diffusion constant in the stroma, C_a its final concentration at the point of application, and x the distance along the strip from this point. In the case of radioactive substances it is easier to measure the quantity

$$\int C_a e^{-x^2/4Dt} dx$$

by gradually exposing the strip to a Geiger Müller counter from under a mask. This function gives a linear relationship against x when plotted on probability graph paper. Three radioactive ions were tested in this way, Cs^{134}, Br^{82}, and Na^{24}. A typical result, illustrated in Fig. 1, shows that the diffusion law is quite strictly obeyed.

It would be interesting to compare the rate of diffusion along the stroma, obtained by this method, with the rate of diffusion of the same substances across the stroma. Adequate methods have not been developed for the latter measurement. If the epithelium and endothelium remain in position they introduce a large resistance and an indeterminate delay into the movement of substances from one side of the cornea to the

other. If these layers are removed, on the other hand, the stroma will absorb water rapidly over its bare surfaces.

Measurements of electrical resistance, however, can be made in a matter of seconds, before an appreciable amount of swelling can take place. It is possible, therefore, to compare the resistance to ionic movement in the two directions in the stroma by comparing the corresponding electrical conductivities.

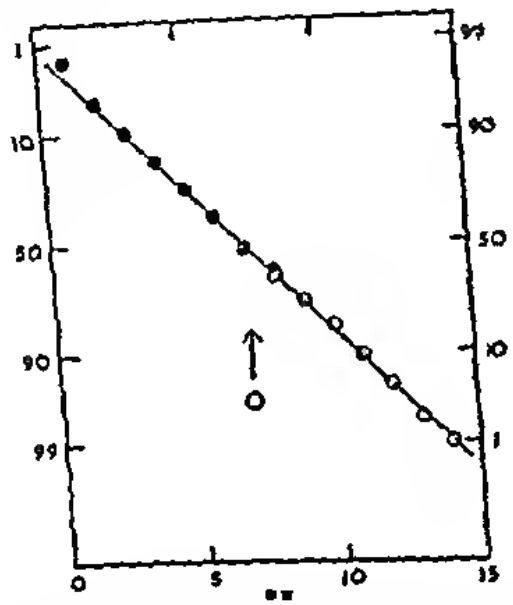

FIG 1 Diffusion of Cs^{134} along corneal strip. Abscissa: distance along strip. O represents point of application of Cs^{134} at start of experiment. Ordinate: percentage of total radioactivity beyond given point on strip after 1 hr 12 min at 37°C. Different circles correspond to exposing each end of strip in turn from under radiopaque mask. Slope of curve leads to diffusion coefficient of 1.07×10^{-5} cm²/sec.

To determine the resistance along the stroma, a cornea was excised, its cellular layers were removed, and a strip was cut about 4 mm wide with parallel sides The strip was quickly weighed, and placed between saline soaked wicks in an electrical circuit passing a measured DC current (Fig 2). The potential gradient along the strip was then rapidly determined by touching it at measured distances along its length with a fine wire connected to a high-impedance millivoltmeter. The resistance of unit length of the strip can be calculated from the electrical observations, and its cross-sectional area from its weight, length, and specific gravity The conductivity of the tissue then follows immediately.

The transverse conductivity was measured also under DC conditions with the arrangement shown in Fig 3. Current was passed between two electrodes each consisting of a 5-mm diameter tube containing agar gel. The electrodes dipped below a solution of 0 9% saline which also saturated the gel. Finely drawn polyethylene tubes pass centrally down

each electrode as far as its face. They are filled with saline and make connection through calomel-KCl junctions with a millivoltmeter. If the electrodes are sufficiently close, the current density in the gap between their faces is constant, and the voltage recorded is proportional to the resistance within this gap. By moving the electrodes relatively to one

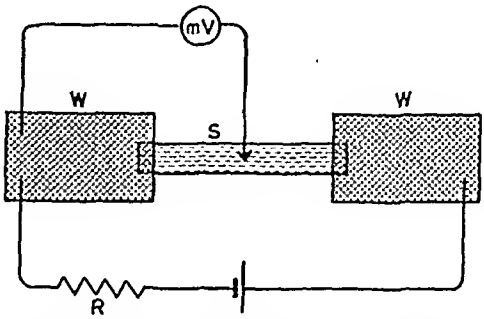

FIG. 2. Electrical circuit for measuring electrical conductivity in plane of stroma. Ends of strip of stroma, S, lie under saline wicks, W. Voltage gradient along stroma measured with fine wire probe and compared with voltage across resistance, R.

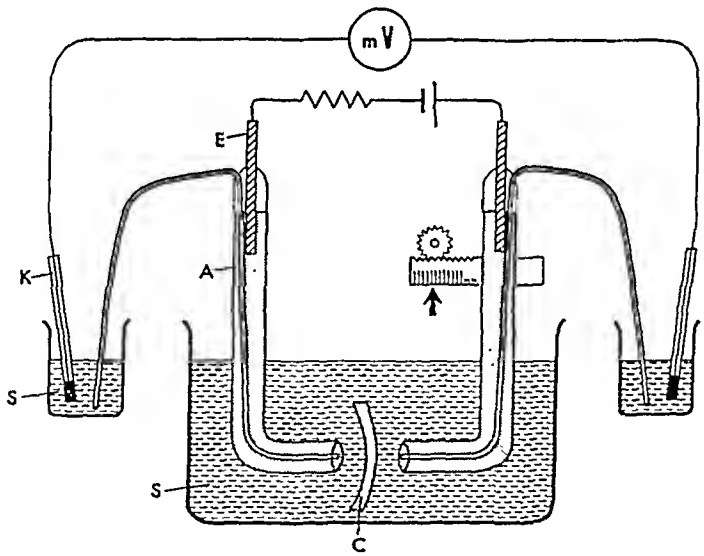

FIG. 3. Electrical circuit for measuring conductivity across stroma. Current is passed via silver-silver chloride electrodes, E, through saline in agar gel, A. Very fine polyethylene tubes record potential across gap through calomel-KCl electrode system, K. S, saline; C, cornea.

another, the voltage developed across unit thickness of saline was measured. The stroma, with both cellular layers rubbed off, was then introduced into the gap and an increase of potential was recorded which could be expressed as the equivalent of a certain thickness, t, of saline. Previously, the thickness of the stroma, d, was measured optically (Maur-

ice and Giardini, 1951). The conductivity of the stroma is equal to $d/(t + d)$ times that of the saline.

Descemet's membrane can be peeled off from the stroma, and the proportion of the increase of thickness attributable to it determined by introducing it alone into the gap.

Results

Table I summarizes the rates of diffusion found for the radioactive ions. Values obtained previously for fluorescein and proteins are also shown. The figures are expressed as the obstruction of the stroma to diffusion—how many times slower the substance diffuses in the stroma than it does in free solution.

TABLE I

Obstruction of Corneal Stroma to Diffusion of Various Substances

Substance	Diameter, Å	Obstruction[a]	
Cs^{134}	~ 5	2.3 ± 0.05	S.E.M.[e]
Br^{82}	~ 5	2.7 ± 0.1	
Na^{24}	6 6	1.9 ± 0.2	
Fluorescein[b]	11	5	
Albumin[c]	74	8	
Mammalian[d] hemoglobin	64	10	
Planorbis[d] hemoglobin	185	∞	

[a] Obstruction defined as how many times diffusion in tissue is slower than diffusion in saline at the same temperature. Small ionic diameters and diffusion coefficients from Robinson and Stokes (1959)

[b] Maurice (1960a)

[c] Maurice (1960b).

[d] Maurice (1957)

[e] S E M = standard error of the mean

The electrical conductivity of the tissue in the plane of the cornea ranged from 2 3 to 2 6 times less than that of aqueous humor in four experiments The transverse conductivity was 2.4 to 2.6 times less in four experiments The resistance of Descemet's membrane could not be determined very accurately by this technique, but it represented only a few per cent of that of the stroma

Discussion

These results do not support the hypothesis that diffusion in the stroma takes place in canals of microscopic size, as has been suggested from time to time If this were true two results might be expected. First, visible particles should be capable of movement. In fact, the largest

molecules which can diffuse are between 60 and 185 Å in diameter. Secondly, since the canals are described as running along the stroma, the movement of solutes should be easier in this direction than across it. However, the electrical measurements show the resistance to be equal in the two directions; furthermore, if the diffusion of a small drop of concentrated hemoglobin introduced into the cornea is observed, it appears to diffuse uniformly in all directions (Maurice, 1957).

Diffusion must, therefore, take place through the substance of the stroma, and solutes must pass through or around the collagen fibrils. Since it is inconceivable that proteins could diffuse through the fibrils, the gaps between them must be at least 70 Å across. The very hydrated structure necessitated by a uniform refractive index throughout the stroma is, therefore, not possible. This is in accordance with the double refracting properties of the stroma which suggest a collagen hydration of only 60% (Maurice, 1957).

This conclusion is supported by the similar values for the conductivity along and across the tissue. If the collagen occupied a fraction f of the total volume, the electrical resistance in a direction perpendicular to the axis of a bundle of fibrils will be approximately $1 + f$ times that in a direction parallel to the axis (Rayleigh, 1892). Across the cornea the current flows through every bundle of fibrils perpendicularly to their axes; along the cornea the current flows in part parallel. It follows that if the difference between the electrical resistance in the two directions is not large, the fraction f also cannot be large.

A further reason for supposing that the collagen is not very hydrated, lies in a comparison of the obstruction the tissue offers to electrical current and the diffusion of small ions. The concentration of diffusible ions in the ground substance cannot be very different from that in the aqueous humor, since they are in osmotic equilibrium across the endothelium. If a large fraction of the volume of the tissue is occupied by fibrils, the number of ions available for carrying current is proportionally decreased. The apparent obstruction of the tissue to current should be greater than that to the diffusion of ions by the same fraction. The similarity of the figures for the obstruction in the two cases suggests that the volume fraction, f, of the fibrils should not be very much greater than its unhydrated value, 15%.

The obstruction diminishes with the size of the diffusing particles as they are more able to circumvent the fibrils. The obstruction offered to the small ions could represent either the remaining hindrance of the fibrils or the resistance offered by the ground substance. The latter alternative is the more probable, since Woodin (1952) has shown that the mucoid extracted from the cornea has an appreciable viscosity.

It is a matter of speculation why planorbis hemoglobin, diameter 185 A, does not diffuse in this structure where the gaps between the fibrils should be about 300 A. Possibly, each fibril is surrounded by a sheath of mucopolysaccharide, as suggested by the micrographs of Van den Hooff (1952), which is sufficiently dense to prevent the movement of proteins but allows free passage to small ions.

Endothelium

The resistance to the movement of dissolved substances across the posterior surface of the cornea could lie in either Descemet's membrane or the endothelium. Measurements of the electrical resistance of these layers show that Descemet's membrane forms a negligible fraction of the barrier, at least as far as small ions are concerned.

The interpretation of measurements of the permeability of a cellular barrier in terms of simple diffusion must be carried out with great caution, because of the possibility that cellular activity may modify it. However, there is evidence in the literature that many substances of small ionic diameter penetrate the endothelial barrier at about the same rate, suggesting that they diffuse through pores (Maurice, 1953). On the assumption that the pores are the intercellular spaces, it was calculated that the separation between adjoining cells walls was about 60 A. Electron micrographs have since shown an intercellular spacing of about 80 A. This correspondence has encouraged a closer examination of the subject.

Methods

The method used previously (Maurice, 1951, 1955) in determining the endothelial permeability was used in about half the experiments. The test substance in a solution isotonic to 0.9% saline, was allowed to come into contact with the epithelial surface for 10 min and the amount penetrating into the cornea and aqueous humor determined. Alternatively, identical experiments were carried out except that the epithelium was scraped off and the test solution was applied directly to the bare stroma. The values obtained for the endothelial permeability by the two methods were in fair agreement.

One group of experiments was carried out with anesthetized animals or with eyes enucleated and maintained at body temperature. In an equal number the animal was killed and the eye and the test solution were refrigerated beforehand, in the majority of cases the temperature of the solution was found to be from 2 to 8°C during the course of the experiment.

The radioactive ions Na^{24}, Br^{82}, and Cs^{134} were used as test sub-

stances in most of the experiments. Some experiments with inert Sr, assayed by flame photometry, were carried out with epithelium-free eyes only.

In order to calculate the permeability of the endothelium to each ion it is necessary to know the ratio of its concentration in the aqueous humor and corneal stroma tissue fluid when it is in equilibrium between them. The determination of this ratio by allowing the ion to attain full equilibrium in the living animal, permitted a considerable interference from the cellular elements of the stroma. Accordingly, the ratio was derived from a comparison of the concentrations of the ions in the stroma in those experiments where it was directly in contact with the test solution, the value of the ratio for Na assumed previously (Maurice, 1951) being accepted. In fact, these ratios did not appear to differ markedly for the four ions tested.

Results

The permeability of the endothelium to the various ions in the cold is shown in Table II. The results are expressed in terms of the obstruction of the membrane—how many times less permeable it is to the ion than a layer of saline of the same thickness, 5 μ, at the same temperature.

TABLE II

Obstruction of Corneal Endothelium to Ions Around 5°C

Ion	Diameter, Å	Obstruction[a]
Cs^{134}	~ 5	1800
Br^{82}	~ 5	1900
Na^{24}	6.6	1700
Sr	8.4	3300

[a] Obstruction defined as how many times less permeable the cell layer is to the ion than a layer of saline of the same thickness at the same temperature.

These mean values are each subject to a standard error of the order of 100, and so the figures for the first three ions are not significantly different. A constant value for the obstruction for all ions below a certain size would be expected for a system of relatively large uncharged pores. The results suggest, therefore, that at this temperature, where cellular activity is suppressed, the endothelium acts as a simple porous membrane. The higher obstruction to Sr may be a result either of its larger size or of its double charge.

The results of the experiments at body temperature are summarized in Table III.

A value obtained in a separate series of experiments for radioactive albumin is also included. Its very slow passage, together with the value for the obstruction of Sr, seem to rule out the possibility of pinocytosis

as a controlling factor in the movement. This mechanism would give a lower obstruction for the larger ions than for the smaller.

The obstruction encountered by the small ions is similar to that in the cold, suggesting that at least the greater part of their movement across the endothelium under normal conditions is by way of the same system of pores. Since it is unlikely that movement through cell walls could be through pores, it would appear that only a small fraction of the transfer of these ions across the barrier can take place through the cells. It must be concluded that the movement of ions across the membrane is predominantly by diffusion through the intercellular spaces.

TABLE III

OBSTRUCTION OF CORNEAL ENDOTHELIUM TO IONS AT 37°C

Ion	*Diameter, A*	*Obstruction*
Cs^{134}	~5	2100
Br^{82}	~5	2100
Na^{24}	6.6	1700
Sr	8.4	2600
Albumin	74	⩾ 250,000

The endothelial cells are hexagonal in outline and are each about 20 μ across. The total intercellular boundary length is, then, 1000 cm for each square centimeter of endothelial area. The width of the intercellular spaces can then be calculated, adopting the same assumptions that were made previously (Maurice, 1953)—that the spaces are uniformly wide over the cell interfaces, that diffusion within them is unrestricted, and that they run perpendicularly across the cell layer. Taking an average figure for the obstruction, 2000, the value for the intercellular spacing becomes 50 A.

A few electron micrographs are available (Garron *et al.*, 1959) in which the endothelial cell boundaries may be clearly seen. The cell boundary membranes appear to be very similar in form and dimensions to those described in the ciliary epithelium by Holmberg (1957), for example, accordingly, the intercellular spaces will be uniform and about 80 A in width. However, these same sections and those of Speakman (1959) show that the cell interfaces do not run perpendicularly across the layer but pursue a wavy course. The total length of the boundary varies from 6 to 13 μ at the five interfaces where measurements are possible, but it is not evident to what extent these figures may have been influenced by shrinkage of the specimen or obliquity of the section. Clearly, however, the estimate of 50 A derived from the permeability data will have to be increased to account for the longer diffusion path; if, for example, the true average length of the cell boundaries was 8 μ

the calculated spacing would be 80 Å, in agreement with its electron micrograph appearance.

Speakman (1959) was able to demonstrate the course of the cell boundaries, under the light microscope, by bringing polychrome methylene blue into contact with the inner face of the cornea in fresh, flat specimens. The dye penetrates only between the cells and, as it does so, develops a characteristic wavy outline. Toward Descemet's membrane the boundaries appear to evolve into a very complicated pattern which spreads over the entire anterior surface of the cells. This probably corresponds to what, under the electron microscope, appears to be interdigitation between the cells at this level. Special care may be needed, therefore, in obtaining a correct estimate of the diffusion path length.

We may conclude provisionally from these studies that the intercellular material of the endothelium does not restrict the diffusion of small ions to any great extent. A more detailed study of the tissue under the electron microscope is necessary, however, before this can be firmly established.

Summary

Measurements on the diffusion rates of various substances in the corneal stroma show (1) that diffusion takes place in the substance of the tissue and not in canals; (2) its constituent collagen fibrils are in a relatively low state of hydration. Both these conclusions are supported by a comparison of the electrical conductivity of the stroma across and in the plane of the tissue which shows it is equal in the two directions.

The permeability of the corneal endothelium to various ions in the cold and at body temperature has been determined. The results indicate that the greater part of the ionic movement is by diffusion through the intercellular spaces. Calculation of the size of these spaces from the values of the permeability gives a value comparable to that shown by the electron microscope. This agreement suggests that diffusion in the intercellular spaces is not restricted.

Acknowledgments

The experiments on endothelial permeability were carried out in collaboration with Dr. C. B. Taylor. The strontium determinations were kindly performed by Dr. D. F. Cole. Technical assistance was provided by Mrs. S. Beech and Miss G. Gregg-Smith.

References

Garron, L. K., Hogan, M. J., McEwen, W. K., Feeney, M. L., and Esperson, J. (1959). *A.M.A. Arch. Ophthalmol.* **61**, 647.

Holmberg, A. S. (1957). "Ultrastructural Changes in the Ciliary Epithelium Following Inhibition of Secretion of Aqueous Humour in the Rabbit Eye." Thesis. Karolinska Institutet, Stockholm.

Jakus, M. A. (1954). *Am. J. Ophthalmol.* **38**, 40.
Maurice, D. M (1951). *J. Physiol. (London)* **112**, 367.
Maurice, D. M. (1953). *Ophthal. Lit. (London)* **7**, 3.
Maurice, D. M. (1955). *Brit. J. Ophthalmol.* **39**, 463.
Maurice, D. M. (1957). *J. Physiol (London)* **136**, 263.
Maurice, D. M. (1960a). *Am. J. Ophthal.* **49**, 1011.
Maurice, D. M. (1960b). In preparation.
Maurice, D. M., and Giardini, A. A. (1951). *Brit. J. Ophthalmol.* **35**, 169.
Rayleigh, Lord (1892). *Phil. Mag.* [5] **34**, 481.
Robinson, R. A., and Stokes, R. H (1959). "Electrolyte Solutions," 2nd ed. Academic Press, New York.
Schwarz, W. (1953). *Z. Zellforsch* **38**, 26.
Speakman, J. S. (1959). *A.M.A. Arch. Ophthalmol.* **62**, 882.
Van den Hooff, A (1952). *Proc. Koninkl. Ned. Akad. Wetenschap.* **55**, 628.
Woodin, A. M (1952). *Biochem. J.* **51**, 319.

Discussion

Dr Tousimis [Armed Forces Institute of Pathology, Washington, D. C.]: We have measured the space between the endothelial cells of the human and monkey cornea. It is about 100 Å.

Dr. Maurice [London, England]. Have you measured their tortuosity or the distance from the anterior chamber to the Descemet's membrane side of the cell?

Dr Tousimis: The cells interdigitate in a three-dimensional pattern so that it would be difficult to carry out such measurements

Dr Kinsey [Kresge Eye Institute, Detroit, Michigan]: Why doesn't the current short-circuit around the cornea?

Dr. Maurice. The electrodes are in plastic tubes 5 mm in diameter and placed about 1 mm apart The current goes straight across from one side to the other because the stromal resistance is very low

Dr. Herrmann [Storrs, Conn.]: Several investigators have suggested that water bound by proteins may assume a state similar to ice Would you say that this may be the case with the water in the corneal stroma?

Dr Maurice Certainly, I can't rule that out. Some of the water may be bound in the fibrils and there is also probably a mucopolysaccharide sheath around them which might obstruct the movement of ions. I don't think the greater part of the water would be bound in that way.

Dr Coulombre [Yale University, New Haven, Conn.]: Would your calculations be altered if the space between the cells were filled with an aqueous fluid or with a mucoid?

Dr Maurice I am assuming the space to be filled with aqueous fluid but if it were a viscous mucoid the figures would be altered in proportion to the difference in viscosity If the viscosity were twice that of water, the spaces would have to be twice as large.

Electron Microscopical Studies of the Fibrillogenesis in the Human Cornea

W. SCHWARZ

Forschungsabteilung für Elektronenmikroskopie der Freien Universität Berlin, Berlin, Germany

Introduction

THE *SUBSTANTIA PROPRIA* of the cornea consists of an avascular connective tissue which is transparent to light. In addition, this tissue is of such a firm consistency that under conditions of a normal intraocular pressure the curvature of the cornea remains unchanged which is of importance to the refraction of light. The fibers form flat bundles whose small edges join to make up lamellae. The lamellae contain the usual two components of the intercellular substance of connective tissue, i.e., fibrils and cement substance (van den Hooff, 1952, 1957; Schwarz, 1952, 1953a, 1957) The fibrils are thin and have in a dried state a thickness averaging 290 Å and vary from 250 to 330 Å. This thickness has been reached already in a fetus of 8.5 cm in length and does not change any more (Schwarz, 1953b). The fibrils are closely packed and parallel within the lamellae (Jakus, 1955). The cement substance is abundant and keeps the fibrils together in the fibers, the fibers in flat bundles, and finally the bundles in lamellae. It is firmly attached to the fibrils, not easily removable, and contains acid mucopolysaccharides such as chondroitin, chondroitinsulfate A, and keratosulfate. Fifty per cent of the mucopolysaccharides is keratosulfate (Meyer *et al.*, 1957).

The formation of this connective tissue has to be subdivided into fibrillogenesis (formation of fibrils) and *cementogenesis* (production of cement substance) Most investigations dealing with the formation of connective tissue describe fibrillogenesis only. All investigators claim the fibroblasts to be involved in the production of fibrils. There are great differences in opinion, as to whether the fibrils of a certain thickness and period are formed within the cell or only their precursors which then form the fibrils outside the cell. Many investigations were made. But the results are diverse [Gieseking, 1959 (chick embryo dermis), Fitton-Jackson, 1956 (avian tendon), Fitton-Jackson, 1957 (bone in embryonic fowl), Kajikawa *et al*, 1959 (skin of mice); Knese and Knoop, 1958 (bone in embryonic rat), Nemetschek, 1958 (rat tail tendon); Policard *et al*, 1957 (silicotic granuloma); Porter and Pappas, 1959 (chick embryo dermis), Schwarz, 1959 (embryonic aorta); Schwarz and Merker,

1958 (embryonic lung); Wassermann and Kubota, 1956 (tendon of chick embryo)]. Kajikawa, Nemetschek, Policard, Porter, and Schwarz hold the opinion that only the precursors of the fibrils are formed intracellularly whereas the formation of the fibrils takes place extracellularly. Porter considers the cellular surface to be an important factor in this process. Gieseking and Wassermann, on the other hand, claim that the fibrils develop to a certain stage within the cell and then protrude from the cell by the breakdown of the outer layer of the cellular protoplasm (Gieseking). Jackson and Knese assume that an intra- and extracellular formation of fibrils exists. According to Gieseking, Knese, Porter, and Schwarz the endoplasmic reticulum is involved in the intracellular synthesis of collagen. The production of cement substance is disregarded my most authors. Schwarz considers the endoplasmic reticulum to be the site of production of the cement substance. Both fibrillogenesis and cementogenesis take place simultaneously within the cornea. All types of connective tissue in the fetus possess first a high percentage of cement substance. While this portion undergoes an involution with further development, a high percentage of it remains preserved within the cornea up to old age. This fact should be kept in mind when considering the physical qualities of the cornea.

Material and Methods

The cornea of fetuses, 6, 8, and 20 cm in length, have been investigated by means of electron microscopy. The specimens were fixed and embedded according to the method of Palade and Fitton-Jackson. The sections were made with Porter-Blum and Sjöstrand microtomes. The sections were stained with a 1% solution of uranyl acetate or PTA (phosphotungstic acid). All micrographs were taken with a Zeiss electron microscope (Type EM 8/II) at 40 kv.

Key to lettering on Plates I to IV.

cf = fibrils	N = nucleus
cs = circumnuclear space	n = nerve
er = endoplasmic reticulum	Pg = Palade granules
M = mitochondrion	sg = small granules
mv = microvesicles	c = cisterna

PLATE I

Section through the cornea of a human fetus, 6 cm in length. At the lower left corner is a portion of a nerve. In the center is a fibroblast with nucleus and narrow endoplasmic reticulum. At the right are some processes of fibroblasts with narrow endoplasmic reticulum. Between the processes there are collagen fibrils, single and in bundles. Magnification: × 20,000.


cf
er
N
cf
M
M
n

Results

Within the substantia propria of the cornea of a human fetus 6 cm in length, there is already an intercellular substance which consists of fibrils and cementing substance. The corneal cells are flat cells with long processes which run in all directions and are in contact with the neighboring cells. The nucleus is oval or spherical in shape depending on the plane of the section (Plate I). The surface membrane of the cell varies between 120 and 160 Å. At some sites it makes a sharp turn. If this is the case, the cellular surface membrane runs back into the interior of the cell in an archlike fashion and there forms a sac which opens outward (Plate II). Only a few mitochondria possessing few and mostly short cristae are present in the protoplasm. The endoplasmic reticulum of the corneal cells is a widely branching system of hollow spaces, varying in shape in different cells. Some portions of the reticulum are narrow (Plate I), others are ballooned (Plate III). In addition, there are cells which have only a narrow reticulum, others whose reticulum is ballooned. Sometimes the ballooning is of such a degree that the term "cisternae" would be appropriate. Some processes of the cytoplasm and cristae protrude into these already light microscopically visible intracellular spaces (Plate III). The borderline between this system of hollow space and the cytoplasm of the cell is formed by a membrane 80 Å in thickness. In the outer surface of these membranes there are in the cytoplasm Palade granules 180 Å in size. Their distribution is regular at many sites, the distance between two Palade granules being 140 Å. However, a portion of these granules is smaller and 60 to 80 Å in size. In flat sections of the membranes their distribution appears especially regular. They are mostly arranged in parallel rows. At other sites the granules show a filigreelike pattern (Plate IV). At some sites the membranes are not studded with Palade granules. Instead there are microvesicles on the membranes measuring 240 to 320 Å in diameter. The wall of these

---

PLATE II

Top: section through a process of a fibroblast. Narrow endoplasmic reticulum. Some membranes of the er are cut obliquely. The membranes are studded with Palade granules, small granules (60–80 Å) in filigreelike patterns, and microvesicles. Magnification: × 30,000. (For key to lettering, see legend to Plate I.)

Inset at lower right: the cell surface of a fibroblast. The endoplasmic reticulum contacts the cell surface (arrows). Collagen fibrils are near the cell surface. Magnification: × 25,000.

Inset at lower left: a section of the process of a fibroblast. The membrane of the cell surface runs back into the interior of the cell (arrow). Magnification: × 25,000.

vesicles is smooth and 40 Å in thickness. Those and larger vesicles occur separated from the membranes in the cytoplasm. The content of the endoplasmic reticulum in the narrow portions is homogeneous and granular. In the wide portions the content is granular. However, these granules are frequently arranged in chains (Plate III). In some sections the outer nuclear membrane is continuous with the membranes of the endoplasmic reticulum. In those cases the space of the endoplasmic reticulum is continuous with the space between the nuclear membranes. This becomes distinctly visible in cells which possess a balooned endoplasmic reticulum. In a few cells large vacuoles are found measuring 0.8 μ in diameter. Their wall is formed by a membrane which is smooth and 100 Å in thickness. Their interior may be empty or contain granular material.

All visible fibrils lie outside of the cells. Their thickness varies from 120 to 200 Å. The longitudionally sectioned fibrils show a period varying from 400 to 500 Å. At the cellular surface or close to the cells the fibrils occur as single fibers or in bundles. In addition, bundles of fibrils are located distant from the cells which run in various directions. Fetuses 8 and 20 cm in length present a different picture. The fibrils are more densely packed in bundles. The bundles are already arranged in lamellae, but the hexagonal packing is not as yet seen. The cells are in several layers parallel to the corneal surface. The cellular processes are very thin and their number has decreased. The endoplasmic reticulum in the cells is well developed, but the ballooning of the reticulum is no longer observed.

Discussion

The formation of the fibrils takes place outside of the cells. The protoplasm itself contains no fibrils, although there is a great number of fibrils between the cells and the cornea is in a very active state of fibrillogenesis. The first visible fibrils occur singly at the cellular surface. Here they are apparently loosely bundled and shifted into the intercellular space. These findings are in agreement with the opinion of Porter (Porter and Pappas, 1959). The cellular membrane, therefore, is

---

PLATE III

A fibroblast with ballooned endoplasmic reticulum and a "cisterna" with a process of the cytoplasm. The circumnuclear space is also ballooned at some places.

Inset at upper right: a section through the ballooned endoplasmic reticulum containing granules and chains of granules as precursors of the ground substance of the connective tissue of the cornea. Magnification: × 30,000. (For key to lettering, see legend to Plate I.)

important for the formation and direction of the fibrils. The endoplasmic reticulum is undoubtedly involved in fibrillogenesis. In favor of this view are the pronounced development and the alternating content of

the tubular system. However, no cross-striated fibrils are found in the endoplasmic reticulum, rather their content is homogeneous and granular. This content is at some sites so increased that vacuoles become visible with the light microscope. Probably they are identical with the vacuoles in fibroblasts which may be seen with the light microscope and have been described by Fitton-Jackson (1955), and Gersh and Catchpole (1949). They are PAS-positive and contain, besides protein, polysaccharides which can be discharged outward. It is difficult to obtain a true picture on the dynamics of those processes. However, the saclike indentations of the outer cellular membrane may represent the momentary picture of a depletion of the vacuoles or the endoplasmic reticulum, respectively.

The Palade granules with their content of ribonucleic acid (RNA) are associated with the protein syntheses (Siekevitz, 1959). The large amount of Palade granules found at the membranes of the endoplasmic reticulum in the fibroblasts of the fetal cornea is an expression of a highly efficient protein synthesis. In fact, a large amount of protein is produced by the fibroblasts of the fetal cornea, i.e., the collagen for the fibrils of the substantia propria. This amount is considerable, since the collagen in the cornea amounts to 78.5% later on (Schaeffer and Murray, 1950). Therefore the pronounced endoplasmic reticulum with its richness in Palade granules is in good agreement with the intense formation of collagen. The synthesis of collagen up to a stage unknown so far is a prerequisite for the formation of collagenous fibrils. Besides the typical Palade granules (160 Å), there are additional smaller ones (60–80 Å) which are grouped in special patterns at the membranes. Their significance is not understood as yet. For the osteoblasts in the embryonic fowl similar structures have been described by Fitton-Jackson (1957). Instead of the Palade granules small vesicles on the membranes of the endoplasmic reticulum are visible at times. Membranes without Palade granules are termed smooth membranes which together with adjacent macro- and microvesicles have been designated as the Golgi zone (Dalton and Felix, 1956; Sjöstrand and Hanzon, 1954). A distinctly defined Golgi zone is still absent in the fibroblasts of the fetal cornea. However, in the fibroblasts of the fetal cornea there are membranes visible, which

---

PLATE IV

Top: a section of a fibroblast. Narrow endoplasmic reticulum, partly cut obliquely. The membranes are studded with Palade granules and microvesicles.

Bottom: a membrane of the endoplasmic reticulum cut nearly tangential. Small granules (60–80 Å) at the outside of the membrane are arranged in a filigreelike pattern. Magnification: × 30,000. (For key to lettering, see legend to Plate I.)

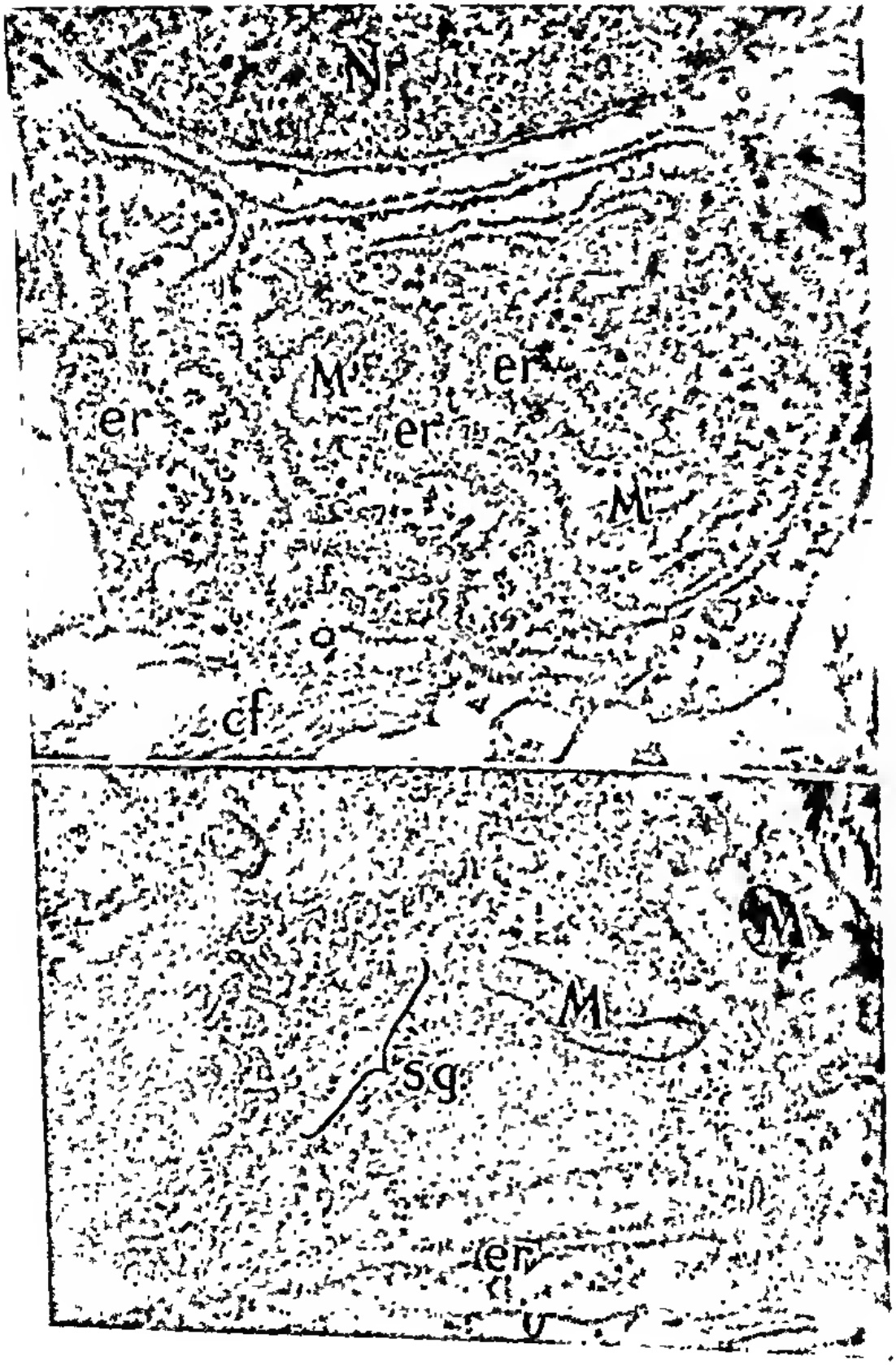
N
M
er
er
er
M
cf
M
M
sg
er

possess Palade granules and microvesicles as well, and belong therefore to the endoplasmic reticulum. The fetal corneal cell has no Golgi zone, which can be demonstrated light microscopically in the corneal cell of the adult organism. The components of a normal Golgi zone, the micro- and macrovesicles, are disseminated in the fetal corneal cell. Probably the microvesicles are involved in the production of the intercellular substance. The fibroblasts produce besides the collagen of the fibrils some other material which later forms the interfibrillar substance. This cementing substance contains various substances of which the mucopolysaccharides are the most important. The site of their origin is not as yet known. The microvesicles may produce these substances. They are not proteins and may, therefore, be formed independently of the Palade granules. These microvesicles resemble those which have been described for the pinocytotic processes. They would then be of importance in the transportation mechanism within the fibroblasts.

Summary

The cornea of the human fetuses 6, 8, and 20 cm in length have been investigated by electron microscopy. The cells form a network and possess a pronounced endoplasmic reticulum whose content is varied. The membranes of the reticulum are studded with Palade granules (160 Å), smaller granules (60–80 Å), and microvesicles. The reticulum contains a homogeneous and granular substance and is held responsible for the synthesis of collagen and the formation of the intercellular substance. The Palade granules, smaller granules, and the microvesicles may be involved in these synthetic processes. The content of the endoplasmic reticulum is discharged outward. This mechanism is not clear as yet. The fibrils are formed outside of the cell. The cellular surface is of importance for the formation and arrangement of the fibrils.

Acknowledgments

This investigation has been supported by grants of the "Deutsche Forschungsgemeinschaft," Germany. The author wishes to thank Dr. H. W. Boschann, Chefarzt der geburtshilfl., gynäkolog. Abt. am Rudolf-Virchow-Krh. and Prof. Dr. H. Lax, Chefarzt der Frauenklin. im Städt. Krh. Berlin-Moabit, for the supply of material.

References

Dalton, A. J., and Felix, M. D. (1956). *J. Biophys. Biochem. Cytol.* 2 (Suppl.), 79-84.
Fitton-Jackson, S. (1955). *Nature* **175**, 39-53.
Fitton-Jackson, S. (1956). *Proc. Roy. Soc.* **B144**, 556-572.
Fitton-Jackson, S. (1957). *Proc. Roy. Soc.* **B146**, 270-280.
Gersh, J., and Catchpole, H. R. (1949). *Am. J. Anat.* **85**, 457-521.

Gieseking, R. (1959). *Verhandl. deut. Ges. Pathol.* **43**, 56-60.
Jakus, M. A. (1955). *XVII Concilium Ophthalmol. Acta* **2**, 461.
Kajikawa, K., Tani, T., and Hirono, R. (1959). *Acta Pathol. Japon.* **9**, 61-80.
Knese, K.-H., and Knoop, A.-M. (1958). *Z. Zellforsch.* **48**, 455-478.
Meyer, K., Hoffmann, P., and Linker, A. (1957). *In* "Connective Tissue" (R. E. Tunbridge, ed.), pp. 86-96 Blackwell, Oxford.
Nemetschek, Th. (1958). *Z. Naturforsch.* **13b**, 225-234.
Policard, A., Collet, A., Prégermain, S., and Renet, C. (1957). *Bull. microscop. appl.* [2]**7**, 73-75.
Porter, K. R., and Pappas, G. D. (1959). *J. Biophys. Biochem. Cytol.* **5**, 153-166.
Schaeffer, A., and Murray, J. P. (1950). *A.M.A. Arch. Ophthalmol.* **44**, 833-841.
Schwarz, W. (1952). *Verhandl. Anat. Ges., Marburg, 1952*, pp 263-265.
Schwarz, W. (1953a). *Z. Zellforsch* **38**, 26-49
Schwarz, W. (1953b). *Z. Zellforsch.* **38**, 78-86.
Schwarz, W. (1957). *In* "Connective Tissue" (R. E. Tunbridge, ed.), pp. 144-156. *Blackwell, Oxford.*
Schwarz, W. (1959). *Verhandl. Anat. Ges., Zürich, 1959.* In press.
Schwarz, W., and Merker, H. J. (1958). *Beitr. Silikose-Forschung* **III**, 103-117.
Siekevitz, P. (1959). *Ciba Foundation on Cell Metabolism* pp 17-45.
Sjostrand, F. S., and Hanzon, V. (1954). *Exptl. Cell Research* **7**, 415-429.
van den Hooff, A. (1952). *Konnkl. Ned. Akad Wetenschap. Ser. C* **55**, 628.
van den Hooff, A. (1957). *In* "Connective Tissue" (R. E. Tunbridge, ed.), pp. 172-176. *Blackwell, Oxford*
Wassermann, F., and Kubota, L. (1956) *J. Biophys. Biochem. Cytol.* **2** (Suppl.), 67-72.

Discussion

Dr. Cogan [Harvard University, Cambridge, Mass.]: Do corneal cells differ in any way from other connective tissue cells?

Dr. Schwarz [Berlin, Germany]. Only small differences are apparent if different types of embryonic connective tissue are examined. In this embryo, one can differentiate between the fibroblasts in the cornea and the dermis

Dr Hebrmann [Storrs, Conn.] From your pictures it seemed that corneal *stroma cells had no mitochondria Is this actually so? In addition, do the* dermal fibroblasts have mitochondria?

Dr. Schwarz: All embryonic cells have a few mitochondria. There are mitochondria in embryonic corneal fibroblasts but they are very rare. These mitochondria have connections with the endoplasmic reticulum Sometimes they are surrounded by the lamellae of the endoplasmic reticulum. These mitochondria are large and oval. They belong to the "cristae type" but have less cristae than the mitochondria of renal cells and pancreatic cells The course of the cristae is often irregular. Very little matrix between the cristae is found

The Development of the Structural and Optical Properties of the Cornea[1]

ALFRED J. COULOMBRE AND JANE L. COULOMBRE

Department of Anatomy, Yale University School of Medicine, New Haven, Connecticut

Introduction

THE SEVERAL OPTICAL PROPERTIES of the vertebrate cornea which affect the transmission of an image include: (a) its refractive index, (b) its curvature, (c) its transparency, and (d) its interference pattern. Much information concerning the factors which underlie and maintain these properties has accrued from the experimental study of adult corneas. However, an even wider scope for the study of these properties is offered by using embryonic material. With the addition of the embryonic time parameter, one can establish the sequence in which these factors come into operation, and one may detect temporal developmental correlations not accessible with adult material.

This report will summarize some of the work on the development of the curvature, the transparency, and the polarization properties of the cornea, and will correlate these changes with structural maturation. The bulk of the data presented is drawn from work on the chick embryo. The developmental ages of the chick embryos are all given as days following the onset of incubation.

Corneal Curvature

The shape of the cornea (especially the curvature of its outer surface) is critical in roughly focusing the visual image at the retina since, among terrestrial vertebrates, its surface is the locus of strongest refraction. In keeping with this important optical function the adult cornea approximates a spherical segment whose radius of curvature is less than the remainder of the eye. Some of the mechanisms involved in appropriately shaping the developing cornea are suggested by the following observations and experiments.

---

[1] Work from our laboratory which is reported here was supported in part by Grant B-870(c) USPHS, and in part by a grant from the Connecticut Lions Eye Research Foundation.

Description of the Development of the Corneal Curvature

Between the fourth and the eighth days of incubation the eye is spherical in outline and the cornea has the same radius of curvature as the posterior segment. The corneal curvature first appears on the eighth day and thereafter its radius of curvature is less than that of the scleral segment (Coulombre and Coulombre, 1958a) (Fig. 1).

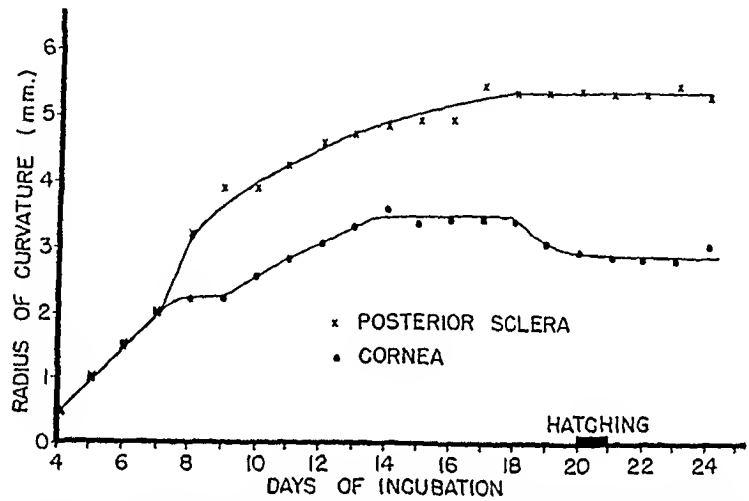

Fig. 1. The radii of curvature of the posterior sclera, and of the cornea are given as functions of age. Each point represents the mean of measurements on at least ten specimens.

The Mechanics of Development of the Corneal Curvature

It is obvious that many factors are involved in the growth and shaping of the cornea. With no intention of minimizing other factors, attention is here focused on the mechanical influences which operate during development.

Following separation of the lens vesicle from the overlying ectoderm, and subsequent closure of the choroid fissure, the eye of the chick embryo becomes a closed chamber. Elaboration of vitreous humor within this chamber increases intraocular pressure, brings the eye wall under tension, and results in a progressive increase in eye size. That intraocular pressure supplies the motive power for this expansion of the eye wall can easily be demonstrated. If, at 4 days, following closure of the choroid fissure, an artificial opening is made in the wall of the eye, either by tearing it (Weiss and Amprino, 1940), or by introducing an indwelling drainage tube (Coulombre, 1956a), vitreous humor will escape as it is formed. Under such conditions intraocular pressure fails to develop, the eye wall is not brought under tension and the eye does not enlarge. Suitable controls indicate that the trauma of the operation has nothing

to do with these results. The cornea, as part of the eye wall, is subjected to the same tangential forces as the rest of its envelope. It is, then, not surprising that experiments reveal that increase in the area of the cornea is dependent on intraocular pressure (*Coulombre, 1957*).

The differential shaping of the eye wall cannot be solely a function of the intraocular hydrostatic pressure, since this acts equally in all directions. Internal pressure acting on an envelope that offers equal resistance to distortion at all points will expand the envelope as a sphere. Therefore deviation from the spherical shape as development proceeds must result from regional changes in the eye coats which occasion differential resistance to distortion under pressure. That the structural properties of the sclera are important is suggested by the fact that prior to the eighth day, when this coat is in its soft, precartilaginous, mesenchymal state, the eye grows very rapidly. However, with the advent of cartilagenous differentiation in the sclera, on the eighth day, the rate of enlargement of the eye is abruptly slowed (Coulombre, 1955). More direct evidence for the morphogenetic role of the differentiating sclera derives from defect experiments. If, at 4 days, a small patch of prescleral mesenchyme is removed the subsequently developing sclera is thin or lacking in the region of the lesion. Under the impetus of intraocular pressure, and in the presence of a local decrease in resistance, the remaining layers of the eye wall bulge out more and more markedly in the region of the defect during the ensuing days (Coulombre, 1956a).

These observations support the notion that the driving force for enlargement of the eye is intraocular pressure, and that the forces that shape the expanding eye derive from local changes in resistance in the eye wall. To see how this applies to the shaping of the cornea it is necessary to detail the changes which occur in the sclera at the time the corneal bulge first appears (Coulombre and Coulombre, 1958a) (Fig. 2). Prior to the eighth day the sclera is mesenchymatous and soft and the eye expands rapidly as a sphere. On the eighth day, cartilage begins to differentiate in the perilimbic region nasal to the site of the choroid fissure. Before the day is over, cartilage encircles the cornea. This tough ring of cartilage expands less rapidly than the rest of the eye wall. As a result the posterior (scleral) segment expands as a segment of a larger sphere, and the cornea expands anteriorly as a segment of a smaller sphere. If steps are taken to prevent the development of intraocular pressure, the tissues of the eye, including the scleral ring, differentiate on schedule, but no corneal bulge appears. In mammalian eyes, which lack an ocular skeleton, the role of the perilimbic scleral cartilage may be played by deposits of collagen as was pointed out by Smelser (1958).

Once the corneal curvature appears it is remarkably resistant to

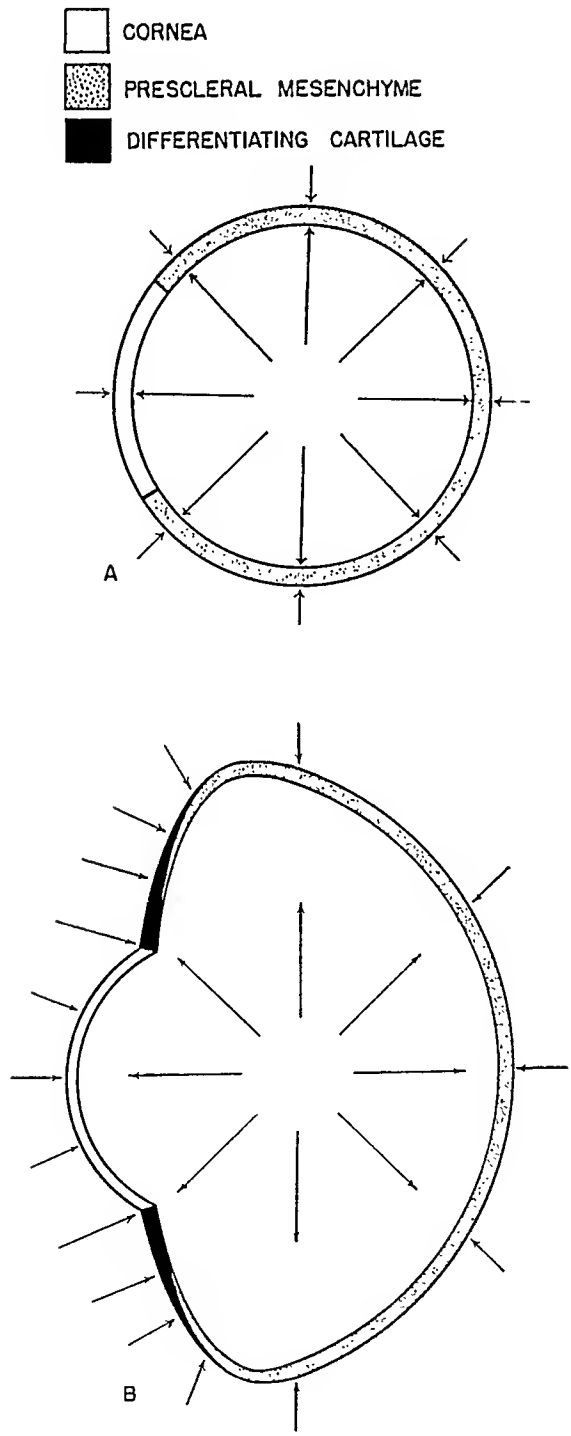

FIG. 2. These diagrams represent sections of the eye in an axial plane, and illustrate the mechanism which brings the corneal curvature into being (see text). The arrows indicate the directions and relative magnitudes of the forces generated within the eye and within its wall. A, stages prior to day 8; B, stages following day 8.

distortion. If, by experimental intervention, the eye is caused to develop in an abnormal shape the cornea tends to retain its shape which approximates a spherical segment. A possible basis for this phenomenon is suggested below. This characteristic of the developing cornea is of importance in view of the dominant role played by the corneal surface in the refraction of the adult eye.

Corneal Transparency

Despite statements to the contrary (e.g., Mann, 1950) the cornea of the vertebrate eye goes through a phase of relative opacity during development before it becomes transparent (van den Hooff, 1951; Coulombre, 1956b; Coulombre and Coulombre, 1958b, Smelser, 1958; Smelser and Ozanics, 1956). In the chick embryo the ability of the cornea to transmit white light was used as a quantitative index of its transparency. The transparency begins to increase on about the fourteenth day. By the eighteenth or nineteenth day the adult transparency has been achieved (Fig. 3).

Knowing the time during development at which the cornea achieves transparency, it is appropriate to search out correlated changes which may be involved causally in this process. It is natural that attention turned first to the corneal water content and to the mucopolysaccharide components of the stroma, two factors of importance for the transparency of the adult cornea.

The Water Content of the Cornea

Under appropriate conditions the adult cornea is capable of absorbing amounts of water equal to many times its own weight. Yet, normally only about 75% of its weight is water. If the water content is increased even slightly there is some loss of transparency. The metabolic mechanism, which maintains the cornea in the state of deturgescence essential to transparency, is known to be temperature and oxygen dependent (Smelser, 1952, Smelser and Ozanics, 1952; Davson, 1955), and to be localized at the outer and inner surfaces of the cornea (Harris, 1957)

The corneal water content in the chick embryo was followed during the period when the cornea was becoming transparent. The corneal dry weight increases steadily between the tenth and the twenty-fourth day. In contrast, the wet weight increases rapidly until the fourteenth day and thereafter much more slowly. As a consequence the amount of water per unit dry weight (specific hydration) decreases as development proceeds. The period of most rapid relative deturgescence is between the

fourteenth and the nineteenth days, the period during which the cornea is assuming adult transparency. By 19 days the cornea contains about 75% by weight of water, the adult level (Fig. 3). At least two factors come into operation to produce corneal deturgescence. In the first place, during this period there is a decrease in the avidity with which the

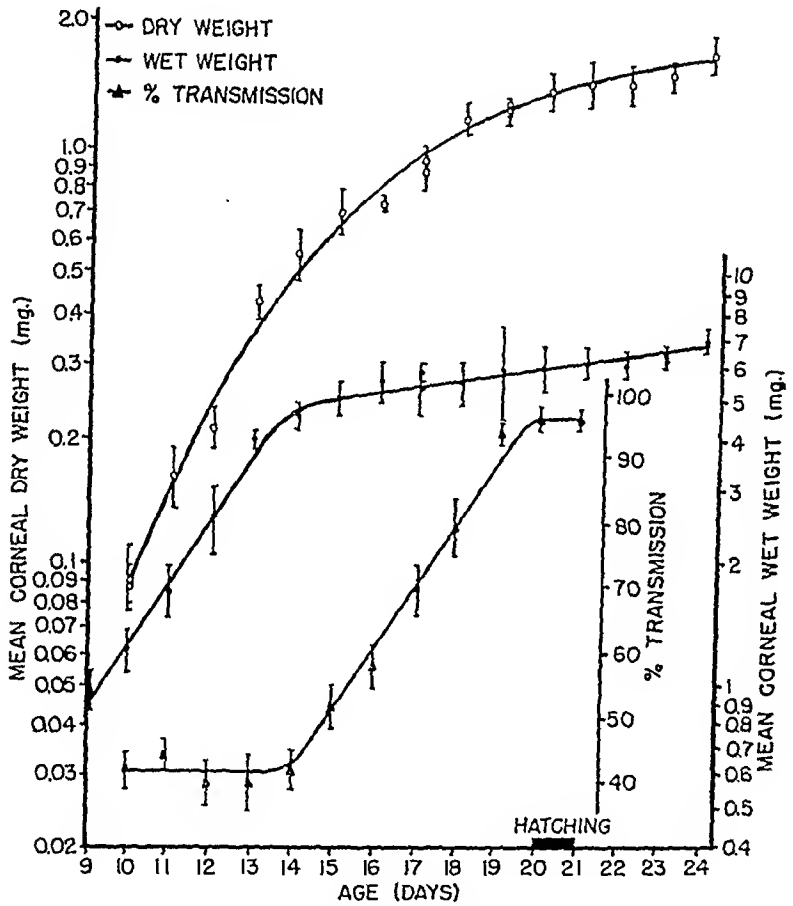

FIG. 3. Three variables (the wet weight, dry weight, and per cent transmission of the cornea) are plotted as functions of age. The weight data are plotted semilogarithmically. Each point represents the mean of measurements on 10 corneas. The vertical lines represent the standard deviation.

cornea absorbs water. Despite the fact that younger corneas contain large amounts of water (up to 96% of their weight), they have a total capacity for water per unit dry weight (when they are brought into equilibrium with distilled water) which is far in excess of more mature corneas. This phenomenon may reflect changes in the stroma which progressively limit the capacity of the water-binding sites, or it may result from a relatively greater increase in collagen than in the more hydrophilic components of the stroma as development proceeds (Smel-

ser, 1958). Whatever its basis, it is insufficient to account fully for the maintenance of deturgescence in mature corneas. While the total water-binding capacity of the mature cornea is smaller than that of younger corneas, it is still appreciable. Thus, an additional factor must be involved in the deturgescence of the fully transparent cornea. It is probable that the water-limiting systems, mentioned above, which are localized at the corneal surfaces, are involved not only in the maintenance of adult corneal deturgescence, but also in the progressive loss of water which occurs as the embryonic cornea becomes transparent. Smelser (1958) has demonstrated in the rabbit that the water-limiting systems are operative quite early in development and presumably play a role in the progressive deturgescence of the developing cornea.

The question of what relationship exists between transparency and hydration can be answered by eliminating the age variable and plotting transparency as a function of specific hydration. The transparency of the developing cornea is an inverse linear function of the hydration. The progressive dehydration of the cornea is a concomitant of the rise in transparency. An experimentally induced increase in corneal water at any age following the fourteenth day results in a loss of the transparency that has already been achieved (Coulombre and Coulombre, 1958c).

Metachromasia of the Corneal Stroma

The adult cornea contains several mucopolysaccharides. These have been isolated from the beef cornea by Meyer, Linker, Davidson, and Weissmann (1953) Keratosulfate, chondroitin and chondroitin sulfate A are present in the ratio 2 1 1. Smits (1957) analyzed the developing beef cornea for collagen (hydroxyproline) and mucopolysaccharide (hexosamine). He found that the hexosamine content of sclera, tendon, and skin decreased as development proceeded whereas the hexosamine content of cornea underwent a transient decrease followed by a marked increase This increase is reflected histochemically in the spread of metachromasia through the cornea during development in mammals (Aurell and Holmgren, 1953, Alagna, 1954; Gemolotto and Patrone, 1955, Seo, 1955, Smelser and Ozanics, 1956, 1957, 1959), and in the chick (van Walbeek *et al*, 1950, van den Hooff, 1951; Coulombre, 1956b; Chiarugi and Bergamini, 1957, Coulombre and Coulombre, 1958b). Smelser and Ozanics (1957) have correlated the spread of metachromasia with the uptake of radiosulfate during development.

In the chick periodic acid-Schiff-positive substances are present in the stroma from very early stages In addition, a faint toluidine blue metachromasia is associated with stromal collagen from the time it first appears However, it is not until the fourteenth day that intense meta-

chromasia appears. It is first localized in a zone at the endothelial surface of the stroma. During subsequent days this intense metachromasia spreads toward the epithelial surface of the stroma, and fills it at about the time adult transparency is achieved. The significance of this change is, at present, a matter of speculation. It is possible, however, that the local increase in metachromasia does not reflect an increase in the rate of synthesis of acid mucopolysaccharides but rather an increase in regional concentration of these substances by a tighter packing of the collagenous lamellae. On the fourteenth day as its last lamella is formed, and as it loses water, the cornea begins to become thinner. This is accompanied by a compacting of the deeper layers of stromal collagen, a change which would bring pre-existing metachromatic material into higher concentration locally and thus account for the intense metachromasia.

The role or roles played by the mucopolysaccharide is still open to question. That it may bring the interfiber and interfibrillar spaces to the same refractive index as collagen is one possibility. Alternatively, or at the same time, it may play a role in establishing the uniform spacing of collagen fibrils that Maurice (1957) has suggested is essential for corneal transparency. In any event the appearance of intense metachromasia at the time the cornea becomes transparent reflects changes in the stroma which are intimately connected with the development of transparency.

The Collagenous Fiber Pattern

Save for water, collagen is the most abundant substance in the corneal stroma, constituting about 80% of its dry weight (Krause, 1934). The manner in which this substance is disposed in space is importantly involved in several optical properties of the cornea. Since collagen has a high tensile strength and a low limit of elasticity it will, in large part, determine the structural properties of the cornea, its response to mechanical distortion, and its ability to retain a near spheroidal shape. In addition, Maurice (1957) has presented evidence suggesting that the geometry of the fibril lattice within the collagen fibers constitutes the physical basis of corneal transparency. Kikkawa (1959) has pointed out that stromal collagen is disposed as a double lattice, and that, in addition to the fibrillar lattice (within the fibers), the lattice formed by the fibers themselves must be considered relative to transparency. Finally, the interference pattern which is observed when the cornea is viewed in polarized light (see below) has its physical basis in the patterns formed by stromal collagen (Stanworth and Naylor, 1950; Kikkawa, 1955).

Attempts to determine stromal fiber patterns have hitherto been

confined to adult specimens and have been of two types. Some workers (e.g., Stanworth and Naylor, 1950, Kikkawa, 1955) have attempted to deduce the probable pattern of the collagen fibers from the optical properties of the cornea. The models that have been arrived at in this way are at variance in detail with those from studies which have resorted to direct observation of the fiber patterns in microscopic sections. The most thorough study of the latter type (Fuchs as cited by Rochon-Duvigneaud, 1943) revealed that in the frog the collagen fibers are disposed parallel to the corneal surface. Within each lamella they form an orthogonal gridwork. As one moves in through the thickness of the cornea successive lamellae are not in register. Their grid axes deviate progressively about 12.5° from those in the next most superficial lamella.

In the chick embryo serial sections made in a plane tangent to the corneal midpoint reveal a somewhat similar situation. Prior to the eighth day the collagenous fibers and cells of the corneal stroma appear randomly oriented in tangential sections. The first patterning that can be seen in the light microscope begins to emerge early on the eighth day. The fully developed pattern is orthogonal, that is, within any one lamella the fibers are disposed in only two directions and intersect to form a right-angled grid. The cells are evenly scattered and lie along the fibers, half of them with their long cell axes parallel to one grid coordinate, and the rest with axes parallel to the other coordinate. This regular pattern is seen at all levels in the 8-day stroma except for the region immediately under the epithelium, a region that shows random organization throughout development. The collagenous gridworks at successive levels in the stroma are *roughly* in register at this early age, and will form the innermost lamellae of the mature cornea. The more superficial lamellae are deposited in sequence beneath the epithelium as development proceeds The grid axes of each of the more superficial lamellae are rotated with respect to those previously deposited. If one views the cornea from its enothelial side, the direction of the progressive rotation is clockwise as the stroma is traversed from its endothelial to its epithelial surface Also the increment of angular deviation becomes progressively greater (Figs. 4 and 5) It is most noteworthy that the direction of rotation of the grid axes is the same in both eyes and is therefore asymmetric with respect to the body midline.

Because of the curvature of the cornea, the plane of section is parallel to the corneal surfaces only toward the center of the section. For this reason only this region was used for the above analysis. The question arises whether the grid pattern is peculiar to the center of the cornea, as claimed by Kikkawa (1956) for the rabbit, or whether it extends within each lamella from limbus to limbus. The question was settled

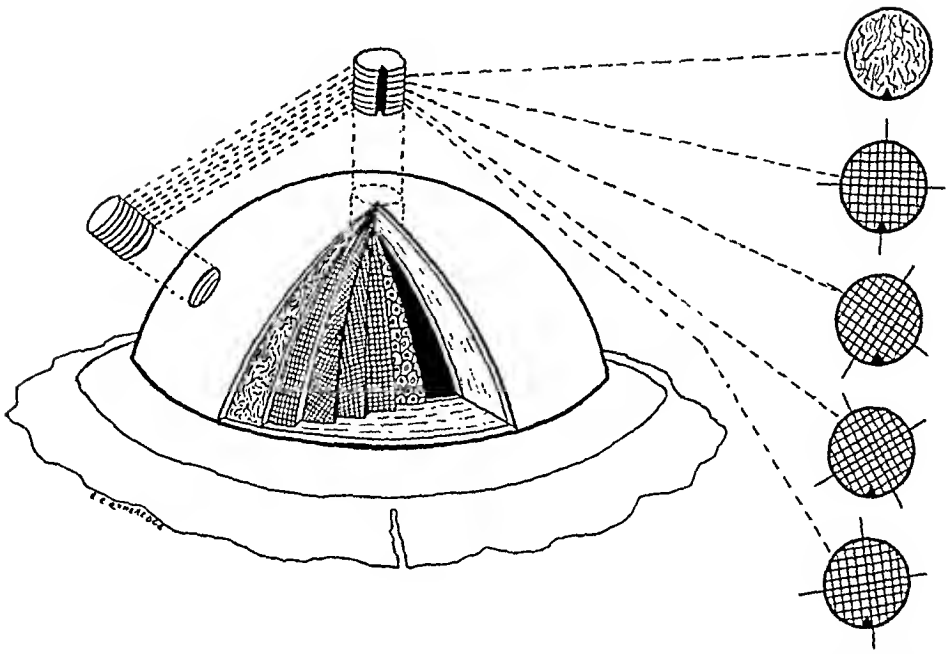

FIG. 4. This diagram demonstrates the spatial distribution of collagen fibers in the stroma. For clarity the thickness of the cornea has been exaggerated and the number of lamellae drastically curtailed. The patterns seen in serial sections made in a plane tangent to the corneal surface are represented in circles at the right. The black notch at the circumference of each circle represents the direction of the choroid fissure. The radial extensions denote the major axes of each grid.

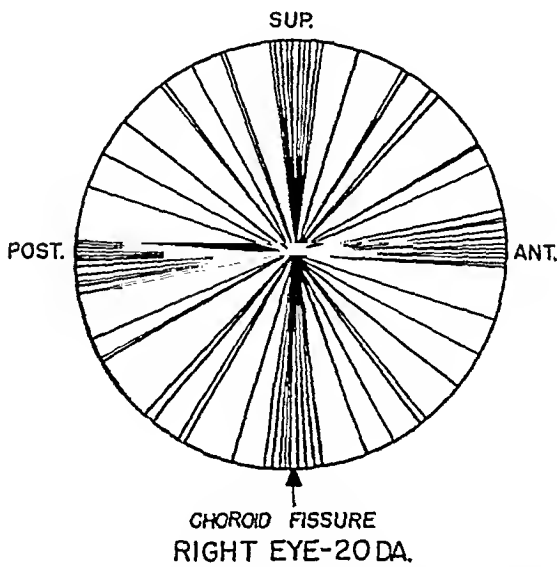

FIG. 5. The major grid axes of all the lamellae are projected onto a common plane tangent to the corneal midpoint. The deeper lamellae have axes that are closer to register than those of the superficial lamellae.

for the chick by cutting a series of eyes in planes tangent to different points on the corneal surface. Since in all of these cases the center of each section showed a rectilinear orthogonal grid it is clear that the gridwork of each lamella stretches from limbus to limbus (Fig. 4).

The most superficial lamella of collagen has been deposited by the fourteenth day. Since collagen synthesis (determined as hydroxyproline) continues unabated until after hatching (Herrmann, 1958) one must conclude that collagen deposition is intralamellar following the fourteenth day. It would be of great interest to know whether this is accomplished by increase in the diameter of the fibrils, by increase in the number of fibrils, or by both.

It is clear that collagen is intimately involved in most, if not all, of the optical properties of the cornea. Before we can fully understand the latter it will be necessary inter alia, to completely quantify the architecture of this substance at the molecular, fibrillar, and fiber levels. If this is done within a developmental context it will be possible to utilize the sequential stages of development of the collagen pattern for experiments that would be impossible with adult material.

Interference Pattern

The isolated adult cornea exhibits a characteristic interference figure when viewed in polarized light. This phenomenon has recently been intensively investigated (Stanworth, 1950, 1953; Stanworth and Naylor, 1950, 1953; Naylor, 1953a, b; Kikkawa, 1955). Cogan (1941) has demonstrated the interference pattern in intact eyes. In all of the forms studied the interference figure consists of two dark rectangular hyperbolas. In the rabbit, dog, cat, and man the apices of the hyperbolas meet at the center of the cornea and the pattern becomes a cross. In these forms the pattern undergoes little change as the cornea is rotated between the crossed polarizer and analyzer. In other species, with more radially asymmetric (elliptical) corneas, such as ox and sheep, the hyperbolas are more widely separated The chick exhibits an interesting combination of these patterns, and what follows deals with the embryonic development of the interference pattern in this species.

In the chick the interference pattern undergoes a progressive, cyclical change as the cornea is rotated about its axis between the crossed polarizers. The cornea can be so rotated until a position is reached at which the interference pattern is a simple cross with its intersection at the center of the cornea. In this position one pair of opposite arms lie in the plane of vibration of the polarizer, while the other pair lie in the plane of vibration of the crossed analyzer. One arm of the cross reaches

the corneal circumference at a point near the anterior extension of the choroid fissure (elongated insertion of the optic nerve). If this point on the corneal margin is used as a reference point and is rotated about the corneal axis 45° in either a clockwise or an anticlockwise direction there is a gradual shift in the pattern from the cross to the separated hyperbola condition. Further rotation to 90° results in a shift back to the cross pattern. Thus the cross appears at 0°, 90°, 180°, and 270°, and the opposed hyperboloid pattern at 45°, 135°, 225°, and 315°. Intermediate positions yield intermediate patterns. This description coincides in part with that given by Kikkawa (1955) for the rabbit. It may be, therefore, that the differences in interference pattern between corneas of the human type and those of the chick type are simply a matter of degree. The two paraboloids are always located in the superior anterior and the posterior inferior quadrants of the chick cornea, with respect to its anatomical position on the eye. In this respect, therefore, the pattern in the two eyes is symmetrical (mirror imaged) with respect to the body midline.

To determine which of the layers of the cornea contributed to the pattern, the different layers were isolated and viewed between crossed Nicols. Only the stroma exhibited the pattern and is, therefore, responsible for it. This is true of all developmental ages at which the pattern is in evidence. Furthermore, the shape and positioning of the pattern are not altered by allowing the stroma to imbibe water and swell.

The only stromal constituent with a sufficiently high coefficient of birefringence, and which is present in high enough concentration to account for the pattern, is collagen. Further support for the involvement of collagen derives from the observation that the pattern makes its first appearance in the chick embryo on the eighth day, the day on which the collagenous gridwork of the stroma is first detected. It is, then, in the disposition in space of the collagen molecules, fibrils and fibers that we must seek the explanation for two phenomena.

The first question deals with the physical basis of the relatively constant location of the cross pattern with respect to the choroid fissure. The cross bears a constant relationship to the grids of collagenous fibers in the deeper lamellae (compare Fig. 5 with Fig. 6). It is presumably the orientation of the gridworks of collagen in these lamellae which determine the positioning of the arms of the cross pattern with respect to the corneal perimeter.

The second question concerns the physical basis of the hyperboloid pattern. The polarization optics underlying this pattern have been elegantly treated by Kikkawa (1955). We need concern ourselves here only with the symmetry of this pattern around the body midline. This

symmetry is in startling contrast to the asymmetry, noted above, of the rotation of the collagenous gridworks of the lamellae. This discrepancy can only mean that the rotation of the axes of these gridworks in successive lamellae has little bearing on the symmetry of the hyperboloid interference pattern. This pattern may depend on the departure of the cornea from sphericity. Two observations suggest this. Stanworth and

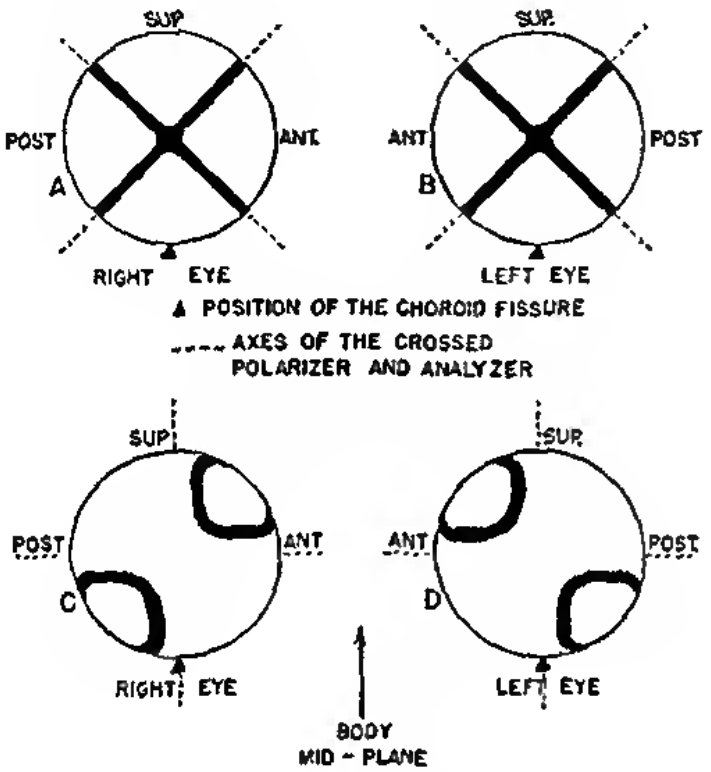

FIG. 6 The isogyres, which are seen when the isolated cornea is viewed between crossed polarizers, are represented in heavy black The circles represent the cornea, on whose periphery the point opposite the choroid fissure is used as an anatomic marker. The cross pattern (A, B) is seen whenever the choroid fissure is 45° removed from any arm of the crossed axes of the polarizer and analyzer. The hyperboloid isogyres are fully developed when the marker coincides with any arm of the axes of the crossed Nicols (C, D) Note the symmetry of the hyperboloid pattern about the body midplane (C, D)

Naylor (1950) point out that the more axially asymmetric the cornea, the larger the separation between the hyperbolic isogyres. In addition to this, appropriate distortion of the isolated cornea of the chick causes the hyperbolic interference patterns to migrate from the superior anterior and posterior inferior quadrants (anatomically) to the remaining two quadrants. Physical distortion of the rabbit cornea leads to a similar inversion (Kikkawa, 1955)

References

Alagna, G. (1954). *Arch. ottalmol.* **58**, 259-271.

Aurell, C., and Holmgren, H. (1953). *Acta Ophthalmol.* **31**, 1-28.

Cogan, D. G. (1941). *A.M.A. Arch. Ophthalmol.* **25**, 391-400.

Coulombre, A. J. (1955). *Am. J. Anat.* **96**, 153-189.

Coulombre, A. J. (1956a). *J. Exptl. Zool.* **133**, 211-225.

Coulombre, A. J. (1956b). *Anat. Record* **124**, 278.

Coulombre, A. J. (1957). *A.M.A. Arch. Ophthalmol.* **57**, 250-253.

Coulombre, A. J., and Coulombre, J. L. (1958a). *A.M.A. Arch. Ophthalmol.* **59**, 502-506.

Coulombre, A. J., and Coulombre, J. L. (1958b). *J. Cellular Comp. Physiol.* **51**, 1-12.

Coulombre, A. J., and Coulombre, J. L. (1958c). *Am. J. Ophthalmol.* **46**, 276-280.

Davson, H. J. (1955). *Biochem. J.* **59**, 24-28.

Gemolotto, G., and Patrone, C. (1955). *Giorn. ital. oftalmol.* **8**, 42-55.

Ghiani, P., and Bergamini, G. (1957). *Atti accad. ligure sci. e lettere (Genoa)* **14**, 298-301.

Harris, John E. (1957). *Am. J. Ophthalmol.* **44**, 262-280.

Herrmann, H. (1958). *In* "A Symposium on the Chemical Basis of Development" (W. D. McElroy and B. Glass, eds.), pp. 329-338. Johns Hopkins Press, Baltimore, Maryland.

Kikkawa, Y. (1955). *Japan. J. Physiol.* **5**, 167-182.

Kikkawa, Y. (1956). *Japan. J. Physiol.* **6**, 300-312.

Kikkawa, Y. (1959). *J. Clin. Ophthalmol. (Japan)* **13**, 1409-1421.

Krause, A. C. (1934). "The Biochemistry of the Eye." Johns Hopkins Press, Baltimore, Maryland.

Mann, I. C. (1950). "The Development of the Human Eye," 2nd ed., pp. 38-39. Grune & Stratton, New York.

Maurice, D. M. (1957). *J. Physiol. (London)* **136**, 263-286.

Meyer, K., Linker, A., Davidson, E. A., and Weissmann, B. (1953). *J. Biol. Chem.* **205**, 611-616.

Naylor, E. J. (1953a). *Brit. J. Ophthalmol.* **37**, 77-84.

Naylor, E. J. (1953b). *Quart. J. Microscop. Sci.* **94**, 83-88.

Rochon-Duvigneaud, A. (1943). "Les Yeux et la Vision des Vertébrés," p. 61. Masson et Cie., Paris.

Seo, S. (1955). *Kyûshû Mem. Med.* **5**, 169-182.

Smelser, G. K. (1952). *A.M.A. Arch. Ophthalmol.* **47**, 328-343.

Smelser, G. K. (1960). *In* "Corneal Transpareney," A symposium organized by C. I. O. M. S. Knokke, Belgium, Sept. 1958. (Sir Stewart Duke-Elder, and E. S. Perkins, eds.), pp. 125-130. Blaekwell, Oxford.

Smelser, G. K., and Ozanies, V. (1952). *Science* **115**, 140.

Smelser, G. K., and Ozanies, V. (1956). *Anat. Record* **124**, 362.

Smelser, G. K., and Ozanies, V. (1957). *Am. J. Ophthalmol.* **44**, 102-110.

Smelser, G. K., and Ozanies, V. (1959). *Am. J. Ophthalmol.* **47**, 100-101.

Smits, G. (1957). *Biochim. et Biophys. Acta* **25**, 542-548.

Stanworth, A. (1950). *Acta XVI Concilium Ophthalmologicum (Britannica)* pp. 1368-1376.

Stanworth, A. (1953). *J. Exptl. Biol.* **30**, 164-169.

Stanworth, A., and Naylor, E. J. (1950). *Brit. J. Ophthalmol.* 34, 201-211.
Stanworth, A., and Naylor, E. J. (1953). *J. Exptl. Biol.* 30, 160-163.
van den Hooff, A. (1951). *Ned. Tijdschr. Geneesk.* 95, 2491-2494.
van Walbeek, K., Neumann, H., Winkelman, J. E., Ruyter, J. H. G., and van den Hooff, A. (1950). *Koninkl. Vlaam. Acad. Gen. Belg* 12, 226-238.
Weiss, P., and Amprino, R. (1940). *Growth* 4, 245-258

Discussion

Dr. Maurice [London, England]. Dr. Coulombre suggests that the stimulus affecting the orientation of the corneal fibers is due to intraocular pressure itself on the cornea. It seems much more likely that it is the resulting tension in the cornea which is the factor.

Dr. A. J. Coulombre [Yale University, New Haven, Conn.]: You are perfectly right, but the tension is generated by an expanding vitreous.

Dr. Maurice: What is the nature of the gridwork you describe? Is it seen in the electron microscope?

Dr. Jakus [Retina Foundation, Boston, Mass.]: Yes, the only difference is that these sections are thicker. The fibers forming the grid are thin bands of parallel collagen fibrils.

Dr. Rohen [Mainz, Germany]. Is there any similarity in the pattern of corneal fibers which you have described to that found in other species?

Dr. A. J. Coulombre: The only others we have examined, are one or two specimens of Rhesus monkey cornea. In these, the patterns were different in that they were much more irregular and, therefore, I do not know how widely applicable the system described in developing chick eye can be. Cartilaginous or bony support in the sclera is not found in mammals. Dr. Smelser has extensively studied development of the cornea in rabbits and has suggested that collagen fibers might well serve a similar function in mammals that the embryonic cartilage appears to do in the chick.

Dr. Langham [Baltimore, Md.]: How do you measure light transmission in these corneas? In problems of corneal transparency one is particularly concerned with the light scattered by the stroma, rather than the amount of light transmitted. Have you observed the appearance of the corneal stroma?

Dr. A. J. Coulombre: We have measured the transmission of light under conditions which do not control scatter or diffraction. The corneas were placed in an appropriate solution held between two plane glass surfaces. The beam of light passed through a very long narrow channel, through the glass, solution, and cornea and fell upon a photo cell. I don't know how much light scatter we avoided.

Dr. Rohen: Are there any changes that could be seen by looking at the cornea?

Dr. A. J. Coulombre: We haven't examined the corneas with a slit lamp. The opacity we referred to is, of course, quite readily visible.

Dr. Balazs [Retina Foundation, Boston, Mass.]: I should like to ask you what pH you used in the metachromatic staining of these immature corneas. We found that the bovine cornea does not bind cationic dyes below pH 4, and at around pH 3.5 the amount of dye bound is only half the amount bound at pH 7. This was quite surprising, since one would expect that the mucopolysaccharides of the cornea having ester sulfate groups, would bind cationic dyes at lower pH's. In other tissues such as cartilage or aorta wall, also containing sulfated polysaccharides, the amount of cationic dye bound is considerable even at pH 2.

Dr. A. J. Coulombre: We have stained only at pH 3.5 to 4.5.

References

Alagna, G. (1954). *Arch. ottalmol.* **58**, 259-271.

Aurell, G., and Holmgren, H. (1953). *Acta Ophthalmol.* **31**, 1-28.

Cogan, D. G. (1941). *A.M.A. Arch. Ophthalmol.* **25**, 391-400.

Coulombre, A. J. (1955). *Am. J. Anat.* **96**, 153-189.

Coulombre, A. J. (1956a). *J. Exptl. Zool.* **133**, 211-225.

Coulombre, A. J. (1956b). *Anat. Record* **124**, 278.

Coulombre, A. J. (1957). *A.M.A. Arch. Ophthalmol.* **57**, 250-253.

Coulombre, A. J., and Coulombre, J. L. (1958a). *A.M.A. Arch. Ophthalmol.* **59**, 502-506.

Coulombre, A. J., and Coulombre, J. L. (1958b). *J. Cellular Comp. Physiol.* **51**, 1-12.

Coulombre, A. J., and Coulombre, J. L. (1958c). *Am. J. Ophthalmol.* **46**, 276-280.

Davson, H. J. (1955). *Biochem. J.* **59**, 24-28.

Gemolotto, G., and Patrone, C. (1955). *Giorn. ital. oftalmol.* **8**, 42-55.

Ghiani, P., and Bergamini, G. (1957). *Atti accad. ligure sci. e lettere (Genoa)* **14**, 298-301.

Harris, John E. (1957). *Am. J. Ophthalmol.* **44**, 262-280.

Herrmann, H. (1958). *In* "A Symposium on the Chemical Basis of Development" (W. D. McElroy and B. Glass, eds.), pp. 329-338. Johns Hopkins Press, Baltimore, Maryland.

Kikkawa, Y. (1955). *Japan. J. Physiol.* **5**, 167-182.

Kikkawa, Y. (1956). *Japan. J. Physiol.* **6**, 300-312.

Kikkawa, Y. (1959). *J. Clin. Ophthalmol. (Japan)* **13**, 1409-1421.

Krause, A. C. (1934). "The Biochemistry of the Eye." Johns Hopkins Press, Baltimore, Maryland.

Mann, I. C. (1950). "The Development of the Human Eye," 2nd ed., pp. 38-39. Grune & Stratton, New York.

Maurice, D. M. (1957). *J. Physiol. (London)* **136**, 263-286.

Meyer, K., Linker, A., Davidson, E. A., and Weissmann, B. (1953). *J. Biol. Chem.* **205**, 611-616.

Naylor, E. J. (1953a). *Brit. J. Ophthalmol.* **37**, 77-84.

Naylor, E. J. (1953b). *Quart. J. Microscop. Sci.* **94**, 83-88.

Rochon-Duvigneaud, A. (1943). "Les Yeux et la Vision des Vertébrés," p. 61. Masson et Cie., Paris.

Seo, S. (1955). *Kyûshû Mem. Med.* **5**, 169-182.

Smelser, G. K. (1952). *A.M.A. Arch. Ophthalmol.* **47**, 328-343.

Smelser, G. K. (1960). *In* "Corneal Transparency," A symposium organized by C. I. O. M. S. Knokke, Belgium, Sept. 1958. (Sir Stewart Duke-Elder, and E. S. Perkins, eds.), pp. 125-130. Blackwell, Oxford.

Smelser, G. K., and Ozanics, V. (1952). *Science* **115**, 140.

Smelser, G. K., and Ozanics, V. (1956). *Anat. Record* **124**, 362.

Smelser, G. K., and Ozanics, V. (1957). *Am. J. Ophthalmol.* **44**, 102-110.

Smelser, G. K., and Ozanics, V. (1959). *Am. J. Ophthalmol.* **47**, 100-101.

Smits, G. (1957). *Biochim. et Biophys. Acta* **25**, 542-548.

Stanworth, A. (1950). *Acta XVI Concilium Ophthalmologicum (Britannica)* pp. 1368-1376.

Stanworth, A. (1953). *J. Exptl. Biol.* **30**, 164-169.

Stanworth, A., and Naylor, E. J. (1950). *Brit. J. Ophthalmol.* **34**, 201-211.
Stanworth, A., and Naylor, E. J. (1953). *J. Exptl Biol.* **30**, 160-163.
van den Hooff, A. (1951). *Ned. Tijdschr. Geneesk.* **95**, 2491-2494.
van Walbeek, K., Neumann, H., Winkelman, J. E., Ruyter, J. H. C., and van den Hooff, A. (1950). *Konnkl. Vlaam. Acad. Gen. Belg.* **12**, 226-238.
Weiss, P., and Amprino, R. (1940). *Growth* **4**, 245-258.

Discussion

Dr. Maurice [London, England]. Dr. Coulombre suggests that the stimulus affecting the orientation of the corneal fibers is due to intraocular pressure itself on the cornea. It seems much more likely that it is the resulting tension in the cornea which is the factor.

Dr. A. J. Coulombre [Yale University, New Haven, Conn.]: You are perfectly right, but the tension is generated by an expanding vitreous.

Dr. Maurice. What is the nature of the gridwork you describe? Is it seen in the electron microscope?

Dr. Jakus [Retina Foundation, Boston, Mass.]. Yes, the only difference is that these sections are thicker. The fibers forming the grid are the bands of parallel collagen fibrils.

Dr. Rohen [Mainz, Germany]. Is there any similarity in the pattern of corneal fibers which you have described to that found in other species?

Dr. A. J. Coulombre. The only others we have examined, are one or two specimens of Rhesus monkey cornea. In these, the patterns were different in that they were much more irregular and, therefore, I do not know how widely applicable the system described in developing chick eye can be. Cartilaginous or bony support in the sclera is not found in mammals. Dr. Smelser has extensively studied development of the cornea in rabbits and has suggested that collagen fibers might well serve a similar function in mammals that the embryonic cartilage appears to do in the chick.

Dr. Langham [Baltimore, Md.]. How do you measure light transmission in these corneas? In problems of corneal transparency one is particularly concerned with the light scattered by the stroma, rather than the amount of light transmitted. Have you observed the appearance of the corneal stroma?

Dr. A. J. Coulombre. We have measured the transmission of light under conditions which do not control scatter or diffraction. The corneas were placed in an appropriate solution held between two plane glass surfaces. The beam of light passed through a very long narrow channel, through the glass, solution, and cornea and fell upon a photocell. I don't know how much light scatter we avoided.

Dr. Rohen. Are there any changes that could be seen by looking at the cornea?

Dr. A. J. Coulombre. We haven't examined the corneas with a slit lamp. The objects we referred to is, of course, quite readily visible.

Dr. Balazs [Retina Foundation, Boston, Mass.]: I should like to ask you what pH you used in the metachromatic staining of these immature corneas. We found that the bovine cornea does not bind cationic dyes below pH 4, and at around pH 5.5 the amount of dye bound is only half the amount bound at pH 7. This was quite surprising, since one would expect that the mucopolysaccharides of the cornea, having ester sulfate groups, would bind cationic dyes at lower pH's. In other tissues, such as cartilage or aorta wall, also containing sulfated polysaccharides, the amount of cationic dye bound is considerable even at pH 2.

Dr. A. J. Coulombre. We have stained only at pH 3.5 to 4.5.

DR. COGAN [Harvard University, Cambridge, Mass.]: You have shown that you can see a cross when the cornea is placed between polaroids. This is compatible with the radial arrangement of the corneal fibers you describe. Have you observed that when you look at an eye with the polarizer and analyzer in an ophthalmoscope, you may see a cross projected on the iris? This is surprising since the cornea is not between the polarizing lenses and we know that the iris will depolarize any light reflected from its surface.

DR. A. J. COULOMBRE: No, we have not looked for this, although we are aware of your own studies which demonstrated the phenomenon.

DR. MAURICE: There has recently been a very full mathematical explanation of this phenomenon by Dr. S. Mishima. It is published in *Advances in Ophthalmology*. (The use of polarized light in the biomicroscopy of the eye, **10**, 1-31, 1960.)

Tissue Interaction and Differentiation in the Corneal and Scleral Stroma

HEINZ HERRMANN

Department of Zoology, Institute of Cell Biology, University of Connecticut, Storrs, Connecticut

Introduction

MANY ORGANS AND TISSUES have as their main components a mesodermal stroma and an ectodermal epithelium. Frequently these components are so closely interdigitated that they cannot be sharply or quantitatively separated. In the cornea, however, a histologically simple boundary is found between the stroma and epithelium and it is easy to scrape off the epithelium and to separate quantitatively the stroma and epithelium from each other. This provides an opportunity to investigate, in a model system, whether there are metabolic interactions between the histologically related cells of the mesodermal and ectodermal components of a tissue.

Early Studies

The first data in the analysis of the cornea which suggested the possibility of a stroma-epithelium metabolic relationship were found during explorations of the metabolism of this tissue (Herrmann and Hickman, 1948a, b, c) and of the effects of local anesthetics (Herrmann *et al.*, 1942) and of mustard gas (Herrmann and Hickman, 1948d) upon it. In the course of these analyses, it was found that about 90% of the oxygen consumption of the bovine cornea was associated with the epithelium and only 10% with the stroma (Herrmann and Hickman, 1948a). Also, in the excised, but intact, bovine cornea carbohydrate reserves of both tissue components were found to be rapidly depleted. In particular, the lactate content of both the stroma and the epithelium decreased rapidly when the isolated beef corneas were maintained *in vitro*. Removal of the epithelium, however, led to a very marked retardation of the disappearance of lactate (Herrmann and Hickman, 1948a, b). Also exogenously supplied pyruvate was found to disappear from the stroma at a very rapid rate in the presence of the epithelium and a much slower rate after removal of the epithelium (Table I). Exposure of beef corneas to mustard gas greatly inhibited lactate disappearance from the stroma while lactate utilization in the epithelium was impaired to a negligible

extent (Table I). It was concluded from these studies that lactate, a product of glycolysis, which was formed in the stroma cannot be further metabolized in this tissue component because of a deficiency of the required components for enzymatic oxidations. It became apparent that oxidation of metabolites formed in the stroma was mediated through the epithelium.

TABLE I[a]

THE UTILIZATION OF LACTATE AND PYRUVATE BY THE EXCISED BEEF CORNEA AS INFLUENCED BY THE PRESENCE OF EPITHELIUM AND MUSTARD GAS

Substrate	Tissue Analyzed	Condition	μg Utilized/hr
Endogenous lactate	Stroma	Presence of epithelium	25
		Absence of epithelium	5
Injected pyruvate	Stroma	Presence of epithelium	124
		Absence of epithelium	14
Endogenous lactate	Epithelium	Mustard treated	19
		Control	22
	Stroma	Mustard treated	6
		Control	26

[a] The data are compiled from measurements reported by Herrmann and Hickman (1948a, b, c, d).

Recent Studies

Later experiments suggested that the epithelium returns some metabolic energy for use in synthetic processes in the stroma. As evidence for such a role of the epithelium it was found that in the absence of the epithelium, incorporation of glycine-1-C^{14} into a collagen fraction (Herrmann, 1957) and of inorganic sulfate-S^{35} into the mucopolysaccharides (Smelser, 1959) of the stroma was greatly diminished.

In the intact cornea, incorporation of amino acids into proteins of the corneal stroma depends not only on the presence of epithelium but also upon the presence of oxygen (Table II). Since the oxygen consumption of the cornea is mainly associated with the epithelium (Herrmann and Hickman, 1948a), the anaerobic suppression of amino acid incorporation into the collagen of the stroma provides additional evidence for its dependence upon epithelial oxidations. The data in Table II also show that the mesodermal cells of the sclera can incorporate amino acids in the absence of ectodermal cells. The oxygen dependence of the incorporation in the sclera shows that enzymatic oxidations which are necessary for syntheses take place in the scleral mesoderm itself.

The necessity of oxygen for the incorporation of amino acid into both the epithelium and the stroma of the cornea gives rise to the ques-

tion whether the oxidative pathways by which energy is liberated for use in synthetic activities in the two cell types are identical. Experiments with metabolic inhibitors show that this does not seem to be the case.

TABLE II

COMPARISON OF GLYCINE INCORPORATION INTO COLLAGEN FRACTION OF CHICK SCLERA AND CORNEA DURING INCUBATION IN AIR AND NITROGEN

(The figures indicate counts/min/μg protein N)

	Sclera		Cornea
	11-Day embryo	4-Day hatched chick	4-Day hatched chick
Air	42 6	7.0	6.1
	52 5	8 6	5.0
	44 3	9 0	4.7
N_2	3 8	1 4	0.3
	2 2	1 6	0.5
	1 6	1.4	0.5

NOTE: The incubations in the presence of glycine-1-C^{14} were carried out in Warburg flasks Six scleras from the embryo, one-third of the sclera, and a single cornea of the hatched chick were used for a single determination. The incubation medium and the analytical procedures were the same as those used in previous experiments (Herrmann, 1958).

The data in Table III indicate that substances like dicumarol and dinitrophenol, which are regarded as inhibitors of the terminal electron transport system, equally diminish amino acid incorporation into proteins of the epithelium and of the stroma. Substances which are mostly used as inhibitors of TCA (tricarboxylic acid) cycle reactions (fluoroacetate, malonate, *trans*-aconitate), suppress the incorporation into the stroma somewhat more than in the epithelium. Arsenite, supposedly an inhibitor of the ketoglutaric dehydrogenase (Neilands and Stumpf, 1955), is a much stronger inhibitor of amino acid incorporation into the stroma than into the epithelium. Arsenite is also known to react with —SH groups in general and to inhibit, therefore, enzymatic reactions dependent on —SH groups (Arnon, 1956). The effect of arsenite on amino acid incorporation in the cornea is comparable to that of several substances which react with —SH groups. The —SH binding reagents (nitrogen mustard, chloromercuribenzoate, and iodoacetate) tested so far at low concentrations, inhibit the amino acid incorporation into stroma proteins to a much greater extent than the incorporation into the proteins of the epithelium. This observation suggests that —SH groups involved in the energy supply for amino acid incorporation into stroma proteins are more sensitive to —SH inhibitors than —SH groups involved in the amino acid incorporation into epithelium proteins. Chlorpromazine (Kar-

TABLE III

EFFECT OF DIFFERENT COMPOUNDS ON INCORPORATION OF GLYCINE-1-C^{14} INTO TOTAL PROTEINS OF THE CORNEAL EPITHELIUM AND THE COLLAGEN FRACTION OF THE CORNEAL STROMA OF THE 2- TO 6-DAY HATCHED CHICK

(Incorporation into controls is set equal to 100)

Compound	Epithelium	Stroma	Loosening
Trypsin 2 mg/2 ml Incubation medium	100	100	++
Collagenase 2 mg/ml Incubation medium	82	61	±
Hyaluronidase 2 mg/ml Incubation medium	100	100	—
Dicumarol			
5×10^{-5}	24	29	—
2.5×10^{-5}	43	43	—
Dinitrophenol			
1×10^{-4}	84	85	
5×10^{-5}	50	44	
Chlorpromazine			
1×10^{-4}			+
2.5×10^{-5}	65	27	±
2×10^{-5}	64	30	—
1×10^{-5}	65	54	—
Methylene blue			
3×10^{-4}	54	32	
2.9×10^{-4}	69	35	
1.8×10^{-4}	93	43	
1.2×10^{-4}	75	63	
0.6×10^{-4}	76	78	
Aminobenzothiazole			
5×10^{-3}	15	20	—
1×10^{-3}	100	100	—
1×10^{-4}	100	100	—
1×10^{-5}	100	100	—

TABLE III (*Continued*)

Compound	Epithelium	Stroma	Loosening
Malonate			
1×10^{-2}	82	52	±
Arsenite			
1×10^{-3}	10	0	
4×10^{-4}	79	21	
trans-Aconitate			
5×10^{-2}	53	36	±
1.2×10^{-2}	94	114	−
Fluoroacetate			
5×10^{-4}	63	40	+
5×10^{-5}	75	50	±
Fluoride			
1×10^{-3}	64	39	++
7.5×10^{-4}	77	94	±
3.75×10^{-4}	117	114	±
1×10^{-4}	94	130	−
Iodoacetate			
1×10^{-3}	32	3	++
1×10^{-4}	90	35	±
1×10^{-5}	80	74	−
Chloromercuribenzoate			
2.9×10^{-4}	10	6	++
1.4×10^{-4}	31	12	+
7×10^{-5}	71	33	±
3×10^{-5}	83	55	−
Nitrogen mustard			
1×10^{-4}	83	50	+
7.5×10^{-5}	110	70	+
Na I			
1×10^{-2}	100	73	−

KEY: ++ = *No noticeable adhesion of epithelium except peripherally.*
+ = *Adhesion markedly diminished.*
± = *Decrease of adhesion barely noticeable.*

NOTE. *The effect of the three enzymes was tested after pre-incubation for one-half hour with the enzyme without glycine-1-C*^{14} *followed by short washing in the incubation medium and incubation for 1 hr without enzyme and with glycine-1-C*^{14}. *The other reagents were present during the 1-hr incubation period with glycine-1-C*^{14}. *The incubation conditions were described previously (Herrmann, 1958).*

roman *et al.*, 1959) and methylene blue, both phenothiazine derivatives, have reactive electron systems and may interfere at low concentrations by virtue of one or both of these properties with electron transport from the stroma to the epithelium. Aminobenzothiazole and NaI have been considered in connection with certain forms of energy transmission (Szent-Györgyi, 1957), but have no effect on the protein synthesis in the corneal stroma at lower concentrations.

It was of interest that in comparing qualitatively the adhesiveness of the epithelium to the stroma a maximal loss (Herrmann and Hickman, 1948e) of adhesion was found after 1 hr incubation of the corneas in a solution of the —SH binding reagents (Table III). A maximal loosening[1] was also observed after incubation in a trypsin solution, whereas a solution of collagenase and of hyaluronidase did not affect the epithelial adhesion to the same extent. The results obtained with trypsin and hyaluronidase corroborate earlier observations on beef cornea (Herrmann and Hickman, 1948e). From these findings it can be seen that mere loosening of the epithelium does not diminish the maintenance by the epithelium of amino acid incorporation in the stroma. For example, complete loosening by trypsin does not alter the amino acid incorporation in the stroma. It can therefore be concluded that the loosening after incubation in —SH binding reagents is not necessarily a factor for the interruption of amino acid incorporation in the stroma. Thus, the effect of —SH binding reagents suggests a role of —SH groups not only in the adhesion of the epithelial cells but also in the metabolic interaction between epithelium and stroma. An effect of —SH binding reagents on the intercellular adhesion of sea urchin blastomers should be pointed out (Mazia, 1959).

Discussion

Metabolic interactions between mesodermal and ectodermal tissue components have been suggested previously as the basis of functional activities of the kidney (Flexner, 1939), the ciliary body (Friedenwald and Stiehler, 1938) and the chorioplexus (Stiehler and Flexner, 1938). The dependence in one cell type upon the metabolism of another cell type for synthesis of macromolecules—and thus of growth—seems to be essentially a newly observed phenomenon. In view of the importance of protein synthesis for growth and differentiation, the present results

[1] Under conditions of maximal loss of adhesiveness large sheets of epithelium can be pulled off with forceps and on removal of the epithelium by scraping with an iris knife no distinct resistance can be noticed. However, no spontaneous separation occurs between epithelium and stroma on incubation of corneas with maximally loosened epithelium.

prompt an inquiry into the developmental implication of the observed cell interactions in the cornea. The establishment of the histological organization of the cornea during embryogenesis of the chick is a relatively late event. No corneal mesoderm is present up to the sixth day of development; but after this period there is a substantial migration of cells from the head mesenchyme to the region covered by the presumptive corneal ectoderm (Redslob, 1935). Parts of the remaining head mesenchyme give rise to the sclera. When measured as relative increases in ribonucleic acid, deoxyribonucleic acid, and protein nitrogen contents, the growth of the sclera and of the corneal stroma and epithelium are quite comparable between the tenth day of embryonic development and the eighth to tenth day after hatching (Table IV). Protein synthesis in the corneal stroma and in the scleral mesoderm seems to depend on entirely different mechanisms of energy supply. Incorporation of labeled amino acids into proteins by the mesodermal cells in the cornea was

TABLE IV

CONTENTS OF RIBONUCLEIC ACID (RNA), DEOXYRIBONUCLEIC ACID (DNA), PROTEIN NITROGEN (PN), AND PROTEIN HYDROXYPROLINE (PHP) IN THE SCLERA, THE CORNEAL EPITHELIUM, AND THE CORNEAL STROMA OF THE CHICK EMBRYO AND THE YOUNG CHICK

(The figures indicate μg in a single sclera, corneal epithelium, and corneal stroma, respectively)

	Sclera			Cornea					
				Stroma			Epithelium		
	RNA	DNA	PHP	RNA	DNA	PHP	RNA	DNA	PN
10-Day embryo	55	39	11 4	4 7	2 6	2 0	0 60	0 28	1.1
16-Day embryo		59	126	12 5	6 9	20 0	2 8	1 9	5.7
1–2-Day hatched chick		80	350	9 9	8 0	47 4	4.7	2.1	11 3
8–10-Day hatched chick	180	78	510	10 7	7 6	51.5	5 0	2 3	15.1

NOTE. Twenty-four, ten, and one cornea were used per sample for the 10-day and 16-day embryo and the hatched chicks, respectively. The extraction was carried out with 2 × 0 1 ml of 5% trichloracetic acid (TCA) at 90° and 2 × 0.1 ml of 5% TCA at room temperature The extracts were made up to 0.5 ml and aliquots of 0 1 ml were used for the colorimetric determinations following Schneider's method (1945) for determination of DNA, the procedure of von Euler and Hahn (1946) for RNA, and the techniques described previously (Herrmann, 1958) for PHP. The final volumes were adjusted to 1 0 ml, 0 3 ml, and 1 2 ml for the determination of RNA, DNA, and PHP, respectively. Two scleras per sample were used for the 10-day embryo and one sclera per sample for the 16-day embryo and the hatched chick. The scleras were extracted with a total of 1 0 ml of 5% TCA and suitable aliquots were used for the colorimetric determinations.

found to be dependent upon the presence of an epithelial layer as early as the eighth day of development, that is, 2 days after the onset of migration of these cells from the head mesenchyme into the corneal area (Herrmann, 1958). Therefore, the metabolic interaction between the two tissue components is established, presumably, shortly after the mesodermal cells reach the corneal area. In contrast, the cells of the head mesenchyme, which develop into the scleral cartilage, seem to maintain practically all or at least a high proportion of amino acid incorporation into proteins without an epithelium (Table II).

The high degree of autonomy in protein synthesis in the sclera, and the almost complete epithelium dependence of amino acid incorporation in the corneal stroma are distinct indices of the divergent chemical differentiation of the head mesenchyme into scleral or corneal mesoderm. Apparently in establishing a close spatial relationship to the epithelium the corneal stroma becomes deficient in its capacity to oxidize intermediates of carbohydrate metabolism and to produce energy for enzymatic syntheses. Evidence has accumulated that the stroma of the beef cornea has a glycolytic system and a lactic acid dehydrogenase (Herrmann and Hickman, 1948a, b). In addition, Kuhlman and Resnik (1958) have demonstrated the presence of appreciable amounts of the enzymes[2] of the TCA cycle in the stroma of the rat cornea. Therefore, the negligible oxygen uptake in the stroma may be due to a defect in the terminal electron transport system. If this is the case, it can be postulated that the electron transport system of the corneal epithelium compensates for this defect in the stroma. Such a scheme would presuppose that electrons are transported in some manner from the stroma cells through a noncellular matrix of the ground substance of the stroma to the epithelial cells. An electron transmission along nondiffusible structural elements of the ground substance has been suggested from radioautographic studies (Herrmann and Love, 1959).

A speculative scheme for the metabolic organization of the cornea is given in Fig. 1, which can be regarded as a working hypothesis for further investigation. In accordance with recent findings of Kinoshita (1957) and Kuhlman and Resnik (1959) the pentose shunt, the glycolytic pathway, and the TCA cycle can be regarded as the main sources of oxidizable substrate for the terminal electron transport in the epithelium. In the stroma only the glycolytic pathway and TCA cycle enzyme activities have been demonstrated. In the scheme no functioning

2 The decrease of enzymatic activities in the corneal stroma of the newly born rat, which is found when calculated on a dry weight basis, may be due in part to the rapid increase in extracellular material such as collagen. If calculated on a per cell basis the levels of these enzymes may show only a small decrease.

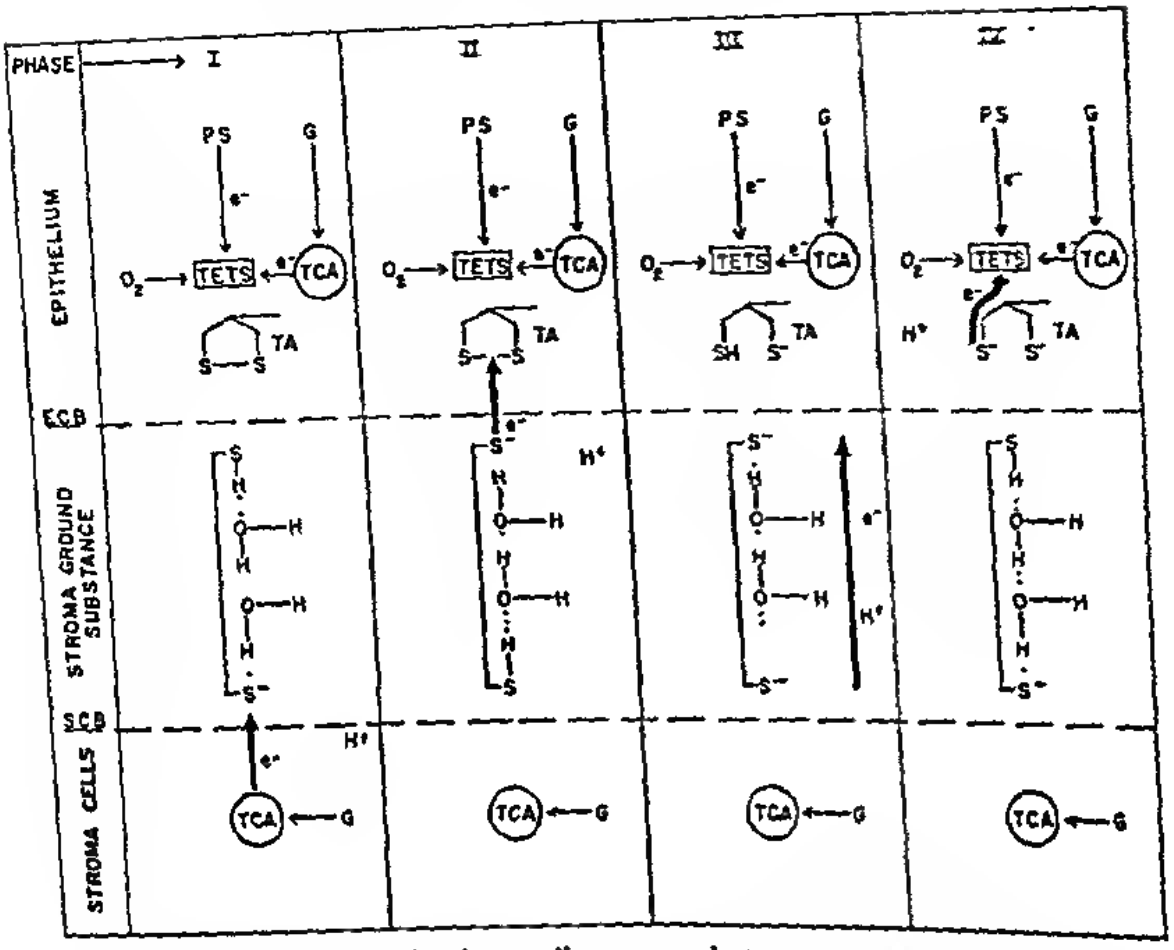

FIG 1 Hypothetical scheme illustrating electron transport from the stroma cells through the ground substance of the stroma to the epithelium cells.

Phase I. Epithelium Indicated are the pentose shunt pathway (PS), the glycolytic pathway (G), the tricarboxylic acid cycle (TCA), and the terminal electron transport system (TETS) Electrons are transferred from PS and TCA via TETS to oxygen Oxidized thioctic acid (TA) is given as example of an electron transfer system at the boundary between epithelium and stroma.

Ground Substance Illustrated is a structural protein molecule with bound water, reduced —SH groups at epithelial cell boundary (ECB) and oxidized —S— groups at stroma cell boundary (SCB).

Stroma Cell Electrons are produced by G and TCA and used in part for reduction of protein —S— in the ground substance

Phase II. Epithelium —S—S— bond in TA is broken in the course of reduction by electrons transmitted from protein —SH groups in ground substance.

Ground Substance. The protein —SH at ECB releases electrons for reduction of TA in epithelium.

Phase III Epithelium. Thioctic acid is partially reduced by gain of one electron.

Ground Substance. Transfer of electrons from protein —SH at SCB to protein —S— at ECB is accomplished by shifting of H bonds (modification of a system described by KUHZ *et al*, 1958).

Phase IV Epithelium Electrons are transferred from TA to TETS with re-oxidation of TA. Return of all three compartments of the cornea to the transition stage shown in phase I.

terminal electron transport system is indicated in the stroma in accordance with the observed defect in its oxygen uptake. Instead, it is proposed that structural elements such as —SH of proteins or bound ascorbic acid, are the mediators by which electrons are transported between the stroma and epithelium. The presence of a structural, nondiffusible electron carrier would conform to the autoradiographic appearance (Herrmann and Love, 1959) of the metabolic effect of the epithelium. In addition, it would explain the sensitivity to —SH binding reagents of the epithelium-dependent protein synthesis in the stroma.

The hypothetical large molecular —SH compound may be reduced on the surface of the stroma cells like the —SH proteins in bacterial cell walls (Falcone and Nickerson, 1959). Transport of electrons along structural —SH-containing elements may follow the model system described by Klotz *et al.* (1958). At the epithelial cell boundary, oxidation of reduced —SH groups would take place by reduction of some suitable electron receptor in the epithelial cell surface. Numerous such systems could be proposed. In completing this scheme, however, it is suggested that thioctic acid may be one of several electron acceptors on the epithelial side of the tissue boundaries. Because the thioctic acid molecule is partly hydrophilic and partly hydrophobic it could be located in a lipoidal cell structure like a cell surface. In this position the —S—S— group of thioctic acid could be expected to react with the reduced —SH groups of the large molecular constituents of the matrix, and thus serve in this way as the first link in the intraepithelial transport of electrons from the stroma.

In concluding, the data presented in this paper and their tentative interpretations may be relevant in two respects. First, the cornea may represent a model system of wider significance for the study of developmental processes. Development and morphogenesis of certain embryonic mesodermal tissues (Zwilling, 1956; Saunders *et al.*, 1958), as well as the regeneration of the mesoderm of limbs (Thornton, 1956), depends upon the presence of an epithelial component. Second, the demonstration of metabolic interactions between cells mediated by structural elements across a known cellular ground substance would emphasize the unity between histological organization, of ultrastructure, and of functional energy transfer.

Addendum

The question has been raised whether the described effect of the epithelium on the maintenance of protein synthesis in the corneal stroma could be explained by prevention of a loss of diffusible substances from the stroma cells. This, however, seems unlikely. Measurements of the

amino acid concentration in the stroma show practically equally rapid equilibration in the absence or presence of the epithelium.

Also, the effect of the epithelium was fully maintained under conditions under which diffusion from the stroma was greatly facilitated. Six corneas from 5-day hatched chicks were cut into five long, connected strips, like a glove with five long fingers and a small palm. The epithelium was removed from three of these cut corneas. Each group of three corneas (with or without epithelium) were placed on one end of a microscopic slide. In each cornea the strips were spread apart to allow for an easy penetration of a tracer solution between the strips. A volume of 0.01 ml of a solution containing 1 μC of glycine-1-C^{14} was evenly distributed along the outline of each group of the split corneas.

Under these conditions only little material could be lost from the stromas into the relatively small volume of tracer solution. Whatever diffusion did take place from the stroma had to be independent of the presence or absence of the epithelial cover. The corneas were incubated by placing the microscope slide into a petri dish which was adapted as a moist chamber and was kept at 37.5°C. for 1 hr. After this incubation period the collagen fractions from the corneal stromas of the three epithelium covered corneas gave counts per minute of 340, 353, and 695 while the collagen fractions from the stromas after incubation without epithelium gave counts per minute of 13, 15, and 5. These results indicate that the effect of the epithelium on incorporation of glycine into the collagen fraction of the stroma does not seem to be related to a control of the diffusion of some substances in or out of the stroma.

Acknowledgments

Original work reported in this paper was carried out with the aid of grants B-549 and B-2238 of the National Institute of Neurological Diseases and Blindness of the U. S. Public Health Service.

The sample of chlorpromazine (Thorazine) was obtained by courtesy of Dr. K. E. Keeler of Smith, Kline and French Laboratories.

References

Arnon, D. I. (1956). *In* "Enzymes. Units of Biological Structure and Function" O. H. Gaebler, ed.), pp. 279-305. (Table IX, p. 302.) Academic Press, New York.

Falcone, G., and Nickerson, W. J. (1959). *In* "Biochemistry of Morphogenesis," Vol. VI, pp. 65-70. Proc. IVth International Congress of Biochemistry, Vienna, 1958. Pergamon Press, New York.

Flexner, L. B. (1939). *J. Biol. Chem.* **131**, 703-711.

Friedenwald, J. S., and Stiehler, R. D. (1938). *Arch. Ophthalmol.* 20, 761-786.

Herrmann, H. (1957). *Proc. Natl. Acad. Sci. U. S.* **43**, 1009-1011.

Herrmann, H. (1958). *In* "A Symposium on the Chemical Basis of Development" (W. D. McElroy and B. Glass, eds.), pp. 329-338. Johns Hopkins Press, Baltimore, Maryland.
Herrmann, H., and Hickman, F. H. (1948a). *Bull. Johns Hopkins Hosp.* **82**, 225-250.
Herrmann, H., and Hickman, F. H. (1948b). *Bull. Johns Hopkins Hosp.* **82**, 260-272.
Herrmann, H., and Hickman, F. H. (1948c). *Bull. Johns Hopkins Hosp.* **82**, 273-286.
Herrmann, H., and Hickman, F. H. (1948d). *Bull. Johns Hopkins Hosp.* **82**, 251-259.
Herrmann, H., and Hickman, F. H. (1948e). *Bull. Johns Hopkins Hosp.* **82**, 182-207.
Herrmann, H., and Love, D. S. (1959). *J. Biophys. Biochem. Cytol.* **6**, 135-136.
Herrmann, H., Moses, S. G., and Friedenwald, J. S. (1942). *Arch. Ophthalmol.* **28**, 652-660.
Karreman, G., Isenberg, I., and Szent-Györgyi, A. (1959). *Science* **130**, 1191-1192.
Kinoshita, J. H. (1957). *J. Biol. Chem.* **228**, 247-253.
Klotz, I. M., Ayres, J., Ho, J. Y. C., Horowitz, M. G., and Heiney, R. E. (1958). *J. Am. Chem. Soc.* **80**, 2132-2141.
Kuhlman, R. E., and Resnik, R. A. (1958). *Am. J. Ophthalmol.* **46**, 47-55.
Kuhlman, R. E., and Resnik, R. A. (1959). *Arch. Biochem. Biophys.* **85**, 29-36.
Mazia, D. (1959). *In* "Sulfur in Proteins" (R. Benesch *et al.*, eds.), pp. 367-389. Academie Press, New York.
Neilands, J. B., and Stumpf, P. K. (1955). "Outlines of Enzyme Chemistry," p. 269. Wiley, New York.
Redslob, E. (1935). *Arch. Anat. Histol. Embryol.* **19**, 135-229.
Saunders, J. W., Gasseling, M. T., and Gfiller, M. (1958). *J. Exptl. Zool.* **137**, 39-74.
Schneider, W. C. (1945). *J. Biol. Chem.* **161**, 293-303.
Smelser, G. K. (1959). *Trans. N. Y. Acad. Sci.* **21**, 575-577.
Stiehler, R. D., and Flexner, L. B. (1938). *J. Biol. Chem.* **126**, 603-617.
Szent-Györgyi, A. (1957). "Bioenergetics." Academic Press, New York.
Thornton, C. S. (1956). *J. Exptl. Zool.* **133**, 281-300.
von Euler, H., and Hahn, L. (1946). *Svensk. Kem. Tidskr.* **58**, 251-265.
Zwilling, E. (1956). *Am. Naturalist* **90**, 257-265.

Discussion

Dr. Meyer [Wayne State University, Detroit, Michigan]: Do you not find that collagen synthesis occurs before the corneal corpuscles enter the cornea?

Dr. Herrmann [Storrs, Conn.]: We could demonstrate collagen synthesis on the eighth day of incubation. I imagine that radioautographic methods would allow this to be done earlier but I have not done it myself, have you?

Dr. Meyer: I have only the evidence obtained by histological techniques.

Dr. Herrmann: Perhaps Dr. O'Rahilly could confirm my opinion that migration of mesenchyme cells into the cornea occurs before the sixth day and that they deposit the initial lamellae. Is that correct?

Dr. O'Rahilly [Wayne State University, Detroit, Michigan]: Mesenchymal cells invade the substantia propria during the sixth day.

Incorporation of Tritium-Labeled Thymidine by Rabbit Corneal Endothelium

NANCY L. MILLS AND ANTHONY DONN

Department of Ophthalmology, College of Physicians and Surgeons, Columbia University, New York, New York

THE PROBLEM of regeneration and replacement of corneal endothelial cells is still unsolved. It is generally held that there is no evidence of mitosis in the endothelium of adult animals (Ballowitz, 1900, Cogan, 1951; Stocker, 1953), although Ballowitz (1900) had observed mitoses in young cats and recently von Sallmann (1960) has reported a mitotic index of 2/100,000 in "young adult rabbits." Binder and Binder (1957) described only "amitotic" cell division in uninjured rabbit endothelium but both "mitotic and amitotic cell division" in the endothelium 12 hr after injury with a blunt spatula. Following irrigation of the anterior chamber by α-chymotrypsin, von Sallmann (1960) observed greatly increased mitotic activity in some localized areas of Descemet's endothelium.

Harding *et al.* (1960) have recently shown that the very weak β-radiation from tritiated thymidine can be detected, by means of autoradiography, in whole mount preparations of lens epithelium. By this method, incorporation of tritiated thymidine by any cell in the entire lens epithelium can be detected. This procedure was applied in a study of Descemet's endothelium. Synthesis of deoxyribonucleic acid (DNA) is a necessary precursor to cell division. The pyrimidine thymidine is incorporated in DNA, and if the thymidine is labeled with tritium those nuclei which have formed new DNA can be detected autoradiographically. Once thymidine has been taken up by the DNA in the cell nuclei it theoretically remains in the cell permanently unless it becomes diluted by subsequent cell divisions (Hughes *et al.*, 1958).

Materials and Methods

The anterior chambers of healthy anesthetized rabbits of specified ages were evacuated with a 27-gage needle inserted at the limbus and refilled with 0.1 to 0.2 ml of tritiated thymidine (20 μC/ml). The thymidine was made up in Eagle's basal medium and had a specific activity of 0.36, 1.9, or 2.7 curies per millimole.

In some cases the endothelium was injured 4 to 48 hr before injecting thymidine with a small blunt probe which was passed into the

anterior chamber through a limbal incision. A linear path was denuded of endothelium.

Two hours after thymidine was injected into the anterior chamber the animal was killed, and the cornea with an adjacent scleral ring was gently dissected away in a bath of normal saline. The tissue was fixed in glacial acetic acid/absolute alcohol, 1:3 for 24 hr, stored in 70% alcohol at least 24 hr and flattened by cutting radial slits in the periphery. After softening the tissue by soaking it for 5 min in water a very thin portion of the posterior cornea (endothelium, Descemet's membrane, and some stromal fragments) was stripped from the preparation (Binder and Binder, 1957; Stocker, 1953) and placed endothelial side up in a drop of water on a gelatin-coated glass slide. In most cases the entire area of the endothelial surface was thus preserved.

Autoradiographs were prepared using Kodak stripping film AR 10 (Kodak Limited, London). After exposing the film for 1 to 2 weeks (depending upon the specific activity of the thymidine) the preparation was developed, washed, stained for 30 minutes with Harris' hematoxylin, 1:3, and mounted in a synthetic resin (Permount) according to the method of Harding *et al.* (1960).

Results

In experiments on 22 uninjured eyes no cell division or thymidine incorporation was observed in the corneal endothelium of adult rabbits (approximately 3 kg body weight). Figure 1 shows a typical preparation magnified 185 ×; the small scattered black dots represent the background exposure. In rabbits 3 months and younger, however, thymidine incorporation by the endothelium was noted in all 34 uninjured eyes. In general there was a greater and more diffuse uptake in the very

---

FIG. 1. Uninjured adult Descemet's endothelium which had been exposed to tritiated thymidine for 24 hr. There are no labeled nuclei; the silver grains scattered throughout the preparation represent background exposure. Magnification: × 185.

FIG. 2. A central area of corneal endothelium of an 11-day-old rabbit which had been exposed to tritiated thymidine for 2 hr. In addition to the background there are many clusters of silver grains directly over nuclei which had incorporated thymidine. Magnification: × 185.

FIG. 3. Large numbers of labeled nuclei in the path of an endothelial abrasion which was exposed to thymidine 24 hr after injury. Magnification: × 60.

FIG. 4. An edge of the same 24 hour wound. Magnification: × 185.

FIG. 5. A 24 hour endothelial wound showing mitotic figures (arrows) and radioactive nuclei. Magnification: × 560.

anterior chamber through a limbal incision. A linear path was denuded of endothelium.

Two hours after thymidine was injected into the anterior chamber the animal was killed, and the cornea with an adjacent scleral ring was gently dissected away in a bath of normal saline. The tissue was fixed in glacial acetic acid/absolute alcohol, 1:3 for 24 hr, stored in 70% alcohol at least 24 hr and flattened by cutting radial slits in the periphery. After softening the tissue by soaking it for 5 min in water a very thin portion of the posterior cornea (endothelium, Descemet's membrane, and some stromal fragments) was stripped from the preparation (Binder and Binder, 1957; Stocker, 1953) and placed endothelial side up in a drop of water on a gelatin-coated glass slide. In most cases the entire area of the endothelial surface was thus preserved.

Autoradiographs were prepared using Kodak stripping film AR 10 (Kodak Limited, London). After exposing the film for 1 to 2 weeks (depending upon the specific activity of the thymidine) the preparation was developed, washed, stained for 30 minutes with Harris' hematoxylin, 1:3, and mounted in a synthetic resin (Permount) according to the method of Harding *et al.* (1960).

Results

In experiments on 22 uninjured eyes no cell division or thymidine incorporation was observed in the corneal endothelium of adult rabbits (approximately 3 kg body weight). Figure 1 shows a typical preparation magnified 185 ×; the small scattered black dots represent the background exposure. In rabbits 3 months and younger, however, thymidine incorporation by the endothelium was noted in all 34 uninjured eyes. In general there was a greater and more diffuse uptake in the very

---

FIG. 1. Uninjured adult Descemet's endothelium which had been exposed to tritiated thymidine for 24 hr. There are no labeled nuclei; the silver grains scattered throughout the preparation represent background exposure. Magnification: × 185.

FIG. 2. A central area of corneal endothelium of an 11-day-old rabbit which had been exposed to tritiated thymidine for 2 hr. In addition to the background there are many clusters of silver grains directly over nuclei which had incorporated thymidine. Magnification: × 185.

FIG. 3. Large numbers of labeled nuclei in the path of an endothelial abrasion which was exposed to thymidine 24 hr after injury. Magnification: × 60.

FIG. 4. An edge of the same 24 hour wound. Magnification: × 185.

FIG. 5. A 24 hour endothelial wound showing mitotic figures (arrows) and radioactive nuclei. Magnification: × 560.

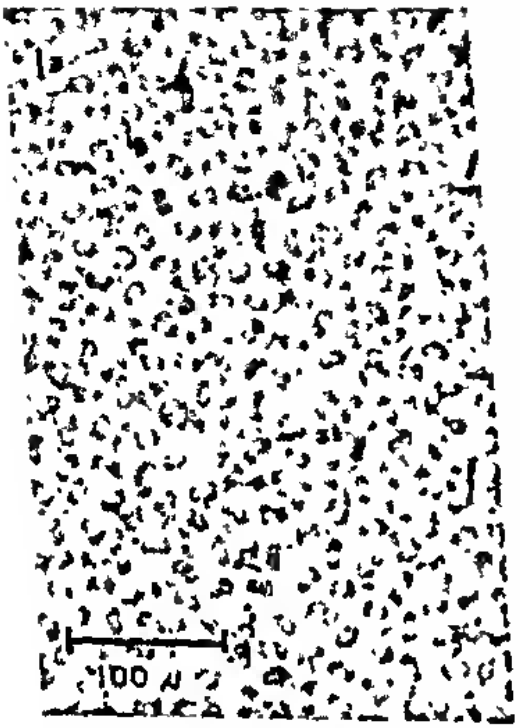
100 Å


200 Å

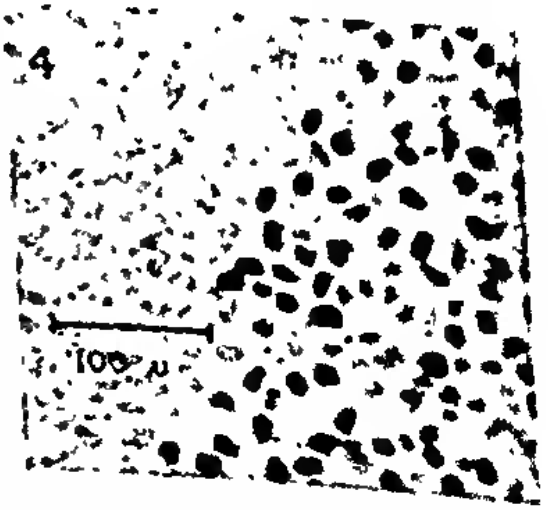
100 Å

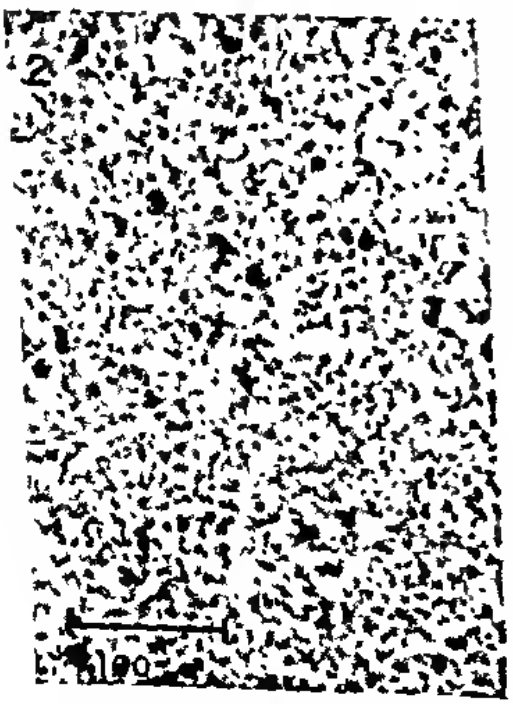
100 Å

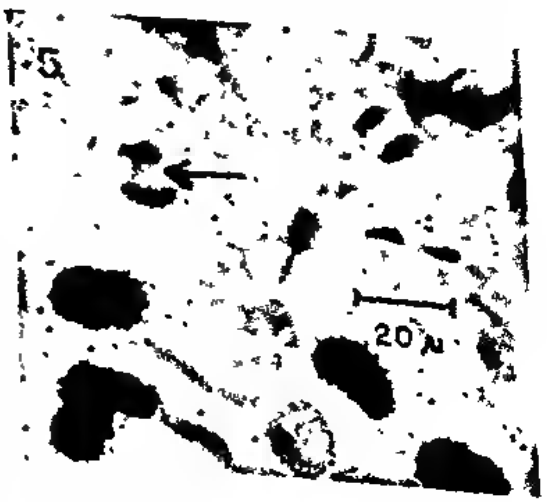
20 Å

When the corneal endothelium of adult rabbits had been previously injured, large numbers of radioactive nuclei and many mitotic figures were seen in the wound path. Maximum thymidine incorporation occurred 24 to 48 hr after injury. At 4, 8, and 12 hr after wounding there was an organization and streaming of the nuclei at the wound edge, but little uptake or mitosis was observed. The path of a 24-hr wound is shown in Fig. 3 magnified 60 ×. Figure 4 shows the edge of the same wound under 185 × magnification. Figure 5 illustrates mitotic cell division occurring along with thymidine uptake in the path of a 24-hr wound magnified 560 ×.

Discussion

Since thymidine incorporation occurs during the synthetic phase of cell division, which is much longer than the dividing phase (Painter and Drew, 1959), and since the availability time of the thymidine in these experiments is estimated at 1 hr, the probability of recording mitotic activity by this method is much greater than by counting mitoses. In all preparations there were many more radioactive nuclei than mitotic figures. Thus the absence of nuclei labeled with incorporated radioactive thymidine in adult corneal endothelium is more significant than the absence of visible mitotic figures; this provides substantial support for the view that the replacement rate of normal adult endothelium is very low or that, as in neural tissue, no replacement occurs. The presence of numerous radioactive nuclei in the endothelium of young and injured corneas indicates that uptake would have been recorded if mitosis had occurred in adult uninjured animals, and these observations confirm the histologic work of others (Ballowitz, 1900; Binder and Binder, 1957; Nagano, 1914; von Sallmann, 1960).

Unlike the lens epithelium which responds to injury with a marked increase in mitotic activity of the neighboring cells (Harding *et al.*, 1959), it appears that the corneal endothelium shows mitotic activity only within the confines of the wound. The enormous numbers of radioactive nuclei which appear in the adult endothelial wound are in marked contrast to their absence in the uninjured neighboring cells.

Summary

The incorporation of tritium-labeled thymidine was studied in the rabbit corneal endothelium. Radioactive nuclei were not found in normal adult endothelium but were observed in the endothelium of rabbits 3 months old and younger and in corneas 24 hr after endothelial abrasion.

291.
Binder, R. F., and Binder, H. F. (1957). *A.M.A. Arch. Ophthalmol.* 57, 11-17.
Cogan, D. C. (1951). *Trans. Am. Acad. Ophthalmol. Otolaryngol.* 55, 228-237.
Harding, C. V., Donn, A., and Srinivasan, B. D. (1957). *Exptl. Cell Research* 13, 582-585.
Harding, C., Hughes, W. L., Bond, V. P., and Schaal, P. (1960). *A.M.A. Arch. Ophthalmol.* 63, 58-65.
Hughes, W. L., Bond, V. P., Brecher, G., Cronkite, E. P., Painter, R. B., Quastler, H., and Sherman, F. G. (1955). *Proc. Natl. Acad. Sci. U. S.* 41, 179-193.
Nagano. (1914). *Arch. Augenheilk.* 76, 28-69.
Painter, R. B., and Drew, R. M. (1959). *Lab. Invest.* 8, 237-253.
Stocker, F. W. (1953). *Trans. Am. Ophthalmol. Soc.* 51, 69-87.
von Sallmann, L. (1960). *Trans. Am. Acad. Ophthalmol. Otolaryngol.* 64, 220-232.

moving aqueous through a second needle. Then the eye was cut in half through the equator and the anterior cup so formed, in some instances with but in others without the lens, was cut into quarters. Fixation was continued in the cold fixative (0° to 4°C.) for 2 to 3 hr. Dehydration was carried out in graded ethanol, finally in 20:80 methyl:butyl methacrylate and embedded in prepolymerized 20:80 methyl:butyl methacrylate containing 1% by weight, Lupereo (50% 2,4-dichlorobenzoyl peroxide with dibutyl phthalate). Alcohol-dehydrated tissue was also embedded in Araldite following standard procedures (Glauert *et al.*, 1956). Both radial and tangential sections were made perpendicular to the surface plane of the iris with the Porter-Blum (Porter and Blum, 1953) type microtome set at 1/40 μ, using a glass knife. They were floated on 10% acetone-water mixture and placed on Formvar and then on carbon-coated (Bradley, 1954) 200-mesh copper grids. The sections were flattened with xylene (Satir and Peachey, 1958) to reduce compression artifacts produced in cutting.

The RCA instruments EMU 3B and 3D, equipped with 10-mil platinum condenser apertures and 40 μ diameter objective diaphragms were used. Micrographs made at magnifications between 1,700 and 30,000 diameters were enlarged photographically either for study or for the illustrations of this paper.

Results and Discussion

The pigment epithelium of the iris in the rhesus monkey and man consists of two layers of cells, the anterior and posterior layers. The posterior layer is composed of cuboidal to cylindrical cells which are filled with pigment granules (Fig. 1). The free posterior surface of these cells faces the posterior chamber. Their nuclei are generally round and frequently indented. Smaller indentations are sometimes in juxtaposition to pigment granules, suggesting the relatively greater hardness of the pigment granules as compared with that of the nuclear envelope and its contents. The nucleus appears to be limited by a double membrane. Its internal contents, both granular and filamentous, are fairly uniform in appearance. At least one marginal nucleolus is present.

Most of the cytoplasm is occupied by the pigment granules. These are fairly uniform in size and shape. In sections the majority appear round but isolated pigment granules obtained from both the rhesus monkey and man, include spherical and ovoid forms. The dimensions of these granules observed in sectioned tissue are similar to those of isolated granules. When a comparison is made between the pigment granules in the posterior epithelial layer of the rhesus monkey and of man, no

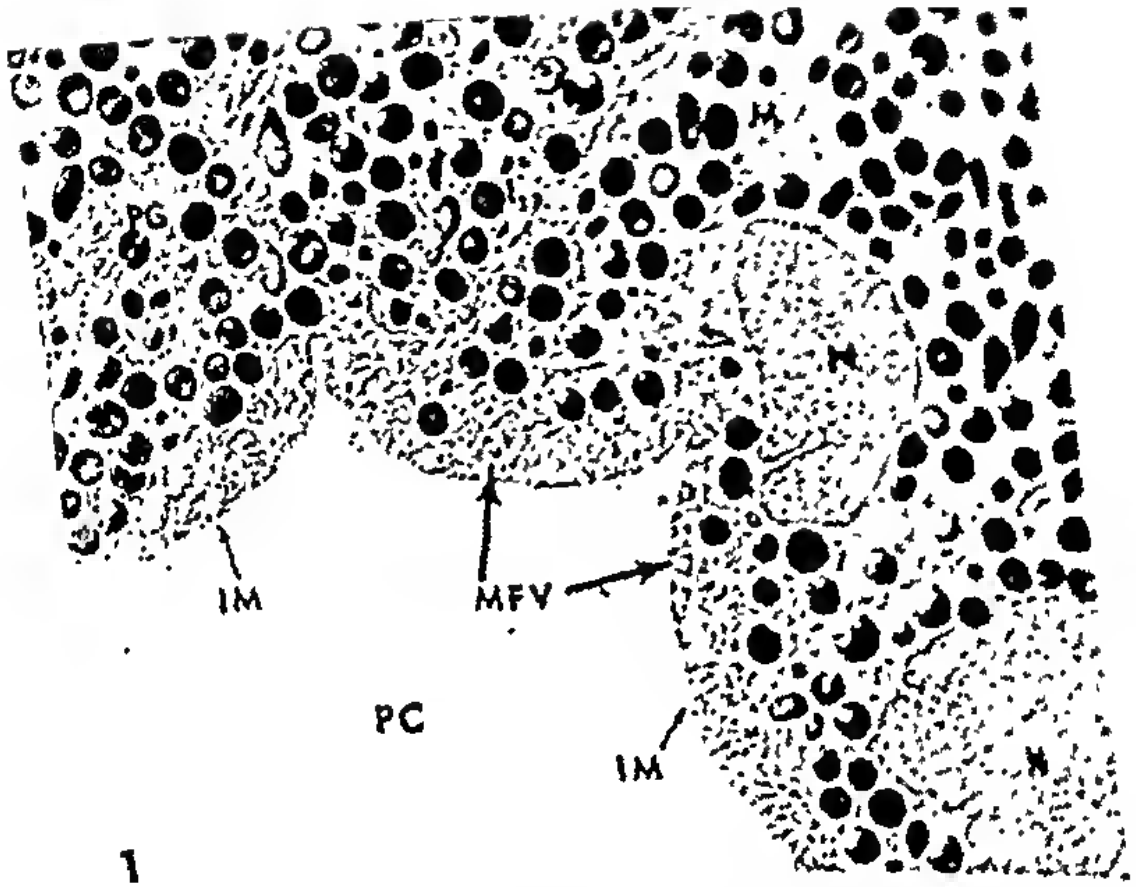

1

FIG 1. Electron micrograph showing a portion of the posterior layer of pigment epithelium from the iris of a 42-year-old man. In the cytoplasm of the cells there are many dense pigment granules (PG) and very few mitochondria (M). The plasma membrane, facing the posterior chamber (PC), is infolded, resulting in a network of irregularly arranged villi (MFV). A basement membrane (the internal limiting membrane, IM), covers the entire posterior surface without discontinuities. Internal contents of the nuclei (N) appear granular, while the nuclear envelopes show two types of indentations, the usual epithelial cell nuclear membrane infoldings which are characteristic for these cells and certain nuclear surface depressions associated with the presence of pigment granules. Intercellular spaces (I_{sp}) are seen between adjacent cells and extending up to the internal limiting membrane. Magnification. × 9100.

granular component, usually less than 100 Å in width, is distributed throughout the cytoplasm of these cells. No specific orientation of this component has been observed. A structure similar to the Golgi apparatus of other cells has been observed only occasionally. Numerous small vesicles appear throughout the cytoplasm of most of these cells.

The posterior surface of these cells occasionally appears fairly flat with very few infoldings of the plasma membrane but more often contains numerous infoldings. These are villus-like cytoplasmic projections of irregular shape and orientation. As a rule, they are best seen in somewhat tangential sections of the posterior surface (Fig. 2). Interdigitated infoldings of the plasma membrane between adjacent cells

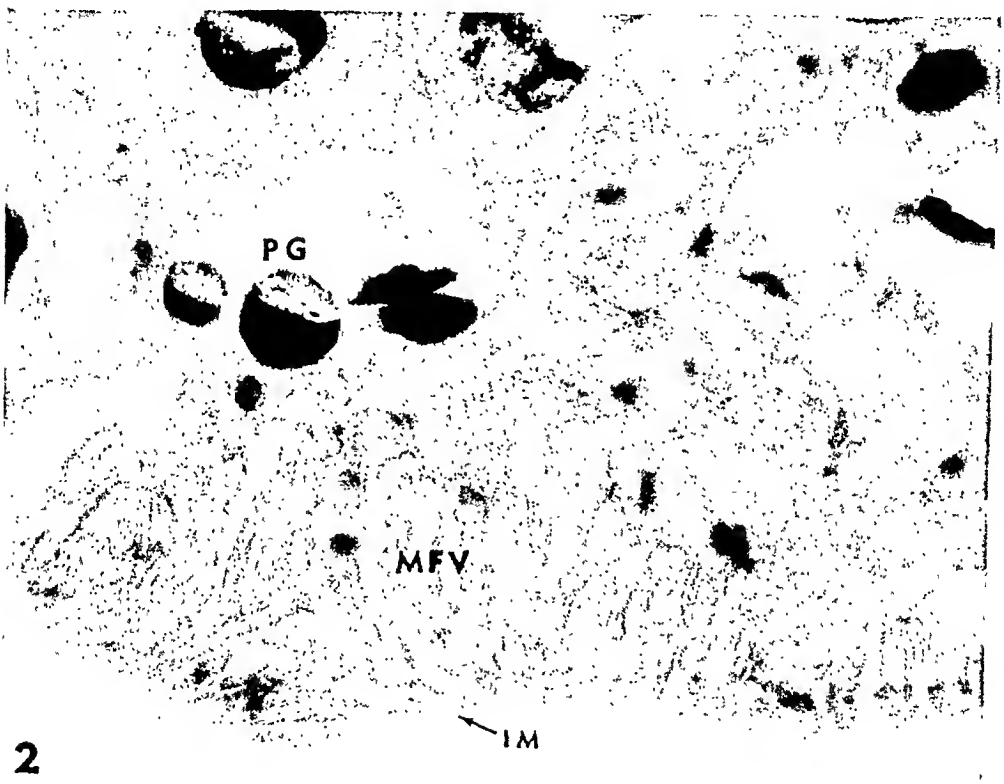

FIG. 2. Posterior surface of the pigment epithelium showing plasma membrane infoldings, forming a network of irregularly arranged villi (MFV). The appearance of the internal limiting membrane (IM) suggests that this section is somewhat tangential. Both mitochondria and pigment granules (PG) are found up to and within the infolded membrane. Small granules of 50 Å or less in size, appear within the folded and/or branched villi. A 42-year-old human iris. Magnification: × 19,600.

similar to those found in the nonpigmented epithelium of the ciliary body (Pease, 1956; Holmberg, 1957; Pappas and Smelser, 1958) are not observed.

Intercellular spaces measuring up to about 1 μ in width are found between the cells of this layer. Within these spaces, a few microvilli can be seen (Figs. 3 and 4). Similar observations were made using various fixatives (e.g., osmium tetroxide and potassium permanganate in isotonic

Covering the entire posterior surface of the iris there is a filamentous structure resembling a basement membrane, the "internal limiting membrance" (Salzmann, 1912). This filamentous membrane frequently appears multilayered and continues without interruption over the free surface and villus-like processes of the pigment cells (Fig. 5). This

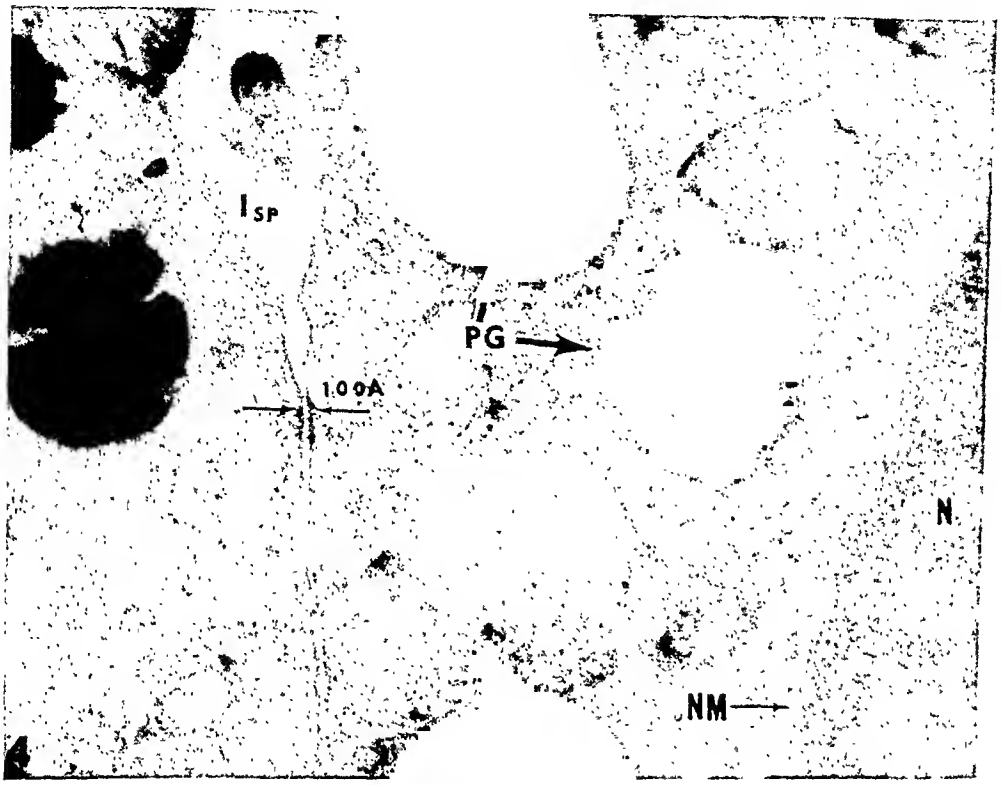

FIG. 4. The granular-appearing nucleus (N) of the posterior layer pigment cell is limited by a double discontinuous nuclear membrane (NM). Pigment granules (PG), in the cytoplasm of the two adjacent cells, show certain distortions probably due to cutting. In general the periphery of these granules is not well defined. Occasionally, a very dense granular material (of 50 Å size or less) appears to be condensed around some of the pigment granules (PG). Intercellular spaces (Isp) are observed between epithelial cells, however, the plasma membranes are also found to approach one another very closely leaving only a 100 Å space in-between. Vesicles and the filamentous-granular component (less than 100 Å) comprise the remaining cytoplasm. Rhesus monkey iris. Magnification: × 49,000.

material does not extend into the spaces between the cells. The presence of such a multilayered basement membrane could help support the rather loosely connected cells of the pigment epithelium during constriction and dilatation of the iris.

The intercellular spaces between the anterior and posterior cell layers are even more prominent than the spaces between cells within

each layer (Fig. 6). They are fairly irregular and larger where microvilli are present. The microvilli project into each cavity from the anterior surface of the posterior layer and to a lesser extent from the posterior surface of the anterior layer. These microvilli are fairly uniform in width (about 1000 Å) and length (up to 1 μ).

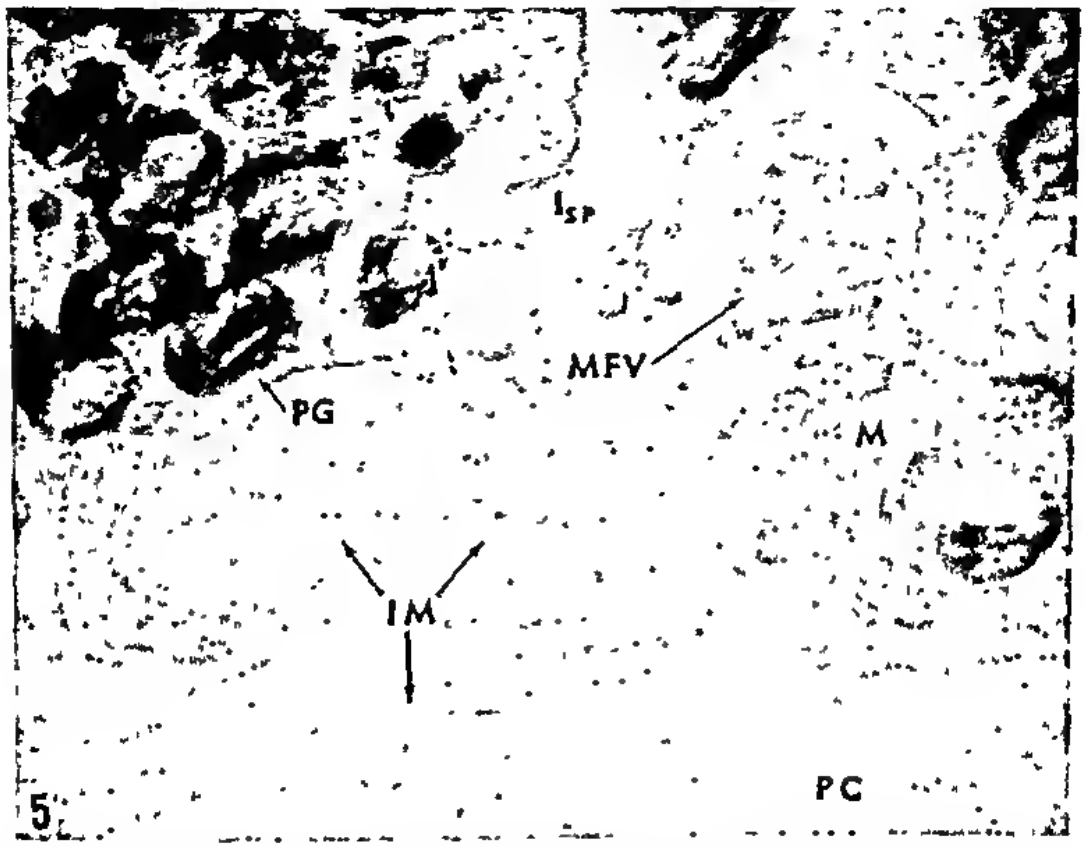

FIG 5 Posterior surface of the pigment epithelium (rhesus monkey) showing a multilayered internal limiting membrane (IM). Both pigment granules (PG) and mitochondria (M) are found near the infolded cytoplasmic membrane (MFV). Openings of the intercellular spaces (I_{SP}) are covered by the internal limiting membrane which shows a filamentous appearance at this magnification. The posterior chamber (PC) is shown. Magnification: × 27,400.

The cells forming the anterior layer of pigment epithelium are more cuboidal and only about one-half as tall as those in the posterior layer; thus the anterior layer accounts for approximately one-third the total thickness of the pigment epithelium. Ribbonlike cytoplasmic prolongations project from the anterior surface of these cells (Tousimis and Fine, 1959a). These cytoplasmic prolongations become continuous with the dilator muscle fibers. Overlapping of these cytoplasmic prolongations gives the impression of a multilayered dilator muscle (Fig. 6) extending from the iris root to the region of the sphincter muscle.

Covering the entire posterior surface of the iris there is a filamentous structure resembling a basement membrane, the "internal limiting membrance" (Salzmann, 1912). This filamentous membrane frequently appears multilayered and continues without interruption over the free surfaee and villus-like processes of the pigment cells (Fig. 5). This

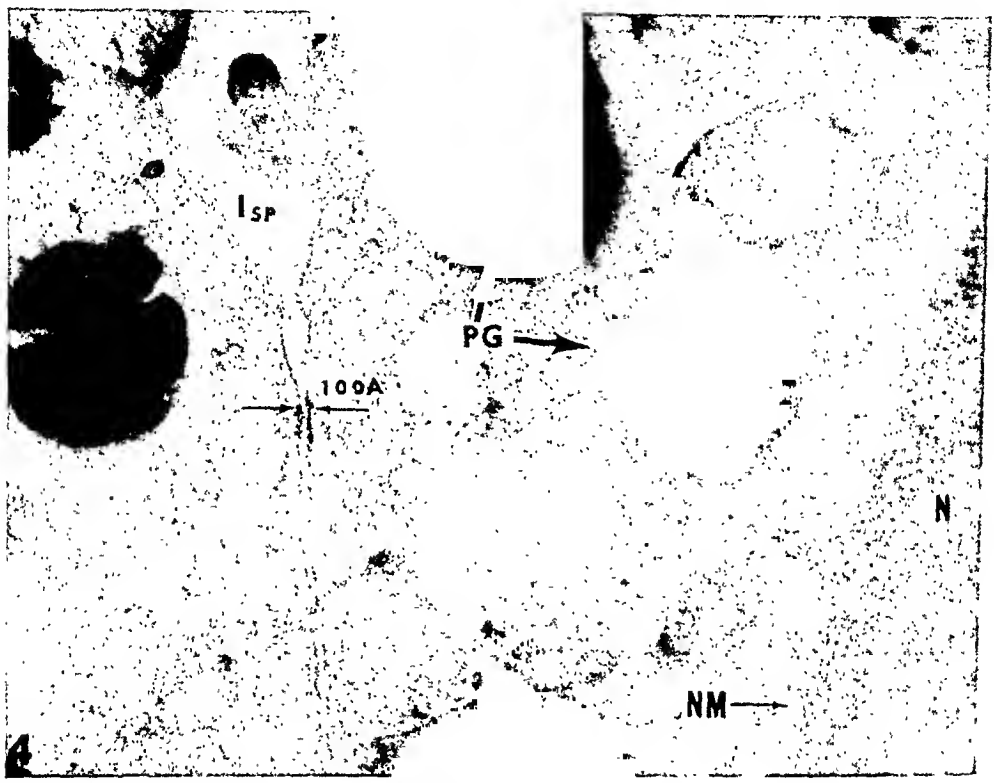

FIG. 4. The granular-appearing nucleus (N) of the posterior layer pigment cell is limited by a double discontinuous nuclear membrane (NM). Pigment granules (PG), in the cytoplasm of the two adjacent cells, show certain distortions probably due to cutting. In general the periphery of these granules is not well defined. Occasionally, a very dense granular material (of 50 Å size or less) appears to be condensed around some of the pigment granules (PG). Intercellular spaces (Isp) are observed between epithelial cells, however, the plasma membranes are also found to approach one another very closely leaving only a 100 Å space in-between. Vesicles and the filamentous-granular component (less than 100 Å) comprise the remaining cytoplasm. Rhesus monkey iris. Magnification: × 49,000.

material does not extend into the spaces between the cells. The presence of such a multilayered basement membrane could help support the rather loosely connected cells of the pigment epithelium during constriction and dilatation of the iris.

The intereellular spaces between the anterior and posterior cell layers are even more prominent than the spaces between cells within

each layer (Fig. 6). They are fairly irregular and larger where microvilli are present. The microvilli project into each cavity from the anterior surface of the posterior layer and to a lesser extent from the posterior surface of the anterior layer. These microvilli are fairly uniform in width (about 1000 A) and length (up to 1 μ).

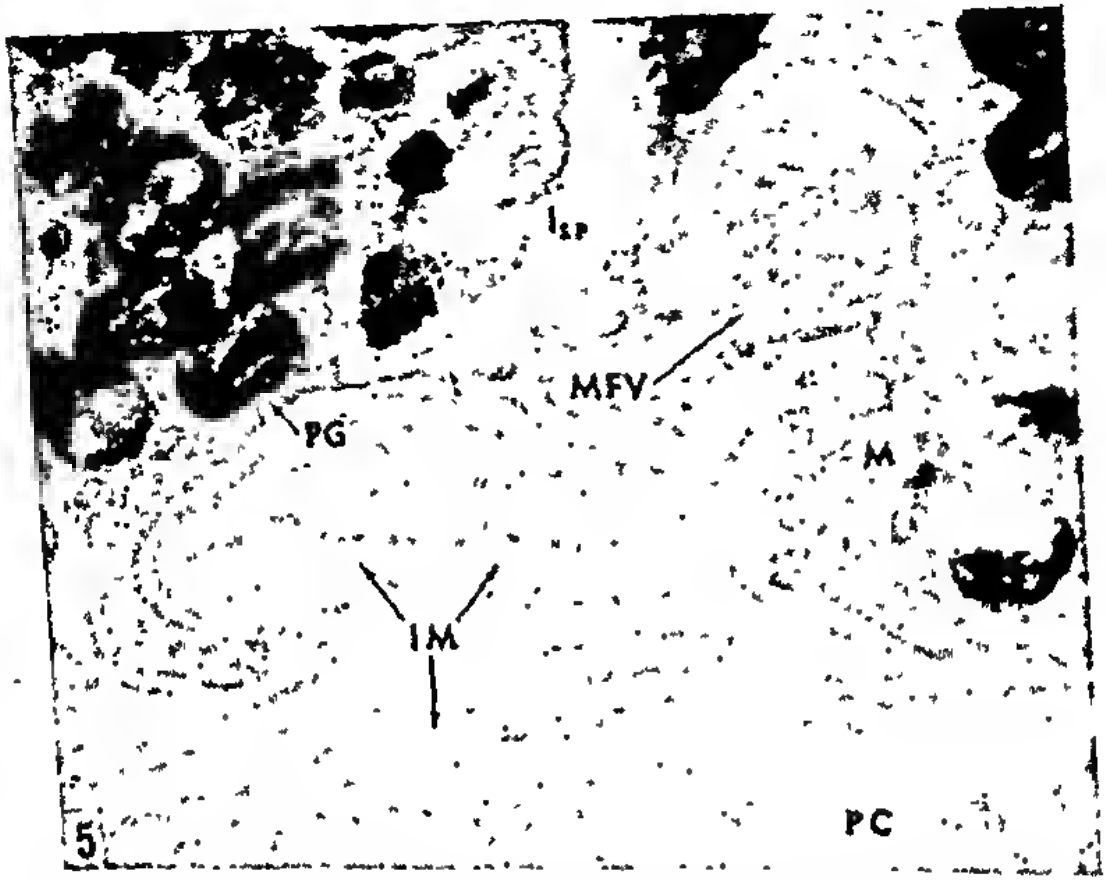

FIG. 5 Posterior surface of the pigment epithelium (rhesus monkey) showing a multilayered internal limiting membrane (IM). Both pigment granules (PC) and mitochondria (M) are found near the infolded cytoplasmic membrane (MFV). Openings of the intercellular spaces (I_{sp}) are covered by the internal limiting membrane, which shows a filamentous appearance at this magnification. The posterior chamber (PC) is shown. Magnification. × 27,400.

The cells forming the anterior layer of pigment epithelium are more cuboidal and only about one-half as tall as those in the posterior layer; thus the anterior layer accounts for approximately one-third the total thickness of the pigment epithelium. Ribbonlike cytoplasmic prolongations project from the anterior surface of these cells (Tousimis and Fine, 1959a). These cytoplasmic prolongations become continuous with the dilator muscle fibers. Overlapping of these cytoplasmic prolongations gives the impression of a multilayered dilator muscle (Fig. 6) extending from the iris root to the region of the sphincter muscle.

Long mitochondria oriented in the direction of the major axis of the cytoplasmic prolongations forming the dilator muscle are found in a matrix of myofibrils. Many vesicles are also present throughout this cytoplasm. The nucleus of these cells is contained within the posterior portion of the cell. It is usually elongated and flattened in the direction

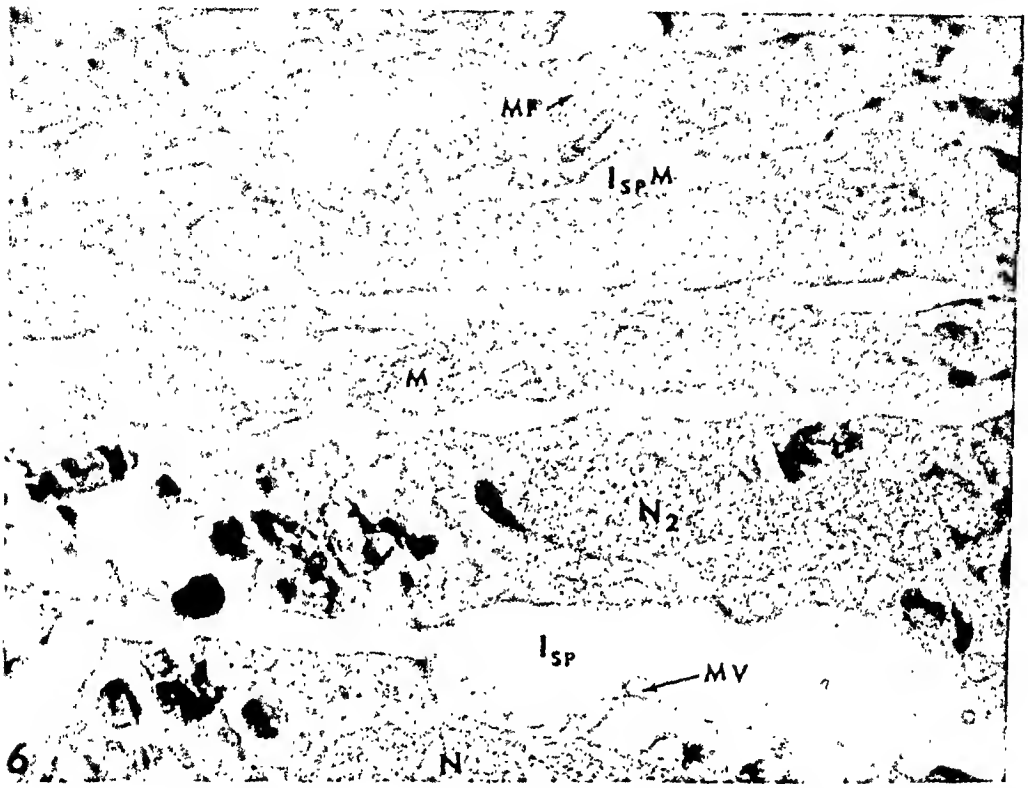

FIG. 6. Dilator muscle of both rhesus monkey or human eye iris consists of cytoplasmic processes of the anterior pigment epithelium layer. These processes are ribbonlike and extend over the rest of the remaining pigmented cell and other prolongations. Only a few pigment granules are found within the dilator muscle process. These granules are similar in size, shape, and internal composition to those of the remaining cell. Both myofibrils (MF) and mitochondria (M) are similar to those found in the sphincter smooth muscle with their long axis in the direction of the cytoplasmic prolongation. Nuclei (N_2) of the anterior pigment epithelium layer are flattened and oriented in the direction of their cytoplasmic process. The nucleus (N) of the cell from the posterior layer is shown in the lower portion of the electron micrograph. A typical intercellular space (I_{SP}) between the posterior and anterior layers appears in the lower right side of the figure. Delicate microvilli are present in the enlarged portions of these intercellular spaces (MV). Interdigitation between cytoplasmic processes (dilator muscle ribbons) is frequently seen. A well-defined intercellular space ($I_{SP}M$) is always present in between. This "space" contains a basement membrane-type material similar to that found between the smooth muscle cells of the iris sphincter. Rhesus monkey iris. Magnification: × 16,800.

of the cytoplasmic process. Numerous pigment granules and larger mitochondria are present about the nucleus. The mitochondria appear larger than those of the posterior epithelial layer. Within the dilator muscle, there are a few pigment granules, similar in size, shape, and internal composition to those found in the pigment epithelium.

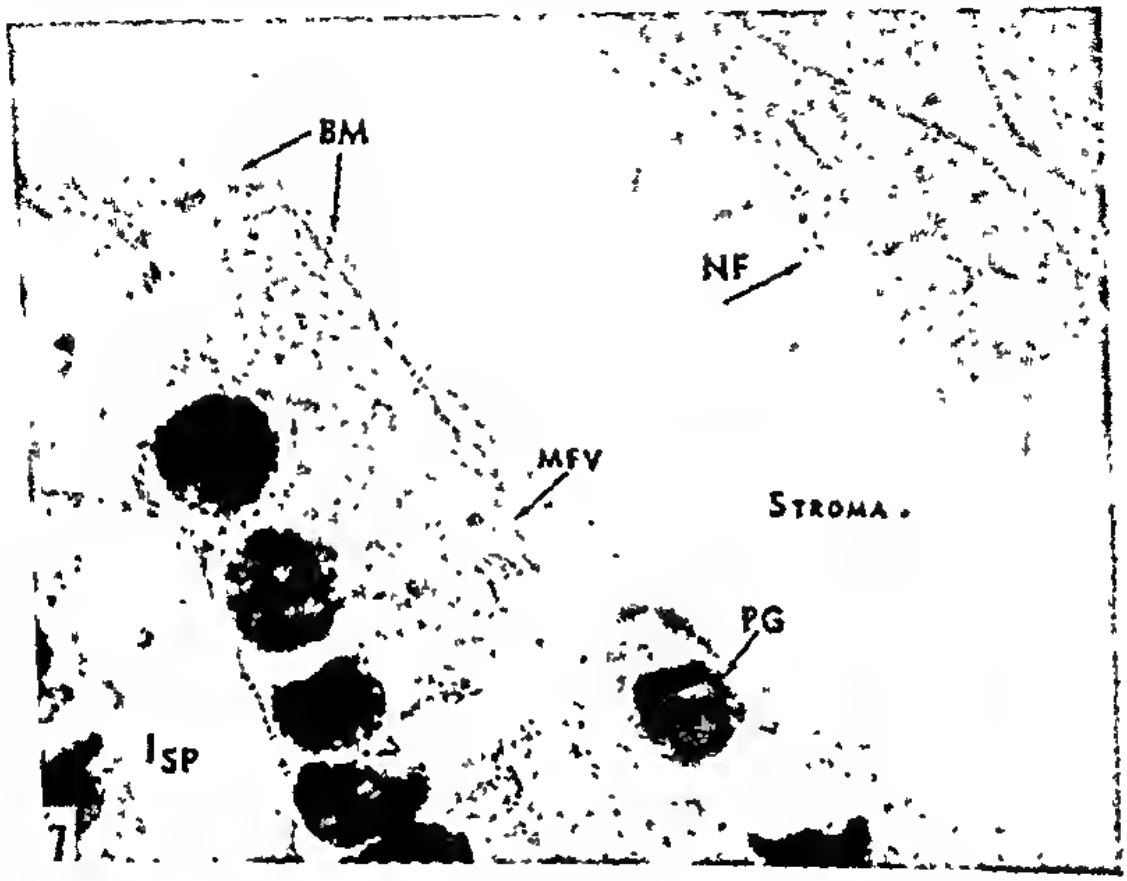

FIG 7. The anterior pigment epithelium, at the pupillary zone directly posterior to the sphincter muscle, lacks smooth muscle cytoplasmic prolongation and is covered by a basement membrane (BM). The cytoplasm of these cells contains pigment granules (PG) similar in size, shape, and internal structure to those of the posterior pigment epithelium layer. Intercellular spaces (I_{SP}) extend up to the anterior limiting membrane. Few plasma membrane foldings, villi (MFV) are present both within the intercellular spaces and near the anterior surface. A filamentous granular component is seen within the cytoplasm of these cells. A somewhat tangentially cut nonmyelinated nerve fiber (NF) appears at the upper right portion of this electron micrograph. Rhesus monkey iris. Magnification: × 27,400

Between the muscle ribbons (anterior cell layer processes) there is a fibrillar semiopaque material (Fig. 6). Preliminary examination at higher magnification suggests that this intercellular substance is similar to other basement membranes such as those found about capillaries. Nonmyelinated nerve fibers are observed within and on the surface of

the dilator muscle. Focal collections of intracytoplasmic microvesicles resembling synaptic vesicles (De Robertis and Bennett, 1954; Palade and Palay, 1954) are present in these nerve fibers.

At the pupillary margin the anterior epithelial layer lacks the cytoplasmic prolongations which give rise to the dilator muscle, and in

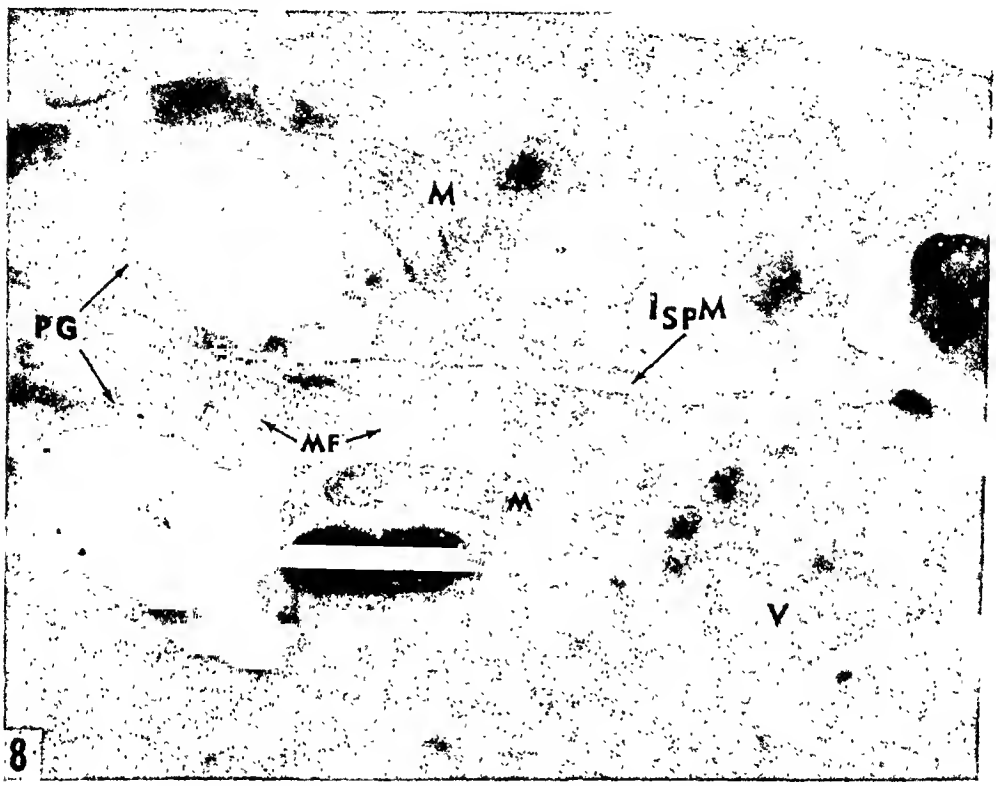

FIG. 8. Electron micrograph showing portions of two longitudinally sectioned cytoplasmic prolongations of sphincter muscle cells. They contain many myofibrils (MF) oriented parallel to the long axis of the processes and numerous vesicles (V). Some of these vesicles appear near to or originate at the plasma membrane of the cell. Mitochondria (M) with many internal cristae are elongated and oriented in the direction of the muscle fiber. Pigment granules (PG) found within the cytoplasm of these cells, are similar in size, shape (section), and internal structure to those of the pigment epithelium layers. Intercellular spaces ($I_{SP}M$) contain a fairly uniform, fibrillar semiopaque substance. Iris from the human eye. Magnification: × 28,000.

general resembles more closely the posterior layer. Intercellular spaces are as prominent as those of the posterior layer (Fig. 7) and the anterior surface in the pupillary zone is covered with a basement membrane.

The sphincter muscle consists of smooth muscle cells whose nuclei are elongated in the direction of their long axes (concentric with the pupil). Many elongated mitochondria, similar to those of the dilator

That is what the Greek words mean. That is a sufficient definition. I think it is good to think of all the different attachment bodies in one category. Terminal bars and the nodes of Bizzozero can be considered as desmosomes of different geometric manifestations. Amongst desmosomes there are some which do indeed show the extra layers to which you referred, though I do not wish to concur in the interpretation you gave to those layers. Some desmosomes have the characteristic appearance which you have shown. Thus I am quite comfortable in calling your structures desmosomes and in interpreting them as attachment areas between adjacent epithelial cells.

DR. TOUSIMIS: By the same definition, however, one will have to call every single portion of the two cell membranes or two plasma membranes that come close together desmosomes.

DR. BENNETT: On the contrary. That is neither the purpose nor the intent of my definition. I refer to a desmosome as a region where two plasma membranes are attached together and not as a region where they just lie in apposition. For example, you may have a group of lymphocytes in a lymph node lying together without a single desmosome in sight. In your pictures you showed some regions where the membranes were like that. But in the particular regions where the special densities appeared, one could discern the characteristic features of desmosomes. Thus there are regions where the membranes merely lie close together, and other regions which are characterized by the characteristic densities of desmosomes. I am comfortable in regarding these latter regions as attachment areas and not as areas where the membranes merely lie together in apposition without attachment.

DR. TOUSIMIS: Well, it's just a matter of interpretation, I think, what one calls desmosomes. I agree with you on the meaning of the word, desmosome as an attachment body, but I still fail to see from our electron micrograph, shown here, that they are desmosomes, that is, special attachment bodies.

The Fine Structure of the Ciliary Epithelium in Relation to Aqueous Humor Secretion[1]

GEORGE D. PAPPAS AND GEORGE K. SMELSER

Departments of Anatomy and Ophthalmology, College of Physicians and Surgeons, Columbia University, New York, New York

IT IS WELL KNOWN THAT INFOLDED cell membranes are found in epithelia noted for their water transport (Pease, 1956). Such elaborate cell membranes are found in the cell epithelium facing the posterior chamber of the eye and have been shown to change under conditions which affect aqueous humor secretion (Holmberg, 1957b; Pappas and Smelser, 1958).

It has recently been shown that the two types of membrane elaborations, the surface infoldings facing the posterior chamber, and the interdigitated margins of adjacent epithelial cells, may function differently in the formation of aqueous humor (Pappas *et al.*, 1959). In order to determine the functions of these types of membrane elaborations, Thorotrast was injected into the posterior chamber. Electron-opaque thorium dioxide particles were found to be reabsorbed at the site of the surface infoldings but not at the marginal folds which interdigitate with the neighboring cells.

Further observations on the reabsorptive processes of the elaborated membranes as a function of secretion are reported in this communication. It is suggested that the surface infoldings reabsorb materials from the provisional aqueous humor. A consideration of the marginal interdigitations as site of formation of the provisional aqueous humor is presented.

Materials and Methods

The ciliary processes studied were from (2.5 to 3.0 kg) adult albino rabbits. The rabbits were anesthetized with pentobarbital (Nembutal), and dibucaine (Nupercainal) was applied topically.

A solution of 1% osmium tetroxide in 1/14 *M* (barbital) Veronal acetate buffer, pH 8.1, was used as a fixative. The tissues were always fixed by injecting this solution through the cornea and pupil into the posterior chamber of the eye. Excess fixative drained away through a keratome incision in the cornea. The eye was then rapidly enucleated, opened, and the processes and iris flooded with additional fixative. Small pieces of the ciliary processes were fixed for 20 to 30 min. The tissue

[1] Supported by Grant B-1202 of the United States Public Health Service.

was subsequently dehydrated in ethyl alcohol and embedded in a mixture of 90% butyl and 10% methyl methacrylate. The blocks were polymerized overnight at 45°C. Thin sections were cut on a Porter-Blum microtome and examined with an RCA-EMU-3C electron microscope.

When Thorotrast (Testagar & Co., Detroit, Michigan), a colloidal suspension of thorium dioxide particles, was used, it was introduced into the posterior chamber by a transcorneal injection. Approximately 0.1 ml of aqueous humor was removed and replaced by a similar amount of the Thorotrast solution.

In the experiments with acetazolamide (Diamox), 100 mg/kg was injected intravenously. The eye was fixed 20 min later.

Elevation of intraocular pressure was accomplished by inserting a 27-gage hypodermic needle into the anterior chamber of the normal eye and connecting the needle to a column of Ringer's solution rising about 100 cm above the level of the eye. Thirty minutes later, the eye was fixed.

Observations

It is well established that aqueous humor is secreted by the ciliary body, which, in many species, shows great elaboration of its surface, forming the ciliary processes. The functional unit of the ciliary process is the tissue lying between the lumen of the ciliary capillaries and the posterior chamber. The capillaries are extremely large, and have a very thin wall (Fig. 1). Pores of considerable size have been described (Pappas, 1959; Pappas *et al.*, 1959; Holmberg, 1959b) in these typically thin endothelial walls. Similar capillary structure is also found in other areas where considerable amounts of fluid are transferred (Bennett *et al.*, 1959).

Various cells (fibroblasts, histiocytes) can be found in the connective tissue stroma. The relatively coarse collagen fibers of the con-

---

FIG. 1. Electron micrograph of a section of a ciliary process of an albino rabbit. Two layers of cells make up the ciliary epithelium. One layer of epithelial cells (E) faces the posterior chamber (PC). The other layer (P) which is pigmented in nonalbino animals, faces the connective tissue stroma (CT). A portion of a thin-walled capillary (Cap), containing red blood cells, is seen. The ciliary epithelium is lined on both surfaces by basement membranes. The internal limiting membrane (ILM) lines the cells facing the posterior chamber, and the external limiting membrane (ELM), the connective tissue basement membrane, lines the pigment cell layer. Elaborate interdigitated margins (I) are evident between the epithelial cells facing the posterior chamber. Magnification: × 8500.

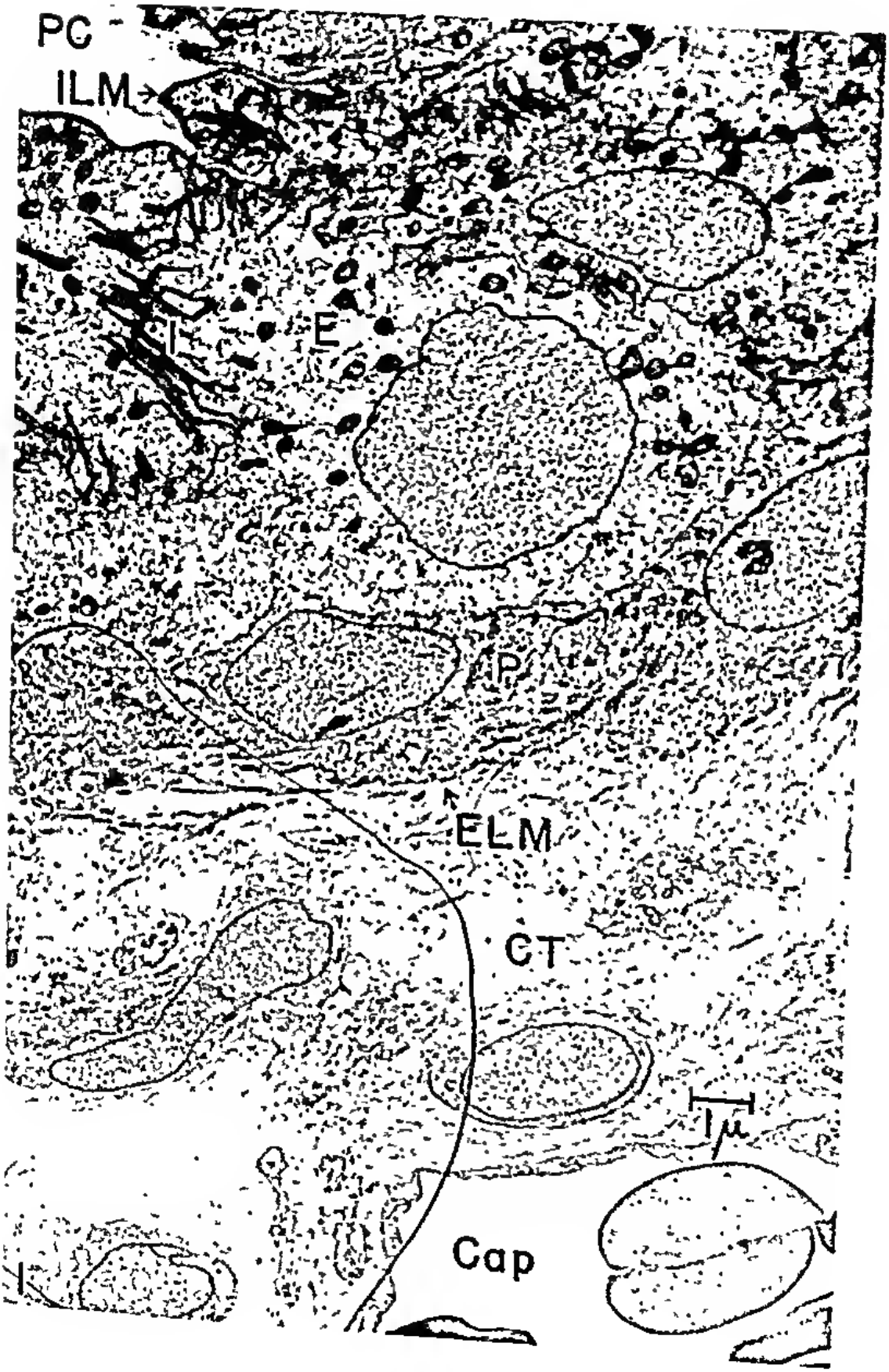
PC
ILM
E
IP
ELM
CT
1μ
Cap

nective tissue have been shown to be in close association with the finely fibrous basement membrane (Pappas and Smelser, 1958).

The two epithelial cell layers of the ciliary processes develop from the single sheet of neuroectoderm, which forms the optic cup. By folding upon itself, this sheet forms both of these layers. Therefore, the surface of the pigment epithelium (P) which rests upon the connective tissue is continuous with the inner layer of the optic cup which faces the posterior chamber (PC) (Fig. 1). The surface of the epithelial cell facing the posterior chamber is also covered by a "basement membrane"—the internal limiting membrane (ILM in Figs. 1 and 2). Zonular fibers do not penetrate into or between the epithelial cells but rather terminate at the internal limiting membrane (Pappas and Smelser, 1958).

The most striking feature of the epithelial cell layer facing the posterior chamber is the extensive elaborations of the membranes. These elaborations are of two types: (a) the highly interdigitated membranes forming the margins between these cells (Figs. 1 and 2), and (b) infoldings of the surface facing the posterior chamber (Fig. 3).

About two-thirds of the apical margins of the epithelial cells are highly interdigitated (Figs. 1 and 2). The intercellular space (S) between adjacent cells varies greatly in width (Fig. 2). In the normal adult rabbit, rows of vesicles (R) are occasionally found alongside these interdigitated borders (Fig. 2).

The surface of these cells facing the posterior chamber (PC) has many infoldings (I) of the limiting membrane. When Thorotrast is injected into the posterior chamber of the normal eye, thorium dioxide particles adhere to the internal limiting membrane and also enter the infoldings (Fig. 3). Note that many vesicles (V) containing thorium dioxide particles are found in the cytoplasm. This suggests that some of the vesicles found normally in the area of the infoldings are formed by pinching off from the infolded membranes (Fig. 3). However, no thorium dioxide particles have been found to enter the interdigitated margins of these cells (Pappas *et al.*, 1959).

It was reported previously that when normal aqueous humor secretion is altered experimentally by a number of methods, the infoldings and interdigitations tend to disappear, and that large numbers of vesicles

---

FIG. 2. Electron micrograph of a margin between two ciliary epithelial cells which face the posterior chamber (PC). The surface is lined with the internal limiting membrane (ILM). The elaborate interdigitations of the limiting membranes characterize the margins (at arrow) of these cells. The intercellular space (S) between adjacent cells varies greatly in width. In the normal adult rabbit, rows of vesicles (R) are occasionally found alongside these interdigitated borders. Magnification: × 33,000.

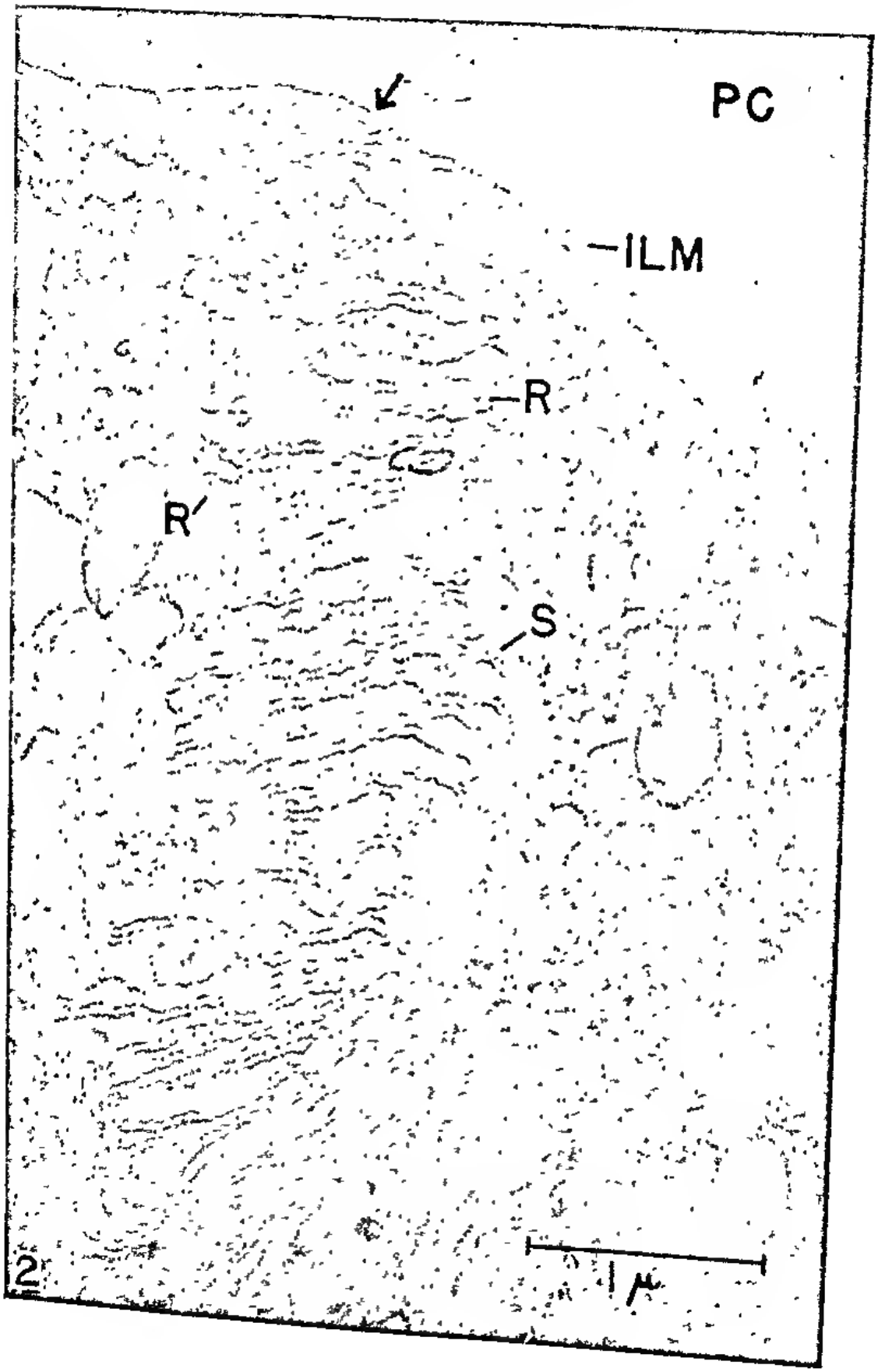
PC
ILM
R
R'
S
2
1 μ

are found in these areas (Smelser, 1958; Pappas and Smelser, 1958; Pappas *et al.*, 1959). Another method of altering normal secretion, described in this paper, is by greatly increasing intraocular pressure. The electron micrograph of Fig. 4 shows the alterations which occur in the fine structure of the cells, when this procedure is followed. These changes are very similar to the changes seen when other experimental methods are used.

Rows of vesicles (V) are found in the areas of the infoldings, which are now not as numerous as in the normal. Not all of the cellular constituents appear to be altered by the increase in intraocular pressure, the Golgi complex (G), for example, appears to be more or less intact.

In order to establish more clearly the relationship between vesicles and infoldings, Thorotrast was injected into the posterior chamber followed immediately by an intravenous injection of Diamox. About 20 min later the eye was fixed and enucleated. Figure 5 illustrates the changes that took place. Rows of vesicles containing thorium dioxide particles are found in the areas where infoldings are normally present. This shows clearly that the rows of vesicles must have been formed by the pinching-off of the infolded cell membranes facing the posterior chamber. It was also observed that the rows of vesicles in the areas of the interdigitations did not contain thorium dioxide particles.

Discussion

Cells active in fluid transport typically have elaborated cell membranes. This is seen, for example, in the cells lining the nephron (Rhodin, 1954; Pease, 1955), in the choroid plexus (Maxwell and Pease, 1956), in the salivary gland (Scott and Pease, 1959), and in the ciliary epithelium (Holmberg, 1957b; Pappas and Smelser, 1958).

There is no secretion of aqueous humor in the newborn rabbit, and the ciliary epithelial cells have simple nonelaborated margins (Pappas *et al.*, 1959). Aqueous secretion starts by the seventh postnatal day (Kinsey, 1950). At this time the cells begin to develop the elaborated membranes characteristic of the adult ciliary epithelium. It thus appears that an elaborated cell membrane may be essential to, or at least facil-

---

FIG. 3. The surface of the ciliary epithelium facing the posterior chamber (PC) shows infoldings (I) of the cell membrane. This electron micrograph was taken from tissue fixed 20 min after the injection of Thorotrast into the posterior chamber. Thorium dioxide particles adhere to the internal limiting membrane lining the free surface. The infoldings also contain these particles. Reabsorption takes place in the infoldings. Note the numerous vesicles (V) containing thorium particles in the cytoplasm. M = mitochondria. Magnification: × 33,000.


PC
I
I
V
M
V
V
M
1 μ
×3

itate, the process of secretion although the precise mechanism is not clear. The advantages of increased surface area for the transport of material from the cytoplasm to the surrounding milieu have not been demonstrated. On the other hand, adsorption of material does occur from the milieu onto the elaborated outer membrane surface of cells (Brandt and Pappas, 1960). Brandt (1958) demonstrated that the first step in pinocytosis is the attachment of solute (such as protein) onto the cell membrane from the surrounding milieu. This step is followed by the uptake of the solute into pinocytosis vesicles in the cytoplasm of the cell. Palay and Karlin (1959) and Clark (1959) have shown the "absorption" of fat at the microvillus border of the cells lining the small intestine. Tennyson (1960) has demonstrated the attachment of thorium dioxide particles from the cerebrospinal fluid onto the surface of the polypoid processes of the choroid plexus cells. Following this surface attachment, the thorium particles are taken into the cytoplasm via membrane-bound vesicles. A similar process occurs in the surface ciliary epithelial cells (Pappas *et al.*, 1959). Note that some particles appear in the infoldings and in the vesicles in the cytoplasm (Fig. 3).

However, Thorotrast is neither accumulated in nor reabsorbed by the interdigitations (Pappas *et al.*, 1959; Pappas, 1959). This differential reabsorption of Thorotrast suggests that the surface infoldings differ from the marginal interdigitations in their reabsorptive capacity.

An important aspect of secretion in the nephron tubules, or in tubular glands such as the salivary gland, is the process of the reabsorption of materials from an initial filtrate or actively secreted "crude" product. In the ciliary process, the net result of the activity of the two epithelial cell layers is the secretion of aqueous humor. It is therefore reasonable to suggest that the adsorption of thorium dioxide onto the surface of the epithelial cell with its many infoldings, and the subsequent uptake of the particles into cytoplasmic vesicles may indicate that this is a site of reabsorption. In contrast, the marginal interdigitations seen in cells in the normal eye do not reabsorb the thorium dioxide.

After normal aqueous secretion has been altered, reabsorption of thorium dioxide particles does not occur. In contrast to the normal eye, the thorium dioxide particles adhere poorly to the cell membrane. None

---

FIG. 4. Electron micrograph of a portion of the ciliary epithelium facing the posterior chamber (PC). Before fixation, the intraocular pressure was experimentally elevated for 30 min. This was accomplished by inserting a hypodermic needle into the anterior chamber of the normal eye. The needle was connected to a 100-cm column of Ringer's solution. Many of the infoldings are no longer present. The rows of vesicles (V) are found in the areas of the infoldings. The Golgi complex (G) appears normal and not dispersed. Magnification: × 36,000.


PC
V
V
V
G
4
1 μ

of the particles are found in the remaining infoldings or in vesicles in the cytoplasm. This suggests that when normal aqueous formation is altered, there is a concomitant interference with the function of the remaining surface infoldings.

It has been shown that most of the cell infoldings and marginal interdigitations disappear when normal aqueous secretion is altered by a variety of methods. These include (1) injection of Diamox (Fig. 5); (2) injection of *Shigella* endotoxin; (3) blocking the drainage angle; (4) decreased intraocular pressure; and (5) increased intraocular pressure (Fig. 4). Large numbers of vesicles appear in the cytoplasm when normal secretion is altered (Pappas and Smelser, 1958; Pappas *et al.*, 1959; Pappas, 1959). While similar vesicles are normally present, they are not found in such large numbers.

Holmberg (1957b) suggested that the increased number of vesicles after Diamox injection may be due to the breakdown of the Golgi complex. In our observations made with the light and electron microscopes, the Golgi complex is not extensively developed in the ciliary epithelium. The breakdown of the Golgi complex would not account for the very large numbers of vesicles present.

Figure 4 shows a portion of a ciliary epithelial cell taken from a rabbit after increased intraocular pressure was induced experimentally. Many vesicles are seen in linear arrangement in the areas where surface infoldings would be present in normal, unaltered cells. It is interesting to note that elements of the Golgi complex are also present, even though it is difficult to determine whether the entire complex of the cell is still intact.

More recently, the vesicles found in the cytoplasm of the surface ciliary epithelial cells have been interpreted as secretory vesicles because Diamox, which partially inhibits normal aqueous secretion, causes these vesicles to accumulate in the cytoplasm (Holmberg, 1959a). However, if thorium dioxide is injected into the posterior chamber, followed by a systemic injection of Diamox, the vesicles which are found in linear arrangements, in the areas where infoldings are normally present, contain thorium dioxide particles (Fig. 5). This shows that the vesicles are

---

FIG. 5. Electron micrograph of the ciliary epithelium facing the posterior chamber (PC). Thorotrast was injected into the posterior chamber and this was followed by an intravenous injection of Diamox. Twenty minutes after Diamox injection, the tissue was fixed. Rows of vesicles (V) containing thorium dioxide particles are found in the areas where infoldings are normally present. This shows clearly that the rows of vesicles were formed by the breakdown of the infoldings. M = mitochondria. Magnification: × 29,000.

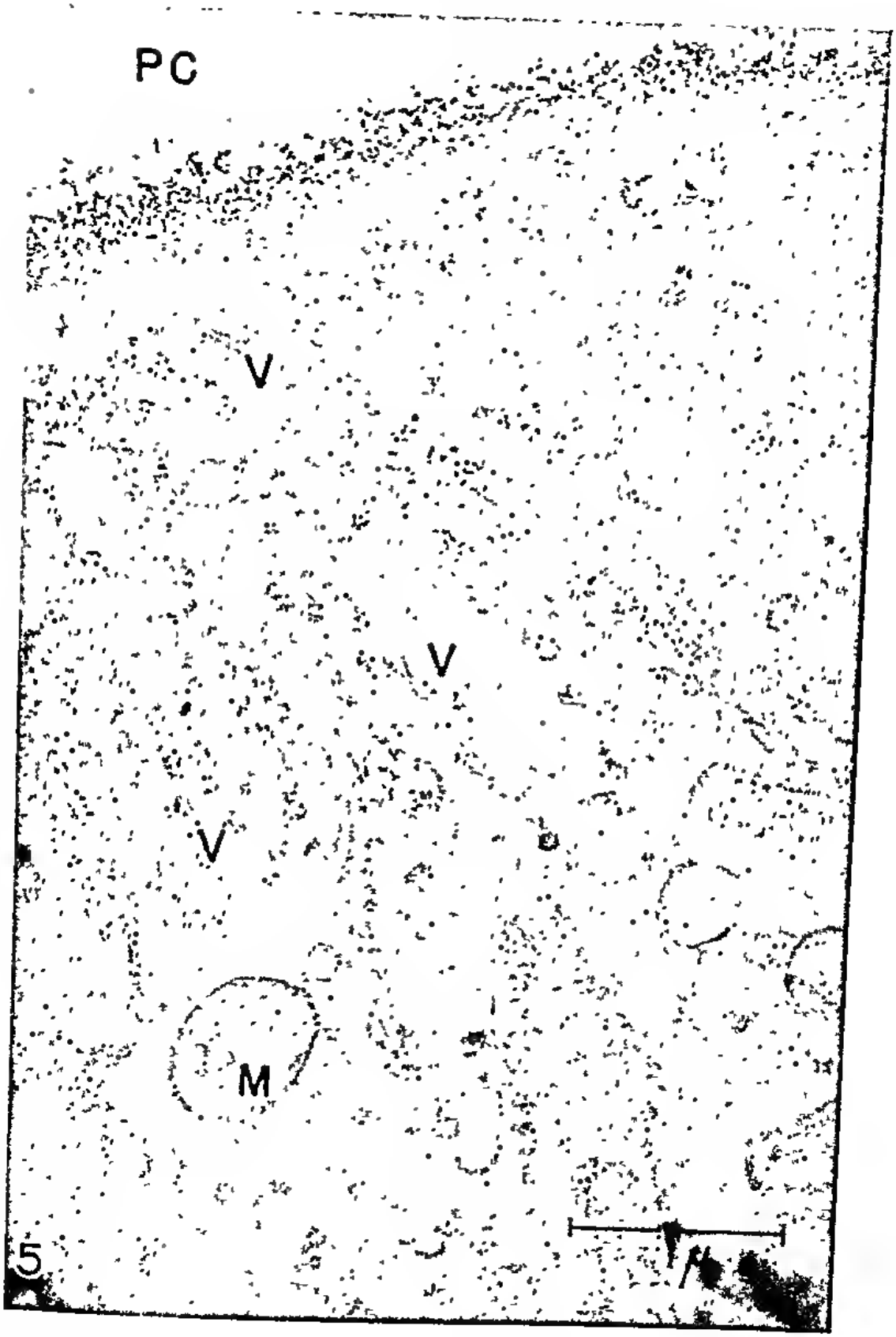
PC
V
V
V
M
5

formed by the breakdown of the surface infoldings and therefore represent reabsorption vesicles rather than secretion vesicles.

The interdigitations of the margins of the surface epithelial cells may function as a site of secretory activity. The very long, tortuous, extracellular channels delimited by the elaborate interdigitated cell membranes may be the pathway traveled by fluids diffusing from the connective tissue spaces to the posterior chamber. Along the way solutes (e.g., proteins), which may be present as normal constituents of extracellular tissue fluids, may accumulate onto the cell membranes and never reach the posterior chamber proper and other materials may be added.

Recently Fawcett (1959) described some experiments in which frogs were injected with Thorotrast. He reported that the glomerular filtrate contained small amounts of thorium dioxide particles, which were subsequently found between the interdigitated surface of adjacent cells of the tubule epithelium. He concluded that "it is not unreasonable to believe that the intercellular pathway may be importantly involved in transport of fluids and ions."

Figure 2, an electron micrograph of the ciliary epithelium of a normal adult rabbit, shows the elaborate marginal interdigitations of adjacent surface cells in the posterior chamber. The linear arrangements of vesicles (R) suggests that intercellular material may also be incorporated into the cytoplasm by the pinching-off of vesicles from the interdigitated cell margins.

In summary, it is proposed that the two types of elaborations of surface epithelial cell membranes play different roles in the secretion of aqueous humor. The marginal interdigitations provide an elaborate intercellular pathway in which materials may be selectively modified by pinocytosis. This process results in the secretion of a provisional aqueous humor. The apical infoldings facing the posterior chamber then reabsorb from the provisional aqueous—resulting in the final product (aqueous humor).

In the evidence and discussion presented so far with respect to the secretory function of the ciliary epithelium, it appears that much reabsorbed material must accumulate in the cytoplasm. It is not inconceivable that a similar reflux of surface membrane molecules may also be involved in transporting material out of the cell.

Summary

The ciliary epithelial cells facing the posterior chamber have extensive elaborations of their cell membranes. These elaborations are of two types: (a) the highly interdigitated membranes forming their margin and (b) infoldings of the surface facing the posterior chamber.

When Thorotrast is injected into the posterior chamber, thorium dioxide particles first become concentrated in the surface infoldings. They are then found in the cytoplasm in vesicles derived from the membranes of the infoldings. Thorotrast is not accumulated in or reabsorbed by the interdigitations.

It is suggested that the marginal interdigitations may be involved with the secretion of a provisional aqueous. The surface infoldings, facing the posterior chamber, then modify the provisional aqueous humor by reabsorbing some materials, leaving the final product (aqueous humor).

References

Bennett, H. S., Luft, J. H., and Hampton, J. C. (1959). *Am. J. Physiol.* **196**, 381-390

Brandt, P. W. (1958). *Exptl. Cell Research* **15**, 300-313.

Brandt, P. W., and Pappas, G. D. (1960). *Anat. Record* **136**, 169-170.

Clark, S. L., Jr. (1959). *J. Biophys. Biochem. Cytol.* **5**, 41-50.

Fawcett, D. W. (1959). *In* "The Microcirculation" (Proceedings of the Fifth Conference on Microcirculatory Physiology and Pathology, S. R. M. Reynolds and B. W. Zweifach, eds.), pp. 1-27. Univ. of Illinois Press, Urbana, Illinois.

Holmberg, A. (1957a). *In* "Electron Microscopy" (Proceedings of the Stockholm Conference, Sept., 1956. F. S. Sjostrand and J. Rhodin, eds.), pp. 139-141. Academic Press, New York.

Holmberg, A. (1957b). Ultrastructural changes in the ciliary epithelium following inhibition of secretion of aqueous humor in the rabbit eye. Thesis. Karolinska Institutet, Stockholm.

Holmberg, A. (1959a). *Am. J. Ophthalmol.* **48**, 428-438.

Holmberg, A. (1959b). *A.M.A. Arch. Ophthalmol.* **62**, 949-951.

Kinsey, V. E. (1950). *A.M.A. Arch. Ophthalmol.* **44**, 215.

Maxwell, D. S., and Pease, D. C. (1956). *J. Biophys. Biochem. Cytol.* **2**, 467-471.

Palay, S. L., and Karlin, L. J. (1959). *J. Biophys. Biochem. Cytol.* **5**, 373-384.

Pappas, G. D. (1959). *In* "Glaucoma" (Transactions of the Fourth Conference, March 1959. F. W. Newell, ed.), pp. 141-178. Josiah Macy Jr. Foundation, New York.

Pappas, G. D., and Smelser, G. K. (1958). *Am. J. Ophthalmol.* **46** (Part II), 299-318.

Pappas, G. D., Smelser, G. K., and Brandt, P. W. (1959). *A.M.A. Arch. Ophthalmol.* **62**, 959-965.

Pease, D. C. (1955). *J. Histochem. and Cytochem.* **3**, 295.

Pease, D. C. (1956). *J. Biophys. Biochem. Cytol.* **2** (Suppl.), 203-208.

Rhodin, J. (1954). Correlation of ultrastructural organization and function in normal and experimentally changed proximal convoluted tubule cells of the mouse kidney. Thesis. Karolinska Institutet, Stockholm.

Scott, B. L., and Pease, D. C. (1959). Electron microscopy of the salivary and lacrimal glands of the rat. *Am. J. Anat.* **104**, 115-161.

Smelser, G. K. (1958). *In* "Glaucoma" (Transactions of the Third Conference). Josiah Macy Jr. Foundation, New York.

Tennyson, V. M. (1960). *Anat. Record* **136**, 290.

Discussion

Dr. Fine [Armed Forces Institute of Pathology, Washington, D. C.]: What is the relationship of the fibrillar component of the zonule to the material which makes up the basement membrane?

Dr. Pappas [Columbia University, New York]: The internal limiting membrane surrounds and is in very close approximation to the cell membrane, facing the posterior chamber. This surface is very irregular. The meshwork of fibers, on the surface, is in continuity with zonular fibers. If you think of a glove, for instance, with threads coming out of the glove, this is then the "attachment."

Dr. Maumenee [London, England]: Are they the same material?

Dr. Pappas: Morphologically, they (the fibers of the internal limiting membrane, and the zonular fibers) seem to be of the same diameter, although I have not been able to see very well the fibrils of the internal limiting membrane, since they are not oriented as are the zonular fibers. I have not been able to see periodicity. It appears to be the same kind of material—a kind of collagen.

Dr. Cohen [Washington University, St. Louis, Missouri]: Professor Wislocki showed that the outer zonular portion of the equatorial lens capsule was metachromatic and the inner capsule was not, although both were PAS-positive. We have recently studied the development of the lens and observed that the basement membrane of the embryonic ectoderm continues onto the surface of the lens vesicle and constitutes the first lamina of the lens capsule. This further relates the inner capsule to basement membrane. I think, therefore, that while these mucoproteins may all look alike in the electron microscope, it might be well to consider that zonular protein is not identical with lens capsule protein or basement membrane.

Dr. Pappas: I believe that the internal limiting membrane is also PAS-positive.

Dr. Cohen: The basement membrane of the embryonic ectoderm appears to pass onto the surface of the neural tube at the anterior neuropore. This occurs before there is an optic cup. When this forms, the neural tube basement membrane continues onto the optic cup and completely envelops it. This further relates Dr. Pappas' "internal limiting membrane" to a basement membrane.

Dr. Maumenee: I would like to point out that the aqueous humor is not only relatively free from proteins, but from all large molecules, for example foreign polysaccharides, introduced into the blood. If you postulate that proteins are removed by an adsorption mechanism, it is reasonable to go further and assume other large molecules are removed in the same way. What kind of adsorptive surface are you proposing that selects only on a basis of molecular size? It seems far more probable that proteins are filtered from the aqueous humor at some point.

Dr. Pappas: This is not the only aspect of secretion of aqueous humor. As I said, there is a basement membrane, and there is the pigment cell layer, which we didn't take into consideration in this paper. It was our attempt, when we saw these elaborated membranes, to try to put some reason to them. Either fluids pass through the cell, which doesn't really make too much sense, because all the vesicles we have been able to identify are reabsorption vesicles, or it goes out between the cells. This was the basis for mentioning this as a hypothesis of the function of the elaborated membranes.

Dr. Wanko [National Institutes of Health, Bethesda, Md.]: May I ask Dr. Pappas whether any other structures bordering the anterior and posterior chamber show the presence of Thorotrast particles?

Dr. Pappas: I would rather not comment on that, because our work is very preliminary. We have looked at the other structures very superficially.

DR. WANKO: Do the particles leave the eye along the physiologic ways of outflow?

DR PAPPAS: Do you mean whether they went out Schlemm's canal? We haven't looked at Schlemm's canal We don't know that.

DR FLEMING [General Electric, Cleveland, Ohio]: How is intraocular pressure maintained prenatally if aqueous is not secreted until the seventh day?

DR PAPPAS: I don't know

DR COULOMBRE [Yale University, New Haven, Conn.]: In answer to Dr. Fleming, I may say that the pressure I was speaking about is vitreous pressure or assumed vitreous pressure, and has nothing to do necessarily with the aqueous.

DR. MAURICE: It is not necessary to assume that the aqueous humor is transported as a whole by the ciliary epithelium. It could be that an ion or some ions are actively moved and that the water followed by the osmotic force

DR. PAPPAS. What evidence do you have?

DR MAURICE. I am not presenting any evidence for it. I said it could be.

Electron Microscope Observations on the Origin, Development, and Genetic Control of Melanin Granules in the Mouse Eye[1,2]

FRANK MOYER

Department of Biology, The Johns Hopkins University, Baltimore, Maryland

Introduction

MELANIN GRANULES are characteristic cytoplasmic inclusions of the cells comprising the pigment epithelium of the retina. An understanding of the origin and development of these granules is therefore important to an understanding of the normal and pathological morphology of the retina. But of even more fundamental interest is the fact that melanin granules are organelles which apparently represent the end product of cytodifferentiation in a specialized cell line. For this reason, an understanding of granule origin and of the effect of different genes on the course of granule development may be expected to yield important information on the genetic control of cytodifferentiation

The literature contains numerous reports on the origin of melanin granules. Guttes (1953) critically reviewed much of this work, and the papers of Weissenfels (1956) and Barnicot and Birbeck (1958) contain valuable discussions and references. Observations of light microscopists have led to three major theories of granule origin These are the "nuclear origin theory" in which granules are supposed to form from extruded nuclear material, the "theory of mitochondrial origin" in which mitochondria are believed to change into melanin granules, and the "theory of Golgi origin" which postulates that early granule stages form in the Golgi apparatus

Information on melanin granule fine structure obtained with the electron microscope falls into three categories as follows: (1) studies on the structure of mature granules using shadowed preparations of isolated granules, (2) studies of sectioned tissue containing melanocytes, and (3) studies not concerned with melanin granules but providing information on granule structure because the tissues used contained melanocytes.

Observations of isolated granules by Mason *et al.* (1947) and Lion

[1] This investigation was supported in part by a National Science Foundation Grant, and by grants H3141 and CF9040 of the National Institutes of Health

[2] This work will be submitted to the Faculty of Arts and Sciences at Johns Hopkins University in partial fulfillment of the requirements for the Ph D degree.

et al. (1956) showed no reeognizable internal structure in the granules. Laxer *et al.* (1954) observed granules isolated from the hair of various mammals and found pronouneed interspeeifie variation in size and shape. Correlations of granule size with the color of alkaline solutions of the granule pigment, and examination of bleached granules, led them to conelude "that the natural melanin granule is a composite strueture eomposed of a eolorless matrix and a colored melanin sheath." Carr (1957), using chickens, examined isolated granules and also studied the granules *in situ* by direct observation of barbs and barbules. His pictures show a dense granule with a faintly reticular core.

Observations of sectioned material by Dalton and Felix (1953), Falk and Rhodin (1956), Lion *et al.* (1956), Porter (1957), Yamada *et al.* (1958), and Eakin and Westfall (1959) show no internal structure in pigment granules. In most cases this ean be attributed to the fact that only mature granules were observed. Barnicot, Birbeck, and their eo-workers did an extensive series of studies on human melanin granules (Barnieot *et al.*, 1955; Birbeek *et al.*, 1956; Barnicot and Birbeck, 1958; Birbeck and Barnieot, 1959). They studied granules isolated from hair by various teehniques, and fine sections of hair folliele melanoeytes. They eoneluded that the granule forms from eolorless thiek-walled "hollow ellipsoids" in whieh a fibrous matrix is laid down, and that melanin is deposited on this matrix. They suggest a Golgi origin for the progranule and therefore agree with Güttes (1953). They were unable to find any evidenee for granule formation from extruded nuelear material or for stages intermediate between mitochondria and granules. This latter point was speeifically investigated by Dalton and Felix (1953) in thin sections of mouse melanomas. They found no evidence of the formation of melanin granules from mitochondria.

Wellings and Siegel (1959), and Dalton (1959) also propose a Golgi origin for melanin granules, but their evidence is not very convineing.

Weissenfels (1956) studied the formation of propigment granules (early unpigmented granule stages) and pigment granules in tissue cultures of chick neural crest and retina. He correlated phase contrast observations on vitally stained melanoblasts with standard histological and electron microscope studies. His results suggest that propigment granules are formed at multiple sites (Pigmentbildungzentren) in the cytoplasm. He states that these centers are easily distinguished from the Golgi apparatus and bear no relationship to it. Furthermore he finds no evidence of granules arising from either nucleus or mitochondria. His pictures suggest definite internal structure in the developing granule.

The literature also contains several papers on topics not related to

melanogenesis in which the published pictures show developmental stages of melanin granules (Bernstein and Pease, 1959; Charles and Ingram, 1959; Karasaki, 1959).

Recent observations of sectioned material suggest, then, that melanin granules have a definite fine structure and develop from a pigmentless and relatively structureless ellipsoidal precursor. The theories of nuclear and mitochondrial origin may be safely abandoned, but the theory of Golgi origin requires more critical examination. Furthermore, a new theory, that of multiple granule forming sites, has been proposed (Weissenfels, 1956).

The effects of genes on pigment granule structure in the mouse are well known. The most comprehensive review of mouse genetics is that of Gruneberg (1952), which contains two chapters on pigment mutants. The classic work of Russell (1946, 1948, 1949a, b) clearly showed that size, shape, number, and distribution of granules were under genetic control. She carried out detailed quantitative histological studies on the hair pigment of mice bred especially to show the effects of individual pigment mutations as well as the effects produced by the interaction of mutations at different loci. Markert and Silvers (1956, 1959) compared the differentiation of melanoblasts in different tissue environments in fifty different mouse genotypes They combined these observations with the results of grafting experiments and concluded that four cellular properties are of primary importance in determining the course of melanoblast differentiation. These are. (1) the genetic constitution and (2) the developmental history of the melanoblasts, and (3) the genetic constitution and (4) the state of differentiation of the tissue environment in which the melanoblast is differentiating

The electron microscope also provides evidence of fine structural differences in melanin granules attributable to different genotypes. Barnicot and Birbeck (1958) observed that pigment granules from human red hair differed in their fine structure from those in dark hair, and that the hair follicle melanocytes of human albino subjects showed early programule stages which never became pigmented. Similar observations were made by Nissen (1958) who studied pigmentation in the feathers of normal and albino parakeets. He found a colorless precursor granule on which pigment was normally deposited, but in the albino, although the precursor formed, no pigment was deposited and the precursor ultimately deteriorated.

Markert and Abramowitz, in exceptionally clear, unpublished electronmicrographs of mouse retina, iris, and choroid, observed definite stages in granule development, and differences in these stages in material

from mice of different genetic strains.[3] These observations suggested that genes might effect the sequence of granule development.

The foregoing information clearly indicates that genes influence the differentiation of melanoblasts and that this influence is reflected in the fine structure of the differentiating cell. Accordingly, this study was initiated to: (1) describe, as accurately as possible, the origin and development of the melanin granule, (2) integrate structural and biochemical data on melanogenesis, (3) determine how different pigment mutations affect the normal developmental sequence, and (4) thus derive more accurate information on how the various pigment mutations act on the fine structure of the cell to produce their observed gross phenotypic effects.

Materials and Methods

Inbred mice of strains carrying various pigment mutations and ranging in age from 15 days *in utero* to 15 days *post partum* were used for these studies. Mice not available from our own stocks were purchased from the Roscoe B. Jackson Memorial Laboratory at Bar Harbor, Maine. Tissue was prepared by enucleating the eye and fixing the wall in such a way that melanocytes of the pigment epithelium and dendritic melanocytes of neural crest origin, located in the choroid, could be observed in the same section (Fig. 1). Conventional fixatives were used and followed by rapid dehydration in graded alcohols. Embedding in 3 parts methyl: 7 parts butyl methacrylate allowed sectioning without shattering the melanin granules. Material was sectioned on a Porter-Blum microtome using glass or diamond knives, mounted on Formvar-, or carbon-

[3] I wish to thank Dr. C. L. Markert and Mr. Harry Abramowitz for the loan of unpublished data and photographs.

PLATE I

FIG. 1. A low-power view of the area of the eye used in these investigations. Red blood cells (RBC) and a dendritic melanocyte of neural crest origin (DM) may be seen on the right in the choroid. The masses of pigment granules in the left half of the picture are in the cells of the pigment epithelium (RPE). The tissue is from a DBA/1 mouse (genotype: *aabbdd*) 2.5 days *post partum*, and was fixed in buffered isotonic OsO_4. The scale line represents 1 μ.

FIG. 2. High-power view of the stage 1 granule (S1). Note the typical double membrane bounding the structure. It is thicker and denser than the membranes bounding mitochondria in these cells. Some of the small vesicles within the granule are faintly visible and have begun to coalesce to form fibers. The tissue is pigment epithelium from a C57/Br/cd mouse (genotype: *aabb*) 16.5 days *in utero*, and was fixed in buffered isotonic OsO_4. The scale line represents 1 μ.

coated, 200-mesh copper grids, and observed in an RCA EMU-3c electron microscope. Best results were obtained using a platinum, 25 μ, objective aperture.

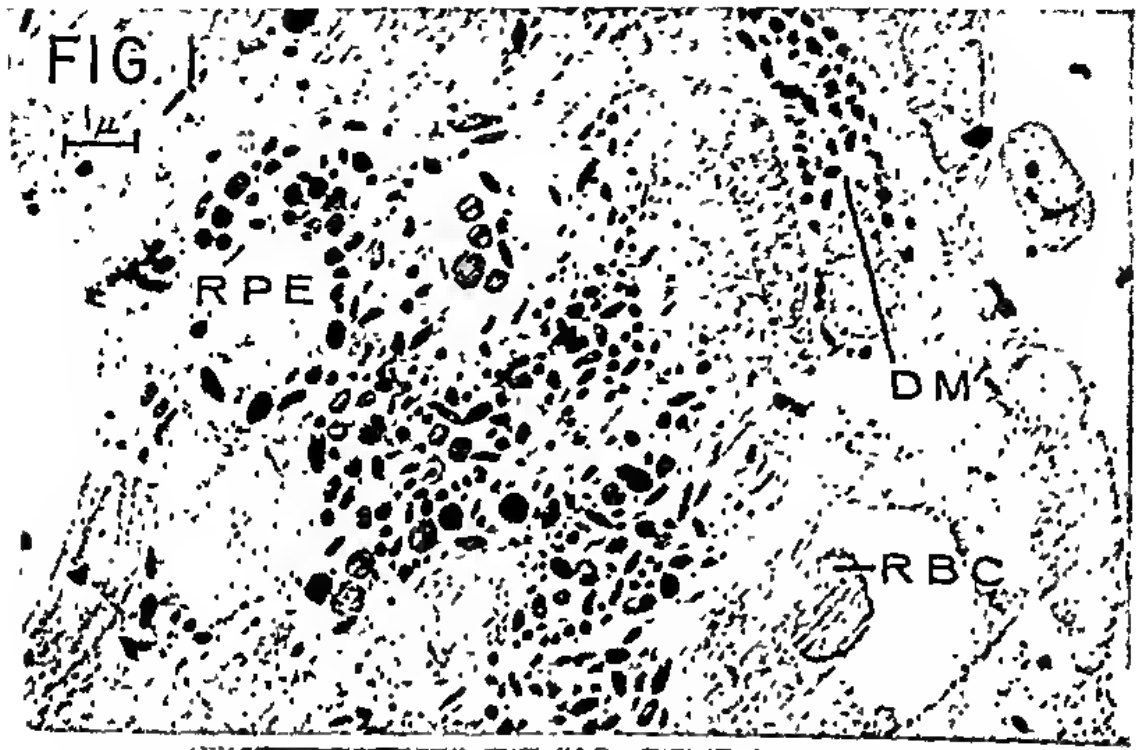

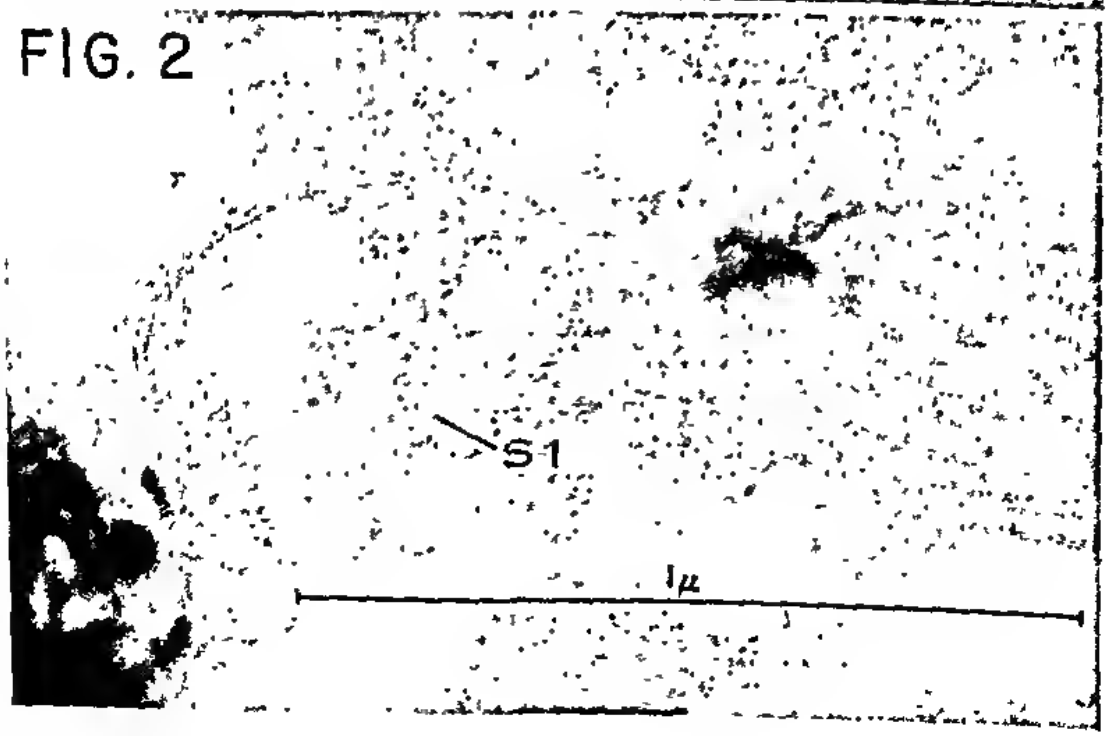

from mice of different genetic strains.[3] These observations suggested that genes might effect the sequence of granule development.

The foregoing information clearly indicates that genes influence the differentiation of melanoblasts and that this influence is reflected in the fine structure of the differentiating cell. Accordingly, this study was initiated to: (1) describe, as accurately as possible, the origin and development of the melanin granule, (2) integrate structural and biochemical data on melanogenesis, (3) determine how different pigment mutations affect the normal developmental sequence, and (4) thus derive more accurate information on how the various pigment mutations act on the fine structure of the cell to produce their observed gross phenotypic effects.

Materials and Methods

Inbred mice of strains carrying various pigment mutations and ranging in age from 15 days *in utero* to 15 days *post partum* were used for these studies. Mice not available from our own stocks were purchased from the Roscoe B. Jackson Memorial Laboratory at Bar Harbor, Maine. Tissue was prepared by enucleating the eye and fixing the wall in such a way that melanocytes of the pigment epithelium and dendritic melanocytes of neural crest origin, located in the choroid, could be observed in the same section (Fig. 1). Conventional fixatives were used and followed by rapid dehydration in graded alcohols. Embedding in 3 parts methyl: 7 parts butyl methacrylate allowed sectioning without shattering the melanin granules. Material was sectioned on a Porter-Blum microtome using glass or diamond knives, mounted on Formvar-, or carbon-

[3] I wish to thank Dr. C. L. Markert and Mr. Harry Abramowitz for the loan of unpublished data and photographs.

PLATE I

FIG. 1. A low-power view of the area of the eye used in these investigations. Red blood cells (RBC) and a dendritic melanocyte of neural crest origin (DM) may be seen on the right in the choroid. The masses of pigment granules in the left half of the picture are in the cells of the pigment epithelium (RPE). The tissue is from a DBA/1 mouse (genotype: *aabbdd*) 2.5 days *post partum*, and was fixed in buffered isotonic OsO_4. The scale line represents 1 μ.

FIG. 2. High-power view of the stage 1 granule (S1). Note the typical double membrane bounding the structure. It is thicker and denser than the membranes bounding mitochondria in these cells. Some of the small vesicles within the granule are faintly visible and have begun to coalesce to form fibers. The tissue is pigment epithelium from a C57/Br/cd mouse (genotype: *aabb*) 16.5 days *in utero*, and was fixed in buffered isotonic OsO_4. The scale line represents 1 μ.

coated, 200-mesh copper grids, and observed in an RCA EMU-3c electron microscope Best results were obtained using a platinum, 25 μ, objective aperture.

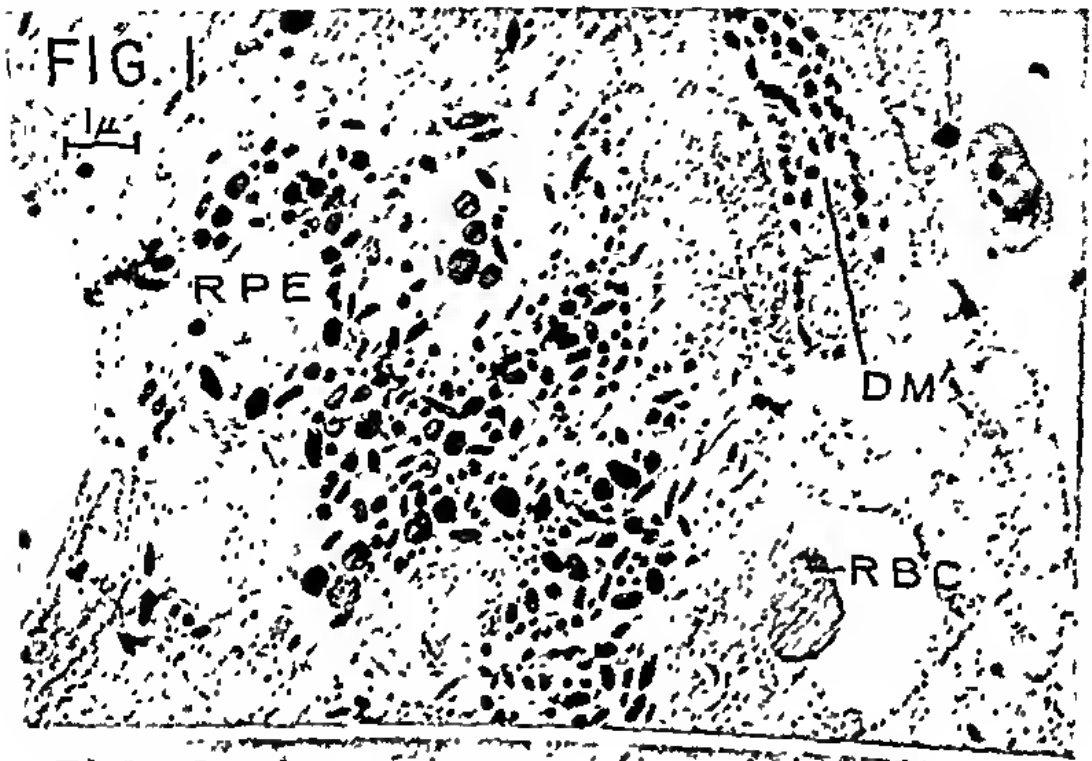

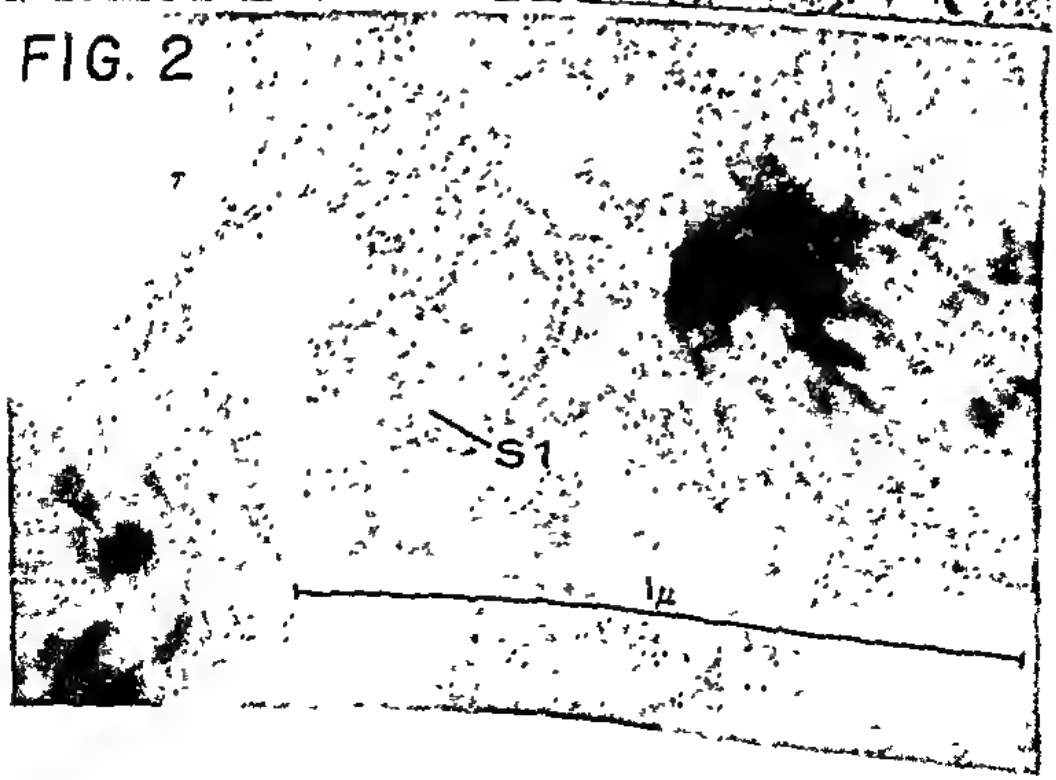

Results

The Developmental Sequence

We have previously described a sequence of four morphologically well-defined stages in the development of the melanin granule (Moyer, 1959). This description can now be expanded on the basis of more recent findings.

The earliest evidence of granule formation (the stage 1 granule) is an ellipsoid bounded by a typical double membrane. The region enclosed by the double membrane usually contains small membranous vesicles and randomly oriented bits of fibrous material (Fig. 2). The bounding membranes themselves are usually smooth. Depending on the plane of sectioning it is sometimes possible to see one or more dense areas in the material enclosed by the membrane, and furthermore, to see that the bounding membranes are continuous at several points with the cytoplasmic membrane system of the cell. The size of stage 1 granules appears generally to be smaller than later granule stages.

The next stage (stage 2) remains bounded by membranes which usually still retain their continuity with the cell membrane system, but the enclosed area has become filled with regularly oriented fibers. These fibers are arranged parallel to each other as can be seen in a longitudinal section such as that in Fig. 3. The diameter of the granule is usually greater in the middle than at the ends, and this is probably due to branching of the fibers. Points where branching is apparent are indicated by arrows in Fig. 3. The fibers are roughly 50 Å in diameter and often show a regular wavy appearance in longitudinal section suggesting an helical orientation. Cross-linking between fibers is also evident in places.

The stage 3 granule differs distinctly from the stage 2 granule because the fibers may be four to six times as thick as stage 2 fibers. Observation of intermediate forms indicates that this change in size and

---

PLATE II

Fig. 3. Stage 2 (S2), stage 3 (S3), and early stage 4 (ES4) granules from the pigment epithelium of a C57/Bl/6 mouse (genotype: *aaBB*) 16.5 days *in utero*. Note branching of the fibers in the stage 2 granule (arrows). The zig-zag appearance of the fiber is faintly visible (h) and suggests an helical orientation. Fixed in buffered isotonic OsO_4. The scale line represents 1 μ.

Fig. 4. Granule stages from the pigment epithelium of a DBA/1 mouse 2.5 days *post partum*. A longitudinal section of a stage 3 granule (L) shows the characteristic arrangement of its fibers. Cross-linking between fibers is evident. In the upper right of the picture a granule intermediate between stage 1 and stage 2 is evident. A granule intermediate between stage 2 and stage 3 is seen at the extreme left. Fixed in buffered isotonic OsO_4. The scale line represents 1 μ.

density is due to the deposition of dense material on the stage 2 fiber. Stage 3 fibers cut longitudinally show parallel arrangement and again there is cross-linking between the fibers (Fig. 4). In cross section the fibers are also seen to be linked to each other (Fig. 5). Formaldehyde fixation shows that the dense material of stage 3 granules has an intrinsic

FIG. 3.

FIG. 4.

electron density and is not an artifact of osmium tetroxide fixation (Fig. 6). Since mature melanin granules are well known to be intrinsically dense to the electron beam, we consider the change between stage 2 and stage 3 to be due to the deposition of melanin on the stage 2 fibers. In very thin sections such as that of Fig. 3, stage 3 fibers show a less dense center, due, no doubt, to the fact that the stage 2 fiber remains as a core and is now surrounded by a cortex of melanin. In most cases some evidence of the bounding membrane remains on the stage 3 granule, but connections with the cell membrane system are not nearly as frequent as before.

In the stage 4 granule the fibrous matrix is completely obscured by melanin, and the granule has achieved the homogeneous appearance of maturity frequently described in the literature. In rare cases, evidence of the bounding membranes and vestiges of their attachment to the cell membrane system remain. Figure 3 shows a granule in early stage 4.

These results are in good agreement with those of Barnicot, Birbeek and their co-workers, cited above.

The development of different parts of single granules does not necessarily proceed synchronously; thus one part of a granule may be in stage 2 while other parts are in stage 3. The stages described here correspond to easily recognized stages of development which are, however, of very short, and not necessarily equal duration. Furthermore, the fact that most of the stage 2 and stage 3 granules observed show orientation of fibers intermediate between the parallel pattern described for longitudinal sections and the "beaded" pattern characteristic of trans-

---

PLATE III

FIG. 5. A transverse section through a stage 3 granule (T) in the same cell as the granules of Fig. 4. The cut ends of the fibers are clearly visible as is the cross-linking between fibers. A mitochondrion (m) is visible on the left. Fixation and magnification are the same as in Fig. 4.

FIG. 6. Granules from a C57/Bl/6 mouse (genotype: *aaBB*) 18.5 days *in utero*. This material was fixed in buffered 4% formaldehyde but the osmotic pressure was not adjusted. Preservation is adequate to show that stage 2 (S2) and stage 3 (S3) granules are intrinsically dense to electrons. This is taken to mean that the dense material is melanin. The nucleus (N) is visible on the left. Scale line represents 1 μ.

FIG. 7. Pigment epithelium from a 2.5-day-old DBA/1 mouse (genotype: *aabbdd*) showing many different granule stages. Early granules (EGS) seem to be localized in groups in this picture. Note that no characteristic Golgi apparatus is apparent here. Numerous mitochondria, cytoplasmic membranes, and the cell nucleus (N) are also visible. Fixed in buffered isotonic OsO_4. Scale line represents 1 μ.

verse sections, indicates that the orientation of these granules within the cytoplasm is random (Fig. 7).

Observations of dendritic melanocytes in the choroid coat show that the details of granule development are essentially the same in these cells of neural crest origin, as in the cells of the pigment epithelium.

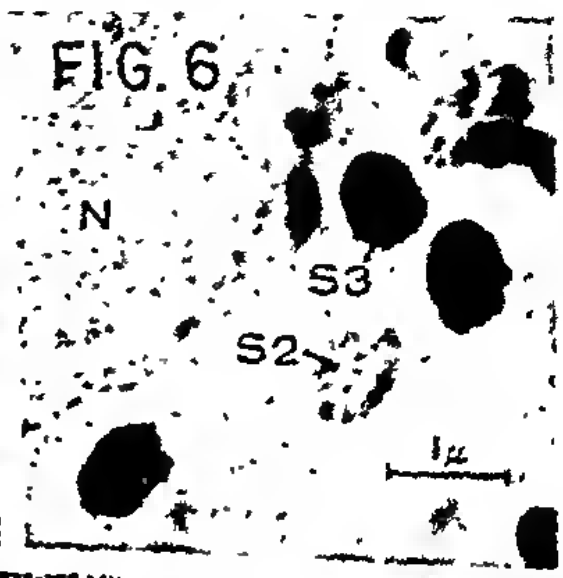

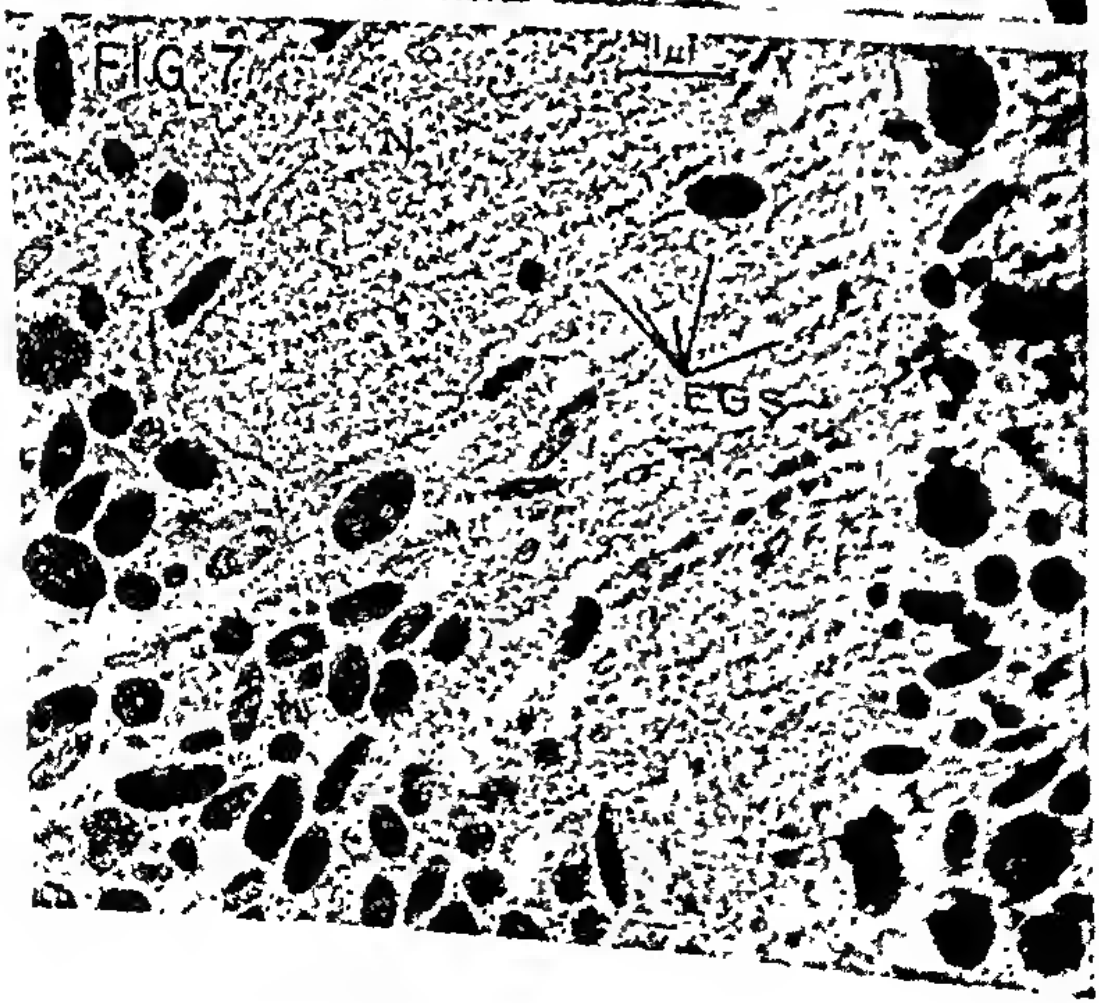

The Influence of Pigment Mutations

The information on gene effects presented here is preliminary in nature. A detailed consideration of these effects will be published at a later date.

The genes so far investigated are confined to four loci, each of which is in a different linkage group. The effects of the alleles for black (*B*) and brown (*b*) at the *B* locus, the alleles for non-albino (*C*), chinchilla (c^{ch}), extreme dilution (c^{e}), and albino (*c*) at the *C* locus, the gene for dilute (*d*) and the gene for ruby-eye (*ru*) are reported here. In all cases the mice observed were homozygous for non-agouti (*a*) at the agouti locus. All characteristics observed are compared to those of non-agouti brown mice (*aabb;* strain C57/Br/cd) which were used as "controls." Table I summarizes the data.

Table I shows that in nearly every case the gene effect was on number, size, or distribution of the granules, *not on the fine structure of the individual granule.* The albino gene (*c*) is an exception in that it also results in failure of the progranules to become melanized. The single most important fact emerging from these studies is that in all cases except the albino, the sequence of fine structural changes in the forming granule appears to be the same (Figs 3, 7, and 8).

Discussion

The Evidence for a Developmental Sequence

The fact that so many of the granules observed in melanocytes represent forms intermediate between the proposed stages in the developmental sequence is the strongest evidence that a developmental sequence really exists. The evidence from a count of relative frequencies of the different granule stages during the course of pigmentation shows that the numbers of stage 1 and stage 2 granules are always low in comparison to the number of stage 3 granules present. This data is summarized in Table II.

The low counts of early granules may be due to the fact that there are discrete sites of granule formation in the cytoplasm as Weissenfels (1956) proposes, and the limited sampling employed in this work does not reflect the true frequency of early granules. On the other hand it may be that the rate of conversion of early granules to the later stages is rapid enough to keep the total number of early granules at a relatively constant, low value. At any rate the data from frequency counts do not deny the developmental sequence in the early stages, and definitely support it in stages 3 and 4.

TABLE I

SUMMARY OF GENE INDUCED CHANGES IN PIGMENT GRANULI ATTRIBUTES[a]

Strain	Genotype	Effect of gene responsible for phenotype difference	Average granule size	Granule number	Granule distribution
C57/Br/cd	*aabb*	None (e g strain used as arbitrary basis of comparison)	—	—	Random
C57/Bl/6	*aaBB*	Color of pigment is black	Greater than *aabb*	Equals *aabb*	Random
SEC	*aabbc^{ch}c^{ch}*	Granules smaller and fewer than *aabb*	Less than *aabb*	Less than *aabb*	Random
CE	*aabbc^{e}c^{e}*	Granules smaller and fewer than *aabbc^{ch}c^{ch}*	Less than *aabbc^{ch}c^{ch}*	Less than *aabbc^{ch}c^{ch}*	Random
A/Jax	*aabbc*	Early granules do not become melanized	Size of early granules less than *aabbc^{e}c^{e}*	Number of early granules less than *aabbc^{e}c^{e}*	Random
DBA/1	*aabbdd*	Clumping of granules	Less than *aabb*	Less than *aabb*	Clumped closely on basal side of nucleus in retina
Black Rubies	*aabbrurn*	Delayed onset of pigmentation Small size and number of granules	Less than *aabb*	Less than *aabb*	Random

[a] The C57/Br/cd strain (genotype: *aabb*) was used as the basis of comparison See text for details.

The Chemical Interpretation of Granule Structure

It is generally agreed that naturally occurring melanin is a polymer of indole-5,6-quinone which copolymerizes with protein. Indole-5,6-quinone is formed, through a series of intermediates, from the oxidation of tyrosine by the enzyme tyrosinase [see Lerner (1953) and Mason (1955), for reviews of the literature]. Most of the tyrosinase activity from mammalian preparations is concentrated in a particulate fraction (Brown *et al.*, 1959), and preparations of isolated granules from the retinas of chick embryos show tyrosinase activity (Fitzpatrick and Kukita, 1959). Fitzpatrick and his co-workers (Fitzpatrick *et al.*, 1958; Fitzpatrick and Kukita, 1959) have suggested that the protein matrix of the granule has tyrosinase activity and that melanin polymerizes directly onto it, eventually blocking the active sites, so that a mature melanocyte, in which granule development has ceased, will no longer have tyrosinase activity. Our observations support this idea and suggest that the fibers of stage 2 granules are protein which has tyrosinase activity; that melanin is deposited directly on the stage 2 fibers to eventually form stage 3 fibers; and that presumably by stage 4, tyrosinase activity has ceased, since no more melanin is formed and the underlying protein matrix is totally obscured. However, more experimental evidence is needed to support these speculations.

TABLE II

The Relative Frequencies of Granule Stages Present at Different Times during the Course of Differentiation of the Mouse Pigment Epithelium[a]

Granule stage	Age of mouse			
	17 Days *in utero*	0.5 Days *post partum*	2.5 Days *post partum*	15 Days *post partum*
1	10.5%	7.8%	7.3%	0.0%
2	6.9%	6.1%	5.2%	0.0%
3	77.9%	85.3%	86.6%	0.0%
4	4.6%	0.7%	0.9%	100.0%
Total granules counted	86	307	232	142

[a] Frequencies are expressed as per cent of total granules counted in randomly selected sections.

The Origin of the Stage 1 Granule

None of the observations reported here support the three classic theories of granule origin. Intermediate stages between mitochondria and melanin granules have never been observed, and mitochondria are clearly distinguishable from melanin granules. Granules have never been seen to be associated with material extruded from the nucleolus or any

part of the nucleus. Whenever any structure resembling Golgi apparatus in its morphology (Dalton and Felix, 1957; Lacy and Challice, 1957) was observed, a careful check was made to see if early granule stages were more frequent in the immediate vicinity, or if they were associated with the structure in any way. In all such cases the results were negative. This implies that the Golgi apparatus is not involved in granulogenesis, but serial sectioning and special staining techniques will be required to settle the issue.

The work of Weissenfels, cited previously, suggests that granules originate in multiple centers in the cytoplasm. Occasionally, in our material, an area is found that seems to have an unusually high number of early granule stages (such an area is shown in Fig. 7), and, as mentioned above, the low relative frequency of early granule stages may reflect the localization of these stages within the cell which our limited sampling may have missed.

The most striking single feature of the early granule stages is their relationship to the cytoplasmic membrane system. On the basis of osmium tetroxide-fixed material from the genotypes studied, these membranes may be tentatively identified as the endoplasmic reticulum, since they fit the generally accepted description of this ubiquitous structure (Palade, 1955, Porter, 1957) This leads to the speculation that a melanin granule originates when a protein having tyrosinase activity is synthesized in an intracisternal dilation of the endoplasmic reticulum in a manner not unlike that recently suggested for the synthesis of zymogen granules in the exocrine cells of the pancreas (Palade, 1956). In this connection it is an interesting fact that stage 1 granules bear striking similarities to structures found in a variety of different secretory cells (cf Yamada, 1955, Rouiller and Bernhard, 1956; Robertson, 1959). If tyrosinase were synthesized in this way it is easy to see how melanin could be immediately deposited on it, if substrate was available, and a granule in the exocrine cells of the pancreas (Palade, 1956). In this the cells of the pigment epithelium would be considered "frustrated secretory cells," in that their secretory product immediately reacts with available substrate to form an insoluble substance which remains in the cell where it originates This analogy gains support from the fact that the pigment epithelium has several features in common with secretory epithelia in general, such as a highly convoluted basal plasma membrane bordering on a well-developed basement membrane (Yamada *et al.*, 1958) (see Fig. 8). The analogy between dendritic melanocytes and secretory cells, pointed out by Birbeck and Barnicot (1959), is even more striking since such melanocytes actually supply the pigment granules which are taken up by epidermal cells.

Observations of pigment epithelium from embryonic retinas lend credence to these speculations on granule origin. In material from fetal stages one often finds vesicular dilations in the endoplasmic reticulum that are approximately the same size as stage 1 granules. Such a dilation may be seen in Fig. 9. These dilations usually appear empty but occasionally show traces of very thin fibers and small vesicles in the lumen. It is significant that such dilations are not found in the cells of the choroid or of the neural retina at this time. The integration of the speculations and observations discussed here leads to a new theory of the origin of melanin granules, namely that they form in intracisternal dilations of the endoplasmic reticulum. Granule origin and development is represented schematically in Fig. 10.

The Genetic Control of Granule Synthesis and Development

It is evident from Table I that every gene tested in this study showed multiple effects, as, for instance, dilute (*d*), which changes granule size, number, and distribution. Such multiple effects might be called "intracellular pleiotropism." Since the morphological sequence of granule development is the same for all of the genes tested except the albino gene, the implication is clear that most of these genes act on processes other than those which directly determine the fine structure of the granule. This implies that the control of phenotype involves more than genic intervention in the synthetic pathways leading to characteristic cell products. Current ideas on the direction of protein synthesis by "template" ribonucleic acid localized in ribosomes [see Anfinsen (1959), for a stimulating discussion and review] account for the transfer of information necessary to the formation of specific proteins. Nevertheless, these ideas do not, by themselves, provide for the obvious necessity of mechanisms to localize and coordinate such proteins within the cytoplasm in a way that allows them to form characteristic cell struc-

---

PLATE IV

FIG. 8. The basal border of a cell in the pigment epithelium of a C57/Br/cd mouse (genotype: *aabb*) 16.5 days *in utero*. Note the extremely convoluted plasma membrane (arrows) bordering on the basement membrane (BM). Stage 1 (S1) and stage 3 (S3) granules, and a mitochondrion (m) may also be seen. Fixed in buffered isotonic OsO_4. Scale line represents 1 μ.

FIG. 9. An intracisternal dilation (ID) in a pigment epithelium cell of a C57/Br/cd mouse 16.5 days *in utero*. The point where the *cisterna* expands is clearly evident (arrow). The dilation contains material similar to that found in a stage 1 melanin granule. A mitochondrion (m) and two stage 3 granules (S3) are also present. Fixed in buffered isotonic OsO_4. Scale line represents 1 μ.

tures like mitochondria, endoplasmic reticulum, and pigment granules. That such mechanisms exist is obvious. Intracellular pleiotropism indicates that they are complex mechanisms, extremely sensitive to genetic control. We may expect that careful observation of fine structural and biochemical variation in organisms amenable to accurate genetic analysis

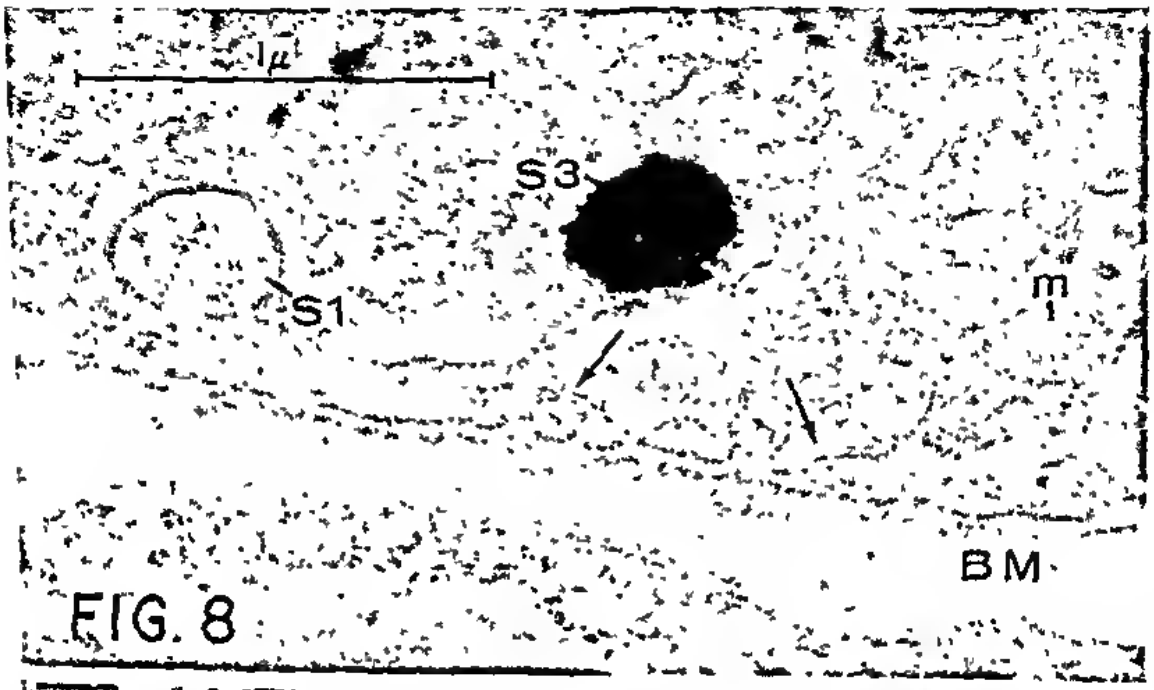

FIG. 8

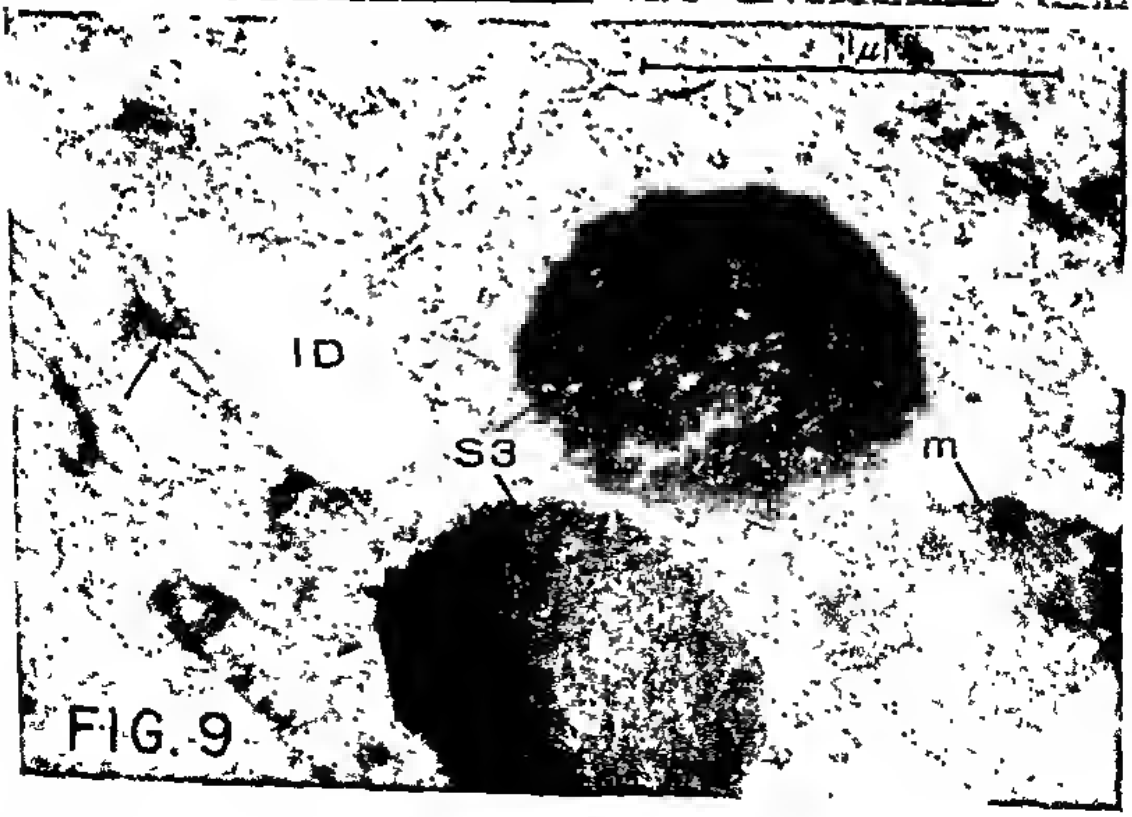

FIG. 9

Markert, C. L., and Silvers, W. K. (1959). *In* "Pigment Cell Biology" (M. Gordon, ed.), p. 241. Academic Press, New York.
Mason, H. S. (1955). *Advances in Enzymol.* **16**, 106.
Mason, H. S., Kahler, H., MacCardle, R. C., and Dalton, A. J. (1947). *Proc. Soc. Exptl. Biol. Med.* **66**, 421.
Moyer, F. (1959). *Anat. Record* **134**, 612 (Abstract).
Nissen, Th. (1958). *Mikraskopie* **13**, 1.
Palade, G. E. (1955). *J. Biophys. Biochem. Cytol.* **1**, 567.
Palade, G. E. (1956). *J. Biophys. Biochem. Cytol.* **2**, 417.
Porter, K. R. (1957). *Harvey Lectures, Ser.* **51**, 175.
Robertson, J. D. (1959). *Biochem. Soc. Symposia (Cambridge, Engl.)* **16**, 3.
Roniller, C., and Bernhard, W. (1956). *J. Biophys. Biochem. Cytol.* **2**, Suppl. p. 355.
Russell, E. S. (1946). *Genetics* **31**, 327.
Russell, E. S. (1948). *Genetics* **33**, 228.
Russell, E. S. (1949a). *Genetics* **34**, 146.
Russell, E. S. (1949b). *Genetics* **34**, 146.
Weissenfels, N. (1956). *Z. Zellforsch. u. Mikroskop. Anat.* **45**, 60.
Wellings, S. R., and Siegel, B. V. (1949). *J. Ultrastruct. Research* **3**, 147.
Yamada, E. (1955). *J. Biophys. Biochem. Cytol.* **1**, 445.
Yamada, E., Tokuyasu, K., and Iwaki,, S. (1958). *J. Electron Microscopy* **6**, 42.

Discussion

Dr. Dowling [Harvard University, Cambridge, Mass.]: I have seen pigment granules in the adult rat (4 months old) showing the same fine structure as seen in Mr. Moyer's type III pigment granules in the embryonic mouse. We have also looked at the pigment epithelium of albino rats and have not seen the type I or II "pigment granules" which he reports. We have found no evidence of any type of pigment granule in our albino animals.

Mr. Moyer [Johns Hopkins University, Baltimore, Md.] We see stage I and II granules only in embryonic and neonatal albino mice. They are gone by 10 to 15 days postpartum which perhaps explains their absence in your adult rats.

Dr. Dowling: Would you care to comment on the presence of stage III granules in our quite mature animals? I thought you intimated that they had disappeared as the animals matured?

Mr. Moyer: Possibly melanization which occurs between stage III and IV proceeds more slowly in the rat.

Dr. Coulombre [Yale University, New Haven, Conn.]: Since you suggest that the pigment granules arise as cisternal enlargements in the agranular reticulum, how do you explain the double membrane you see occasionally?

Mr. Moyer: All I can say is that the inner lamella may be formed inside the cisterna. If we had a cisterna, for instance, with vesicular material inside, and the vesicular material—we don't know what it is—coalesced as fat droplets sometimes do, until one big droplet formed, then the interface between this droplet and the substance filling the intracisternal space could represent one of the lamellae of the double membrane, while the membrane bounding the cisterna would represent the other.

Now, in Dr. Palade's well-known papers on the development of zymogen granules in the pancreas (*J. Biophys. Biochem. Cytol.* **2**, 417-422, 1956; **4**, 203-218, 1958; **4**, 309-318, 1958), he finds that intracisternal granules do have a membrane. Perhaps this membrane is an interface also. I must confess I am baffled as to how it is formed.

Histogenesis of Mouse Retina Studied with Thymidine-H^3*

RICHARD L. SIDMAN

Laboratory of Cellular Neuropathology, Harvard Medical School, Boston, Massachusetts

Introduction

THE CELLS OF THE VERTEBRATE RETINA are arranged in three strata: the ganglion cell layer, the bipolar layer, and the photoreceptor layer. The distribution of cell types in each layer has been reviewed by Polyak (1957) and Ramon y Cajal (1960). The present study concerns the patterns of histogenesis by which the stratified retina of the mouse develops in the embryonic and early postnatal periods. We asked, where do cells form and how do they reach their final positions in the mature retina?

These questions were studied by marking cells with radioactive thymidine and locating them subsequently in autoradiograms. Tritium-labeled thymidine (thymidine-H^3), when injected, is taken up almost exclusively by cells synthesizing new deoxyribonucleic acid (DNA) as a prelude to cell division Once incorporated, the radioactive label remains in the nuclear DNA, though the label becomes diluted in half during each cell division subsequent to the time of labeling (Hughes *et al*, 1958). After a single injection into a mammal, the thymidine-H^3 is available to cells for less than one hour, and only cells synthesizing DNA during that limited time become labeled (Quastler and Sherman, 1959) If animals are killed within a few hours after exposure to thymidine-H^3 and autoradiograms of their tissues are examined, one can observe where cells are forming, and approximately in what numbers. If animals are killed after longer intervals, the labeled cells can be traced as they migrate and differentiate. This autoradiographic method is particularly suited to the analysis of histogenesis in the nervous system, as many of the neural cells divide but seldom while migrating and differentiating. Also, the mammalian embryonic nervous system is inaccessible with most other experimental methods. The present study of retinal histogenesis is one of a series on histogenesis in the mammalian nervous system (Sidman *et al*, 1959, Sidman and Miale, 1959, Sidman, 1960).

* Supported in part by Grant No B1938 from the National Institutes of Health, Bethesda, Maryland

Data on formation of the retina obtained by classic methods of histology form a baseline for the present study. Ramon y Cajal (1960) and others observed that the ganglion cell layer forms during embryonic life and that the remaining retinal cells separate into two additional layers much later, postnatally in many mammalian species. In the mouse, mitoses are found in the retina continuously from the eleventh day of gestation until several days after birth. Almost all mitotic figures are located at the outer surface of the developing retina, the surface analogous to the ventricular surface of the brain (Fürst, 1904; Detwiler, 1932). After mitosis, cells migrate inward and differentiate into the various special cell types of the retina. Ramon y Cajal (1960) recognized that the ganglion and amacrine cells are the first retinal neurons to differentiate, and that they begin to differentiate while migrating from the outer toward the inner surface of the developing retina. During embryonic life the developing processes of ganglion and amacrine cells form the inner plexiform layer. Ramon y Cajal also recognized that in the newborn mouse the Müller cells, horizontal cells, and bipolar cells of the future bipolar layer, and the rod and cone cells of the future photoreceptor layer, are mixed without apparent order in the broad zone of undifferentiated cells between the outer retinal surface and the inner plexiform layer. He described repeated extension and retraction of dendrite branches during the first few postnatal weeks, until the mature alignment of cell processes is finally attained. He deduced that cell bodies also must migrate, since cells of a given class were found scattered through various retinal planes at one stage of development, and were concentrated in a single plane at a later stage. However, the extent of the cell migrations, as well as the timing and the number of cells involved, become much clearer with the use of autoradiography after injection of thymidine-H^3.

Material and Methods

Inbred mice at timed stages of pregnancy were injected intravenously with 5 μC of thymidine-H^3 (specific activity 890 mC/mM) per gram of mouse, as in previous studies (Sidman *et al.*, 1959). Young postnatal mice were injected subcutaneously (Miale and Sidman, 1960). Mice were killed at the times recorded in Table I. The eyes were fixed in Bouin's fluid, dehydrated, and embedded in polyester wax. Sections cut at 5 μ were mounted on microscope slides, dewaxed, and dipped into Kodak NTB 3 bulk emulsion, according to Messier and Leblond (1957). Slides were exposed in the dark at —70°C. in the presence of a CO_2 gas phase for 7 to 28 days (average 16 days), and then were developed in the standard way with Kodak Dektol developer. After treat-

TABLE I

SCHEDULE OF EXPERIMENTS

Thymidine-H³ injected on		Animals killed on	
		Embryonic days	Postnatal days
Embryonic day	11	11, 12, 13, 17	1, 10, 30
	12		30
	13	13	1, 10, 30
	15	15	1, 10, 30
	17	17	1
	18		1, 2, 3, 6, 10, 30
Postnatal day	1		2, 10, 30
	2		4, 10, 30
	4		5, 10, 30
	5		6, 10, 30
	6		10, 15, 30
	10		15, 20, 30
	15		20, 30
	20		30
	30		

ment with hypo and thorough washing in water, slides were stained by the Cason method (Sidman *et al.*, 1959). The slides were dehydrated in ethanol, cleared in xylene and cover slips were applied with Permount.

Results

The gestation period of our mice was 19 days. By the eleventh day of gestation the optic cup was well developed, though still continuous with the diencephalon via the optic stalk. Numerous mitotic figures were easily recognized at this time near the external surface of the retinal anlage, and were seen continuously until about a week after birth. Differentiation proceeded slowly compared to most other organs. Even at birth the retina was quite immature, a ganglion cell layer had formed but the bipolar and photoreceptor layers were still represented by a single broad, undifferentiated zone. The inner segments of photoreceptor cells formed during the first postnatal week. The outer segments began to form on the eighth day after birth and then elongated progressively over the subsequent few weeks. The patterns of cell division, migration, and differentiation as observed in the autoradiograms were considered against this general framework.

To-and-Fro Migrations in the Primitive Ependymal Zone

Pregnant mice were injected with a single dose of thymidine-H³ and the embryos were removed and fixed one hour later, in order to

locate the nuclei synthesizing DNA. Labeled cells were not detected in retinas exposed to thymidine-H^3 on the tenth day of gestation. At all embryonic stages from the eleventh day of gestation on, a broad band of labeled nuclei was found part way between the outer and inner surfaces of the retina and extending from one edge of the ora serrata to the other (Figs. 1, 2, 10, and 13). Within an average of about 6 hr after uptake of thymidine-H^3 for DNA synthesis, the labeled nuclei migrated to the outer retinal surface and divided. After mitosis most of the nuclei migrated back toward the inner parts of the retina, where they either began to synthesize DNA again in preparation for another mitotic cycle or migrated farther inward and differentiated. This pattern of somewhat synchronous to-and-fro migrations in relation to mitosis is identical with the pattern described in the primitive ependymal zone of the neural tube (Sauer and Walker, 1959; Sidman *et al.*, 1959). In fact, the nuclei synthesizing DNA from thymidine-H^3 in the retina formed a continuous band with the nuclei engaged in similar activity in the adjacent evaginated brain wall of the young embryo (Figs. 1 and 2). In older embryos the retina and the brain wall no longer were continuous, but both continued to generate new cells by comparable means in a pseudostratified primitive ependymal zone. The immature retina was correctly interpreted by Lebouecq (1909) as a pseudostratified epithelium with mitoses limited to one surface.

The number of retinal cells synthesizing DNA at any given time increased dramatically from the eleventh day of gestation until after birth (Table II). The concentration of labeled nuclei per unit volume of retinal primitive ependyma was fairly constant through most of the formative period (Figs. 1, 2, 10, 13), but the volume of the retina in-

---

FIG. 1. Mouse injected with thymidine-H^3 on the eleventh day of gestation; embryos fixed one hour later. Retina and adjacent diencephalon show extensive labeling in the primitive ependymal zone (pe). Epidermal cells, mesenchymal cells, and many blood cells in the hyaloid and other vessels also are labeled. p, primitive optic papilla surrounded by cavity of primary optic vesicle; v, third ventricle bounded by wall of diencephalon. Magnification: × 195.

FIG. 2. Mouse injected with thymidine-H^3 on the thirteenth day of gestation; embryos fixed one hour later. Retina shows band of labeled nuclei in inner part of primitive ependymal zone. Unlabeled retinal nuclei in outer part of primitive ependymal zone (near pigmented cells of pigment epithelium) had completed DNA synthesis before exposure to thymidine-H^3 and are immediately pre- or postmitotic. The unlabeled cells in mantle zone (m) are differentiating ganglion and amacrine cells which had formed in the primitive ependymal zone prior to the thirteenth day. The band of labeled cells (arrows) along the optic stalk represents a narrow primitive ependymal zone still continuous with both retina and diencephalon. Magnification: × 195.


v
pe
1
m
2

creased manyfold. Hicks and D'Amato (1960) have described the corresponding rate of increase in volume of the developing retina in the rat.

TABLE II
RELATIVE NUMBERS OF RETINAL CELLS FORMING ON VARIOUS DAYS

		Number of labeled cells per section	Number of sections per eye	Number of labeled cells per eye
Embryonic day	11	138	25	3,500
	13	267	67	18,000
	15	910	131	119,000
	17	507	228	115,500
Postnatal day	0	686	230	158,000
	2	577	270	156,000
	4	175	285	50,000
	6	43	380	17,000

NOTE: Embryos were killed 1 hr, and postnatal animals 2 hr, after exposure to thymidine-H^3. The number of cells labeled after a single injection of thymidine-H^3 represents only a fraction of the cells forming on a given day, since the thymidine-H^3 is available for incorporation for less than 1 hr (Quastler and Sherman, 1959; Miale and Sidman, 1960).

During the first week after birth mitotic aetivity deereased, first near the eenter of the retina and then progressively toward the ora serrata (Fig. 15). In miee killed 2 hr after injeetion of thymidine-H^3 on the sixth day after birth, only about 40 labeled eells were seen per section of retina. They were limited to the region of the ora serrata. Rare labeled eells were found in the retina after injection on the tenth postnatal day, and none when thymidine-H^3 was injeeted into older miee. The pattern of to-and-fro migrations persisted postnatally, but was more eomplex because the migrating cells crossed regions in which cells were already differentiating, as described below.

FATE OF CELLS FORMING ON THE ELEVENTH AND TWELFTH EMBRYONIC DAYS (TABLE III)

The fate of eells labeled by a single injection of thymidine-H^3 on the eleventh day of gestation was studied after various time intervals (Table I). Forty-eight hours after injection, the majority of retinal cells were labeled, and had begun to separate into two main groups (Fig. 3). One group of cell nuelei occupied the inner parts of the retina; these nuclei were heavily labeled. The other group occupied the outer two-thirds of the retina; many of these nuclei were less intensely labeled and

presumably had divided at least once more than the others. Segregation of the two groups was incomplete at 13 days. By the seventeenth day of gestation the two groups of cells were more clearly separated (Fig. 4). The inner third of the retina was occupied by heavily labeled cells. Most of the cells in the outer two-thirds were less intensely labeled, though some cells were heavily labeled.

TABLE III

FATE OF CELLS INCORPORATING THYMIDINE-H^3

Thymidine-H^3 injected on	Labeled cells differentiating after few further mitoses (heavily labeled)	Labeled cells differentiating after many further mitoses (weakly labeled)
Embryonic day 11	Large ganglion cell neurons; some amacrine and perhaps some horizontal cells	Many cells of ganglion, bipolar, and photoreceptor layers
Embryonic day 13	Large ganglion cell neurons; amacrine cells, horizontal cells, some photoreceptor cells	Some ganglion cells; many cells of bipolar and photoreceptor layers
Embryonic days 15–18	Large and small ganglion cell neurons, amacrine cells, other cells of inner halves of bipolar and photoreceptor layers, scattered other photoreceptor cells	Cells of bipolar and photoreceptor layers, especially in outer parts
Postnatal days 0–6	Neuroglial cells of ganglion cell layer, bipolar and photoreceptor neurons, especially in outer halves of the two layers	

Most of the cells in the inner zone were destined to become retinal ganglion cells, and were assuming their final positions and morphology in the retinas of newborn (Fig. 5) and 10-day-old mice (Fig. 6). The labeled ganglion cells became separated from each other and were compressed into one or two rows as the eye enlarged postnatally (Figs. 5 and 6). Crude counts indicated that the total number of labeled cells in the ganglion cell layer remained constant postnatally.

The cells which occupied the outer two-thirds of the retina in the 17-day embryo were more difficult to trace (Figs. 5 and 6). The few heavily labeled cells in this zone eventually came to reside either at the inner or outer margins of the bipolar layer, or were scattered in the photoreceptor layer. The more numerous, weakly labeled cells became distributed throughout the bipolar and photoreceptor layers. Their con-

centration of radioactive DNA was just above threshold, presumably because of further mitoses. No attempt was made to account quantitatively for this population of cells.

Thus cells originating on the eleventh day of gestation either migrated to the ganglion cell layer with relatively little further mitosis, or continued to divide and became distributed in the bipolar and photoreceptor layers (Table III).

Essentially the same results were obtained with a single litter of mice exposed to thymidine-H^3 on the twelfth day of gestation.

Fate of Cells Forming between the Thirteenth and Eighteenth Embryonic Days (Table III)

Many more cells formed on the thirteenth than on the eleventh day of gestation (Table II, and Fig. 2 compared to Fig. 1). The cells which incorporated thymidine-H^3 on the thirteenth day also were destined to reach all 3 layers of the differentiated retina (Fig. 7). Many became large ganglion cells with few if any mitoses after the thirteenth day. Other heavily labeled cells assumed the position of amacrine cells, along the inner edge of the bipolar layer. A few heavily labeled cells took up positions along the outer edge of the bipolar layer, and probably were horizontal cells; others remained in the photoreceptor layer. Weakly labeled cells were distributed in the bipolar and photoreceptor layers.

Figures 3 to 6 illustrate retinas of mice exposed once to thymidine-H^3 on the eleventh day of gestation; they may be compared with Fig. 1, in the same series.

Fig. 3. Embryo killed on day 13 of gestation. The most heavily labeled retinal cells are entering the mantle zone (m). Many cells in the primitive ependymal zone (pe) have already divided a second time, as judged by the decreased numbers of silver grains over their nuclei. Many blood cells in the hyaloid vessels along the right edge of the tissue are intensely labeled. The pigment epithelial cells along the left margin already contain pigment, not to be confused with the silver grains over cell nuclei. The autoradiograms of retina and cerebral vesicle are almost indistinguishable at this stage (see Fig. 1D in Sidman *et al.*, 1959). Magnification: × 490.

Fig. 4. Embryo killed on day 17 of gestation. Oblique section, showing heavily labeled cells in developing ganglion cell layer (g) and some in primitive ependymal layer (pe). Magnification: × 195.

Fig. 5. Mouse killed one day after birth. Bipolar and photoreceptor layers have not yet separated from each other. Magnification: × 310.

Fig. 6. Mouse killed 10 days after birth. The ganglion cell layer (on the right) is becoming more attenuated and the labeled cells more widely spaced as the eye enlarges. The bipolar (b) and photoreceptor (ph) layers have formed and contain many weakly labeled cells. Magnification: × 310.

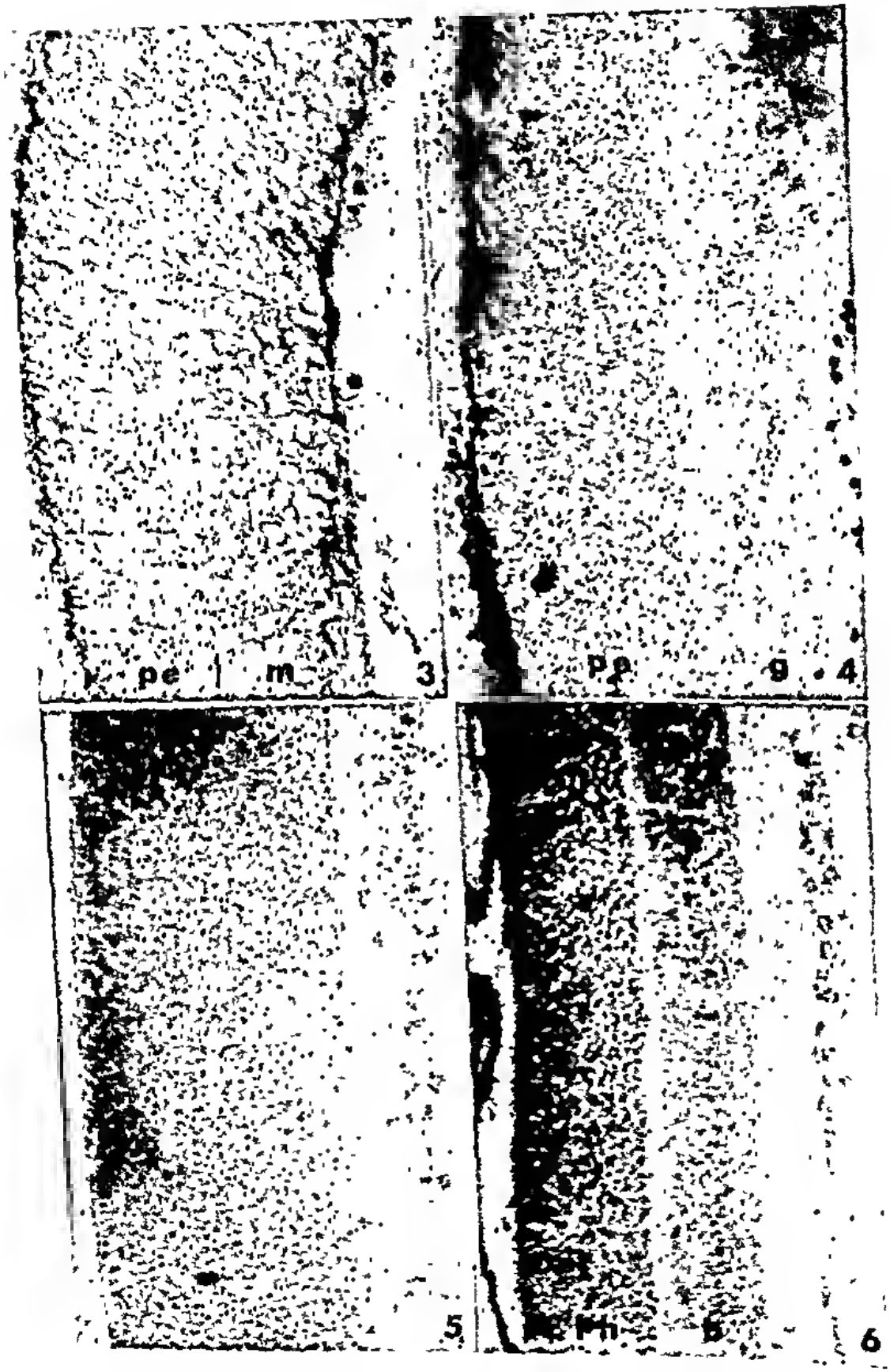
pe
m
3
pp
9
4
5
Ph
6

All of these labeled cells had reached their final positions by the tenth day after birth.

Cells labeled on the fifteenth day of gestation became similarly distributed in the differentiated retina, except that somewhat fewer entered the ganglion cell layer and relatively more entered the bipolar and photoreceptor layers, especially their inner halves (Fig. 8). Both large and small neurons of the ganglion cell layer were labeled (Fig. 9), whereas cells of the ganglion cell layer which became labeled at earlier embryonic stages were almost all large neurons.

Cells labeled on the seventeenth and eighteenth days of gestation were found one day after birth mainly in the combined bipolar and photoreceptor layer (Fig. 11). The lowest concentration of labeled nuclei was in the middle third of this layer. A small percentage of labeled cells were in the ganglion cell layer 48 hr after labeling, and others were in transit across the inner plexiform zone (Fig. 11). By the tenth postnatal day, the greatest number of heavily labeled nuclei was in the inner half of the photoreceptor layer, somewhat fewer were in the inner half of the bipolar layer, and relatively few were in the ganglion cell layer (Fig. 12). An occasional labeled nucleus was still in the inner plexiform layer. Compared to the distribution of cells derived from the 15-day stage, cells formed at 17 days were destined in greater numbers for the photoreceptor layer and in lesser numbers for the ganglion cell layer.

Fate of Cells Forming Postnatally (Table III)

At birth the retina contained a ganglion cell layer and a combined bipolar-photoreceptor layer (Figs. 5, 11, 13). Within the bipolar-photoreceptor layer the innermost few rows of nuclei belonged mainly to amacrine cells, which had formed in an earlier embryonic period. About midway between inner and outer margins were nuclei of differentiating horizontal cells (Figs. 5 and 7; see also Figs. 187 and 188 in Ramon y Cajal, 1960). Nuclei incorporating thymidine-H^3 during the first post-

---

Fig. 7. Mouse injected with thymidine-H^3 on the thirteenth day of gestation; offspring killed 30 days after birth. Heavily labeled cells are large neurons of the ganglion cell layer (g), amacrine cells along the inner edge of the bipolar layer (a), occasional horizontal cells along the outer edge of the bipolar layer (h), and scattered cells in the photoreceptor layer (ph). Magnification: × 780.

Fig. 8. Mouse injected with thymidine-H^3 on the fifteenth day of gestation; offspring killed 10 days after birth. Fewer labeled ganglion cells are seen, but more cells are labeled in the innermost part of the bipolar layer and in all parts of the photoreceptor layer. Some photoreceptor cells are much more heavily labeled than the others. Magnification: × 490.

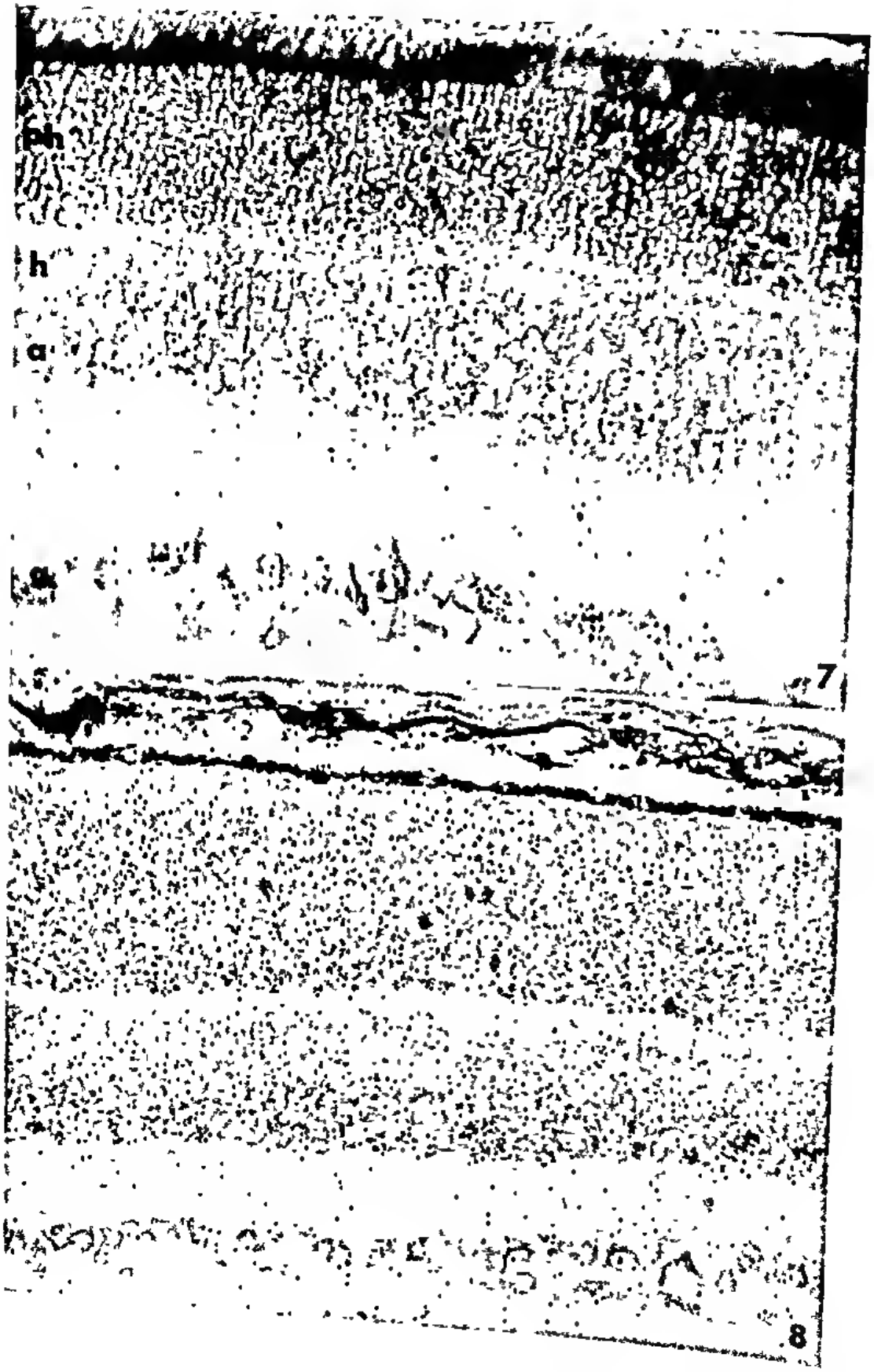
Bh
h
a
7
8

natal week occupied the territory between the amacrine and horizontal cell nuclei (Figs. 13 and 15). These nuclei moved outward past the differentiating horizontal and photoreceptor cells, and divided in typical fashion at the outer retinal surface. In a retina exposed to thymidine-H^3 on the fifth postnatal day and fixed 5 hr later, only about one-third of the labeled nuclei were near the outer retinal surface; the others had not yet migrated significantly. At early embryonic stages, by contrast, the nuclei moved more quickly and more synchronously to the outer retinal surface for mitosis.

After mitosis the cells forming postnatally moved inward from the outer retinal surface and separated into two groups (Figs. 14 and 16). One group of nuclei migrated inward past the horizontal cells and differentiated mainly or entirely into bipolar neurons. The second group of nuclei migrated inward only a short distance and differentiated into photoreceptor cells. Cells forming on the day of birth had reached their final positions in the bipolar and photoreceptor layers less than 72 hr later. The majority of the bipolar neurons of the bipolar layer and almost all the photoreceptor cells in the outer half of the photoreceptor layer formed in this way during the week after birth.

Differentiation was more advanced near the posterior pole of the retina than near the ora serrata, as many previous authors have noted. By the fourth postnatal day the cell population of the bipolar and photoreceptor layers was complete at the posterior pole, and the outer plexiform zone was forming between these two nuclear layers. Cell prolifera-

---

FIG. 9. Same specimen as in Fig. 8, different field. Both large and small ganglion cell neurons are labeled. The heavily labeled cells in the inner part of the bipolar layer (left side of figure) are identified tentatively as amacrine cells. Magnification: × 780.

FIG. 10. Mouse injected with thymidine-H^3 on the seventeenth day of gestation; embryos fixed one hour later. The band of labeled nuclei deep in the primitive ependymal zone extends from one edge of the ora serrata to the other. Cells of the lens epithelium are heavily labeled. Magnification: × 120.

FIG. 11. Mouse injected with thymidine-H^3 on the seventeenth day of gestation; offspring killed one day after birth. Many heavily labeled cells are in the combined bipolar-photoreceptor layer, particularly in its inner and outer thirds. The middle third is occupied mainly by nuclei making DNA at the time of death (see Fig. 13) and therefore contains but few labeled nuclei in this specimen. Magnification: × 310.

FIG. 12. Mouse injected with thymidine-H^3 on the seventeenth day of gestation; offspring killed 10 days after birth. Labeled neurons are found in all three retinal layers. Fewest are in the ganglion cell layer and most are in the photoreceptor layer. Labeled nuclei are concentrated in the inner halves of the bipolar and photoreceptor layers. Magnification: × 310.

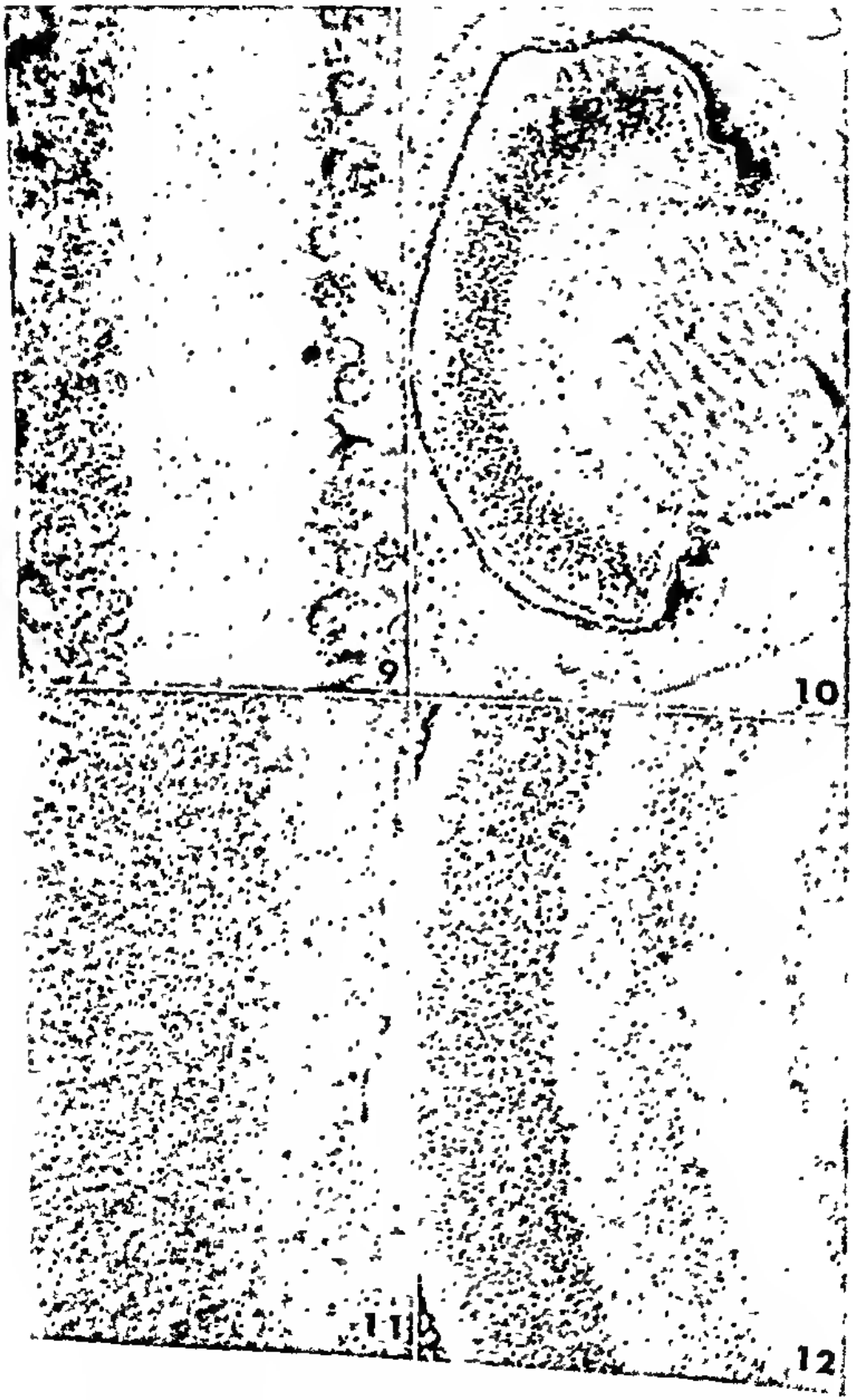
9
10
11
12

tion, as indicated by thymidine-H^3 incorporation, was still prominent laterally toward the ora serrata, where no outer plexiform zone was yet to be seen. The posterior region which contained a developing plexiform zone overlapped slightly with the lateral region which contained cells incorporating thymidine-H^3. Thus some of the labeled nuclei migrated across a developing outer plexiform zone before dividing at the outer retinal surface. Since the plexiform zone was extending laterally at a rapid pace, even more of the postmitotic nuclei migrating back to the bipolar layer would have crossed the plexiform zone.

At 6 days after birth, cells incorporating thymidine-H^3 were confined to the region of the ora serrata (Fig. 16). A retina exposed to thymidine-H^3 on the tenth postnatal day and fixed a month later, contained only one heavily labeled bipolar cell in the 5 sections examined. These late-forming cells probably do not undergo to-and-fro migrations, but divide *in situ*.

In addition to the cells forming in the photoreceptor and bipolar layers, some nuclei of the ganglion cell layer became labeled when thymidine-H^3 was injected postnatally (Figs. 15 and 16). These were small, often elliptical, nuclei disposed between the ganglion cell neurons and the inner surface of the retina. They formed in greatest number in the latter half of the first postnatal week. At the time of their formation these cells could not always be distinguished from endothelial cells of

---

FIG. 13. Mouse injected with thymidine-H^3 on the day of birth and killed 2 hr later. The combined bipolar-photoreceptor layer is still largely a primitive ependymal zone. Labeled nuclei occupy the territory between the already formed amacrine cells and horizontal cells. Thus the zone of DNA synthesis at this time is actually within the presumptive bipolar layer. Magnification: × 490.

FIG. 14. Mouse injected with thymidine-H^3 2 days after birth and killed at 30 days of age. The labeled nuclei occupy the outer halves of the bipolar and photoreceptor layers. Magnification: × 310.

FIG. 15. Mouse injected with thymidine-H^3 4 days after birth and killed 2 hr later. The field lies about half way between the posterior pole of the eye, where thymidine-H^3 incorporation has ended, and the ora serrata, where the primitive ependymal zone continues in full activity. The outer plexiform zone is forming nearer the posterior pole, and will reach the field shown here before all the labeled nuclei have completed their to-and-fro migration. The heavily labeled cells on the right margin of the retina are neuroglial cells. Magnification: × 195.

FIG. 16. Mouse injected with thymidine-H^3 six days after birth and killed at 30 days of age. On the 6th postnatal day, thymidine-H^3 uptake is confined to cells near the ora serrata. These cells also divide at the outer retinal surface and then separate into two groups, which come to occupy the outer halves of the bipolar and photoreceptor layers. A heavily labeled neuroglial cell with an elongated nucleus is seen in the ganglion cell layer, at the lower right. Magnification: × 195.


13
14
15
16

the proliferating vitreal capillaries (Fig. 13). However, in mature eyes which had incorporated thymidine-H^3 during the first postnatal week, the labeled cells were identified more securely as neuroglial cells in the nerve fiber zone of the ganglion cell layer (Fig. 16).

Discussion

One of the limitations in the study of histogenesis by means of autoradiography with tritiated thymidine is that the radioactivity per nucleus is halved with each cell division. Our mice were exposed to relatively high doses of tritium, but many mature retinal cells containing tritiated thymidine were only slightly above the threshold of detection by autoradiography, and others almost surely were undetected. Further limitations, especially concerning quantitation, are discussed by Miale and Sidman (1960). Despite these limitations, autoradiography with thymidine-H^3 is a very powerful method for the study of histogenesis in mammals.

We were surprised to learn that cells destined for all three retinal layers are forming simultaneously through most of the developmental period. However, the relative numbers of cells destined for each layer changes with time. The ganglion cell layer attains its full complement of neurons earlier than the other layers, and the photoreceptor layer receives a majority of the cells forming at any given moment during the last two-thirds of the developmental period. This pattern of development might differ in certain details in vertebrate species with relatively more cells in the bipolar layer than in the photoreceptor layer.

The developmental history of almost all cell types in the mouse retina can now be described. The large ganglion cell neurons originate in the primitive ependymal zone of the retina on the eleventh to seventeenth days of gestation and migrate inward to the ganglion cell layer without further mitotic division. A few are still migrating in the early postnatal period. Small neurons of the ganglion cell layer form mainly between the fifteenth and eighteenth days of gestation. Neuroglial cells of the ganglion cell layer form postnatally, with the peak in the latter half of the first week after birth. These cells incorporate thymidine-H^3 while in the ganglion cell layer.

Amacrine cells, located along the inner margin of the bipolar layer in the mature retina, form at the same time and place as the ganglion cell neurons. Some of the cells labeled on embryonic day 11 divide two or three times more before differentiating into amacrine cells. Most of the ones labeled on days 13 or 15 divide only once after incorporating thymidine-H^3, and then differentiate. Many horizontal cell neurons,

located along the outer margin of the bipolar layer, form on embryonic day 13. Horizontal cells are too difficult to identify in our material to warrant a more complete description of the period in which they form. Cells destined to become the bipolar neurons of the bipolar layer migrate to-and-fro and divide many times in the primitive ependymal zone during the embryonic period; the majority cease dividing and differentiate postnatally.

The future photoreceptor cells also divide repeatedly in the primitive ependymal zone during the embryonic period. By the seventeenth day of gestation a significant percentage of the cells whose nuclei will occupy the inner half of the photoreceptor zone are dividing for the last time. Bipolar neurons with nuclei in the inner half of the bipolar layer form at the same time and place. Most of the cells with nuclei in the outer half of the photoreceptor zone complete their mitoses in the first postnatal week. They arise in common with those bipolar neurons whose nuclei take positions in the outer half of the bipolar layer. Presumably these potential photoreceptor and bipolar cells which are making DNA postnatally, comprise the radiosensitive population described by Glucksman and Tansley (1936) and Hicks and D'Amato (1960).

The origin of Muller's cells is not clear in our material. Ramon y Cajal (1960) described the early formation of Muller's cells, with protoplasmic processes extending to both inner and outer surfaces. Muller's cells were thought to be capable of division, and it is interesting to note that double telophase nuclei were illustrated only near the outer retinal surface. Probably many or most of the elongated cells stained by the reduced silver methods were not Muller's cells, but were undifferentiated primitive ependymal cells at various phases of the to-and-fro migration cycle related to mitosis (see, for example, Figs. 168, 169, 172, and 173 in Ramon y Cajal, 1960) Since the primitive ependymal zone persists into the postnatal period, this interpretation would account also for Ramon y Cajal's uncertainty in identifying early stages of bipolar neurons and photoreceptor neurons, and in distinguishing them from "imperfectly impregnated Muller's cells."

An Hypothesis Concerning the Origin of Synaptic Specificity

The simultaneous origin in space and time of nerve cells with close functional relationships may be more than coincidental. Many ganglion cell neurons and amacrine cells simultaneously become labeled with thymidine-H^3 (Fig 9) A ganglion cell and an amacrine cell might be daughters of a common parent cell which incorporated thymidine-H^3 while in the primitive ependymal zone. The cell bodies of these daughter cells migrate apart and their cytoplasmic processes form the inner plexi-

form layer. The two cells might maintain contact across the inner plexiform layer even while the cell bodies are separating. Appropriate synaptic contacts could be established and, in this way, the vexing problem circumvented of what specific attractive forces secondarily draw selected nerve cells into synaptic relationships.

The simultaneous formation of inner bipolar and inner photoreceptor cells during the late embryonic period (Fig. 12), and of outer bipolar and outer photoreceptor cells during the postnatal period (Fig. 14), may have a similar significance. Other instances are seen during histogenesis of the central nervous system. For example, the Purkinje cells of the cerebellar cortex and the neurons of the cerebellar roof nuclei arise simultaneously on the eleventh and twelfth days of gestation and migrate apart over the next several days (Miale and Sidman, 1960). No other cell type of the cerebellum forms in significant quantity on those embryonic days. The two cell types are well known to be in direct synaptic contact.

The hypothesis that synaptic specificity might arise by contact between daughter cells from the time of their origin is offered very tentatively. The hypothesis has the merit of being testable. However, even if the hypothesis should prove valid, it can have only limited applicability within circumscribed regions of the nervous system; it could not account, for example, for the specificity of synaptic relations between retinal ganglion cells and neurons in visual centers of the brain.

Summary

Autoradiographic studies after injection of tritiated thymidine into mice have given data on the time, place, and rate of formation of various retinal cell types. Cells destined for all three retinal layers form simultaneously through most of the developmental period. Cell nuclei synthesize DNA while positioned deep in the primitive ependymal zone; they then migrate to the outer retinal surface, divide, and migrate inward again to repeat the cycle or to differentiate. Ganglion cell neurons and amacrine cells form early, as do many horizontal cell neurons. Cells with nuclei in the inner halves of the bipolar and photoreceptor zones form simultaneously in the late embryonic period, and cells whose nuclei are destined to occupy the outer halves of the bipolar and photoreceptor layers form simultaneously in the first week after birth. Crude calculations were made of the relative numbers of cells forming at each stage of the developmental period. A tentative hypothesis is suggested, that specificity of synaptic connections in a circumscribed region of the nervous system might arise by maintenance of contact between daughter

cells as their cell bodies migrate from the common site of origin to separate positions in the mature tissue.

References

Detwiler, S. R (1932). *J. Comp. Neurol.* **55**, 473-492.

Furst, C. M. (1904) *Lunds Univ. Arsskr.* **40**, 1-45

Glucksman, H , and Tansley, K. (1936). *Brit. J. Ophthalmol* 20, 497-509.

Hicks, S P., and D'Amato, C. J. (1960). *2nd Intern. Symposium Phakomatoses Cerebrales, Paris, October, 1959.* In press

Hughes, W L , Bond, V. P , Brecher, G., Cronkite, E. P., Painter, R. B , Quastler, H , and Sherman, F. G. (1958). *Proc. Natl. Acad. Sci. U. S* **44**, 476-483.

Lebouerq, C. (1909). *Arch. anat. microscop.* **10**, 555-605

Messier, B , and Leblond, C P (1957). *Proc. Soc. Exptl. Biol. Med.* **96**, 7-10.

Miale, I., and Sidman, R L (1960). *Exptl. Neurol* Submitted for publication.

Polyak, S. L. (1957). "The Vertebrate Visual System." University of Chicago Press, Chicago, Illinois

Quastler, H , and Sherman, F. G. (1959). *Exptl Cell Research* **17**, 420-438.

Ramón y Cajal, S R. (1960) "Studies on Vertebrate Neurogenesis" (L Guth, transl.), pp. 353-405 C. C Thomas, Springfield, Illinois.

Sauer, M. E , and Walker, B E. (1959) *Proc Soc. Exptl. Biol. Med.* **101**, 557-560.

Sidman, R L. (1960) *Anat Record* **136**, 276-277.

Sidman, R. L , and Miale, I (1959). *Anat Record* **133**, 429-430

Sidman, R. L., Miale, I., and Feder, N (1959). *Exptl Neurol.* **1**, 322-333.

Discussion

Dr von Sallmann [National Institutes of Health, Bethesda, Md.]. How do you explain that you label only the cells of one generation in tissue cultures, although thymidine is available?

Dr. Sidman [Harvard Medical School, Boston, Mass.] I have no explanation to offer

Dr. von Sallmann Is there any indication that thymidine uptake is not limited to the premitotic stage in dividing cells?

Dr. Sidman. S R Pelc has presented the best evidence for thymidine turnover *independent of cell division (Lab Invest 8, 225-236, 1959).* He found synthesis or exchange of DNA out of proportion to the slight mitotic activity in mouse seminal vesicle (*Exptl Cell Research* **14**, 301-315, 1958) We have seen apparent cytoplasmic labeling of blood cells after exposing young mouse embryos to thymidine H^3 In the retina, however, we have a nuclear label which *remains stable through at least* the period of morphogenesis The label is always in cell nuclei, and the number of labeled cells is usually about ten times the number of mitotic figures I would feel reasonably confident that in the retina we are labeling a premitotic population of cells and retaining that label in DNA.

Dr Cohen [Washington University, St. Louis, Missouri] *All the cells that* line the ventricle of the lumen of the neural tube or the cavity of the optic cup have terminal bars *Dr* Sidman's work would indicate that a cell could wander up to the surface, fit in, form terminal bars, divide, break down its terminal bars, and move out, in which case the attachment sites are pretty labile

Dr. Sheiser [Columbia University, New York] I just wanted to comment

that in the last year and a half, Miss Ozanics and I have been working on precisely the same problem that Dr. Sidman has been discussing, and our observations confirm his in every respect. We have not determined the length of time between DNA synthesis and mitosis as he did, but in general our data are the same.

DR. COULOMBRE [Yale University, New Haven, Conn.]: Do the cells which later migrate back into the ganglion cell layer and the cells which remain superficially belong either totally to the rod system or totally to the cone system?

DR. SIDMAN: Possibly the small number of heavily labeled cells forming at embryonic stages could belong to the cone system, as there is one cone per 10 or 20 rods in the mature eye. We have no direct information on rod versus cone systems.

Production of Congenital Eye Malformations, Particularly in Rat Fetuses

H. TUCHMANN-DUPLESSIS AND L. MERCIER-PAROT

Laboratoire d'Embryologie, Faculté de Médecine, Paris, France

At the present time, study of the cause of malformations assumes a medicosocial importance of the first order. Because of effective methods of prevention of infectious diseases, malformations have become the chief cause of infant mortality and of serious infirmities. Anomalies of vision are particularly frequent, for apart from the central nervous system the eye is the organ which proves to be most sensitive to the harmful action of external factors.

According to Berens *et al.* (1955), 67% of blind children of preschool age are affected by prenatal blindness. It is hard to know what proportion of malformations are of genetic origin as compared with those due to an external teratogenous factor. Opinions of writers vary, but it seems that genetic origin has been proved with certainty only in about 20% of the cases.

The appearance of certain anomalies in the course of successive pregnancies may suggest an hereditary origin. However, as a result of the work of Hale, Warkany, Giroud, Nelson, and Wilson, we know that numerous ocular anomalies considered to be of genetic origin may also be due to infections, intoxications, or unsuspected deficiencies. In human beings ocular anomalies resulting from infection by German measles offer a well-known example.

The importance of external factors in the production of ocular malformations is eloquently attested by experimental results. As Wilson noted (1959), analysis of the literature on the subject reveals that about 60 different methods have been successfully employed to obtain malformations in laboratory animals.

The most varied factors, physical, chemical, nutritional, infectious, as well as metabolic disorders and disorders of the endocrine glands, can affect the development of the eye and cause malformations. In the occurrence of these malformations, as in that of all other anomalies, the sensitivity of the primordium, which varies in the course of development, and the specific toxicity of each teratogenous agent, must be considered of particular importance. To these essential factors must evidently be added the animal's genotype, which influences more or less

appreciably the reaction to the teratogenous agent, and can therefore result in considerable variations in the degree and type of malformations.

In the restricted scope of this article we shall briefly summarize results obtained by numerous authors experimenting in mammals, which all bear witness to the vulnerability of the ocular apparatus.

That the optic primordium is of great sensitivity is proved by the malformations obtained by various methods. The action of X-rays gives us a very clear demonstration of this. According to Wilson *et al.* (1953), 25 r are sufficient to disturb ocular development, whereas the teratogenous amounts for other organs are of 100 r or more.

Numerous examples of the close correlation between the date of occurrence of the teratogenous factor and the nature of the malformation are known. Experiments using X-rays, the amount and action of which can be measured with precision, are eloquent on this matter. Hicks (1953, 1954), by means of a single irradiation of 100 r of rats on the tenth day of pregnancy obtained anophthalmia. More or less complex damage to the retina was obtained after irradiation on the eleventh and twelfth days.

Similar observations made by Giroud and Martinet (1956) show that a hypervitaminosis A from the fifth to the eighth day results in anophthalmia, from the eighth to the eleventh day in anophthalmia and microphthalmia, and from the eleventh to the fourteenth day, aplasias of the eyelids, and only cataract if the treatment is applied from the eighteenth to the twenty-first day.

When using x-methylfolic acid for production of ocular malformations, Nelson *et al.* (1955) observed that the most vulnerable stage of the ocular primordia was on the eighth and ninth days.

Review of the Chief Factors Which May Bring About Ocular Malformations

Physical Factors

X-radiation

The ocular primordium is very vulnerable to *radiation*. With amounts varying from 100 to 200 r a great variety of ocular anomalies have been produced in laboratory animals (Wilson *et al.*, 1953; Hicks, 1953; Rugh, 1958, 1959; Rugh and Clugston, 1954; Rugh and Wolff, 1955).

Irradiations early in pregnancy result in total absence of development of the optic primordium, primary anophthalmia, or microphthalmia with various other anomalies, among them the persistence of the choroid fissure.

Irradiations later, after the eye is formed, produce different kinds of

damage to the retina including rosettes, as Rugh and Wolff have shown (1955). When mice are irradiated on the thirteenth day of gestation to the extent of 300 r, massive destruction of the future retinal cells is observed 4 hr after the treatment; about 50% of them are pycnotic. After 24 hr the cellular disintegration continues and active phagocytosis appears; 72 hr after irradiation, however, the majority of fetus eyes prove to have been capable of repairing the lesions produced by the radiation, so that the retina appears almost normal; the eye remains small, there is a slight microphthalmos but its general morphological proportions are not modified.

Certain agents (cysteamine) diminish and others such as cortisone (Woolam *et al.*, 1959), augment sensitivity to X-rays.

The eye of the human embryo is likewise very sensitive to X-rays, and numerous accidents, especially microphthalmia, have been reported in children born to women who have undergone therapeutic irradiations during the first weeks of pregnancy.

Engelking (1935) has described a case of bilateral microphthalmos with microcephalus in a child whose mother had undergone such treatment in about the seventh or eighth week of pregnancy.

Rugh (1958), based on results of irradiation obtained experimentally and on data relating to the embryonic development of the human, thought that the fetal eye must be particularly vulnerable to the effect of radiation around the twenty-eighth day of pregnancy.

Hypothermia

Working on hamsters, Smith (1957) established that "deep freezing" resulting in a lowering of body temperature below zero centigrade for 45 min between days 1½ and 8½ caused malformations, among which were unilateral or bilateral anophthalmia.

Hypoxia

Werthemann and Reiniger (1950) observed various malformations among rats subjected to low pressures (460 to 350 mm of mercury) between the first and eighth days of pregnancy. "Puckering" of the retina and degeneration of the lens were among these.

Ingalls *et al* (1952) submitted mice to low atmospheric pressure of 280–260 mm of mercury for 5 hr on the eighth day of gestation, and obtained fetuses of which the eyes were open, exhibiting lesions of the lens and of the retina. The authors thought that the malformations thus obtained exhibited analogies to retrolental fibroplasia. It is however rather an excess of oxygenation or its abrupt variation which causes this condition. Retrolental fibroplasia is a disease of the premature which

appears usually 4–5 weeks after birth. However, it can be related to congenital malformations because of the incomplete development of the eye, which may favor the formation of lesions of the vitreous body.

Even though a great amount of work was done in recent years, there is still no agreement concerning the etiology and pathogenesis of this condition.

Many observations, however, strongly point out an influence of environmental oxygen in the production of the disease. There is a correlation between the use of high oxygen concentration in incubators and the incidence of the disease (Symposium: Retrolental Fibroplasia, 1955).

Similar but not identical lesions to retrolental fibroplasia have been produced by various conditions: hypoxia of the mother hyperoxia of the newborn (Gyllensten and Hellström, 1956, in mice), vitamin deficiencies, and hypervitaminosis A. Giroud and Martinet (1959a) have observed after hypervitaminosis A in rabbits, hemorrhagic eyes, fibrosis of the vitreous body, alterations and hemorrhagic lenses, and detachment of the retina followed by degeneration.

Chemical Substances

As experimentation proceeds, the number of chemical substances capable of producing ocular malformations increases.

Trypan Blue

This is well known as a teratogenic agent (Gillman *et al.*, 1948; Wilson, 1955; Hamburgh, 1954; Tuchmann-Duplessis and Mercier-Parot, 1956). Gilbert and Gillman (1954) have analyzed in detail all known types of ocular malformations which can be observed in rats: anophthalmia, microphthalmia, anomalies of the retina—sometimes with eversion. We have likewise observed microphthalmia, anophthalmia, and exophthalmia in rats (Tuchmann-Duplessis and Mercier-Parot, 1956). Analogous results have been obtained with mice (Hamburgh, 1954).

Various *antimitotics* have likewise proved to be harmful to the eye. In the course of our researches we have observed ocular malformations with the following: 1 methyl-4-aminopyrazolo(3.4d)-pyrimidin and triethylenmelamin (Tuchmann-Duplessis and Mercier-Parot, 1958c).

Hoskins (1948), Thiersch (1954, 1957), and Murphy (1959; Murphy and Karnofsky, 1956) have examined a long series of antimetabolites, "anti-growth" substances, and "alkylating agents," of which several have proved teratogenous to rats, without their effect on the eye having been studied, however.

The effects on the eye of *hypoglycemic sulfonamides* and of *actinomycin D* which we have observed are described below.

Maternal Nutritional Deficiencies

During the last 15 years this problem has been studied extensively in the laboratories of Warkany, Giroud, and Nelson. Ferraro and Roizin (1947) obtained anomalies of the cornea and crystalline lens following tryptophan deficiency. Among work on food deficiency, let us draw attention to the observations of Pike (1951), which report cataracts after a diet deficient in tryptophan. Certain sugars, such as galactose, produced cataracts in rats (Bannon *et al.*, 1945). Recently de Meyer (1959) has also observed in rats treated with galactose the same lesions of the lens with various degrees of vacuolization and of necrosis. He has also noted that the migration of the optic fibers toward the diencephalon is defective or even absent.

Vitamins

Hale (1935) showed that microphthalmia in pigs could be due to a lack of vitamin A. In rats, vitamin A deficiency, as Warkany and Schraffenberger (1946) have shown, results in multiple malformations of the eye, particularly colobomas, fibroses of the vitreous body, and puckering of the retina.

Deficiency in pantothenic acid entails anophthalmia and microphthalmia (Lefebvres, 1951, Giroud, 1957). This writer has been able to find examples demonstrating phenomena of induction of the lens as known among the lower animals. absence of the optic cup resulting in absence of the crystalline lens, and reduction of the cup causing the appearance of a small crystalline lens only Likewise he finds proof of the independent development of the ocular annexes vis-à-vis the optic primordium, as observed experimentally in birds by Amprino (1949). In cases of anophthalmia, indeed, where all ocular primordium is absent, the eyelids, the tear glands, and the eye muscles are present.

Deficiency of folic acid (A. Giroud *et al.*, 1954) often results in complex malformations of the eye, due to eversions and folding of the retina arising from colombas. These malformations provide an opportunity to observe what happens in the coloboma The eversion of the retina, that is to say its external exposure at the location of the external opening, tends normally to form in pigs and in birds at the upper part of the choroid fissure (Mann, 1957) It attains its fullest extent in malformed eyes. It appears to result from the limited growth of the pigment epithelium relative to the retinal layer.

From these data, Giroud has been able to find arguments in support of theories concerning the mechanism of formation of the choroid. He also has had opportunity to observe abnormal evolutions of the primordia

of the lens: it may remain in continuation with the epithelium of the palpebral chamber or, in detaching itself, may permit the formation of a supernumerary lens (Fig. 1).

Nelson *et al.* (1955) observed colobomas with eversion and retinal cysts engendered by x-methylfolic acid administration. Using the same method, Tuchmann-Duplessis and Lefebvres-Boisselot (1957) have observed the production of microphthalmia in the cat.

Vitamin B_2 deficiency obtained by use of an anti-vitamin, galactoflavin, produces some ocular malformations (Nelson *et al.*, 1956; Kalter and Warkany, 1957).

An excess of vitamin can also prove teratogenous, which is the case with A hypervitaminosis (Cohlan, 1953; Giroud and Martinet, 1954). Anophthalmia and a whole series of microphthalmia have been observed in the rat and rabbit (Giroud and Martinet, 1959b) where this excess can cause colobomas, as well as fibrosis of the vitreous body, inducing folding of the retina and intraocular hemorrhages (Fig. 2).

Hormonal Factors

Unbalanced thyroid activity (hypo- or hyperactivity) has been shown to have a definite influence on the development of the eye. Giroud and his co-workers (1951–1954) have obtained cataracts after administration of thyroxine. So far, malformations of the eye have not been reported after administration of antithyroid substances. We have not found any ocular anomalies in the rat after administration of propylthiouracil. In hypothyroidism obtained by thyroidectomy, however, Langman and van Paassen (1955) have observed numerous ocular malformations in the rat, particularly retinal folds. Clinical workers have also considered unbalanced thyroid activity responsible for malformations, without, however, advancing strict proof.

The action of other hormones, such as the corticosteroids, sexual hormones, pituitary-stimulating substances, and insulin, still remains a matter for controversy. It is worth recalling that disturbances of hydrocarbon metabolism, in particular diabetes and prediabetes, have often been thought responsible for embryopathies which are said to be three times more frequent in these conditions than among normal women (Hoet, 1959).

Infections

Since the observations made by Gregg (1942), it is known that rubella causes single or bilateral cataracts with atrophic appearance of the iris. Sometimes microphthalmia or buphthalmia or retinal dystrophy may be observed. Their frequency depends on the period of gestation at

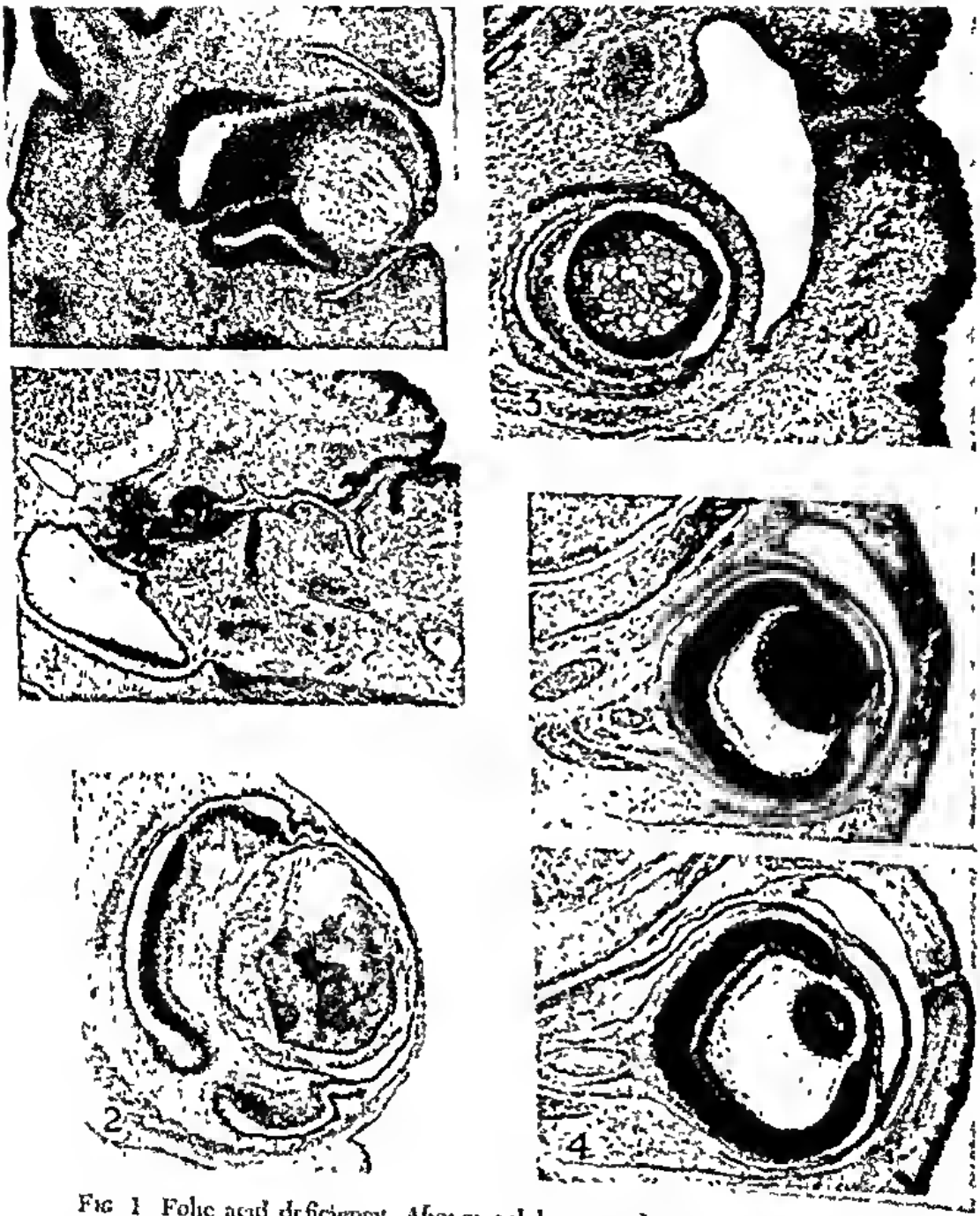

FIG 1 Folic acid deficiency *Above:* coloboma and supernumerary lens *Below:* lens not separated from the epidermis, on the left a part of the eye. (From Giroud and Lefebvres, unpublished)

FIG 2. *Hypervitaminosis* A on rabbit Coloboma, fibrosis of vitreous and hemorrhagic lens (From Giroud and Martinet, 1959b.)

FIG 3 Carbutamide BZ 55 Microphthalmia, undifferentiated epithelium, lens without fibrous differentiation.

FIG. 4 Carbutamide BZ 55. *Above* eye with abnormal migration of the retinal fibers and with aplasia of the optic nerve *Below:* normal eye for the comparison of the optic nerve

which the attack of rubella occurs, which varies from 20 to 100% (Waardenburg, 1955).

Microphthalmia, persistence of the pupillary membrane, and especially chorioretinitis have been observed in cases of toxoplasmosis (Bamatter, 1947). After infecting rats with *Toxoplasma gondii,* P. Giroud *et al.* (1954) observed only cataracts. Waardenburg (1955), analyzing the data to be found in the literature of the subject, found that in 78 proven cases of toxoplasmosis, there were 37 cases of microphthalmia and 33 cases of eyes with atrophia.

The fragile character of the ocular primordium is thus shown by the multiplicity of agents capable of disturbing its development, as is also shown in the following experiments.

Action of Hypoglycemic Sulfonamides and Actinomycin D

Our experiments with the hypoglycemic sulfonamides have been carried out on the rat; but the studies with actinomycin D have been made on both rats and rabbits.

The hypoglycemic sulfonamides used included: carbutamide BZ 55, tolbutamide D 860, 2259 R.P. and chlorpropamide. All were administered orally in daily doses of from 60 to 350 mg per animal, from the first to the twelfth day of gestation. The mothers were generally sacrificed between the sixteenth and twentieth days of gestation.

Only two of these four substances proved to be teratogenous and 200 mg per day caused the maximum frequency of malformations. The carbutamide causes, depending on the strain of rats, 11 to 39% of macroscopically observable malformations and tolbutamide only 2 to 4% of anomalies. Ninety-five per cent of the anomalies produced by carbutamide BZ 55 concerned the eye (Tuchmann-Duplessis and Mercier-Parot, 1958a, b, c).

It has not yet been possible to determine the mechanism of the teratogenous action of this sulfonamide, but it does not seem to be connected with its hypoglycemic properties, nor with a modification of the glucidic metabolism of the retina, as suggested by the observations of Trerotoli (1956).

Ocular anomalies caused by BZ 55 are both unilateral and bilateral; when unilateral, they affect the left side in 90% of the cases.

Histological study of 16-day fetuses revealed only microphthalmia, the retinal epithelium of which often remained undifferentiated (Fig. 3). Sometimes pigmentary and retinal differentiation occurred, but the choroid fissure remained more or less open. The size of the lens was generally proportionate to that of the optic vesicle.

The 20-day fetus eyes are of normal appearance, though sometimes of slightly diminished size, but reveal important anomalies of the optic nerve which may be atrophied or even absent. Among such eyes we observe that, besides the fibers which normally go toward the diencephalon, a number of nerve fibers take the opposite direction and emerge on the side of the iris (Fig. 4). They may then either introduce themselves between the two layers of the retina, or emerge through the pupil and make their way toward the cornea. In extreme cases all the nerve fibers have an abnormal centrifugal pattern of emergence, and in consequenee there is complete absence of the optie nerve (Fig. 5).

In a comparison of the 16- and 20-day fetuses, marked aggravation of oeular lesions proportionate to the age of the fetus was noticed. This suggests a process of secondary destruction, which is diseussed below. Some mothers were allowed to bear their young, and we were able to see the final development of cases of microphthalmia (Fig. 6).

Analogous, but in general much more serious, malformations were obtained by use of actinomycin D (Tuchmann-Duplessis and Mercier-Parot, 1958d, 1959a, b) The highest percentage of malformations (56%) was obtained by intraperitoneal injection of 20 μg on the eighth and ninth days of gestation.

In the majority of cases the anomalies were considerable, whether single or multiple, some concerned the eye, with a predominance of anophthalmia. Various malformations were to be observed, such as colobomas, abnormal orientations of the primordia, wrinkling of the retina, and various deteriorations of the lens. Anomalies of the optie nerve with centrifugal emergence of optic fibers (Fig. 7) were also observed.

Conclusion

The facts related demonstrate the high degree of sensitivity of the eye to the action of very varied external factors. The anomalies prove to be most serious when the teratogenous action is greatest, and when its action occurs at the earlier stages of morphogenesis.

As the different stages of ocular development succeed one another, various types of malformation may occur successively. Very early teratogenous action may result in anophthalmia, and later action produces various types of microphthalmia Later still they cause deterioration of the retina, particularly abnormal development of the visual fibers. The situation is complicated by the possibility of secondary regressions. Our observations emphasize this.

Comparison of embryos of 16 and 20 days gestation has shown that,

in the first, anophthalmia is not to be found, but only fairly marked microphthalmia, whereas anophthalmia are frequently met in the second. This leads us to suppose that secondary regressions have occurred, and that the observed anophthalmia would seem not to be original ones. This interpretation is supported by the fact that when examined histologically the microphthalmic eye may be found to have an incomplete stalk, which is present near the diencephalon and is observed near the optic cup. As it was certainly complete in the beginning, there can be no doubt of its secondary regression.

These facts should be compared with the observations of Browman and Ramsey (1943) on microphthalmic rats. The eye is well developed at first, but in a second phase it regresses, apparently due to insufficient development of the vessels.

Our information does not allow us to hold any definite opinion on the mechanism, but a secondary regression or atrophy is indicated. The simultaneous development of an optic nerve of reduced size and an emergence of the visual fibers in the anterior pole of the eye is more complex. Such an abnormal emergence of the fibers was also observed in the regenerating eye of *Rana pipiens* (van Campenhout, 1935) and in rats by de Meyer and Isaac-Mathy (1958). This curious behavior of the visual fibers must be related to the more general problem of the orientation of the nerve fibers. It is well known that in the growing fetus the nerve fibers make their way toward the somites. The correlation between the orientation of the nerve fibers and the position of the primordia which they innervate has been well shown by Detwiler (1936). When, indeed, these primordia are displaced, the new medullary segments opposite which they are grafted emit their fibers in their direction. These facts allow us to suppose the existence of a neurotropic stimulant. Such a possibility is now supported by the observations of Levi-Montalcini (1958), who has suggested the possibility of a selective stimulation of the growth of the cells and nerve fibers by certain proteins.

On the basis of these facts, we can envisage that the abnormal emergence of the optic fibers may arise from a disturbance of their sensitivity to the growth stimulant. It may be due equally to insufficient production of stimulating substance in the optic peduncle, or even to the appearance of similar substances at an abnormal place.

This brief review demonstrates the high degree of sensitivity of the eye to the noxious action of external factors. The seriousness of malformations is proportionate to the time at which the teratogenous agent acts, as well as to its nature. In addition, as numerous observations show, the frequency of anomalies may vary to an important degree with respect to the genotype of the individual.

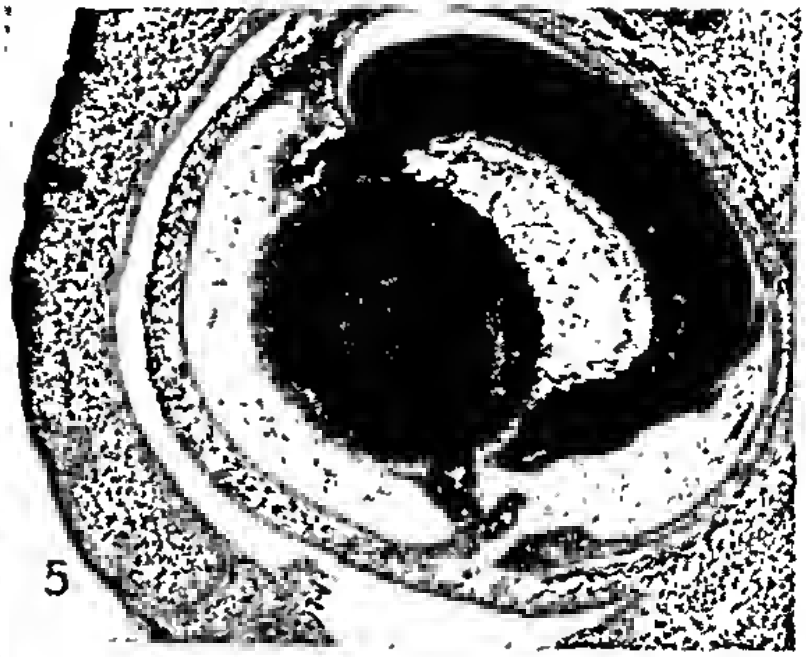

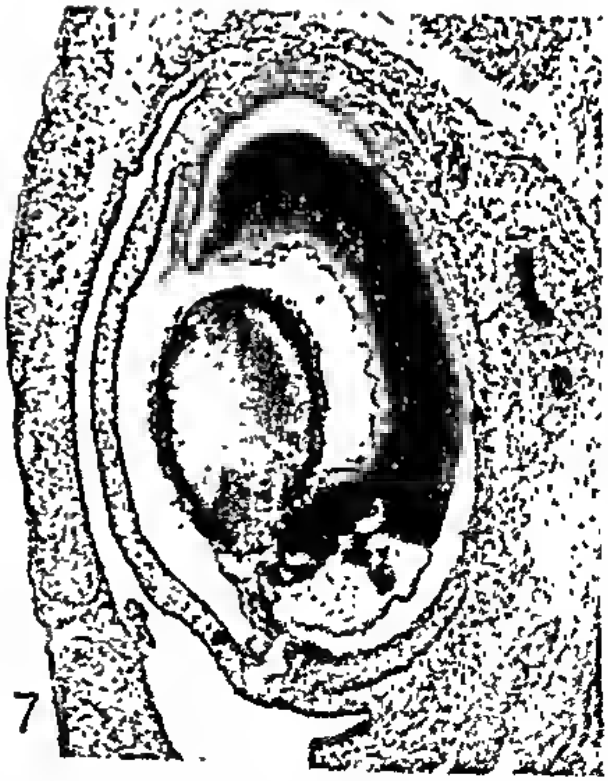

FIG. 5. Carbutamide BZ 55. Abnormal migration of the retinal fibers between the pigmented epithelium and the retina and into the cornea.

FIG. 6. Carbutamide BZ 55. Rat 40 days with microphthalmia, right eye, ventral view of the brain showing atrophy of the optic nerve on the right.

FIG. 7. Actinomycin D. Eye with abnormal migration of retinal fibers between the retina and pigmented epithelium and in the cornea.

References

Amprino, R. (1949). *Bull. Assoc. Anat.* **56**, 3-11.

Bannatter, F. (1947). *Acta Ophthalmol.* **114**, 340-358.

Bannon, S. L., Higginbottom, R. M., McConnel, J. M., and Kaan, H. W. (1945). *Arch. Ophthalmol.* **33**, 224-228.

Berens, C., Franklin, M. D., Foote, M., and Kerby, C. E. (1955). *J. ophtalmol. sociale* **15**, 3-12.

Browman, L. G., and Ramsey, F. (1943). *Arch. Ophthalmol.* **30**, 338-351.

Cohlan, S. Q. (1953). *Science* **117**, 535-536.

de Meyer, R. (1959). *Ann. endocrinol. (Paris)* **20**, 203-211.

de Meyer, R., and Isaac-Mathy, M. (1958). *Ann. endocrinol. (Paris)* **19**, 167-172.

Detwiler, S. R. (1936). "Neuroembryology: An Experimental Study." Macmillan, New York.

Engelking, E. (1935). *Klin. Monatsbl. Augenheilk.* **94**, 151-163.

Ferraro, A., and Roizin, L. (1947). *A.M.A. Arch. ophthalmol.* **38**, 331-335.

Gilbert, C., and Gillman, J. (1954). *S. African J. Med. Sci.* **19**, 147-154.

Gillman, J., Gilbert, C., Spence, I., and Gillman, T. (1948). *S. African J. Med. Sci.* **13**, 47-90.

Giroud, A. (1957). *Acta Anat.* **30**, 297-306.

Giroud, A., and de Rothschild, B. (1951). *Compt. rend. soc. biol.* **145**, 525-526.

Giroud, A., and Martinet, M. (1954). *Arch. Ophtalmol. (Paris)* **14**, 247-258.

Giroud, A., and Martinet, M. (1956). *Arch. anat. microscop. et morphol. exptl.* **45**, 77-98.

Giroud, A., and Martinet, M. (1959a). *Bull. soc. ophtalmol. Paris* **3**, 1-11.

Giroud, A., and Martinet, M. (1959b). *Bull. soc. ophthalmol. Paris*, **3**, 191-201.

Giroud, A., Deimas, A., Lefebvres, J., and Prost, H. (1954). *Arch. anat. microscop. et morphol. exptl.* **43**, 21-41.

Giroud, P., Giroud, A., and Martinet, M. (1954). *Bull. soc. pathol. exotique* **47**, 505-508.

Gregg, N. M. (1942). *Trans. Ophthalmol. Soc. Australia* **3**, 35-46.

Gyllensten, L. J., and Hellström, B. E. (1956). *J. Ophthalmol.* **41**, 619-627.

Hale, F. (1935). *Am. J. Ophtholmol.* **18**, 1087-1093.

Hamburgh, M. (1954). *Anat. Record* **119**, 409-427.

Hicks, S. P. (1953). *Am. J. Roentgenol., Radium Therapy Nuclear Med.* **69**, 272-293.

Hicks, S. P. (1954). *J. Cellular Comp. Physiol.* **43**, 151-178.

Hoet, J. P., Hoet, J. J., and Gommers, A. (1959). *Proc. Roy. Soc. Med.* **52**, 813-816.

Hoskins, D. (1948). *Anat. Record* **102**, 493-512.

Ingalls, T. H., Curley, F. J., and Prindle, R. A. (1952). *New Engl. J. Med.* **247**, 758-768.

Kalter, H., and Warkany, J. (1957). *J. Exptl. Zool.* **136**, 531-566.

Langman, J., and van Paassen, F. (1955). *Am. J. Ophtholmol.* **40**, 65-76.

Lefebvres, J. (1951). *Ann. Med.* **52**, 225-299.

Levi-Montalcini, R. (1958). "A Symposium on the Chemical Basis of Development" (W. D. McElroy and B. Glass, eds.), pp. 646-664. The Johns Hopkins Press, Baltimore, Maryland.

Mann, I. (1957). "Development Abnormalities of the Eye," pp. 1-419. British Medical Association, London.

Murphy, M. L. (1959). *Pediatrics* **23**, 231-244.
Murphy, M. L., and Karnofsky, D. A. (1956). *Cancer* **9**, 955-962.
Nelson, M. M., Wright, H. V., Asling, C. W., and Evans, H. M. (1955). *J. Nutrition* **56**, 349-370.
Nelson, M. M., Baird, C. D. C, Wright, H. V, and Evans, H. M. (1956). *J. Nutrition* **58**, 125-134.
Pike, R. L. (1951). *J. Nutrition* **44**, 191-204.
Rugh, R. (1958). *J. Pediatrics* **52**, 531-538.
Rugh, R. (1959). *Military Med.* **124**, 401-416.
Rugh, R., and Clugston, H. (1954). *Radiation Research* **1**, 437-447.
Rugh, R., and Wolff, J. (1955). *A.M.A. Arch. Ophthalmol.* **54**, 351-359.
Smith, A. U. (1957). *J. Embryol. Exptl. Morphol* **5**, 311-323.
Symposium: Retrolental Fibroplasia (1955). *Trans. Am. Acad. Ophthalmol. Otolaryngol* **59**, 7-41.
Thiersch, J. B. (1954). *Proc. Soc. Exptl. Biol. Med.* **87**, 571-577.
Thiersch, J. B. (1957). *Proc. Soc. Exptl. Biol. Med.* **94**, 24-32, 40-43.
Trerotoli, L. P. (1956). *Ann. ottalmol. e clin. oculist.* **82**, 479-504.
Tuchmann-Duplessis, H., and Lefebvres-Boisselot, J. (1957). *Compt. rend. soc. biol.* **151**, 12, 2005-2008.
Tuchmann-Duplessis, H., and Mercier-Parot, L. (1956). *Gazette hop.* **12**, 511-518.
Tuchmann-Duplessis, H., and Mercier-Parot, L. (1958a). *Compt. rend. acad. sci.* **245**, 156-158.
Tuchmann-Duplessis, H., and Mercier-Parot, L. (1958b). *Compt. rend. acad. sci.* **247**, 1134-1137.
Tuchmann-Duplessis, H., and Mercier-Parot, L. (1958c). *Compt. rend. acad. sci.* **247**, 152-154.
Tuchmann-Duplessis, H., and Mercier-Parot, L. (1958d). *Compt. rend. acad. sci.* **247**, 2,200-2,203.
Tuchmann-Duplessis, H., and Mercier-Parot, L. (1959a). *J. Physiol. (Paris)* **51**, 65-83.
Tuchmann-Duplessis, H., and Mercier-Parot, L. (1959b). *Compt. rend. soc. biol.* **153**, 386-388.
Tuchmann-Duplessis, H., and Mercier-Parot, L. (1959d). *Compt. rend. acad. med.* **249**, 1160-1162.
van Campenhout, E. (1935). *Anat. Record* **61**, 351-358.
Waardenburg, P. J. (1955). *Fortschr. Augenheilk.* **4**, 175-240.
Warkany, J., and Schraffenberger, E. (1946). *Arch. Ophthalmol.* **35**, 150-169.
Werthemann, A., and Reuniger, M. (1950). *Acta Anat.* **11**, 329-347.
Wilson, J. G. (1955). *Anat. Record* **123**, 313-333.
Wilson, J. G. (1959). *J. Chronic Diseases* **10**, 111-130.
Wilson, J. G., Jordan, H. C., and Brent, R. L. (1953). *Am. J. Anat.* **92**, 153-187.
Woolam, D. H. M., Millen, J. W., and Hovard, J. A. F. (1959). *Brit. J. Radiol.* **32**, 47-48.

Discussion

Dr. Carpenter (Tufts University, Boston, Mass.): Professor Detwiler showed that there was no specific stimulus which attracted nerves. For example, a brachial nerve grows readily to a transplanted eye. There may be something in the optic cup which normally directs the centripetal growth of the fibers and perhaps your experimental treatment interfered with it.

Dr. Tuchmann-Duplessis [Paris, France]: Yes, that is my feeling. At first, we thought there might be some mechanical factor which prevented the optic nerve fibers from going directly to the brain but this idea has been discarded.

Dr. Linksz [New York City]: Where do the anomalous optic nerve fibers actually end?

Dr. Tuchmann-Duplessis: They end in the cornea.

Dr. Cogan [Harvard University, Cambridge, Mass.]: I am not aware of such an anomaly in the pathology of the human eye.

Dr. Tuchmann-Duplessis: I have never heard of a human case.

Editor's Note: Dr. Tuchmann-Duplessis inquired of Professor Mawas (Paris), who was present, if he had any knowledge of such an anomaly in the human. Professor Mawas replied that he had not.

The Fine Structure of Vertebrate and Invertebrate Photoreceptors As Revealed by Low-Temperature Electron Microscopy[1]

H. FERNÁNDEZ-MORÁN

Mixter Laboratories for Electron Microscopy, Neurosurgical Service, Massachusetts General Hospital, Boston, Massachusetts, and Department of Biology, Massachusetts Institute of Technology, Cambridge, Massachusetts

Introduction

THE HIGH DEGREE of structural regularity underlying functional specialization in the photoreceptors has been of central interest ever since these cell organelles were recognized as primary sites of the visual process, where "nerve can be excited by light" (W. Kuhne, 1878). Photoreceptors generally exhibit marked birefringence as an expression of their compact paracrystalline structure, and natural dichroism resulting from oriented inclusion of the photosensitive pigments within the organized matrix. In view of the key role played by visual pigments in the photochemistry and physiology of vision (Wald, 1936, 1938, 1951, 1953, 1954, 1958, 1959; Wald *et al*, 1950), detailed elucidation of their organization and characteristic relationship with other components at the molecular level has now become a major task of ultrastructure research

On the basis of classic polarized light studies W. J. Schmidt (1934, 1935a, b, c, 1937, 1938, 1951) predicted that the outer limbs of visual cells are built up by compact layers of longitudinally oriented lipid molecules alternating with transversally arranged protein layers, and including the oriented visual pigments as an integral part of the ordered lamellar structure

Direct visualization of the postulated lamellar structures in photoreceptors and related systems was subsequently achieved by electron microscopy The investigations of Sjöstrand (1949, 1953) and others (Fernández-Morán, 1954, De Robertis, 1956) revealed that the outer segments of retinal rods and cones consist of several hundred or thousand double-membrane unit disks piled up in compact array. Both these layered structures and the corresponding tubular compartments of invertebrate photoreceptors (Fernández-Morán, 1956b, 1958, Goldsmith

[1] This work was supported by Atomic Energy Commission Contract AT(30-1)-2278 and by a grant (B-2460) from the National Institutes of Health.

and Philpott, 1957; Miller, 1957; Wolken *et al.*, 1957b) are considered to be specialized membrane derivatives, formed by multiple foldings or invaginations of the essentially continuous receptor cell membrane (Sjöstrand, 1959; Moody and Robertson, 1960). Moreover, this repetitive arrangement of ordered lipoprotein layers apparently represents a basic structural pattern common to a wide variety of "lamellar systems" including photoreceptors, chloroplasts, the myelin sheath, and mitochondria—all of which are primarily concerned with energy transfer or transduction in living organisms (Fernández-Morán, 1959b).

All of these interesting findings are based mainly on examination of standard osmium-fixed preparations, which have already shown significant limitations and proved to be inadequate in a study of the myelin sheath (Fernández-Morán, 1959b, c). Similarly, standard preparations of photoreceptors merely preserve an osmium-stabilized lipoprotein framework, while largely obliterating or masking the organized fine structure within the unit layers which may be related to the important visual pigment constituents. Instead of the continuous paracrystalline structure with exceptionally high concentration of solids characteristic of fresh rod outer segments, we find only a loose system of relatively "empty" double-membrane profiles with wide interspaces when examining serial sections of osmium-fixed rods. Therefore, despite impressive initial gains, it must be admitted that electron microscopy has not succeeded as yet in matching the performance of polarization and dichroism analysis regarding localization of the visual pigments either *in situ* or even less *in vivo*.

In order to achieve this essential correlation, present sources of preparation artifacts and specimen damage must first be considerably reduced before the main objective of photopigment localization can be profitably approached. Guided by these considerations, improved low-temperature preparation techniques have been developed during the past years (Fernández-Morán, 1959a, e), which consistently yield better morphological and histochemical preservation of photoreceptors and other lamellar systems than the standard procedures. These "cryofixation techniques" are based on rapid freezing of fresh or glycerinated specimens with liquid helium II at 1° to 2° K, followed by freeze-substitution and embedding in plastics at low temperatures, under conditions which minimize ice crystal formation, chemical fixation, extraction, and embedding artifacts (Fernández-Morán, 1959d, 1960). This preparative approach was supplemented by cooling the specimen support with a modified liquid nitrogen stage during observation of delicate sections in the electron microscope with a microbeam of extremely low intensity (Fernández-Morán, 1959e, 1960), thus appreciably reducing irradiation damage and specimen contamination. The term "low-temperature electron

microscopy" is therefore used here in a broader sense to encompass the two complementary aspects of this experimental approach aimed at minimizing artifact sources.

The first cryofixation preparations of rod outer segments disclosed a dense intermediate layer and other structural details of the unit disks which had not been observed previously in standard preparations (Fernández-Morán, 1959a). Since these techniques permitted controlled fixation with heavy metals and halogens at low temperatures, a comparative investigation of various types of dark- and light-adapted vertebrate and invertebrate photoreceptors was undertaken to provide supplementary data for localization of the oriented photopigment complexes within the planes of the layers. Collateral studies of the characteristic birefringence and dichroism changes observed in these photoreceptors after treatment with heavy metal salts (W. J. Schmidt, 1935a, c) served as valuable controls for evaluation of oriented structures in the different types of electron microscope preparations.

In the present report a preliminary account will be given of certain reproducible findings observed in the course of these studies which are being carried out as part of a more extensive methodological and comparative survey of lamellar systems in photoreceptors. Improved preservation of the disk and interdisk substance in rod and cone outer segments has disclosed the presence of organized electron-dense components associated with the unit layers. These components are particularly noticeable in dark-adapted outer segments, and appear to be related to the photopigment complexes, as suggested by collateral data derived from polarization analysis and controlled rhodopsin extraction with digitonin solutions.

After fixation with platinum chloride and other heavy metal compounds, characteristic modifications were detected in dark- and light-adapted visual cells. Condensation of the layers and dense inclusion bodies were produced by these agents particularly in dark-adapted frog visual cell outer segments, while they were not encountered or appeared to be less pronounced in the corresponding light-adapted retinas. Crystalline lamellar structures which are closely associated with the pigment granules and outer segments were frequently observed in fresh retinal rod preparations examined directly by low-temperature electron microscopy. Characteristic electron diffraction patterns could be recorded from these lamellae and are now being evaluated.

Bearing in mind the preliminary character of these observations and the numerous inherent artifact sources, it is evident that further investigations are required before definite conclusions can be drawn. It is hoped nevertheless that this survey may serve to illustrate the poten-

tialities of low-temperature preparation techniques in correlative studies of photoreceptor structures.

Materials and Methods

Materials

This report is based mainly on examination of representative specimens selected in the course of experimental studies of photoreceptor structures from frogs (65 *Rana pipiens* and 35 *Rana catesbiana*), guinea pigs (10), rabbits (10), chickens (2), compound eyes of the housefly (*Musca domestica*), and worker honeybee (*Apis mellifera*) (8).

Preparation of the Retinas

In order to establish a comparison with the standard preparations described in previous electron microscope studies, the first series of retinas was processed under conditions corresponding to partial light adaptation. Subsequently, however, only retinas from animals in a well-defined state of light or dark adaptation were chosen for investigation. The animals were light adapted at room temperature (20°–25° C) by placing them under two 100-watt lamps for 1–2 hr prior to swift decapitation and careful removal of the retinas with adjacent pigment epithelium. The retinas from dark-adapted animals kept in light-tight boxes in a darkroom at 20° C for 6 to 12 hr were processed under dim red light (Wratten filter, series II). In some cases the retinas were either frozen *in situ* (by regional flooding with liquid nitrogen-Freon 22 and subsequent block dissection of the fundus in a bath of this refrigerant) or, alternatively, fixed with cold liquids or vapors after removal of the cornea and lens in the anesthetized animal. However, in most cases the whole retina was gently stretched out over thin plastic strips or fenestrated Formvar films mounted on wire loops, and processed throughout as an intact unit at low temperatures in the special embedding chambers described below. This is essential for adequate preservation of structural integrity and critical relationships which are often deranged in the standard procedures when the retina is cut up into strips for embedding in capsules. Fresh preparations of detached visual cell outer segments and other retinal structures were mounted on thin films and examined directly by low-temperature electron microscopy. Suspensions of isolated rod outer segments prepared by differential centrifugation using the sugar gradient method of Collins, Love, and Morton (1952) are particularly suitable for ultrarapid freezing by the microdroplet spraying technique (Fernández-Morán, 1960). Excellent preservation of the com-

pound eyes was obtained by placing the light- or dark-adapted insects in closed chambers (at 0°–4° C) containing osmium tetroxide, formalin, bromine, or tetraethyllead vapors for 30 to 60 min, followed by low-temperature dehydration and embedding of the compound eye segments. The tubular network of the insect tracheal system considerably facilitates rapid freezing with gaseous refrigerants under reduced pressure, or chemical fixation with cold vapors.

Low-Temperature Preparation Techniques

The special low-temperature preparation techniques have been described in previous publications (Fernández-Morán, 1959a, b, c, d, e, 1960). However, in view of the operational significance of the methods in evaluating the present findings, an outline of the main preparation procedures will be given. The basic low-temperature cryofixation technique involves sequential application of: (a) rapid or ultrarapid freezing of the fresh retinas, or sprayed microdroplets of retinal rod suspensions, with liquid helium II at 1° to 2° K, or alternatively with liquid nitrogen-Freon 22 mixtures at —160° C, (b) staining at —150° C with halogens or organometallic compounds dissolved in isopentane; (c) substitution of the ice matrix with solutions (1–2%) of platinum chloride, osmium tetroxide, gold chloride, and other heavy metal salts in acetone-alcohol-ethyl chloride mixtures at —130° to —80° C; (d) infiltration of the specimens at —100° to —75°C with mixtures of methyl acrylate and butyl-methyl-methacrylate monomers, (e) final embedding by photopolymerization with ultraviolet light using low-temperature catalysts (i e, benzoin) at —80° to —20° C

The best structural and histochemical preservation of the retinas was obtained with an important variant which reduces chemical fixation and ice artifacts to a minimum by infiltration of the fresh specimens with buffered (pH 7.4) glycerol-Ringer solutions of gradually increasing concentration up to 50–60% at —20° C prior to freezing in liquid helium II. Freezing in liquid nitrogen cooled under reduced pressure close to its fusion temperature (—210° C) or in liquid nitrogen-Freon 22 was also carried out. All chemical fixation and staining processes are avoided during the subsequent freeze-substitution and low-temperature embedding in this method. As described earlier (Fernández-Morán, 1959a, c, d), thin sections of these "unfixed" specimens can then be subjected to controlled staining, extraction, enzymatic digestion, and appropriate histochemical procedures. Since the entire processing cycle at low temperatures may require several weeks when dealing with large bullfrog retinas, special equipment was developed for routine preparations.

This "cryofixation assembly" may be used for semiautomatic freeze-substitution and photopolymerization embedding within a modified Harris refrigeration unit designed to constantly maintain —100° C. The specimens are placed after rapid freezing in sealed chambers which are connected by Teflon tubing and valves to a series of large separation funnels containing the substitution fluids and monomers. By regulating successive flow of the various liquids through simple manipulation of the valves at prescribed intervals (12–24 hr) in this closed system, the complete freeze-substitution and photopolymerization embedding is readily carried out at low temperatures without danger of ice formation or temperature fluctuation. Since the tissue matrix remains uniformly congealed during polymerization at low temperatures, the embedded specimen which emerges ready for sectioning at room temperature exhibits an exceptional degree of three-dimensional preservation of the native cellular fine structure and histological organization. The rectangular specimen chamber (approximately 9 × 6 cm and 2–3 cm thick), specially designed to make use of this unique feature, consists of two thin Plexiglas sheets firmly pressed agains an intercalated Teflon gasket by two sturdy aluminum frames clamped together by large screws. This type of chamber has proved to be essential for all types of preparations involving low-temperature dehydration and photopolymerization, since large specimens can be embedded *in toto* within the thick plastic slab which is easily detached from the bounding Teflon-plastic frame by disassembling the frame. Whole retinas or an entire eye fundus could thus be routinely embedded, and the selected segments were then cut out from the plastic block with a fine jig saw, without distortion, for precise orientation and sectioning in any desired direction. The required anhydrous substitution and embedding fluids, with less than 10 parts per million water content, were prepared by treatment with Linde 4A molecular sieves, followed by ultrafiltration to remove suspended particles.

Chemical Fixation Combined with Low-Temperature Dehydration and Embedding

In order to obviate ice crystal formation and other freezing effects while still retaining the advantages of low-temperature dehydration and embedding, a modification of these procedures was used in combination with standard chemical fixation. This valuable modification yields better preservation of fine structure than the standard procedures, mainly because of the characteristic reduction of extraction and embedding artifacts at low temperatures. Since it is relatively simple and requires only a freezer and other standard laboratory equipment it can be strongly recommended as one of the best approaches to the more complex cryo-

fixation techniques. The exposed retinas were fixed *in situ* or after mounting on thin plastic strips with either one of the following groups of reagents: (a) osmium tetroxide, bromine, or iodine vapors applied in a closed moist chamber, or with a "vapor gun" consisting of a glass tube containing glass wool soaked with the reagent, which is then gently blown as moist vapor onto the specimen by a steady current of cold air. At 0° C fixation times are of the order. 30–45 minutes for the largest specimens. (b) The retinas are first fixed in a 1–2% platinum chloride-Veronal buffer solution (pH 7.2) at 0° C for 10 min, rinsed briefly in buffered saline, and transferred directly to a 2% osmium tetroxide solution adjusted with Veronal buffer (pH 7.2) at 0° C, remaining here about 30 min. Fixation with 1% solutions of gold chloride, silver nitrate, and potassium dichromate was also used in control experiments involving polarization analysis and dichroism studies of the type described by W. J. Schmidt (1935a, b, c). Dehydration of the specimens was carried out in graded series of acetone or methanol, starting at 0° C with 30–40% and proceeding toward higher concentrations at progressively lower temperatures of —5° to —25° C. The dehydrated specimens were infiltrated at —25° C with a mixture of methyl acrylate (5–10 ml), *n*-butyl methacrylate (75–85 ml), and methyl methacrylate (10–15 ml) for approximately 24 to 48 hr; followed by a further 48 to 72 hr at —25° C in a similar mixture containing 0.2–0.3% benzoin and 1% benzoyl peroxide as catalysts. Final embedding was carried out in a fresh change of this mixture, using the described specimen chambers, by photopolymerization with ultraviolet light (4 small fluorescent tubes of 6–8 watts symmetrically arranged around each chamber) at —25° C or at —55° C (using a stronger ultraviolet source). Special precautions were taken to maintain the temperature of the specimens constant (below —10° to —40° C) throughout the entire process, by attaching a thin copper-constantan thermocouple to the irradiated chamber areas and recording the temperatures periodically. Polymerization was usually completed after 48–72 hr at —25° C.

Extraction Experiments

Following essentially the procedures described by Collins *et al.* (1952) for preparation of rhodopsin, dark- and light-adapted bullfrog retinas (either fresh, or preferably after fixation at 0° C with 4% potash alum and 10% neutral formalin solution for 1 hr) were extracted with 1 or 2% aqueous digitonin solutions (prepared immediately before use) for 1 hr at 20° C. The extracted retinas, and the untreated control retinas, were then fixed with 1% buffered platinum chloride-2% buffered osmium tetroxide solutions at 0° C, followed by low-temperature dehydration

and embedding. In view of the friable character of the extracted retina with extensive fragmentation of the outer segments, the relative stabilization achieved at low temperatures was particularly important for establishing a comparison with the untreated control retinas. The extracted rhodopsin was examined directly by low-temperature electron microscopy and subjected to controlled modifications in a series of experiments which will be described in a separate publication.

Standard Preparation Methods

Standard preparation methods were used systematically to serve as controls. Fixation of the retinas in 1 or 2% osmium tetroxide in isotonic Veronal-acetate buffer (pH 7.2) at 1°–4° C was followed by dehydration in acetone or methanol and embedding in *n*-butyl methacrylate or in Araldite at 45° C. Gelatin embedding according to the procedure described by Fernández-Morán and Finean (1957) was found to be particularly useful for preparation of fresh isolated rod outer segments.

Microtomy

Serial ultrathin sections of the suitably oriented blocks were prepared with a Morán-Leitz ultramicrotome equipped with a diamond knife (Fernández-Morán, 1953, 1956a). Routine preparation of undistorted transverse serial sections (100–300 Å) through the whole retina was made possible by the exceptional cutting properties of the diamond knife and the stability of the ultramicrotome. The sections were picked up directly on distilled water without acetone or alcohol, since cryofixation and related preparations are particularly sensitive to the effects of these solvents and of the xylol or chloroform vapors commonly used for extending thin sections. In certain cases (unfixed, dark-adapted retinas) sectioning was carried out under dim red light with the variable-speed motor drive, and the sections picked up directly on the dry diamond edge, lightly coated with a thin glycerol or silicon film. The sections were deposited on thin Formvar or carbon films of the smooth and fenestrated type, mounted on copper grids or on platinum disks to avoid contamination when treating the specimens with heavy metal compounds or halogen vapors.

Electron Microscopy

A Siemens Elmiskop 1 operating at 40 to 100 kv and provided with multiple objective apertures of 30–50 μ (Fernández-Morán, 1959e) was used. In the latter part of this study, improved pointed filaments of tungsten with a tip radius of 1–10 μ were developed and used with the double condenser system of this microscope to provide extremely intense

microbeam illumination of low angular divergence. With this arrangement enhanced contrast and improved resolution of the order of 8–10 Å were obtained in suitably thin sections. Even at the highest electron optical magnifications (80,000–160,000 ×) the image brightness is adequate for obtaining satisfactory electron micrographs with Ilford high-resolution plates (8–15 sec exposures) which can be subsequently enlarged to yield far higher useful magnifications than ordinary plates.

Low-Temperature Electron Microscopy

Specimen damage by irradiation can be considerably reduced by suitable combination of low-intensity electron optics and improved specimen cooling devices. With the new pointed filaments and the double condenser system fitted with apertures of 50–20 μ it is also possible to obtain microbeams of 0·5–3 μ diameter and of extremely low intensity. By focusing on adjacent specimen areas and then shifting the low-intensity microbeam, useful micrographs were recorded on high-speed emulsions (i.e, Tri-X, sensitized with gold thiocyanate solutions) from extremely labile components. A Leisegang liquid nitrogen stage was used to cool the thermally insulated specimen support (—70° to —130° C) provided with a special shielding device consisting of several superimposed copper or platinum apertures which protect the specimen from contamination with residual vapors in the microscope column (Fernández-Morán, 1960). Recently, vacuum-tight microchambers of special design with "windows" of impermeable single-crystal films of graphite or mica have made it possible to perform direct electron microscope observations of partially hydrated biological systems, including certain components of photoreceptors Several of these techniques have been applied in a preliminary investigation of crystalline lamellar structures observed in fresh retinal rod preparations.

Electron Diffraction

The microbeam illumination of very low intensity and low divergence obtained with the described arrangement has proved to be particularly useful for electron diffraction studies of organic crystals. Thus, by combining low-temperature electron microscopy with low-intensity microbeam illumination it was possible to record successively electron micrographs of the sensitive crystalline lamellar structures, and the corresponding selected-area electron diffraction patterns from individual crystals on high-speed 35 mm films and on plates. By using longer exposures, useful electron diffraction patterns with a complete two-dimensional reciprocal lattice net have been recorded from these lamellae and from labile organic crystals, which normally would have suffered com-

plete loss of their diffracting power. Evaporated gold films were used for calibration of the patterns, and special precautions were taken to keep the specimen film position constant within certain limits, while trying to reduce the numerous other sources of error in a preliminary evaluation of the patterns.

Observations

Comparison of the Fine Structure of Visual Cell Outer Segments in Standard and Low-Temperature Preparations

Standard Osmium Fixation

Most of the retinas in this control group were partially light adapted, since the standard specimen preparations are generally carried out under variable experimental conditions which preclude reproducible attainment of complete light adaptation. In thin longitudinal sections of osmium-fixed guinea pig retinas the rod outer segments display the characteristic pattern of uniform double-membrane disks, arranged in parallel series to form a continuous pile. As already described by Sjöstrand (1953), these flattened disks or sacs are approximately 130–150 Å thick, and consist of two dense outer layers delimiting a light intermediate space about 70 to 80 Å wide which is usually filled with a homogeneous material of very low density. The "interdisk spaces" are recognized as intercalated gaps of widely varying dimensions (100 to 500 Å width, depending on the degree of specimen preparation) alternating regularly with the unit disk profiles. These interspaces are largely devoid of structure, and Sjöstrand (1959) has suggested that they "are filled mainly with an aqueous, ionic medium containing little or no lipids" (p. 304).

The rod outer segments of the frog are much larger (approximately 6 μ in diameter and 50 μ long), and the unit disks have a typical lobulated shape with numerous incisions which show up in thin sections as a mosaic formed by segmented columnar arrays of double-membrane profiles

---

Fig. 1. Longitudinal section through outer and inner segments of guinea pig retinal rods, showing improved preservation of general integrity and fine structure of the photoreceptor components. Specimen rapidly frozen in liquid helium II, followed by osmium-cryofixation and low-temperature embedding. Magnification: × 20,000.

Fig. 2. High-resolution electron micrograph of rod outer segment from light-adapted frog retina showing profiles of the double membrane disks which appear relatively devoid of internal structure and flattened as a result of partial extraction in this standard osmium-fixed preparation. Magnification: × 280,000.

Fig. 3. Pile of rod unit disks in low-temperature preparation of frog retina, which exhibit by contrast a compact granular fine structure with formation of dense intermediate strata, and indications of orientation in the plane of the layers. Osmium fixation, low-temperature dehydration and embedding. Magnification: × 300,000.

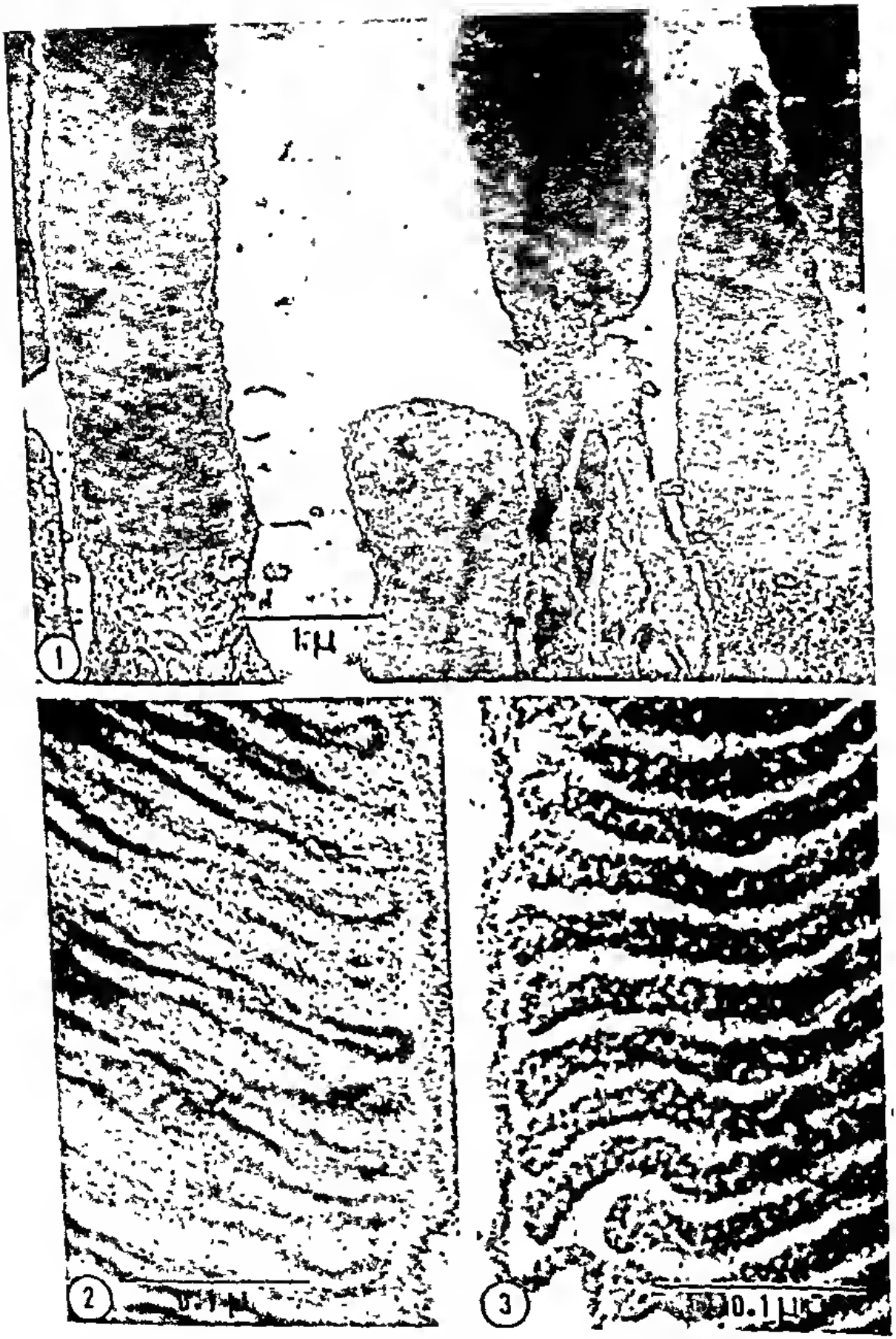
1
1μ
2
0.1μ
3
0.1μ

(Fernández-Morán, 1954, 1959b). As seen in Fig. 2 each of the unit disks contains two uniform dense layers (30–40 Å thick) which fuse at the edges in characteristic loop formations, enclosing an intermediate region partly filled with low-density granular components. The irregular interdisk spaces show sparse granular aggregates, and contain numerous blank areas featuring a uniform matrix texture which is indistinguishable from the untreated plastic medium of control sections. A related masking effect of the embedding matrix, involving compensation of shrinkage artifacts produced in the myelin sheath by standard preparation techniques, has been studied quantitatively by X-ray diffraction and electron microscopy (Fernández-Morán and Finean, 1957). Since the lamellar structures represent only a fraction of the over-all outer segment patterns observed in thin sections, extensive removal of the aqueous medium and other important labile components would be required to account for this diminished residual framework. Moreover, subsequent permeation with the homogeneous embedding matrix would effectively mask the corresponding tissue losses. On the basis of these considerations and of supporting collateral evidence, it can therefore be assumed that major constituents of the photoreceptor structures are either missing or partly effaced in standard preparations.

Low-Temperature Preparations

In contrast to standard specimens, low-temperature preparations show marked improvement of structural preservation and stabilization of spatial relationships at all levels of photoreceptor organization. This is mainly due to the combination of freeze-substitution or subzero dehydration with low-temperature polymerization embedding of the whole retina, which prevents extraction and rearrangement of the labile components. The layered structure of the visual cell outer segments consistently exhibits unmarred regularity and compactness (Fig. 1) in osmium-cryofixation preparations, differing substantially from the vacuolated and distended piles commonly encountered in standard controls. Even the largest frog retinal rods are so well preserved that it is possible to follow a continuous series of 500–1000 or more intact unit disks stacked up in flawless compact array, with precisely aligned marginal loop formations. The individual retinal elements appear to be immobilized in definite configurations, because the critical transition from the frozen state to the block embedding in a plastic matrix takes place uniformly at low temperatures without thawing. This is one of the most important potential advantages of the cryofixation procedures; and further methodological advances may eventually permit us to analyze the morphological and histochemical correlates of sequentially arrested states of activity in

rapidly congealed and stabilized tissues. Preliminary applications of these techniques have already disclosed new aspects of the local and regional patterns of visual cell organization, including their relation with the pigment epithelium (Fernández-Morán, 1959c). An interstitial material of varying composition and distribution has also been found permeating the visual cell-pigment epithelium zone. This material corresponds essentially to the interstitial matrix of light microscopy, as recently described by R. L. Sidman and Feder and Sidman (1958) in their comprehensive histochemical studies of photoreceptors using improved freeze-substitution techniques.

Comparative evaluation of the photoreceptor structures as revealed by improved methods demonstrates significant differences which refer specifically to enhanced structural definition and preservation of the unit disk organization, the interdisk spaces, the textural pattern of the visual cell outer segments, and relationship with the cell membrane.

Organization of the Unit Disks

Confirming previous observations (Fernández-Morán, 1959a, c, 1960), the apparently simple double-membrane disks in visual cell outer segments of the frog, guinea pig, and rabbit are actually found to be composite elements with a highly differentiated microstructure. The compact internal disk structure is characterized by dense particulate constituents organized within the plane of the layers. A dense intermediate layer is located in the middle of this intradisk space (Fernández-Morán, 1959a) demarcating the junctional region where the two unit membranes are held closely together to form the "compound" unit disks. It was pointed out earlier (Fernández-Morán, 1959c) that this arrangement strikingly resembles the close apposition of two asymmetric unit membranes as seen in the myelin sheath and in chloroplasts (Hodge, 1959) thus suggesting a common origin as derivatives of the cell membrane.

As shown in Figs. 2 and 3 adequate preservation of the disk structures does not depend primarily on the effects of freezing or fixation at low temperatures. Although in this case both specimens were initially subjected to the same type of osmium tetroxide fixation, subsequent low-temperature dehydration and embedding conserved most of the unit disk organization, as demonstrated in Fig. 3. However, processing of the control specimen by standard dehydration and polymerization at 45° C. sufficed to bring about massive extraction or removal of the internal disk and interdisk components over large areas of the rod outer segment (Fig. 2). A comparison of the flattened disks in standard specimens (110–150 Å. thick), with the corresponding values measured in Fig. 3 (160–200 Å. marginal loops: 200–250 Å.), indicates an average difference of

50Å. This represents a marked shrinkage in a direction normal to the disk planes of approximately 20 to 30%, which is mainly due to loss of material. If allowance is made for the spurious masking effects of the embedding matrix the actual losses may turn out to be even greater.

In all variants of the low-temperature preparations a prominent granular structure is regularly found as an integral component of the rod or cone unit layers, mainly in unbleached or partly bleached retinas. The dense particles, about 20 to 30 Å in diameter, of polyhedral or slightly elongated shape, are either closely associated with the outer and intermediate disk layers, or may actually contribute to their formation (Figs. 3, 5, and 8). The granular elements show indications of regular orientation parallel to the rod axis, and are often aligned in linear arrays normal to the smooth or segmented transverse layers. After treatment with heavy metal compounds, the dense particles exhibit substructure of the order of 10 to 15 Å, and appear embedded in a homogeneous intradisk matrix of less density. In thin planar sections through the unit disks a pattern of regular condensation zones can be discerned, featuring ordered conglomerates of dense granules surrounded by this homogeneous or extremely fine particulate material. A continuous or segmented dense intermediate layer of 15 to 20 Å can usually be detected in the middle of the intradisk space, and is most conspicuous in cryofixation preparations (Fernández-Morán, 1959a, 1960). In certain preparations of bleached retinas (Figs. 4a, b), a thin uniform fissure of corresponding dimensions is seen extending from the central gap of the marginal loop formations, clearly separating the two constituent membranes of each disk. The structures described by Moody and Robertson (1960) in amphibian photoreceptors fixed with $KMnO_4$ are, in general, similar to these findings, except as regards the lack of preservation of the important particulate disk components in their preparations.

The interdisk spaces are more uniform, of less width (50–100 Å), and appear to be filled with a homogeneous substance of varying density,

---

FIG. 4. Sections of rod (a, b) and cone (c) outer segments from light-adapted frog retinas showing granular unit layer structure of comparatively lower density. The wide interdisk spaces (a, b) contain a light homogeneous material. Osmium and platinic chloride (Pt/Os) fixation, low-temperature preparations. Magnification: × 130,000 (4a, b); × 190,000 (4c).

FIG. 5. Corresponding areas of rod (a, b) and cone (c) outer segments from dark-adapted frog retinas featuring a more compact granular fine structure of the unit disks, with prominent intermediate layers and dense interdisk substance. The arrow (b) indicates a region of condensed layers resulting from extensive apposition (c) of adjacent unit disks. Pt/Os, low-temperature preparations. Magnifications: × 130,000 (5a, b); × 190,000 (5c).

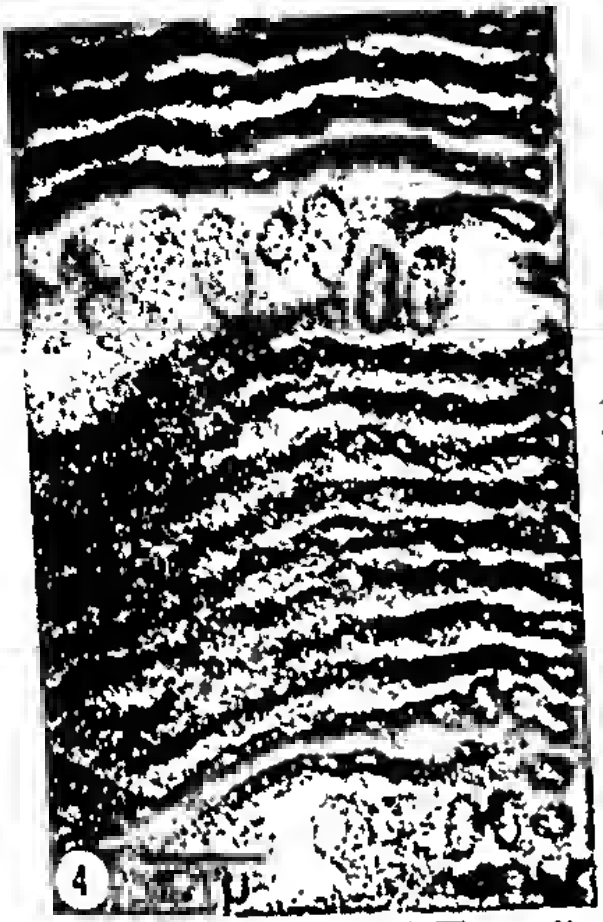
4
0.1μ


5
0.1μ

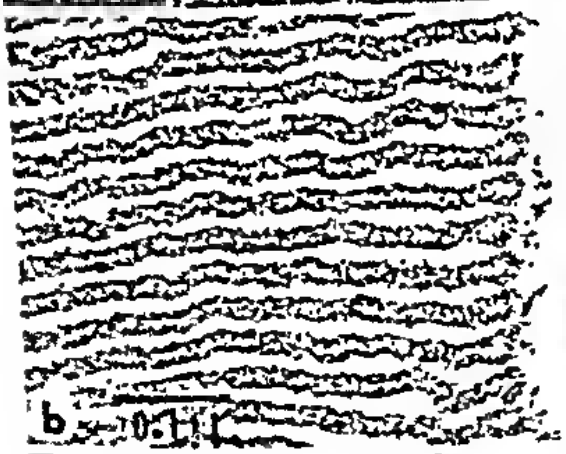
b
0.1μ


b
0.1μ

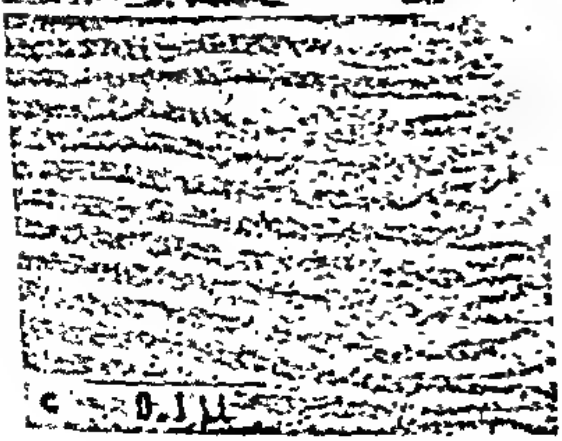
c
0.1μ


c
0.1μ

which is frequently associated with the interstitial matrix around the visual cells. The interdisk substance is more noticeable in platinum-osmium preparations of unbleached retinas (Figs. 5 and 8), and is apparently related to the cytoplasmic ground substance. Considerable narrowing or impregnation of the interdisk spaces may lead to the formation of condensed layered structures which closely resemble the compact lamellar system of the myelin sheath. In cone outer segments this regional condensation of multilayers is particularly marked (Fig. 5c).

Organization of the Outer Segments and Cell Membrane Relationships

Longitudinal and oblique serial sections through the rod outer segments reveal an intricate system of interstices and channels which follow the course of the numerous disk incisions. The deep fissures (about 1–3 μ long and 100–200 Å wide) are lined with symmetrically disposed rows of marginal loops, indicating that hundreds of superimposed unit disks must be in accurate three-dimensional register along their edge cords and incision margins. The columnar arrays of double loops are frequently associated with annular profiles (Fig. 4a) which correspond to cross-sectioned tubular extensions of the lobulated segments and incisions. The tubular formations, considered as differentiated invaginations of the cell membrane, would contribute together with the numerous disk incisions to increase the available inner surface of the compact outer segments. As already pointed out by Wald (1958), this would facilitate diffusion processes and metabolic interchanges with the surrounding cell systems. Similar tubular structures and vesicular complexes are also found in the basal region of guinea pig rod outer segments (Fernández-Morán, 1959b), and may possibly reflect active membrane formation processes in these areas. Confirming the observations of Sjöstrand (1959) and Moody and Robertson (1960) direct continuity of the cell membrane with the layered structures of the rod and cone outer segments can be seen, particularly in the latter. As a result of the better over-all preservation, however, more extensive transitional sites along the borders and apical regions of the outer limbs can be detected. Closely packed tubular or annular profiles and dense granular bodies, 150–200 Å in diameter, are found in the basal regions adjacent to the inner segments where the cell membrane connections are most evident.

Fine Structure of Dark-Adapted Visual Cell Outer Segments

Earlier investigations (Fernández-Morán, 1959a, c) had shown that dark-adapted guinea pig and frog retinas which were rapidly frozen with liquid helium II or liquid nitrogen and examined at —150° C in a special

low-temperature stage retained the characteristic salmon-pink color of the native photopigment complex essentially unaltered over extended periods. However, in the subsequent process of freeze-substitution with acetone or alcohols a distinct change to an orange or pink-yellow color was noted, indicating that the labile photopigment complexes suffer definite alterations even at low temperatures.

No further modifications were detected in this yellow color of the photoreceptor layer, and the embedded dark-adapted retinas can therefore be readily distinguished from the bleached control specimens. Attempts have now been made to preserve major components of the labile photopigment complexes and their derivatives in a form more suitable for electron microscopy, by treatment with halogens and organometallic compounds at —150° C before initiating additional staining with heavy metal compounds introduced during the process of freeze-substitution.

Parallel controls by polarized light microscopy carried out during the various preparation stages demonstrate that the dichroism and birefringence changes occurring at low temperatures are markedly different from those introduced during standard fixation and dehydration. Preliminary evaluation of these results tends to confirm that the organized photopigment complexes or their derivatives are better preserved within the lipoprotein lamellar system in low-temperature preparations. However, interpretation of the artificial dichroism produced by oriented heavy metal impregnation is rendered difficult by the presence of anomalous polarization effects, which are partly due to the strong negative form birefringence of the well-preserved lipoprotein layers in these specimens. A correlation with the corresponding results obtained by Schmidt (1934, 1937, 1938, 1951) in rod outer segments stained with heavy metals after lipid extraction must therefore await detailed quantitative polarized light analysis of the type already carried out on photoreceptors by Denton (1959).

In connection with the present studies the most interesting results were obtained when applying a combination of platinum chloride and osmium tetroxide either in the process of freeze-substitution at —130° to —80° C, or at 0° C followed by low-temperature dehydration and embedding. This combination has the advantage of preserving the characteristic interaction of platinum chloride with the photopigment complex, while stabilizing the underlying lipoprotein matrix of the visual cell outer segments.

Dark-adapted rod and cone outer segments are distinguished by a characteristic compact appearance due to enhanced staining and conservation of the intradisk structures, the interdisk spaces, and the enveloping interstitial material. As shown in Figs. 5 and 8, the granular

disk components already observed in partly light-adapted specimens appear more accentuated, and are embedded in an extremely fine particulate matrix of 10 to 15 Å. The prominent intermediate layers (arrows) can now be regularly found in most of the unit disks, and are often segmented and wider (20–30 Å) occupying a larger part of the middle zone. Except for the central gaps in the marginal loop formations the entire unit disks appear to be densely packed with these granular and layered constituents. The reduced interdisk spaces (30–60 Å wide) are uniformly filled with a diffuse ground substance, replete with dense 10 to 15 Å particles, which stain intensely with heavy metal reagents. This interdisk substance extends into the peripheral boundary regions of the outer segments and the plasma membrane, blending into the interstitial zone (Fig. 5a, arrow). Impregnation of the interdisk space is especially marked in the cone outer segments (Fig. 5c), and contributes largely to the over-all impression of a continuous multilayered system. In addition to the more common type of a uniformly well-preserved compact layered structure, irregular condensation areas are also found in certain specimens (Fig. 5b), interspersed with gaps and other evidence of local extraction and rearrangements. There are also regional condensation zones (Fig. 6) with enhanced staining, and transitions to the paracrystalline inclusions which will be described separately.

Comparison of Dark- and Light-Adapted Outer Segments

In view of the variations encountered in adjacent outer segments of the same specimen, and of the relatively limited samples available for comparison by electron microscopy, it is difficult at this stage to establish significant structural differences between light- and dark-adapted photoreceptors. Only when strongly light-adapted and completely bleached retinas are compared with dark-adapted control specimens fixed under

---

Fig. 6. Section of cone outer segment in dark-adapted frog retina showing characteristic regional condensation of layers and sites of enhanced staining with heavy metal salts. Platinic chloride-osmium (Pt/Os), low-temperature preparation. Magnification: × 100,000.

Fig. 7a and b. Residual structure of unit disks in the rod outer segments of dark-adapted frog retina after extraction of rhodopsin with (2%) aqueous digitonin solution. Most of the granular disk components have been removed, and only marginal fragments of the refractory dense outer layers are detected. Pt/Os, low-temperature preparation. Magnification: × 250,000.

Fig. 8. Control preparation of rod outer segment from dark-adapted frog retina. Comparison of the dense granular structures of these unit disks with the corresponding "empty regions" (arrow) of extracted specimens furnishes supplementary evidence on localization of the visual pigment complex within the plane of the layers. Pt/Os, low-temperature preparation. Magnification: × 250,000.

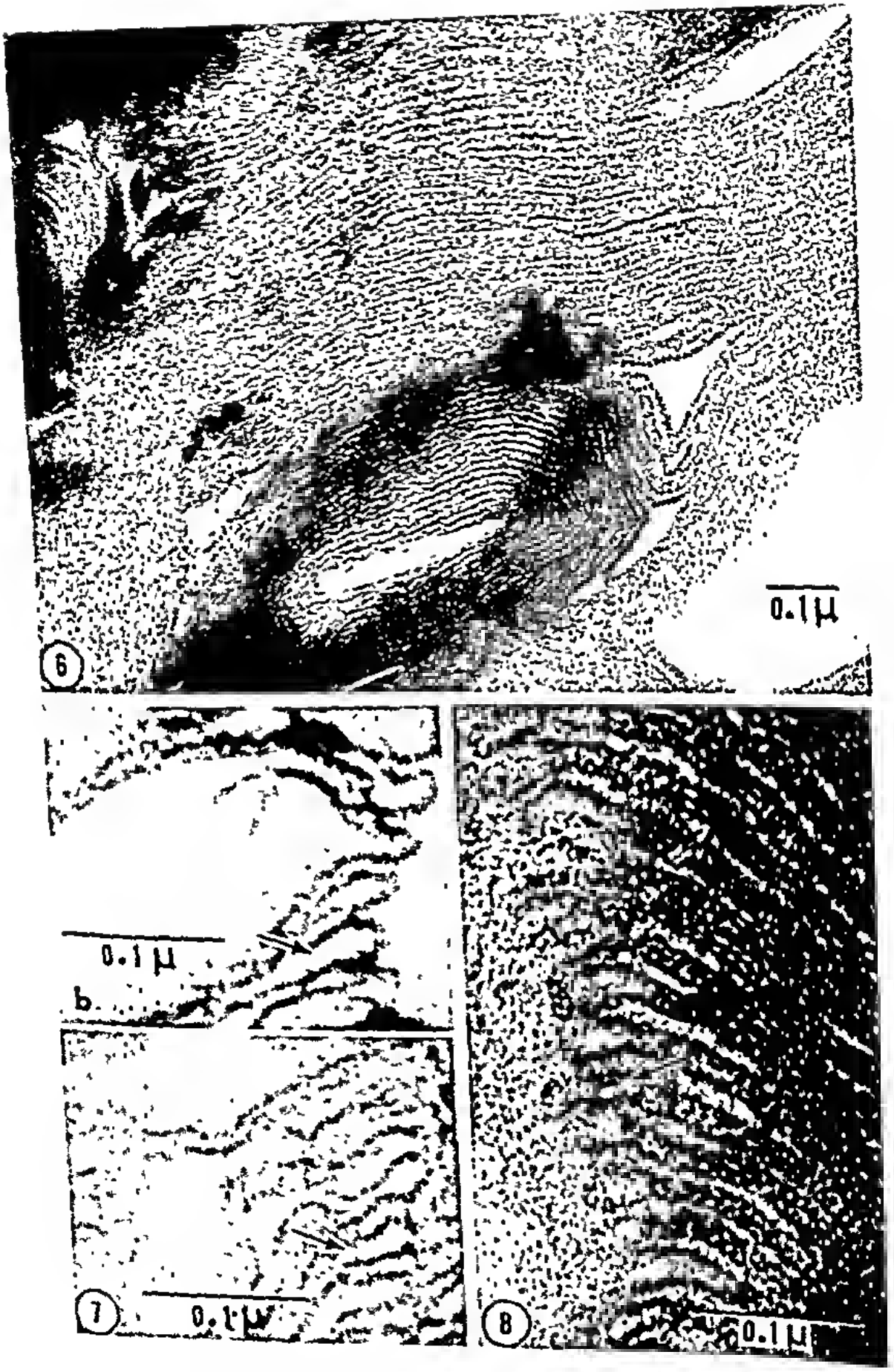
0.1μ
6
0.1μ
b
7
0.1μ
8
0.1μ

optimum conditions can certain differences be detected. With these reservations in mind, the specimens shown in Figs. 4 and 5 have been selected from a larger series of transitional forms to illustrate representative differences which are discernible with our present methods. In light-adapted rod and cone outer segments (Figs. 4a, b, c) the granular components and associated particulate matrix of the unit disks are usually less numerous (and of slightly reduced dimensions) than in the corresponding dark-adapted specimens (Figs. 5a, b, c). The intermediate layers are only partly preserved or generally replaced by a clear central fissure. The interdisk spaces are wider and contain a homogeneous substance of low density. In contrast to the compact and dense dark-adapted outer segments, the light-adapted specimens disclose a general "depleted" appearance, as if certain constituents which stain preferentially with halogens and heavy metals were missing. This may not necessarily represent the actual organization of the native visual cell outer segments, but reveal instead some form of "equivalent state" or "developed latent configuration" brought forth by the preparation procedures. Thus, the vitamin A liberated by bleaching is known to leave the retina of the strongly light-adapted frog eye and diffuse into the pigment epithelium (Wald, 1936, 1958). It is therefore conceivable that the release of vitamin A, and modification of the state of association of other photopigment derivatives in completely bleached retinae, would render them more vulnerable to the selective extraction and dissociation effects of the fixation and dehydrating agents.

Effects of Extraction with Digitonin Solutions

Since rhodopsin is considered to be one of the principal structural components of the rods, representing about 40% of the dry weight of the frog rod outer segment (Hubbard, 1954; Wald, 1959), treatment with an extractant for visual pigments like digitonin should produce marked fine structural changes. Investigation of the effects of this extractant on the granular components and associated layered structures of the unit disks would therefore be of particular interest.

When dark-adapted frog retinas are extracted with 2% aqueous digitonin solutions, preferably after pretreatment with alum-formalin, and then subjected to fixation and low-temperature embedding, the congealed tissue matrix acts as a stabilizing support, thus preventing more extensive losses and rearrangements than would otherwise occur if isolated rods were extracted. It is nevertheless obvious that considerable extraction has taken place, as shown by the extensive fenestration, irregular gap formation and general disruption of the outer segments, adjacent myeloid bodies, and other retinal components. In the residual framework the

marginal parts of the unit disks and the characteristic loop formations are most commonly preserved (Fig. 7a), appearing as hollow shells (arrows). The intradisk granular components, the particulate matrix, and the intermediate layer have been completely removed. The residual dense outer layers are smooth, thinner (about 20–30 Å), and appear to split or fray out into tenuous ribbons resembling the membrane patches (Figs. 7a, b) seen in other types of extracted lamellar systems. The other middle portions of the disks are largely obliterated, but numerous vesicular and contorted tubular formations can still be recognized.

Upon comparing these residual marginal formations with the corresponding unextracted regions of the dark-adapted control specimens (Fig. 8), and drawing on the collateral evidence of rhodopsin localization in the layers, it may be tentatively assumed that the intradisk particulate and layered structures are either directly related or in some way associated with the photopigment complex. However, in view of the considerable modifications introduced by these procedures, and the possibility that digitonin may extract or dissociate other substances in addition to the visual pigments (Dartnall, 1957), much further work is required to support this assumption. Supplementary experimental approaches are now designed to perform a more gentle extraction with digitonin and related compounds after stabilizing the tissue matrix at moderately low temperatures, while following the different stages by polarized light and electron microscopy.

Paracrystalline Inclusions in Visual Cell Outer Segments Fixed with Heavy Metal Compounds

Characteristic condensation zones and dense paracrystalline inclusion bodies are regularly found in the visual cell outer segments of dark-adapted frog retinas which have been subjected to prolonged treatment (mainly at 0° C) with platinum chloride, osmium tetroxide, and other heavy metal solutions including gold, silver, and chromate compounds. Numerous transitions can be observed between the dense condensation regions, as commonly seen in cone outer segments (Fig. 6), and the paracrystalline inclusions (Figs. 9 and 10) which are encountered more frequently in rod outer limbs. The condensation zones result from regional apposition and fusion of adjacent dense outer layers and concomitant accentuation of the intermediate layers to give a fairly regular period of 60 to 120 Å. The paracrystalline inclusions apparently derive from the condensed patches by intensification of the intermediate layers and development of periodic structure within the plane of the lamellae.

These dense bodies are recognized as irregular inclusions, about 0.2 to 2 μ in diameter, firmly embedded without loss of continuity in the

well-preserved layered structure of the outer segments. Fifty to one hundred layers with a regular period of 50–60 Å can be clearly discerned in the larger inclusions which stand out plainly because of enhanced staining with heavy metal salts. The individual layers display regular fine structure of the order of 15 to 25 Å, leading to the two-dimensional periodicity characteristic of paracrystalline structures (Figs. 10b, c). Although the boundary regions still preserve direct continuity with the unit layers (Fig. 10a, arrow) and similar orientation, the core of the inclusions often show irregular whorl formations. Only small gaps, which are hardly in proportion to the mass of the inclusion, may be seen at the margins, and the integrated enclosure of these bodies without producing major distortions in the compact photoreceptor texture is noteworthy. One gains the impression that the constituent material of these inclusions has exuded and "crystallized out," without having been removed too far from its site of origin within the unit layers. In specimens which have been treated with silver nitrate or gold chloride the inclusion bodies contain oriented colloidal precipitates. The described inclusion bodies have been predominantly found in dark-adapted rod outer segments, and occasionally in partly bleached retinas; they occur sparsely in completely light-adapted receptors. Similar inclusions were also frequently encountered in dark-adapted frog retinas which had been bleached under intense light immediately after removal and kept at 0° C during the process of light adaptation.

The largest inclusions (Fig. 9b) are readily visible with the light microscope, and resemble the droplets, first described by Kolmer (1909, 1925), in association with the rod outer segment and pigment epithelium processes of various vertebrate retinas. In a series of comprehensive investigations, Detwiler (1932), Detwiler and Zwemer (1937), and Johnson and Detwiler (1942) have shown that these droplets are demonstrable only in retinas which have been fixed with bichromate-acetic acid solution or in platinum chloride. The droplets are abundantly present in frog rod outer segments after dark adaptation at room temperature, and

---

FIG. 9. Dense paracrystalline inclusion bodies found predominantly in the rod outer segments of dark-adapted frog retinas. These inclusion bodies (0.2–2 μ diameter) appear to arise from condensation and fusion of the unit layers in regions which stain intensely with heavy metal salts. The larger inclusions (b) would resemble the "Kolmer droplets" of light microscopy. Pt/Os, low-temperature preparation. Magnifications: × 150,000 (9a); × 15,000 (9b).

FIG. 10. High-resolution electron micrographs of the dense inclusion bodies exhibiting a regular paracrystalline structure with a period of 50 to 60 Å in certain areas. Pt/Os, low-temperature preparations. Magnifications: × 250,000 (10a); × 400,000 (10b, c).

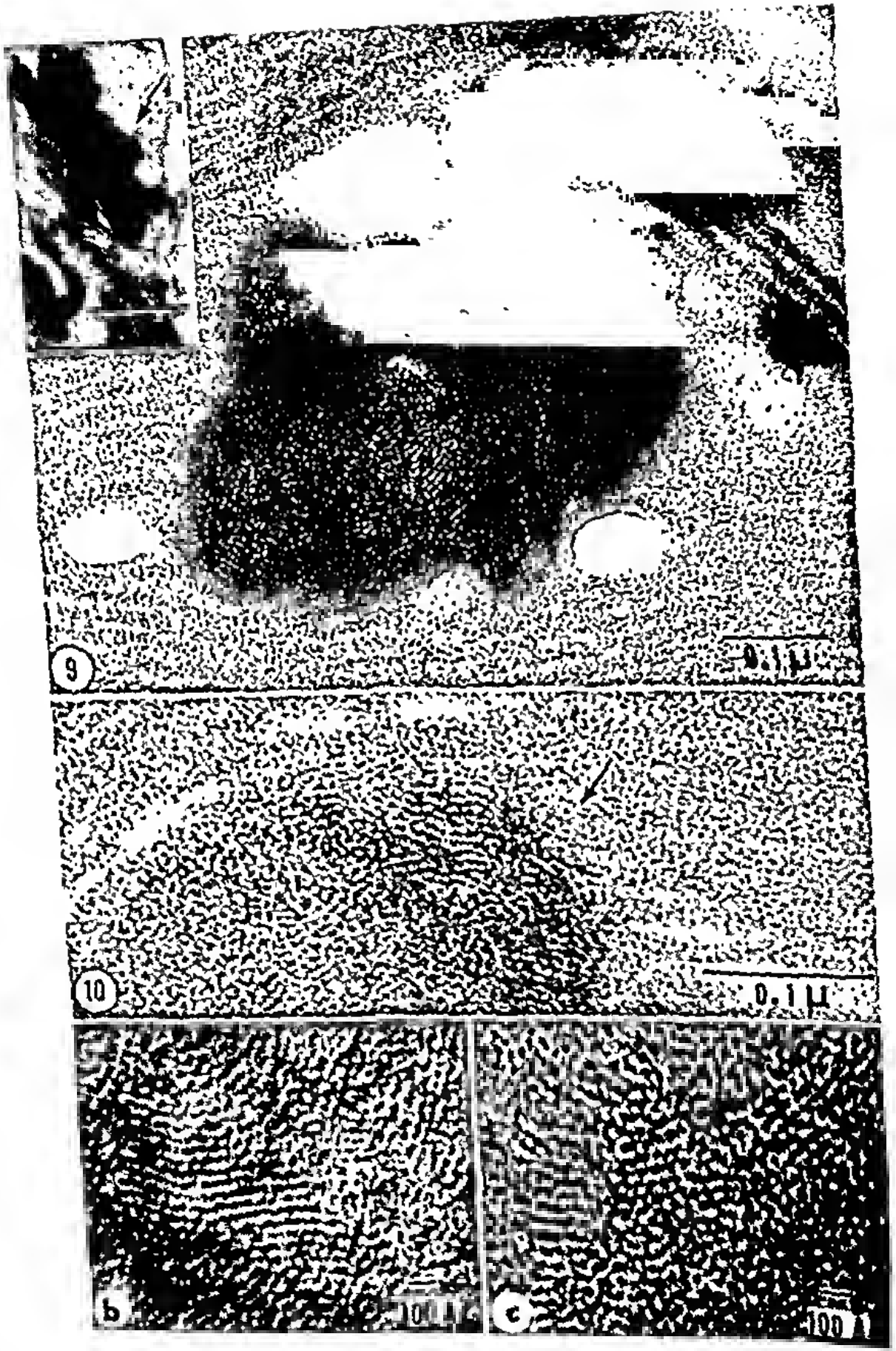
9
0.1 μ
10
0.1 μ
b
100 Å
c
100 Å

after light adaptation at 0° C in retinas which had been previously dark adapted at room temperature; while they are less numerous in retinas light adapted at room temperature (Johnson and Detwiler, 1942). These authors suggest that, on the basis of their common properties and analogous behavior under similar conditions of illumination and temperature, "the droplets are histological entities which may be identified with retinene" (Johnson and Detwiler, 1942, p. 247).

Although the possible contribution of artifacts in the formation of these droplets must be kept in mind (Walls, 1939), the demonstration by electron microscopy of similar, well-defined paracrystalline inclusions embedded within the organized lamellar structure of the outer segments, would indicate that we are dealing with some derivative (i.e., retinene or conjugated protein compound) of the photopigment complex still bearing a significant measure of topographical relationship with its original localization in the layered photoreceptor structure.

Lamellar Inclusions in Dark-Adapted Visual Cell Inner Segments

Variants of the low-temperature preparations involving combined fixation with heavy metals and halogens reveal characteristic structures in the rod and cone inner segments, which have been more regularly found in dark-adapted frog retinas than in the corresponding completely light-adapted controls. Although other interesting structural differences have been noted in these preparations, description will be limited here to the dense bodies seen in the mitochondria, and the adjacent cytoplasmic inclusions.

As shown in Fig. 11, the closely packed large mitochondria of the ellipsoid region contain numerous spherical or polyhedral bodies, approximately 300 to 600 Å in diameter, which stain intensely with halogens (iodine, bromine) and with heavy metal compounds. These "intramitochondrial bodies" exhibit a particulate substructure of 15 to 20 Å, which is densely packed in fairly regular patterns (Fig. 11b). They are often lodged in rows of 6 or more elements (lower arrow in Fig. 11a) between

---

Fig. 11. Section of rod inner segment from dark-adapted frog retina displaying numerous dense granules within the mitochondria and compact multilayered inclusion bodies. The round intramitochondrial granules, 300 to 600 Å in diameter, exhibit a regular internal fine structure (b). Pt/Os, low-temperature preparation. Magnifications: × 80,000 (11a); × 350,000 (11b).

Fig. 12. Dense multilayered inclusion bodies found close to the mitochondria in rod inner segments of dark-adapted frog retina. These bodies, about 0.1 to 0.5 μ in diameter, are formed by concentrically arranged layers with a regular period of 50 to 60 Å which stain intensely with heavy metal compounds. Pt/Os, low-temperature preparation. Magnifications: × 300,000 (12a); × 200,000 (12b).

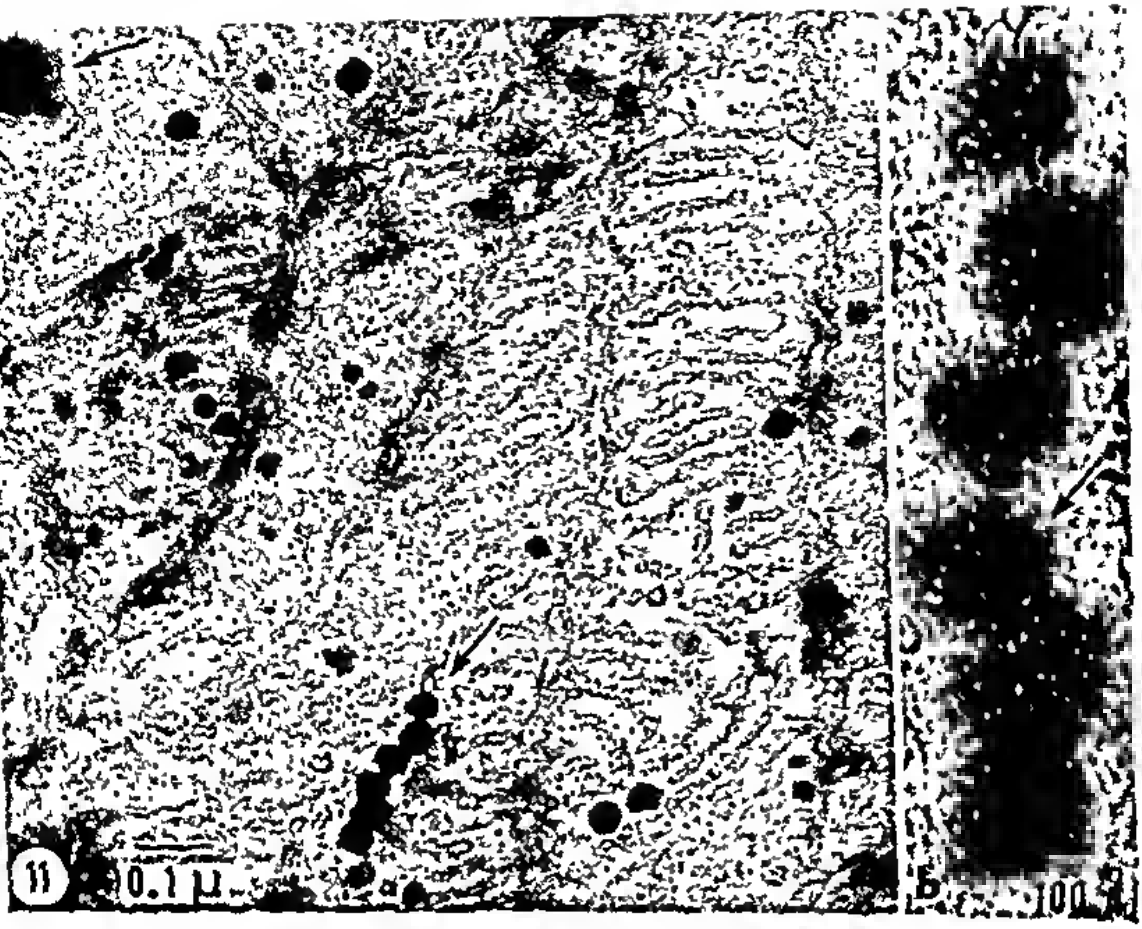
11
0.1 μ
a
b


0.1 μ
12
0.1 μ
b

the internal mitochondrial membranes and appear embedded in the general matrix. Morphologically, these dense granules would correspond essentially to the intramitochondrial granules, described by Sjöstrand (1959) and other authors, in various types of cells. The relatively large number of intramitochondrial granules found in the inner segments of dark-adapted visual cells, as compared with their sparse distribution in light-adapted controls, may be an expression of important functional activity.

Dense multilayered inclusion bodies (Figs. 11a and 12b) are also abundantly present around the mitochondria and in close association with the endoplasmic reticulum of the visual cells in this region. The oval or round lamellar bodies, about 0.1 to 0.5 μ in diameter, are formed by multiple layers with a regular period of 50 to 60 Å concentrically arranged or spirally wrapped around a light core (Fig. 12a). The dense osmiophilic layers (20–30 Å thick) display a segmented or granular fine structure of 15 to 20 Å. Similar lamellar bodies have been described previously in the marginal zones of insect retinula cells (Fernández-Morán, 1958).

Fine Structure of Pigment Granules and Relationship with Photoreceptors

Important structural features of the formed cellular elements and the surrounding interstitial matrix can now be investigated in the exceptionally well-conserved zone between pigment epithelium and visual cell outer segments, as seen in low-temperature preparations. In frog and guinea pig retinas the slender projections of the pigment epithelium cells which invest the outer and inner segments of the visual cells, contain specialized lamellar components and numerous dense granules. The hard pigment or fuscin granules, measuring approximately 0.3 to 2 μ, which only show small particulates or embedded tubular networks (Yamada *et al.*, 1958) in standard preparations, reveal instead a distinct paracrystalline structure with a regular period of 50 to 60 Å in cryofixation preparations of guinea pig retinas (Fernández-Morán, 1959c). These pigment granules are generally enveloped by multiple membranes which appear to be gradually reduced while going through certain transitional phases. In frog retinas the dense pigment granules do not usually exhibit this high degree of order, containing rather poorly defined internal lamellar structures with a period of 50 to 60 Å, surrounded by a dense granular shell (Fig. 13).

In light-adapted frog retinas these granules with associated cytoplasmic membranes of the pigment epithelium projections are often seen to be in direct contact with the peripheral layers of the rod outer segment. A similar relationship is also observed in preparations of dark-

adapted retinas rapidly frozen or fixed *in situ*, followed by low-temperature block embedding which preserves the delicate connections of the pigment epithelium with the outer segment region far better than any of the standard techniques. In thin sections of these dark-adapted specimens (Fig. 13), the pigment granules still appear to be closely attached to the tips of the rod outer segments. Important histological and physiological interrelations have already been established between the pigment epithelium and the photoreceptors (Wald, 1958; Hubbard, 1956). Further investigation of the intimate association of pigment granules, myeloid bodies, and other differentiated pigment epithelium constituents with the highly organized lamellar systems in visual cells may therefore lead to a better understanding of the metabolic interactions and specialized transport mechanisms operative at the submicroscopic level.

Fine Structure of Photoreceptors in the Insect Compound Eye

The rhabdomeres of the 7 or 8 sensory retinula cells in each ommatidium of the insect compound eye are built up of closely packed tubular compartments, 400 to 1200 Å in diameter, which are oriented in highly regular arrangement (Fernández-Morán, 1956b, 1958, Goldsmith and Philpott, 1957, Wolken *et al.*, 1957a, b, Wolken, 1958). As described earlier, the compartment walls "exhibit a dense boundary line of 20 to 30 Å combined with a less dense layer of about 60 Å in osmium-fixed preparations" (Fernández-Morán, 1958, p. 640). This less dense outer layer is therefore definitely not an "60 Å gap" as incorrectly stated by Moody and Robertson (1960, p 88), but represents instead a clearly depicted component which was actually considered as corresponding to the lipoprotein layers of the photoreceptors (Fernández-Morán, 1958, p 637)

In order to investigate these important tubular constituents with *improved low-temperature techniques, special* precautions were now taken to ensure a well-defined state of light or dark adaptation prior to preparation When dark-adapted housefly compound eyes are fixed *in situ* by rapid freezing or treatment with cold osmium tetroxide or halogen vapors, followed by low-temperature dehydration and embedding, the rhabdomere tubules show characteristic structures. As seen in Fig. 14a, the double-contoured walls of the cross-sectioned tubules display a prominent granular or segmented fine structure of 20 to 30 Å. Apposition of the outer layers of adjacent tubular compartments leads to the formation of dense intermediate strata, 30 to 40 Å wide (Fig. 14b, arrow), which are usually embedded in a less dense homogeneous or particulate substance. This arrangement resembles the structure of cross-sectioned octopus "rhabdome" tubules, as described by Moody and Robertson (1960). However,

when strongly light-adapted compound eyes are examined under identical conditions as the dark-adapted controls, the intermediate layer is no longer uniformly well preserved. Even in partly light-adapted specimens this junctional intermediate zone is only incompletely conserved. It is therefore conceivable that the marked intermediate layer resulting from the apposition or fusion of adjacent unit membrane components may bear some relation to the dark-adapted, or partially light-adapted state. The variance of the intermediate layer and of the distinctive granular elements is in many respects similar to the differences observed in the corresponding structural features of dark- and light-adapted vertebrate photoreceptors. The interior of the tubular compartments appears to be partly filled with an extremely fine particulate component which shows varying degrees of association with a homogeneous material of reduced density.

By virtue of its pervading tracheolar network the intact living insect is uniquely suited for very rapid fixation or freezing *in toto* of the labile photoreceptors with cooled vapors or gaseous refrigerants, thus eliminating the deleterious solvent effects of liquid fixatives. These preparative advantages may prove to be of decisive value in connection with future studies on localization of the unusually soluble retinene-protein complex, and other photosensitive pigments described in the compound eyes and ocelli of honeybees by Goldsmith (1958a, b).

Crystalline Lamellar Structures in Unfixed Preparations of Fresh Frog Retina

In order to obviate major artifact sources inherent in all present techniques for thin sectioning, unfixed preparations of fresh retinal rods and associated pigment components were examined directly by low-intensity or low-temperature electron microscopy. By carefully depositing a coated specimen grid on the exposed receptor layer of a fresh frog retina contained in a cool moist chamber, and then removing the grid with a gentle sliding and inverting motion (preferably carried out under binocular microscope control) a large number of detached, intact rod outer segments and attached particulate elements were found to adhere

---

Fig. 13. Oblique section through tips of rod outer segments from dark-adapted frog retina showing close structural relationship of the pigment granules with the rod layers. These granules of the pigment epithelium exhibit indications of an internal lamellar fine structure. Pt/Os, low-temperature preparation. Magnification: × 100,000.

Fig. 14. Cross-sectioned rhabdomere tubules of dark-adapted housefly retinula demonstrating double-contoured walls with associated granular components. The dense intermediate line (b, arrow) results from apposition or fusion of the outer layers of adjacent tubular compartments. Osmium vapor fixation, low-temperature dehydration and embedding. Magnifications: × 300,000 (14a); × 400,000 (14b).

(13)

(14)

readily to the thin carbon or plastic specimen film. In this way excellent preparations, which are thin enough for electron microscopy in many areas, can be rapidly obtained with a minimum of manipulation, and without introducing any extraneous material. The isolated rod outer limbs suspended in their native fluid medium can be examined in a simple microchamber with the polarized light microscope, and exhibit unaltered natural birefringence and dichroism indicative of an intact submicroscopic organization. Numerous pigment granules and minute birefringent crystalline components (Fig. 15) are also regularly seen in these preparations. In this connection it is interesting to point out that examination of the fresh retinal receptor layer under a low-power binocular microscope reveals characteristic scintillation effects around the exposed outer segments. The effect is apparently derived from extensive random reflections by rapidly shifting minute particles, and is strikingly reminiscent of the intense twinkling observed in microcrystalline suspensions. It is therefore possible that this scintillation effect may be due to the large number of suspended microcrystalline components surrounding the outer limbs.

When the corresponding air-dried (or frozen-dried) preparations are examined by electron microscopy (Fig. 16) characteristic thin crystalline lamellae (arrow) are regularly found in close association with the elongated pigment granules, and the opaque outer segments. The crystalline lamellae, approximately 0.5 to 3 μ long, are often stacked up in piles of different thickness (from about 20–50 Å upward) (Figs. 16 and 17), and display partly well-developed crystalline shapes, with sharp angular contours, and measurable interfacial angles in certain regions. These

---

FIG. 15. Phase contrast micrograph of wet, unfixed rod outer segment from fresh frog retina preparation, showing minute crystalline components (arrow) which are generally found near the photoreceptor layer in close association with pigment granules. Magnification: × 1400.

FIG. 16. Electron micrograph of native pigment granules with attached crystalline lamellae (arrow) which are regularly observed when fresh rod outer segment preparations (Fig. 15) are mounted and dried on specimen films without fixation. Magnification: × 12,000.

FIG. 17. These crystalline lamellae, which are extremely sensitive to irradiation effects, can be adequately examined only with low intensity electron optics and preferably by cooling the specimen holder. They are quite different from surrounding salt crystals, and yield characteristic electron diffraction patterns. Magnification: × 20,000.

FIG. 18. Selected area electron diffraction pattern recorded from crystalline lamellae (adjacent specimen Fig. 17) with electron microbeam of very low intensity. These crystalline components show diffraction patterns which give interplanar distances along two axes of 16.6 and 9.1 Å. Further evaluation is now in progress in an attempt to identify these lamellar components.


1μ
15
16
17

lamellae, which are extremely sensitive to the effects of irradiation can only be adequately examined by low-intensity microbeam illumination, and preferably with concomitant cooling of the specimens. The thin lamellae are quite different from the crystalline deposits of precipitated salts which rapidly sublimate under an intense electron beam; while under similar conditions the crystalline layers preserve their outer structure but immediately lose their diffracting power and characteristic electron optical behavior. Moreover, these lamellae exhibit typical crystallinity phenomena such as extinction contours, reflection images, and occasionally, when piled up on top of each other in favorable orientation also characteristic moiré patterns.

By using a microbeam of very low intensity characteristic electron diffraction patterns (Fig. 18) have been recorded from the crystalline lamellae, and a correlation could be established with the individual crystals by selected area diffraction. In a preliminary evaluation, carried out in collaboration with Dr. Murray V. King, it was found that the diffraction patterns give interplanar distances along two axes of 16.6 and 9.1 Å. The 16.6 axis shows absence of the odd orders, indicating the presence of a screw axis or a glide plane. The patterns show a complete two-dimensional reciprocal lattice net with a limiting resolution of the order of 1.8 Å. This resolution of the transmission electron diffraction patterns compares favorably with the X-ray diffraction patterns given by more complex substances such as proteins. Identification of the crystalline lamellae has not progressed beyond this very preliminary stage. Thus, although the dimensions are compatible with the tentative assumption of a carotenoid, numerous other substances could also fit these parameters. It may nevertheless be possible to compare these patterns systematically with the corresponding electron diffraction and X-ray diffraction patterns of important carotenoid compounds and their derivatives. Thanks to the described low-intensity electron optics and the specimen cooling devices, useful electron diffraction patterns can now be recorded from very sensitive crystalline substances like vitamin A, examination of which was precluded by immediate melting and volatilizing under the electron beams of normal intensity used in routine electron microscopy.

Most of the observations were made on crystalline lamellae from partly or completely light-adapted frog retinas, since dark-adapted specimens have not been adequately investigated. Throughout these studies the possibility was carefully considered that we may be dealing with extraneous components or other sources of contamination; but critical evaluation and repetition of the experiments under controlled conditions has essentially confirmed the initial results. It is realized, however, that conclusive proof and characterization of these crystalline structures will

largely depend on successful isolation of the crystalline lamellae by differential ultracentrifugation and supplementary techniques.

Summary

Improved low-temperature preparation technique and standard methods have been applied in electron microscope studies of frog, guinea pig, and rabbit visual cells, and photoreceptors of insect compound eyes. The investigations were supplemented by direct observation of unfixed native specimens in the electron microscope at temperatures of —80° C to —130° C using a special cold stage and low intensity electron optics. A comparative survey is given of the oriented electron-dense components and the intermediate structures observed in the unit layers of the visual cell outer segments and the rhabdomere tubules, which consistently exhibit better morphological and histochemical preservation in cryofixation and related low-temperature preparations. Characteristic differences detected in the fine structure of the unit membranes in light- and dark-adapted photoreceptors are correlated with the available evidence on localization of the photopigments within the planes of the layers. Condensation of the layers and dense paracrystalline inclusions were produced by treatment with platinum chloride and other heavy metal compounds particularly in dark-adapted frog visual cell outer segments. Crystalline lamellar structures which are closely associated with the pigment granules and outer segments were frequently observed in preparations of fresh frog retinas examined directly by low-temperature electron microscopy and electron diffraction. Characteristic electron diffraction patterns were recorded from these crystalline components which give interplanar distances along two axes of 16.6 and 9.1 Å.

A critical evaluation is presented of possible artifact sources, and illustrations given of the potentialities of low-temperature preparation techniques in elucidating the macromolecular organization of photoreceptor structures during various states of activity.

Acknowledgments

The author is particularly obliged to Professor Samuel C. Collins, Director of the Cryogenic Engineering Laboratory, Massachusetts Institute of Technology, for his guidance and generous help in making available the facilities of his laboratory during the course of the liquid helium experiments and to his assistant, Mr. Robert Cavileer, for his technical contribution in the instrumentation of the liquid helium experiments. Sincere thanks are also due to Frederick B. Mork and Joanne T. Frederick for their valuable technical assistance, and to Miss Irene Brierley for her kind help in preparing the manuscript. The valuable suggestions and the kind assistance of Dr. Murray V. King of the Orthopedics Research Unit, Massachusetts General Hospital, in connection with evaluation of the electron diffraction patterns are gratefully acknowledged.

References

Ayres, W. C., and Kühne, W. (1878). *Untersuch. Physiol. Inst. Univ. Heidelberg.* **2**, 215-240.

Brenner, S., and Horne, R. W. (1959). *Biochim. et Biophys. Acta* **34**, 103-110.

Broda, E. E., and Goodeve, C. F. (1941). *Proc. Roy. Soc.* **A179**, 151-159.

Broida, H. P. (1957). *Ann. N.Y. Acad. Sci.* **67**, 530-545.

Bullivant, S. (1960). *Abstracts, 4th Ann. Meeting Biophys. Soc., Philadelphia, February 24-26, 1960* p. 6.

Calvin, M. (1959a). *Revs. Modern Phys.* **31**, 147-156.

Calvin, M. (1959b). *Revs. Modern Phys.* **31**, 157-161.

Collins, F. D., and Morton, R. A. (1950a). *Biochem. J.* **47**, 3.

Collins, F. D., and Morton, R. A. (1950b). *Biochem. J.* **47**, 10-18.

Collins, F. D., Love, R. M., and Morton, R. A. (1952). *Biochem. J.* **51**, 292-298.

Dartnall, H. J. A. (1957). "The Visual Pigments." Wiley, New York.

Dartnall, H. J. A., Goodeve, C. F., and Lythgoe, R. J. (1938). *Proc. Roy Soc.* **A164**, 216-230.

Denton, E. J. (1959). *Proc. Roy. Soc.* **B150**, 78-94.

Denton, E. J., and Wyllie, J. H. (1955). *J. Physiol. (London)* **127**, 81-89.

De Robertis, E. (1956). *J. Biophys. Biochem. Cytol.* **2**, 319-329.

Detwiler, S. R. (1932). *J. Comp. Neurol.* **55**, 473-492.

Detwiler, S. R., and Zwemer, R. L. (1937). *Anat. Record* **67**, 295-303.

Dowling, J. E., and Wald, G. (1958). *Ann. N.Y. Acad. Sci.* **74**, 256-265.

Ewald, A., and Kühne, W. (1878). *Untersuch. physiol. Inst. Heidelberg.* **1**, 139-218, 248-290, 370-455.

Favard, P., and Carasso, N. (1958). *Arch. anat. microscop. morphol. exptl.* **47**, 211-234.

Feder, N., and Sidman, R. L. (1958). *J. Biophys. Biochem. Cytol.* **4**, 593-600.

Fernández-Morán, H. (1953). *Exptl. Cell. Research* **5**, 255.

Fernández-Morán, H. (1954). *Progr. Biophys. and Biophys. Chem.* **4**, 112-147.

Fernández-Morán, H. (1956a). *Ind. Diamond Rev.* **16**, 128-133.

Fernández-Morán, H. (1956b). *Nature* **177**, 742-743.

Fernández-Morán, H. (1957). *In* "Metabolism of the Nervous System" (E. Richter, ed.), pp. 1-34. Pergamon Press, London.

Fernández-Morán, H. (1958). *Exptl. Cell Research Suppl.* **5**, 586-644.

Fernández-Morán, H. (1959a). *Science* **129**, 1284.

Fernández-Morán, H. (1959b). *Revs. Modern Phys.* **31**, 319-330.

Fernández-Morán, H. (1959c). *In* "Proceedings Sixth Annual Symposium Origin and Role of Complex Macromolecular Aggregates in Development," (M. V. Edds, ed.), Session II, Society of General Physiologists, September 8, 1959. Ronald Press, New York. In press.

Fernández-Morán, H. (1959d). *J. Appl. Phys.* **30**, 2038.

Fernández-Morán, H. (1959e). Progr. 17th Ann. Meeting, Electron Microscope Society of America, Columbus, Ohio, September 9, 1959, *J. Appl. Phys.* **30**, 2028.

Fernández-Morán, H. (1960). Conference on Freezing and Drying of Biological Materials, Session III, The New York Academy of Sciences, Section of Biological and Medical Sciences, October 1, 2, 1959. *Ann. N.Y. Acad. Sci.* **85**, 689-713.

Fernández-Morán, H., and Finean, J. B. (1957). *J. Biophys. Biochem. Cytol.* **3**, 725-748.

Finean, J. B., Sjöstrand, F. S., and Steinman, E. (1953). *Exptl. Cell Research* **5**, 557.

Goldsmith, T. H. (1958a). *Proc. Natl. Acad. Sci. U.S.* **44**, 123.

Goldsmith, T. H. (1958b). *Ann. N.Y. Acad. Sci.* **47**, 223-229.
Goldsmith, T. H., and Philpott, D. E. (1957). *J. Biophys Biochem. Cytol.* **3**, 429-440.
Granit, R., Holmberg, T., and Zewi, M. (1938). *J. Physiol.* (*London*) **94**, 430-440.
Hecht, S., and Pickles, E. G. (1938). *Proc Natl. Acad Sci. U.S.* **24**, 172-176.
Hodge, A. J. (1959). *Revs. Modern Phys.* **31**, 331-341.
Hubbard, R. (1954). *J. Gen. Physiol.* **37**, 381-399.
Hubbard, R. (1956). *J. Gen. Physiol.* **39**, 935-962
Hubbard, R., and Kropf, A. (1958). *Proc Natl. Acad. Sci. U.S.* **44**, 130-139.
Johnson, M. L., and Detwiler, S. R (1942). *J. Exptl. Zool.* **89**, 233-249.
Klotz, I. M. (1958). *Science* **128**, 815.
Kolmer, W. (1909). *Pflüger's Arch ges Physiol.* **129**, 35-45.
Kolmer, W. (1925). *Arch. Ophthalmol Graefe's* **115**, 310-313
Kropf, A., and Hubbard R (1958). *Ann. N.Y Acad. Sci.* **74**, 266-280
Kuhne, W. (1878a). "On the Photochemistry of the Retina and on Visual Purple" (*Trans by M Foster*). Macmillan, London.
Kuhne, W. (1878b) *Untersuch Physiol Inst. Univ. Heidelberg* **1**, 15
Kuhne, W. (1879). *In* "Handbuch der Physiologie" (L. Herman, *ed.*), Vol 3, p. 235. Vogel, Leipzig
Kuhne, W. (1895) *Z Biol* **32**, 21
Lythgoe, R J (1937). *J Physiol* **89**, 331-358.
Lythgoe, R J., and Quilliam, J P (1938) *J. Physiol.* (*London*) **94**, 399-410.
Mendelssohn, K (1956). *In* "Handbuch der Physik," Encyclopedia of Physics. XV. *Low Temperature Physics* (S Flugge, *ed.*), Vol. II, pp. 370-461. Springer, Berlin.
Muller, W H (1957) *J Biophys Biochem Cytol* **3**, 421-427.
Moody, M F., and Robertson, J D (1960) *J Biophys Biochem. Cytol.* **7**, 87-92.
Robertson, J D (1959) *Biochem Soc Symposia* (*Cambridge, Engl.*) **16**, 3-43.
St George, R C C (1952) *J Gen Physiol* **35**, 495-517
Saito, Z (1938) *Tôhoku J Exptl Med* **32**, 432-446.
Schmidt, W J (1934) *Naturwissenschaften* **22**, 206.
Schmidt, W J (1935a) *Z. Zellforsch u mikroskop Anat* **22**, 485-522.
Schmidt, W J (1935b) *Zool Anz* **109**, 245-251
Schmidt, W J (1935c) *Z wiss Mikroskop* **52**, 8-23
Schmidt, W. J (1937) "Die Doppelbrechung von Karyoplasma, Zytoplasma und Metaplasma" Gebruder Borntraeger, Berlin
Schmidt, W J (1938) *Kolloid-Z* **85**, 137-148
Schmidt, W J (1951) *Pubbl staz zool Napoli* **23**, 158-183.
Sjostrand, F. S (1949) *J Cellular Comp Physiol* **33**, 383
Sjostrand, F S (1953) *J Cellular Comp Physiol* **42**, 15-44
Sjostrand F S. (1959) *Revs Modern Phys* **31**, 301-318
Smith, E L., and Pickles, E G (1940) *Proc Natl Acad Sci. U S.* **26**, 272-277.
Stern, R (1905) *Arch Ophthalmol Graefe's* **61**, 561-563
Tansley, K (1931) *J Physiol* (*London*) **71**, 442-458
Tansley, K (1933) *Proc Roy Soc* **B114**, 79-103.
Wald, G. (1936) *J Gen Physiol* **19**, 781-795.
Wald, G. (1938) *J Gen Physiol* **21**, 795-832
Wald G (1951) *J. Opt Soc Am* **41**, 949-956
Wald, G. (1953) *Ann Rev Biochem* **22**, 497-526
Wald, G (1954) *Am Scientist* **42**, 73-95.
Wald, G (1958). *Exptl Cell Research Suppl* **5**, 389-410.

Wald, G. (1959). *Handbook of Physiol.* (*Neurophysiol.* **1**), pp. 671-692.
Wald, G., Durell, J., and St. George, R. C. C. (1950). *Science* **111**, 179-181.
Walls, G. L. (1939). *Anat. Record* **73**, 373-385.
Walls, G. L. (1942). *Cranbrook Inst. Sci. Bull.* **19**, 785 pp.
Wolken, J. J. (1958). *Ann. N.Y. Acad. Sci.* **74**, 164-181.
Wolken, J. J., Mellon, A. D., and Contis, G. (1957a). *J. Exptl. Zool.* **134**, 383-410.
Wolken, J. J., Capenos, J., and Turano, A. J. (1957b). *J. Biophys. Biochem. Cytol.* **3**, 441-447.
Yamada, E., Tokuyasu, K., and Iwaki, S. (1958). *J. Electronmicroscopy* (*Chiba*) **6**, 42-46.

Discussion

Dr. Thornberg [Dartmouth Medical School, Hanover, New Hampshire]: Could you comment on the fixation of the carotenoids?

Dr. Fernández-Morán [Cambridge, Mass.]: The stains and heavy metal compounds used in our electron microscope and free-substitution work are not considered to be specific for the carotenoids. However, it might be possible to identify retinene and other photopigment derivatives, if they can be isolated in crystalline form or specific heavy metal complexes prepared, by combining electron microscopy with selected area electron diffraction studies. Thus, although vitamin A crystals melt at 63°–64°C, useful electron diffraction patterns can be recorded from microcrystalline deposits by cooling the specimen holder and illuminating with an electron microbeam of very low intensity.

Dr. Wolken [University of Pittsburgh, Penn.]: How did you get these pictures?

Dr. Fernández-Morán [Cambridge, Mass.]: The electron diffraction patterns of the crystalline components were all recorded from native, unfixed and unstained frog retinas prepared immediately after removal from the living animal. When the exposed layer of retinal receptors is gently touched or stroked with carbon-coated specimen grids, the rod outer segments and associated pigment and crystalline components adhere to the thin films, and are then suitable for low-temperature electron microscopy.

AUTHOR INDEX

Numbers in italics indicate the pages on which the references are listed.

A

Adler, F. H., 142, 150
Akiya, H., 168, 170
Alagna, G., 411, 418
Alexander, H. E., 235, 246
Allen, R. A., 161, 162, 170
Alter, A. J., 259, 271
Amprino, R., 406, 419, 511, 518
Anfinsen, C. B., 161, 170, 482, 485
Anger, H. O., 259, 271
Appelmans, M., 284, 290
Arnon, D. I., 423, 431
Ashton, N., 311, 320, 324, 335, 340
Asling, C. W., 508, 512, 519
Attfield, M., 32, 49
Auerbach, T., 250, 253, 256
Aurell, G., 411, 418
Ayres, J., 429, 430, 432
Ayres, W. C., 554

B

Baesch, P., 207, 210, 218
Bahr, G. F., 37, 42, 48
Baird, C. D. C., 512, 519
Baker, J. R., 37, 44, 48
Baker, R. F., 12, 49
Balazs, E. A., 290, 294, 297, 300, 301, 303, 304, 305, 306, 308, 309
Ballowitz, E., 435, 438, 439
Bamatter, F., 514, 518
Bannon, S. L., 511, 518
Bárány, E. H., 311, 324, 338, 340
Barber, A. N., 441, 451
Barnett, N. A., 469, 470, 471, 481, 485
Baumann, M., 283, 290, 295, 308
Bembridge, B. A., 283, 291
BenGeren, B., 2, 27
Bennett, H. S., 20, 27, 37, 48, 450, 451, 454, 465
Bensusan, H. B., 299, 308
Berens, C., 507, 518
Bergamini, G., 411, 418
Berggren, L., 319, 324
Berman, M. D., 46, 49
Bernd, A. H., 209, 218
Bernhard, W., 481, 486
Bernstein, M. H., 142, 143, 144, 150, 471, 485
Beyer, H., 55, 69
Binder, H. F., 435, 436, 438, 439
Binder, R. F., 435, 436, 438, 439
Birbeck, M. S. C., 469, 470, 471, 481, 485
Blanchard, J., 108, 115
Blockeel, J., 284, 290
Bloom, G., 301, 303
Bloom, W., 143, 150
Blum, J., 442, 451
Boell, E. J., 161, 163, 171
Bolck, F., 318
Bonanto, M. V., 250, 256
Bond, V., 273, 274, 281
Bond, V. P., 273, 277, 281, 435, 436, 439, 487, 505
Bornschein, H., 202, 205
Bowness, J. M., 176, 191
Bradley, D. E., 442, 451
Brandt, P. W., 453, 454, 456, 458, 460, 462, 465
Brecher, C., 273, 277, 281, 435, 439, 487, 505
Brenner, S., 554
Brent, R. L., 508, 519
Brini, A., 311, 320, 324, 335, 340
Broda, E. E., 554
Broda, H. P., 554
Brownman, L. G., 516, 518
Brown, F. C., 480, 485
Brown, G. W., Jr., 160, 164, 170
Brown, P. K., 105, 115, 183, 191
Brunet, P., 480, 485
Bullivant, S., 554
Bunney, D. M., 304, 308
Burky, E. L., 240, 246, 249, 257
Burstone, M., 160, 170
Burtner, H. J., 160, 164, 170

C

Calvin, M., 47, 49, 554
Capenos, J., 176, 191, 522, 547, 556
Carasso, N., 554
Carr, J. G., 470, 485

Casearano, J., 68, *69*
Catchpole, H. R., 400, *402*
Caulfield, J. B., 368, *377*
Challice, C. E., 481, *485*
Charles, A., 471, *485*
Cheng, C.-S., 55, *70*
Chesterman, W., 213, *218*
Ciaccio, C., 37, *48*
Clark, S. L., Jr., 460, *465*
Clugston, H., 508, *519*
Cogan, D. G., 53, 54, 66, *69*, 97, *98*, 104, *115*, 167, *170*, 259, *271*, 415, *418*, 435, *439*
Cohen, A., 235, *247*
Cohen, A. I., 151, 156, *158*
Cohen, C., 294, *308*
Cohlan, S. Q., 512, *518*
Collet, A., 393, *403*
Collins, F. D., 46, *48*, 524, 527, *554*
Colman, A. D., 111, *115*
Cone, W., 126, *136*
Coutis, G., 547, *556*
Cooper, S. N., 250, *256*
Coulombre, A. J., 406, 407, 409, 411, *418*
Coulombre, J. L., 406, 407, 409, 411, *418*
Crawford, G. N. C., 283, *291*
Cronkite, E. P., 273, 277, *281*, 435, *439*, 487, *505*
Crosby, E. C., 126, *136*
Crozier, W. J., 207, *218*
Cuckow, F. W., 470, *485*
Curley, F. J., 509, *518*

D

Dalton, A. J., 151, *158*, 400, *402*, 469, 470, 481, *485*, *486*
D'Amato, C. J., 492, 503, *505*
Danielli, J. F., 4, *27*
Dartnall, H. J. A., 541, *554*
Davey, J. B., 32, *49*
Davidson, E. A., 411, *418*
Davson, H. J., 4, *27*, 409, *418*
Day, T. D., 302, 307, *308*
Defendi, V., 164, *171*
Deimas, A., 511, 512, *518*
Del Castillo, J., 20, *27*
del Rio Hortega, P., 117, *136*
de Meyer, R., 511, 516, *518*
Denton, E. J., 537, *554*
De Robertis, E., 6, 17, 20, *27*, 29, 30, 32, 36, 37, 42, 47, *48*, 62, *69*, 96, *98*, 139, 140, 141, *150*, 151, *158*, 168, *170*, 173, 174, *191*, 450, *451*, 521, *554*
DeRoche, M. H., 304, *308*
De Roetth, A., Jr., 161, *170*
de Rothschild, B., 512, *518*
de Souza, E., 55, *70*
Detwiler, S. R., 488, *505*, 516, *518*, 542, 544, *554*, *555*
Devik, F., 260, *271*
Dodt, E., 126, *136*, 202, *205*
Donaldson, D. D., 259, *271*
Donn, A., 273, *281*, 438, *439*
Dowgjallo, N. D., 329, *333*
Dowling, J. E., 85, 86, 97, *98*, 104, 110, 111, *115*, *554*
Drance, S. M., 260, *271*
Drew, R. M., 279, 280, *281*, 438, *439*
Drungis, A., 259, *271*
Ducrest, P., 255, *257*
Duke-Elder, W. S., 82, *83*, 126, *136*, 207, *218*, 283, *291*, 294, *308*
Durrell, J., 521, *556*

E

Eagle, H., 274, *281*
Eakin, R. M., 470, *485*
Eaves, G., 302, *308*
Eckl, E. A., *301*
Eichner, D., 161, 162, *170*
Engelking, E., 509, *518*
Engström, A., 46, *48*
Engström, H., 20, *28*
Eränkö, O., 161, *170*
Esperson, J., 389, *390*
Euler, H. von, 427, *431*
Evans, H. M., 508, 512, *519*
Ewald, A., *554*

F

Falcone, G., 430, *431*
Falk, S., 470, *485*
Favard, P., *554*
Fawcett, D. W., 230, 232, 252, *266*, 464, *465*
Feder, N., 63, *69*, 487, 488, 489, 490, 492, *505*, 533, *554*

Feeney, M. L., 311, *324*, 343, *366*, 370, *377*, 389, *390*
Felix, M. D., *400*, *402*, 470, 481, *485*
Fernández-Morán, H., 4, *27*, 173, 176, *191*, 285, *291*, 521, 522, 523, 524, 525, 528, 529, 532, 533, 534, 536, *548*, 547, *554*
Ferraro, A., 511, 518
Ferry, J. D., 294, *308*
Fessler, J. H., 299, 307, *308*, *309*
Fine, B. S., 301, 309, 441, 443, 447, *451*
Finean, J. B., 4, *27*, 42, *46*, *48*, 528, 532, *554*
Fitton-Jackson, S., 393, *400*, *402*
Fitzgerald, P. L., 250, 251, *256*
Fitzpatrick, T. B., *150*, 480, *485*
Flexner, L. B., 426, *431*, *432*
Flocks, M., 335, *340*, *377*
Foote, M., 507, *518*
Fortin, E. P., *377*
Fozzard, J. A. F., *509*, *519*
Franchi, G. M., 17, *27*, 30, *48*, 62, *69*
Francis, C. M., 53, *69*, 101, 102, 163, 167, *170*
François, J., *240*, *246*, 250, *256*
Franklin, M. D., 507, *518*
Freund, J., 250, *256*
Friedenwald, J. S., 126, *136*, 161, 162, *170*, 421, *426*, *431*, *432*
Furst, C. M., 488, *505*
Futterman, S., 167, *170*

G

Galfaso, G., 37, 42, *48*
Garron, L. K., 311, *324*, 343, *366*, *370*, *377*, 389, *390*
Gasseling, M. T., *430*, *432*
Gavin, M. A., 221, 222, 224, *232*
Gellert, A., 207, 210, *218*
Gemelotto, G., 411, *418*
Gerchtzoff, M. A., 161, 166, *170*
Gergely, J., *308*, *308*
Gersh, I., 400, *402*
Gfeller, M., 430, *432*
Ghiara, P., 411, *418*
Gierdin, A. V., 385, *391*
Gerter, T., 6, 28
Gieseking, R., 393, *403*
Gilbert, C., 510, *518*
Gillman, J., 510, *518*
Gillman, T., 510, *518*
Giroud, A., 508, 510, 511, 512, 513, 514, *518*
Giroud, P., 512, 514, *518*
Glauert, A. M., 87, *98*, 344, *366*, 442, *451*
Glauert, R. H., 87, *98*, 344, *366*, 442, *451*
Glenner, G. G., 160, 164, *170*
Glucksman, H., *503*, *505*
Goedbloed, J., 295, 296, *308*
Goldmann, H., 259, *271*
Goldsmith, R. L., 125, *137*
Goldsmith, T. H., 176, *191*, 521, 547, 548, 554, 555
Gomez, C. J., *37*, 42, *48*
Gommers, A., 512, *518*
Gomori, G., 159, 170
Gonzalez, P., *255*, *257*
Goodeve, C. F., *554*
Granit, R., 18, *27*, 203, *205*, *555*
Graymore, C. N., 60, *69*
Greenfield, P., 161, 163, *171*
Greff, R., 120, *136*
Gregg, N. M., 512, *518*
Gregory, W. K., 255, 256
Griffin, A. C., 480, *485*
Grignolo, A., 283, 284, *291*, 301, *308*
Gross, J., 284, *291*, 294, 299, *308*
Gruneberg, H., 471, *485*
Guttes, E., 469, 470, *485*
Gustavson, K. H., 295, 309
Gyllensten, L. J., 510, *518*

H

Hagans, W. A., *115*
Hahn, L., 427, *431*
Halbert, S. P., *250*, 251, 253, *256*
Hale, F., 511, *518*
Hamburg, A., 301, *309*
Hamburger, V., *209*, *218*
Hamburgh, M., 510, *518*
Hamilton, V. L., 209, *218*
Hampton, J. C., *454*, *465*
Hanzon, V., 400, *403*
Harding, C. V., 273, 274, *281*, 435, 436, 438, 439
Harris, J. E., 409, *418*
Harthine, H. K., 22, *27*
Hassal, A. H., 374, *377*
Haye, G., 343, *366*

Hebb, C. O., 101, 162, *170*
Hecht, S., 107, *115*, *555*
Hedges, E., 186, *191*
Heidelberger, M., 249, *256*
Heine, L., *377*
Heiney, R. E., 429, 430, *432*
Hektoen, L., 249, 256
Hellström, B. E., 510, *518*
Henle, J., 374, *377*
Hermans, P. H., 294, *309*
Herrmann, H., 415, *418*, 421, 422, 423, 425, 426, 427, 428, 430, *431*, *432*
Hess, R., 160, *170*, *171*
Heydenreich, A., 144, *150*
Hickman, F. H., 421, 422, 426, 428, *432*
Hicks, S. P., 492, 503, *505*, 508, *518*
Higginbottom, R. M., 511, *518*
Highberger, J. H., 299, *308*
Hirono, R., 393, *403*
Ho, J. Y. C., 429, 430, *432*
Hodge, A. J., 42, *48*, 112, *115*, 533, *555*
Hoet, J. J., 512, *518*
Hoet, J. P., 512, *518*
Hoffmann, P., 393, *403*
Hogan, M. J., 311, *324*, 370, *377*, 389, *390*
Holmberg, Å., *340*, 389, *390*, 444, *451*, 453, 454, 458, 462, *465*
Holmberg, T., *555*
Holmgren, H., 411, *418*
Horne, R. W., *554*
Horowitz, M. C., 429, 430, *432*
Hoskins, D., 510, *518*
Howard, A., 259, 261, *271*, 274, *281*
Howard-Flanders, P., 260, *271*
Hoyt, B. L., 299, *308*
Hubbard, R., 105, 109, 111, *115*, 168, *170*, 180, 183, 184, *191*, 540, 547, *555*
Huber, C. C., 126, *136*
Hughes, W. L., 273, 274, 276, 277, *281*, 435, 436, *439*, 487, *505*

I

Ingalls, T. H., 509, *518*
Ingelstam, E., 24, *27*
Ingram, J. T., 471, *485*
Isaac-Mathy, M., 516, *518*
Isenberg, I., 426, *432*
Ishida, T., 343, *366*
Iwaki, S., 73, 82, *83*, 96, *99*, 139, 143, 144, *150*, 470, 481, *486*, 546, *556*

J

Jackson, D. S., 299, *309*
Jakus, M. A., 343, *366*, 367, 370, *377*, 381, *391*, 393, *403*
Janeső, N., 322, *324*
Jennings, W. H., *115*
Johnson, M. L., 85, *99*, 542, 544, *555*
Jokl, A., 207, 209, *218*
Jordan, H. C., 508, *519*
Jusélius, E., *282*

K

Kaan, H. W., 511, *518*
Kahler, H., 469, *486*
Kajikawa, J., 207, 213, *218*
Kajikawa, K., 393, *403*
Kallam, F., 42, *49*
Kalter, H., 512, *518*
Kaminski, M., 250, *256*
Kappers, C. U., 126, *136*
Karasaki, S., 471, *485*
Karli, P., 32, *48*
Karlin, L. J., 460, *465*
Karnofsky, D. A., 510, *518*
Karreman, C., 426, *432*
Karrer, H. E., 230, *232*
Katz, B., 20, *27*
Katzin, H. M., 343, *366*
Kauth, H., 207, *218*
Keeler, C. E., 32, *48*
Kerby, C. E., 507, *518*
Khalaf, K. T., 176, *191*
Kikkawa, Y., 412, 413, 415, 416, 417, *418*
Kimura, S. F., 259, *271*
Kinoshita, J. H., 167, *170*, 428, *432*
Kinsey, V. E., 266, *271*, 458, *465*
Klotz, I. M., 429, 430, *432*, 555
Knese, K.-H., 393, *403*
Knoch, M., 284, *291*
Knoop, A.-M., 393, *403*
Koelle, G. B., 159, 160, 161, 162, 164, *170*
Koller, P. C., 32, *49*
Kolmer, W., 542, 555
Kopriwa, B., 277, *281*
Korngold, L., 239, *246*

Krause, A C, 412, *418*
Krinsky, N. I, 46, 48, 105, *115*
Kropf, A, 105, 109, *115*, 180, 183, *191*, 585
Kubik, I, 333
Kubota, L, 394, *403*
Kuhne, W, 143, *150*, 521, *554*, 555
Kuhlman, R. E, 428, *432*
Kukita, A, 480, *485*
Kulkarni, M. E, 250, *256*
Kuwahara, T., 53, 54, 66, 69, 167, *170*
Kuyken, M., 235, *246*

L

Lacy, D, 481, *485*
Ladman, A J., 58, *69*, 168, *170*
Lajtha, L G., 266, *271*
Landsteiner, K, 249, 256
Langman, J., 235, 236, 237, 239, 242, *246*, 512, 518
Lasansky, A., 29, 32, 36, 37, 42, *48*, 131, *158*
Lauber, H, 126, *136*, 283, 284, *291*
Laurent, T C, 304, 300, *308*, *309*
Laurent, U B G, 304, *308*
Lawn, A M, 151, 158
Lawrentjew, A P., 329, *333*
Lazer, G., 470, 485
Leach, E H, *213*, *218*
Leblond, C P, 277, *281*, 488, *505*
Leboucq, G, *490*, *505*
Lecomte du Nouy, P, 188, *191*
Lefebvres, J, 511, *512*, 513, *518*
Lefebvres-Bausselot, J, 512, *519*
Leinfelder, P J, 259, 270, *271*
Leplat, G, 161, 160, *170*
Lerner, A B, 480, *485*
Levi-Montalcini, R, 516, *518*
Lewis, C, 29, *48*, 66, *70*, 168, *170*
Liechti A 259, *271*
Lillie R D 46, *48*
Lindahl C, 207, 209, *218*
Linker, A 393, *403*, 411, *418*
Lion G, 469, 470, *485*
Lison L 37, *48*, 215, *218*
Liss, L 122 126, 128, *136*, *137*
Lloyd B J, 222, *232*
Locatcher-Khorazo, D, 250, *256*
Love, D S, 428, 430, *432*
Love, R M, 46, *48*, 524, 527, *554*
Lowry, O. H, 29, *48*, 66, *70*, 168, *170*
Lucas, D. R., 32, *49*
Luthy, H., 46, *48*
Luft, J. H, 441, 451, 454, *465*
Lythgoe, R J, *554*, *555*

M

MacCardle, R. C., 469, *486*
McConnell, J. M., 511, *518*
McEwen, W. K., 311, *324*, 370, *377*, 389, *390*
McGovern, V. J., 322, *324*
McKeehan, M S, 235, *247*
McLean, J. D, 42, 48, 112, 115
MacMillan, J A, 126, *136*
Maetlens, C, 470, *485*
Maisel, H, *239*, *246*
Mann, I C., 207, 209, 210, 212, 218, 409, *418*, 441, *451*, 511, *518*
Manski, W., 250, 253, *256*
Marchesani, O, 125, *136*
Markert, C L, 471, *485*, *486*
Martinet, M, 508, 510, 512, 513, 514, *518*
Masek, B, 160, *171*
Mason, H S, 469, 480, 486
Matoltsy, A G, 284, *291*, 294, *308*, *309*
Maurice, D M., 381, 382, 384, 385, 386, 387, 388, 389, *391*, 412, *418*
Mawas, J, 146, *150*
Maximow, A A, 143, *150*
Maxwell, D S, 458, *465*
Maynard, E A., 17, 27
Mazia, D, 426, *432*
Mellon, A D, 547, 556
Mendelssohn, K, *555*
Mercer, E H., 470, *485*
Mercer, F V., 42, *48*, *112*, *115*
Mercier-Parot, L., 510, 514, 515, *519*
Merker, H J, 393, *403*
Messier, B, 277, *281*, 488, *505*
Meyer, D B, 209, *218*
Meyer, K, 393, *403*, 411, *418*
Miale, I, 487, 488, 489, 490, 492, 494, 502, 501, *505*
Michaelis, L., 441, *451*
Michaelson, I C, 142, *150*
Millen, J. W, 509, *519*
Miller, W H, *522*, *555*
Mishuna, S., *420*

Miyamoto, M., *150*
Moody, M. F., 6, 27, 151, *158*, 522, 534, 536, 547, *555*
Moran, H., 42, *48*
Morton, R. A., 46, *48*, 524, 527, *554*
Moses, S. G., 421, *432*
Mowry, R. W., 214, 215, *218*
Moyer, F., 474, 485
Munoz, C. M., 259, *271*
Murphy, M. L., 510, *518*
Murray, J. P., 400, *403*

N

Nachlas, M. M., 55, *70*
Nagano, 438, *439*
Naylor, E. J., 412, 413, 415, 417, *418*, *419*
Neetens, A., 240, *246*
Nelson, M. M., 508, 512, *519*
Nemetschek, Th., 393, *403*
Neumann, H., 411, *419*
Nickerson, W. J., 430, *431*
Nielands, J. B., 423, *432*
Nissen, T., 471, *486*
Noell, W. K., 29, 32, 34, 36, *48*, 97, *99*, 103, *115*, 203, *205*
Novikoff, A. B., 160, *170*, *171*
Nuttall, G. H. F., 249, *256*

O

Offret, C., 343, *366*
Ogston, A. G., 304, 305, *309*
O'Rahilly, R., 209, *218*
Ouchterlony, O., 239, *247*, 249, *256*
Ozanics, V., 409, 411, *418*

P

Paassen, van F., 512, *518*
Painter, R. B., 273, 277, 279, 280, *281*, 438, *439*, 487, *505*
Palade, G. E., 144, *150*, 221, *232*, 441, 450, *451*, 481, *486*
Palay, S. L., 450, *451*, 460, *465*
Palmgren, A., 325, 333
Pappas, G. D., 393, 398, *403*, 444, *451*, 453, 454, 456, 458, 460, 462, *465*
Patrone, C., 411, *418*
Peachey, L. D., 442, *451*
Pearse, A. G. E., 55, 56, 68, *70*, 159, 160, 161, *170*, *171*
Pearson, B., 164, *171*
Pease, D. C., 17, *27*, 142, *143*, 144, *150*, 444, *451*, 453, 458, *465*, 471, *485*
Pele, S. R., 277, *281*, *505*
Pepler, W. G., 161, *171*
Petit, 207, *218*
Phillips, R. I., 125, *137*
Philpott, D. E., 522, 547, *555*
Pickles, E. G., 555
Pietruszkiewicz, A., 304, *309*
Pike, R. L., 511, *519*
Pirenne, M. H., 107, *115*
Pirie, A., 159, *171*, 260, 266, *271*, 283, *291*, 294, 295, *309*
Policard, A., 393, *403*
Polyak, S. L., 92, *99*, 117, 126, *136*, 139, *150*, 487, *505*
Poppe, E., 259, 264, *271*
Porter, K. R., 38, 42, *48*, *49*, 73, 74, 78, 80, 82, *83*, 96, 97, *99*, 139, 144, *150*, 393, 398, *403*, 442, *451*, 470, *481*, *486*
Posarelli, A., 284, *291*
Prégermain, S., 393, *403*
Prince, J. H., 230, *232*
Prindle, R. A., 509, *518*
Pringle, B. H., 239, *247*
Prost, H., 511, 512, *518*
Puntenney, I., 259, *271*
Pyl, T., *55*, *69*

Q

Quastler, H., 273, 277, *281*, 435, *439*, 487, 492, *505*
Quilliam, J. P., *555*

R

Rabaey, M., 240, *246*, 250, *256*
Radhakrishnan, M. R., 250, *256*
Ramón y Cajal, S. R., 117, *136*, 487, 488, 496, 503, *505*
Ramsey, F., 516, *518*
Rao, S. S., 250, 256
Ratliff, F., 22, *27*
Rayleigh, Lord, 386, *391*
Redslob, E., 319, *324*, 427, *432*
Reiniger, M., 509, *519*
Reuet, C., 393, *403*
Resnik, R. A., 428, *432*
Rhodin, J., 3, *28*, 458, *465*, 470, *485*
Richards, R. D., 259, 270, *271*

Riley, E. F., 259, 270, 271
Roberts, N. R., 29, *48*, 66, *70*, 168, *170*
Robertson, J. D., 3, 4, 6, 27, 151, *158*, 481, *486*, 522, *534*, *536*, 547, *555*
Robinson, C., 188, 191
Robinson, R. A., 385, 391
Rochon-Duvigneaud, A., 325, 333, 413, *418*
Rogers, G. E., 344, 366, 442, *451*
Rohen, J., 311, 320, 322, *324*, 335, *340*
Rorzin, L., 511, *518*
Romanoff, A. L., 209, *218*
Romeis, B., 325, 333
Roseman, S., 305, *309*
Rouget, C., 130, *136*
Roullier, C., 481, *486*
Rugh, R., 508, 509, *519*
Rushton, W. A. H., 108, *115*
Ruska, H., 291
Russell, E. S., *471*, *486*
Ruyter, J. H. C., 411, *419*
Ryan, M., 304, 309

S

St. George, R. C. C., 521, *555*, *556*
Saito, Z., 555
Salzmann, M., 367, 376, *377*, 446, *451*
Satir, P. G., 442, *451*
Sauer, M. E., 490, *505*
Saunders, J. W., 430, *432*
Scarpelli, D. G., 100, *170*, *171*
Schaeffer, A., *400*, *403*
Schalekamp, M., 235, *246*
Schaly, G. A., 130, *136*
Scharenberg, K., 117, 118, 128, 130, 132, 136
Scheer, I. J., 176, *191*
Schmke, R. T., 29, *49*
Schmidt, G., 294, 295, *309*
Schmidt, W. J., 5, 27, 36, *49*, 178, *191*, 521, 523, 527, 537, *555*
Schmitt, F. O., 299, *308*
Schneider, W. C., 427, *432*
Schork, P., 273, 274, 281, 435, 436, *439*
Schraffenberger, E., 511, *519*
Schuchardt, E., 283, 284, *291*
Schulhof, K., 249, *256*
Schultz, R. L., 17, 27
Schwarz, W., 283, 284, 285, *291*, 294, 301, *309*, 381, *391*, 393, *403*
Scott, B. L., 148, *150*, 458, *465*
Seegal, B., 250, *256*
Seligman, A. M., 55, 70
Seo, S., 411, *418*
Shanes, A. M., 46, *49*
Shen, S.-C., 161, 163, *171*
Sherman, F. G., 273, 277, 281, 435, *439*, 487, 492, 505
Shin, E., 174, *191*
Shlaer, S., 107, *115*
Shoch, D., 259, *271*
Sidman, R. L., 37, 46, *49*, 53, 63, 68, *69*, 71, 163, 167, *171*, 487, 488, 489, 490, 492, 494, 502, 504, 505, 533, 554
Siegel, B. V., 470, *486*
Siekevitz, P., 400, *403*
Sikorski, J., 470, *485*
Silver, A., 161, 162, 170
Silvers, W. K., *471*, *485*, *486*
Sjostrand, F. S., 2, 3, 4, 5, 6, 8, 10, 14, 16, 17, 18, 20, 22, 24, 26, 27, 28, 30, 38, 42, *49*, 90, *99*, *105*, *115*, 139, *150*, 151, *158*, 168, *171*, 173, *191*, 400, *403*, 521, 522, 530, 536, 546, *554*, *555*
Slonaker, J. R., 209, *218*
Smelser, G. K., 240, *247*, 407, 409, 410, 411, *418*, 422, *432*, 444, *451*, 453, 454, 456, 458, 460, 462, *465*
Smith, A. U., 509, *519*
Smith, E. L., *555*
Smith, R., 311, 320, *324*, 335, *340*
Smuts, G., 411, *418*
Sogo, P. B., 47, *49*
Sommer, H., 207, 218
Sorsby, A., 32, *49*
Speakman, J. S., 311, 320, *324*, 389, 390, *391*
Spence, I., 510, *518*
Spicer, S. S., 216, *218*
Srinivasan, B. D., 273, *281*, 438, *439*
Stanworth, A., 412, 413, 415, *418*, *419*
Steinman, E., *554*
Stern, K. H., 186, *191*
Stern, R., 555
Stiehler, R. D., 426, *431*, *432*
Stocker, F. W., 435, 436, *439*
Stoeckenius, W., 37, 42, *49*
Stokes, R. H., 385, *391*

Strampelli, B., 284, *291*
Strömberg, R., 283, *291*
Stumpf, P. K., 423, *432*
Swan, A. A. B., 161, 162, *170*
Swick, L., 250, *256*
Sylvén, B., 285, *291*
Szabó, J., *333*
Szegvári, G., 202, *205*
Szent-Györgyi, A., 426, *432*
Szirmai, J. A., 294, 297, 301, *308*, *309*

T

Tanii, T., 393, *403*
Tansley, K., 32, *49*, 85, *99*, 503, *505*, *555*
Teng, C. C., 343, *366*
Tennyson, U. M., 460, *465*
Thiersch, J. B., 510, *519*
Thiessen, R., 283, *290*
Thornburg, W., 42, *49*
Thornton, C. S., 430, *432*
Tobias, C. A., 259, *271*
Tokuyasu, K., 30, *49*, 73, 82, *83*, 96, *99*, 139, 143, 144, *150*, 151, *158*, 470, 481, *486*, 546, *556*
Tollin, G., 47, *49*
Tomita, K., 53, *70*
Toth, L. Z. J., *301*
Tousimis, A. J., 301, *309*, 441, 443, 447, *451*
Trerotoli, L. P., 514, *519*
Tsou, K.-C., 55, *70*
Tuchmann-Duplessis, H., 510, 512, 514, 515, *519*
Turano, A. J., 522, 547, *556*
Turano, A. M., 176, *191*

U

Uhlenhuth, P. T., 249, *257*
Unger, H. H., 322, 324, 335, *340*
Uzman, L. L., 343, *366*

V

Valk, A. de T., 160, 164, *170*
van Campenhout, E., 516, *519*
Van den Hooff, A., 387, *391*, 393, *403*, 409, 411, *419*
Vandermeersche, G., 470, *485*
van Deth, J. H. M. G., 235, *247*
Van Heyningen, R., 159, *171*
van Paassen, F., 512, *518*
van Walbeek, K., 411, *419*
Varga, L., 306, *308*
Veen, R., 235, *246*
Vogt, A., 283, *291*
von Euler, H., 427, *431*
von Sallmann, L., 240, *247*, 259, 262, 264, 265, *271*, 274, *281*, 296, 309, 435, 438, *439*
von Szily, A., 209, *218*
Vrabec, F., 311, 320, 321, *324*, 325, 333

W

Waardenburg, P. J., 514, *519*
Wachtl, C., 266, *271*
Waddington, C. H., 235, *247*
Wagner, H. G., 22, *27*
Wald, G., 24, *28*, 57, *70*, 73, 83, 85, 86, 96, 97, *98*, *99*, 102, 104, 105, 109, *115*, 143, 144, *150*, 169, *171*, 173, 174, 180, 183, *191*, 521, 536, 540, 547, *554*, *555*, *556*
Walker, B. E., 490, *505*
Walls, G. L., 142, *150*, 207, *218*, 315, *324*, 544, *556*
Walsch, E. G., 161, 162, *170*
Walther, J. B., 202, *205*
Wanko, T., 221, 224, *232*
Ward, D. N., 480, *485*
Ward, J. C., 188, *191*
Warkany, J., 511, 512, *518*, *519*
Wassermann, F., 394, *403*
Waters, J. W., 294, 295, *309*
Watson, D., 305, *309*
Watson, M. L., 368, *377*
Weiss, P., 235, *247*, 406, *419*
Weissenfels, N., 469, 470, 471, 478, *486*
Weissmann, B., 411, *418*
Welch, C., 259, *271*
Wellings, S. R., 470, *486*
Wersäll, J., 20, 28
Werthemann, A., 509, *519*
Westfall, J. A., 470, *485*
Whewell, C. S., 470, *485*
Wieme, R. J., 240, *246*, 250, *256*
Wilson, J. G., 507, 508, 510, *519*
Wilson, M. L., 239, *247*
Wilson, W. W., 120, 124, *137*
Winkelman, J. E., 411, *419*
Winkler, C. H., 215, *218*
Wirth, A., 202, *205*
Wislocki, G., 37, *49*, 53, 68, *70*, 163, 167, *171*

Witmer, R. H., 250, 251, 253, 256, 257
Wolf, E., 207, *218*
Wolfand, L., 101, 162, *170*
Wolff, J., 508, 509, *519*
Wolken, J., 36, *49*, 174, 175, 176, 182, 183, 184, 188, *191*, 522, 547, *556*
Wolman, E., 255, *257*
Wolpers, C., 284, *291*
Wolter, J. R., 118, 120, 121, 122, 124, 125, 120, 128, 130, 132, 134, *136*, 137
Woodin, A. M., 386, *391*
Woods, A. C., 240, *246*, 249, 257
Woods, E. F., 305, *309*
Woods, H. J., 470, *485*
Woolam, D. H. M., 509, *519*
Wright, H. V., 508, 512, *519*

Y

Yamada, E., 30, 38, *49*, 73, 74, 78, 80, 82, 83, 96, *99*, 139, 143, 144, *150*, 151, *158*, 470, 481, *486*, 546, *556*

Z

Zeman, W., 117, *118*, 128, 130, 132, *136*
Zewi, M., *555*
Zimm, B. M., 190, *191*
Zimmermann, H., 68, 70
Zimmermann, K. W., 130, *137*
Zimmermann, L. E., 336, *340*, 441, *451*
Zweifach, B. W., 68, *69*
Zwemer, R. L., 542, *554*
Zweng, H. C., *377*
Zwilling, E., 430, *432*

SUBJECT INDEX

A

Accommodation, 232, 328
Anophthalmia, 508, 510
Anterior chamber angle, 314
  annular ligament of, 312, 313
  comparative anatomy of, 312-317, 326
  evolution of, 322
  glycogen in, 319
Aqueous humor, 453
Aqueous veins, 311
Autoradiography, 273-280, 435-440, 487-506

B

Basement membrane, 456
Bergmeister's papilla, 209
Blood-brain barrier, 17
Buphthalmia, 512

C

C3H mice, 30, 32, 47
Capillaries, 212, 364
  pores in, 76, 142, 454
Carbonic anhydrase, 207
Cataract formation, 270
Chloroplasts, 112, 533
Choroid, 139
  Bruch's membrane, 74, 125, 130, 143
  chorioeapillaris, 74, 139, 142, 146
  pericytes of, 130
  pigment granules in, 472
Choroid fissure, 207, 406, 416, 508
Ciliary body, 316, 325
Ciliary epithelium, 453, 464
  acetazolamide (Diamox) effect on, 454, 458, 462
  cell membrane elaborations of, 453
  Golgi complex in, 458, 462
  Shigella endotoxin effect on, 462
Collagen synthesis, 415, *see also* cornea
Compound eyes, 174
Cornea, 365, 393, 409
  anomalies of, 511
  basement membrane of, 343, 350
  Bowman's membrane, 343, 348, 350
  canals in, 132, 386
  cells of, 132, 348, 352
  cementogenesis in, 393
  chondroitin in, 411
  chondroitinsulfate in, 393, 411
  collagen fibrils of, 398
  collagenous fiber patterns of, 412
  curvature of, 405, 413
  development of, 427
  diffusion in, 381, 390
  electrical properties of, 383, 385
  epithelial adhesiveness, 426
  epithelial cells, 343, 344
  fibrillar lattice of, 412
  fibrillogenesis in, 393
  hydration of, 386, 390, 393, 411, 422
  interference pattern of, 405, 415
  interfibrillar spaces of, 412
  keratosulfate in, 393, 411
  lamellae of, 393
  long-spacing collagen fibers in, 343, 352, 365, 370, 372, 376
  mast cells in, 352
  metabolic organization of, 428
  mucopolysaccharides in, 364, 365, 409, 411
  nerves of, 132
  protein synthesis in, 427
  refractive index of, 405
  scars in, 365
  Schwalbe's line, 134, 367, 372
  Schwann cells in, 132
  stroma, 346, 381
  stroma-epithelium metabolic relationship, 421
  transparency of, 381, 405, 409, 411, 412
  water content of, 409
  water-limiting systems of, 411
Cornea guttata, 376
Crampton's muscle, 316, 326, 327
Cryostat sections, 56
Cysteine, mitotic inhibition by, 266

D

Dark adaptation, 110, 111, 193, 197, 200, 538
DBA mice, 30
Descemet's endothelium, 134, 350, 370, 376, 387, 435, 437, 438
  intercellular spaces in, 388, 390
  mitotic figures in, 435, 438
  regeneration of, 435

Descemet's membrane, 321, 348, 352, 354, 364, 365, 367, 368, 370, 372, 376
Desmosomes, 344, *see also* lens
Diamox, see ciliary epithelium
Dilator muscle, 441, 447, 450
Diurnal vision, 193
DNA, 273, 276, 280, 281, 487, 490

E

Electron diffraction patterns, 552
Electroretinogram, 85, 193, 197, 198, 199, 200, 203, 204
  bipolar layer and, 203
  off-effect, 200
Endoplasmic reticulum, 364, 398, 402
Evolutionary pathways, 253
Exophthalmia, 510

F

Flicker fusion, 202
Fluid transport, 458
Freeze substitution, 50, 522, 525

G

Golgi apparatus, 469, 470, *see also* ciliary body, retina

H

Hassal-Henle bodies, 352, 364, 372, 374, 376
Hyaloid artery 210
Hyaluronic acid, 302, 304, 305, 306, *see also* vitreous humor

I

Immunoelectrophoretic methods, 251, 258
Immunological techniques, 239, 249
Internal limiting membrane, 146
Intraocular pressure, 406, 407
Intrascleral canal, 318
Ions, diffusion of, 387

K

Kayser-Fleischer ring, 365
Kolmer's droplets, 542

L

Lamina cribrosa, 125
Lamina vitrea, 143
Lens, 235
  alpha crystallin, 240, 245, 253, 257
  antigens, 235, 239, 250
  antiserum to, 235
  beta crystallin, 240, 245, 253, 257
  cataract, 259
  cell interdigitations, 224
  cell migration in, 261
  in cephalopods, 255
  cortical fibers of, 221
  desmosomes, 230, 232
  epithelium, 224, 273
  epithelium flat preparations, 259
  explants cultured, of, 236
  fibers, 222, 224, 232
  formation *in vitro* of, 237
  gamma crystallin, 240, 246, 253, 257
  germinative zone of, 259, 264
  heterologous and homologous antisera to, 250
  induction of, 235
  invertebrate lenses, 255, 256
  mechanical injury to, 273
  mitochondria of, 224
  mitotic counts in, 259, 260
  organ specificity of, 249
  species specificity of, 249
  sutures of, 221, 222, 224
Liesegang ring, 186
Liquid crystals, 37, 188, 190
Lymphatic vessels, 333

M

Metachromasia, 411, 412
Microphthalmia, 508, 509, 510, 512
Microvilli, 447
Mitochondria, 76, 78, 364, 396, *see also* lens, pigment epithelium, retina, rods and cones
Mitosis, 268, 275, 279, 280, 488, *see also* Descemet's endothelium, lens, radiation damage, retina, trabecular meshwork
Mucopolysaccharides, 412, 422, *see also* cornea
Myelin, 2, 102, 533

N

Neurolemma, 101
Nonneural retina, 146

O

Ocular malformations, 507, 508
Ommatidia, 174
Opsin, 104
Optic disk, 125, 207
Optic nerve glia, 125, 126
Ora serrata, 146, 492
Ouchterlony, double diffusion, method of, 239

P

PAS, 214
Pecten, 82, 207, 210, 212
Photoreceptors, 173, 180, 521, 534
  evolution and comparative anatomy of, 174-176, 547-548
Pigment epithelium, 67, 73, 102, 139, 441, 442, 446, 533, 546, *see also* vitamin A deficiency
  cell processes of, 80
  endoplasmic reticulum in, 80, 144
  fuscin granules, 80, 144
  melanin granules in, 469
  microvilli, 444
  mitochondria, 144
  myeloid bodies, 78, 96-97, 112, 144, 546
  oxidative enzymes in, 67
  pigment granules, 148, 442, 546, 550
  relation of photoreceptors to, 144
Pigment granules, 80, 210, 443, *see also* pigment epithelium
  development of, 474
  effect of genes on, 471, 478
  structure of, 470
Pinocytosis, 388, 402, 460
Plasma membrane, 2
  molecular structure of, 2
Polarized light, 415, 521
Posterior chamber, 456, 458, 464
Potassium permanganate fixation, 3
Precipitin reactions in agar gels, 250
Pseudoreplica technique, 312, 320
Purkinje shift, 193, 197

R

Radiation damage, 259
  cell density and, 261
  cysteine, treatment of, 260, 265, 266, 267, 268
  lens, shielding of, 260
  mitosis, effect on, 264
  nuclear fragmentation, 261, 262, 265
Radiosulfate, 411
Resistance to outflow, 338
Retina, 16, 17, 82, 207, 521-556
  amacrine cells, 161, 194, 204, 488, 494, 502
  amplification in, 109
  bipolar cells, 17, 29, 194, 195, 204, 487, 488, 489, 493, 496, 498, 502, 503
  brightness contrast, 22
  Cajal, end bulbs in, 129
  central retinal artery, 203
  centrifugal nerve fibers in, 126
  centripetal fibers of, 129
  in C3H mice, 103
  cholinergic transmission mechanism, 162
  cilia, 16
  circuit diagram of, 22
  citric acid cycle in, 68
  degeneration of, 87-90
  development of, 30, 32, 60, 64, 487
  DPN in, 72, 166, 167
  enzymes in, 53-72, 159-172
  enzyme turnover in, 109
  external limiting membrane, 67
  extracellular space in, 16, 17
  fatty acid metabolism of, 68
  fovea, 143
  ganglion cells, 67, 203, 487, 488, 489, 493, 496, 502, 504
  ganglion cells, degeneration of, 203
  glia of, 17, 117, 120, 124, 502
  glycolytic activity in, 170
  Golgi apparatus in, 16
  horizontal cells, 194, 195, 503
  inner nuclear layer, 161, 195, 198, 203, 204
  inner plexiform layer, 20, 67, 161, 488, 496
  metabolic exchange in, 82
  metabolic pathways in, 170
  mitochondria in, 16
  mitotic figures in, 489
  Müller's cells and/or fibers, 1, 17, 66, 72, 167, 488, 503
  nerve impulses, transmission of, 166
  nutrition of, 207

outer plexiform layer, 67, 161, 500
oxidative activity in, 68
pentose cycle activity in, 68
photoreceptors in, 29, 487, 489, 493, 496, 502
primary synapses in, 29
pure-cone, 194, 197
pure rod, 18
radial fibers in, 118
regeneration of, 129
rosettes of, 509
Schwann cells, 17
structural organization of, 23
synapses in, 17, 504
synaptic bodies and vesicles in, 18, 20
TPN in, 166, 167
vitamin A deficiency and, 90
Retinitis pigmentosa, 97, 101
Retrolental fibroplasia, 509
Rhabdomeres, 174, 176, 553
Rhodopsin, 10, 104, 109, 173-183, 193, 527, 540
RNA, 78
Rods and cones, 5, 140, 151, 193, 532, 534
analysis with polarized light, 5
anatomical degeneration of, 97
chemistry of lamellae in, 42
cone-like rods, 18
cones, 10, 18, 82, 101, 108, 173, 195, 196
crystal-like structure of, 46
development of, 30, 96
disk geometry, 178
disks of, 8, 178, 521, 533
double cones, 10
double row of cones, 190, 202
ellipsoids, 68
energy transfer in, 47
fine structure of, 37
fresh preparations of, 523, 529
inner segments of, 67, 146, 151, 544
inter- and intra-saccular spaces in, 40
lamellae of, 101, 522, 529, 548
lipoprotein, structure of, 16, 36
mitochondria in, 151, 544
molecular architecture of, 5
outer segments of, 5, 10, 108, 151, 523, 530, 536, 541, 548
plasma membrane of, 1, 8
quantum mechanics, in relation to, 101, 107, 108, 109
quasi-crystalline structures of, 103
rod sacs, 30, 151, 156
rods, 18, 101, 108, 173
vitamin A-deficiency and, 103

S

Schlemm's canal, 326, 328, 333
Schwann cells, 1
Sciuridae, 193
Sclera, 365, 407
cartilagenous differentiation in, 407
Scotopic vision, 108
Sensory corpuscles
of Herbst, 325, 326, 327
of Krause, 325
of Vater-Pacini, 329
Sheath, of Schwann, 101
Spectral sensitivity curve, 193
Sphincter muscle, 441

T

Tapetum, 143
Teratogenic agents, 508-514
Thorotrast, 453
Thymidine-H3, 273, 277, 435, 438, 487, 490, 492, 496, 500
Trabecular meshwork, 132, 134, 311, 319, 320, 322, 326, 335, 336, 354, 367, 370, 377
argyrophilic fiber system of, 335
cellular elements of, 320
cement substance of, 322
corneoscleral part, 336
"glass membranes" of, 335
mitotic division in, 322
nerve supply of, 134
phagocytic activity in, 322
pores in, 319, 330, 340, 377

V

Visual pigments, 104-107, 173, 193, 544
Vitamin A, 85, 87, 104, 105
Vitamin A deficiency
Muller's fibers in, 92
myeloid bodies in, 103
opsin in, 97
outer segments regeneration following, 96

pigment epithelium in, 90
retinal recovery from, 94
Vitreous humor, 207, 283, 289, 406
cells in, 294, 301, 307
collagen of, 294
cortical layer, 294, 300, 302
fibrils, 283, 284, 285, 289
fibrous bands of, 307
gel state of, 294
heat shrinkage of, 295
hyaloid membrane, 301
hyaluronic acid in, 284, 296, 304
hydroxyproline-containing filaments of, 295
interfibrillar substance, 285
liquid vitreous, 307
membrana plicata, 283, 290, 301
model gel, 299
postlenticular space, 290, 301

W

Wilson's disease, 365

X

X-ray diffraction, 2

Z

Zonular fibers, 456